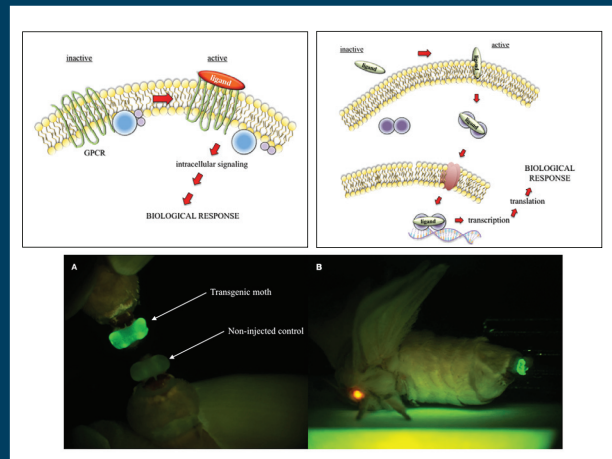


frontiers

RESEARCH TOPICS



MOLECULAR MECHANISMS UNDERLYING INSECT BEHAVIORS: RECEPTORS, PEPTIDES, & BIOSYNTHETIC PATHWAYS

Topic Editors

Shogo Matsumoto and Joe Hull



frontiers in
ENDOCRINOLOGY



frontiers

FRONTIERS COPYRIGHT STATEMENT

© Copyright 2007-2013
Frontiers Media SA.
All rights reserved.

All content included on this site, such as text, graphics, logos, button icons, images, video/audio clips, downloads, data compilations and software, is the property of or is licensed to Frontiers Media SA ("Frontiers") or its licensees and/or subcontractors. The copyright in the text of individual articles is the property of their respective authors, subject to a license granted to Frontiers.

The compilation of articles constituting this e-book, wherever published, as well as the compilation of all other content on this site, is the exclusive property of Frontiers. For the conditions for downloading and copying of e-books from Frontiers' website, please see the Terms for Website Use. If purchasing Frontiers e-books from other websites or sources, the conditions of the website concerned apply.

Images and graphics not forming part of user-contributed materials may not be downloaded or copied without permission.

Individual articles may be downloaded and reproduced in accordance with the principles of the CC-BY licence subject to any copyright or other notices. They may not be re-sold as an e-book.

As author or other contributor you grant a CC-BY licence to others to reproduce your articles, including any graphics and third-party materials supplied by you, in accordance with the Conditions for Website Use and subject to any copyright notices which you include in connection with your articles and materials.

All copyright, and all rights therein, are protected by national and international copyright laws.

The above represents a summary only. For the full conditions see the Conditions for Authors and the Conditions for Website Use.

ISSN 1664-8714

ISBN 978-2-88919-179-6

DOI 10.3389/978-2-88919-179-6

ABOUT FRONTIERS

Frontiers is more than just an open-access publisher of scholarly articles: it is a pioneering approach to the world of academia, radically improving the way scholarly research is managed. The grand vision of Frontiers is a world where all people have an equal opportunity to seek, share and generate knowledge. Frontiers provides immediate and permanent online open access to all its publications, but this alone is not enough to realize our grand goals.

FRONTIERS JOURNAL SERIES

The Frontiers Journal Series is a multi-tier and interdisciplinary set of open-access, online journals, promising a paradigm shift from the current review, selection and dissemination processes in academic publishing.

All Frontiers journals are driven by researchers for researchers; therefore, they constitute a service to the scholarly community. At the same time, the Frontiers Journal Series operates on a revolutionary invention, the tiered publishing system, initially addressing specific communities of scholars, and gradually climbing up to broader public understanding, thus serving the interests of the lay society, too.

DEDICATION TO QUALITY

Each Frontiers article is a landmark of the highest quality, thanks to genuinely collaborative interactions between authors and review editors, who include some of the world's best academicians. Research must be certified by peers before entering a stream of knowledge that may eventually reach the public - and shape society; therefore, Frontiers only applies the most rigorous and unbiased reviews.

Frontiers revolutionizes research publishing by freely delivering the most outstanding research, evaluated with no bias from both the academic and social point of view.

By applying the most advanced information technologies, Frontiers is catapulting scholarly publishing into a new generation.

WHAT ARE FRONTIERS RESEARCH TOPICS?

Frontiers Research Topics are very popular trademarks of the Frontiers Journals Series: they are collections of at least ten articles, all centered on a particular subject. With their unique mix of varied contributions from Original Research to Review Articles, Frontiers Research Topics unify the most influential researchers, the latest key findings and historical advances in a hot research area!

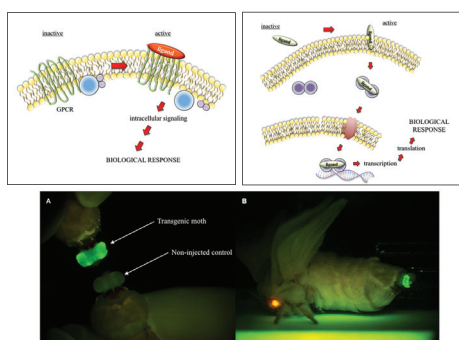
Find out more on how to host your own Frontiers Research Topic or contribute to one as an author by contacting the Frontiers Editorial Office: researchtopics@frontiersin.org

MOLECULAR MECHANISMS UNDERLYING INSECT BEHAVIORS: RECEPTORS, PEPTIDES, & BIOSYNTHETIC PATHWAYS

Topic Editors:

Shogo Matsumoto, Advanced Science Institute – RIKEN, Japan

Joe Hull, USDA Agricultural Research Service, USA



Upper right panel – Schematic diagram of G protein-coupled receptor signaling. A GPCR, which consists of seven transmembrane domains with alternating extracellular and intracellular loops, binds extracellular ligands (i.e. peptides, neurotransmitters, etc). Ligand binding promotes dissociation of a heterotrimeric G protein complex. This in turn activates downstream effectors that trigger an intracellular signaling cascade culminating in a biological response. **Upper left panel – Schematic diagram of nuclear receptor signaling.** In this example, a lipophilic compound crosses the plasma membrane and binds to a cytosolic nuclear hormone receptor. Ligand binding promotes translocation to the nucleus and binding to a specific sequence of DNA. This leads to transcription of downstream DNA into RNA and the subsequent translation of the RNA message into protein, which triggers a cellular change culminating in a biological response. **Lower panel – Enhanced green fluorescent protein expression in the PG of G1 female adults.** (A) EGFP expression was visible in the PG of transgenic moths but not non-injected controls. (B) The expressions of two reporter genes via whole-body fluorescence imaging. Red fluorescence is derived from DsRed expressed in the compound eye and green fluorescence is derived from EGFP expressed in the PG of the transgenic *B. mori*. Figure from this issue - Moto K-I and Matsumoto S (2012) Construction of an *in vivo* system for functional analysis of the genes involved in sex pheromone production in the silkworm, *Bombyx mori*. *Front. Endocrin.* 3:30. doi: 10.3389/fendo.2012.00030.

Countless studies utilizing a diversity of insect species have significantly contributed to our understanding at both the molecular and cellular levels of how an extracellular signal is turned into a cellular response. These studies have spawned a wide-ranging multi-disciplinary research field that has its roots in the elucidation of chemical structures and biosynthetic pathways but which has since branched out to incorporate cellular and molecular dynamics, metabolic engineering, population genetics, and RNA-dependent gene silencing. Research into other signals and their cognate receptors has led to the realization that these interactions govern nearly every facet of insect life from growth and development to homeostasis and reproductive behavior. As a consequence, significant efforts have been made to further our knowledge of signaling pathways and how they impact insect physiology and behavior as a means of facilitating the development of the next generation of biorationally-designed insect control agents. The same linear dependence on signaling also makes insects excellent models for the basic endocrine mechanisms underlying lipid and cellular biology and can provide insights into lipid uptake, lipogenesis, hormone-regulated lipolysis, membrane trafficking, and intracellular calcium signaling in organisms from other phyla. It is the aim of this Research Topics forum to celebrate the advancements seen in insect endocrinology via review papers and original articles as well as to highlight recent developments in fundamental and applied insect-based endocrine research.

Table of Contents

- 06 *Molecular Mechanisms Underlying Insect Behaviors: Receptors, Peptides, and Biosynthetic Pathways***
Joe Hull and Shogo Matsumoto
- 08 *Functional Characterization of Hypertrehalosemic Hormone Receptor in Relation to Hemolymph Trehalose and to Oxidative Stress in the Cockroach *Blattella germanica****
Jia-Hsin Huang, Xavier Bellés and How-Jing Lee
- 19 *Re-Evaluation of the PBAN Receptor (PBANR) Molecule: Characterization of PBANR Variants Expressed in the Pheromone Glands of Moths***
Jae Min Lee, J. Joe Hull, Takeshi Kawai, Chie Goto, Masaaki Kurihara, Masaru Tanokura, Koji Nagata, Hiromichi Nagasawa and Shogo Matsumoto
- 31 *Establishment of Sf9 Transformants Constitutively Expressing PBAN Receptor Variants: Application to Functional Evaluation***
Jae Min Lee, J. Joe Hull, Takeshi Kawai, Kazuhide Tsuneizumi, Masaaki Kurihara, Masaru Tanokura, Koji Nagata, Hiromichi Nagasawa and Shogo Matsumoto
- 39 *Select Neuropeptides and Their G-Protein Coupled Receptors in *Caenorhabditis Elegans* and *Drosophila Melanogaster****
William G. Bendena, Jason Campbell, Lian Zara, Stephen S. Tobe and Ian D. Chin-Sang
- 51 *Cytoplasmic Travels of the Ecdysteroid Receptor in Target Cells: Pathways for Both Genomic and Non-Genomic Actions***
Xanthe Vafopoulou and Colin G.H. Steel
- 67 *The Arginine Residue With in the C-Terminal Active Core of Bombyx Mori Pheromone Biosynthesis-Activating Neuropeptide is Essential for Receptor Binding and Activation***
Takeshi Kawai, Jae Min Lee, Koji Nagata, Shogo Matsumoto, Masaru Tanokura and Hiromichi Nagasawa
- 72 *Molecular Structure and Diversity of PBAN/Pyrokinin Family Peptides in Ants***
Man-Yeon Choi and Robert K. Vander Meer
- 80 *Effects of Starvation on Brain Short Neuropeptide F-1, -2, and -3 Levels and Short Neuropeptide F Receptor Expression Levels of the Silkworm, *Bombyx mori****
Shinji Nagata, Sumihiro Matsumoto, Tomohiro Nakane, Ayako Ohara, Nobukatsu Morooka, Takahiro Konuma, Chiaki Nagai and Hiromichi Nagasawa

- 88** *Regulatory Role of PBAN in Sex Pheromone Biosynthesis of Heliothine Moths*
Russell Jurenka and Ada Rafaeli
- 96** *Screening for the Genes Involved in Bombykol Biosynthesis: Identification and Functional Characterization of Bombyx Mori Acyl Carrier Protein*
Atsushi Ohnishi, Misato Kaji, Kana Hashimoto and Shogo Matsumoto
- 105** *Construction of an in Vivo System for Functional Analysis of the Genes Involved in Sex Pheromone Production in the Silkworm, Bombyx Mori*
Ken-Ichi Moto and Shogo Matsumoto
- 115** *Biosynthetic Pathway for Sex Pheromone Components Produced in a Plusiinae Moth, Plusia festucae*
Hayaki Watanabe, Aya Matsui, Sin-ichi Inomata, Masanobu Yamamoto and Tetsu Ando
- 122** *Prostaglandins and Their Receptors in Insect Biology*
David Stanley and Yonggyun Kim
- 133** *Recent Topics on the Regulatory Mechanism of Ecdysteroidogenesis by the Prothoracic Glands in Insects.*
Yoshiaki Tanaka
- 139** *Wolbachia as an "Infectious" Extrinsic Factor Manipulating Host Signaling Pathways*
Ilaria Negri



Molecular mechanisms underlying insect behaviors: receptors, peptides, and biosynthetic pathways

J. Joe Hull^{1*} and Shogo Matsumoto^{2†}

¹ USDA-ARS, US Arid Land Agricultural Research Center, Maricopa, AZ, USA

² Molecular Entomology Laboratory, RIKEN Advanced Science Institute, Wako, Japan

*Correspondence: joe.hull@ars.usda.gov

†Retired

Edited by:

Cunming Duan, University of Michigan, USA

Keywords: intracellular signaling, neuropeptide, receptor, biosynthetic pathway, insect

Intracellular signaling pathways govern nearly every facet of insect life. As a consequence, significant effort has been made to expand our understanding (for both basic and applied purposes) of these pathways at the molecular and cellular levels. It is the aim of this Research Topic to highlight recent developments in insect systems that address fundamental questions of how chemical signals trigger biological/physiological responses. The articles presented here have been loosely grouped into three topics: receptors, ligands, and intracellular pathways/mechanisms.

The first section (four Original Articles and one Review Article) is “receptor-centric” with four papers discussing G protein-coupled receptors (GPCRs) and the other reporting on an intracellular nuclear receptor. Hypertrehalosemic hormone (HTH) is a peptide hormone recently implicated in some systems in the cellular response to oxidative stress. Huang et al. (1) report identification of a GPCR for HTH in the German cockroach (*Blattella germanica*). Based on RNAi-mediated knockdown of the ligand-receptor pair, the authors conclude that HTH and its receptor are critical for mediating anti-oxidative responses in *B. germanica*. Lee et al. (2) examined the expression of a different peptide hormone receptor, pheromone biosynthesis activating neuropeptide receptor (PBANR). They showed that four alternatively spliced variants, differentiated only by the length of their carboxyl terminal tails, are concomitantly expressed in the pheromone glands of multiple moth species. This finding addresses concerns regarding the biological significance of PBANR isoforms identified previously. To further evaluate the functionality and regulation of those PBANR variants, Lee et al. (3) established cultured insect lines constitutively expressing the receptor variants. Functional characterization of the receptors revealed that the “long” and “short” variants utilize different downstream effectors and regulatory mechanisms. Departing from the Original Article format of the previous entries, Bendena et al. (4) present a short review of select neuropeptides [NPF/Y, short neuropeptide F (sNPF), FMRFamide, pigment dispersing hormone, cholecystokinin, and allatostatin-like peptides] and their GPCRs in *Drosophila melanogaster* and *Caenorhabditis elegans*. The final paper in the receptor grouping used confocal scanning laser-based immunohistochemical imaging to examine nuclear trafficking of the ecdysteroid receptor (EcR) in *Rhodnius prolixus* cells (5). Co-localization of EcR with microtubules, Hsp90, FKBP52, and a component of dynein, along with impeded EcR nuclear localization following disruption of

the microtubule network, led the authors to propose that EcR translocates to the nucleus along microtubules via a cytosolic dependent protein complex.

The second section (two Original Articles and one Review Article) of this issue focuses on neuropeptide ligands, in particular pheromone biosynthesis activating neuropeptide (PBAN) and sNPF. In most species of moths, PBAN controls biosynthesis of the chemical compounds (i.e., sex pheromones) that females use to attract conspecific males. To develop a more nuanced understanding of how PBAN interacts with its receptor [i.e., PBANR; see (2, 3)], Kawai et al. (6) sought to clarify the role of the Arg residue in the FxPRLamide active core of PBAN. Structure-function analyses revealed the importance of this residue in PBANR binding and activation. PBAN/pyrokinin peptides, which are characterized by the FxPRLamide motif, are present in multiple insect orders. In their Review Article, Choi and Vander Meer (7) discuss recent research on the molecular structure and diversity of PBAN/pyrokinin peptides in ants, in particular the fire ant, *Solenopsis invicta*. The final paper of this section examines the role of sNPFs in governing feeding behavior in the silkworm, *Bombyx mori* (8). MALDI-TOF mass spectrometric profiling revealed that brain sNPF levels decreased following starvation but returned to basal levels after feeding, while direct injection of sNPFs into larvae stimulated feeding.

The final section (two Review Articles, three Original Articles, one Mini-Review, and one Perspective) of this issue centers on a number of diverse intracellular pathways/mechanisms. The opening quartet of articles in this section focuses on the intracellular pathways associated with moth sex pheromone biosynthesis. The first article by Jurenka and Rafaeli (9) provides an extensive review of the role PBAN has in heliothine moth biosynthetic pathways, and discusses recent findings implicating PBAN involvement in male pheromone production. Ohnishi et al. (10) present an Original Article describing their use of *B. mori* EST databases in conjunction with RNAi screening to identify transcripts involved in *B. mori* sex pheromone production. Subsequent characterization of one such transcript identified an acyl carrier protein essential for biosynthesis of the *B. mori* sex pheromone precursor. In an Original Article, Moto and Matsumoto (11) address the limitation of unequivocally demonstrating the *in vivo* functionality of genes linked to sex pheromone biosynthesis in systems such as moths that lack the desired genetic malleability. They describe the development of a transgenic system in *B. mori* utilizing the piggyBac transposon in conjunction

with a pheromone gland-specific desaturase promoter region. In the final article of the quartet, Watanabe et al. (12) present chemical evidence for the biosynthetic pathway utilized by the female rice looper (*Plusia festucae*) to generate ω 7-unsaturated sex pheromone components. Intriguingly, comparative analysis with another Plusiinae species suggested that different β -oxidation systems are utilized. The Review Article by Stanley and Kim (13) moves the focus away from moth sex pheromone production and places it on the biological role of prostaglandin receptor-mediated events in insect physiology. Among the topics reviewed are the role of prostaglandins in egg-laying in crickets and insect egg development in general, a prostaglandin receptor in tick salivary glands and prostaglandin receptor-mediated action in insect immunity. In a Mini-Review Article, Tanaka (14) describes recent studies on the regulatory mechanism underlying ecdysteroidogenesis (i.e., the production of compounds critical to insect molting and metamorphosis). The author further highlights studies in *B. mori* that have examined the role of humoral factors and neural control on ecdysteroidogenesis. Negri (15) presents the last paper in this issue, a Perspective Article reviewing data implicating the involvement of *Wolbachia*, a widespread endosymbiont of arthropods, in modulating host insulin and ecdysteroid hormonal pathways. The author concludes by presenting a model illustrating a possible mechanism for direct bacterial influence on host ecdysone signaling and epigenetic regulation.

REFERENCES

- Huang J-H, Bellés X, Lee H-J. Functional characterization of hypertrehalosemic hormone receptor in relation to hemolymph trehalose and to oxidative stress in the cockroach *Blattella germanica*. *Front Endocrinol (Lausanne)* (2012) 2:114. doi: 10.3389/fendo.2011.00114
- Lee JM, Hull JJ, Kawai T, Goto C, Kurihara M, Tanokura M, et al. Re-evaluation of the PBAN receptor molecule: characterization of PBANR variants expressed in the pheromone glands of moths. *Front Endocrinol (Lausanne)* (2012) 3:6. doi: 10.3389/fendo.2012.00006
- Lee JM, Hull JJ, Kawai T, Tsuneizumi K, Kurihara M, Tanokura M, et al. Establishment of Sf9 transformants constitutively expressing PBAN receptor variants: application to functional evaluation. *Front Endocrinol (Lausanne)* (2012) 3:56. doi: 10.3389/fendo.2012.00056
- Bendena WG, Campbell J, Zara L, Tobe SS, Chin-Sang ID. Select neuropeptides and their G-protein coupled receptors in *Caenorhabditis elegans* and *Drosophila melanogaster*. *Front Endocrinol (Lausanne)* (2012) 3:93. doi: 10.3389/fendo.2012.00093
- Vafopoulou X, Steel CGH. Cytoplasmic travels of the ecdysteroid receptor in target cells: pathways for both genomic and non-genomic actions. *Front Endocrinol (Lausanne)* (2012) 3:43. doi: 10.3389/fendo.2012.00043
- Kawai T, Lee JM, Nagata K, Matsumoto S, Tanokura M, Nagasawa H. The arginine residue within the C-terminal active core of *Bombyx mori* pheromone biosynthesis-activating neuropeptide is essential for receptor binding and activation. *Front Endocrinol (Lausanne)* (2012) 3:42. doi: 10.3389/fendo.2012.00042
- Choi M-Y, Vander Meer RK. Molecular structure and diversity of PBAN/pyrokinin family peptides in ants. *Front Endocrinol (Lausanne)* (2012) 3:32. doi: 10.3389/fendo.2012.00032
- Nagata S, Matsumoto S, Nakane T, Ohara A, Morooka N, Konuma T, et al. Effects of starvation on brain short neuropeptide F-1, -2, and -3 levels and short neuropeptide F receptor expression levels of the silkworm, *Bombyx mori*. *Front Endocrinol (Lausanne)* (2012) 3:3. doi: 10.3389/fendo.2012.00003
- Jurenka R, Rafaeli A. Regulatory role of PBAN in sex pheromone biosynthesis of heliothine moths. *Front Endocrinol (Lausanne)* (2011) 2:46. doi: 10.3389/fendo.2011.00046
- Ohnishi A, Kaji M, Hashimoto K, Matsumoto S. Screening for the genes involved in bombykol biosynthesis: identification and functional characterization of *Bombyx mori* acyl carrier protein. *Front Endocrinol (Lausanne)* (2011) 2:92. doi: 10.3389/fendo.2011.00092
- Moto K-I, Matsumoto S. Construction of an *in vivo* system for functional analysis of the genes involved in sex pheromone production in the silkworm, *Bombyx mori*. *Front Endocrinol (Lausanne)* (2012) 3:30. doi: 10.3389/fendo.2012.00030
- Watanabe H, Matsui A, Inomata S-I, Yamamoto M, Ando T. Biosynthetic pathway for sex pheromone components produced in a Plusiinae moth, *Plusia festucae*. *Front Endocrinol (Lausanne)* (2011) 2:74. doi: 10.3389/fendo.2011.00074
- Stanley D, Kim Y. Prostaglandins and their receptors in insect biology. *Front Endocrinol (Lausanne)* (2011) 2:105. doi: 10.3389/fendo.2011.00105
- Tanaka Y. Recent topics on the regulatory mechanism of ecdysteroidogenesis by the prothoracic glands in insects. *Front Endocrinol (Lausanne)* (2011) 2:107. doi: 10.3389/fendo.2011.00107
- Negri I. *Wolbachia* as an “infectious” extrinsic factor manipulating host signaling pathways. *Front Endocrinol (Lausanne)* (2012) 2:115. doi: 10.3389/fendo.2011.00115

Received: 23 August 2013; accepted: 28 August 2013; published online: 12 September 2013.

Citation: Hull JJ and Matsumoto S (2013) Molecular mechanisms underlying insect behaviors: receptors, peptides, and biosynthetic pathways. *Front. Endocrinol.* 4:120. doi: 10.3389/fendo.2013.00120

This article was submitted to *Experimental Endocrinology*, a section of the journal *Frontiers in Endocrinology*.

Copyright © 2013 Hull and Matsumoto. This is an open-access article distributed under the terms of the Creative Commons Attribution License (CC BY). The use, distribution or reproduction in other forums is permitted, provided the original author(s) or licensor are credited and that the original publication in this journal is cited, in accordance with accepted academic practice. No use, distribution or reproduction is permitted which does not comply with these terms.



Functional characterization of hypertrehalosemic hormone receptor in relation to hemolymph trehalose and to oxidative stress in the cockroach *Blattella germanica*

Jia-Hsin Huang¹, Xavier Bellés² and How-Jing Lee^{1*}

¹ Department of Entomology, National Taiwan University, Taipei, Taiwan

² CSIC-UPF, Institute of Evolutionary Biology, Barcelona, Spain

Edited by:

Joe Hull, USDA Agricultural Research Service, USA

Reviewed by:

Dalibor Kodrik, University of South Bohemia, Czech Republic
Gerd Gäde, University of Cape Town South Africa

*Correspondence:

How-Jing Lee, Department of Entomology, National Taiwan University, No. 1, Sec. 4, Roosevelt Road, Taipei 106, Taiwan.
e-mail: m480@ntu.edu.tw

Hypertrehalosemic hormone (HTH) is a peptide hormone that belongs to the adipokinetic hormone/red pigment concentrating hormone (AKH/RPCH) family, which exerts pleiotropic actions related to catabolic reaction and stress response. AKH peptides have been demonstrated to participate in stress response including oxidative stress in several insects. In order to study the signaling pathway of HTH involved in anti-oxidative stress, we have characterized a HTH receptor cDNA in *Blattella germanica* (*Blage-HTHR*) in structural and in functional terms using RNA interference (RNAi). *Blage-HTHR* is expressed in various female adult tissues (brain–CC–CA, ventral nerve cord, midgut, fat body, oviduct), but maximal expression is observed in the fat body. RNAi-mediated knockdown of *Blage-HTHR* expression results in a significantly lower level of hemolymph trehalose, even though HTH is exogenously administered. Paraquat elicits lethal oxidative stress in *B. germanica*, and co-injection of paraquat and HTH reduces this detrimental effect and extends the median survival time. Interestingly, the “rescue” effect of HTH on mortality caused by paraquat is diminished in specimens with depleted expression of *Blage-HTH* and *Blage-HTHR*. Finally, lipid peroxidation in the hemolymph increases 4 h after paraquat treatment, in comparison with control specimens or with HTH-treated specimens. However, lipid peroxidation induced by paraquat was not “rescued” by HTH in *Blage-HTH* and *Blage-HTHR* knockdown specimens. Our results demonstrate that HTH acts as a stress hormone mediating anti-oxidative protection in *B. germanica*, and that its receptor, *Blage-HTHR*, is essential for this action.

Keywords: adipokinetic hormone, paraquat, RNA interference, hypertrehalosemic hormone receptor, German cockroach

INTRODUCTION

The adipokinetic hormone/red pigment concentrating hormone (AKH/RPCH) family is one of the extensively characterized group of neuropeptides whose members play important roles on energy homeostasis, as well as on other physiological and behavioral processes in insects (Schooley et al., 2005). AKH peptides are 8- to 10-amino acid long, with a pyroglutamate blocked N-terminus and an amidated C-terminus, aromatic residues at positions 4 and 8, and a glycine residue at position 9, when present (Gäde, 2009). Among them, the peptides that primarily induce trehalose efflux into hemolymph are referred to as a hypertrehalosemic hormone (HTH).

Recently, AKHs have been related to stress response, through mechanisms involving the stimulation of catabolic reactions while inhibiting synthetic reactions by increasing available energy (Kodrik, 2008). Earlier studies have related the release of AKHs as a result of insecticide poisoning through recording the increase of metabolites such as trehalose and lipids in the hemolymph of the cockroach *Periplaneta americana* (Granett and Leeling, 1972) and the locust *Schistocerca gregaria* (Samaranayaka, 1974). Direct measurement of AKH titer increase after insecticide exposure has

been further reported in a number of insects, including the locust *S. gregaria* and the bug *Pyrrhocoris apterus* (Candy, 2002; Kodrik and Socha, 2005; Velki et al., 2011). In addition, AKHs participate in anti-oxidative mechanisms by increasing reduced glutathione efflux and decreasing protein carbonyl levels in response to treatment with paraquat (PQ), a bipyridylum herbicide that is currently used to elicit oxidative stress in animals through redox-cycling reactions (Hassan, 1984); it has been used in this way, for example, in the potato beetle *Leptinotarsa decemlineata* (Kodrik et al., 2007) and in *P. apterus* (Vecera et al., 2007).

Oxidative stress is a type of stressor that causes neurodegeneration of brain cells under severe stress condition (Chaudhuri et al., 2007); it also affects a number of physiological processes, including an adaptive compensatory specific response of the organism that is activated to sustain homeostasis (Valko et al., 2007). Reactive oxygen species, such as superoxide anion radicals, hydroxyl radical, and hydrogen peroxide, represent a class of molecules that are derived from the normal metabolism of oxygen in the majority of aerobic organisms. Reactive oxygen species arise as endogenous by-products of metabolic reactions in the cells, and from exogenous exposure to environmental pollutants, ionizing radiation,

and others. Excess of reactive oxygen species and/or deficit of scavenging antioxidants results in oxidative stress, which may impair correct regulation of lipids, proteins, and DNA (Halliwell and Gutteridge, 2007).

Most of the previous studies show that AKHs are involved in antioxidant protection mechanisms used biochemical experimental approaches such as monitoring AKH titer changes or exogenously applying AKH under oxidative challenges (Kodrik et al., 2007; Vecera et al., 2007). Thus, little information is available at the molecular level on the relation of AKH with antioxidant protection mechanisms. In this context, we aim to provide molecular evidence that the signaling pathway of HTH is involved in the antioxidant protection mechanisms, using the cockroach *Blattella germanica* as model. Previously, we had cloned the hypertrehalosemic hormone (*Blage-HTH*) cDNA in *B. germanica* (Huang and Lee, 2011). In the present study we report the cloning of the cDNA of the HTH receptor (*Blage-HTHR*) and the effect of PQ when both *Blage-HTH* and *Blage-HTHR* expression are silenced by RNA interference (RNAi) in *B. germanica*, a species that is particularly sensitive to this knockdown technique (Belles, 2010).

MATERIALS AND METHODS

INSECTS

A colony of the German cockroach, *B. germanica* (L.), was maintained in environmental chambers at 28°C under L:D = 16:8 h conditions. Dog chow and water were provided *ad libitum*. Nymphs and adults were reared in groups, but adults were separated by sex to keep them in virgin state. Detailed information about rearing has been described previously (Lee and Wu, 1994).

RNA EXTRACTION AND REVERSE TRANSCRIPTION TO cDNA

All RNA extractions were performed using TRIzol Reagent (Invitrogen) following the supplier's protocol. Possible genomic DNA contamination was removed by DNase I (Promega) treatment. One microgram of total RNA was reverse transcribed using High Capacity cDNA Reverse Transcription Kits (ABI).

CLONING OF THE HTH RECEPTOR

The first primer set was designed based on the known AKH receptor sequences of other insects, including *P. americana* (DQ217786), *Apis mellifera* (AY898652), *Tribolium castaneum* (DQ422965), and *Bombyx mori* (AF403542). The primer sequences were as follows: 5'-TCC ACG TGG AGG AGC ACC C-3' forward; and, 5'-TTC TTC CAS STG GAG GRR CAC CCC-3' reverse. The amplified fragment (420 bp) was subcloned into the pGEMT-easy vector (Promega) and sequenced. To complete the sequence, the GeneRacer Kit (Invitrogen) for rapid amplification of cDNA ends (RACE) was used following the manufacturer's protocol. For 5'-RACE, the reverse primer was 5'-GAC TCA GCT GTA CCA GTT CTG GTA CAG GA-3', and for 3'-RACE, the forward primer was 5'-GTC TGA ACT GAG CTG ATA TCT GCG A-3'. All PCR products were subcloned into pGEMT-easy vector (Promega) and sequenced.

PHYLOGENETIC ANALYSIS

The amino acid sequences of all known insect AKH receptors were obtained from GenBank and aligned using the Clustal X

1.18 program (Thompson et al., 1997). The resulting alignment was manually edited using the GeneDoc program (Nicholas et al., 1997) and analyzed by the Neighbor-joining method for construction of a phylogenetic tree. The AKH receptor of the insect species with the GenBank accession numbers are *Drosophila melanogaster* (AAF52426), *Anopheles gambiae* (ABD60146), *Aedes aegypti* (CAY77164 and CAY77166), *Glossina morsitans* (AEH25943), *B. mori* (AAL95712), *Manduca sexta* (ACE00761), *A. mellifera* (AAX83121), *Nasonia vitripennis* (NP_001161243), *T. castaneum* (ABE02225), *Acyrtosiphon pisum* (XP_001945436), *Pediculus humanus* (EEB15485), *P. americana* (ABB20590), and *B. germanica* (ADL60118). Five-letter abbreviations used for these AKH receptors and species are indicated in **Figure 1B**. Phylogenetic trees based on the resulting alignment were constructed using MEGA version 5 (Tamura et al., 2011). The gonadotropin-releasing hormone receptor of *Caenorhabditis elegans* (Caeel-GnRHR, GenBank accession number NP_506566) was used as outgroup. The robustness of phylogenetic analysis was evaluated by bootstrapping using 1000 replicates.

BLAGE-HTHR EXPRESSION ANALYSIS

We performed semiquantitative RT-PCR to investigate the distribution of *Blage-HTHR* in different tissues of 7-day-old adult female *B. germanica* and to assess the effects of RNAi. Thus, the 25 µl PCR mixture for amplifying the *Blage-HTHR* fragment included 1 µl of cDNA, 10 pmol of forward primer (5'-GAC TCA GCT GTA CCA GTT CTG GTA-3'), 10 pmol of reverse primer (5'-GGG AAA TGT CTT GTG AAC CAG GTC-3'), and 5 µl of Taq polymerase mixture (Protech). The PCR (30 cycles) was performed as follows: denaturation at 94°C for 30 s, annealing at 58°C for 30 s, extension at 72°C for 1 min. Expression of *BgActin* (GenBank EU514491) was used as reference. PCR products were separated and visualized on a 1.5% agarose gel.

Quantitative real-time PCR measurements were carried out in triplicate in Applied Biosystems StepOnePlus real-time PCR systems with Fast SYBR Green Master Mix (Applied Biosystems). The primers used to measure *Blage-HTHR* mRNA were as follows: 5'-TCT ATC GGG ACA ACA GCA ACC AGA-3' forward, and 5'-TGC TTC AGG AAC TTC ACT CAC AGT-3' reverse. The efficiency of this primer set was first validated by constructing a standard curve through five serial dilutions. The expression levels were normalized to *BgActin* expression using 2^{(-Delta Delta C(T))} method (Pfaffl, 2001). The PCR program began with a single cycle at 95°C for 3 min, 40 cycles at 95°C for 15 s, and 60°C for 30 s. Afterward, PCR products were heated to 95°C for 15 s, cooled to 60°C for 30 s and increasing the temperature 0.5°C/min in order to measure the dissociation curves and to determine an unique PCR product for each gene. A template-free control was performed in each batch.

RNA INTERFERENCE

The *Blage-HTHR* cDNA of the German cockroach was first cloned into the pGEMT-easy vector (Promega, Madison, WI, USA). Then, a 528 bp fragment targeting the 3'-UTR of *Blage-HTHR* mRNA was amplified by PCR. The primers (which contained the T7 promoter sequence: TAATACGACTCACTATAG) used in this PCR reaction were as follows: 5'-TGG ATA GAC CAG CAG TCT GCT

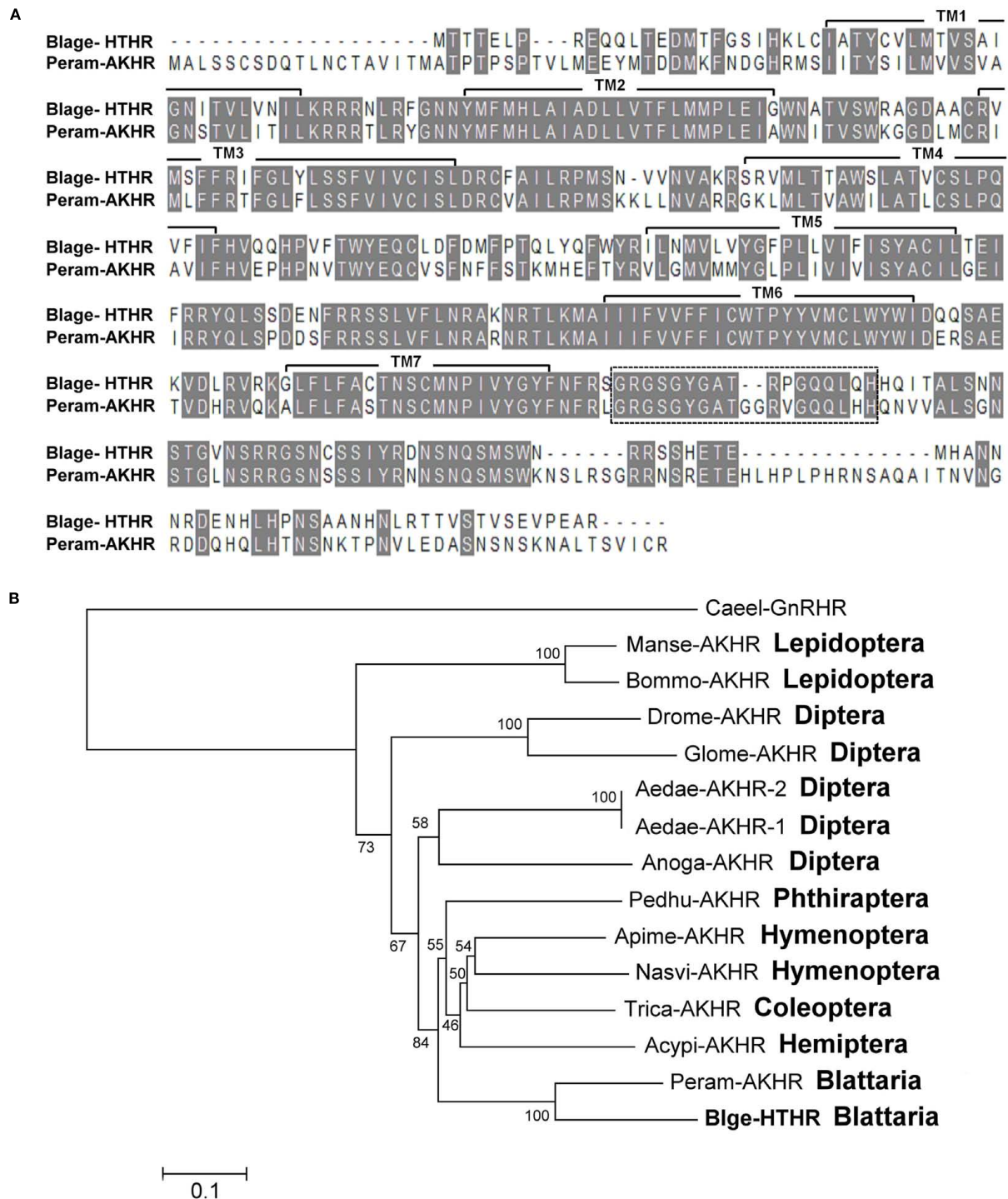


FIGURE 1 | (A) Alignment of the deduced amino acid sequences of the *Blattella germanica* HTH receptor (Blage-HTHR, GenBank GU591493) with the *Periplaneta americana* AKH receptor (Peram-AKHR, GenBank ABB20590). Identical amino acid residues are highlighted in gray. The seven transmembrane α -helices are indicated by TM1-7. The dotted-line rectangle indicates an insertion present in both cockroach species. **(B)** Neighbor joining tree of AKH receptor insect sequences. The tree was generated using MEGA 5 with 1000 bootstrap replicates. The evolutionary distance is given in units of the number of amino acid substitutions per site. The

abbreviated names of insect AKHR are: Acypi-AKHR (*Acyrtosiphon pisum*), Aedae-AKHR-1 and Aedae-AKHR2 (*Aedes aegypti*), Anoga-AKHR (*Anopheles gambiae*), Apime-AKHR (*Apis mellifera*), Blage-HTHR (*Blattella germanica*), Bommo-AKHR (*Bombyx mori*), Drome-AKHR (*Drosophila melanogaster*), Glome-AKHR (*Glossina morsitans*), Manse-AKHR (*Manduca sexta*), Nasvi-AKHR (*Nasonia vitripennis*), Pedhu-AKHR (*Pediculus humanus*), Peram-AKHR (*Periplaneta americana*), and Trica-AKHR (*Tribolium castaneum*). Gonadotropin-releasing hormone receptor of *Caenorhabditis elegans* (Caeel-GnRHR) was used as outgroup.

GAA-3' forward primer, and 5'-GGG AAA TGT CTT GTG AAC CAG GTC-3' reverse. The MEGAscript RNAi Kit (Ambion) was used to generate the dsRNA following the manufacturer's protocol. The dsRNA solution was stored at -20°C until use. A dose of 1.5 μg of the 528 bp dsRNA targeting the *Blage-HTHR* mRNA was injected into the abdomen of newly emerged adults. As dsRNA control, the enhanced green fluorescence protein (EGFP) sequence was used at the same dose. *Blage-HTHR* expression in the fat body was determined by semiquantitative RT-PCR within the following days after dsRNA treatment.

To investigate the role of HTH against oxidative stress, we injected 1.5 μg of both, dsHTHR and dsHTH, the latter being prepared according to the protocol previously described (Huang and Lee, 2011), into newly emerged male *B. germanica*. *Blage-HTHR* expression in the fat body and *Blage-HTH* expression in the whole head were determined by semiquantitative RT-PCR at the 10th day after dsRNA treatment.

TREHALOSE DETERMINATION

Trehalose in the hemolymph was determined following the protocol previously described (Huang and Lee, 2011). Briefly, 5 μl hemolymph was obtained from the hind leg coxae. Then, the hemolymph was incubated overnight at 37°C with 2 μl porcine kidney trehalase (Sigma) to convert trehalose into glucose. The amount of glucose in 50 μl of the above solution was measured using the Glucose Assay Kit (Sigma). Glucose concentration was corrected by deducting the amount of glucose from the same supernatant prepared under identical conditions but without trehalase.

OXIDATIVE STRESS TREATMENTS

The insects were individually injected with 1 μl solution of 20 mM PQ (paraquat: 1,1'-dimethyl-4,4'-bipyridylum dichloride hydrate) to cause oxidative stress, or with 1 μl Ringer saline as control. To study the effect of HTH against oxidative stress, the insects were injected with 1 μl solution containing synthetic HTH peptide (pGlu-Val-Asn-Phe-Ser-Pro-Gly-Trp-Gly-Thr-NH₂) of *B. germanica* at various concentrations (10, 40, and 80 pmol) in combination with 20 nmol PQ (1:1 in volume). The number of dead cockroaches were recorded every day. All chemicals used in the experiments and assays were obtained from Sigma-Aldrich Chemical Company (St. Louis, MO, USA) unless otherwise stated.

LIPID PEROXIDATION MEASUREMENT

We used lipid peroxidation as specific test to measure the level of oxidative stress. A total of 15 μl hemolymph from a pool of eight specimens was collected at 4 h post inoculation of oxidative stress treatment and diluted with 30 μl PBS containing 1% butylated hydroxytoluene to prevent further oxidation of lipid during further processing. The diluted hemolymph was shaken vigorously and centrifuged ($10,000 \times g$ for 10 min at 4°C). To determine the levels of malondialdehyde as indicator of lipid peroxidation, the supernatants were processed using the OxiSelect TBARS (thiobarbituric acid reactive substances) assay kit (Cell Biolabs) following the manufacturer's instructions.

STATISTICAL ANALYSIS

The results in the figures represent the mean \pm SEM. Statistical analyses were performed using computing software R. Statistical significance of results were evaluated using unpaired *t*-test between two groups and one-way ANOVA followed by Tukey's HSD *post hoc* test for multiple comparisons. The analyses of survival curves were carried out using Kaplan–Meier test for median survival time, the Log-rank test for testing the differences among treatment groups, and the Kruskal–Wallis rank sum test for post-test calculations.

RESULTS

CLONING AND EXPRESSION PATTERN OF *BLAGE-HTH* RECEPTOR

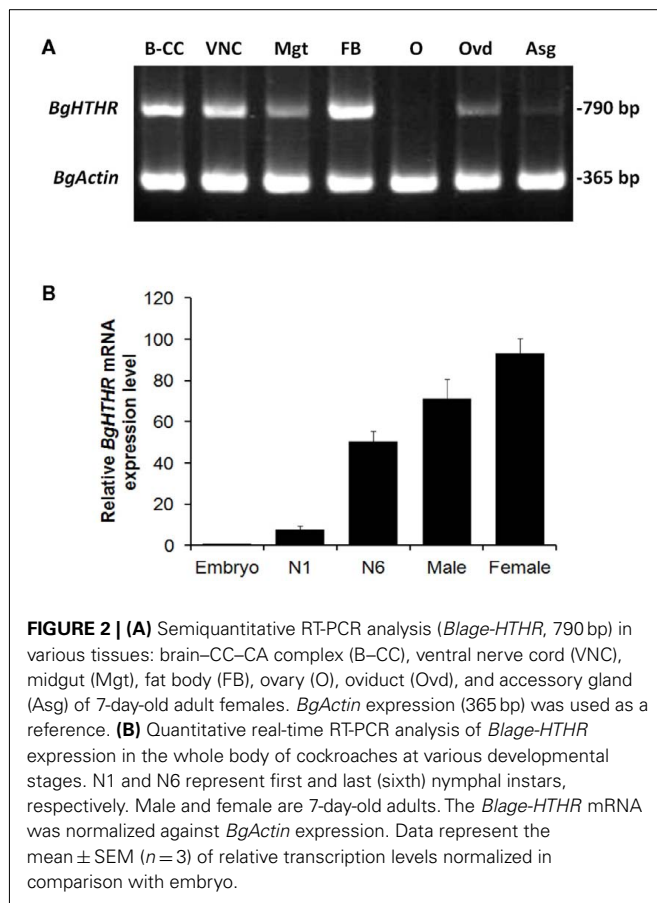
Cloning of the HTH receptor (*Blage-HTHR*) cDNA of *B. germanica* was accomplished by a RT-PCR approach, combining the use of degenerate primers based on AKHR conserved motifs to obtain a partial sequence, and 5'-RACE and 3'-RACE experiments to complete it. These amplifications rendered a full-length cDNA of 1,769 bp encoding a predicted 406 amino acid protein (*Blage-HTHR*; GenBank accession number GU591493; **Figure A1** in Appendix). According to BLAST searches, cDNA sequence of *Blage-HTHR* was very close (71.0% identity, 81.5% similarity) to *P. americana* AKH receptor (*Peram-AKHR*; GenBank accession number ABB20590). In addition, the alignment of receptor proteins of the two cockroach species showed values of 62.4% identity and 72% similarity (**Figure 1A**). The deduced amino acid sequence of *Blage-HTHR* exhibits the typical structural features of G protein-coupled receptors including an extracellular N-terminus, seven transmembrane regions, and an intracellular C-terminus.

Neighbor-joining analysis of insect AKH receptor sequences gave a tree (**Figure 1B**) showing that *Blage-HTHR* clusters with *Peram-AKHR* from *P. americana*, as expected. Indeed, these two cockroach receptors have an additional consensus sequence in the intracellular C-terminus that is characteristic of them, and which is not present in other insect AKH receptor sequences (**Figure A2** in Appendix). The sister group of the cockroach node is composed by phylogenetically distal hemimetabolous species (Phthiraptera, Hemiptera) and basal holometabolous species (Coleoptera, Hymenoptera), and these two nodes have the more modified holometabolous species (Lepidoptera and Diptera) as sister group. In general, the topology of the tree approximately follows the phylogenetic relationships of the insect orders currently established.

The expression of *Blage-HTHR* was detected and quantified in various tissues and stages (**Figure 2**). Concerning the adult, the expression was observed in practically all studied tissues, but the strongest expression was found in the fat body (**Figure 2A**). Conversely, expression in the ovary was practically absent, and that in the accessory glands was very faint. Comparing different life cycle stages (**Figure 2B**), expression was very low in embryos and relatively low in the first instar nymph. Values were much higher in the last instar (N6) nymph, and in the adult stage of both sexes.

RNAI-MEDIATED KNOCKDOWN OF *BLAGE-HTHR* REDUCES THE TREHALOSEMIC EFFECT OF HTH

We first studied the function of *Blage-HTHR* in *B. germanica* in relation to trehalose regulation by depleting its expression by

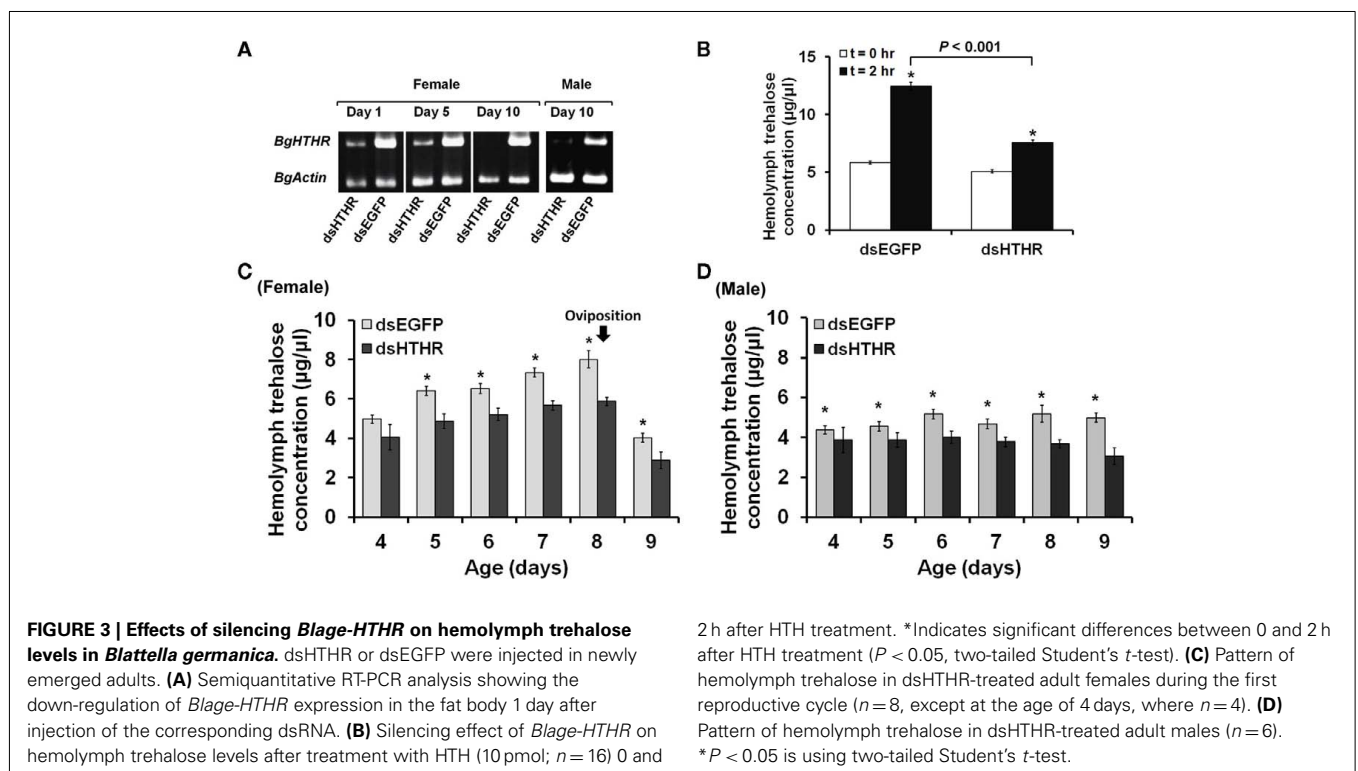


RNAi. *Blage-HTHR* mRNA was measured in the fat body 1, 5, and 10 days after the treatment with dsHTHR, and results (**Figure 3A**) showed that expression was clearly reduced in comparison with controls (dsEGFP-treated) on days 1 and 5, and it was practically undetectable on day 10, either in females as well as in males. The function of *Blage-HTHR* as HTH receptor was illustrated by the significant reduction of trehalose titers in the hemolymph after injection of HTH in dsHTHR-treated females (**Figure 3B**). The injection of 10 pmol of HTH resulted in the increase of hemolymph trehalose up to 113% 2 h later in dsEGFP-treated females. In contrast, the hemolymph trehalose increased significantly less (49%) in dsHTHR-treated females 2 h after the HTH injection. These results suggest that the remarkable increase of hemolymph trehalose elicited by HTH requires a high expression of its receptor, *Blage-HTHR*.

The titer of hemolymph trehalose displayed a steady increase and peaked at day 8 in the first reproductive cycle of female adults, either in controls (dsEGFP-treated) as in specimens treated with dsHTHR (**Figure 3C**), although the levels are lower in the latter. The hemolymph trehalose pattern is coincident with that of ovarian development. In adult males, the hemolymph trehalose levels practically do not fluctuate, either in controls (dsEGFP-treated) as in specimens treated with dsHTHR (**Figure 3D**); again, the levels were significantly lower in dsHTHR-treated specimens (**Figure 3D**).

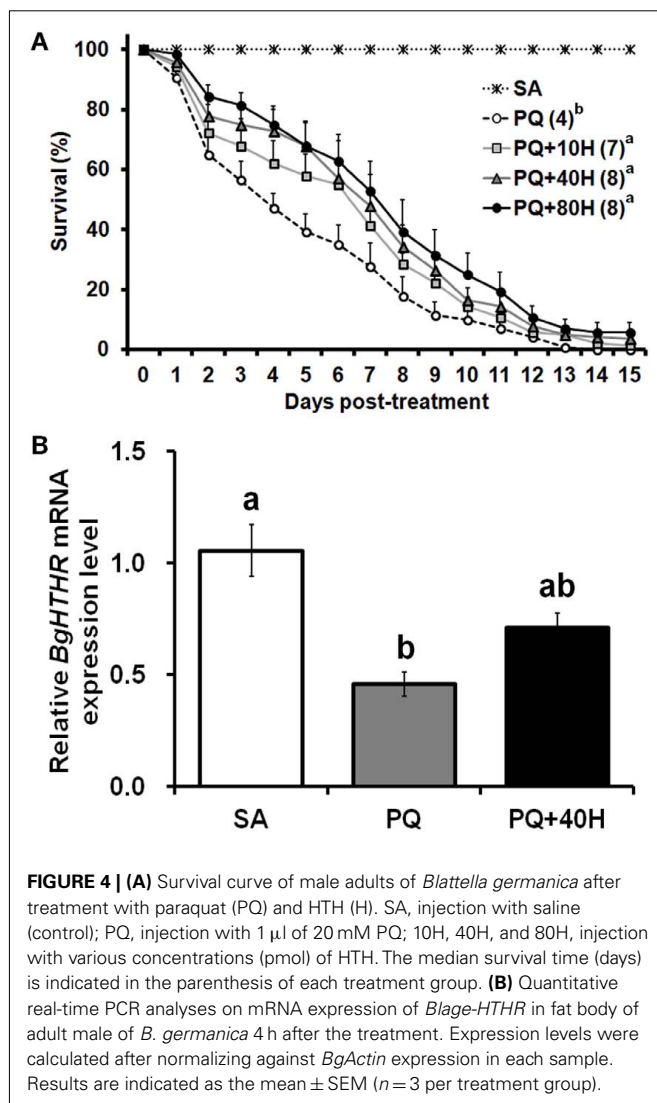
ROLE OF HTH AS RELIEVER OF OXIDATIVE STRESS

Subsequently, we studied the potential roles of HTH as reliever of oxidative stress. Given that female *B. germanica* exhibits a varied ability against oxidative stress during the reproductive cycle



(unpublished data), we chose only males to conduct the following experiments. The injection of 20 nmol of PQ on 10-day-old male adults caused a mortality that rapidly increased with time, thus median survival time was attained on day 4 (**Figure 4A**). However, exogenous HTH at 10, 40, and 80 pmol concentrations significantly reduced the speed of mortality increase, with median survival time attained around day 7 (**Figure 4A**), thus, the protective effect of HTH did not show significant differences among the three concentrations used.

To further assess the possible protective role of HTH against oxidative stress, the expression of *Blage-HTHR* after PQ treatment was studied (**Figure 4B**). Injection of PQ (20 nmol) caused a significant reduction of the *Blage-HTHR* expression in the fat body 4 h later. Mean value of *Blage-HTHR* mRNA was also decreased in the specimens injected with PQ and 40 pmol HTH, which extended the life span under the provoked oxidative stress. But the level of *Blage-HTHR* in PQ co-injected with HTH was not significantly different from that in either control or PQ treatment.



RNAi-SILENCED HTH SIGNALING REDUCES ANTI-OXIDATIVE PROTECTION

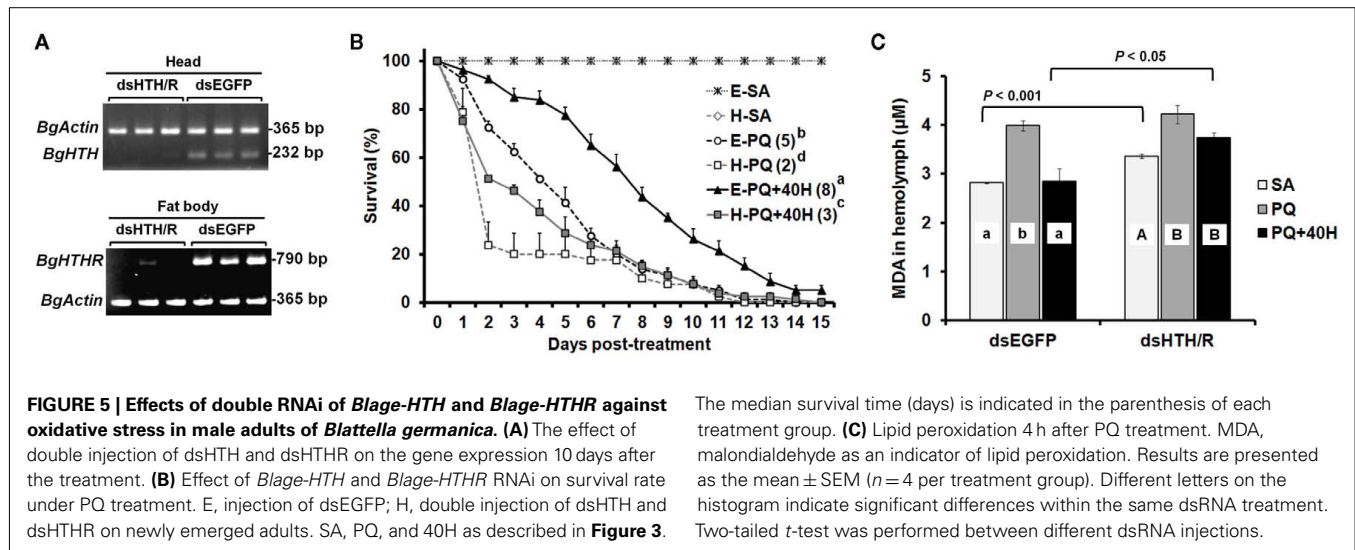
We further assessed the protective role of HTH on oxidative stress in specimens where *Blage-HTH* and *Blage-HTHR* mRNA levels had been simultaneously depleted by RNAi. A treatment of 1.5 μ g of dsHTH and 1.5 μ g of dsHTHR (dsHTH/R) was administered to newly emerged males of *B. germanica*, and the corresponding expression of *Blage-HTH* and *Blage-HTHR* was undetectable 10 days later in the tissues where these transcripts are most expressed: *Blage-HTH* in the head and *Blage-HTHR* in the fat body (**Figure 5A**). There were no lethal effects when the expression of both genes was knocked down, as all specimens survived in apparently healthy conditions at least during 25 days after the dsRNA injections. However, PQ treatment elicited a faster mortality in the specimens knockdown for *Blage-HTH* and *Blage-HTHR* (median survival time was attained on day 2 after PQ treatment), than in controls (dsEGFP-treated; median survival time attained on day 5; **Figure 5B**). Moreover, a dose of 40 pmol of HTH significantly relieved the detrimental effect elicited by PQ in control specimens (median survival time attained on day 8), but this “rescue” effect of HTH was milder in the specimens knockdown for *Blage-HTH* and *Blage-HTHR* (median survival time attained on day 3; **Figure 5B**).

Finally, the anti-oxidative stress function of *Blage-HTH* and *Blage-HTHR* was further demonstrated by measuring malondialdehyde as indicator of lipid peroxidation under oxidative stress caused by PQ, using specimens where *Blage-HTH* and *Blage-HTHR* expression had been depleted by RNAi, and applying exogenous HTH. Results (**Figure 5C**) show that without PQ, the malondialdehyde titer in the group of specimens knockdown for *Blage-HTH* and *Blage-HTHR* was higher than that of the dsEGFP-treated group. PQ elicited and increased the titer of malondialdehyde in both groups, but differences between them were not statistically significant. Finally, exogenous HTH significantly counteracted the effects of PQ in the dsEGFP-treated group, but not in the group of *Blage-HTH* and *Blage-HTHR* knockdowns.

DISCUSSION

About 50 peptides belonging to the AKH family have been identified in insects (Gäde, 2009) since the first hyperglycemic factor was discovered in the cockroach *P. americana* (Steele, 1961). The physiological function of these peptides on energy homeostasis as well as on signal transduction at the cellular level have been thoroughly reviewed by a number of authors (Van der Horst et al., 2001; Gäde and Auerwald, 2003; Schooley et al., 2005). However, studies at molecular level of AKH receptors have been conducted more recently in the fruit fly *D. melanogaster* and in the silkworm *B. mori* (Staubli et al., 2002). In cockroaches, only the AKH receptor cDNA of *P. americana* has been characterized (Hansen et al., 2006; Wicher et al., 2006). The present contribution reports the characterization of the HTH receptor in another cockroach, *B. germanica*, which is structurally close to that of *P. americana* AKH receptor (**Figure 1**).

Alignment of all known AKH/HTH receptor protein sequences shows a large region of evolutionary conserved residues in the transmembrane domain, but a highly diversified region in the C-terminus, which is associated to intracellular signaling (**Figure A2**



in Appendix). The phylogenetic analysis indicates that the intracellular C-terminus has considerably diverged in different insect orders, and this might have derived in different signal transduction mechanisms in different orders. Interestingly, an additional sequence at the beginning of the intracellular C-terminus in cockroaches might be related to the export of the receptor to the cell membrane, as an equivalent sequence in the C-terminal end of the AKH receptor of *B. mori* serves for this function (Huang et al., 2011).

The most abundant expression of *Blage-HTHR* in the fat body among the tissues tested (Figure 2A) is in agreement with the fact that HTH is the major regulator of energy metabolism in insects. This is also supported by the increasing expression level of *Blage-HTHR* from nymphal to adult stage which coincides with increasing locomotion which occurs in parallel (Yang et al., 2009), and which requires increasing energy expenditure. Our previous results showed that depletion of *Blage-HTH* expression results in a delay of oviposition in virgin females of *B. germanica* (Huang and Lee, 2011). In the present study, we observed *Blage-HTHR* expression in the oviduct, but not in ovary (Figure 2A), which suggests that *Blage-HTH* release could stimulate the contraction of oviduct muscles during basal oocyte extrusion. Indeed, a myoactive effect of AKHs on the dorsal vessel has been demonstrated in *P. americana* (Scarborough et al., 1984).

The canonical function of *Blage-HTHR* as HTH receptor in *B. germanica* has been demonstrated by injecting HTH in specimens where *Blage-HTHR* had been depleted by RNAi, and observing that mobilization of trehalose in the hemolymph was impaired (Figure 3B). Equivalently, the malaria mosquito *A. gambiae* with lowered expression of AKH receptor (Anoga-AKHR) also fails to mobilize the glycogen reserves in the fat body after injection of Anoga-AKH-I (Kaufmann and Brown, 2008). However, the occurrence of a significant elevation of hemolymph trehalose in dsHTHR-treated group was likely considered as incomplete silencing of *Blage-HTHR* expression because RNAi does not completely knockout gene expression. In addition, studies *in vitro* demonstrate that reduced

expression of the *Bombyx* AKHR on the cell membrane results in lower levels of intracellular cAMP (cyclic adenosine monophosphate) formation after AKH stimulation (Huang et al., 2011). Therefore, a maximal action of HTH would require an adequate expression of its receptor to trigger signal transduction.

RNA interference-mediated depletion of *Blage-HTHR* mRNA was found to decrease hemolymph trehalose levels in the adult of both sexes (Figures 3C,D), although the female displays fluctuations of trehalose related to the reproductive cycle. Our present results of *Blage-HTHR* RNAi (Figure 3C) supports our previous hypothesis postulating that HTH induces hemolymph trehalose mobilization during the reproductive cycle in virgin females (Huang and Lee, 2011). The results suggest that HTH plays a critical role in carbohydrate homeostasis, as occurs in AKH-cell-deficient *D. melanogaster* that has relatively low hemolymph trehalose levels (Lee and Park, 2004).

The involvement of AKH peptides in antioxidant protection in insects was inferred from the increase in AKH titer after exposure to oxidative stress (Kodrik et al., 2007; Vecera et al., 2007). The same authors showed that exogenous AKH application enhanced the efflux of reduced glutathione to the hemolymph and maintained the normal levels of protein carbonyl, a marker of oxidative stress. In the present study, we have fully demonstrated the protective role of HTH upon oxidative stress under different experimental approaches, first, through experiments of co-injection of PQ and HTH on control specimens (Figure 4A), and secondly, in specimens with the expression levels of *Blage-HTH* and *Blage-HTHR* depleted by RNAi (Figure 5B). These results provide a new and relevant information supporting that *Blage-HTH* potentiates a stress hormone on anti-oxidative stress response in *B. germanica*. The promoter of oxidative stress used in our experiments has been PQ, which acts on the redox-cycling reactions, thus eliciting free radicals as well as causes oxidative modification of macromolecules, such as lipid peroxidation (Hassan, 1984). Accordingly, we examined lipid peroxidation in the hemolymph 4 h after PQ treatment (Figure 5C). Levels of lipid

peroxidation in the hemolymph increased significantly after PQ injection in dsEGFP and dsHTH/R groups. However, the co-injection of HTH maintained the lipid peroxidation at a normal level in controls but not in the *Blage-HTH* and *Blage-HTHR* knockdowns, which suggests that HTH lowers the oxidative damage in *B. germanica*. A likely mechanism might be that HTH induces the efflux of glutathione into the hemolymph, as demonstrated in other insect AKHs (Kodrik et al., 2007; Vecera et al., 2007). However, the significant reduction of *Blage-HTHR* expression after PQ treatment (Figure 4B), suggests that the oxidative stress directly impairs its expression. The less severe reduction of *Blage-HTHR* expression observed after co-injecting PQ and HTH (Figure 4B) might be the outcome of downstream response induced by HTH to relieve the oxidative damage. Moreover, genome-wide analysis in *D. melanogaster* after PQ treatment have shown that cytochrome P450 genes become up- and

down-regulated (Girardot et al., 2004), and it has been additionally reported that HTH stimulates cytochrome P450 expression in the cockroach *Blaberus discoidalis* (Lu et al., 1995). Therefore, we further speculate that HTH might induce the expression of P450 genes, thus contributing to decrease the oxidative stress in *B. germanica*.

ACKNOWLEDGMENTS

We are grateful to Chin-Cheng Yang for his help with the phylogenetic analyses. Support for this research was provided by National Science Council of Taiwan (NSC 97-2313-B-002-031 and NSC 100-2923-B-002-002 to How-Jing Lee; NSC 98-2917-I-002-147 to Jia-Hsin Huang for working one year in Barcelona), and the Spanish MICINN (grant CGL2008-03517/BOS to Xavier Bellés) and by the CSIC (grant 2010TW0019, from the Formosa program, to Xavier Bellés).

REFERENCES

- Belles, X. (2010). Beyond *Drosophila*: RNAi in vivo and functional genomics in insects. *Annu. Rev. Entomol.* 55, 111–128.
- Candy, D. J. (2002). Adipokinetic hormones concentrations in the haemolymph of *Schistocerca gregaria*, measured by radioimmunoassay. *Insect Biochem. Mol. Biol.* 32, 1361–1367.
- Chaudhuri, A., Bowling, K., Funderburk, C., Lawal, H., Inamdar, A., Wang, Z., and O'Donnell, J. M. (2007). Interaction of genetic and environmental factors in a *Drosophila* parkinsonism model. *J. Neurosci.* 27, 2457–2467.
- Gäde, G. (2009). Peptides of the adipokinetic hormone/red pigment-concentrating hormone family: a new take on biodiversity. *Ann. N. Y. Acad. Sci.* 1163, 125–136.
- Gäde, G., and Auerswald, L. (2003). Mode of action of neuropeptides from the adipokinetic hormone family. *Gen. Comp. Endocrinol.* 132, 10–20.
- Girardot, F., Monnier, V., and Tricoire, H. (2004). Genome wide analysis of common and specific stress responses in adult *Drosophila melanogaster*. *BMC Genomics* 5, 74. doi:10.1186/1471-2164-5-74
- Granett, J., and Leeling, N. C. (1972). A hyperglycemic agent in the serum of DDT-prostrate American cockroaches, *Periplaneta americana*. *Ann. Entomol. Soc. Am.* 65, 299–302.
- Halliwell, B., and Gutteridge, J. M. C. (2007). *Free Radicals in Biology and Medicine*, 4th Edn. Oxford: Clarendon Press.
- Hansen, K. K., Hauser, F., Cazzamali, G., Williamson, M., and Grimmelikhuijzen, C. J. P. (2006). Cloning and characterization of the adipokinetic hormone receptor from the cockroach *Periplaneta americana*. *Biochem. Biophys. Res. Commun.* 343, 638–643.
- Hassan, H. M. (1984). Exacerbation of superoxide radical formation by paraquat. *Meth. Enzymol.* 105, 523–532.
- Huang, H., Deng, X., He, X., Yang, W., Li, G., Shi, Y., Shi, L., Mei, L., Gao, J., and Zhou, N. (2011). Identification of distinct c-terminal domains of the Bombyx adipokinetic hormone receptor that are essential for receptor export, phosphorylation and internalization. *Cell. Signal.* 23, 1455–1465.
- Huang, J.-H., and Lee, H.-J. (2011). RNA interference unveils functions of the hypertrehalosemic hormone on cyclic fluctuation of hemolymph trehalose and oviposition in the virgin female *Blattella germanica*. *J. Insect Physiol.* 57, 858–864.
- Kaufmann, C., and Brown, M. R. (2008). Regulation of carbohydrate metabolism and flight performance by a hypertrehalosemic hormone in the mosquito *Anopheles gambiae*. *J. Insect Physiol.* 54, 367–377.
- Kodrik, D. (2008). Adipokinetic hormone functions that are not associated with insect flight. *Physiol. Entomol.* 33, 171–180.
- Kodrik, D., Krishnan, N., and Habus-tova, O. (2007). Is the titer of adipokinetic peptides in *Leptinotarsa decemlineata* fed on genetically modified potatoes increased by oxidative stress? *Peptides* 28, 974–980.
- Kodrik, D., and Socha, R. (2005). The effect of insecticide on adipokinetic hormone titre in the insect body. *Pest Manag. Sci.* 61, 1077–1082.
- Lee, G., and Park, J. H. (2004). Hemolymph sugar homeostasis and starvation-induced hyperactivity affected by genetic manipulations of the adipokinetic hormone-encoding gene in *Drosophila melanogaster*. *Genetics* 167, 311–323.
- Lee, H. J., and Wu, Y. L. (1994). Mating effects on the feeding and locomotion of the German cockroach, *Blattella germanica*. *Physiol. Entomol.* 19, 39–45.
- Lu, K.-H., Bradfield, J. Y., and Keeley, L. L. (1995). Hypertrehalosemic hormone-regulated gene expression for cytochrome P4504C1 in the fat body of the cockroach *Blaberus discoidalis*. *Arch. Insect Biochem. Physiol.* 28, 79–90.
- Nicholas, K. B., Nicholas, H. B., and Deerfield, D. W. (1997). GeneDoc: analysis and visualization of genetic variation. *Embnet News* 4, 14.
- Pfaffl, M. W. (2001). A new mathematical model for relative quantification in real-time RT-PCR. *Nucleic Acids Res.* 29, e45.
- Samaranayaka, M. (1974). Insecticide-induced release of hyperglycaemic and adipokinetic hormones of *Schistocerca gregaria*. *Gen. Comp. Endocrinol.* 24, 424–436.
- Scarborough, R. M., Jamieson, G. C., Kalish, F., Kramer, S. J., McEnroe, G. A., Miller, C. A., and Schooley, D. A. (1984). Isolation and primary structure of two peptides with cardioacceleratory and hyperglycemic activity from the corpora cardiaca of *Periplaneta americana*. *Proc. Natl. Acad. Sci. U.S.A.* 81, 5575–5579.
- Schooley, D. A., Horodyski, F. M., and Coast, G. M. (2005). "Hormones controlling homeostasis in insects," in *Comprehensive Molecular Insect Science*, eds L. I. Gilbert, K. Iatrou, and S. S. Gill (Amsterdam: Elsevier Press), 493–550.
- Staubli, F., Jorgensen, T. J. D., Cazzamali, G., Williamson, M., Lenz, C., Sondergaard, L., Roepstorff, P., and Grimmelikhuijzen, C. J. P. (2002). Molecular identification of the insect adipokinetic hormone receptors. *Proc. Natl. Acad. Sci. U.S.A.* 99, 3446–3451.
- Steele, J. E. (1961). Occurrence of a hyperglycaemic factor in the corpus cardiacum of an insect. *Nature* 192, 680–681.
- Tamura, K., Peterson, D., Peterson, N., Stecher, G., Nei, M., and Kumar, S. (2011). MEGA5: molecular evolutionary genetics analysis using maximum likelihood, evolutionary distance, and maximum parsimony methods. *Mol. Biol. Evol.* 28, 2731–2739.
- Thompson, J. D., Gibson, T. J., Plewniak, F., Jeanmougin, F., and Higgins, D. G. (1997). The CLUSTAL_X windows interface: flexible strategies for multiple sequence alignment aided by quality analysis tools. *Nucleic Acids Res.* 25, 4876–4882.
- Valko, M., Leibfritz, D., Moncol, J., Cronin, M. T., Mazur, M., and Telser, J. (2007). Free radicals and antioxidants in normal physiological functions and human disease. *Int. J. Biochem. Cell Biol.* 39, 44–84.
- Van der Horst, D. J., Van Marrewijk, W. J. A., and Diederens, J. H. B. (2001). "Adipokinetic hormones of insect: release, signal transduction, and responses," in *International Review of Cytology – A Survey of Cell Biology*, ed. K. W. Jeon (San Diego, CA: Academic Press), 179–240.
- Vecera, J., Krishnan, N., Alquicer, G., Kodrik, D., and Socha, R. (2007). Adipokinetic hormone-induced enhancement of antioxidant capacity of *Pyrrhocoris apterus* hemolymph in response to oxidative stress. *Comp. Biochem. Physiol. C Toxicol. Pharmacol.* 146, 336–342.

- Velki, M., Kodrik, D., Vecera, J., Hackenberger, B. K., and Socha, R. (2011). Oxidative stress elicited by insecticides: a role for the adipokinetic hormone. *Gen. Comp. Endocrinol.* 172, 77–84.
- Wicher, D., Agricola, H. J., Sohler, S., Gundel, M., Heinemann, S. H., Wollweber, L., Stengl, M., and Derst, C. (2006). Differential receptor activation by cockroach adipokinetic hormones produces differential effects on ion currents, neuronal activity, and locomotion. *J. Neurophysiol.* 95, 2314–2325.
- Yang, Y. Y., Wen, C.-J., Mishra, A., Tsai, C.-W., and Lee, H.-J. (2009). Development of the circadian clock in the German cockroach, *Blattella germanica*. *J. Insect Physiol.* 55, 469–478.
- Conflict of Interest Statement:** The authors declare that the research was conducted in the absence of any commercial or financial relationships that could be construed as a potential conflict of interest.
- Received: 28 October 2011; paper pending published: 18 November 2011; accepted: 20 December 2011; published online: 09 January 2012.
- Citation: Huang J-H, Bellés X and Lee H-J (2012) Functional characterization of hypertrehalosemic hormone receptor in relation to hemolymph trehalose and to oxidative stress in the cockroach *Blattella germanica*. *Front. Endocrin.* 2:114. doi: 10.3389/fendo.2011.00114
- This article was submitted to *Frontiers in Experimental Endocrinology*, a specialty of *Frontiers in Endocrinology*. Copyright © 2012 Huang, Bellés and Lee. This is an open-access article distributed under the terms of the Creative Commons Attribution Non Commercial License, which permits non-commercial use, distribution, and reproduction in other forums, provided the original authors and source are credited.

APPENDIX

1 5' -AATATGAATCTAACAAGCTATCATACTTCT
 31 CTTATGGCTGGAGGAGCGGAAAAATCTGCAGTGTAGAAAAAGCGATAACATTCTAAGAACAACTGAATGATTAGACAAATCAAATGT
 121 TCGAGAATTTATTCAACGAAGATTGAAGTGATGAACGAATTAGTTCTAACAGTGAAATGGAAGAGACGAAGTGATGATTTCGCTTAGTGAA
 211 ACAGTGGCATGGAAGAATTTGGGTGTTGGTAATCTTGATTTCATCTTTCAACTGTCAACATTTTGACATGAGCATTTGACAGGAACCCAAG
 301 **ATG**ACGACTACAGAGCTGCCCCGTGAGCAGCAGCTGACTGAGGACATGACTTTTGGCTCCATACATAAGTTATGTATCGCCACGTATTGC
 M T T T E L P R E Q Q L T E D M T F G S I H K L C I A T Y C
 391 GTTCTCATGACTGTATCTGCAATTGGCAACATCACGGTCTCTGGTCAACATACTCAAGAGACGCCGCAACCTTCGTTTTGGGAACAACTAC
 V L M T V S A I G N I T V L V N I L K R R R N L R F G N N Y
 481 ATGTTTCATGCATCTTGCCATAGCAGACCTATTGGTGACTTTTCTCATGATGCCGCTAGAAATCGGCTGGAATGCAACAGTGTCTTGAGA
 M F M H L A I A D L L V T F L M M P L E I G W N A T V S W R
 571 GCCGGTGACGCTGCTTGCGAGTGATGTGTTCTTCAGGATATTCGGCCTCTATCTGTCTAGCTTCGTAATTGTGTGCATCAGTCTGGAC
 A G D A A C R V M S F F R I F G L Y L S S F V I V C I S L D
 661 CGCTGTTTCGCCATTCTAAGGCCCATGTGCAACGTCGTCAACGTCGCCAAACGCAGCAGAGTAATGCTGACCACTGCCTGGTCATTGGCC
 R C F A I L R P M S N V V N V A K R S R V M L T T A W S L A
 751 ACTGTTTGTAGTTTACCTCAGGTGTTTCATCTTCCACGTACAACAGCATCCCGTTTTTCACATGGTATGAGCAGTGTTCGACTTCGACATG
 T V C S L P Q V F I F H V Q Q H P V F T W Y E Q C L D F D M
 841 TTTCC**GACTCAGCTGTACCAGTCTGGTA**CAGGATATTAATATGGTTCAGTGTACGGTTTCCCACTCCTCGTCATTTTCATCTCATAC
 F P T Q L Y Q F W Y R I L N M V L V Y G F P L L V I F I S Y
 931 GCCTGTATCCTCACAGAGATTTTTCGAGATATCAGCTCAGTTCAGACGAAAACCTCCGGAGATCGAGCCTGTGTTCCTGAACAGAGCC
 A C I L T E I F R R Y Q L S S D E N F R R S S L V F L N R A
 1021 AAAAATAGGACGCTCAAAATGGCCATCATAATATTCGTAGTGTCTTCATCTGCTGGACTCCCTACTATGTGATGTGTCTCTGGTACT**TCG**
 K N R T L K M A I I I F V V F F I C W T P Y Y V M C L W Y W
 1111 **ATAGACCAGCAGTCTGCTGAAAAGGTTGACTTGCGCGTGAGAAAAGGCTGTCTCTGTTGCTTGTACCAATTCCGTGTATGAACCCGATT**
 I D Q Q S A E K V D L R V R K G L F L F A C T N S C M N P I
 1201 **GTGTACGGGTACTTCAACTTCCGTTCAAGACGGGGAAGTGGTTATGGTGCAACAAGACCAGGGCAGCAGTTACAGCATCATCAAATAACT**
 V Y G Y F N F R S G R G S G Y G A T R P G Q Q L Q H H Q I T
 1291 **GCATTGAGCAATAACTCAACGGGAGTTAACAGCCGAAGGGGAAGCAACTGCAGCAGCATCTATCGGGACAACAGCAACCAGAGCATGTCC**
 A L S N N S T G V N S R R G S N C S S I Y R D N S N Q S M S
 1381 **TGGAATCGCGAAGCAGCCATGAAACAGAAATGCACGCCAATAACAATCGAGACGAAAATCACTTACACCCCAACTCAGCTGCGAACCAC**
 W N R R S S H E T E M H A N N N R D E N H L H P N S A A N H
 1471 **AATTTGCGAACTACAGTATCTACTGTGAGTGAAGTTCCTGAAGCAAGATGAGGTTTACTCCTTGTGCTTCGAAATTATACTATCAGTGAT**
 N L R T T V S T V S E V P E A R *
 1561 **AAACATTGCCAATGTAATTAAACATTAATGTTCTAGTCTAAGACTTGACATGACCTGGTTCACAAGACATTTC** AAGAGAGTGAACAAA
 1651 ACAATTGAATTGGTATAAACATGTGTTAACTAATGTACAATACACTCAACAGTTTTACACAAAAATAAATTTATTATTTTGTG
 1741 CCACTAAAAAAAAAAAAAAAAAAAAA-3'

FIGURE A1 | Nucleotide sequence of cDNA encoding the open-reading frame for *B. germanica* HTHR with flanking 5'- and 3'-UTR sequences (GenBank accession number GU591493). Start and stop codon are indicated by yellow background. The primer pair for

qRT-PCR is shown in underlined bold type. The primer pair for semiquantitative PCR is boxed. The fragment encompassed by the dsHTHR used in the RNAi experiments is shown in green background.



FIGURE A2 | Alignment of the AKH receptor protein sequences from insects and gonadotropin-releasing hormone receptor of *Caenorhabditis elegans* used in the phylogenetic analysis. The alignment was carried out using ClustalW program. A black background

indicates the amino acids are identical among species, whereas a gray background shows similarity among residues. The red underline indicates the insertion present in both cockroach species. The abbreviated names of sequences used are provided in **Figure 1B**.



Re-evaluation of the PBAN receptor molecule: characterization of PBANR variants expressed in the pheromone glands of moths

Jae Min Lee^{1†}, J. Joe Hull^{2*†}, Takeshi Kawai³, Chie Goto⁴, Masaaki Kurihara¹, Masaru Tanokura³, Koji Nagata³, Hiromichi Nagasawa³ and Shogo Matsumoto^{1*}

¹ Molecular Entomology Laboratory, RIKEN Advanced Science Institute, Wako, Japan

² Agricultural Research Service, United States Department of Agriculture, Arid Land Agricultural Research Center, Maricopa, AZ, USA

³ Department of Applied Biological Chemistry, Graduate School of Agricultural and Life Sciences, The University of Tokyo, Tokyo, Japan

⁴ Agricultural Research Center, National Agriculture and Food Research Organization, Tsukuba, Japan

Edited by:

Akiyoshi Takahashi, Kitasato University, Japan

Reviewed by:

Honoo Satake, Suntory Institute for Bioorganic Research, Japan
Hiroyuki Kaiya, National Cerebral and Cardiovascular Center Research Institute, Japan

Tsuyoshi Ohira, Kanagawa University, Japan

*Correspondence:

J. Joe Hull, Agricultural Research Service, United States Department of Agriculture, Arid Land Agricultural Research Center, 21881 N Cardon Lane, Maricopa, AZ 85138, USA.
e-mail: joe.hull@ars.usda.gov;
Shogo Matsumoto, RIKEN Advanced Science Institute, 2-1 Hirosawa, Wako, Saitama 351-0198, Japan.
e-mail: smatsu@riken.jp

[†]Jae Min Lee and J. Joe Hull have contributed equally to this work.

Sex pheromone production in most moths is initiated following pheromone biosynthesis activating neuropeptide receptor (PBANR) activation. PBANR was initially cloned from pheromone glands (PGs) of *Helicoverpa zea* and *Bombyx mori*. The *B. mori* PBANR is characterized by a relatively long C-terminus that is essential for ligand-induced internalization, whereas the *H. zea* PBANR has a shorter C-terminus that lacks features present in the *B. mori* PBANR critical for internalization. Multiple PBANRs have been reported to be concurrently expressed in the larval CNS of *Heliothis virescens*. In the current study, we sought to examine the prevalence of multiple PBANRs in the PGs of three moths and to ascertain their potential functional relevance. Multiple PBANR variants (As, A, B, and C) were cloned from the PGs of all species examined with PBANR-C the most highly expressed. Alternative splicing of the C-terminal coding sequence of the PBAN gene gives rise to the variants, which are distinguishable only by the length and composition of their respective C-terminal tails. Transient expression of fluorescent PBANR chimeras in insect cells revealed that PBANR-B and PBANR-C localized exclusively to the cell surface while PBANR-As and PBANR-A exhibited varying degrees of cytosolic localization. Similarly, only the PBANR-B and PBANR-C variants underwent ligand-induced internalization. Taken together, our results suggest that PBANR-C is the principal receptor molecule involved in PBAN signaling regardless of moth species. The high GC content of the C-terminal coding sequence in the B and C variants, which makes amplification using conventional polymerases difficult, likely accounts for previous “preferential” amplification of PBANR-A like receptors from other species.

Keywords: PBAN, receptor, alternative splicing, pheromone gland, receptor internalization, confocal microscopy, GC-rich sequence

INTRODUCTION

In most moth species, a 33–34 aa neuropeptide termed pheromone biosynthesis activating neuropeptide (PBAN) regulates sex pheromone production and release. First isolated from *Helicoverpa zea* (Raina et al., 1989) and *Bombyx mori* (Kitamura et al., 1989), PBAN has subsequently been identified in a variety of species. PBAN is a member of the pyrokinin/PBAN family of peptides that are characterized by a FXPRamide C-terminal pentapeptide motif. This motif is essential for biological activity, which, in addition to regulation of moth sex pheromone biosynthesis, includes melanization in lepidopteran larvae, induction of embryonic diapause in *B. mori*, and ecdysone biosynthesis in prothoracic glands of *B. mori* (Rafaeli, 2009). The role of PBAN in sex pheromone biosynthesis is governed by species-specifically defined photoperiods in which PBAN is released from the subesophageal ganglion into the hemolymph. Circulating PBAN acts directly on the modified epidermal cells

of the eighth and ninth abdominal segment that comprise the pheromone gland (PG) via its cognate G protein-coupled receptor (GPCR). The pheromone biosynthesis activating neuropeptide receptor (PBANR) consequently plays a pivotal role in turning the extracellular PBAN signal into the biological response of sex pheromone production. Indeed, *in vivo* dsRNA-mediated knock-down of PBANR reduced sex pheromone production in the silkworm (*B. mori*; Ohnishi et al., 2006) and negatively affected mating frequency in the diamondback moth (*Plutella xylostella*; Lee et al., 2011).

Pheromone biosynthesis activating neuropeptide receptor was initially cloned from PGs of the corn earworm, *H. zea* (Choi et al., 2003) and *B. mori* (Hull et al., 2004). While the two PBANRs share significant sequence similarity (82%), the *B. mori* PBANR (BommoPBANR) is structurally differentiated by a 67-aa C-terminal extension that is absent in the *H. zea* PBANR (HelzePBANR). BommoPBANR, like most GPCRs,

undergoes ligand-induced internalization, a common endocytotic regulatory mechanism involved in GPCR desensitization (Moore et al., 2007; Marchese et al., 2008). Truncation of the BommoPBANR C-terminal extension prevented this internalization event (Hull et al., 2004). Further studies revealed that a 10 residue segment (Arg358–Gln367) of the BommoPBANR C-terminal extension is essential for internalization and that endocytosis was phosphorylation dependent, proceeded via clathrin-coated pits, and involved a YXX Φ motif (Hull et al., 2005).

Pheromone biosynthesis activating neuropeptide receptors that have C-terminal sequences more similar to HelzePBANR than to BommoPBANR have since been cloned from other moth species (Rafaeli et al., 2007; Zheng et al., 2007; Cheng et al., 2010; Lee et al., 2011). However, multiple PBANR subtypes have recently been identified in the tobacco budworm *Heliothis virescens* and the tobacco hornworm *Manduca sexta* (Kim et al., 2008). Similar to HelzePBANR, *H. virescens* PBANR (HelviPBANR)-A has a relatively short C-terminus, while HelviPBANR-C has an extended C-terminus that is ~78% identical to BommoPBANR and which contains the YXX Φ motif. Surprisingly, even though *H. virescens* and *H. zea* are closely related species, the HelviPBANR-C variant rather than HelviPBANR-A (the HelzePBANR ortholog) was preferentially amplified from *H. virescens* PGs (Kim et al., 2008). Sequence analyses suggest that the HelviPBANR subtypes arise from alternative splicing, a common transcriptional regulation event in GPCR genes (Minneman, 2001; Markovic and Challiss, 2009). Because alternative splicing can generate protein isoforms that are structurally, functionally, and/or spatially distinct, the presence of multiple PBANR variants raises questions regarding the functional role and relevance of the individual variants in regulating sex pheromone biosynthesis. To address these questions, we sought to examine and characterize PBANR variants from the PGs of multiple moth species.

MATERIALS AND METHODS

INSECTS

Insects were maintained in a rearing chamber at 25°C under a 16L (light): 8D (dark) regime. Larvae of the inbred p50 strain of *B. mori* were reared on an artificial diet as described previously (Fónagy et al., 1992). Pupal age was determined based on morphological characteristics as described (Matsumoto et al., 2002). Larvae of *Pseudaletia separata* and *Helicoverpa armigera* were reared on an artificial diet (Insecta-LFS; Nihon Nosan Kogyo Ltd., Yokohama, Japan) under the same conditions as described (Fónagy et al., 2011). Pupae were sexed such that the newly emerged females were collected and kept separately in boxes and provided with a special sucrose solution energy drink (Pocari sweat®; Otsuka Pharmaceutical Co., Ltd, Tokyo, Japan). The newly emerged females were designated as day 0. *H. zea* pupae were purchased from Benzon Research (Carlisle, PA, USA) and maintained in a rearing chamber at 25°C under a 16L (light): 8D (dark) regime until adult emergence.

DEGENERATE PCR AND RACE-BASED CLONING OF PBANR VARIANTS

Total RNA was isolated from PGs of *B. mori* (p50), *P. separata*, *H. armigera*, and *H. zea* with first strand cDNAs synthesized

using a SMARTer™ RACE cDNA Amplification kit (Clontech, Palo Alto, CA, USA) according to the manufacturer's instructions. Fragments of *Pseudaletia separata* PBANR (PsesePBANR) and *Helicoverpa armigera* PBANR (HelarPBANR) transcripts were amplified with Advantage 2 polymerase (Clontech, Palo Alto, CA, USA) using multiple combinations of degenerate oligonucleotide primers described previously (Hull et al., 2004). PCR products of the expected sizes were sub-cloned using a TOPO TA cloning kit (Invitrogen Co., Ltd., Tokyo, Japan) and sequenced. RACE was performed using cDNAs generated above with Advantage 2 polymerase in conjunction with adaptor specific primers (UPM and NUP) and gene-specific primers (Table 1; P1–P7). Thermacycler conditions consisted of 94°C for 2 min, followed by 35 cycles at 94°C for 30 s, 65°C for 30 s, and 68°C for 3 min, and a final extension at 68°C for 7 min. PCR products were sub-cloned as before and sequenced.

Table 1 | Species-specific PCR primers used to amplify the PBANR variants.

Primer	Name	Sequence (5'-3')
P1	BommoPBANR3'F1	CAGGAACGCTTTCAGGTAAGATTAAA CTAG
P2	PsesePBANR3'F1	CACACCATGTCGAAGCTGTCAAGAG
P3	PsesePBANR3'F2	GCATCTCCAACCTCCAGTCTTCGCGAG
P4	PsesePBANR5'R	CAACTTAATGCCTATCAACGCGTACAAC
P5	HelarPBANR3'F1	GCGATGCGAGTTCGGTATAGTGTCTGAT
P6	HelarPBANR3'F2	GCATCTCCAACCTCCAGTCTTCGCGAG
P7	HelarPBANR5'R	GCATCTGACCAAGGTCTTTCATTGCT
P8	BommoPBANR	ATGATGGCAGATGAAACCGTCAAC
P9	BommoPBANR-As-A	CCTTTAAGAGTTTCGTACTAGTTAATCT TACC
P10	BommoPBANR-B-C	TCCTAATGAAACCCACAACAGCTGAATC
P11	PsesePBANR	ATGACCTTACCAGCGCTCCGAGCATC
P12	PsesePBANR-As-A	CAGTCAGCCGGCTGCCGGCCTGAAT
P13	HelarPBANR	ATGACATTGTGAGCGCCCCGAGCATCG
P14	HelarPBANR-As-A	TTAATCATAGACTCTTACCTTAAAGGC GTTC
P15	PsesePBANR-B-C	TCAGGTGAGTCCGCCGATGTTACAGTTC
P16	Bommo-AF	CGTATTTTGCATCCCGTTAAGAAGCTG
P17	Bommo-AR	CCTTTAAGAGTTTCGTACTAGTTAATC TTACC
P18	Bommo-BCF	TCGTTTTTCATCTGTTGGGCTCCATT
P19	Bommo-BR	ATCGCGATTTTGGTAGCACTGCG
P20	Bommo-CR	CGCGATTTTGGTAGCACTCACCT
P21	Psese-AF	TGATAGGCATTAAGTTGCGGACCTCTC
P22	Psese-AR	GTTCCGCGAGGTAACAATACAAGTAG
P23	Psese-BCF	TGCAGTATAGGAACGGAGCATCACA
P24	Psese-BR	CGCGCCCGTTGTAGCACTGCG
P25	Psese-CR	GCCCGTTGTAGCACTCACCTG
P26	Helar-AF	CAGTGTGTACGCGTTGATAGGCATT
P27	Helar-AR	GTCGTGAGATGTAAGACAACAAGGAG
P28	Helar-BCF	AGTCATCAGAATGCTCGTTGCACTG
P29	Helar-BR	CGCGCCCGTTGTAGCACTGCG
P30	Helar-CR	GCCCGTTGTAGCACTCACCTG

SPECIFIC AMPLIFICATION OF BOMMO, PSESE, HELAR, AND HELZE PBANR VARIANTS

To amplify the BommoPBANR variants, total RNA was isolated from 10 *B. mori* (p50) PGs immediately after adult eclosion with first strand cDNAs synthesized as before. BommoPBANR-As and BommoPBANR-A were amplified using Advantage 2 polymerase with a general BommoPBANR sense primer (Table 1; P8) and a short variant antisense primer (Table 1; P9), while BommoPBANR-B and BommoPBANR-C were amplified using the same sense primer and a long variant antisense primer (Table 1; P10). Thermacycler conditions consisted of 94°C for 2 min, followed by 35 cycles at 94°C for 30 s, 62°C for 30 s, and 68°C for 3 min with a final extension at 68°C for 7 min. PCR products were sub-cloned as before and sequenced. To amplify the PsesePBANR, HelarPBANR, and HelzePBANR variants, total RNA was isolated from 120 *P. separate*, 850 *H. armigera*, and 30 *H. zea* PGs dissected 1–3 days after adult eclosion. First strand cDNA was synthesized as before. PsesePBANR-As and PsesePBANR-A transcripts were amplified using Advantage 2 polymerase with a general PsesePBANR sense primer (Table 1; P11) and a short variant antisense primer (Table 1; P12). Thermacycler conditions consisted of 94°C for 2 min, followed by 35 cycles at 94°C for 30 s, 65°C for 30 s, and 68°C for 2 min with a final extension at 68°C for 7 min. HelarPBANR-As and HelarPBANR-A were amplified using a general HelarPBANR sense primer (Table 1; P13) and a short variant antisense primer (Table 1; P14). The resulting PCR products were sub-cloned and sequenced. Full-length PsesePBANR-B and PsesePBANR-C transcripts were amplified using a GC-optimized polymerase, KOD-FX (Toyobo, Osaka, Japan), with the previous PsesePBANR sense primer and a long variant-specific antisense primer (Table 1; P15) with thermacycler conditions consisting of 94°C for 2 min, followed by 32 cycles at 98°C for 10 s, 65°C for 30 s, and 68°C for 2 min with a final extension at 68°C for 7 min. HelarPBANR-B and HelarPBANR-C transcripts were similarly amplified using the HelarPBANR sense primer and the long variant-specific PsesePBANR antisense primer (Table 1; P15). Transcripts for the HelzePBANR variants were amplified using PCR conditions identical to those of the HelarPBANR variants. All resulting PCR products were sub-cloned and sequenced. The sequences reported in this paper have been deposited in the GenBank database (*B. mori* accession nos. JN228346–228349; *H. armigera* accession nos. JN228350–228353; *P. separate* accession nos. JN228354–JN228357; *H. zea* accession nos. JN206677 and JQ255024).

PRIMER CHECK PCR USING GENE-SPECIFIC PRIMERS

Primer check PCR was performed using 1 ng plasmid DNA containing the full-length sequence of each PBANR variant (PBANR-As, -A, -B, or -C) as template with primer sets designed for specific amplification of each PBANR sequence (Table 1; P16–P30). Primer check PCR using a general polymerase, Ex Taq DNA polymerase (Takara Bio Inc., Otsu, Japan), was performed using thermacycler conditions consisting of 94°C for 2 min, followed by 30 cycles at 94°C for 30 s and 68°C for 1 min. Primer check PCR using KOD-FX was performed using thermacycler conditions consisting of 94°C for 2 min, followed by 30 cycles at 98°C for 10 s and

68°C for 1 min. PCR products were analyzed on a 2% agarose gel and visualized with ethidium bromide.

RT-PCR TISSUE EXPRESSION ANALYSIS

Total RNAs isolated using TRIzol reagent (Invitrogen) were prepared from various newly emerged adult *B. mori* female tissues or adult female *P. separate* and *H. armigera* tissues 3 days after adult eclosion. cDNAs were generated using a Onestep RT-PCR kit (Qiagen, Tokyo, Japan) with RT-PCR performed using HotStarTaq DNA polymerase (Qiagen) and primer sets designed for specific amplification of each PBANR sequence (Table 1; P16–P30). Thermacycler conditions consisted of reverse transcription for 30 min at 50°C, then 95°C for 15 min followed by 20–30 cycles at 94°C for 30 s, 62°C for 30 s, and 72°C for 1 min. PCR products were analyzed on a 2% agarose gel and visualized with ethidium bromide. A separate cDNA synthesis was carried out in parallel using 500 ng total RNA with an RNA PCR kit (Takara Bio Inc.,) according to the manufacturer's instructions. RT-PCR with Ex Taq DNA polymerase was performed using thermacycler conditions consisting of 94°C for 2 min, followed by 26–32 cycles at 94°C for 30 s and 68°C for 1 min. RT-PCR using KOD-FX DNA polymerase was performed with thermacycler conditions consisting of 94°C for 2 min, followed by 26–32 cycles at 98°C for 10 s and 68°C for 1 min. PCR products were analyzed on a 2% agarose gel and visualized with ethidium bromide.

SEQUENCE ANALYSIS

The guanine–cytosine (GC) content of the full-length cDNA sequences for the PBANR-As, -A, -B, and -C variants of *B. mori*, *P. separate*, and *H. armigera* was determined following alignment of the putative translation initiation sites. The average GC content was calculated using 100 base windows over a range of 700 bases. GC content distribution diagrams were generated using GENETYX-MAC Version 12.0.0 (Genetyx, Tokyo, Japan).

CONSTRUCTION OF EXPRESSION PLASMIDS

Expression plasmids encoding the respective BommoPBANRs, PsesePBANRs, and HelarPBANRs fused at their respective C termini to enhanced green fluorescent protein (EGFP) were generated using a pIB/V5-His-TOPO TA Expression kit (Invitrogen). Chimeric genes were constructed via overlap extension PCR using plasmid DNAs with KOD-*plus* (Toyobo) and KOD-FX. Gene-specific primers described above were used with species-specific chimeric primers (Table 2) and an EGFP antisense primer. The resulting products were sub-cloned into the pIB/V5-His expression vector and sequenced to confirm presence and orientation of the insert.

PREPARATION OF A FLUORESCENT PBAN ANALOG

A fluorescent PBAN analog was prepared from a synthetic peptide corresponding to the terminal 10 residues of *B. mori* PBAN (i.e., SRTRYFSPRLamide) with Lys substitution of Arg2. The Lys residue was labeled with Rhodamine Red succinimidyl ester (Molecular Probes, Eugene, OR, USA) following overnight incubation in 0.1 M sodium bicarbonate (pH 8.2). The conjugated peptide, designated RR-C10PBAN_{R2K}, was purified by reversed-phase high-performance liquid chromatography on a Senshu

Table 2 | Primer sets used for generating fluorescent PBANR chimeras.

Name	Orientation	Sequence (5'-3')
BommoPBANR-As-EGFP	Sense	CTGATACATTTTATCTGGTAATGGTGAGCAAGGGC
BommoPBANR-As-EGFP	Antisense	GCCCTTGCTCACCATTACCAGATAAAATGTATCAG
BommoPBANR-A-EGFP	Sense	TTTCAAGGTAAGATTAAACATGGTGAGCAAGGGC
BommoPBANR-A-EGFP	Antisense	GCCCTTGCTCACCATTGTTTAACTTACCTTGAAA
BommoPBANR-B-EGFP	Sense	TAATATAGAAGGACTTACCATGGTGAGCAAGGGC
BommoPBANR-B-EGFP	Antisense	GCCCTTGCTCACCATTGGTAAGTCCTCTATATTA
BommoPBANR-C-EGFP	Sense	ATCGCGATCTCTCCAATGGTGAGCAAGGGC
BommoPBANR-C-EGFP	Antisense	GCCCTTGCTCACCATTGGAGAGATCGCGAT
PsesePBANR-As-EGFP	Sense	CTTTTACCTGGTAAACTTGATGGTGAGCAAGGGC
PsesePBANR-As-EGFP	Antisense	GCCCTTGCTCACCATTCAAGTTTACCAGGTAAG
PsesePBANR-A-EGFP	Sense	CGGCTTTGTTTATTAATACTTATGGTGAGCAAGGGC
PsesePBANR-A-EGFP	Antisense	GCCCTTGCTCACCATAAGTATTAAACAAAGCCG
PsesePBANR-B-EGFP	Sense	ATCGGCGGACTCACCATTGGTGAGCAAGGGC
PsesePBANR-B-EGFP	Antisense	GCCCTTGCTCACCATTGGTGAGTCCGCCGAT
PsesePBANR-C-EGFP	Sense	CCTACATGTACCACGATGGTGAGCAAGGGC
PsesePBANR-C-EGFP	Antisense	GCCCTTGCTCACCATTGGTGATACGTAGG
HelarPBANR-As-EGFP	Sense	GGAATCTATAGATACATGGTGAGCAAGGGC
HelarPBANR-As-EGFP	Antisense	GCCCTTGCTCACCATTGATCTATAGATTCC
HelarPBANR-A-EGFP	Sense	GTAAGAGTCTATGATATGGTGAGCAAGGGC
HelarPBANR-A-EGFP	Antisense	GCCCTTGCTCACCATTATCATAGACTCTTAC
HelarPBANR-B-EGFP	Sense	ATCGGCGGACTCACCATTGGTGAGCAAGGGC
HelarPBANR-B-EGFP	Antisense	GCCCTTGCTCACCATTGGTGAGTCCGCCGAT
HelarPBANR-C-EGFP	Sense	CCTACATGTACCACGATGGTGAGCAAGGGC
HelarPBANR-C-EGFP	Antisense	GCCCTTGCTCACCATTGGTGATACGTAGG
EGFP	Antisense	TTACTTGTACAGCTCGTCCAT

The EGFP portion of the chimeric oligonucleotides is underlined.

Pak PEGASIL ODS column (10 mm × 150 mm; Senshu Scientific Co., Ltd., Tokyo, Japan) with absorbance monitored at 225 nm. RR-C10PBAN_{R2K} was stored at 4°C until needed.

FLUORESCENT CONFOCAL MICROSCOPY IMAGING

A monolayer of adherent Sf9 insect cells (Smith et al., 1985) was transfected with 1 µg plasmid DNA encoding the respective fluorescent PBANR chimeras and 8 µl Cellfectin II (Invitrogen) according to the manufacturer's instructions. Ligand-induced internalization of the fluorescent PBANR chimeras was performed as described previously using a Leica TCS NT confocal system (Hull et al., 2004) but with 50 nM RR-C10PBAN_{R2K}. Fluorescence images were obtained. Images were processed using Photoshop 6.0 (Adobe Systems Inc., San Jose, CA, USA).

NORTHERN BLOT ANALYSIS

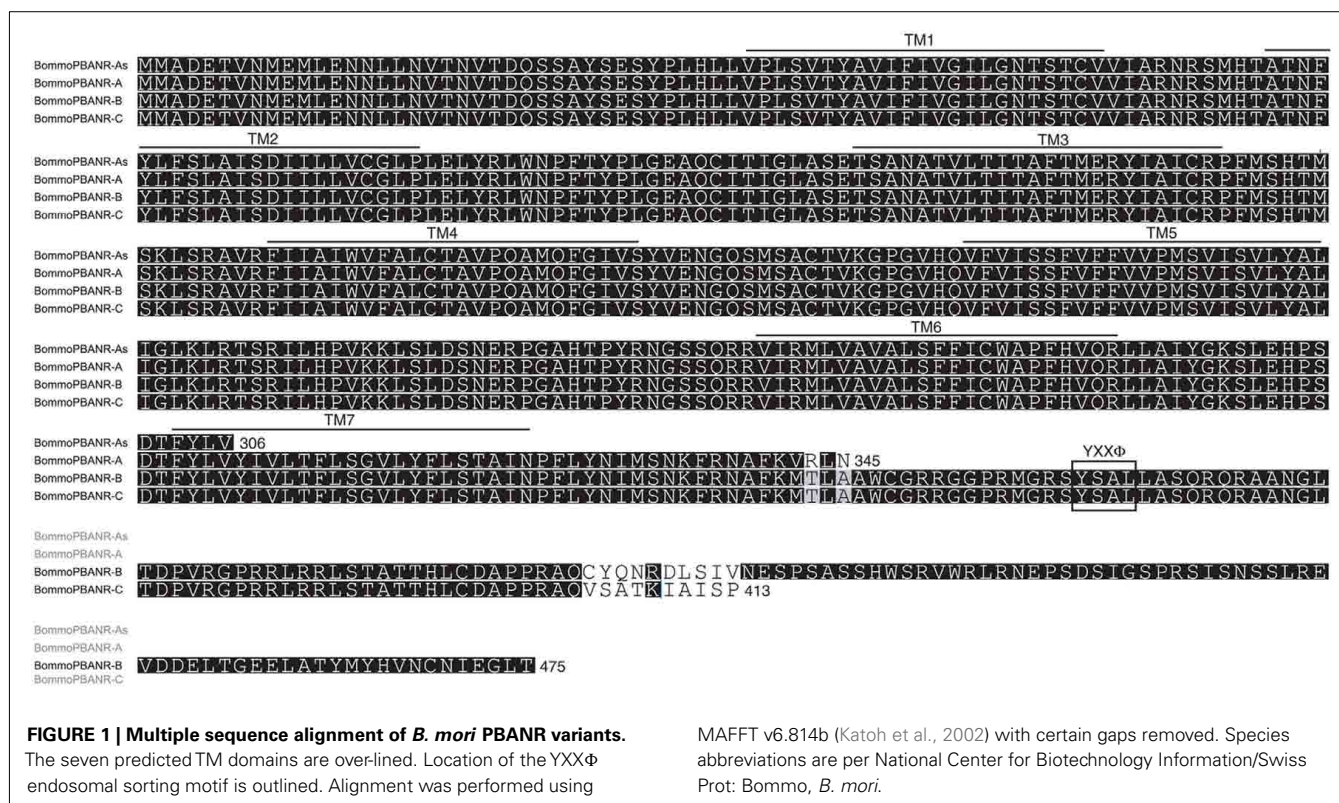
Northern blots were performed using denatured total RNAs (1 µg of each) prepared from various *B. mori*, *P. separata*, and *H. armigera* tissues electrophoresed on a 1.0% gel in 2 M formaldehyde/1X MOPS buffer and then transferred to a nylon membrane (Hybond N⁺, Amersham Biosciences, Piscataway, NJ, USA) by capillary blotting. cDNA probes (BommoPBANR-A nt 1–1265, BommoPBANR-C nt 1591–2616, PsesePBANR-A nt 254–1378, PsesePBANR-C nt 1586–2608, HelarPBANR-A nt 242–1282 and HelarPBANR-C nt 1574–2597) were labeled with DIG (digoxigenin-11-UTP) using a DIG northern starter kit (Roche

Applied Science, Indianapolis, IN, USA). Probe hybridization was performed at 68°C for 18 h at which point the blot was washed twice in an initial solution of 0.1% SDS/2 × SSC for 5 min at 22°C and then transferred to 0.1% SDS/0.1 × SSC for two 15 min washes at 68°C. Signals were detected using a LAS-3000 image analyzer (Fujifilm, Tokyo, Japan).

RESULTS

IDENTIFICATION OF MULTIPLE BOMMOPBANR VARIANTS

To determine if multiple PBANR variants are expressed in the *B. mori* PG, we PCR-screened our *B. mori* PG cDNA library (Yoshiga et al., 2000) using primers designed to BommoPBANR (AB181298). Sequencing multiple cDNA clones resulted in the identification of transcripts encoding the 413-aa BommoPBANR reported previously (Hull et al., 2004) and a new 475-aa protein (Figure 1). Despite large differences in the amino acid sequences of the respective C-terminal tails, the nucleotide sequence of the clones differed by five nucleotides. The larger cDNA was only present in ~10% of the clones sequenced, suggesting that it was poorly represented in our cDNA library and thus that its PG transcript levels are lower than the 413-aa variant. Because the 475-aa variant exhibited significant homology (82%) to HelviPBANR-B, we sought to present a uniform nomenclature system for the PBANR variants. Consequently, we designated the 475-aa variant as BommoPBANR-B and the 413-aa variant,



which shares 81% sequence homology with HelviPBANR-C, as BommoPBANR-C.

PCR primers designed from *B. mori* genomic data based on sequence similarity with HelviPBANR-A lead to the identification of cDNA clones encoding 345-aa and 306-aa proteins. Because the 345-aa variant is similar in size to HelviPBANR-A, we designated it BommoPBANR-A. The 306-aa variant, which has an incomplete seventh transmembrane domain (TM7), was designated BommoPBANR-As. The four BommoPBANR variants identified in these experiments are differentiated only by the size and sequence of their respective C-terminal tails (Figure 1). The sequence data for all four variants have been deposited with GenBank (JN228346–228349).

GENOMIC STRUCTURE AND ALTERNATIVE SPLICING OF THE BOMMOPBANR GENE

Using the Silkworm Genome Research Program (<http://sgp.dna.affrc.go.jp/KAIKObase/>), we localized the *BommoPBANR* gene to scaffold Bm_scaf84 of chromosome 12 and determined that it is composed of six exons and five introns covering >50 kb of sequence (Figure 2). The majority of the BommoPBANR coding sequence (N-terminus through TM7) is carried on exons 2–4 while exons 5–6 encode the C-terminal tail and exon 1 the 5' untranslated region. BommoPBANR-As and A arise from alternative splice events that retain introns 3 and 4 respectively. The inclusion of intron 3 introduces a premature stop codon (TGA) in BommoPBANR-As that truncates TM7 at residue 306, whereas the inclusion of intron 4 in BommoPBANR-A results in a premature stop codon (TAG) that truncates the protein at residue 345. BommoPBANR-C arises from an insertion of 5 nt at the 3' end

of exon 5 that shifts the reading frame of the last 10-aa (residues 404–413) and introduces a stop codon (TAG) that generates a C-terminal tail truncated 62-aa compared to BommoPBANR-B (Figure 1).

EXPRESSION ANALYSIS OF BOMMOPBANR VARIANTS

RT-PCR analyses showed that all four PBANR variants are preferentially expressed within the PG (Figure 3A). Amplification of BommoPBANR-As and -A was barely detectable at cycle 30 while BommoPBANR-B generated a robust, but non-saturating, signal (Figure 3A). In contrast, BommoPBANR-C was saturating by PCR cycle 28, indicating that it is the most abundant PBANR transcript expressed in the PG. Amplimers corresponding to the PBANR-B and C variants were also amplified in other tissues, albeit at significantly lower levels (Figure 3A). The amplification of lower abundance PBANR transcripts in non-PG tissues is not without precedence (Rafaeli et al., 2007; Watanabe et al., 2007) and may either reflect a novel regulatory role for the receptor in those tissues or may be an indication of leaky transcription and thus are of questionable physiological relevance. Regardless, our results, and those of others, clearly demonstrate that PBANR expression in adult moths is predominantly PG-directed, which is congruous with its role in mediating sex pheromone production.

Consistent with our previous report, which described the developmental profile of the BommoPBANR-C transcript (Hull et al., 2004), all four BommoPBANR variants are up-regulated on the day preceding adult emergence (Figure 3B). Similar up-regulation has been observed for other genes crucial to *B. mori* pheromonogenesis, i.e., pgFAR, Bmpgdesat1, pgACBP, BmFATP,

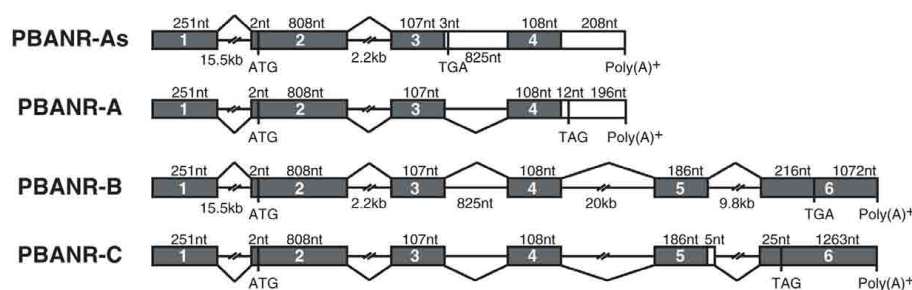


FIGURE 2 | Schematic diagram of the *B. mori* PBANR genomic structure and alternative splice sites. The four BommoPBANR variants (As, A, B, and C) are depicted. The filled boxes represent exons. Initiation (ATG) and stop sites (TGA or TAG) are indicated by their respective codons.

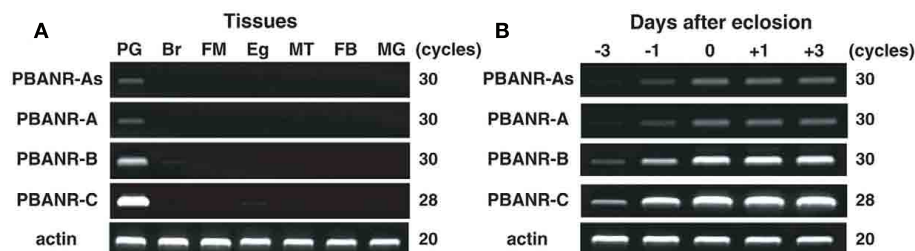


FIGURE 3 | Expression profile of BommoPBANR transcripts in adult female tissues. (A) Expression in adult tissues. Tissues were dissected from newly emerged (day 0) p50 female moths. PG, pheromone gland; Br, brain; FM, flight muscle; Eg, unfertilized egg; MT, Malpighian tubule; FB, fat body; MG, midgut. **(B)** Expression in the PG at different

developmental stages. PGs were dissected from p50 female pupae at 3 days (–3) and 1 day (–1) before eclosion and from p50 adults at 0 day (0), 1 day (+1), and 3 days (+3) after eclosion. cDNAs were normalized to actin expression levels. The PCR cycle number is indicated to the right of the gels.

and BmLsd1 (Matsumoto et al., 2001; Moto et al., 2003, 2004; Ohnishi et al., 2009, 2011).

IDENTIFICATION OF PBANR VARIANTS IN NOCTUID SPECIES

We next investigated the pervasiveness of PBANR splice variants in three other moths. In the Oriental armyworm, *P. separata*, we identified clones encoding 374-aa and 309-aa proteins with 98 and 82% identity to HelviPBANR-A and BommoPBANR-As respectively, which we designated PsesePBANR-A and PsesePBANR-As (Figure 4). Initial attempts to identify PsesePBANR-B and PsesePBANR-C variants via 3'-RACE using conventional polymerases were unsuccessful. Because conventional polymerases often fail to amplify GC-rich targets, we switched to a commercially available GC-optimized polymerase to identify the 469-aa PsesePBANR-C and the 476-aa PsesePBANR-B (Figure 4). As before, sequencing of multiple clones suggested that PsesePBANR-C was the predominantly expressed variant. Applying the same cloning strategy to females of the cotton bollworm, *H. armigera*, we isolated four PBANR variants from a PG-specific cDNA library: a 330-aa protein designated HelarPBANR-As, a 346-aa protein designated HelarPBANR-A, a 476-aa protein designated HelarPBANR-B, and a 469-aa protein designated HelarPBANR-C (Figure 5). HelarPBANR-A is 99% identical to the deposited HelarPBANR (AY792036) with nucleotide sequence variations largely restricted to the third codon position; the lone exception was Leu substitution of Trp118 (Figure 5). The sequence data for the *H. armigera* and *P. separata* PBANR variants have been

deposited with GenBank (*H. armigera* – JN228350–228353 and *P. separata* – JN228354–JN228357).

Because the only PBANR identified in *H. zea* to date corresponds to the PBANR-A variant, we sought to determine if the longer PBANR-B and PBANR-C variants are also expressed in the PG of this species. Using RT-PCR methods as above, we identified *H. zea* homologs of both variants (Figure 6). HelzePBANR-B (JQ255024) is a 476-aa protein with 99% sequence identity to HelviPBANR-B while HelzePBANR-C (JN206677) is a 469-aa protein with 98% sequence identity to HelviPBANR-C. Based on our results and those of Kim et al. (2008), the concurrent expression of multiple PBANR variants that arise from alternative splicing of the 3' coding region appears to be extremely prevalent, if not absolute, across moth species.

RT-PCR EXPRESSION ANALYSES OF PBANR VARIANTS

Sequence analyses revealed that, regardless of moth species, the ~300-nt coding sequence unique to the PBANR-B and -C variants (Figure 7, red bars) is GC-rich. In *P. separata* and *H. armigera*, the GC content of this region ranges from 65–80% while that of the *B. mori* gene is 55–60%. The C-terminal coding sequence of the PBANR-As and -A variants, in contrast, is more AT-rich (Figure 7). In preliminary experiments, we confirmed that species-specific primer sets capable of amplifying both PBANR-A and -As (Figure 8, primer set A) generated distinct amplicons of the expected sizes for each transcript from each species assayed. We also found that while the PBANR-B and -C

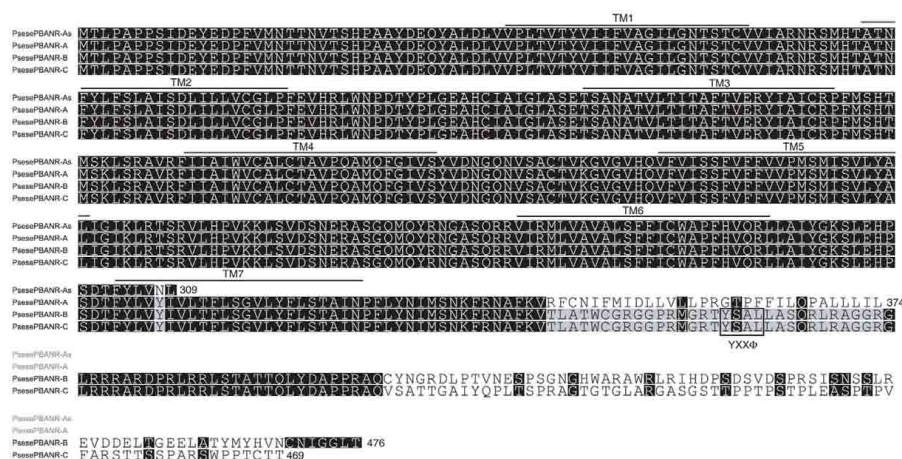


FIGURE 4 | Multiple sequence alignment of the *P. separata* PBANR variants. The seven predicted TM domains are over-lined. Location of the YXXΦ endosomal sorting motif is outlined. Alignment was performed using

MAFFT v6.814b (Katoh et al., 2002) with certain gaps removed. Species abbreviations are per National Center for Biotechnology Information/Swiss Prot: Psese, *Pseudaletia separata*.

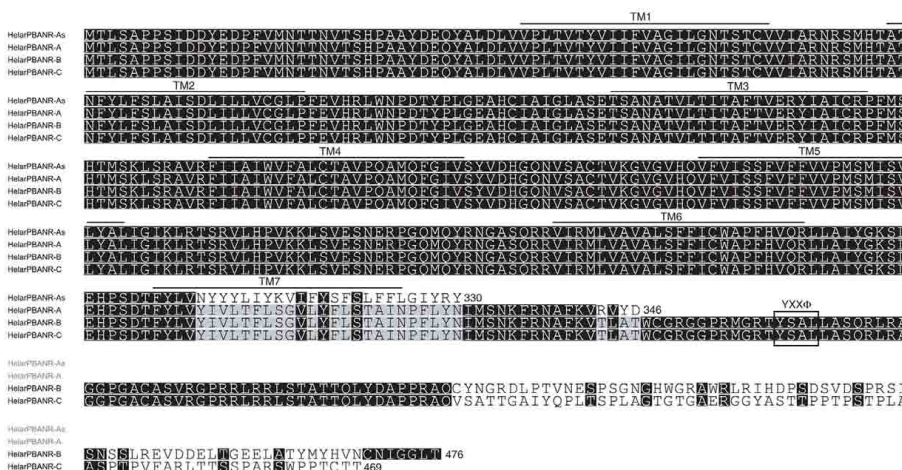


FIGURE 5 | Multiple sequence alignment of the *H. armigera* PBANR variants. The seven predicted TM domains are over-lined. Location of the YXXΦ endosomal sorting motif is outlined. Alignment was performed using

MAFFT v6.814b (Katoh et al., 2002) with certain gaps removed. Species abbreviations are per National Center for Biotechnology Information/Swiss Prot: Helar, *Helicoverpa armigera*.

variants were poorly amplified from *P. separata* with a conventional polymerase, both were robustly amplified with a commercially available GC-optimized polymerase (Figure 8). Based on these results, we performed RT-PCR using PG cDNAs with both the GC-optimized polymerase as well as the conventional DNA polymerase (Figure 9). In all moth species, we observed higher expression levels for PBANR-C than either of the shorter variants. To further confirm the expression levels of PBANR isoforms in the three moth species, we performed Northern blots using total RNA prepared from PGs during pheromonogenesis. Using probes that recognize the “short” (PBANR-As and A) and “long” (PBANR-B and C) variants, we detected a single band corresponding to the “long” variant transcript of 3.4–4.1 kb in the PG of each species (Figure 10A). No bands corresponding to the “short” variant transcript were detected. Furthermore, Northern blots using

total RNAs prepared from various female tissues during this same time period confirmed PG-specific expression of the long variants as single bands were only detected in PGs (Figure 10B).

CELL SURFACE LOCALIZATION AND FUNCTIONAL ACTIVATION OF THE PBANR VARIANTS

To confirm the functionality of the PBANR variants, cultured Sf9 insect cells were transfected with plasmid DNAs encoding fluorescent chimeras of the *B. mori*, *P. separata*, and *H. armigera* PBANR variants in which EGFP was fused in frame to the receptor C-terminus. Cell surface localization of each variant was confirmed using laser confocal microscopy (Figure 11). Regardless of moth species, the PBANR-B and -C variants localized exclusively to the plasma membrane (Figure 11A). The BommoPBANR-A and HelarPBANR-A variants exhibited varying degrees of intracellular

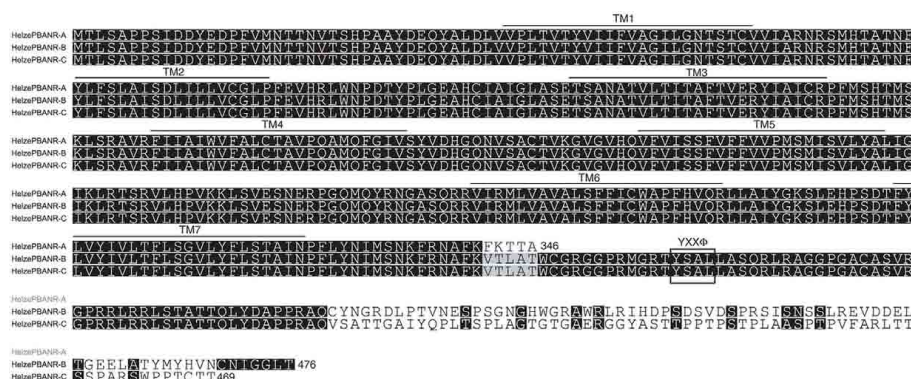


FIGURE 6 | Multiple sequence alignment of the *H. zea* PBANR variants. The seven predicted TM domains are over-lined. Location of the YXXΦ endosomal sorting motif is outlined. Alignment was performed using MAFFT

v6.814b (Kato et al., 2002) with certain gaps removed. Species abbreviations are per National Center for Biotechnology Information/Swiss Prot: Helze, *Helicoverpa zea*.

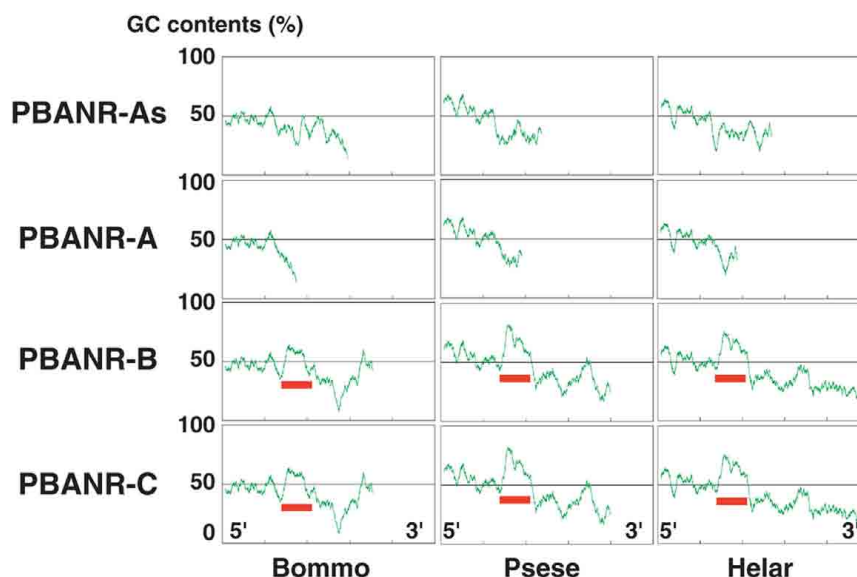


FIGURE 7 | Guanine–cytosine content distribution diagrams of PBANR variants. The distribution of GC content in full-length cDNA sequences for the PBANR variants of *B. mori*, *P. separata*, and *H.*

armigera was calculated using 100 base windows over a range of 700 bases. Red bars indicate the ~300-nt coding sequence unique to the PBANR-B and -C variants.

localization with some cell surface localization (Figure 11A). The PsesePBANR-A variant, in contrast, was completely intracellular (Figure 11A), as were all of the PBANR-As variants (Figure 11A), suggesting that an intact TM7 is necessary for cell surface trafficking and localization.

Ligand-induced receptor internalization is a key element in regulating the strength and duration of receptor-mediated cell signaling. We have previously shown that PBAN induces BommoPBANR-C (formerly referred to as BomPBANR) internalization (Hull et al., 2004, 2005, 2011). We consequently sought to determine if the other PBANR variants are regulated in a similar fashion. Cells transiently expressing the fluorescent PBANR variant chimeras were incubated with a Rhodamine Red-labeled PBAN derivative (RR-C10PBAN_{R2K}). RR-C10PBAN_{R2K} induced

internalization of the PBANR-C and -B variants from each species as evidenced by the intracellular accumulation of red fluorescent vesicles that co-localized with the EGFP chimera-derived green fluorescent signals (Figure 11B). In contrast, despite clear cell surface binding, RR-C10PBAN_{R2K} failed to induce internalization of BommoPBANR-A and HelarPBANR-A (Figure 11B). In addition, consistent with a lack of cell surface localization, no RR-C10PBAN_{R2K} binding was observed in cells expressing PsesePBANR-A (Figure 11B).

DISCUSSION

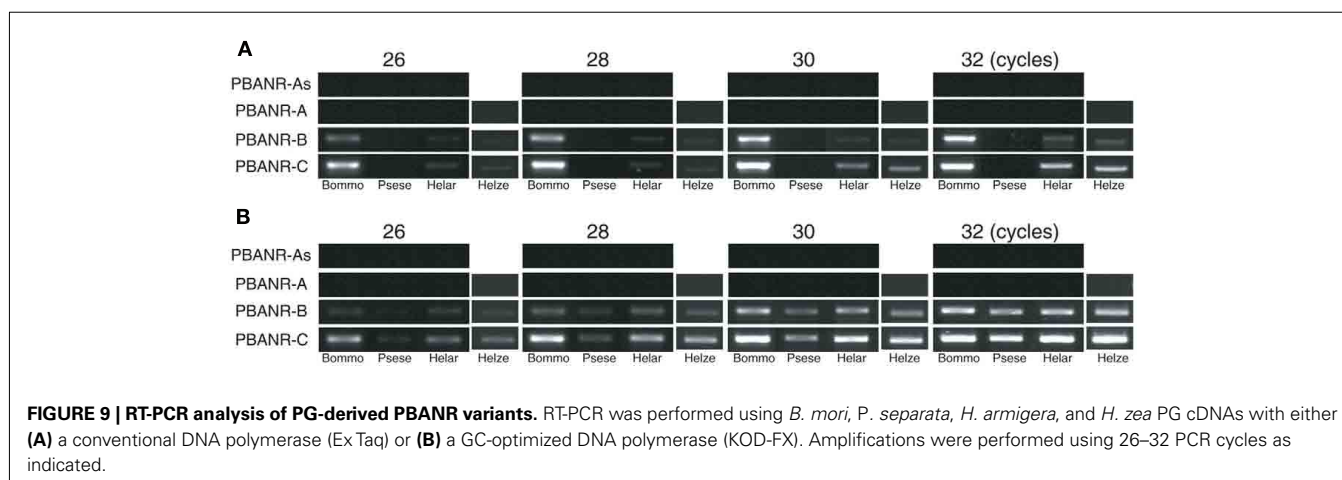
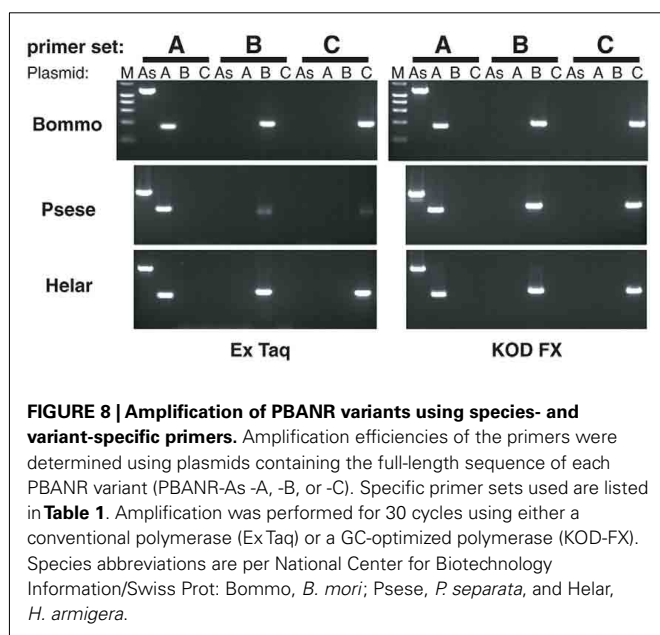
Following ligand binding, receptor trafficking is crucial for the temporal and spatial control of GPCR signaling. The magnitude and duration of GPCR signaling is tightly regulated by

mechanisms that terminate initial signaling and prime the cells to respond to new ligand exposure. Consequently, endocytosis of GPCRs from the cell surface allows for the fine-tuning of signal magnitude and duration by playing a crucial role in signal desensitization, re-sensitization, and down-regulation (Moore et al., 2007; Marchese et al., 2008). Initially, our understanding of the molecular mechanisms underlying PBANR signaling was restricted to the PBANRs identified in *H. zea* and *B. mori* (Choi et al., 2003; Hull et al., 2004). These receptors, however, are structurally differentiated by a 67-aa C-terminal extension in BommoPBANR that is essential for receptor internalization (Hull et al., 2004). Given the significance of GPCR endocytotic trafficking in signal termination, it seems clear that the C-terminal extension present in BommoPBANR plays an essential role in regulating the duration of the PBAN signal. This conclusion, however, raises questions regarding PBANR signaling in general given that HelzePBANR lacks this domain. The functional significance of the two receptor subtypes was initially ascribed to differences in signal transduction cascades

activated (*H. zea*: cAMP dependent vs. *B. mori*: cAMP independent). However, it was recently reported that multiple PBANRs, two of which have extended C-terminal tails and YXXΦ endosomal sorting motifs similar to BommoPBANR, are concurrently expressed in the *H. virescens* larval CNS (Kim et al., 2008). The presence of multiple PBANR transcripts that are concomitantly expressed and that differ only in the length of their C-terminal loop suggests that our understanding of PBAN signaling may be more incomplete than previously thought and raises questions regarding their physiological role.

In the current study, we sought to assess the prevalence of PBANR variants in the PGs of various moth species, and found that multiple variants were expressed in the PGs of every moth examined (Figures 1, 4–6). Genomic structure analysis of the *B. mori* gene showed that the PBANR variants arise from alternative splicing at the 3'-end of the receptor gene on chromosome 12 (Figure 2). Taken together, our findings and those of Kim et al. (2008) provide clear evidence that the PBANR gene in moths undergoes a number of alternative splice events involving the 3'-portion of the gene and suggest that expression of multiple PBANR variants in moth PGs is pervasive.

To determine the potential functionality of the PBANR variants, we expressed EGFP-tagged PBANR variants in Sf9 cells and examined their localization and ability to undergo ligand-induced internalization (Figure 11). The PBANR-As from all the species studied failed to localize to the plasma membrane, a functional deficiency likely attributable to the incomplete TM7 (Markovic and Challiss, 2009). Even though the PBANR-A variant of *H. armigera* and *B. mori* partially localized to the plasma membrane and specifically bound RR-C10PBAN_{R2K}, there was no indication of ligand-induced internalization (Figure 11B). In contrast, all of the PBANR-B and -C variants localized to the plasma membrane and exhibited ligand-induced internalization (Figure 11B). Because internalization is dependent on an active signaling cascade (Hull et al., 2005, 2011), we concluded that the PBANR-A variant is either functionally deficient or has distinct intracellular signaling properties. The lack of an internalization response in cells expressing the PBANR-A variants, however, was not completely unexpected as C-terminal truncations lacking the YXXΦ motif, which is present in the PBANR-B and -C



variants but not the PBANR-A variants, exhibited drastically different internalization kinetics (Hull et al., 2005). Interestingly, while capable of mobilizing extracellular Ca^{2+} in response to PBAN, the initial HelzePBANR variant identified by Choi et al. (2003) also lacks this motif. This suggests that functional differences between the *H. zea* receptor and the *B. mori* receptor likely extend beyond the C-terminus. Notable sequence variations between BommoPBANR-A and HelzePBANR-A include the last four to five residues (BommoPBANR-A: VRLN vs. HelzePBANR: FKTTA) of the respective C-terminal tails and a four residue span in the third intracellular loop (BommoPBANR-A: AHTP vs. HelzePBANR: QMQ). What role, if any, these residues may play in PBANR signal transduction remains to be determined.

In the course of our efforts to clone transcripts encoding PBANR variants, we found that conventional 3'-RACE PCR failed to amplify cDNAs for the PBANR-B and -C variants. In addition, RT-PCR using gene-specific primers with conventional polymerases likewise failed to amplify the cDNAs encoding PsesePBANR-B and -C. In contrast, these transcripts were successfully amplified with a GC-optimized polymerase (Figure 9). Regardless of moth species, the coding sequence unique to the PBANR-B and -C variants is GC abundant, while the C-terminal coding sequence of the PBANR-As and -A variants is AT-rich (Figure 7). We speculate that this may be the reason why transcripts encoding PBANR-A have been so frequently amplified (Rafaeli et al., 2007; Zheng et al., 2007; Cheng et al., 2010; Lee et al., 2011) despite the higher expression levels of PBANR-B and -C (see Figure 9). As a consequence, we believe that conclusions drawn regarding the *in vivo* functional role of the PBANR-A variant should be reconsidered within the context of coincident PBANR-B and -C expression.

While evidence for the four PBANR splice variants is currently limited to the transcript level, their conservation across multiple species, in conjunction with similar observations of conserved splicing patterns in mammalian receptors (Markovic and Grammatopoulos, 2009), suggests that the variants are likely physiologically relevant. Concomitant expression of the multiple variants within a single cell type could represent a fine-tuning mechanism for cellular responsiveness to the extracellular signal. In one scenario, a non-responsive receptor (e.g., BommoPBANR-A) expressed at the cell surface might function as a decoy receptor that competes with the wildtype receptor (e.g., BommoPBANR-C) for ligand binding. The net result would be less bioactive peptide available to trigger the cellular response thus decreasing overall sensitivity. Alternatively, heterodimerization of the short receptors (e.g., BommoPBANR-A and/or -As) with the longer wildtype receptors (e.g., BommoPBANR-C or -B) could trap the active receptors within the secretory pathway, thereby decreasing the pool of available receptor for ligand binding and effectively decreasing overall cellular sensitivity. Truncated variants of the calcitonin receptor, corticotropin releasing factor receptor type 1, and, more recently, growth hormone secretagogue receptor type 1a have all been shown to exhibit dominant negative effects on signaling when co-expressed with wildtype variants (Seck et al., 2005; Zmijewski and Slominski, 2009; Chow et al., 2012). Receptor variants have also been shown to be functionally distinct with respect to spatial and temporal expression, ligand binding, regulation, and

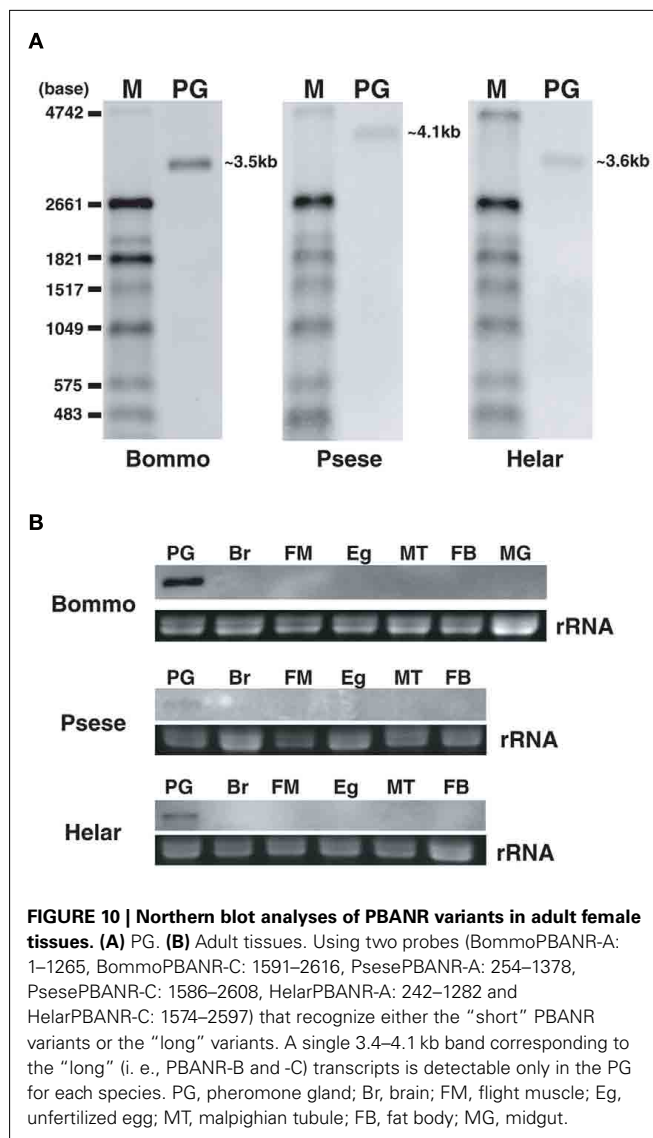


FIGURE 10 | Northern blot analyses of PBANR variants in adult female tissues. (A) PG. **(B)** Adult tissues. Using two probes (BommoPBANR-A: 1–1265, BommoPBANR-C: 1591–2616, PsesePBANR-A: 254–1378, PsesePBANR-C: 1586–2608, HelarPBANR-A: 242–1282 and HelarPBANR-C: 1574–2597) that recognize either the “short” PBANR variants or the “long” variants. A single 3.4–4.1 kb band corresponding to the “long” (i. e., PBANR-B and -C) transcripts is detectable only in the PG for each species. PG, pheromone gland; Br, brain; FM, flight muscle; Eg, unfertilized egg; MT, malpighian tubule; FB, fat body; MG, midgut.

downstream effector pathways (Markovic and Challiss, 2009). A naturally occurring variant of the neurokinin 1 receptor that essentially lacks a C-terminus has been shown to mediate intracellular signaling mechanisms distinct from those initiated by the full-length receptor including: an inability to mobilize extracellular Ca^{2+} , decreased protein kinase δ phosphorylation, slowed activation of the extracellular signal-regulated kinase (ERK) pathway, and decreased desensitization and internalization (DeFea et al., 2000; Lai et al., 2008). A similar differentiation in signaling pathways activated downstream of ligand binding has been observed for the PBANR variants. When expressed in mammalian CHO-WTA11 cells, only the HelviPBANR-C variant generated a robust Ca^{2+} signal in response to PBAN, little to no Ca^{2+} mobilization was observed in cells expressing the HelviPBANR-A or -B variants (Kim et al., 2008). Furthermore, given the pleiotropic nature of PBAN and PBAN-like peptides (Rafaeli, 2009), it is likely that PBANR variants expressed in other tissues/developmental stages may govern tissue-dependent physiological functions. Indeed, the

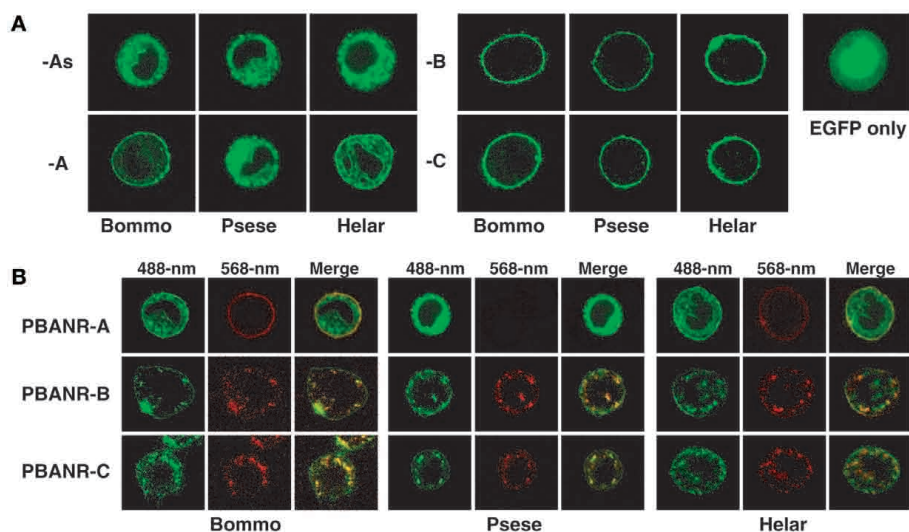


FIGURE 11 | Confocal imaging of fluorescent chimeras of the PBANR variants transiently expressed in Sf9 cells. (A) Localization of EGFP-tagged PBANR variants. For control purposes, Sf9 cells were transfected with an

expression plasmid containing EGFP. **(B)** Ligand-induced internalization of EGFP-tagged PBANR variants. Internalization was triggered with 50 nM RR-C10PBAN_{R2K}. Co-localization is indicated by yellow in the merged images.

PBANR-A variant in *Spodoptera littoralis* was cloned from fifth instar larvae as part of an effort to identify the receptor responsible for cuticular pigmentation, a physiological effect mediated by the PBAN family of peptides (Zheng et al., 2007).

In conclusion, our results show that PBANR-C is the predominant variant expressed in the PG during pheromonogenesis regardless of moth species, and, given the functional significance of the C-terminus (Hull et al., 2004, 2005, 2011), strongly suggest that this variant is the principal receptor molecule involved in PBAN signaling. This conclusion is supported by Northern blot analyses (Figure 10) as well as specific photoaffinity-based binding of biotin-labeled PBAN to a membrane-bound protein of ~50 kDa in *H. armigera* PGs (Rafaeli et al., 2003), which is more consistent with the molecular weight of HelarPBANR-C (51.1 kDa) than

HelarPBANR-A (38.7 kDa). Furthermore, preferential amplification of the PBANR-C variant was also demonstrated in *H. virescens* PGs (Kim et al., 2008). Lastly, in contrast to PBANR-C, the shorter PBANR-A variant localizes poorly at the cell surface and fails to undergo typical ligand-induced internalization (Figure 11), which suggests that desensitization of this variant either does not occur, or at the very least that its regulation is mediated by a distinct intracellular pathway.

ACKNOWLEDGMENTS

This work was supported by the Lipid Dynamics Research Program from RIKEN and the Targeted Proteins Research Program (TPRP) from the Ministry of Education, Culture, Sports, Science, and Technology of Japan.

REFERENCES

- Cheng, Y., Luo, L., Jiang, X., Zhang, L., and Niu, C. (2010). Expression of pheromone biosynthesis activating neuropeptide and its receptor (PBANR) mRNA in adult female *Spodoptera exigua* (Lepidoptera: Noctuidae). *Arch. Insect Biochem. Physiol.* 75, 13–27.
- Choi, M. Y., Fuerst, E. J., Rafaeli, A., and Jurenka, R. (2003). Identification of a G protein-coupled receptor for pheromone biosynthesis activating neuropeptide from pheromone glands of the moth *Helicoverpa zea*. *Proc. Natl. Acad. Sci. U.S.A.* 100, 9721–9726.
- Chow, K. B. S., Sun, J., Chu, K. M., Cheung, W. T., Cheng, C. H. K., and Wise, H. (2012). The truncated ghrelin receptor polypeptide (GHS-R1b) is localized in the endoplasmic reticulum where it forms heterodimers with ghrelin receptors (GHS-R1a) to attenuate their cell surface expression. *Mol. Cell. Endocrinol.* 348, 247–254.
- DeFea, K. A., Vaughn, Z. D., O'Bryan, E. M., Nishijima, D., Déry, O., and Bunnett, N. W. (2000). The proliferative and antiapoptotic effects of substance P are facilitated by formation of a β -arrestin-dependent scaffolding complex. *Proc. Natl. Acad. Sci. U.S.A.* 97, 11086–11091.
- Fónagy, A., Matsumoto, S., Uchiumi, K., Orikasa, C., and Mitsui, T. (1992). Action of pheromone biosynthesis activating neuropeptide on pheromone glands of *Bombyx mori* and *Spodoptera litura*. *J. Pest Sci.* 17, 47–54.
- Fónagy, A., Moto, K., Ohnishi, A., Kurihara, M., Kis, J., and Matsumoto, S. (2011). Studies of sex pheromone production under neuroendocrine control by analytical and morphological means in the oriental armyworm, *Pseudaletia separata*, Walker (Lepidoptera: Noctuidae). *Gen. Comp. Endocrinol.* 172, 62–76.
- Hull, J. J., Lee, J. M., and Matsumoto, S. (2011). Identification of specific sites in the third intracellular loop and carboxyl terminus of the *Bombyx mori* pheromone biosynthesis activating neuropeptide receptor crucial for ligand-induced internalization. *Insect Mol. Biol.* 6, 801–811.
- Hull, J. J., Ohnishi, A., and Matsumoto, S. (2005). Regulatory mechanisms underlying pheromone biosynthesis activating neuropeptide (PBAN)-induced internalization of the *Bombyx mori* PBAN receptor. *Biochem. Biophys. Res. Commun.* 334, 69–78.
- Hull, J. J., Ohnishi, A., Moto, K., Kawasaki, Y., Kurata, R., Suzuki, M. G., and Matsumoto, S. (2004). Cloning and characterization of the pheromone biosynthesis activating neuropeptide receptor from the silkworm, *Bombyx mori*: significance of the carboxyl terminus in receptor internalization. *J. Biol. Chem.* 279, 51500–51507.
- Katoh, K., Misawa, K., Kuma, K., and Miyata, T. (2002). MAFFT: a novel method for rapid multiple sequence alignment based on fast Fourier transform. *Nucleic Acids Res.* 30, 3059–3066.
- Kim, Y. J., Nachman, R. J., Aimanova, K., Gill, S., and Adams, M. E. (2008). The pheromone biosynthesis activating neuropeptide (PBAN) receptor of *Heliothis virescens*: identification, functional expression, and structure-activity relationships of ligand analogs. *Peptides* 29, 268–275.

- Kitamura, A., Nagasawa, H., Kataoka, H., Inoue, T., Matsumoto, S., Ando, T., and Suzuki, A. (1989). Amino acid sequence of pheromone-biosynthesis-activating neuropeptide (PBAN) of the silkworm, *Bombyx mori*. *Biochem. Biophys. Res. Commun.* 163, 520–526.
- Lai, J.-P., Lai, S., Tuluc, F., Tansky, M. F., Kilpatrick, L. E., Leeman, S. E., and Douglas, S. D. (2008). Differences in the length of the carboxyl terminus mediate functional properties of neurokinin-1 receptor. *Proc. Natl. Acad. Sci. U.S.A.* 105, 12605–12610.
- Lee, D. W., Shrestha, S., Kim, A. Y., Park, S. J., Yang, C. Y., Kim, Y., and Koh, Y. H. (2011). RNA interference of pheromone biosynthesis-activating neuropeptide receptor suppresses mating behavior by inhibiting sex pheromone production in *Plutella xylostella* (L.). *Insect Biochem. Mol. Biol.* 41, 236–243.
- Marchese, A., Paing, M. M., Temple, B. R., and Trejo, J. (2008). G protein-coupled receptor sorting to endosomes and lysosomes. *Annu. Rev. Pharmacol. Toxicol.* 48, 601–629.
- Markovic, D., and Challiss, R. A. (2009). Alternative splicing of G protein-coupled receptors: physiology and pathophysiology. *Cell. Mol. Life Sci.* 66, 3337–3352.
- Markovic, D., and Grammatopoulos, D. K. (2009). Focus on the splicing of secretin GPCRs transmembrane-domain 7. *Trends Biochem. Sci.* 34, 443–452.
- Matsumoto, S., Fónagy, A., Yamamoto, M., Wang, F., Yokoyama, N., Esumi, Y., and Suzuki, Y. (2002). Chemical characterization of cytoplasmic lipid droplets in the pheromone-producing cells of the silkworm, *Bombyx mori*. *Insect Biochem. Mol. Biol.* 32, 1447–1455.
- Matsumoto, S., Yoshiga, T., Yokoyama, N., Iwanaga, M., Koshiba, S., Kigawa, T., Hirota, H., Yokoyama, S., Okano, K., Mita, K., Shimada, T., and Tatsuki, S. (2001). Characterization of acyl-CoA-binding protein (ACBP) in the pheromone gland of the silkworm, *Bombyx mori*. *Insect Biochem. Mol. Biol.* 31, 603–609.
- Minneman, K. P. (2001). Splice variants of G protein-coupled receptors. *Mol. Interv.* 1, 108–116.
- Moore, C. A., Milano, S. K., and Benovic, J. L. (2007). Regulation of receptor trafficking by GRKs and arrestins. *Annu. Rev. Physiol.* 69, 451–482.
- Moto, K., Suzuki, M. G., Hull, J. J., Kurata, R., Takahashi, S., Yamamoto, M., Okano, K., Imai, K., Ando, T., and Matsumoto, S. (2004). Involvement of a bifunctional fatty-acyl desaturase in the biosynthesis of the silkworm, *Bombyx mori*, sex pheromone. *Proc. Natl. Acad. Sci. U.S.A.* 101, 8631–8636.
- Moto, K., Yoshiga, T., Yamamoto, M., Takahashi, S., Okano, K., Ando, T., Nakata, T., and Matsumoto, S. (2003). Pheromone gland-specific fatty-acyl reductase of the silkworm, *Bombyx mori*. *Proc. Natl. Acad. Sci. U.S.A.* 100, 9156–9161.
- Ohnishi, A., Hashimoto, K., Imai, K., and Matsumoto, S. (2009). Functional characterization of the *Bombyx mori* fatty acid transport protein (BmFATP) within the silkworm pheromone gland. *J. Biol. Chem.* 284, 5128–5136.
- Ohnishi, A., Hull, J. J., Kaji, M., Hashimoto, K., Lee, J. M., Tsuneizumi, K., Suzuki, T., Dohmae, N., and Matsumoto, S. (2011). Hormone signaling linked to silkworm sex pheromone biosynthesis involves Ca^{2+} /Calmodulin-dependent protein kinase II-mediated phosphorylation of the insect PAT family protein *Bombyx mori* lipid storage droplet protein-1 (BmLsd1). *J. Biol. Chem.* 286, 24101–24112.
- Ohnishi, A., Hull, J. J., and Matsumoto, S. (2006). Targeted disruption of genes in the *Bombyx mori* sex pheromone biosynthetic pathway. *Proc. Natl. Acad. Sci. U.S.A.* 103, 4398–4403.
- Rafaeli, A. (2009). Pheromone biosynthesis activating neuropeptide (PBAN): regulatory role and mode of action. *Gen. Comp. Endocrinol.* 162, 69–78.
- Rafaeli, A., Bober, R., Becker, L., Choi, M. Y., Fuerst, E. J., and Jurenka, R. (2007). Spatial distribution and differential expression of the PBAN receptor in tissues of adult *Helicoverpa* spp. (Lepidoptera: Noctuidae). *Insect Mol. Biol.* 16, 287–293.
- Rafaeli, A., Zakharova, T., Lapsker, Z., and Jurenka, R. A. (2003). The identification of an age- and female-specific putative PBAN membrane-receptor protein in pheromone glands of *Helicoverpa armigera*: possible up-regulation by juvenile hormone. *Insect Biochem. Mol. Biol.* 33, 371–380.
- Raina, A. K., Jaffe, H., Kempe, T. G., Keim, P., Bacher, R. W., Fales, H. M., Riley, C. T., Klun, J. A., Ridgway, R. L., and Hayes, D. K. (1989). Identification of a neuropeptide hormone that regulates sex pheromone production in female moths. *Science* 244, 796–798.
- Seck, T., Pellegrini, M., Florea, A. M., Grignoux, V., Baron, R., Mierke, D. F., and Horne, W. C. (2005). The δel3 isoform of the calcitonin receptor forms a six-transmembrane domain receptor with dominant-negative effects on receptor surface expression and signaling. *Mol. Endocrinol.* 19, 2132–2144.
- Smith, G. E., Ju, G., Ericson, B. L., Moschera, J., Lahm, H. W., Chizzonite, R., and Summers, M. D. (1985). Modification and secretion of human interleukin 2 produced in insect cells by a baculovirus expression vector. *Proc. Natl. Acad. Sci. U.S.A.* 82, 8404–8408.
- Watanabe, K., Hull, J. J., Niimi, T., Imai, K., Matsumoto, S., Yaginuma, T., and Kataoka, H. (2007). FXPRL-amide peptides induce ecdysteroidogenesis through a G-protein coupled receptor expressed in the prothoracic gland of *Bombyx mori*. *Mol. Cell. Endocrinol.* 273, 51–58.
- Yoshiga, T., Okano, K., Mita, K., Shimada, T., and Matsumoto, S. (2000). cDNA cloning of acyl-CoA desaturase homologs in the silkworm, *Bombyx mori*. *Gene* 246, 339–345.
- Zheng, L., Lytle, C., Njauw, C. N., Altstein, M., and Martins-Green, M. (2007). Cloning and characterization of the pheromone biosynthesis activating neuropeptide receptor gene in *Spodoptera littoralis* larvae. *Gene* 393, 20–30.
- Zmijewski, M. A., and Slominski, A. T. (2009). CRF1 receptor splicing in epidermal keratinocytes: potential biological role and environmental regulations. *J. Cell. Physiol.* 218, 593–602.

Conflict of Interest Statement: The authors declare that the research was conducted in the absence of any commercial or financial relationships that could be construed as a potential conflict of interest.

Received: 13 December 2011; paper pending published: 26 December 2011; accepted: 09 January 2012; published online: 24 January 2012.

Citation: Lee JM, Hull JJ, Kawai T, Goto C, Kurihara M, Tanokura M, Nagata K, Nagasawa H and Matsumoto S (2012) Re-evaluation of the PBAN receptor molecule: characterization of PBANR variants expressed in the pheromone glands of moths. *Front. Endocrin.* 3:6. doi: 10.3389/fendo.2012.00006

This article was submitted to *Frontiers in Experimental Endocrinology*, a specialty of *Frontiers in Endocrinology*.

Copyright © 2012 Lee, Hull, Kawai, Goto, Kurihara, Tanokura, Nagata, Nagasawa and Matsumoto. This is an open-access article distributed under the terms of the Creative Commons Attribution Non Commercial License, which permits non-commercial use, distribution, and reproduction in other forums, provided the original authors and source are credited.



Establishment of Sf9 transformants constitutively expressing PBAN receptor variants: application to functional evaluation

Jae Min Lee¹, J. Joe Hull^{2*}, Takeshi Kawai³, Kazuhide Tsuneizumi¹, Masaaki Kurihara¹, Masaru Tanokura³, Koji Nagata³, Hiromichi Nagasawa³ and Shogo Matsumoto^{1*}

¹ Molecular Entomology Laboratory, RIKEN Advanced Science Institute, Wako, Japan

² USDA-ARS Arid Land Agricultural Research Center, Maricopa, AZ, USA

³ Department of Applied Biological Chemistry, Graduate School of Agricultural and Life Sciences, The University of Tokyo, Tokyo, Japan

Edited by:

Akiyoshi Takahashi, Kitasato University, Japan

Reviewed by:

Mitsuyo Kishida, Kumamoto University, Japan
Sho Kakizawa, Kyoto University, Japan
Yoonseong Park, Kansas State University, USA

*Correspondence:

J. Joe Hull, USDA-ARS Arid Land Agricultural Research Center, 21881 North Cardon Lane, Maricopa, AZ 85138, USA.
e-mail: joe.hull@ars.usda.gov;
Shogo Matsumoto, RIKEN Advanced Science Institute, 2-1 Hirose, Wako, Saitama, 351-0198, Japan.
e-mail: smatsu@riken.jp

To facilitate further evaluation of pheromone biosynthesis activating neuropeptide receptor (PBANR) functionality and regulation, we generated cultured insect cell lines constitutively expressing green fluorescent protein chimeras of the recently identified *Bombyx mori* PBANR (BommoPBANR) and *Pseudaletia separata* PBANR (PsesePBANR) variants. Fluorescent chimeras included the BommoPBANR-A, -B, and -C variants and the PsesePBANR-B and -C variants. Cell lines expressing non-chimeric BommoPBANR-B and -C variants were also generated. Functional evaluation of these transformed cell lines using confocal laser microscopy revealed that a Rhodamine Red-labeled PBAN derivative (RR-C10PBAN_{R2K}) specifically co-localized with all of the respective PBANR variants at the plasma membrane. Near complete internalization of the fluorescent RR-C10PBAN_{R2K} ligand 30 min after binding was observed in all cell lines except those expressing the BommoPBANR-A variant, in which the ligand/receptor complex remained at the plasma membrane. Fluorescent Ca²⁺ imaging further showed that the BommoPBANR-A cell line exhibited drastically different Ca²⁺ mobilization kinetics at a number of RR-C10PBAN_{R2K} concentrations including 10 μ M. These observations demonstrate a clear functional difference between the BommoPBANR-A variant and the BommoPBANR-B and -C variants in terms of receptor regulation and activation of downstream effector molecules. We also found that, contrary to previous reports, ligand-induced internalization of BommoPBANR-B and BommoPBANR-C in cell lines stably expressing these variants occurred in the absence of extracellular Ca²⁺.

Keywords: PBAN receptor, GPCR, splice variants, ligand-induced internalization, stable transformation

INTRODUCTION

Since mating in insects is often limited to a specific phase of the photoperiod, the biochemical processes that comprise sex pheromone biosynthesis must be precisely regulated. In most moth species, sex pheromone production in pheromone gland (PG) cells is initiated following the activation of a G protein-coupled receptor (GPCR) by a neurohormone termed pheromone biosynthesis activating neuropeptide (PBAN; Raina et al., 1989; Rafaei, 2009). In the silkworm, *Bombyx mori*, activation of the PBAN receptor (PBANR) triggers an intracellular signal transduction cascade that comprises a canonical store-operated channel (SOC) pathway in which Gq-mediated phospholipase C (PLC) activation triggers the coupling of endoplasmic reticulum-resident STIM with cell surface-localized Orai channels. The influx of extracellular Ca²⁺ that follows STIM-Orai coupling drives the species-specific enzymatic reactions that culminate in sex pheromone production and release (Matsumoto et al., 2010). Consequently, PBANR plays a critical role in turning the extracellular PBAN signal into the biological response of sex pheromone production.

Based on predicted structural similarities with the mammalian neuromedin U receptor (Park et al., 2002), PBANRs were cloned from PGs of the corn earworm, *Heliothis virescens*, and *B. mori* (Choi et al., 2003; Hull et al., 2004). Both PBANRs were characterized as rhodopsin-like GPCRs that belong to the neuromedin U receptor family and exhibit significant sequence similarities (76%). The *B. mori* PBANR (BommoPBANR), though, is structurally differentiated by a 67-aa C-terminal extension absent in HelzePBANR that is essential for ligand-induced receptor regulation (Hull et al., 2004, 2005). Until recently, a majority of the PBANRs identified in other moths were of a single isoform that exhibited a truncated C-terminal tail similar to the HelzePBANR, suggesting a potential correlation with species-specific signal transduction pathways (Rafaei, 2009). Multiple PBANR variants (identified as A, B, and C) that arise from alternative splicing at the 3'-end of the PBANR gene, however, were identified in the tobacco budworm *Heliothis virescens* (Kim et al., 2008). The HelviPBANR-A variant is homologous to HelzePBANR, while the HelviPBANR-C variant has an extended C-terminal intracellular loop that shares considerable sequence similarity with BommoPBANR. Intriguingly, despite *H.*

virescens and *H. zea* being derived from the same Heliothinae sub-family, HelviPBANR-C, and not HelviPBANR-A, was preferentially amplified from *H. virescens* PGs (Kim et al., 2008). The expression of multiple PBANR variants (As, A, B, and C) that arise from alternative splicing of the 3'-end of the PBANR gene was recently confirmed in PGs of several moth species including *B. mori*, *Pseudaletia separata* (the Oriental armyworm), *Helicoverpa armigera* (the cotton bollworm), as well as *H. zea* (Lee et al., 2012). The unusually high GC-content of the C-terminal tail coding region of the PBANR gene is thought to have contributed to the previous "preferential" amplification of the PBANR-A variant.

Transient expression of enhanced green fluorescent protein (EGFP) chimeras of the PBANR variants in cultured insect Sf9 cells revealed that regardless of moth species the PBANR-B and -C variants localized to the plasma membrane and internalized upon ligand binding. PBANR-A variants likewise localized to the cell surface, but failed to undergo ligand-induced internalization (Lee et al., 2012). While these transient expression studies afforded the opportunity for fast analysis of gene function, their effectiveness in studies that require more reproducible gene expression levels is limited. In the current study, we sought to expand on our previous studies and establish a more advantageous system for evaluating receptor functionality by generating transformed Sf9 cells that constitutively express the BommoPBANR and *P. separata* PBANR (PsesePBANR) variants.

MATERIALS AND METHODS

CONSTRUCTION OF EXPRESSION PLASMIDS

Chimeric EGFP-fused expression plasmids for the BommoPBANR variants (A, B, and C) and PsesePBANR variants (B and C) were prepared as described (Lee et al., 2012). Non-chimeric expression plasmids for the BommoPBANR variants (B and C) were amplified using a gene specific BommoPBANR sense primer (5'-ATGATGGCAGATGAAACCGTCAAC-3') with either a BommoPBANR-B antisense primer (5'-TCAGGTAAGTCCTTCTATATTACAG-3') or a BommoPBANR-C antisense primer (5'-CTATGGAGAGATCGCGATTTTGG-3') from plasmids containing full-length BommoPBANR-B and BommoPBANR-C, respectively. PCR was performed using thermocycler conditions consisting of 25 cycles at 94°C for 30 s, 60°C for 30 s, and 72°C for 2 min, and a final extension at 72°C for 7 min. PCR products were sub-cloned using a pIB/V5-His-TOPO TA expression kit (Invitrogen Co., Ltd., Tokyo, Japan) and sequenced to confirm the presence and orientation of the inserts.

CELL CULTURE AND TRANSFECTION

Lepidopteran Sf9 insect cells derived from *Spodoptera frugiperda* (Smith et al., 1985) were cultured in IPL-41 insect medium (Invitrogen) at 27°C. Cells were transfected using 1 µg plasmid DNA and 8 µl Cellfectin II (Invitrogen) according to the manufacturer's instruction. Forty-eight hours post-transfection, the transfection medium was replaced with fresh IPL-41 insect medium supplemented with 10% fetal bovine serum. Transfected cells were further incubated for 3 weeks in selective medium containing 80 µg/ml (final concentration) blasticidin S (Invitrogen) at 27°C. The selective medium was replaced every 3–4 days until foci formation. To establish clonal cell lines, individual colonies were

isolated 3 weeks after transfection and the clonal cells were further cultured for 6–24 months in IPL-41 insect medium containing 10 µg/ml (final concentration) blasticidin S at 27°C.

SOUTHERN BLOT ANALYSIS

Genomic DNAs were isolated from cell lines constitutively expressing the PBANR variants as well as untransformed Sf9 cells using a NucleoSpin Tissue kit (TaKaRa Bio Inc., Tokyo, Japan) according to the manufacturer's instruction. Genomic DNAs (10 µg) were digested with *Bam*HI, separated by 0.8% agarose gel electrophoresis and then transferred to a nylon membrane (Hybond N⁺, Amersham Biosciences, Piscataway, NJ, USA) by capillary blotting. The full-length EGFP sequence (720 base-pair) was used as probe. Labeling of the probe, hybridization and signal detection were done using a DIG DNA Labeling and Detection Kit and DIG Easy Hyb (Roche Applied Sciences, Indianapolis, IN, USA) according to the manufacturer's instruction. Probe hybridization was performed at 45°C for 18 h at which point the blot was washed twice in an initial solution of 0.1% SDS/2× SSC for 5 min at 22°C and then transferred to 0.1% SDS/0.1× SSC for two 15 min washes at 65°C. Signal was detected using NBT/BCIP (nitro-blue tetrazolium chloride/5-bromo-4-chloro-3'-indolophosphate *p*-toluidine salt).

PREPARATION OF A FLUORESCENT PBAN ANALOG

To facilitate preparation of a fluorescent analog of a synthetic 10-aa peptide corresponding to the C-terminal part of *B. mori* PBAN (SRTRYFSPRLamide), the Arg at position two was changed to Lys to generate C10PBAN_{R2K} (SKTRYFSPRLamide). Lys2 was then labeled with Rhodamine Red succinimidyl ester (Molecular Probes, Eugene, OR, USA) by overnight incubation in 0.1 M sodium bicarbonate (pH 8.2). The conjugated peptide, designated RR-C10PBAN_{R2K}, was purified by reversed-phase high-performance liquid chromatography on a Senshu Pak PEGASIL ODS column (10 mm × 150 mm; Senshu Scientific Co., Ltd., Tokyo, Japan) with absorbance monitored at 225 nm. RR-C10PBAN_{R2K} was stored at 4°C until used.

CONFOCAL MICROSCOPY

For imaging of ligand-induced internalization of the fluorescent chimera PBANR, Sf9 cells were washed with fresh IPL-41 insect media and incubated in the presence of 50 nM RR-C10PBAN_{R2K} for 1 h at 4°C. Cells were then washed twice with cold phosphate-buffered saline (PBS) to remove unbound label and incubated for 30 min at 27°C in 2 ml IPL-41. At the end of the incubation, cells were fixed for 30 min with 4% paraformaldehyde at 4°C, washed twice with cold PBS, and then imaged. For imaging of Ca²⁺ influx, Sf9 cells stably expressing PBANR variants were incubated in IPL-41 containing 3 µM Fluo4-AM (Molecular Probes) and 0.03% pluronic F-127 (Molecular Probes) for 60 min at 27°C in the dark. Cells were then washed twice with 500 µl IPL-41, incubated in 900 µl insect Ringer's buffer [RB; 35 mM NaCl, 36 mM KCl, 12 mM CaCl₂, 16 mM MgCl₂, 274 mM glucose, and 5 mM Tris (pH 7.5)] for 30 min at room temperature in the dark, and imaged for basal Ca²⁺ levels. For experiments, cells were further incubated for 2–30 min following addition of 100 µl of a 50-nM RR-C10PBAN_{R2K} solution and then imaged. Fluorescence images were obtained with a Leica TCS NT or Olympus FV1000D confocal system as described previously (Hull et al., 2004). Images were

processed using Photoshop 6.0 (Adobe Systems Inc., San Jose, CA, USA). Statistical analyses were performed in GraphPad Prism 4.0 (Graphpad Software Inc., San Diego, CA, USA) and calculated using one-way analysis of variance with Tukey's *post hoc* test for multiple comparisons.

CONFOCAL MICROSCOPY-BASED Ca^{2+} IMAGING

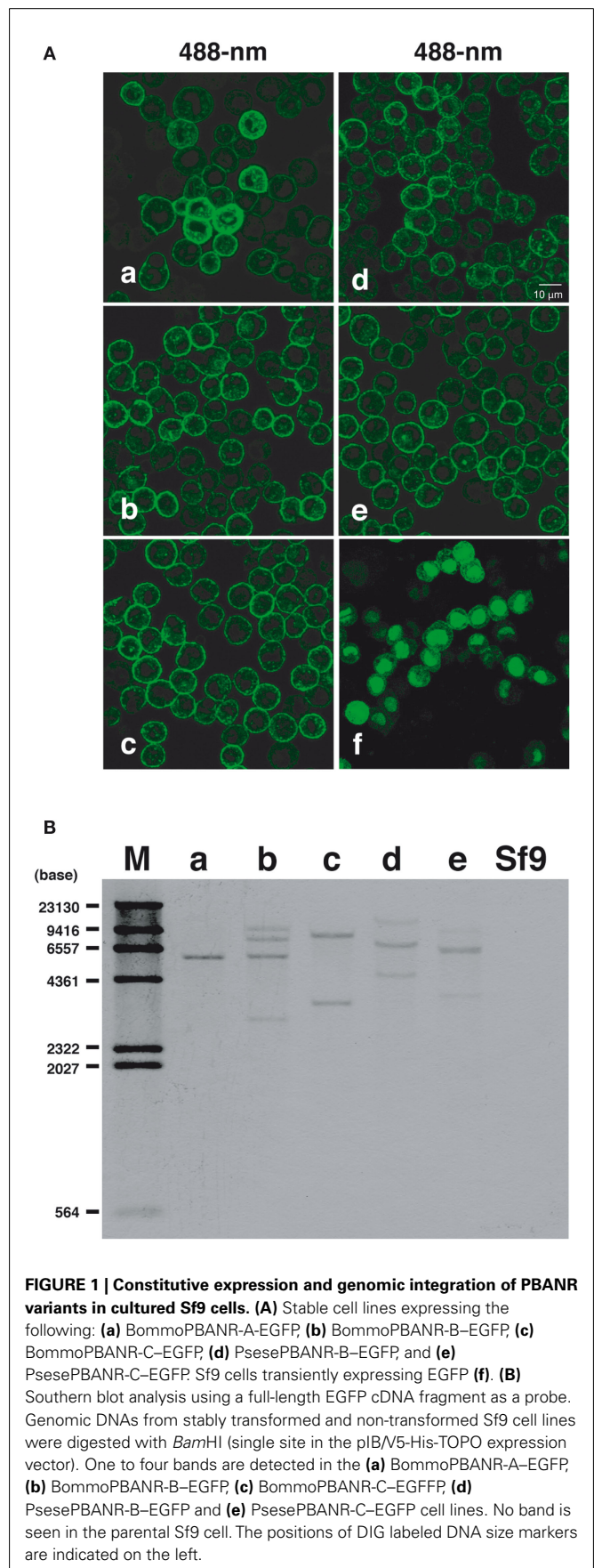
Cell lines constitutively expressing the PBANR variants were harvested and incubated in a 24 well glass bottom plate (AGC, Tokyo, Japan) at 27°C for 2 days with 10% FBS in IPL-41. On the day of the experiment, cells were washed three times with IPL-41 and incubated in 250 μl IPL-41 with 0.75 μl F-127 and 1 mM Fura Red AM (Invitrogen) for 30 min in the dark. After incubation, the cells were washed three times with IPL-41, and 300 μl IPL-41 was added to each well. The plate was left in the dark for 20 min to allow hydrolysis of the Fura Red AM ester bond. EGFP and Fura Red fluorescence were obtained on a FV1000D confocal laser microscope (Olympus, Tokyo, Japan) using 488 and 548 nm laser lines, respectively. To measure receptor activation, fluorescence was monitored for 40 scans (1.08 s/scan) and a 100 μl peptide solution, prepared at concentrations of 1, 10, 100, 1000, and 10000 nM, was added to the well after 10 scans. The Fura Red fluorescence was analyzed using the FV1000D software "Fluoview" (Olympus, Tokyo, Japan).

RESULTS

ESTABLISHMENT OF Sf9 TRANSFORMANTS THAT CONSTITUTIVELY EXPRESS PBANR VARIANTS

We recently demonstrated that multiple PBANR variants (i.e., PBANR-As, -A, -B, and -C) differentiated only by alternative splicing at the 3' end of the PBANR gene are expressed in multiple moth species (Lee et al., 2012). Transient expression assays in Sf9 cells revealed that, unlike the other variants, PBANR-As, which lacks an intact seventh transmembrane domain, failed to localize to the plasma membrane and that PBANR-A failed to undergo ligand-induced internalization. Based on these results, we sought to establish a more advantageous system for characterizing the function and regulation of the PBANR-A, -B, and -C variants by generating transformants of each in Sf9 insect cells.

Cultured Sf9 cells were transfected with plasmid DNAs coding for fluorescent chimeras of the BommoPBANR variants (A, B, and C) and then cultured under selective medium containing blasticidin S (final concentration 80 $\mu\text{g}/\text{ml}$) for 3 weeks. We visually selected 24 colonies for expression of the respective EGFP-fused BommoPBANR variants and separately cultured the colonies for more than 6 months in selective medium to confirm transgene integration. We similarly generated Sf9 cell lines constitutively expressing EGFP-fused PsesePBANR-B and -C. Using this approach, multiple transformed lines for the BommoPBANR variants (four lines for A, six lines for B, and five lines for C) and for the PsesePBANR variants (two lines for B and three lines for C) were generated. There were no noticeable differences in cell morphology and growth time amongst the variant cell lines or compared to the non-transformed parent line. Confocal laser microscopy revealed that both the *B. mori* and *P. separata* derived PBANR variants were predominantly localized to the plasma membrane (Figures 1Aa–e). In contrast, transiently expressed EGFP localized only to the cytosol and nucleus (Figures 1Af). Southern blot analysis using a probe designed to the EGFP coding



sequence confirmed integration of the chimeric transgenes with single to multiple copies present in the genomes of the transformed cell lines but not in the untransformed parental Sf9 cell line (Figure 1B).

FUNCTIONAL CHARACTERIZATION OF STABLY EXPRESSED PBANR-EGFP VARIANTS

We next sought to confirm the functionality of the PBANR variants by assaying for the influx of extracellular Ca^{2+} that occurs in response to PBAN binding, an event that has been well documented in various moth species including *B. mori* (Hull et al.,

2007). Using scanning laser confocal microscopy in conjunction with the fluorescent Ca^{2+} indicator Fluo4-AM, we observed a robust increase (within 2 min) in the intracellular fluorescence of cells expressing BommoPBANR-B-EGFP and BommoPBANR-C-EGFP following the addition of 50 nM of a Rhodamine Red-labeled PBAN derivative (RR-C10PBAN_{R2K}; Figure 2A). This Ca^{2+} -associated intracellular fluorescence persisted for 30 min (Figure 2A). No increase was observed in the absence of extracellular Ca^{2+} . These results are consistent with PBAN triggering an influx of extracellular Ca^{2+} in response to binding and indicate that BommoPBANR-B-EGFP and BommoPBANR-C-EGFP

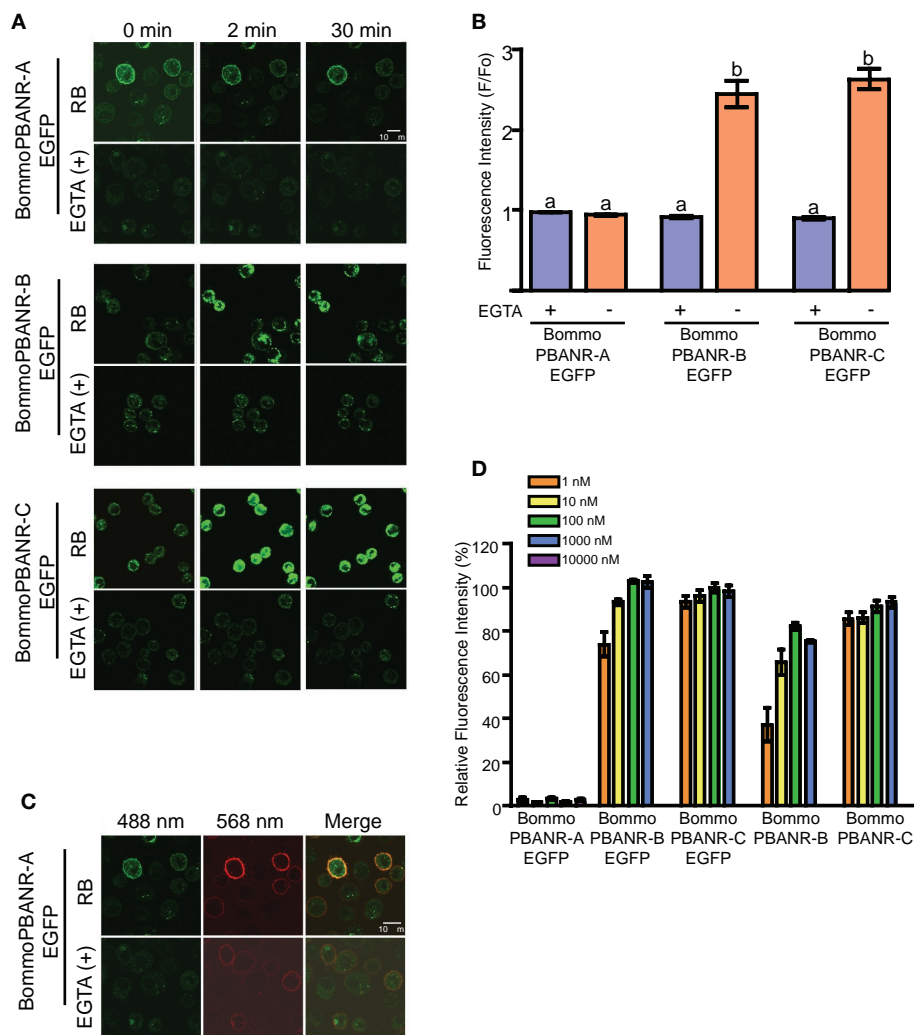


FIGURE 2 | Ligand-induced influx of extracellular Ca^{2+} in stable Sf9 cell lines. (A). RR-C10PBAN_{R2K} (50 nM) induced influx of extracellular Ca^{2+} in Sf9 cell lines stably transformed with BommoPBANR-EGFP fluorescent chimeras. Cells were incubated in insect Ringer's buffer (RB) or Ca^{2+} -free RB buffer supplemented with 3 mM EGTA [EGTA(+)]. Cells were imaged before and after (2 and 30 min) addition of RR-C10PBAN_{R2K} solution. **(B).** The fluorescence intensity profile of BommoPBANR-EGFP Sf9 cell lines calculated as F/F₀ (i.e., fluorescence prior to ligand application and 2 min after ligand application) in response to RR-C10PBAN_{R2K} (50 nM). Bars represent mean values + SEM from independent cells ($n > 8$). **(C).** Confocal imaging

of BommoPBANR-A-EGFP cells incubated with RR-C10PBAN_{R2K} (50 nM) in the presence and absence of extracellular Ca^{2+} . Co-localization is indicated by yellow in the merged images. **(D).** Dose-response profile of BommoPBANR cell lines to increasing concentrations (1 nM–10 μM) of C10PBAN_{R2K}. Fluorescence intensity was measured on a FV1000D confocal laser scanning microscope using Fura Red as the Ca^{2+} indicator. The fluorescence intensity is presented relative to BommoPBANR-C-EGFP activation with 100 nM C10PBAN_{R2K}. Bars represent mean values + SEM of five replicates per peptide concentration. Different letters denote a statistically significant difference for each sample (one-way ANOVA, $p < 0.001$).

are fully functional in our stable cell lines. Surprisingly, despite clear cell surface localization, all four BommoPBANR-A-EGFP cell lines exhibited significantly different Ca^{2+} mobilization kinetics (**Figure 2A**) with no indications of an increase in intracellular Ca^{2+} levels apparent at 2 and 30 min after ligand application. Because no analyses were done at other time points we are unable to rule out the possibilities that: (1) BommoPBANR-A may mediate a more transient Ca^{2+} signal that dissipates before the 2 min or (2) that the BommoPBANR-A Ca^{2+} signal is transient within the time frame between our two assay points. Regardless, it is readily apparent that the BommoPBANR-A cell line exhibits a significantly different Ca^{2+} mobilization profile. Quantitative analyses comparing the levels of fluorescence prior to ligand application and 2 min after ligand application support the results of the imaging experiments (**Figure 2B**). There was no statistical difference in the fluorescence intensity among the three cell lines after 2 min in the presence of the Ca^{2+} chelator EGTA, suggesting that any release of intracellular Ca^{2+} in response to PBAN binding within the first 2 min is below the threshold of detection. In the presence of media replete with Ca^{2+} both the BommoPBANR-B-EGFP and BommoPBANR-C-EGFP cell lines exhibited a dramatic (~ 2.7 -fold) increase in intracellular fluorescence (**Figure 2B**). There, however, was no statistically significant difference between the two lines. As before, there was no PBAN-mediated Ca^{2+} influx in the BommoPBANR-A-EGFP cell line at this time point (**Figure 2B**). This functional difference is not the result of impaired ligand binding as RR-C10PBAN_{R2K} clearly co-localized with BommoPBANR-A-EGFP at the cell surface (**Figure 2C**). To examine the possibility that BommoPBANR-A may be functioning as a low affinity receptor, we measured the relative fluorescence intensities of the respective cell lines (normalized to BommoPBANR-C-EGFP activation with 100 nM C10PBAN_{R2K}) using a different Ca^{2+} indicator, Fura Red, following the addition of varying concentrations (1 nM–10 μM) of C10PBAN_{R2K} (**Figure 2D**). No increase in fluorescence was observed in the BommoPBANR-A-EGFP cell line at the time point assayed even at the 10- μM concentration. The BommoPBANR-B cell lines, both with and without the EGFP tag, exhibited decreased response profiles when challenged with ligand concentrations below 100 nM. In contrast, there was no significant difference in the response profiles amongst the BommoPBANR-C cell lines at any of the concentrations tested, suggesting that the BommoPBANR-C variant is the more responsive variant.

To further examine the utility of the stably transformed lines, we sought to confirm that the pathway underlying PBANR regulation remained functional. We have previously shown that the PBAN-mediated influx of extracellular Ca^{2+} activates a regulatory pathway that promotes endocytosis of PBAN-bound PBANR from the cell surface (Hull et al., 2004, 2005, 2011). Consequently, we used RR-C10PBAN_{R2K} to examine ligand-induced internalization of the fluorescent chimera PBANR variants (**Figure 3**). Consistent with previous results obtained in transient expression assays, we found that all of the expressed PBANR variants specifically bound RR-C10PBAN_{R2K} (**Figures 3Aa–e**), but only the PBANR-B and -C variants underwent RR-C10PBAN-induced internalization, as evidenced by the intracellular accumulation of red fluorescent vesicles that co-localized with the EGFP-derived green fluorescent signals (**Figures 3Bb–e**). RR-C10PBAN_{R2K} binding failed

to induce internalization in cells expressing BommoPBANR-A as the ligand/receptor complex remained at the plasma membrane even 30 min after RR-C10PBAN_{R2K} binding (**Figures 3Ba**). Unexpectedly, we also observed ligand-induced internalization of BommoPBANR-B and BommoPBANR-C in the presence of EGTA (**Figures 3Bg–h**).

FUNCTIONAL CHARACTERIZATION OF STABLY EXPRESSED NON-FLUORESCENT PBANR VARIANTS

To establish Sf9 stable transformants expressing unlabeled (fluorescence-free) PBANR variants, cultured Sf9 cells were transfected with the expression plasmids encoding intact BommoPBANR-B or -C variants and cultured in selective medium containing blasticidin S (final concentration 80 $\mu\text{g}/\text{ml}$) for 3 weeks as described above. To select for the unlabeled BommoPBANR lines, we chose 24 blasticidin-resistant foci and examined ligand-induced PBANR internalization using the RR-C10PBAN_{R2K} fluorescent ligand. This approach allowed us to perform precise selection of unlabeled BommoPBANR lines. As a result, we were able to establish three unlabeled BommoPBANR-B lines and two unlabeled BommoPBANR-C lines. Scanning laser confocal microscopy-based Ca^{2+} influx assays demonstrated that the non-chimeric BommoPBANR-B and BommoPBANR-C lines mobilized extracellular Ca^{2+} in response to RR-C10PBAN_{R2K} stimulation (**Figure 4A**). The cell lines also underwent ligand-induced internalization as evidenced by the accumulation of numerous intracellular red fluorescent red vesicles (**Figure 4B**).

DISCUSSION

Molecular identification of PBANR in moths was initially attained in *H. zea* (Choi et al., 2003) and *B. mori* (Hull et al., 2004). Surprisingly, the respective PBANRs exhibited a striking structural difference at the C-terminus, a 67 amino acid extension in BommoPBANR that is critical for ligand-induced internalization (Hull et al., 2004, 2005). The functional significance of the two receptor subtypes was initially ascribed to differences in signal transduction cascades activated (cAMP dependent/no C-terminal extension vs. cAMP independent/with the C-terminal extension). However, given the significance of GPCR endocytotic trafficking in signal termination, the absence of this domain in HelzePBANR (and many of the other PBANRs identified to date) raises questions regarding receptor regulation. Furthermore, the recent determination that multiple PBANR variants, two of which have C-terminal extensions, are concurrently expressed complicates our understanding of PBANR regulation.

The expression of multiple alternatively spliced PBANR variants (PBANR-As, -A, -B, and -C) appears to be a conserved phenomenon in moths as it has been observed now in six species representing three families (Noctuidae, Sphingidae, and Bombycidae; Lee et al., 2012). Using a transient expression system in cultured insect cells, we initially characterized the functionality of the BommoPBANR variants (Lee et al., 2012). However, while this system provided a rapid means of assessing gene function, we sought a more advantageous system that would offer the opportunity for more complex studies and which could help unravel the current conundrum of PBANR regulation. Consequently, in the current study, our goal was to establish a stable expression

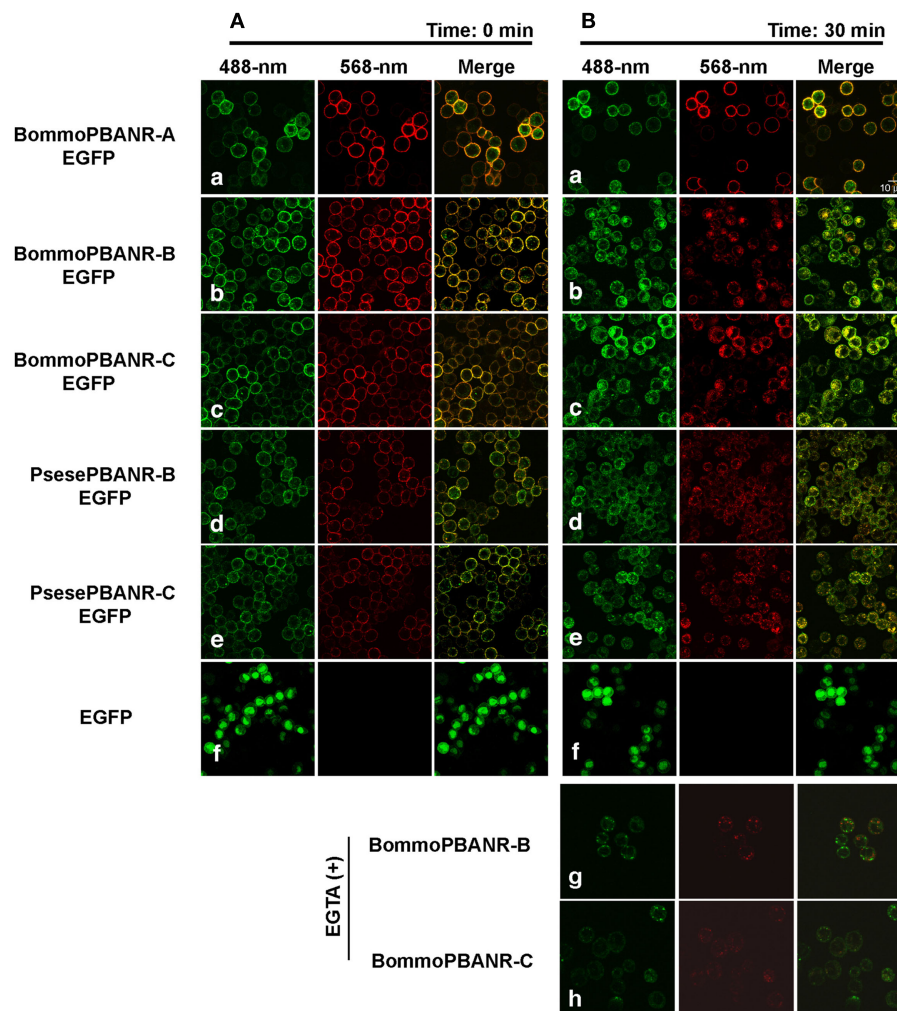


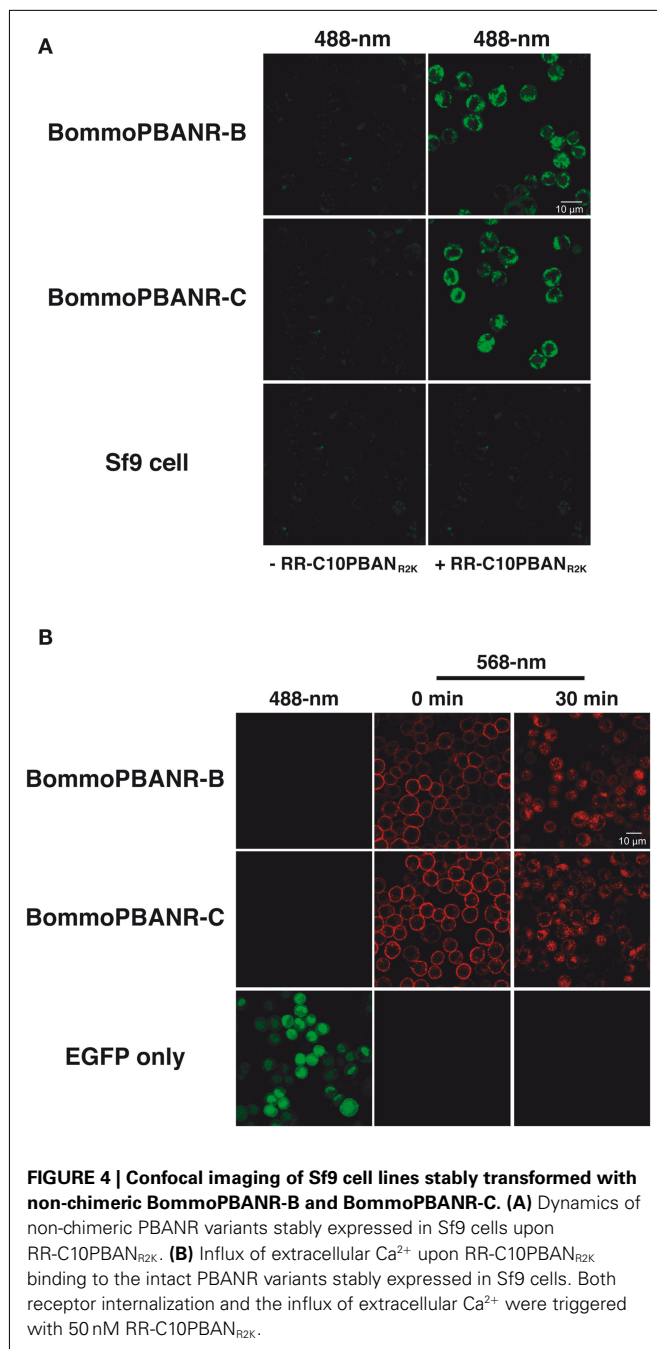
FIGURE 3 | Dynamics of EGFP-tagged PBANR variants stably expressed in Sf9 cells following binding with RR-C10PBAN_{R2K}. (A) Confocal imaging immediately after application of 50 nM RR-C10PBAN_{R2K}. (B) Confocal imaging

30 min after application of 50 nM RR-C10PBAN_{R2K}. For control purposes, Sf9 cells were transfected with an expression plasmid containing EGFP. Co-localization is indicated by yellow in the merged images.

system using insect Sf9 cells to constitutively express three of the *B. mori* PBANR variants and two of the *P. separata* variants. The shortest variant, PBANR-As, which lacks a complete seventh transmembrane domain, was omitted because it fails to localize to the plasma membrane (Lee et al., 2012).

After establishing the respective cell lines, we sought to confirm that the expressed receptors remained capable of mediating the characteristic influx of extracellular Ca^{2+} that occurs in response to PBAN binding. Using the fluorescent Ca^{2+} indicator Fluo4-AM, we observed the robust increase in intracellular fluorescence characteristic of extracellular Ca^{2+} influx in cells expressing BommoPBANR-B or BommoPBANR-C following RR-C10PBAN_{R2K} binding (Figure 2B). Surprisingly, despite clear indications of RR-C10PBAN_{R2K} binding, no increase in fluorescence was observed in cells expressing BommoPBANR-A at the time points assayed (Figures 2A,B). The dramatic difference in extracellular Ca^{2+} mobilization at high concentrations (10 μM) of ligand suggests that the BommoPBANR-A variant most likely does

not function as a low affinity receptor. It is, however, possible that the BommoPBANR-A variant may mediate a more transient Ca^{2+} signal that dissipated prior to our analysis. Because different Ca^{2+} mobilization kinetics were present in all four BommoPBANR-A cell lines, we concluded that the difference is not the result of a deleterious positional effect following gene insertion during generation of the stable lines. These results in conjunction with the finding that the RR-C10PBAN_{R2K}-BommoPBANR-A complex does not undergo endocytotic internalization (Figures 3Ba) suggest that the BommoPBANR-A variant is functionally differentiated from the BommoPBANR-B and -C variants in terms of receptor regulation and activation of downstream effector molecules. Similar differentiation in signaling pathways activated downstream of ligand binding has been reported for the HelviPBANR variants with only the C variant generating a strong Ca^{2+} signal when expressed in mammalian CHO-WTA11 cells (Kim et al., 2008). The presence of multiple receptor variants such as BommoPBANR-A have been hypothesized to represent a means



of fine-tuning responsiveness to extracellular signals with non-responsive receptors potentially functioning to decrease overall cellular sensitivity. Alternatively, the BommoPBANR-A variant may couple to different downstream effector pathways. This latter hypothesis is especially intriguing given the pleiotropic nature of PBAN (Rafaeli, 2009).

Our results have also implicated a role for the BommoPBANR-C-terminus in PBANR signal transduction in addition to signal termination as previously reported (Hull et al., 2004, 2005, 2011). G protein interaction sites have been linked to all three intracellular loops as well as the C-terminal tail of GPCRs (Kristiansen,

2004). The BommoPBANR-A sequence is identical to the B and C variants up to Lys341 (i.e., the cytoplasmic edge of the seventh transmembrane domain) but diverges over its terminal four residues via non-conserved mutations (M342V, T343R, A344N) and C-terminal deletions of 130 and 68 amino acids respectively. Basic residues in the membrane proximal C-terminal tail of the human β 1-adrenergic receptor and rat melanin-concentrating hormone receptor 1 have been implicated in G protein coupling (Tetsuka et al., 2004; Delos Santos et al., 2006). Intriguingly, basic residues (Arg350Arg351) near this region are present in both the BommoPBANR-B and C variants but absent in BommoPBANR-A. What specific role the BommoPBANR-C-terminus plays in mediating G protein coupling remains to be determined; however, it is clear that the absence of this region contributes to the different functionality in BommoPBANR-A. Perpetually, HelzePBANR, which has been shown to mediate PBAN-induced Ca²⁺ influx (Choi et al., 2003), also lacks this region. While the first 16 residues of the severely truncated BommoPBANR-A and HelzePBANR C-terminal tails are identical, the terminal 4–5 residues differ (BommoPBANR-A: VRLN vs. HelzePBANR: FKTTA) with HelzePBANR possessing two threonine residues, the hydroxyl groups of which potentially could function via hydrogen bonds to stabilize G protein coupling. Alternatively, a four residue span in the third intracellular loop (BommoPBANR-A: AHTP vs. HelzePBANR: QMQ) could potentially account for the differences in G protein activation. How these residues affect PBANR-G protein coupling and/or activation, however, remains to be determined. Regardless, our findings strongly suggest that the molecular basis of PBANR activation may be species dependent.

We unexpectedly found that ligand-induced internalization in the BommoPBANR-B and C cell lines proceeded even in the presence of EGTA, which limits the availability of extracellular Ca²⁺. This observation suggests that PBANR internalization may be under the control of intracellular PBAN signaling prior to the influx of extracellular Ca²⁺. While these findings deviate from our previous report regarding the necessity of extracellular Ca²⁺ (Hull et al., 2005), they do not necessarily change our model of the mechanisms underlying PBANR function. We have proposed that PBAN signaling comprises a canonical SOC activation pathway utilizing Gq-mediated PLC activation, followed by a molecular interaction between the SOC-linked proteins STIM and Orai, and a subsequent calcium-signaling pathway associated with an influx of extracellular Ca²⁺ (Matsumoto et al., 2010). A possible explanation for the differing results in the absence of extracellular Ca²⁺ could be related to the levels of the expressed PBANR. Stable cell lines generally have higher expression levels than transient expression systems. It is possible that the efflux of Ca²⁺ from the ER following PLC activation is sufficient to trigger the internalization mechanism via heterologous desensitization, a pathway that has been associated with second messenger dependent kinases (Kristiansen, 2004). Previous studies using pharmacological inhibitors of second messenger kinases, mutation of consensus protein kinase C sites in BommoPBANR-C, and RNA interference-mediated knockdown of Sf9 protein kinase C are consistent with the involvement of the heterologous desensitization pathway (Hull et al., 2005, 2011).

In conclusion, we have established a series of Sf9 cell lines that constitutively express functional BommoPBANR and PsesePBANR variants. Our attempt to utilize these stable transformants for functional evaluation of the PBANR variants confirmed that the cell lines were fully functional and should prove to be viable models for further examining the molecular basis of PBANR activation and regulation. In addition, our current results have further highlighted the functional relevance of both the PBANR-B and PBANR-C variants and raised questions regarding the role of the shorter A variant. It is our expectation that the stable cell lines described will facilitate the development of a more clearly defined

understanding of the molecular mechanisms underlying PBANR regulation and activation. This knowledge can then be used to provide greater insights into the broader physiological roles of PBAN and could potentially serve as the basis for defining key targets for novel agrochemical reagents.

ACKNOWLEDGMENTS

This work was supported by the Lipid Dynamics Research Program from RIKEN and the Targeted Proteins Research Program (TPRP) from the Ministry of Education, Culture, Sports, Science and Technology of Japan.

REFERENCES

- Choi, M. Y., Fuerst, E. J., Rafaei, A., and Jurenka, R. (2003). Identification of a G protein-coupled receptor for pheromone biosynthesis activating neuropeptide from pheromone glands of the moth *Helicoverpa zea*. *Proc. Natl. Acad. Sci. U.S.A.* 100, 9721–9726.
- Delos Santos, N. M., Gardner, L. A., White, S. W., and Bahouth, S. W. (2006). Characterization of the residues in helix 8 of the human β 1-adrenergic receptor that are involved in coupling the receptor to G proteins. *J. Biol. Chem.* 281, 12896–12907.
- Hull, J. J., Kajigaya, R., Imai, K., and Matsumoto, S. (2007). Sex pheromone production in the silkworm, *Bombyx mori*, is mediated by store-operated Ca^{2+} channels. *Biosci. Biotechnol. Biochem.* 71, 1993–2001.
- Hull, J. J., Lee, J. M., and Matsumoto, S. (2011). Identification of specific sites in the third intracellular loop and carboxyl terminus of the *Bombyx mori* pheromone biosynthesis activating neuropeptide receptor crucial for ligand-induced internalization. *Insect Mol. Biol.* 20, 801–811.
- Hull, J. J., Ohnishi, A., and Matsumoto, S. (2005). Regulatory mechanisms underlying pheromone biosynthesis activating neuropeptide (PBAN) induced internalization of the *Bombyx mori* PBAN receptor. *Biochem. Biophys. Res. Commun.* 334, 69–78.
- Hull, J. J., Ohnishi, A., Moto, K., Kawasaki, Y., Kurata, R., Suzuki, M. G., and Matsumoto, S. (2004). Cloning and characterization of the pheromone biosynthesis activating neuropeptide receptor from the Silkworm, *Bombyx mori*: significance of the carboxyl terminus in receptor internalization. *J. Biol. Chem.* 279, 51500–51507.
- Kim, Y. J., Nachman, R. J., Aimanova, K., Gill, S., and Adams, M. E. (2008). The pheromone biosynthesis activating neuropeptide (PBAN) receptor of *Heliothis virescens*: identification, functional expression, and structure-activity relationships of ligand analogs. *Peptides* 29, 268–275.
- Kristiansen, K. (2004). Molecular mechanisms of ligand binding, signaling, and regulation within the superfamily of G-protein-coupled receptors: molecular modeling and mutagenesis approaches to receptor structure and function. *Pharmacol. Ther.* 103, 21–80.
- Lee, J. M., Hull, J. J., Kawai, T., Goto, C., Kurihara, M., Tanokura, M., Nagata, K., Nagasawa, H., and Matsumoto, S. (2012). Re-evaluation of the PBANR receptor (PBANR) molecule: characterization of PBANR variants expressed in the pheromone glands of moths. *Front. Endocrinol.* 3:6. doi:10.3389/fendo.2012.00006
- Matsumoto, S., Ohnishi, A., Lee, J. M., and Hull, J. J. (2010). Unraveling the pheromone biosynthesis activating neuropeptide (PBAN) signal transduction cascade that regulates sex pheromone production in moths. *Vitam. Horm.* 83, 425–445.
- Park, Y., Kim, Y. J., and Adams, M. E. (2002). Identification of G protein-coupled receptors for *Drosophila* PRXamide peptides, CCAP, corazonin, and AKH supports a theory of ligand-receptor coevolution. *Proc. Natl. Acad. Sci. U.S.A.* 99, 11423–11428.
- Rafaei, A. (2009). Pheromone biosynthesis activating neuropeptide (PBAN): regulatory role and mode of action. *Gen. Comp. Endocrinol.* 162, 69–78.
- Raina, A. K., Jaffe, H., Kempe, T. G., Keim, P., Blacher, R. W., Fales, H. M., Riley, C. T., Klun, J. A., Ridgway, R. L., and Hayes, D. K. (1989). Identification of a neuropeptide hormone that regulates sex pheromone production in female moths. *Science* 244, 796–798.
- Smith, G. E., Ju, G., Ericson, B. L., Moschera, J., Lahm, H. W., Chizzonite, R., and Summers, M. D. (1985). Modification and secretion of human interleukin 2 produced in insect cells by a baculovirus expression vector. *Proc. Natl. Acad. Sci. U.S.A.* 82, 8404–8408.
- Tetsuka, M., Saito, Y., Imai, K., Doi, H., and Maruyama, K. (2004). The basic residues in the membrane-proximal C-terminal tail of the rat melanin-concentrating hormone receptor 1 are required for receptor function. *Endocrinology* 145, 3712–3723.

Conflict of Interest Statement: The authors declare that the research was conducted in the absence of any commercial or financial relationships that could be construed as a potential conflict of interest.

Received: 22 December 2011; accepted: 01 April 2012; published online: 18 April 2012.

Citation: Lee JM, Hull JJ, Kawai T, Tsuneizumi K, Kurihara M, Tanokura M, Nagata K, Nagasawa H and Matsumoto S (2012) Establishment of Sf9 transformants constitutively expressing PBAN receptor variants: application to functional evaluation. *Front. Endocrin.* 3:56. doi: 10.3389/fendo.2012.00056

This article was submitted to *Frontiers in Experimental Endocrinology*, a specialty of *Frontiers in Endocrinology*.

Copyright © 2012 Lee, Hull, Kawai, Tsuneizumi, Kurihara, Tanokura, Nagata, Nagasawa and Matsumoto. This is an open-access article distributed under the terms of the Creative Commons Attribution Non Commercial License, which permits non-commercial use, distribution, and reproduction in other forums, provided the original authors and source are credited.



Select neuropeptides and their G-protein coupled receptors in *Caenorhabditis elegans* and *Drosophila melanogaster*

William G. Bendena^{1*}, Jason Campbell¹, Lian Zara¹, Stephen S. Tobe² and Ian D. Chin-Sang¹

¹ Department of Biology, Queen's University, Kingston, ON, Canada

² Cell and Systems Biology, University of Toronto, ON, Canada

Edited by:

Joe Hull, USDA Agricultural Research Service, USA

Reviewed by:

Shinji Nagata, University of Tokyo, Japan

Stephen Garczynski, United States Department of Agriculture, USA

*Correspondence:

William G. Bendena, Department of Biology, Queen's University, Kingston, ON, Canada K7L 3N6.

e-mail: william.bendena@queensu.ca

The G-protein coupled receptor (GPCR) family is comprised of seven transmembrane domain proteins and play important roles in nerve transmission, locomotion, proliferation and development, sensory perception, metabolism, and neuromodulation. GPCR research has been targeted by drug developers as a consequence of the wide variety of critical physiological functions regulated by this protein family. Neuropeptide GPCRs are the least characterized of the GPCR family as genetic systems to characterize their functions have lagged behind GPCR gene discovery. *Drosophila melanogaster* and *Caenorhabditis elegans* are genetic model organisms that have proved useful in characterizing neuropeptide GPCRs. The strength of a genetic approach leads to an appreciation of the behavioral plasticity that can result from subtle alterations in GPCRs or regulatory proteins in the pathways that GPCRs control. Many of these invertebrate neuropeptides, GPCRs, and signaling pathway components serve as models for mammalian counterparts as they have conserved sequences and function. This review provides an overview of the methods to match neuropeptides to their cognate receptor and a state of the art account of neuropeptide GPCRs that have been characterized in *D. melanogaster* and *C. elegans* and the behaviors that have been uncovered through genetic manipulation.

Keywords: invertebrate neuropeptides, G-protein coupled receptor, insects, nematodes, *Caenorhabditis elegans*, *Drosophila melanogaster*

INTRODUCTION

Animals respond to environmental cues through alteration of neural circuits that modify behavior and metabolism. The mechanism underlying the regulation of the neural circuit in response to a simple sensory cue is extremely complex and difficult to disentangle in mammals. The nematode *Caenorhabditis elegans* offers an excellent model organism to analyze neural circuit function. *C. elegans* is 1.3 mm in length and has several desirable features. The hermaphrodite has 959 somatic cells that form different organs and tissues including muscle, hypodermis, intestine, reproductive organs and glands, and the nervous system. The nervous system comprises 302 neurons whose identity and connections have been defined by morphology and ablation studies. *C. elegans* is also transparent such that *in vivo* fluorescent proteins and dyes can be used to visualize gene expression and fat metabolism in the living animal. The advantage over other systems is that alterations within a functional neuron can be studied in the context of the whole organism and rather than measuring changes in fluorescence, the actual behavioral response of the animal can be monitored directly. *Drosophila melanogaster* is more complex in terms of physical organization and behaviors. Some 90,000 neurons of the brain reflect a similar level of complexity as the different neural cell types in humans (Venken et al., 2011). *D. melanogaster*, like *C. elegans*, has a variety of genetic tools that allow for forward (mutagenic screens) and reverse (targeted

gene disruption) genetics. The *Drosophila* UAS-Gal4 system (and derivatives thereof) enable the use of specific promoters to target reporter genes, structural genes (for overexpression), or expression of ds RNA for selected gene inhibition (RNAi) to specific larval or adult tissues (Seroude, 2002). *D. melanogaster* and *C. elegans* have recently emerged as excellent paradigms for identifying the cellular mechanisms underlying human disease. Disease models are possible if the disease can be explained in molecular terms. Both of these non-mammalian genetic models have a strong record of uncovering disease-related genes that have orthologs in the human genome. These include the uncovering of genes involved in Alzheimer's disease (Sundaram and Greenwald, 1993; De Strooper et al., 1999; Chakraborty et al., 2011), Parkinson's (Feany and Bender, 2000), diabetes type II (Nakae et al., 2002), polyglutamine and other triplet repeat expansion diseases (Campesan et al., 2011), depression (Ranganathan et al., 2001; Pandey and Nichols, 2011), epilepsy, and schizophrenia (O'Kane, 2011).

Drosophila melanogaster and *C. elegans* produce and store most classical small molecule neurotransmitters in synaptic vesicles that cluster for release at pre-synaptic sites. These include acetylcholine, γ -aminobutyric acid (GABA), the biogenic amines octopamine, tyramine, dopamine, and serotonin (5-hydroxytryptamine) and glutamate (Bargmann, 2006) function in conjunction with neuropeptides that are produced as precursor proteins that are packed with processing enzymes and stored in large dense core vesicles

in the trans-Golgi network. Release of neuropeptide-containing dense core vesicles is not restricted to nerve terminals and can occur at both axons and dendrites. In *C. elegans*, 113 neuropeptide genes have been identified that potentially produce 250 neuropeptides. These are classified into three groups: the insulin-like peptides (40 *ins* genes), the FMRFamide-related/like peptides (31 *FaRP* or *flp* genes), and the neuropeptide-like peptides (42 *nlp* genes; Nathoo et al., 2001). Two recent reviews summarize the synthesis, processing, and function of *C. elegans* neuropeptides (Husson et al., 2007; Li and Kim, 2008). In *D. melanogaster*, 119 neuropeptide genes have been predicted with 46 neuropeptide families characterized biochemically from 19 precursors (Clynen et al., 2010). In *C. elegans*, there are over 1100 G-protein coupled receptors (GPCRs) with approximately 100 thought to be specific for neuropeptides (Bargmann, 1998). *D. melanogaster* has approximately 160 GPCRs (far less than *C. elegans* with 44 exhibiting characteristics consistent with peptide ligand receptors (Hewes and Taghert, 2001). In both organisms, very few GPCRs have been matched with their respective neuropeptides and much less is known as to how each neuropeptide GPCR functions in neurotransmission or behavior. GPCRs can be separated structurally into several classes or subfamilies. The largest of these are the rhodopsin-like which are activated by small ligands and peptides. The secretin class of GPCRs have large extracellular domains that selectively bind glycoproteins. The metabotropic glutamate/pheromone GPCRs have domains that share sequence similarity with periplasmic binding proteins of bacteria involved in the transport of ions, amino acids, sugars, and peptides. The adhesion and frizzled class of GPCRs also have unique N-terminal binding domains with unique binding properties (Fredriksson et al., 2003; Krishnan et al., 2012). Given the diversity of GPCR types and varied functions this review focuses on some of the genetic and molecular techniques that have been used to specifically de-orphan neuropeptide GPCRs in *C. elegans* and *D. melanogaster* and decipher their role in regulating behavior and physiology.

MATCHING NEUROPEPTIDES TO ORPHAN RECEPTORS

METHODOLOGY

Only a limited number of reverse pharmacological approaches have been applied to match a peptide ligand to its receptor (i.e., de-orphanization) in *D. melanogaster* and *C. elegans*. All approaches are based on expression of the GPCR in a membrane system that will complete a signaling pathway that can be assayed. One of the more common assays used to de-orphan GPCRs is the GTP γ S assay (Larsen et al., 2001). The GTP γ S assay is one of the most sensitive assays for screening GPCRs and is widely used to characterize full and partial agonists and antagonists. In this assay, the GPCR of interest is expressed in mammalian cells such as Chinese hamster ovary (CHO) or human embryonic kidney (HEK293) cells. The plasma membrane replete with the recombinant GPCR of interest is purified and incubated with GDP and a potential neuropeptide ligand. A radiolabeled non-hydrolyzable GTP analog [³⁵S] GTP γ S, is then added. The premise of the assay is that if the neuropeptide has activated the receptor, the G-protein α -subunit exchanges GDP for GTP or in this case [³⁵S]GTP γ S which accumulates in the membrane and is easily measured. A second type of assay monitors cAMP levels. In this case, a receptor expressed in mammalian cells

can be activated by adding a neuropeptide to the culture media. Upon activation, if exchange of GDP to GTP occurs using a $G\alpha_s$ subunit, adenylate cyclase activity will be stimulated, converting ATP to cAMP. Conversely, if the GDP to GTP exchange occurs using a $G\alpha_i$ subunit, adenylate cyclase is inhibited, and cAMP levels decline. In practice, a reporter construct that provides a promoter with multiple cAMP response elements controlling expression of the gene luciferase is co-transfected into cells with the receptor. Enhanced expression of luciferase occurs when cAMP increases. Luciferase catalyzes the oxidation of the firefly specific substrate, D-luciferin, to produce light which can be directly measured. If signaling occurs through $G\alpha_i$, which depresses cAMP levels, cells can be treated with forskolin (which activates adenylate cyclase) prior to neuropeptide application. In this case, cAMP levels can be measured in cell extracts by incubation with a biotinylated-anti-cAMP antibody and an anti-cAMP antibody coupled to an acceptor bead. Streptavidin-coupled to a donor bead is then added to complex with biotin. Excitation of the donor bead with a laser (680 nm) produces singlet oxygen which can travel up to 200 nm and excite the cAMP – antibody bound acceptor bead in the complex. The acceptor bead then emits light which can be directly measured. Intracellular Ca^{2+} can also be used as a measure of GPCRs that couple through G_q . G_q activates phospholipase C β which generates inositol triphosphate and diacylglycerol. Inositol triphosphate activates release of intracellular Ca^{2+} stores from the endoplasmic reticulum. Ca^{2+} can be measured by Ca^{2+} sensitive indicators such as Fluo-4. Alternatively, cells can be co-transfected with a gene that expresses apoaequorin. In the presence of the cofactor coelenterazine, a complex is formed that generates light proportional to the quantity of Ca^{2+} . The relative simplicity of these assays has resulted in their widespread use in matching neuropeptides to their GPCRs, although the expression of *C. elegans* GPCRs in mammalian cells has encountered a number of pitfalls. For example, stable cell lines expressing some GPCRs cannot be generated because of toxicity problems. In addition, some GPCRs appear to be active only if cultured cells are incubated at 28°C rather than the normal 37°C (Harada et al., 1987; Geary et al., 1999; Kubiak et al., 2003a,b).

Drosophila melanogaster GPCRs have also been de-orphaned using a β -arrestin2-green fluorescent protein (GFP) translocation assay (Johnson et al., 2003). In this assay, following ligand-GPCR interaction in mammalian cells, β -arrestin2-GFP translocates from the cytoplasm to the cell membrane or receptor-bearing endosomes as part of termination of signaling (Barak et al., 1997).

G-protein coupled receptors of both *C. elegans* and *D. melanogaster* have also been expressed in *Xenopus laevis* oocytes along with a G-protein-gated inward rectifying potassium channel (GIRK; Harada et al., 1987). Gating results from release of the $G\beta\gamma$ subunits, which, upon receptor activation, then interact with GIRK. Measurement is through whole cell voltage-clamp recordings.

Caenorhabditis elegans GPCRs have been expressed in the pharynx of *C. elegans* by creating a transgenic animal with a GPCR construct that is under the control of a heat shock promoter. Action potentials are measured by placing a microelectrode into an exposed terminal pharyngeal bulb. For *C. elegans* neuropeptide receptor-1 (NPR-1), this method gave slightly different results than

the *Xenopus* assay when the receptor was tested with several peptides (see below). Human somatostatin receptor and chemokine receptor 5 (CCR5) have been expressed in *C. elegans* nociceptive neurons ASH and ADL by transformation of the genes under the control of the *gpa-11* promoter. Transgenic animals showed an avoidance response to the cognate peptide placed between the worms and an attractant (Teng et al., 2006). This study has been extended to show that animals expressing CCR5 in nociceptive neurons will avoid *Escherichia coli* that expressed the natural ligand and MIP-1 α (Teng et al., 2008). As a cautionary note, this approach may only be applicable to non-modified peptides such as MIP-1 α because *E. coli* does not have the enzymes necessary for some modifications, such as C-terminal amidation that some neuropeptides require for activity.

Despite the techniques outlined above, only a very small number of *C. elegans* and *D. melanogaster* receptors have been matched to their cognate ligand. At present, most families of known neuropeptides have been matched to receptors in *D. melanogaster* (Hewes and Taghert, 2001; Johnson et al., 2003; Clynen et al., 2010). The de-orphaning of *C. elegans* neuropeptide receptors has not been as rapid as in *D. melanogaster*. However, some of the *C. elegans* receptors that have been studied have provided better insights into components of the signal transduction pathways. Both model organisms though have advantages in that transgenic animals can be generated that overproduce neuropeptides or GPCRs and the availability of mutants that give rise to specific phenotypes that result from the suppression of neuropeptide and/or GPCR-linked functions.

COMPARING FUNCTION OF STRUCTURALLY CONSERVED PEPTIDES AND RECEPTORS IDENTIFIED IN *DROSOPHILA* AND *CAENORHABDITIS*

Insect systems have proven invaluable in revealing primary peptide structures that define many neuropeptide families and for developing *in vitro* physiological assays that provide clues to *in vivo* functions. The signal transduction pathways for most neuropeptides though are only vaguely understood beyond their interaction with their cognate receptor. Genetic systems such as *D. melanogaster* and *C. elegans* are now extending our understanding of the steps between neuropeptide release to final physiological action. Many of these peptide-GPCR interactions lead to conserved functions. For example, allatostatin-like peptides appear to influence foraging behavior in *D. melanogaster* and *C. elegans*. These systems have also been instrumental in uncovering additional neuropeptide and neuropeptide GPCR functions.

NEUROPEPTIDE F, NPY/NPF PEPTIDES, AND RECEPTORS

In vertebrates, a 36 amino acid neuropeptide Y (NPY) functions as a neuromodulator to stimulate feeding behavior (Clark et al., 1984; Kalra, 1997). Roles of vertebrate NPY include suppression of responsiveness to adverse stimuli and in promotion of food search and acquisition under adverse conditions (Thorsell and Heilig, 2002). Destruction of NPY-expressing neurons in mice results in starvation of the animals (Pedrazzini, 2004). NPY is thought to work through a specific NPY receptor, to repress the activity of inhibitory neural circuits that then promotes feeding behavior (Klapstein and Colmers, 1993; Browning and Travagli, 2003).

In invertebrates, neuropeptide F is an ortholog of vertebrate NPY but differs in a C-terminal phenylalanine rather than tyrosine (Brown et al., 1999). *Drosophila* NPF (DromeNPF) is expressed in the brain and midgut of larvae and adults (Brown et al., 1999). A single receptor, Drome NPF receptor (DromeNPFR) has been identified through expression of the receptor in mammalian cells and binding assays (Garczynski et al., 2002; **Table 1**). In common with vertebrate NPY, DromeNPF, and its receptor have been associated with the control of social and feeding behaviors. DromeNPF levels are high in larvae, when they remain attracted to food, then fall to lower levels in subsequent developmental stages in which feeding is reduced. Overexpression of the DromeNPFR at later developmental stages encourages feeding behaviors that differ from wild type, whereas underexpression of DromeNPFR leads to a food aversion response in earlier larvae that would normally feed (Wu et al., 2003). Food-associated memory is promoted by starvation and inhibited by satiety in *Drosophila*. Stimulation of neurons that express DromeNPF mimics food deprivation and promotes memory performance in satiated flies. This memory performance requires the expression of the DromeNPFR in six dopaminergic neurons whereas blocking these neurons releases memory performance in satiated flies and suppresses memory performance in hungry flies. This suggests that dopamine and DromeNPF act together to coordinate memory performance, based on nutritional status (Krashes et al., 2009). DromeNPF also functions in fly-aversive responses to a variety of stressors. NPF appears to act antagonistically to insulin signaling systems in regulating aversive responses (Wu et al., 2005). In aversion responses, DromeNPF suppresses PAIN neurons through attenuation of transient receptor potential (TRP) channel-induced neuronal excitation (Xu et al., 2010). iDromeNPF signaling has been implicated in a wide range of behaviors and has recently been shown to have a modulatory effect on fly aggression. Drug-induced increases of 5-hydroxytryptamine (serotonin) amplify aggression amongst flies, whereas silencing of the serotonergic circuits leads to a lack of response following application of exogenous serotonin; however, the aggression response still exists. Silencing of the DromeNPF circuit leads to an increase in fly aggression, showing that serotonin and DromeNPF signaling systems act together to regulate fly aggression (Dierick and Greenspan, 2007). The DromeNPF signaling pathways also modulate acute ethanol sensitivity (Wen et al., 2005) and appear to have a male-specific function in courtship behavior. DromeNPF also has a possible role in circadian rhythms (Lee et al., 2006) and is potentially involved in the control of evening activity (Hermann et al., 2012). The signaling pathways regulating these later phenotypes are still poorly understood.

The *C. elegans* GPCR (C39E.6.6 = Cael *npr-1*) shares homology with the vertebrate NPY receptor family. Cael *npr-1* is expressed in at least 20 neurons. Two natural alleles of NPR-1 that differ by a single amino acid at position 215, which likely affects G-protein signaling show two behavioral phenotypes termed “solitary” versus “social.” Animals, typified by the N2 Bristol strain used in most labs as a wild type strain, express Cael *npr-1* with valine at position 215 (Cael *npr-1* 215V). This Cael *npr-1* allele results in animals with reduced locomotory activity on a bacterial lawn and they disperse over the lawn as solitary individuals. Animals such as the Hawaiian isolate CB4856, express Cael *npr-1* with

Table 1 | Receptor-ligand interaction affinities as measured in heterologous expression systems.

Receptor gene	Peptide ligand	Peptide sequence	EC ₅₀	Reference
<i>C. elegans</i>				
Caeel C39E6.6 (NPR-1)	FLP-21	GLGPRPLRFa	215V 2.2–77 nM, 215F 59–370 nM	Kubiak et al. (2003b)
**	FLP-21	GLGPRPLRFa	215V –108, 215F –104	Rogers et al. (2003)
**	FLP-18-1	DFDGAMPGVLRFa	215V –9.3, 215F 0	
**	FLP-18-2	EMPGVLRFa	215V –32, 215F 0	
**	FLP-18-3	SVPGVLRFa	215V –9.7, 215F 0	
**	FLP-18-4	EIPGVLRFa	215V –8, 215F 0	
**	FLP-18-5	SEVPGVLRFa	215V –6.8, 215F 0	
**	FLP-18-6	DVPGVLRFa	215V –9.7, 215F 0	
Caeel <i>npr-2</i> T05A1.1	Unknown			
Caeel <i>npr-3</i> C10C6.2	FLP-15-1	GGPQGPLRFa	162.4 nM	Kubiak et al. (2003a)
	FLP-15-2	RGPSGPLRFa	250.6 nM	
Caeel Y58G8A.4 (<i>npr-5</i>)	FLP-18-6	DVPGVLRFa	a: 32.3 nM; b: 45.9 nM	Rogers et al. (2003)
Splice variants a and b	FLP-18-3	(K) SVPGVLRFa	a: 28.3 nM, b: 48.3 nM	
	FLP-18-3	SVPGVLRFa	a: 14.4 nM, b: 43.3 nM	
	Truncated			
	FLP-18-5	SEVPGVLRFa	a: 25.9 nM, b: 58.4 nM	
	FLP-18-4	EIPGVLRFa	a:117.2 nM, b: 124 nM	
Caeel C26F1.6	FLP-7-2	TPMQRSSMVRFa	1.02 ± 0.24 μM	Mertens et al. (2005b)
	FLP-7 Truncated	SMVRFa	0.096 ± 0.016 μM	
	FLP-11-1	AMRNALVRFa	1.34 ± 0.41 μM	
	FLP-7-1	SPMQRSSMVRFa	Inactive	
	FLP-7-3	SPMDRKMVRFa	Inactive	
	FLP-7-4	SPMERSAMVRFa	Inactive	
Caeel Y59H11AL.1	FLP-7-3	SPMERSAMVRFa	<0.7 [28°C]–1.1 [37°C] μM	Mertens et al. (2006)
	FLP-7-2	TPMQRSSMVRFa	2.5 μM	
	FLP-7-1	SPMQRSSMVRFa	5.0 μM	
	FLP-7-4	SPMDRSKMVRFa	5.0 μM	
	FLP-1-8	KPNFMRYa	0.1 μM	
	FLP-9	KPSFVRFa	5.0 μM	
	FLP-11-1	AMRNALVRFa	0.75 μM	
	FLP-11-2	ASGGMRNALVRFa	2.5 μM	
	FLP-11-3	NGAPQPFVRFa	1.0 μM	
Caeel T19F4.1	FLP-2-1	SPREPIRFa	53.1 ± 7.7 nM	Mertens et al. (2005a)
	FLP-2-2	LRGEPIRFa ²	54.4 ± 6.2 nM	
Caeel C46F4.1 (<i>egl-6</i>)	FLP-10	QPKARSGYIRFa	11 nM	Ringstad and Horvitz (2008)
	FLP-17-1	KSAFVRFa	28 nM	
	FLP-17-2	KSQYIRFa	1 nM	
Caeel C13B9.4 (<i>pdf-1</i>)	PDF-1a	SNAELINGLIGMDLGKLSAVa	127.4 nM	Janssen et al. (2008b)
	PDF-1b	SNAELINGLLSMNLNKLSGAa	360 nM	
	PDF-2 NLP-37	NNAEVVNHILKNFGALDRLGDVa	33.8 nM	
Caeel;Y39A3B.5 (<i>ckr-2</i>)	NLP-12A	DYRPLQFa	56.7 nM	Janssen et al. (2008a)
	NLP-12B	DGYRPLQFa	14.7 nM	
<i>D. melanogaster</i>				
Drome NPFR CG1147	DromeNPF	SNSRPPRKNDVNTMADAYKFL	65 nM*	Garczynski et al. (2002)
	CG10342	QDLDTYYGDRARVRFa		
Drome sNPFR =	Drome sNPF	AQRSPSLRLRFa	5.1 × 10 ^{−8}	Mertens et al. (2002)
NPFR76F CG7395	CG13968	SPSLRLRFa	4.2 × 10 ^{−8}	
		PQRLRWa	3.1 × 10 ^{−8}	
		PMRLRWa	7.5 × 10 ^{−8}	

(Continued)

Table 1 | Continued

Receptor gene	Peptide ligand	Peptide sequence	EC ₅₀	Reference
DromeFR CG2114	Drome FMRF-1	DPKQDFMRFa	2.0 nM	Meeusen et al. (2002)
	Drome FMRF-2	TPAEDFMRFa	2.8 nM	
	Drome FMRF-3	SDNFMRFa	1.9 nM	
	Drome FMRF-4	SPKQDFMRFa	2.5 nM	
	Drome FMRF-5	PDNFMRFa	1.8 nM	
	<i>N. bullata</i>	APPQPSDNFIRFa	3.5 nM	
	<i>N. bullata</i>	pQPSQDFMRFa	2.0 nM	
Drome CG13229	Unknown			
Drome PDFR CG1758	Drome PDF	NSELINSLSLPKNMNDaa	25 nM	Mertens et al. (2005c)
	CG6492			
	Drome DH ₃₁	TVDFGLARGYSGTQAEKHRMG LAAANFAGGPa	218.6 nM	
Drome CCKLR	Drome DSK	FDDY(SO(3)H)GHLRFa	5.3 nM	Kubiak et al. (2002)

*Determined through a competition assay which displaced radioactive peptide from the receptor.

**Values represent alteration of current in response to neuropeptide application in the *Xenopus* assay.

phenylalanine at position 215 (Caeel *npr-1* 215F). Caeel *npr-1* 215F animals display a “bordering” phenotype as they move rapidly on bacterial food to areas where the food is thickest, and burrow. These animals also show social behavior by interacting with each other to form clumps that can contain hundreds of animals (de Bono and Bargmann, 1998). Caeel NPR-1 acts as an inhibitor of social behavior as Caeel *npr-1* loss-of-function (*lf*) mutants display social behavior. This results in part from Caeel *npr-1* (*lf*) exhibiting enhanced attraction to low levels of the ascaroside pheromone (Macosko et al., 2009). The Caeel *npr-1* 215 Valine (V) allele is dominant to the Caeel *npr-1* 215 Phenylalanine (F) allele so that heterozygotes will display solitary behavior. Genetics and targeted expression studies have suggested that NPR-1 acts through neurons AQR, PQR, and URX that are exposed to body fluids (Coates and de Bono, 2002) to suppress aggregation and bordering by inhibiting the expression/activity of two α/β soluble guanylate cyclases GCY-35 and GCY-36 that are required to activate a cGMP-gated ion channel (TAX-2/TAX-4) encoded by the *tax-2* and *tax-4* genes (Cheung et al., 2004; Gray et al., 2005). Social animals may display aggregation and bordering activity as a means of avoiding high O₂ levels (hyperoxia) on food. In solitary Caeel NPR-1 215V animals, food suppresses avoidance of hyperoxia by signaling through Caeel NPR-1 via GCY-35/GCY-36 and the TGF- β homolog DAF-7 (Cheung et al., 2005; Chang et al., 2006). On food, Caeel NPR-1 215V also promotes avoidance of high levels of CO₂ whereas the Caeel NPR-1 215F-bearing animal only exhibits a weak avoidance to CO₂. Indeed, an increase in CO₂ leads to a burst of turning in wild type (N2) worms; however, the Caeel *npr-1* 215F strain does not respond. Up or downshifting of O₂ has a dramatic effect on turning in Caeel *npr-1* 215F. The activity of Caeel NPR-1 may thus serve to integrate inputs from O₂- and CO₂-sensing pathways and generate an appropriate response with respect to availability of food (Bretscher et al., 2008; Chang and Bargmann, 2008; Hallem and Sternberg, 2008). The O₂ and CO₂-sensing pathways may control which peptides become involved in regulating Caeel NPR-1. A globin-like gene (*glb-5*) appears to

cooperate with Caeel *npr-1* to mediate responses to O₂ and CO₂ concentrations. Expression of the globin-like gene (*glb-5*) in animals with a *lf* allele of Caeel *npr-1* showed suppressed aggregation behavior (McGrath et al., 2009).

Caeel NPR-1 has recently been shown to play a role in innate immunity, with Caeel *npr-1* (*lf*) animals showing an increased susceptibility to infection by the bacteria *Pseudomonas aeruginosa*. A similar initial signaling pathway may be used since one of the soluble guanylate cyclases (GCY-35) expressed in AQR, PQR, and URX neurons, and the cGMP-gated ion channel TAX-2/TAX-4 are required (Styer et al., 2008). Caeel *npr-1* has been implicated in hyperoxia avoidance in the presence of an exopolysaccharide matrix characteristic of mucoid bacteria. OSM-9 is part of the TRP Vanilloid (TRPV)-like ion channel that is within the ASH and ADL nociceptive neurons (Kapfhammer et al., 2008). The TRPV-like channel mutant (*osm-9*) mutant exhibited mucoid bacterial avoidance as a consequence of the lack of induction of the Caeel NPR-1 pathway. Worms that lack the TRPV-like channel and guanylate cyclase (*gcy-35*) showed restored Caeel NPR-1-dependent oxygen sensitivity and absence of pathogen avoidance exhibited by TRPV (*osm-9*) mutant (Reddy et al., 2011).

The TRPV-like channel appears to work with Caeel NPR-1 in several instances of behavioral adaptation/acute tolerance. For example, following exposure of wild type *C. elegans* to ethanol, intoxication can occur which is assayed by hyperexcitation followed by inhibition of locomotor activity and egg laying. Decreased intoxication as a result of acute tolerance is observed in Caeel NPR-1 215F animals which show a dramatic recovery to ethanol exposure relative to Caeel NPR-1 215V animals. Ethanol-induced clumping of animals was suppressed by the loss of the cGMP-gated ion channel (*tax-4*) and the TRPV-like channel (*osm-9*; de Bono et al., 2002). Caeel *npr-1* expression in RMG interneurons acts synergistically with TRPV-like channel (*osm-9*) in parallel pathways to regulate aversive behaviors at high temperature with *npr-1* (*lf*) animals show an increased threshold for heat avoidance (Glauser et al., 2011).

The initial study to de-orphan Cael NPR-1 used expression of Cael *npr-1* in a mammalian (CHO) cell line screened with 200 synthetic invertebrate peptide sequences. A single *Ascaris suum* neuropeptide AF9 (Cowden and Stretton, 1995) was identified as an activating ligand. AF9 is a FMRFamide-related peptide (FaRP) unrelated in sequence to NPY. This peptide sequence has been found in the *C. elegans* genome and is known as FMRFamide-like peptide-21 (FLP-21; Kubiak et al., 2003b). FLP-21 activation of Cael NPR-1 results in inhibitory signaling through Gi/Go proteins and inhibition of cAMP production. In GTPγS binding assays, FLP-21 displayed higher activity with Cael NPR-1 215V in comparison to Cael NPR-1 215F (Kubiak et al., 2003b; **Table 1**). Higher FLP-21 activation of Cael NPR-1 215V was also noted when the receptor was expressed in *Xenopus* oocytes and assayed for GIRK channel activation (Rogers et al., 2003; **Table 1**). This is consistent with the observation that social behavior is repressed in Cael NPR-1 215V. In the *Xenopus* assay, in addition to FLP-21, six unique FaRPs encoded by *flp-18* were found to activate Cael NPR-1 215V but not Cael NPR-1 215F (**Table 1**). Using a different assay system in which Cael NPR-1 isoforms were expressed in the *C. elegans* pharynx, both isoforms were activated by the sole FLP-21 peptide and all FLP-18 peptides and signaling may occur through Gα_q (Rogers et al., 2003). The expression patterns of *flp-18* and *flp-21* have limited overlap. *flp-18* is expressed in neurons AVA, AIY, and RIG, motor neurons RIM and pharyngeal neurons M2 and M3. *flp-21* is expressed in sensory neurons ADL, ASE, and ASH, motor neuron MRA and pharyngeal neurons MC. M2 and M4. Deletion of *flp-21* has a limited effect on increasing aggregation and bordering in Cael *npr-1* 215V animals but does enhance aggregation in Cael *npr-1* 215F animals (Rogers et al., 2003). This supports a role for FLP-18 peptides acting in conjunction with FLP-21 to regulate behavior. However, this is not always the case as FLP-21 does not appear to act in acute ethanol tolerance, suggesting that FLP-18 may be the active ligand. FLP-21 may act solely with Cael NPR-1 in adaptation to heat avoidance (Glauser et al., 2011).

C53C7.1 is another *C. elegans* receptor related to the *Drosophila* neuropeptide F-like receptor. Two isoforms of C53C7.1 are generated by alternative splicing. A single patent report identifies a different FMRFamide-like peptide encoded by the *flp-3* gene as the ligand for C53C7 (Lowery et al., 2003).

SHORT NPF AND sNPF RECEPTORS

The *D. melanogaster* gene for short NPF (sNPF) encodes a precursor polypeptide that, upon processing, would release two C-terminal RLRFamides (sNPF-1, sNPF-2) and two RLRWamides (sNPF3, sNPF4; Hewes and Taghert, 2001; Vanden Broeck, 2001). Several thousand neurons in the CNS of *D. melanogaster* express sNPFs suggesting an array of potential functions for these neuropeptides (Nassel et al., 2008). A single neuropeptide GPCR (NPRF76F, CG7395, sNPRF1) is activated by all four sNPFs (Mertens et al., 2002; **Table 1**). Many sNPF-expressing neurons also co-express classic neurotransmitters suggesting that sNPF could act as a co-transmitter or neuromodulator (Nassel et al., 2008). sNPFs are also produced in the hypocerebral ganglion and in the anterior and middle midgut of *D. melanogaster* although the function of sNPF at these sites is unknown (Veenstra et al.,

2008). In *D. melanogaster*, sNPF and sNPF1 regulate body growth and metabolism by activating extracellular signal-related kinases (ERK) that mediate insulin-like peptide signaling (Lee et al., 2004). This response appears to show evolutionary conservation as mammalian NPY also mediates growth, metabolism, and lifespan through ERK-mediated insulin signaling. Olfactory receptor neurons also express sNPF (Carlsson et al., 2010) and this expression is responsible for starvation-dependent enhancement of food searching behavior. Starvation results in an insulin signal that functions via the phosphoinositide 3-kinase pathway to upregulate sNPF1 expression in odorant receptor neurons which in turn sensitizes select sensory neurons to promote food search behavior (Root et al., 2011).

In *C. elegans*, the sequence of NPR-2 (T05A1.1) shares 26% amino acid sequence identity with the *D. melanogaster* sNPF1. Three isoforms of NPR-2, one of 430 aa and two of 387 aa that differ at their amino-terminus, could potentially be generated by alternative splicing. RNAi experiments have demonstrated that knockdown of NPR-2 expression leads to a reduction in locomotion (Keating et al., 2003). Reduction in NPR-2 expression is also associated with an increase in accumulation of intestinal lipid (Cohen et al., 2009). The endogenous ligand is unknown. FLP-18 and FLP-21 were tested in the *Xenopus* oocyte assay and were unable to activate NPR-2 (Cohen et al., 2009).

Caenorhabditis elegans npr-3 (C10C6.2) is currently thought to specify only one GPCR of 376 aa that is expressed in the nerve cord and in excitatory and inhibitory motoneurons in the region of the nerve cord. The NPR-3 sequence, like NPR-2 is most related to the *D. melanogaster* sNPF1 sharing 30% amino acid sequence identity. In *C. elegans*, the functions of this GPCR are still being established. In one RNAi screen, a knockdown of NPR-3 led to abnormal locomotion, with animals exhibiting sluggish behavior and a flat locomotory path as body bends were reduced (Keating et al., 2003). A second RNAi screen found that reduction of NPR-3 in a *lin-35* background (loss of *lin-35* results in enhanced RNAi) led to reduced brood size and protruding vulvas (Ceron et al., 2007). Neuropeptides specified by *flp-15* appeared to be the only peptides that could activate NPR-3 in a GTPγS assay with membranes prepared from *npr-3* transiently transfected CHO cells. In this assay, FLP-15-2 was a more potent activator than FLP-15-1 (**Table 1**). This interaction appears to be specific since a peptide such as FLP-21 (**Table 1**), which shares the carboxyl-terminal GPLRFamide, was inactive. NPR-3 appears to require a distinct conformation as activity was only observed when transiently NPR-3 transfected cells were incubated at 28°C. Membranes prepared from cells incubated at 37°C were inactive. Attempts to make a stably transformed NPR-3 cell line with CHO, HEK293, or COS7 cells were unsuccessful and resulted in cell death. In a transient expression assay; NPR-3 appears to activate via pertussis toxin-sensitive Gi/Go coupled signaling pathways which suggests that NPR-3 action is inhibitory (Kubiak et al., 2003a).

A second potential sNPF-like GPCR in *C. elegans* is Y58G8A.4 (NPR-5). NPR-5 RNA is spliced to generate two receptor isoforms of 397 aa (NPR-5a) and 433 aa (NPR-5b) that differ in sequence at the carboxyl-terminus. NPR-5 is most similar (31% amino acid sequence identity) to the *D. melanogaster* receptor CG7395 that encodes a NPF-like GPCR; that binds sNPF (Mertens et al., 2002).

Both isoforms of NPR-5 were assayed for activation with 150 synthetic peptides in a transient expression system in CHO cells. The most potent activators in a Ca^{2+} mobilization assay were peptides derived from the *flp-18* gene. FLP-18 peptides showed activation with EC_{50} values in the nM range, with most having similar potencies using either NPR-5a or b (Table 1). The least active peptide was the longest FLP-18-1 which is also the least active when assayed with the NPF-like receptor NPR-1 (Rogers et al., 2003). FLP-18-1 has been isolated as a processed peptide with the first three amino-terminal amino acids removed which may result in a more potent form of the peptide (Clynen et al., 2009). The sole FLP-21 peptide, that is the cognate ligand for NPR-1, was found to activate both forms of NPR-5 but with far less potency (Kubiak et al., 2008). This is not surprising since FLP-18 peptides have been shown to activate NPR-1 in oocyte expression assays as well as in a *C. elegans* pharyngeal expression assay (Rogers et al., 2003). It is unclear whether the FLP-18 and FLP-21 peptides work together. The two isoforms of NPR-5 may activate multiple signal transduction pathways as contributions from G_q , G_s , and G_i were observed (Kubiak et al., 2008). Deletion mutants of *flp-18* display no measurable phenotype.

FMRFAMIDES AND FMRFAMIDE-RELATED RECEPTORS

In vertebrate systems, neuropeptides with C-terminal sequence FMRFamide and FaRPs function in regulation of muscle contraction, feeding behavior, and learning and memory (Panula et al., 1996).

In *D. melanogaster*, FMRFamides are expressed from a single gene that encodes a precursor specifying 8 FMRFamide peptides. Five copies of the peptide Drome FMRF-1 would be released from the precursor (Table 1; Schneider et al., 1993). *In vitro* assays have established that FMRFamides function as modulators of muscle contraction, including in larval heart muscle; crop, foregut, and muscle of the body wall (Nichols et al., 2002; Nichols, 2003). The *D. melanogaster* FMRFamide GPCR (CG2114; Drome FR) is expressed in most larval and adult tissues. Drome FR was de-orphaned in two independent studies. In an aequorin bioluminescence assay, Drome FMRFamides 1–5 (numbered as unique FMRFamide-terminating peptide sequences from amino to the carboxyl-terminus of the precursor) were found to elicit a calcium response in a dose-dependent manner in CHO expressing (Table 1). *Neobellieria bullata* FMRFamide peptides were found to be active with the Drome FR with comparable potencies to native Drome FMRFamides (Table 1; Meeusen et al., 2002). Drome FMRFamide-5 was the most potent ligand in both studies (Cazzamali and Grimmelikhuijzen, 2002; Meeusen et al., 2002). Both studies found that the Drome FR can be activated by non-FMRFamide peptides such as Drome sNPF-1 and Drome myosuppressin; however, these peptides require much higher concentrations to elicit a response. Despite the high concentration required, FMRFamides were recently shown to act post-synaptically, inducing slow larval body wall contractions and increased tonus of the body wall muscles. The latter action of Drome FMRFamide requires activation of Drome FR and the Drome myosuppressin GPCR as well as an influx of calcium through L-type calcium channels (Klose et al., 2010). A role in reproduction had been suggested for Drome FR (Meeusen et al., 2002) as it is related in

sequence to a sex peptide receptor (CG16752); however, the Drome FR could not replace the sex peptide receptor in *in vitro* expression assays (Yapici et al., 2008). Drome CG2114 shares 16–20% amino acid identity with *C. elegans* GPCRs F21C10.9 and C26F1.6. Following knockdown of the expression of the *C. elegans* receptor C26F1.6 by RNAi, a hyperactive egg laying phenotype is observed suggesting that this GPCR functions in control of egg production (Keating et al., 2003). Using expression of Cael C26F1.6 in mammalian cells, only two neuropeptide sequences elicited a dose-dependent response Peptide FLP-7-2 which is found as two copies within the *flp-7* gene-encoded precursor was the most active followed by FLP-11-1 which is one of four peptides specified by the *flp-11* gene. Related peptides FLP-7-1, FLP-7-3, and FLP-7-4 processed from the FLP-7 precursor were inactive (Mertens et al., 2004, 2005b; Table 1). The FLP-7-2 peptide is likely cleaved at the arginine at the fifth position from the amino-terminus, as truncating the peptide to the terminal 5 amino acids was more active in receptor activation than the predicted full-length peptide (Mertens et al., 2005b). If processing does occur, all peptides from the FLP-7 precursor could be active peptides for receptor Cael C26F1.6. Alternatively, the unique amino-terminal sequences may be required for targeting.

Cael Y59H11AL.1 is a FaRP receptor that is related to the invertebrate tachykinin/mammalian neurokinin family of receptors. Cael Y59H11AL.1 is most closely related to the *Drosophila* NPY-like receptor (CG5811, DromeNepYr) which is a tachykinin family member. Drome NepYr has not been assigned a functional role. However, the Cael Y59H11AL.1 receptor appears to play a role in growth and reproduction as knockdown of Cael Y59H11AL.1 gene expression results in small animals with a reduced brood size (Ceron et al., 2007). Expression of the Cael Y59H11AL.1 gene results in two potential RNA splice variants that lead to two receptors of 427 aa and 434 aa. The two receptors differ by alteration of peptide sequence at the carboxyl-terminal region of the receptor. Of 68 neuropeptides tested against Cael Y59H11AL.1 expressed in mammalian cells, the Cael *flp-7* gene-encoded peptide FLP-7-3 was the most potent peptide (Table 1; Mertens et al., 2006). Three other peptides processed from the Cael FLP-7 precursor, FLP-7-1, FLP-7-2, and FLP-7-4 were less active. Peptide FLP-7-4 appears to be the only Cael FLP-7 precursor-derived peptide that uniquely activates Cael Y59H11AL.1, as the others activate Cael C26F1.6 as well. This result is surprising since the two receptors share limited sequence identity. Other peptides that showed weak activation of Cael Y59H11AL.1 were Cael FLP-1-8, FLP-9, and FLP-11-1-3 (Table 1; Mertens et al., 2006). Activation by multiple related peptides suggests a functional redundancy in peptide binding or possibly a less selective requirement of the receptor to respond to a variety of signals.

Another FaRP receptor in *C. elegans* is T19F4.1. RNA splice variants give rise to two receptors of 402 aa (Cael T19F4.1a) and 432 aa (Cael T19F4.1b). The difference between the receptors resides with the intracellular carboxy-terminus. After transient expression of each receptor in mammalian cells, two peptides, FLP-2-1 and FLP-2-2 derived from the Cael *flp-2* gene precursor were found to activate in a dose-dependent manner either Cael T19F4.1a or Cael T19F4.1b (Table 1). A stable transformed mammalian cell line expressing Cael T19F4.1b showed far less

activation with FLP-2-1 and was less responsive when challenged with FLP-2-2 (Mertens et al., 2005a). The reasons for this are unclear. In a genome-wide RNAi screen, knockdown of the Cael *flp-2* gene resulted in lethality in the embryo or larval stages or resulted in postembryonic growth defects (Simmer et al., 2003). No visible phenotypes have been identified in a Cael FLP-2 receptor knockdown that would affect both splice variants.

Cael C46F4.1 GPCR was found to be involved in an egg laying-defective phenotype (*egl*) in *C. elegans*. The most related receptor in *D. melanogaster* is Drome CG13229; however, no ligand or function has been ascribed to this unnamed fly receptor. Flyatlas lists low expression in the *D. melanogaster* nervous system. Cael C46F4.1 is equivalent to *egl-6* (Ringstad and Horvitz, 2008) and two receptor isoforms that differ at the amino-terminus are produced by alternative splicing and alternate start sites. Cael *egl-6* is predominately expressed in HSN motor neurons that innervate vulval muscles and glia-like cells located in the head region. Weaker expression was also noted in DVA tail interneurons. Expression was sometimes seen in lateral interneurons SDQL and SDQR (Ringstad and Horvitz, 2008). A gain-of-function mutant (*n592gf*) that results from a single amino acid change, Alanine 135 to Threonine 135, in the third transmembrane domain enhances EGL-6 activity. The result of this receptor activation is an egg laying-defective phenotype. Thus, EGL-6 normally transduces signals that confer inhibitory activity on the HSN motor neurons. This activity is dependent, in part, on G_o signaling. Transgenic overexpression of Cael *flp* and other neuropeptide genes in both wild type and animals that carried an *egl-6* deletion suggested that the ligands for EGL-6 were dependent on Cael *flp-10* and Cael *flp-17* genes. This was further supported by the demonstration that a Cael *flp-10* deletion mutant suppressed the egg laying defect in the gain-of-function mutant and suppression was further enhanced by deletion of the Cael *flp-17* gene. Peptides FLP-10 and two unique peptide sequences FLP-17-1 and 2, proved to be potent activators of EGL-6 when expressed in *X. laevis* oocytes. A GIRK channel assay, used to monitor expression, demonstrated that all peptides were potent activators, with EC_{50} values in the nM range (Table 1). Expression of Cael *flp-17* is confined to anterior BAG sensory neurons and this expression is necessary for EGL-6 function in egg laying. Expression of Cael *flp-10* occurs in numerous neurons ASIL, ASIR, DVB, PVCL, PVCR, PVR as well as in non-neuronal tissues including head mesodermal cells, vulval tissue, uterine cells, and spermathecae. Only non-neuronal expression of Cael *flp-10* appears to be important in EGL-6 action on egg laying (Ringstad and Horvitz, 2008).

PIGMENT DISPERSING FACTOR AND RECEPTOR

Pigment dispersing hormone is a light adapting hormone originally identified as responsible for daily rhythms of color change in Crustacea (Meelkop et al., 2011). Similar peptides known as pigment dispersing factors (PDFs) have been identified in arthropods and they are required for normal circadian control of locomotion. In *D. melanogaster*, the PDF receptor (DromePDFR; CG13758) null mutant does not show any apparent morphological defects. Drome PDFR immunostaining revealed that DromePDFR was localized in 13 neurons in each hemisphere of the adult brain, 4 I-LNV neurons, one of the six LNd neurons, seven neurons

in the DN1 area, and one neuron in the DN3 area. In a 12-h Light/Dark cycle, the receptor null mutants started morning activity later than wild type and began evening activity earlier than wild type. Placing animals in 24 h dark conditions for 8 days resulted in a loss of rhythmic activity. This behavior is seen in *Drosophila* PDF mutants, suggesting that DromePDF and DromePDFR may be part of a pathway that controls rhythmic circadian behavior. DromePDFR can be activated with Drome PDF, pituitary adenylate cyclase activating polypeptide (PACAP), or calcitonin-like peptides (Drome DH₃₁; Mertens et al., 2005c).

A search of the *C. elegans* database for a PDF receptor (PDFR) ortholog using the *Drosophila* PDFR (CG13758) as a query sequence (Renn et al., 1999) resulted in the identification of the gene Cael C13B9.4 as coding for a Cael PDFR. Transcription and alternate splicing of gene Cael C13B9.4 mRNA gives rise to six mRNAs (Wormbase). Two mRNAs that differ by variable length of the 5' untranslated region specifies one of three related receptors. These three receptor isoforms differ at the amino-terminal region of the proteins, generating receptors of 543 aa (Cael PDFR-1a); 536 aa (CaelPDFR-1b), and 541 aa (Cael PDFR-1c). Cael C13B9.4 promoter-driven reporter expression showed that expression of this receptor is extensive. Expression was observed in chemosensory neurons PHA and PHB, mechanosensory neurons PLM, ALM, FLP, OLQD, and OLQV, the ring motor neuron RMED, the I1 pharyngeal interneuron pair, and a single sensory neuron R3 in the male tail. In non-neuronal tissue, expression was found in 95 body wall muscles and two vulval cells (Janssen et al., 2008b). This localization is similar to the localization of PDF-like neuropeptides which are found in neurons involved in chemosensation, mechanosensation, oxygen sensing, and locomotion (Janssen et al., 2008b). Expression of each of the three receptor isoforms in stably transformed CHO cells demonstrated that only three of 156 synthetic *C. elegans* peptides were active in a calcium bioluminescence assay. These included Cael PDF-1a, PDF-1b, and PDF-2 = NLP-37 (Table 1). These three peptides were most active with Cael PDFR-1b but showed reduced activity with Cael PDFR-1a. Cael PDFR-1c was inactive in this assay. In a cAMP activation assay in transiently transfected HEK293 cells, all three receptor isoforms were activated by Cael PDF-1a, Cael PDF-1b, and Cael PDF-2, which suggests signaling through G_{α_s} . In this assay, Cael-PDFR-1b was the most active and responded particularly to Cael PDF-2. Cael PDFR-1c was the least active isoform. Cells expressing Cael PDFR-1 responded to all three peptides in a dose-dependent manner, using the ability to inhibit forskolin-induced cAMP formation, which suggests that Cael PDFR-1c may participate in coupling with additional G-proteins such as $G_{\alpha_{i/o}}$.

A Cael *pdf-1* (*lf*) results in a decrease in the speed of movement of worms, an increase in the reversal frequency and an increase in the frequency of directional change. The net result is that the distance that animals travel in the forward direction is dramatically reduced. These locomotor defects are not seen in animals in which Cael *pdf-1* is over-expressed. In contrast, overexpression of Cael *pdf-2* results in a phenotype equivalent to the Cael *pdf-1* (*lf*). Overexpression of Cael *pdf-1* (expressing all 3 isoforms) results in animals that show a dramatic increase in reversal frequency but lack changes in speed of movement or directional change. The current model is that Cael PDF-1 peptides activate Cael PDFR-1 to

stimulate forward movement and/or inhibit backward movement and this effect is counter-balanced by Cael PDF-2 acting on Cael PDFR-1 to inhibit forward movement and/or stimulate backward movement (Janssen et al., 2008b). *D. melanogaster* clock genes have counterparts in *C. elegans*. Null alleles of *C. elegans* clock genes reduced mRNA levels of Cael *pdf-1a*, *pdf-1b*, and *pdf-2* which implicates Cael PDF-1 and 2 activity as dependent on the clock genes. Cael *pdf-1* appears to work independently of Cael *pdf-2* as the level of one does not affect the other (Janssen et al., 2009).

CHOLECYSTOKININ AND ITS RECEPTOR

Cholecystokinin (CK) is known in vertebrates as a regulator of food intake as it functions to stimulate smooth muscle contraction which, in vertebrates, includes intestinal and gall bladder contractions. CK also stimulates the secretion of digestive enzymes such as α -amylase (Dufresne et al., 2006). The *D. melanogaster* CK-like receptor (Drome CCKLR) was identified based on homology to mammalian CK receptors (CKR) and was found in mammalian expression assays to bind to a sulfated FMRFamide-like peptide, drosulfakinin (Drome DSK). The sulfated form of Drome DSK is necessary to achieve specific interaction with EC50 values in the nM range (Kubiak et al., 2002). Analysis of loss-of-function mutations in either Drome CCKLR or Drome DSK results in neuromuscular junction undergrowth suggesting that both GPCR and ligand are required pre-synaptically to promote neuromuscular junction growth. Genetically, Drome CCKLR and Drome DSK were found to function upstream of G α s which in turn regulates a cAMP-dependent protein kinase which then acts on a transcriptional regulatory protein CREB2 which is the primary effector of the pathway (Chen and Ganetzky, 2012). In *C. elegans*, CaelY39A3B.5 shares 67% similarity with mammalian CKR (CCK2R) and 64% with sulfakinin receptors (DK-R1; Johnsen, 1998; Janssen et al., 2008a). Through computer predicted alternate splicing, Cael Y39A3B.5 produces four isoforms of 582 aa (Y39A3B.5a), 552 aa (Y39A3B.5b), 471 aa (Y39A3B.5c), and 617 aa (Y39A3B.5; Wormbase). Additional isoforms may exist as two further isoforms were identified as a result of sequencing DNA generated experimentally by reverse-transcriptase PCR. Both contained the first eight exons of isoform c but then differed, as one contained the last two exons of isoform b (Y39A3B.5c/b = Cael CKR-2a) and the second the last four exons of isoform d (Y39A3B.5c/d = Cael CKR-2b). These two receptors were de-orphaned by transient expression in CHO cell lines, using a calcium bioluminescence assay. Cael NLP-12a and Cael NLP-12b were the only peptides tested that activated Cael CKRs in a dose-dependent manner (Table 1). The most potent ligand for Cael CKR-2a was Cael NLP-12b whereas NLP-12a showed a higher potency than NLP-12b with CKR-2b. NLP-12 is localized to a tail interneuron DVA and to processes from DVA that extend around the nerve ring. Expression was also observed in all six coelomocytes. In common with vertebrates, Cael NLP-12 can regulate digestion since Cael *ckr-2(lf)* have decreased intestinal α -amylase and both Cael *ckr-2(lf)* and Cael *nlp-12(lf)* animals gain fat even though there is no difference in pharyngeal pumping rate or defecation rate. Cael *ckr-2* and its ligand, Cael *nlp-12*, may also be involved in a mechanosensory feedback loop that couples muscle contraction to changes in pre-synaptic ACh release (Hu et al., 2011).

ALLATOSTATIN-LIKE PEPTIDES AND RECEPTORS

Mammalian galanin is a neuropeptide that regulates numerous physiological processes including neurotransmission, nociception, feeding and metabolism, energy, and osmotic homeostasis as well as learning and memory (Lang et al., 2007). Insect allatostatins (ASTs) have a carboxyl-terminal sequence Y (Xaa) FGL-amide and have multiple functions that include inhibition of juvenile hormone biosynthesis (Bendena et al., 1999; Tobe and Bendena, 2012) inhibition of muscle contraction, regulation of digestive enzymes, and neuromodulation (Tobe and Bendena, 2012). In *Drosophila* Drome FGL-amide ASTs do not inhibit juvenile hormone biosynthesis. RNAi reduction in Drome AST or Drome ASTR transcripts results in reduced locomotory behavior in the presence of food. Locomotion is normal in the absence of food. Reduction in Drome AST and Drome ASTR is correlated with decreased *for* transcript levels which encodes cGMP-dependent protein kinase. A reduction in the *for* transcript is known to be associated with a naturally occurring allelic variation that creates a sitter phenotype in contrast to the rover phenotype which is caused by a *for* allele associated with increased *for* activity (Wang et al., 2012). In *C. elegans* the gene Cael *npr-9* expresses a single GPCR isoform of 444 aa that shares 33 and 37% amino acid sequence identity with mammalian galanin receptor 2 and the Drome allatostatin receptor (Drome ASTR), respectively. Promoter-driven reporter expression suggests that Cael *npr-9* is transcribed exclusively in interneuron AIB. Cael NPR-9 appears to function as an inhibitor of local search behavior in the presence of a food stimulus. In the absence of food, Cael *npr-9 (lf)* mutants display locomotory activity that is identical to wild type animals. Cael *npr-9 (lf)* mutants behave as if AIB is stimulated (increased pivoting and local search). Cael *npr-9(lf)* animals also accumulate fat at an accelerated rate relative to wild type and thus again resemble galanin/allatostatin neuropeptides that affect metabolism. This contrasts with Cael *npr-9(gf)* animals (overexpression of Cael NPR-9) which display enhanced forward locomotion that mimic the phenotype displayed by AIB laser ablation or a mutation in the glutamate receptor-1 (Bendena et al., 2008). Cael *npr-9(gf)* animals travel long distances off food, presumably as a result of over-riding dopamine, and glutamate signals that evoke "area restricted search" behavior in wild type animals. Area restricted search is characterized by frequent reversals and sharp omega-turns that function to maximize the time spent on an abundant food source (Hills et al., 2004). The ligands for Cael NPR-9 have not yet been identified. Two genes, Cael *nlp-5* and Cael *nlp-6*, specify peptides that resemble ASTs. Cael *nlp-5* and Cael *nlp-6* specify peptides with carboxyl-terminal MGLamide and MGFamide, respectively. Cael *nlp-6* encodes a peptide with carboxy-terminal FGFamide. A mutation in Cael *nlp-5* has been reported to result in animals with altered locomotory behavior on food (Bargmann, Wormbase), which appears to be similar to behaviors exhibited by Cael *npr-9(lf)* animals.

PERSPECTIVES

High throughput neuropeptide projects are expected to facilitate de-orphanization of all of the predicted *D. melanogaster* and *C. elegans* neuropeptide receptors. These neuropeptides and their receptors will serve as starting points to understand the functional

significance of these signaling events. Both organisms serve as genetic models not only for matching GPCRs with their respective neuropeptide ligand but offer a means of uncovering signal transduction pathways that lead to novel behaviors. Genetic modifier screens and genome-wide RNAi screens will certainly identify many of the neuropeptide signaling components. *C. elegans* transgenic studies will allow the manipulation of neuropeptide receptor signaling at the level of a single cell or tissue within an entire

organism. As many of these receptors have counterparts in mammals, it will not be surprising to find similar signaling pathways conserved throughout evolution.

ACKNOWLEDGMENTS

This work was supported by Natural Science and Engineering Research Council of Canada (NSERC) grants to William Bendena and Ian Chin-Sang.

REFERENCES

- Barak, L. S., Ferguson, S. S. G., Zhang, J., and Caron, M. G. (1997). A beta-arrestin green fluorescent protein biosensor for detecting G protein-coupled receptor activation. *J. Biol. Chem.* 272, 27497–27500.
- Bargmann, C. I. (1998). Neurobiology of the *Caenorhabditis elegans* genome. *Science* 282, 2028–2033.
- Bargmann, C. I. (2006). Chemosensation in *C. elegans*. *WormBook* 1–29. Available at: <http://www.wormbook.org>
- Bendena, W. G., Boudreau, J. R., Papanicolaou, T., Maltby, M., Tobe, S. S., and Chin-Sang, I. D. (2008). A *Caenorhabditis elegans* allatostatin/galanin-like receptor NPR-9 inhibits local search behavior in response to feeding cues. *Proc. Natl. Acad. Sci. U.S.A.* 105, 1339–1342.
- Bendena, W. G., Donly, B. C., and Tobe, S. S. (1999). Allatostatins: a growing family of neuropeptides with structural and functional diversity. *Ann. N. Y. Acad. Sci.* 897, 311–329.
- Bretscher, A. J., Busch, K. E., and de Bono, M. (2008). A carbon dioxide avoidance behavior is integrated with responses to ambient oxygen and food in *Caenorhabditis elegans*. *Proc. Natl. Acad. Sci. U.S.A.* 105, 8044–8049.
- Brown, M. R., Crim, J. W., Arata, R. C., Cai, H. N., Chun, C., and Shen, P. (1999). Identification of a *Drosophila* brain-gut peptide related to the neuropeptide Y family. *Peptides* 20, 1035–1042.
- Browning, K. N., and Travagli, R. A. (2003). Neuropeptide Y and peptide YY inhibit excitatory synaptic transmission in the rat dorsal motor nucleus of the vagus. *J. Physiol. (Lond.)* 549, 775–785.
- Campesan, S., Green, E. W., Breda, C., Sathyaikumar, K. V., Muchowski, P. J., Schwarcz, R., Kyriacou, C. P., and Giorgini, F. (2011). The kynurenine pathway modulates neurodegeneration in a *Drosophila* model of Huntington's disease. *Curr. Biol.* 21, 961–966.
- Carlsson, M. A., Diesner, M., Schachtner, J., and Nassel, D. R. (2010). Multiple neuropeptides in the *Drosophila* antennal lobe suggest complex modulatory circuits. *J. Comp. Neurol.* 518, 3359–3380.
- Cazzamali, G., and Grimmelikhuijzen, C. J. (2002). Molecular cloning and functional expression of the first insect FMRFamide receptor. *Proc. Natl. Acad. Sci. U.S.A.* 99, 12073–12078.
- Ceron, J., Rual, J. F., Chandra, A., Dupuy, D., Vidal, M., and van den Heuvel, S. (2007). Large-scale RNAi screens identify novel genes that interact with the *C. elegans* retinoblastoma pathway as well as splicing-related components with synMuv B activity. *BMC Dev. Biol.* 7, 30. doi:10.1186/1471-213X-7-30
- Chakraborty, R., Vepuri, V., Mhatre, S. D., Paddock, B. E., Miller, S., Michelson, S. J., Delvadia, R., Desai, A., Vinokur, M., Melicharek, D. J., Utreja, S., Khandelwal, P., Ansaloni, S., Goldstein, L. E., Moir, R. D., Lee, J. C., Tabb, L. P., Saunders, A. J., and Marendza, D. R. (2011). Characterization of a *Drosophila* Alzheimer's disease model: pharmacological rescue of cognitive defects. *PLoS ONE* 6, e20799. doi:10.1371/journal.pone.0020799
- Chang, A. J., and Bargmann, C. I. (2008). Hypoxia and the HIF-1 transcriptional pathway reorganize a neuronal circuit for oxygen-dependent behavior in *Caenorhabditis elegans*. *Proc. Natl. Acad. Sci. U.S.A.* 105, 7321–7326.
- Chang, A. J., Chronis, N., Karow, D. S., Marletta, M. A., and Bargmann, C. I. (2006). A distributed chemosensory circuit for oxygen preference in *C. elegans*. *PLoS Biol.* 4, e274. doi:10.1371/journal.pbio.0040274
- Chen, X., and Ganetzky, B. (2012). A neuropeptide signaling pathway regulates synaptic growth in *Drosophila*. *J. Cell Biol.* 196, 529–543.
- Cheung, B. H., Arellano-Carbajal, F., Rybicki, I., and de Bono, M. (2004). Soluble guanylate cyclases act in neurons exposed to the body fluid to promote *C. elegans* aggregation behavior. *Curr. Biol.* 14, 1105–1111.
- Cheung, B. H., Cohen, M., Rogers, C., Albayram, O., and de Bono, M. (2005). Experience-dependent modulation of *C. elegans* behavior by ambient oxygen. *Curr. Biol.* 15, 905–917.
- Clark, J. T., Kalra, P. S., Crowley, W. R., and Kalra, S. P. (1984). Neuropeptide-Y and human pancreatic-polypeptide stimulate feeding behavior in rats. *Endocrinology* 115, 427–429.
- Clynen, E., Husson, S. J., and Schoofs, L. (2009). Identification of new members of the (short) neuropeptide F family in locusts and *Caenorhabditis elegans*. *Trends Comp. Endocrinol. Neurobiol.* 1163, 60–74.
- Clynen, E., Reumer, A., Baggerman, G., Mertens, I., and Schoofs, L. (2010). Neuropeptide biology in *Drosophila*. *Adv. Exp. Med. and Biol.* 692, 192–210.
- Coates, J. C., and de Bono, M. (2002). Antagonistic pathways in neurons exposed to body fluid regulate social feeding in *Caenorhabditis elegans*. *Nature* 419, 925–929.
- Cohen, M., Reale, V., Olofsson, B., Knights, A., Evans, P., and de Bono, M. (2009). Coordinated regulation of foraging and metabolism in *C. elegans* by RFamide neuropeptide signaling. *Cell Metab.* 9, 375–385.
- Cowden, C., and Stretton, A. O. (1995). Eight novel FMRFamide-like neuropeptides isolated from the nematode *Ascaris suum*. *Peptides* 16, 491–500.
- de Bono, M., and Bargmann, C. I. (1998). Natural variation in a neuropeptide Y receptor homolog modifies social behavior and food response in *C. elegans*. *Cell* 94, 679–689.
- de Bono, M., Tobin, D. M., Davis, M. W., Avery, L., and Bargmann, C. I. (2002). Social feeding in *Caenorhabditis elegans* is induced by neurons that detect aversive stimuli. *Nature* 419, 899–903.
- De Strooper, B., Annaert, W., Cupers, P., Saftig, P., Craessaerts, K., Mumm, J. S., Schroeter, E. H., Schrijvers, V., Wolfe, M. S., Ray, W. J., Goate, A., and Kopan, R. (1999). A presenilin-1-dependent gamma-secretase-like protease mediates release of Notch intracellular domain. *Nature* 398, 518–522.
- Dierick, H. A., and Greenspan, R. J. (2007). Serotonin and neuropeptide F have opposite modulatory effects on fly aggression. *Nat. Genet.* 39, 678–682.
- Dufresne, M., Seva, C., and Fourmy, D. (2006). Cholecystokinin and gastrin receptors. *Physiol. Rev.* 86, 805–847.
- Feany, M. B., and Bender, W. W. (2000). A *Drosophila* model of Parkinson's disease. *Nature* 404, 394–398.
- Fredriksson, R., Lagerström, M. C., Lundin, L., and Schiöth, H. B. (2003). The G-protein-coupled receptors in the human genome form five main families. Phylogenetic analysis, paralogon groups, and fingerprints. *Mol. Pharmacol.* 63, 1256–1272.
- Garczynski, S. F., Brown, M. R., Shen, P., Murray, T. F., and Crim, J. W. (2002). Characterization of a functional neuropeptide F receptor from *Drosophila melanogaster*. *Peptides* 23, 773–780.
- Geary, T. G., Marks, N. J., Maule, A. G., Bowman, J. W., Alexander-Bowman, S. J., Day, T. A., Larsen, M. J., Kubiak, T. M., Davis, J. P., and Thompson, D. P. (1999). Pharmacology of FMRFamide-related peptides in helminths. *Ann. N. Y. Acad. Sci.* 897, 212–227.
- Glauser, D. A., Chen, W. C., Agin, R., MacInnis, B. L., Hellman, A. B., Garrity, P. A., Tan, M., and Goodman, M. B. (2011). Heat avoidance is regulated by transient receptor potential (TRP) channels and a neuropeptide signaling pathway in *Caenorhabditis elegans*. *Genetics* 188, 91–U150.
- Gray, J. M., Hill, J. J., and Bargmann, C. I. (2005). A circuit for navigation in *Caenorhabditis elegans*. *Proc. Natl. Acad. Sci. U.S.A.* 102, 3184–3191.
- Hallem, E. A., and Sternberg, P. W. (2008). Acute carbon dioxide avoidance in *Caenorhabditis elegans*. *Proc. Natl. Acad. Sci. U.S.A.* 105, 8038–8043.
- Harada, Y., Takahashi, T., Kuno, M., Nakayama, K., Masu, Y., and Nakanishi, S. (1987). Expression of two different tachykinin receptors in *Xenopus* oocytes by exogenous mRNAs. *J. Neurosci.* 7, 3265–3273.

- Hermann, C., Yoshii, T., Dusik, V., and Helfrich-Foerster, C. (2012). Neuropeptide F immunoreactive clock neurons modify evening locomotor activity and free-running period in *Drosophila melanogaster*. *J. Comp. Neurol.* 520, 970–987.
- Hewes, R. S., and Taghert, P. H. (2001). Neuropeptides and neuropeptide receptors in the *Drosophila melanogaster* genome. *Genome Res.* 11, 1126–1142.
- Hills, T., Brockie, P. J., and Maricq, A. V. (2004). Dopamine and glutamate control area-restricted search behavior in *Caenorhabditis elegans*. *J. Neurosci.* 24, 1217–1225.
- Hu, Z., Pym, E. C. G., Babu, K., Murray, A. B. V., and Kaplan, J. M. (2011). A neuropeptide-mediated stretch response links muscle contraction to changes in neurotransmitter release. *Neuron* 71, 92–102.
- Husson, S. J., Mertens, I., Janssen, T., Lindemans, M., and Schoofs, L. (2007). Neuropeptidergic signaling in the nematode *Caenorhabditis elegans*. *Prog. Neurobiol.* 82, 33–55.
- Janssen, T., Husson, S. J., Meelkop, E., Temmerman, L., Lindemans, M., Verstraelen, K., Rademakers, S., Mertens, I., Nitabach, M., Jansen, G., and Schoofs, L. (2009). Discovery and characterization of a conserved pigment dispersing factor-like neuropeptide pathway in *Caenorhabditis elegans*. *J. Neurochem.* 111, 228–241.
- Janssen, T., Meelkop, E., Lindemans, M., Verstraelen, K., Husson, S. J., Temmerman, L., Nachman, R. J., and Schoofs, L. (2008a). Discovery of a cholecystokinin-gastrin-like signaling system in nematodes. *Endocrinology* 149, 2826–2839.
- Janssen, T., Husson, S. J., Lindemans, M., Mertens, I., Rademakers, S., Ver Donck, K., Geysen, J., Jansen, G., and Schoofs, L. (2008b). Functional characterization of three G protein-coupled receptors for pigment dispersing factors in *Caenorhabditis elegans*. *J. Biol. Chem.* 283, 15241–15249.
- Johnsen, A. H. (1998). Phylogeny of the cholecystokinin/gastrin family. *Front. Neuroendocrinol.* 19, 73–99.
- Johnson, E. C., Bohn, L. M., Barak, L. S., Birse, R. T., Nassel, D. R., Caron, M. G., and Taghert, P. H. (2003). Identification of *Drosophila* neuropeptide receptors by G protein-coupled receptors-beta-arrestin2 interactions. *J. Biol. Chem.* 278, 52172–52178.
- Kalra, S. P. (1997). Appetite and body weight regulation: is it all in the brain? *Neuron* 19, 227–230.
- Kapfhamer, D., Bettinger, J. C., Davies, A. G., Eastman, C. L., Smail, E. A., Heberlein, U., and McIntire, S. L. (2008). Loss of RAB-3/A in *Caenorhabditis elegans* and the mouse affects behavioral response to ethanol. *Genes Brain Behav.* 7, 669–676.
- Keating, C. D., Kriek, N., Daniels, M., Ashcroft, N. R., Hopper, N. A., Siney, E. J., Holden-Dye, L., and Burke, J. F. (2003). Whole-genome analysis of 60 G protein-coupled receptors in *Caenorhabditis elegans* by gene knockout with RNAi. *Curr. Biol.* 13, 1715–1720.
- Klapstein, G. J., and Colmers, W. F. (1993). On the sites of presynaptic inhibition by neuropeptide-Y in rat hippocampus in vitro. *Hippocampus* 3, 103–112.
- Klose, M. K., Dason, J. S., Atwood, H. L., Boulianne, G. L., and Mercier, A. J. (2010). Peptide-induced modulation of synaptic transmission and escape response in *Drosophila* requires two G-protein-coupled receptors. *J. Neurosci.* 30, 14724–14734.
- Krashes, M. J., DasGupta, S., Vreede, A., White, B., Armstrong, J. D., and Waddell, S. (2009). A neural circuit mechanism integrating motivational state with memory expression in *Drosophila*. *Cell* 139, 416–427.
- Krishnan, A., Almén, M. S., Fredriksson, R., and Schiöth, H. B. (2012). The origin of GPCRs: identification of mammalian like *Rhodopsin*, *Adhesion*, *Glutamate* and *Frizzled* GPCRs in fungi. *PLoS ONE* e29817. doi:10.1371/journal.pone.0029817
- Kubiak, T. M., Larsen, M. J., Bowman, J. W., Geary, T. G., and Lowery, D. E. (2008). FMRFamide-like peptides encoded on the flp-18 precursor gene activate two isoforms of the orphan *Caenorhabditis elegans* G-protein-coupled receptor Y58G8A.4 heterologously expressed in mammalian cells. *Biopolymers* 90, 339–348.
- Kubiak, T. M., Larsen, M. J., Burton, K. J., Bannow, C. A., Martin, R. A., Zantello, M. R., and Lowery, D. E. (2002). Cloning and functional expression of the first *Drosophila melanogaster* sulfakinin receptor DSK-R1. *Biochem. Biophys. Res. Commun.* 291, 313–320.
- Kubiak, T. M., Larsen, M. J., Zantello, M. R., Bowman, J. W., Nulf, S. C., and Lowery, D. E. (2003a). Functional annotation of the putative orphan *Caenorhabditis elegans* G-protein-coupled receptor C10C6.2 as a FLP15 peptide receptor. *J. Biol. Chem.* 278, 42115–42120.
- Kubiak, T. M., Larsen, M. J., Nulf, S. C., Zantello, M. R., Burton, K. J., Bowman, J. W., Modric, T., and Lowery, D. E. (2003b). Differential activation of “social” and “solitary” variants of the *Caenorhabditis elegans* G protein-coupled receptor NPR-1 by its cognate ligand AF9. *J. Biol. Chem.* 278, 33724–33729.
- Lang, R., Gundlach, A. L., and Kofler, B. (2007). The galanin peptide family: receptor pharmacology, pleiotropic biological actions, and implications in health and disease. *Pharmacol. Ther.* 115, 177–207.
- Larsen, M. J., Burton, K. J., Zantello, M. R., Smith, V. G., Lowery, D. L., and Kubiak, T. M. (2001). Type A allatostatins from *Drosophila melanogaster* and *Diptera punctata* activate two *Drosophila* allatostatin receptors, DAR-1 and DAR-2, expressed in CHO cells. *Biochem. Biophys. Res. Commun.* 286, 895–901.
- Lee, G., Bahn, J. H., and Park, J. H. (2006). Sex- and clock-controlled expression of the neuropeptide F gene in *Drosophila*. *Proc. Natl. Acad. Sci. U.S.A.* 103, 12580–12585.
- Lee, K. S., You, K. H., Choo, J. K., Han, Y. M., and Yu, K. (2004). *Drosophila* short neuropeptide F regulates food intake and body size. *J. Biol. Chem.* 279, 50781–50789.
- Li, C., and Kim, K. (2008). Neuropeptides. *WormBook* 1–36. Available at: <http://www.wormbook.org>
- Lowery, D. E., Geary, T. G., Kubiak, T. M., and Larsen, M. J. (2003). *G Protein-Coupled Receptors and Modulators Thereof*. US Patent No. 6,632,621
- Macosko, E. Z., Pokala, N., Feinberg, E. H., Chalasani, S. H., Butcher, R. A., Clardy, J., and Bargmann, C. I. (2009). A hub-and-spoke circuit drives pheromone attraction and social behaviour in *C. elegans*. *Nature* 458, 1171–U110.
- McGrath, P. T., Rockman, M. V., Zimmer, M., Jang, H., Macosko, E. Z., Kruglyak, L., and Bargmann, C. I. (2009). Quantitative mapping of a digenic behavioral trait implicates globin variation in *C. elegans* sensory behaviors. *Neuron* 61, 692–699.
- Meelkop, E., Temmerman, L., Schoofs, L., and Janssen, T. (2011). Signalling through pigment dispersing hormone-like peptides in invertebrates. *Prog. Neurobiol.* 93, 125–147.
- Meeusen, T., Mertens, I., Clynen, E., Baggerman, G., Nichols, R., Nachman, R. J., Huybrechts, R., De Loof, A., and Schoofs, L. (2002). Identification in *Drosophila melanogaster* of the invertebrate G protein-coupled FMRFamide receptor. *Proc. Natl. Acad. Sci. U.S.A.* 99, 15363–15368.
- Mertens, I., Clinckspoor, I., Janssen, T., Nachman, R., and Schoofs, L. (2006). FMRFamide related peptide ligands activate the *Caenorhabditis elegans* orphan GPCR Y59H11AL.1. *Peptides* 27, 1291–1296.
- Mertens, I., Meeusen, T., Janssen, T., Nachman, R., and Schoofs, L. (2005a). Molecular characterization of two G protein-coupled receptor splice variants as FLP2 receptors in *Caenorhabditis elegans*. *Biochem. Biophys. Res. Commun.* 297, 1140–1148.
- Mertens, I., Meeusen, T., Janssen, T., Nachman, R., and Schoofs, L. (2005b). Characterization of an RFamide-related peptide orphan GPCR in *C. elegans*. *Ann. N. Y. Acad. Sci.* 1040, 410–412.
- Mertens, I., Vandingenen, A., Johnson, E. C., Shafer, O. T., Li, W., Trigg, J. S., De Loof, A., Schoofs, L., and Taghert, P. H. (2005c). PDF receptor signaling in *Drosophila* contributes to both circadian and geotactic behaviors. *Neuron* 48, 213–219.
- Mertens, I., Vandingenen, A., Meeusen, T., Janssen, T., Luyten, W., Nachman, R. J., De Loof, A., and Schoofs, L. (2004). Functional characterization of the putative orphan neuropeptide G-protein coupled receptor C26F1.6 in *Caenorhabditis elegans*. *FEBS Lett.* 573, 55–60.
- Nakae, J., Biggs, W. H. III, Kitamura, T., Cavenee, W. K., Wright, C. V., Arden, K. C., and Accili, D. (2002). Regulation of insulin action and pancreatic beta-cell function by mutated alleles of the gene encoding forkhead transcription factor Foxo1. *Nat. Genet.* 32, 245–253.
- Nassel, D. R., Enell, L. E., Santos, J. G., Wegener, C., and Johard, H. A. D. (2008). A large population of diverse neurons in the *Drosophila* central nervous system expresses short neuropeptide F, suggesting multiple distributed peptide functions. *BMC Neurosci.* 9, 90. doi:10.1186/1471-2202-9-90
- Nathoo, A. N., Moeller, R. A., Westlund, B. A., and Hart, A. C. (2001). Identification of neuropeptide-like protein gene families in *Caenorhabditis elegans* and other species. *Proc. Natl. Acad. Sci. U.S.A.* 98, 14000–14005.

- Nichols, R. (2003). Signaling pathways and physiological functions of *Drosophila melanogaster* FMRFamide-related peptides. *Annu. Rev. Entomol.* 48, 485–503.
- Nichols, R., Bendena, W. G., and Tobe, S. S. (2002). Myotropic peptides in *Drosophila melanogaster* and the genes that encode them. *J. Neurogenet.* 16, 1–28.
- O’Kane, C. J. (2011). *Drosophila* as a model organism for the study of neuropsychiatric disorders. *Mol. Funct. Models Neuropsychiatry* 7, 37–60.
- Pandey, U. B., and Nichols, C. D. (2011). Human disease models in *Drosophila melanogaster* and the role of the fly in therapeutic drug discovery. *Pharmacol. Rev.* 63, 411–436.
- Panula, P., Aarnisalo, A. A., and Wasowicz, K. (1996). Neuropeptide FF, a mammalian neuropeptide with multiple functions. *Prog. Neurobiol.* 48, 461–487.
- Pedrazzini, T. (2004). Importance of NPY Y1 receptor-mediated pathways: assessment using NPY Y1 receptor knockouts. *Neuropeptides* 38, 267–275.
- Ranganathan, R., Sawin, E. R., Trent, C., and Horvitz, H. R. (2001). Mutations in the *Caenorhabditis elegans* serotonin reuptake transporter MOD-5 reveal serotonin-dependent and -independent activities of fluoxetine. *J. Neurosci.* 21, 5871–5884.
- Reddy, K. C., Hunter, R. C., Bhatla, N., Newman, D. K., and Kim, D. H. (2011). *Caenorhabditis elegans* NPR-1-mediated behaviors are suppressed in the presence of mucoid bacteria. *Proc. Natl. Acad. Sci. U.S.A.* 108, 12887–12892.
- Renn, S. C., Park, J. H., Rosbash, M., Hall, J. C., and Taghert, P. H. (1999). A pdf neuropeptide gene mutation and ablation of PDF neurons each cause severe abnormalities of behavioral circadian rhythms in *Drosophila*. *Cell* 99, 791–802.
- Ringstad, N., and Horvitz, H. R. (2008). FMRFamide neuropeptides and acetylcholine synergistically inhibit egg-laying by *C. elegans*. *Nat. Neurosci.* 11, 1168–1176.
- Rogers, C., Reale, V., Kim, K., Chatwin, H., Li, C., Evans, P., and de Bono, M. (2003). Inhibition of *Caenorhabditis elegans* social feeding by FMRFamide-related peptide activation of NPR-1. *Nat. Neurosci.* 6, 1178–1185.
- Root, C. M., Ko, K. I., Jafari, A., and Wang, J. W. (2011). Presynaptic facilitation by neuropeptide signaling mediates odor-driven food search. *Cell* 145, 133–144.
- Schneider, L. E., Sun, E. T., Garland, D. J., and Taghert, P. H. (1993). An immunocytochemical study of the FMRFamide neuropeptide gene products in *Drosophila*. *J. Comp. Neurol.* 337, 446–460.
- Seroude, L. (2002). GAL4 drivers expression in the whole adult fly. *Genesis* 34, 34–38.
- Simmer, F., Moorman, C., van der Linden, A. M., Kuijk, E., van den Berghe, P. V., Kamath, R. S., Fraser, A. G., Ahringer, J., and Plasterk, R. H. (2003). Genome-wide RNAi of *C. elegans* using the hypersensitive rrf-3 strain reveals novel gene functions. *PLoS Biol.* 1, e12. doi:10.1371/journal.pbio.0000012
- Styer, K. L., Singh, V., Macosko, E., Steele, S. E., Bargmann, C. I., and Aballay, A. (2008). Innate immunity in *Caenorhabditis elegans* is regulated by neurons expressing NPR-1/GPCR. *Science* 322, 460–464.
- Sundaram, M., and Greenwald, I. (1993). Suppressors of a lin-12 hypomorph define genes that interact with both lin-12 and glp-1 in *Caenorhabditis elegans*. *Genetics* 135, 765–783.
- Teng, M. S., Dekkers, M. P., Ng, B. L., Rademakers, S., Jansen, G., Fraser, A. G., and McCafferty, J. (2006). Expression of mammalian GPCRs in *C. elegans* generates novel behavioural responses to human ligands. *BMC Biol.* 4, 22. doi:10.1186/1741-7007-4-22
- Teng, M. S., Shadbolt, P., Fraser, A. G., Jansen, G., and McCafferty, J. (2008). Control of feeding behavior in *C. elegans* by human G protein-coupled receptors permits screening for agonist-expressing bacteria. *Proc. Natl. Acad. Sci. U.S.A.* 105, 14826–14831.
- Thorsell, A., and Heilig, M. (2002). Diverse functions of neuropeptide Y revealed using genetically modified animals. *Neuropeptides* 36, 182–193.
- Tobe, S. S., and Bendena, W. G. (2012). “Allatostatin in the insects,” in *The Handbook of Biologically Active Peptides*, Chap. 31, ed. A. Kastin (MA, USA: Elsevier Science Press), 201–206.
- Vanden Broeck, J. (2001). Neuropeptides and their precursors in the fruitfly, *Drosophila melanogaster*. *Peptides* 22, 241–254.
- Veenstra, J. A., Agricola, H., and Sellami, A. (2008). Regulatory peptides in fruit fly midgut. *Cell Tissue Res.* 334, 499–516.
- Venken, K. J. T., Simpson, J. H., and Bellen, H. J. (2011). Genetic manipulation of genes and cells in the nervous system of the fruit fly. *Neuron* 72, 202–230.
- Wang, C., Chin-Sang, I., and Bendena, W. G. (2012). The FGLamide-allatostatins influence foraging behavior in *Drosophila melanogaster*. *PLoS ONE* e36059. doi:10.1371/journal.pone.0036059
- Wen, T. Q., Parrish, C. A., Xu, D., Wu, Q., and Shen, P. (2005). *Drosophila* neuropeptide F and its receptor, NPFRI, define a signaling pathway that acutely modulates alcohol sensitivity. *Proc. Natl. Acad. Sci. U.S.A.* 102, 2141–2146.
- Wu, Q., Wen, T. Q., Lee, G., Park, J. H., Cai, H. N., and Shen, P. (2003). Developmental control of foraging and social behavior by the *Drosophila* neuropeptide Y-like system. *Neuron* 39, 147–161.
- Wu, Q., Zhao, Z., and Shen, P. (2005). Regulation of aversion to noxious food by *Drosophila* neuropeptide Y- and insulin-like systems. *Nat. Neurosci.* 8, 1350–1355.
- Xu, J., Li, M., and Shen, P. (2010). A G-Protein-coupled neuropeptide Y-like receptor suppresses behavioral and sensory response to multiple stressful stimuli in *Drosophila*. *J. Neurosci.* 30, 2504–2512.
- Yapici, N., Kim, Y. J., Ribeiro, C., and Dickson, B. J. (2008). A receptor that mediates the post-mating switch in *Drosophila* reproductive behaviour. *Nature* 451, 33–37.

Conflict of Interest Statement: The authors declare that the research was conducted in the absence of any commercial or financial relationships that could be construed as a potential conflict of interest.

Received: 13 March 2012; accepted: 14 July 2012; published online: 09 August 2012.

Citation: Bendena WG, Campbell J, Zara L, Tobe SS and Chin-Sang ID (2012) Select neuropeptides and their G-protein coupled receptors in *Caenorhabditis elegans* and *Drosophila melanogaster*. *Front. Endocrin.* 3:93. doi: 10.3389/fendo.2012.00093

This article was submitted to *Frontiers in Experimental Endocrinology*, a specialty of *Frontiers in Endocrinology*.

Copyright © 2012 Bendena, Campbell, Zara, Tobe and Chin-Sang. This is an open-access article distributed under the terms of the Creative Commons Attribution License, which permits use, distribution and reproduction in other forums, provided the original authors and source are credited and subject to any copyright notices concerning any third-party graphics etc.



Cytoplasmic travels of the ecdysteroid receptor in target cells: pathways for both genomic and non-genomic actions

Xanthe Vafopoulou* and Colin G. H. Steel

Biology Department, York University, Toronto, ON, Canada

Edited by:

Joe Hull, USDA Agricultural Research Service, USA

Reviewed by:

Kirst King-Jones, University of Alberta, Canada

Chantal Dauphin-Villemant, CNRS, France

*Correspondence:

Xanthe Vafopoulou, Biology Department, York University, 4700 Keele Street, Toronto, ON, Canada M3J 1P3.
e-mail: xanthev@yorku.ca

Signal transduction of the insect steroid hormones, ecdysteroids, is mediated by the ecdysteroid receptor, EcR. In various cells of the insect *Rhodnius prolixus*, EcR is present in both the nucleus and the cytoplasm, where it undergoes daily cycling in abundance and cellular location at particular developmental times of the last larval instar that are specific to different cell types. EcR favors a cytoplasmic location in the day and a nuclear location in the night. This study is the first to examine the potential mechanisms of intracellular transport of EcR and reveals close similarities with some of its mammalian counterparts. In double and triple labels using several antibodies, immunohistochemistry, and confocal laser scanning microscopy, we observed co-localization of EcR with the microtubules (MTs). Treatments with either the MT-stabilizing agent taxol or with colchicine, which depolymerizes MTs, resulted in considerable reduction in nuclear EcR with a concomitant increase in cytoplasmic EcR suggesting that MT disruption inhibits receptor accumulation in the nucleus. EcR also co-localizes with the chaperone Hsp90, the immunophilin FKBP52, and the light chain 1 of the motor protein dynein. All these factors also co-localize with MTs. We propose that in *Rhodnius*, EcR exerts its genomic effects by forming a complex with Hsp90 and FKBP52, which uses dynein on MTs as a mechanism for daily nucleocytoplasmic shuttling. The complex is transported intact to the nucleus and dissociates within it. We propose that EcR utilizes the cytoskeletal tracks for movement in a manner closely similar to that used by the glucocorticoid receptor. We also observed co-localization of EcR with mitochondria which suggests that EcR, like its mammalian counterparts, may be involved in the coordination of non-genomic responses of ecdysteroids in mitochondria.

Keywords: microtubules, Hsp90, immunophilin, dynein, nucleocytoplasmic receptor shuttling, mitochondria, steroid hormone, *Rhodnius*

INTRODUCTION

Ecdysteroids, the steroid hormones of insects, coordinate a wide variety of developmental and physiological processes by binding to a specific cellular receptor protein called the ecdysteroid receptor (EcR) and regulate tissue- and stage-specific gene transcription. EcR is a ligand-activated transcription factor and a member of the steroid receptor superfamily (reviewed by Henrich, 2009). The functional ecdysone receptor in insects is a heterodimer of the EcR protein and a RXR homolog, Ultraspiracle (Usp; review by Spindler et al., 2009). EcR and Usp and their isoforms have been cloned from many insects and other arthropods and their differential expression is considered a major factor in regulation of the diversity of cellular responses to ecdysteroids during development (review by Riddiford et al., 2003). There is an extensive literature on the molecular structure, mechanisms of partnership with Usp and transcriptional activity of EcR (e.g., reviews by Henrich, 2009; Nakagawa and Henrich, 2009; Spindler et al., 2009). In mammals, steroid receptors and most of the nuclear factors involved in signaling cascades are continually shuttling between the nucleus and the cytoplasm (review by Echeverria and Picard, 2010). EcR possesses both nuclear localization and nuclear export signals (Gwózdź et al., 2007) and interacts with exportin 1 (Betanska et al., 2011). The

presence of cytoplasmic EcR in insects has been noted but no significance has been attributed to it (Lammerding-Köppel et al., 1998; Gwózdź et al., 2007; Nieva et al., 2007; Betanska et al., 2011). The only evidence that EcR undergoes shuttling derives from evidence in *Rhodnius prolixus* (Vafopoulou and Steel, 2006). More recently, it was found that the orphan nuclear receptor DHR4 also undergoes nucleocytoplasmic shuttling in prothoracic gland (PG) cells of *Drosophila* (Ou et al., 2012) suggesting that shuttling of nuclear receptors may be a common phenomenon in insects.

Rhodnius is a historically favored model system for studies of the hormonal control of insect development (Wigglesworth, 1985). A blood meal is required by each stage to initiate development to the next stage, which results in remarkable synchrony in a group of insects fed simultaneously throughout the 21-days of larval-adult development. This synchrony results in unmatched precision of timing of developmental events. It has also enabled this laboratory to identify the first circadian rhythms in insect hormones, particularly in the levels of the steroid molting hormones (ecdysteroids; Ampleford and Steel, 1985; Vafopoulou and Steel, 1991; review by Steel and Vafopoulou, 2006). Recently we also showed that EcR shuttles between nucleus and cytoplasm of several cell types and that this shuttling occurs with a circadian rhythm.

The abundance of EcR in the nuclei peaks during the night and decays during the day, whereas the abundance in the cytoplasm shows an inverse trend and peaks during the day and reaches low levels in the night. This shuttling rhythm persists in continuous darkness, emphasizing its circadian nature (Vafopoulou and Steel, 2006). The circadian rhythm of shuttling is in synchrony with the circadian rhythm of circulating ecdysteroids (Vafopoulou and Steel, 2006; Vafopoulou, 2009). Circadian shuttling had not been seen previously in any animal. The present paper confirms these initial findings but also shows that shuttling can be restricted to a period of only a few of the 21-days of development in certain cell types, but occurs on every day of development in others.

The mechanisms underlying EcR transport within cells has never been studied. We proposed recently, using double immunolabels, that EcR may utilize molecular machinery involving cytoskeletal tracks, similar to vesicle transport (Vafopoulou, 2009). The cytoskeleton has been implicated as a system for targeted movement of several mammalian steroid receptors. The primary objective of the present article is to investigate the relationship between EcR in the cytoplasm and the motor machinery of microtubules (MTs) and mitochondria in several cell types of *Rhodnius*. We report that EcR in the cytoplasm becomes co-localized with both the chaperone Hsp90 and co-chaperone immunophilin FKBP52 and also with the light chain 1 of the motor protein dynein of microtubules (MTs) and tubulin of MTs, indicating that EcR may form a complex with Hsp90 and FKBP52, similar to that of its mammalian counterparts. This complex may use dynein as the motor protein on MTs for targeted movement to the nucleus. This movement system is very similar to that utilized by the glucocorticoid receptor (GR). We also found that the inferred EcR–Hsp–FKBP52 complex shuttles intact into the nucleus and that EcR dissociates from the chaperones inside the nucleus. These findings bring EcR into closer alignment with the more thoroughly analyzed mammalian steroid hormones.

A second objective of the present work was to examine relationships between EcR and cytoplasmic organelles, to identify potential non-genomic roles for cytoplasmic EcR. Many examples of rapid actions of ecdysteroids cannot be explained by genomic actions and imply potential non-genomic actions of ecdysteroids (reviewed by Schlattner et al., 2006), which indicate a functional significance for the presence of EcR in the cytoplasm. Many actions of ecdysteroids are rapid and transient and usually involve electrochemical changes at the cell membrane (review by Schlattner et al., 2006). Membrane-bound molecules that appear to be related to conventional EcR have been reported (Elmogy et al., 2004, 2007). We reported recently that EcR associates with mitochondria in the cytoplasm of PG cells of *Rhodnius* (Vafopoulou, 2009). Here, we report co-localization of cytoplasmic EcR with mitochondria in all cell types studied, showing that the mitochondria are a potential site for non-genomic actions of ecdysteroids.

MATERIALS AND METHODS

ANIMALS

Fifth (last) larval instar males of *R. prolixus* were raised at 28°C in a 12-h light:12 h dark regime. Animals exist in a state of arrested development until given a blood meal, which initiates larval–adult development. The day of feeding was designated day 0. Days of

development were counted from the day of feeding. Ecdysis is gated with a median on day 21. Tissues were dissected at day 13 after a blood meal.

ANTIBODIES, PROTEINS, AND REAGENTS

A mouse monoclonal EcR antibody (9B9) was purchased from Developmental Studies Hybridoma Bank (University of Iowa). This antibody detects an epitope between residues 127 and 354 of *Manduca sexta* EcR; these sequences are present in all EcR isoforms of *Manduca*, hence they were designated EcR-common (Fujiwara et al., 1995; Jindra et al., 1996). This antibody has been used previously to localize EcR in PG cells (Vafopoulou, 2009). Several lines of evidence validated the specificity of this antibody in recognizing the EcR of *Rhodnius*. First, this antibody recognizes only three proteins in *Rhodnius* PGs on Western blots at 79, 64, and 56 kDa (Vafopoulou, 2009). Proteins of closely similar molecular masses to those above were also identified in various *Rhodnius* tissue extracts using two other antibodies (15C3 and 10F1) which were also produced against the common region of *Manduca* EcR (Vafopoulou et al., 2005). These three immunoreactive proteins possess very similar molecular masses to EcR isoforms reported in other insects and have been considered to represent the isoforms of *Rhodnius* EcR (references in Vafopoulou et al., 2005; Vafopoulou, 2009). Upregulation of EcR was seen with all three antibodies in response to an increase in ecdysteroid levels *in vivo* and *in vitro* (Vafopoulou et al., 2005; Vafopoulou, 2009), as is expected for ligand inducible receptors such as EcR (Henrich, 2009). The 9B9 antibody was used immunohistochemically to demonstrate a circadian rhythm in abundance and cytoplasmic location of EcR in PGs (Vafopoulou, 2009). This circadian rhythm was of the same phase and period length as had been reported earlier using the other two EcR antibodies (Vafopoulou and Steel, 2006). We conclude that all three antibodies recognize the native *Rhodnius* EcR. This antibody was used at a 1:1000 dilution.

A rabbit polyclonal antibody against the whole human Hsp90 was purchased from Stressgen (Enzo Life Science International, Plymouth Meeting, PA, USA) and was used at a 1:250 dilution. This antibody recognizes a protein of about 90 kDa in samples from many eukaryotes, including *Drosophila* (supplier data). Blast searches revealed that Hsp90 is a highly conserved protein among animals; it displays a 60–80% amino acid identity between a variety of mammals and insects. The nucleotide sequences of the Hsp90 genes of insects are highly conserved showing 80–99% identities (see references in Zhang and Denlinger, 2010; Shu et al., 2011). A Blast search of the *Rhodnius* trace archive revealed two sequential, long stretches (total of about 1000 nucleic acids) that share about 73% identity with the Hsp90 genes of humans and insects.

One class of Hsp90-binding co-chaperones is the FK506 immunophilin FKBP52. A rabbit polyclonal antibody against amino acids 1–50 at the amino end of human FKBP52 was purchased from Novus Biologicals (Littleton, CO, USA) and was used at a dilution of 1:100. A Blast search revealed that human FKBP52 shares about 50% amino acid identity with its insect homologs; the amino acid identity in the 1–50 sequence ranges between 30 and 63% between humans and several insect species like *Drosophila*, *Bombyx*, and *Apis*. A Blast search of the *Rhodnius*

trace archive revealed two sequential, highly conserved regions that share 85–100% identity with the coding sequence of the 50 amino acids at the amino end of human FKBP52.

A rabbit polyclonal antibody (DNLL1/2) against the whole molecule (89 amino acids) of human dynein light chain I (DNLL1) was purchased from Santa Cruz Biotechnology (Santa Cruz, CA, USA) and was used at a dilution of 1:100. This antibody also recognizes the closely similar DYNLL2 in humans. DYNLL1 is highly conserved across species. For example, the amino acid sequence of *Drosophila* DYNLL1 shares about 92% similarity with the DYNLL1 of humans, *Chlamydomonas reinhardtii*, and *Caenorhabditis elegans* (Dick et al., 1996). A Blast search of the *Rhodnius* trace archive revealed five sequential regions that share 78–93% identity with the coding sequences of human DYNLL1.

Native human Hsp90 (Enzo Life Science International, Plymouth Meeting, PA, USA), full-length, recombinant, His-tagged FKBP52 (Novus Biologicals, Littleton, CO, USA), and lysate of human DYNLL1 from transfected 293 T cells (Santa Cruz Biotechnology, Santa Cruz, CA, USA) were used as positive controls on Western blots. Each of these proteins produce single bands when they immunoreact with their respective antibodies listed above (manufacturers' data sheets); their respective migration positions correspond to approximately 90 kDa for Hsp90, 54 kDa for FKBP52, and 10 kDa for DYNLL1.

MTs were labeled with a rat monoclonal antibody against tyrosylated α -tubulin (YL 1/2) which was purchased from AbD Serotec (Raleigh, NC, USA) and was used at a 1:400 dilution. This antibody specifically recognizes a linear sequence with an aromatic residue at the C-terminus, with two adjacent, negatively charged, amino acids; this sequence is represented by Gly-Gly-Tyr in tyrosylated α -tubulin (manufacturer's information).

Mitochondria were labeled with a cell-permeant, mitochondria-selective fluorescent dye, MitoTracker Deep Red 633, which has been used before to localize mitochondria in *Rhodnius* PGs (Vafopoulou, 2009). Acidic organelles, including lysosomes, were labeled with a cell-permeant, fluorescent dye LysoTracker Red DND-99. Both dyes were purchased from Molecular Probes (Eugene, OR, USA) and used according to manufacturer's instructions.

For single and double label immunohistochemistry the following fluorescent secondary antibodies were used: an Alexa fluor 488 (green) goat anti-mouse IgG was used to localize EcR; an Alexa fluor 555 (red) goat anti-rat IgG was used to localize tubulin; an Alexa fluor 555 (red) goat anti-rabbit IgG was used to localize Hsp90 and FKBP52. For triple label experiments, an Alexa fluor 488 (green) goat anti-mouse IgG was used to localize EcR, an Alexa fluor 555 (red) goat anti-rat IgG was used to localize tubulin and an Alexa fluor 633 (far red) goat anti-rabbit IgG was used to localize DNLL1. All secondary antibodies were purchased from Molecular Probes (Eugene, OR, USA) and were used at 1:200 dilutions.

Taxol (paclitaxel) and colchicine were purchased from Sigma-Aldrich (St. Louis, MO, USA). Vectashield mounting medium was purchased from Vector Laboratories (Burlingame, CA, USA). PVDF filters were purchased from Millipore (Billerica, MA, USA). Ten percent SDS-PAGE gels, 15% Tris-Tricine gels, and kaleidoscope pre-stained standards were purchased from Bio-Rad (Hercules, CA, USA). Amicon Ultra-0.5 ml (Ultracel-PL membrane)

centrifugal tubes for protein purification and concentration were purchased from Millipore (Billerica, MA, USA). Four types of tubes were used for protein filtration with molecular sizes cut-off at 10, 30, 50, and 100 kDa.

IMMUNOHISTOCHEMISTRY AND IMAGE COLLECTION

Tissues were fixed according to an established protocol (Vafopoulou, 2009). In order to preserve the cytoskeleton and have good visualization of nuclear and cytoplasmic EcR, tissues were dissected in PBS (pH 7.4) containing 10 mM EGTA and 1 mM MgSO₄; MT assembly was induced by decreasing Ca⁺⁺ concentration by addition of the chelating agent EGTA. In single label experiments with anti-EcR (to demonstrate the presence of cytoplasmic EcR), tissues were incubated in PBS at 37°C for 30 min to allow MTs to polymerize. In double label experiments, co-localization of EcR with MTs or mitochondria was visualized in tissues where MTs were stabilized in live cells with 10 μ M taxol in PBS for 1 h at 37°C, prior to fixation. Taxol was obtained from a 10-mM stock solution in dimethyl sulfoxide (DMSO). DMSO was added to aid dissolution of taxol. Likewise, in order to ascertain co-localization of anti-EcR with mitochondria, the taxol-treated tissues were incubated for 45 min at 37°C in 400 nM MitoTracker Deep Red 633, a cell-permeant fluorescent probe specific for mitochondria. This probe was well retained following cell fixation. In order to ascertain co-localization of EcR with acidic organelles (like lysosomes), tissues were incubated for 45 min at 37°C in 50 nM LysoTracker Red DND-99. All tissues were then fixed in freshly prepared 4% paraformaldehyde containing 0.15% glutaraldehyde (2 h at 37°C). Addition of glutaraldehyde to the fixative enhances preservation of MTs by cross-linking them inside the cell. The tissues were washed thoroughly in PBS and then pre-incubated in 5% control serum containing 1% Triton X-100 as a permeabilizing agent followed by secondary antibody incubation (2 h at room temperature). Tissues were mounted in Vectashield.

The pattern of co-localization of EcR with MTs was compared in tissues where MTs were depolymerized with colchicine. Depolymerization was achieved by incubating live cells with 10 μ M colchicine in PBS for 1 h at room temperature. For controls, the primary antibodies were replaced with non-immune serum or the secondary antibodies were replaced with PBS, or MitoTracker Deep Red 633 was omitted. Fluorescence levels in controls were indistinguishable from the background and autofluorescence was not detected. Fluorescence resulting from antibody binding to cells is called here EcR, Hsp90, FKBP52, DYNLL1, or tubulin fluorescence depending on the antibody. Ten animals were dissected at each indicated time point.

Digital optical sections at 1 μ m distances were viewed with an Olympus FV300 confocal laser scanning microscope. Red and green fluorescence were scanned using separate channels to excite Alexa fluor 488 at 488 nm, Alexa fluor 555 at 568 nm, and MitoTracker Deep Red 633 and Alexa fluor 633 at 644 nm. Stringent use of filter blocks was employed to prevent bleed-through between channels. Settings were kept identical for all scanning sessions. Images were processed using Image J 1.41 (NIH) and Adobe Photoshop CS5. Images were modified only to adjust contrast and merge files.

SDS-PAGE AND WESTERN BLOTS

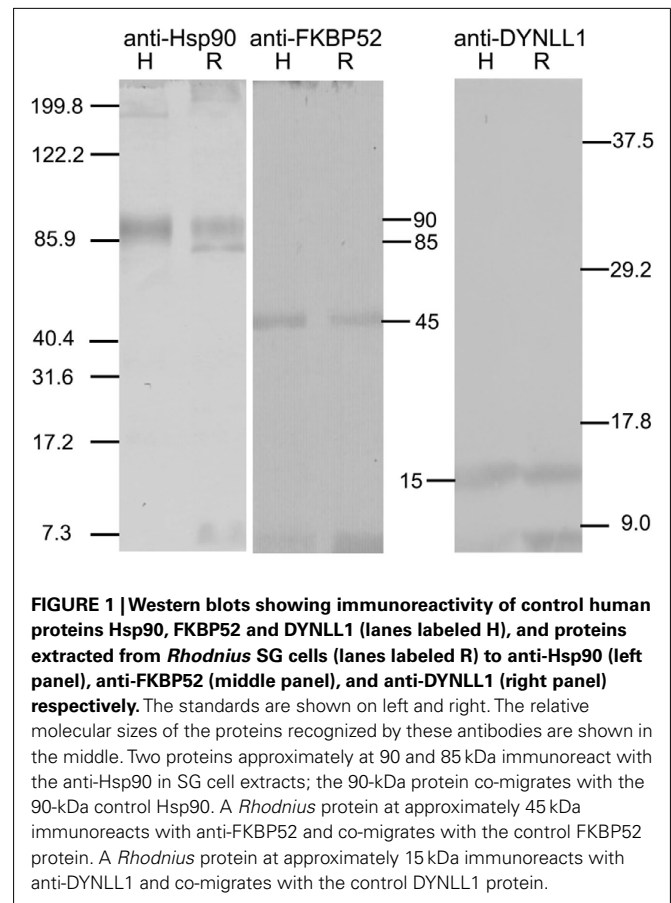
To confirm the specificities of the antibodies against proteins related to human Hsp90, FKBP52, and DYNLL1, protein samples from day 13 salivary glands (SGs) were immunoblotted. Batches of 30 SGs each were homogenized by sonication in lysis buffer (50 mM Tris-HCl pH 7.4; 150 mM NaCl, 1% Triton X-100, 1 mM EDTA, 1 mM dithiothreitol (DTT), 1 mM phenylmethyl sulfonylfluoride (PMSF), 2 µg/ml leupeptin, and 1 mg/ml each antipain, aprotinin, and pepstatin A and centrifuged at $15,000 \times g$ for 10 min at 4°C to remove cell debris. The supernatant was retrieved and fractionated into different molecular size fractions using Amicon Ultra centrifugation tubes. In order to concentrate and partially isolate the Hsp90-related proteins from other proteins, supernatants were centrifuged using a 100-kDa filter membrane. The retentate was discarded to remove proteins >100 kDa and the filtrate was re-centrifuged using a 50-kDa filter membrane to remove proteins <50 kDa. Then the retentate, which contained proteins in the range of 50–100 kDa was used on Western blots. For FKBP52, the supernatant was first centrifuged with a 50-kDa filter membrane to remove proteins >50 kDa and the filtrate was re-centrifuged using a 10-kDa filter membrane. The retentate, which contained proteins in the range of 10–50 kDa was used on Western blots. For DYNLL1, the supernatant was centrifuged using a 30-kDa filter membrane to remove all proteins >30 kDa and the filtrate was used on Western blots. 10% SDS-PAGE was used for identifying Hsp90- and FKBP52-related proteins and 15% Tris-Tricine PAGE was used for identification of DYNLL1-related proteins. Western blots were performed using standard procedures. Proteins were electrophoretically transferred onto PVDF filters. Signal detection on filters was performed using the O-dianisidine reaction. As positive controls, purified proteins for human Hsp90, FKBP52, and DYNLL1 were used.

The Western blots in **Figure 1** show that *Rhodnius* contains proteins that immunoreact with the antibodies against Hsp90 (left blot), FkBP52 (middle blot), and DYNLL1 (right blot). Two immunoreactive protein bands were revealed with anti-Hsp90, a major one at approximately 90 kDa and a minor one at approximately 85 kDa. The major 90 kDa immunoreactive band co-migrated with the single control human Hsp90 band. A single immunoreactive protein band was revealed with anti-FKBP52 that co-migrated with the single control human FKBP52 band at approximately 45 kDa. A single immunoreactive protein band was revealed with anti-DYNLL1 that co-migrated with the single control human DYNLL1 band at approximately 15 kDa. Various gels were prepared using the unused fractions from these fractionations, but were found to contain no bands that were immunoreactive with the relevant antibody. Therefore, the SG cells of *Rhodnius* contain proteins electrophoretically and immunologically related to human Hsp90, FKBP90, and DYNLL1.

RESULTS

CYCLING OF EcR IN RHODNIUS CELLS

We reported before the presence of a circadian rhythm in abundance and subcellular localization in EcR in several different cell types using a different EcR antibody (Vafopoulou and Steel, 2006) and a clear daily rhythm in PG cells using the 9B9 antibody (Vafopoulou, 2009). Presently, we confirmed the presence



of an EcR rhythm in various cell types using the 9B9 EcR antibody (**Figure 2**). Tissues which are known ecdysteroid targets (Vafopoulou et al., 2005), were dissected twice on day 13, in the middle of scotophase (7 h after lights-off) and in the middle of photophase (7 h after lights-on). In scotophase, strong and abundant nuclear EcR fluorescence was observed in all cell types (**Figures 2A,C,E,G,I,K**) accompanied by moderate (arrows in **Figures 2C,E,G**) or nil cytoplasmic EcR fluorescence, suggesting genomic effects of ecdysteroids at this time. Both PG and SG cells possess enormous polyploid nuclei carrying a large number of nucleoli (non-fluorescent areas in nuclei; **Figures 2C,E** respectively); SG cells are binucleate (**Figure 2E**). The nucleoli were not labeled with the exception of oenocytes (**Figure 2K**) suggesting that ecdysteroids may also affect nucleolar activities like rRNA synthesis in this cell type.

In contrast, in photophase, widespread distribution of EcR was evident in the cytoplasm of all cell types (**Figures 2B,D,F,H,J,L**), whereas nuclear EcR fluorescence was significantly diminished, but not entirely absent (e.g., **Figures 2B,D,H,L**). Cytoplasmic EcR usually appeared either as densely packed fluorescent dots and small rods over most of the cytoplasm (**Figures 2F,H**) or diffuse and uniform (**Figures 2B,D**). In several cell types such as the fat body cells (**Figure 2H**) and oenocytes (**Figure 2L**), EcR fluorescence exhibited a distinct pattern of accumulation around the nuclei similar to that seen with the distribution of mitochondria in

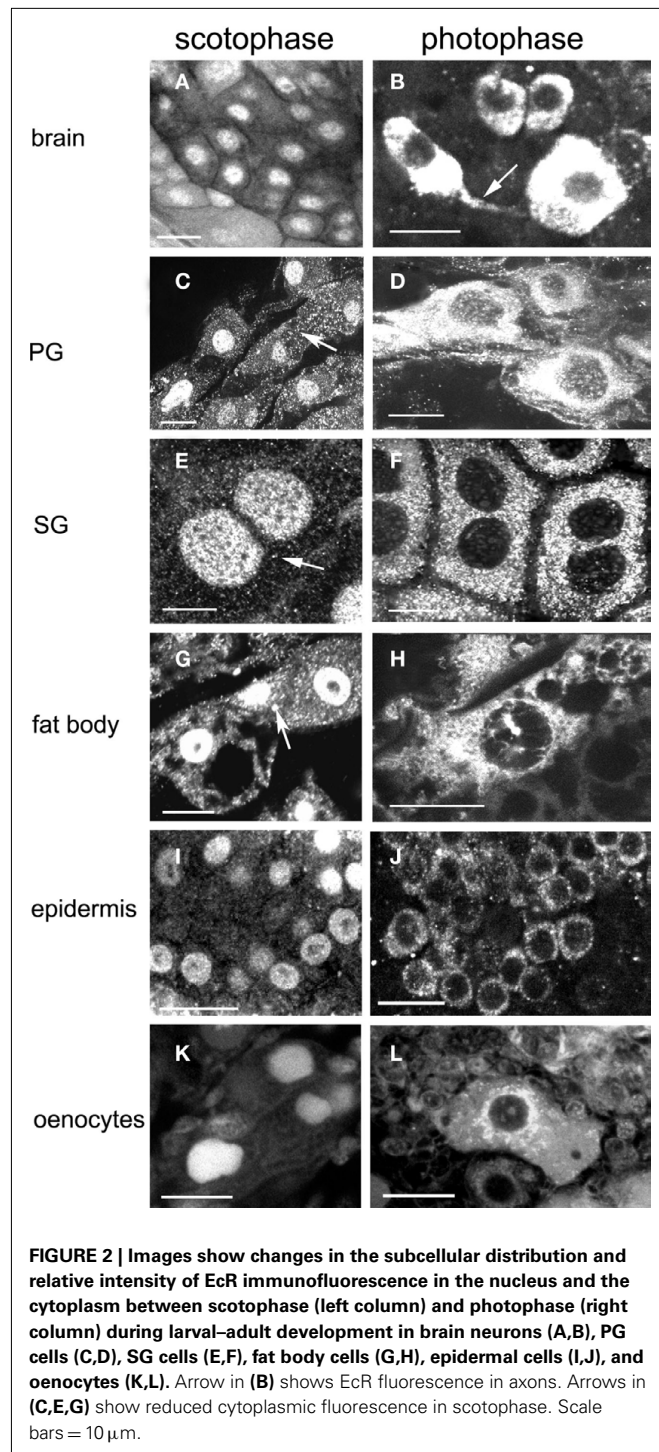


Figure 10. Importantly, EcR fluorescence was also seen in the axons of brain neurons, indicating axonal transport of EcR (Figure 2B, arrow; see Discussion). The cytoplasm of fat body cells was highly vacuolated. These vacuoles represent the areas of fat deposits that were not preserved with paraformaldehyde–glutaraldehyde and were extracted during fixation (Figures 2G,H). Two conclusions are derived from these findings: first, a clear daily rhythm of

nuclear EcR fluorescence exists in many cell types of *Rhodnius* at the beginning of the late period of larval–adult development, confirming our previous findings. Second, this daily rhythm shows daily shuttling of EcR to the nucleus.

DEVELOPMENTAL PROFILES OF EcR FLUORESCENCE IN NUCLEUS AND CYTOPLASM IN DIFFERENT CELL TYPES

Developmental profiles of EcR distribution in the cytoplasm and nuclei of the cell types described in the previous section were constructed based on cytological evaluation for the presence or absence of EcR fluorescence during the entire larval–adult development (Figure 3). Tissues were dissected throughout this period, beginning at 2 h after feeding and every 2 days thereafter until day 18; ecdysis occurred around day 21. Dissections were carried out twice a day, once in middle photophase and once in middle scotophase. These time points were selected because EcR fluorescence is confined at these times to either the nucleus or the cytoplasm (see Figure 2). At each time point, 10 animals were sacrificed and whole mounts of six different tissues were scored for the presence of EcR fluorescence in the nuclei and in the cytoplasm. Cytoplasmic EcR fluorescence was scored from the photophase tissues (light bars in Figure 3) and nuclear EcR fluorescence was scored from the scotophase tissues (dark bars in Figure 3). In both cases, fluorescence was scored as either positive (hatched regions of bars) or as negative (unhatched regions of bars). A positive score required at least one cell in each tissue sample to show fluorescence, while a negative score required all cells in each sample to be devoid of fluorescence. Therefore, the bars in Figure 3 do not imply quantitative differences. The bars show the periods of time (days) during development where nuclear and cytoplasmic EcR fluorescence is present in each of the six tissues. It is striking that this time period is tissue-specific (see below). Daily shuttling of EcR between cytoplasm and nucleus can only occur on days when both light and dark bars are hatched, showing that shuttling is constrained to different developmental times in different tissues (see below).

Two general conclusions can be made: first, within a particular cell type, nuclear EcR fluorescence was restricted to a specific developmental period. For example, abundant nuclear EcR fluorescence was apparent almost throughout development in cells of the PGs, epidermis, and fat body. In contrast, nuclear fluorescence was present during short periods of time in brain neurons, SG cells, and oenocytes. These profiles are in general agreement with previous findings and their importance to development has been discussed elsewhere (Vafopoulou et al., 2005). Second, the profiles of cytoplasmic EcR fluorescence corresponding to a particular cell type are rarely completely coincidental within a day with those of nuclear EcR fluorescence. This is the case for all cell types except PG cells in which both nuclear and cytoplasmic EcR fluorescence were present throughout development. In three cell types, brain neurons, SG cells, and oenocytes the presence of EcR fluorescence in the nuclei was brief whereas the appearance of cytoplasmic EcR fluorescence was significantly longer; in the case of brain neurons in particular, presence of cytoplasmic EcR fluorescence spanned almost throughout development. Curiously, in fat body and epidermal cells nuclear EcR fluorescence appeared almost immediately after feeding, whereas cytoplasmic EcR fluorescence appeared only 6 days later. We conclude, first that

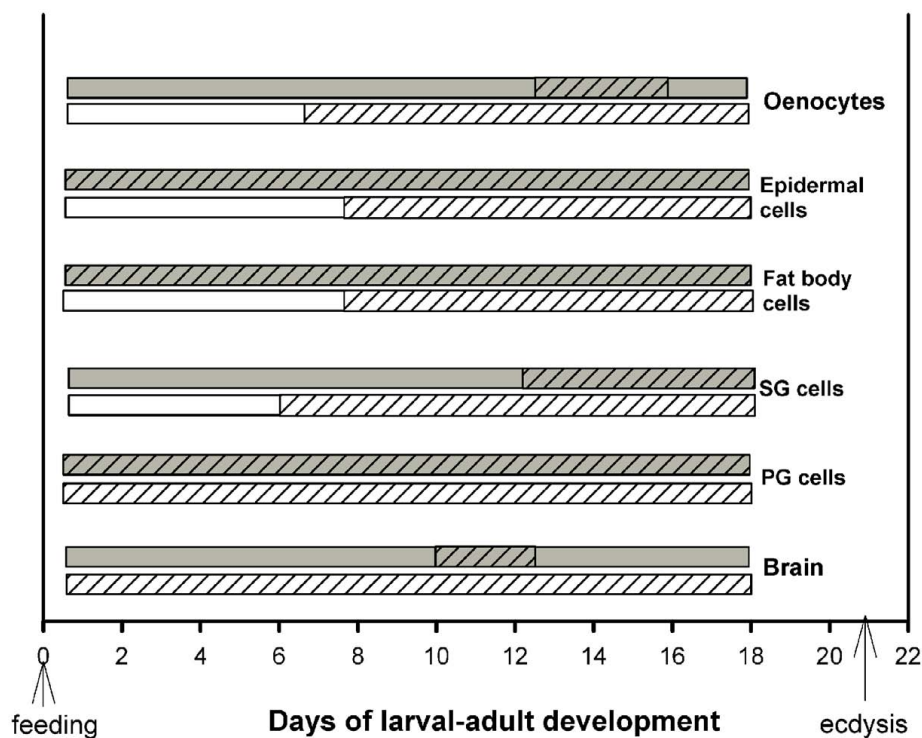


FIGURE 3 | Schematic diagram of the periods during development (in days after feeding) during which cytoplasmic (light bars; day) and nuclear (dark bars; night) EcR fluorescence was found in six different tissues. Hatched areas of each bar show the length of time (in days) during which EcR fluorescence is seen in the cytoplasm during the day and in the

nucleus during the night of each tissue. Note that EcR is present for different lengths of developmental time in different tissues. Cytoplasmic-nuclear shuttling of EcR is necessarily confined to the developmental times when both the light and dark bars are hatched, i.e., EcR is present in both compartments during the same 24 h period. For details, see text.

presence of EcR in the cytoplasm is a widespread phenomenon in *Rhodnius* cells. Second, during larval–adult development nuclear and cytoplasmic EcR are seen in the same 24 h period only at certain cell-specific periods during the course of development. This observation indicates that daily shuttling between cytoplasm and nucleus (see Cycling of EcR in *Rhodnius* cells) is also confined to certain specific time periods during development and that these periods vary between cell types. These periods vary in duration and their position on the developmental time scale depending on the cell type. In general, during development, EcR fluorescence is found more frequently in the cytoplasm than in the nucleus. The finding of cytoplasmic EcR throughout extended periods of development raises interesting questions as to the significance of EcR in the cytoplasm of *Rhodnius* cells. The spatial relationship of EcR with cytoplasmic organelles suggests functions for cytoplasmic EcR.

CO-LOCALIZATION OF EcR WITH MTs

The spatial relationship of cytoplasmic EcR fluorescence with MTs was determined in double label experiments using the EcR antibody and an antibody against tyrosinated α -tubulin (Figures 4 and 5). Tissues were obtained from scotophase animals at day 13. Several types of cells were pre-treated with taxol which stabilizes MTs against disassembly and promotes excess assembly. Taxol caused a marked reduction in the relative intensity of EcR fluorescence in

the nucleus (compare left column of Figure 2 with left columns in Figures 4 and 5). Therefore, it appears that MT stabilization inhibits the accumulation of EcR within the nucleus.

Ecdysteroid receptor fluorescence is shown in the left column (green), tubulin fluorescence is shown in the right column (red). Co-localization is shown as yellow/orange in the merged column; the cytoplasmic areas enclosed in small white rectangles in the merged column are shown enlarged in the enlarged column from the left. Extensive networks of MTs were revealed with anti-tubulin label in PG cells (Figures 4A–C), brain neurons (Figures 4D–I), SG cells (Figures 4J–L), fat body cells (Figures 4M–O), oenocytes (Figures 5A–F), and epidermal cells (Figures 5D–F). In epidermal cells (Figure 5E) and oenocytes (Figures 5C,F) in particular, MTs were arranged radially from well defined centrosomes. Strong cytoplasmic EcR fluorescence is seen in all cell types, which exhibited a closely similar distribution to that of MTs and extensive co-localization with MTs (merged columns in Figures 4 and 5); this is particularly evident in oenocytes (Figures 5A,D) and epidermal cells (Figure 5D), where specks of EcR fluorescence follow closely the radial pattern of MTs within the cell bodies (Figures 5B1,E1, arrows). The enlarged images (enlarged columns) show clearly that EcR fluorescence forms punctate spots that are aligned along MTs. Therefore, an intimate spatial relationship exists between EcR fluorescence and tubulin fluorescence suggesting a potential association between

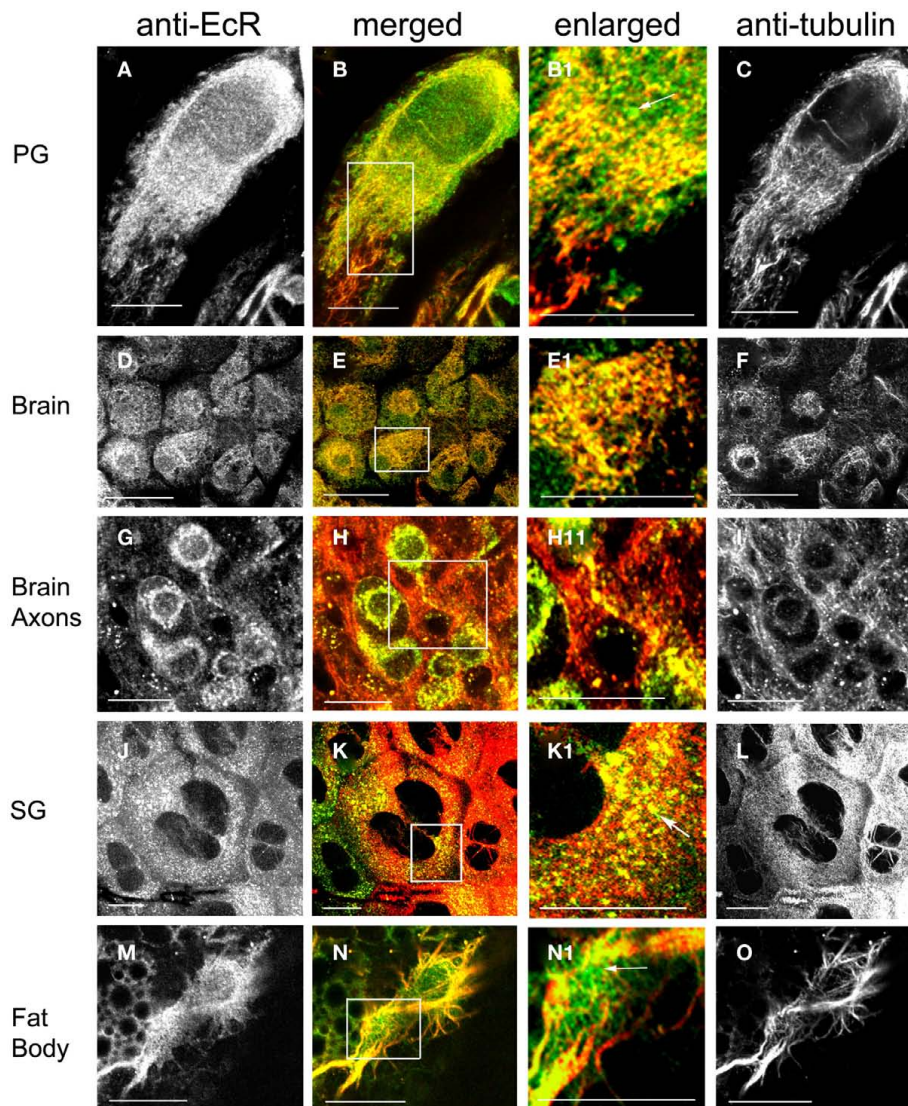


FIGURE 4 | Cells double-labeled with anti-EcR (left column, green) and anti-tubulin (right column, red). Merged images of left and right are shown in the merged column. Co-localization is shown as yellow/orange. Cells were pre-incubated with the MT-stabilizing agent taxol. PG cells (**A–C**), brain neurons (**D–I**), SG cells (**J–L**), fat body cells (**M–O**). Areas enclosed in the white lined boxes in (**B,E,H,K,N**) are

shown in the enlarged column as (**B1,E1,H1,K1,N1**) respectively; these images show details of co-localization of EcR fluorescence with tubulin fluorescence on MTs. Note the alignment of EcR fluorescence with MTs in these images; this is particularly evident in (**H1**) that shows an axon. Arrows in (**B1,K1,N1**) show that not all EcR fluorescence co-localizes with MTs. Scale bars = 10 μ m.

EcR and MTs. This co-localization between MTs and EcR was also observed in axons of brain neurons shown in **Figure 4H1**, suggesting that EcR may be moved along axons (above) by MTs. However, it should be noted that not all cytoplasmic EcR fluorescence co-localized with MTs; this is evident in **Figures 4B1,K1,N1** and **5B1,E1** (arrows).

Pre-treatment of scotophase cells with colchicine, a MT disrupting agent, disrupted the MT network, and anti-tubulin fluorescence became re-distributed into discrete cytoplasmic pockets in the form of bright dots (**Figure 6**, right column). The co-localization of tubulin and EcR fluorescence persisted in these

pockets (**Figure 6**, merged column). Critically, the nuclear EcR fluorescence was greatly diminished (**Figure 6**, left column). This pattern of distribution of EcR fluorescence resembles that of the photophase (see **Figure 2**) rather than the scotophase. Therefore, disruption of MTs causes a loss of nuclear EcR fluorescence (like that with stabilization of MTs by taxol) and a re-distribution of cytoplasmic EcR fluorescence into the photophase configuration rather than that of the scotophase. We conclude that some EcR co-localizes with MTs in various cell types of *Rhodnius*, suggesting that EcR may be transported within the cytoplasm using the MT network.

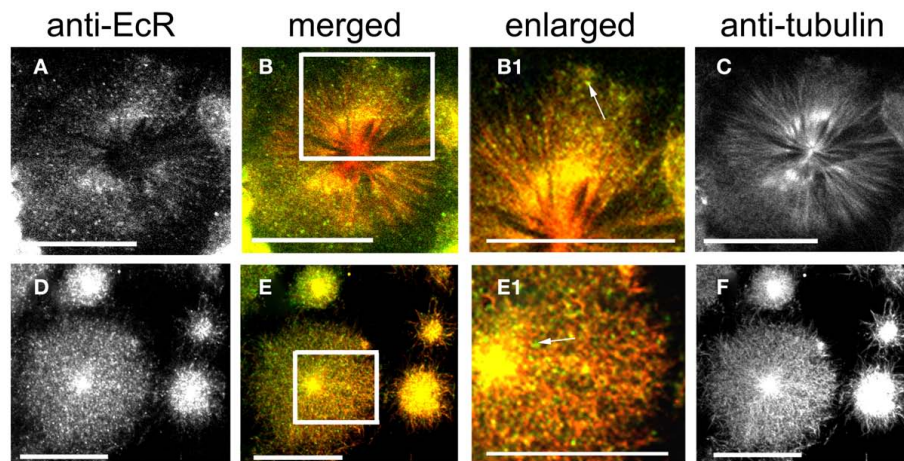


FIGURE 5 | Cells double-labeled with anti-EcR (left column, green) and anti-tubulin (right column, red). The merged column shows merged images of left and right. Co-localization is shown as yellow/orange. Cells were pre-incubated with the MT-stabilizing agent taxol. Large cells are oenocytes and small cells are epidermal cells. Both rows show different aspects of oenocytes. (C,F) Show the radial

arrangement of MTs from a well defined centrosome. Areas enclosed in the white lined boxes in (B,E) are shown in the enlarged column as (B1,E1) respectively. Note the co-localization of EcR fluorescence with MTs (yellow specks) in (B1,E1). Some EcR fluorescence does not associate with MTs [green specks, arrows in (B1,E1)]. Scale bars = 10 μ m.

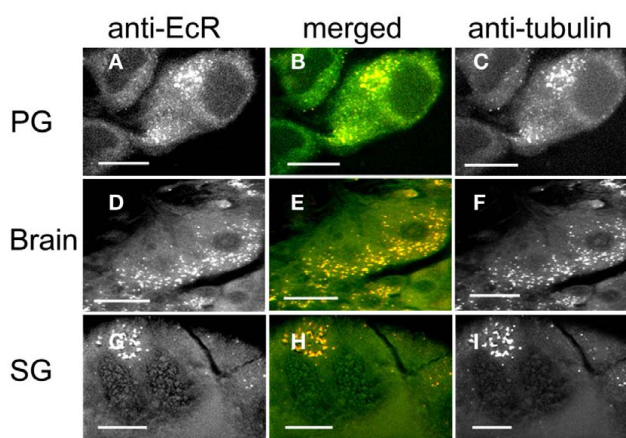


FIGURE 6 | PG cells (A–C), brain neurons (D–F), and SG cells (G–I) pre-treated with colchicine to disrupt MTs and double-labeled with anti-EcR (left column, green) and anti-tubulin (right column, red). Co-localization is shown as yellow/orange in the merged images of left and right in the middle column. Note the disruption of MTs in (C,F,I), which appear as fluorescent specks and re-distribution of tubulin fluorescence. Co-localization is retained after colchicine treatment (B,E,H). Scale bars = 10 μ m.

CO-LOCALIZATION OF EcR WITH THE MOLECULAR CHAPERONE Hsp90

Co-localization of EcR with the molecular chaperone Hsp90 was examined in SG cells. *Rhodnius* SGs consist of a single lobe which is composed of an epithelial monolayer of flat binucleate cells (about 6–8 μ m thick) surrounding the lumen that contains the salivary secretions. These cells are very large (about 40 μ m in diameter) which makes them ideal for cytological analysis of their cytoplasmic constituents. The cellular distribution of Hsp90 (Figure 7 right, red) and its co-localization with EcR (Figure 7 left, green)

were both revealed in double label experiments with antibodies against both proteins (Figures 7A–L). Hsp90 was seen in abundance forming a punctate pattern in the cytoplasm of cells in photophase (Figures 7I,L,M), where much, but not all, Hsp90 co-localized with EcR (EcR seen in Figures 7G,J). Co-localization is seen in particular in the merged images in Figures 7H,K and the enlarged images in Figures 7H1,K1; the abundance of Hsp90 in these images agrees with its ubiquitous presence in animal cells. Likewise, not all of the green specks of EcR fluorescence co-localized with the red specs of Hsp90 fluorescence (Figure 7H1), showing that only a portion of cytoplasmic EcR is associated with Hsp90. This close spatial relationship of EcR with Hsp90 suggests that an EcR–Hsp90 receptor-chaperone complex may be formed, as is common with other steroid receptors (see Discussion).

In nuclei from the scotophase, Hsp90 was found as a diffuse stain in many cells of the same sample (Figure 7F), (but not all, Figure 7C), where it co-localizes with EcR fluorescence (yellow/green nuclei in Figure 7E). When co-localization of Hsp90 and EcR was seen in nuclei, Hsp90 presence in the cytoplasm was considerably reduced (Figure 7E1; compare with Figure 7B1) and no co-localization was seen with EcR, suggesting that most EcR had been transported to the nucleus during the scotophase (compare Figures 7A,D with Figure 7G, which shows nuclei in photophase). Images Figures 7C,F suggest the existence of two different states of Hsp90 in nuclei, one potentially associated with EcR and the other potentially dissociated from it.

In the cytoplasm, pre-treatment with taxol caused a dramatic re-organization of both EcR dots (Figure 7J) and Hsp90 dots (Figure 7L); both formed elongated rods arranged in lines that presumably correspond to MTs. Even after taxol treatment, the cytoplasmic co-localization of Hsp90 with EcR was maintained (Figures 7K,K1). Double labels with anti-Hsp90 and anti-tubulin revealed a co-localization of Hsp90 (Figure 7M) with MTs

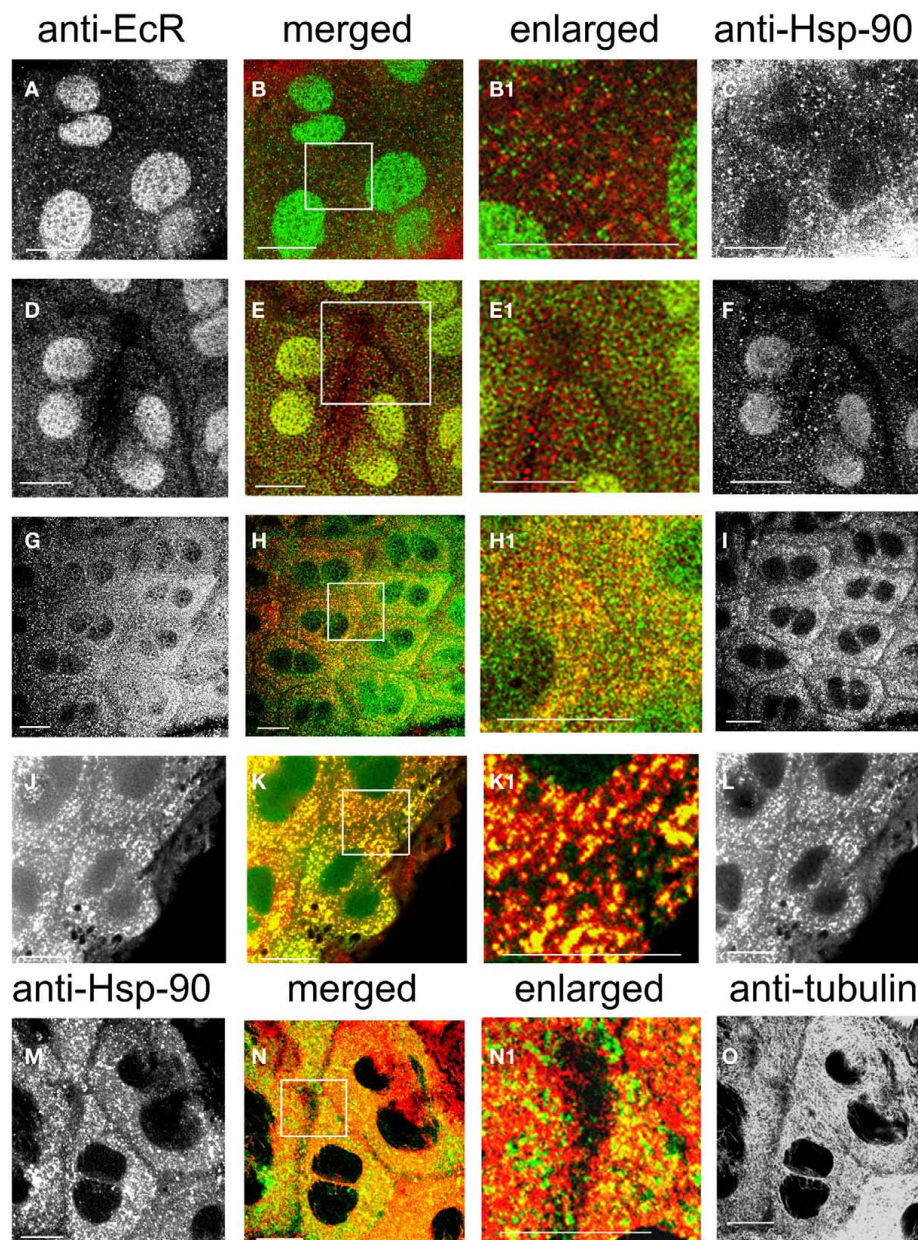


FIGURE 7 | SG cells double-labeled with anti-EcR and anti-Hsp90 (A–L). Anti-EcR is shown on the left column (green) and anti-Hsp is shown on the right column (red). (M–O) Shows double labels with anti-Hsp90 (left, green) and anti-tubulin (right, red). The merged column shows the merged images of left and right. Co-localization is shown as yellow/orange. Areas enclosed in the white lined boxes in (B,E,H,K,N) are shown in the enlarged columns as in (B1,E1,H1,K1,N1) respectively; these images show details of co-localization of EcR fluorescence with Hsp90 fluorescence (B1,E1,H1,K1) and details of

co-localization of Hsp90 fluorescence with anti-tubulin (N1). (A–F) Show SG cells in scotophase and (G–I) shows cells in photophase. Note absence of co-localization in the cytoplasm in scotophase [abundance of red and green specks in (B1,E1)] and widespread co-localization in photophase [abundance of yellow/orange specks in (H1)]. (J–L) Shows cells pre-treated with taxol. Note the arrangement of co-localized EcR and Hsp90 fluorescence in yellow lines (K1). In (N1), note co-localization of Hsp90 fluorescence with tubulin fluorescence (yellow specks along MTs). Scale bars = 10 μ m.

(Figure 7O) as seen in Figure 7N; this co-localization was in the form of fine lines along the tracks of MTs as seen in the enlarged image in Figure 7N1. Therefore, the putative EcR–Hsp90 complex is co-localized with the MT network in the cytoplasm of *Rhodnius* SG cells.

CO-LOCALIZATION OF EcR WITH THE IMMUNOPHILIN FKBP52

The cellular distribution of immunophilin FKBP52 (Figures 8C,F,I, red) and its spatial relationship with EcR (Figures 8A,D,G, green) was revealed with double labels using antibodies against both proteins (Figures 8A–I). FKBP52 fluorescence appears punctate

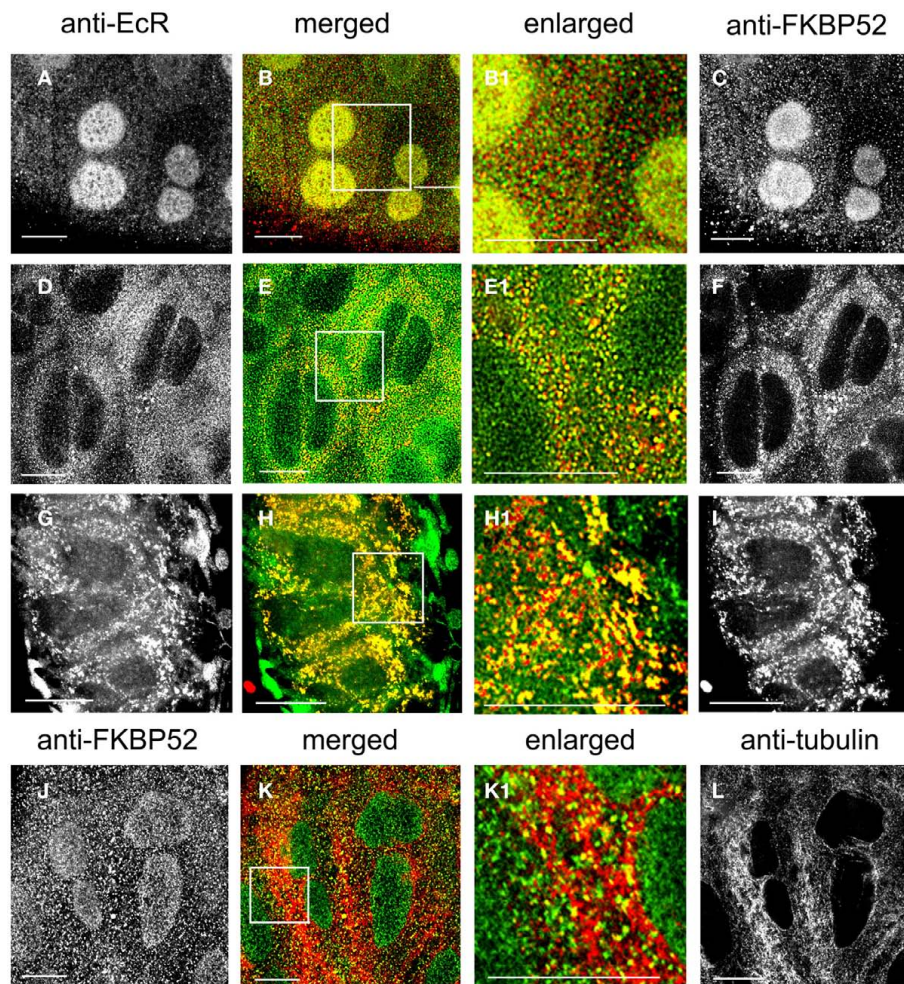


FIGURE 8 | (A–I) Show SG cells double-labeled with anti-EcR (left column, green) and anti-FKBP52 (right column, red). **(J–L)** Show SG cells double-labeled with anti-FKBP52 **(J)**, green] and anti-tubulin **(L)**, red]. The merged column shows merged images of left and right. Co-localization is shown as yellow/orange. Areas enclosed in the white lined boxes in **(B,E,H,K)** are shown enlarged in **(B1,E1,H1,K1)** respectively; these images show details of co-localization of EcR fluorescence with FKBP52 fluorescence **(B1,E1,H1)** and details of co-localization of FKBP52 fluorescence with anti-tubulin **(K1)**.

(A–C) Show scotophase and **(D–F)** show photophase. Note the absence of cytoplasmic co-localization of EcR fluorescence and FKBP52 fluorescence in scotophase and its presence in nuclei [red and green specks in **(B1)**]. In contrast, note extensive co-localization in the cytoplasm in photophase and its absence from nuclei [yellow specks in **(E1)**]. **(G–I)** Show cells pre-treated with taxol. Note the alignment of yellow dots and rods in lines in **(H1)**. In **(K1)**, note co-localization of FKBP52 fluorescence with anti-tubulin (yellow specks along MTs). Scale bars = 10 μ m.

and broadly distributed throughout the cytoplasm in photophase (**Figure 8F**) and is partially co-localized with the green EcR dots (**Figure 8E**). The enlarged image in **Figure 8E1** clearly shows yellow dots, indicating a co-localization of EcR and FKBP52 in the cytoplasm of SG cells. In the nucleus, co-localization is seen in the scotophase, where fluorescence of FKBP52 (**Figure 8C**) co-localizes with that of EcR (**Figure 8A**) as shown in **Figures 8B,B1**, where nuclear stain appears as diffuse yellow/green. In the scotophase, little, or no EcR fluorescence remains in the cytoplasm (see **Figure 8B1**), and the remaining FKBP52 fluorescence appears as red dots (free FKBP52; compare **Figure 8E1** with **Figure 8B**). Two conclusions can be drawn from these findings: first, EcR may form a complex with the co-chaperone FKBP52 in photophase and second, this complex seems to translocate to the nucleus in

scotophase. When photophase SG cells were pre-treated with taxol, the previously scattered dots of EcR and FKBP52 seen in the cytoplasm of untreated cells (see **Figures 8E,E1**), became re-organized to elongated rods (**Figure 8G** for EcR fluorescence and **Figure 8I** for FKBP52 fluorescence) that aligned in tandem in the direction of MTs as seen in the merged images in **Figures 8H,H1**. This alignment of EcR–FKBP52 into rows suggests they may attach to MTs. This inference is supported by double labels of scotophase SGs with anti-FKBP52 (**Figure 8J**) and anti-tubulin (**Figure 8L**), in which FKBP52 fluorescence co-localizes with MTs as shown in the merged image in **Figure 8K** and the enlarged image in **Figure 8K1**. These observations suggest that FKBP52 is probably attached to MTs. We conclude that the inferred EcR–FKBP52 complex co-localizes with MTs.

CO-LOCALIZATION OF EcR WITH LIGHT CHAIN 1 OF DYNEIN

The co-localization of EcR with the light chain 1 of dynein, DYNLL1, was revealed in photophase SG cells with triple labels using antibodies against EcR (Figure 9A; green), tubulin (Figure 9B; red) and dynein (Figure 9C; blue). Staining of cytoplasmic dynein was punctate throughout the cytoplasm (Figure 9B) and co-localized with both EcR and tubulin (Figure 9D). Co-localization of all three appears as white dots throughout the cytoplasm, which appear to follow the tracks of the MT as seen in the enlarged area in Figure 9D1. It is therefore probable that EcR co-localizes with both DYNLL1 and tubulin.

CO-LOCALIZATION OF EcR WITH MITOCHONDRIA

The spatial relationship of EcR and mitochondria was examined in brain neurons (Figures 10A–C), PGs (Figures 10D–F), SGs (Figures 10G–I), epidermal cells (Figures 10J–L), and fat body cells (Figures 10M–O) in double label experiments using anti-EcR (left column, green) and MitoTracker Deep Red 633 (right column, red); co-localization is shown as yellow/orange in the merged column. All dissections were carried out in photophase. Mitochondria were widely distributed in the cytoplasm of all cells forming fluorescent webs with a relatively high density in the perinuclear region; this is particularly evident in PG cells (Figure 10F), epidermal cells (Figure 10L), and fat body cells (Figure 10O). The distribution of mitochondria in fixed cells closely reflects that in live cells, where the mitochondria tend to aggregate in the perinuclear area of cells, showing that fixation preserved organelle structure satisfactorily (not shown). In all cell types there was considerable co-localization of EcR fluorescence with that of MitoTracker (arrows in the merged column). However, not all EcR fluorescence co-localized with mitochondrial fluorescence as it is seen as a widespread green label in Figures 10B,E,H,N. Likewise, not all mitochondrial fluorescence co-localized with EcR

fluorescence (seen as red specks in the middle column). The degree of co-localization depended on the cell type. Brain neurons (Figures 10A–C shows a large neurosecretory cell and smaller neurons), PG cells (Figures 10D–F), SG cells (Figures 10G–I), and fat body cells (Figures 10M–O) showed moderate co-localization whereas, epidermal cells (Figures 10J–L) showed extensive co-localization. Therefore, a considerable amount of, but not all, cytoplasmic EcR fluorescence, co-localizes with mitochondria in *Rhodnius* cells, depending on the cell type.

ABSENCE OF CO-LOCALIZATION OF EcR WITH ACIDIC ORGANELLES

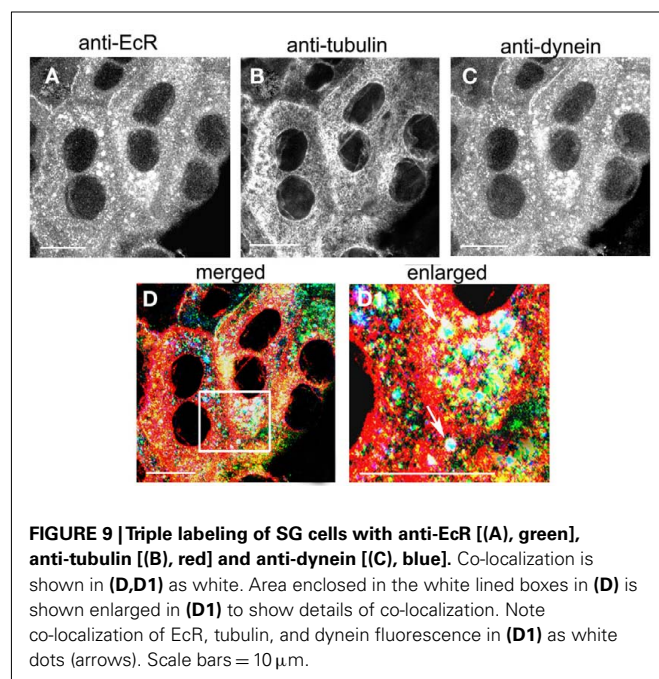
The spatial relationship of EcR with cytoplasmic acidic organelles, such as lysosomes, was examined in double label experiments (Figure 11) using anti-EcR (left column; green) and LysoTracker (right column; red); co-localization is shown in the central column as orange/yellow. Lysosomes have been implicated in EcR elimination in some animals (see Discussion). Animals were selected at the same developmental days as above. None of the cell types tested showed any significant co-localization of EcR fluorescence with LysoTracker fluorescence as in the examples shown Figures 11A–C for brain neurons and Figures 11D–F for SG cells. We conclude that EcR in *Rhodnius* does not appear to associate with acidic organelles.

DISCUSSION

NUCLEOCYTOPLASMIC SHUTTLING OF EcR AND THE ROLE OF MICROTUBULES

The temporal and spatial profiles of EcR reported here during larval–adult development, revealed that shuttling between the nucleus and cytoplasm was restricted to specific developmental periods in most cell types. In many cases, the presence of EcR in the cytoplasm exceeded the period of shuttling. This finding emphasizes that not all of the cytoplasmic EcR is necessarily involved in shuttling. This conclusion raises the prospect that EcR may also be involved in specific cytoplasmic events, i.e., non-genomic actions. Further investigation of the function(s) of cytoplasmic EcR is clearly required. In *Rhodnius*, daily shuttling of EcR to the nucleus implies EcR transport mechanisms. Extensive work with mammalian nuclear receptors has established that receptors employ various methods for nuclear import, including conventional nuclear localization signal machinery or use of cytoskeletal tracks (review by Echeverria and Picard, 2010). Conventional machinery involving nuclear signaling has been until now assumed the only mechanism of intracellular EcR movement (reviews by Henrich, 2009; Nakagawa and Henrich, 2009).

We studied details of nucleocytoplasmic trafficking of EcR in *Rhodnius* cells. We found that in a variety of cell types, substantial amounts of EcR co-localized with the MT network when MTs were stabilized with taxol. In epidermal cells and oenocytes in particular, where well defined centrosomes were present, specks of EcR fluorescence were detected attached to radiating lines of MTs (see Figure 5). This relationship of EcR with the cytoskeleton in insects has only been reported before in *Rhodnius* PG cells (Vafopoulou, 2009). No such association has been reported for any other insect. In contrast, this association is quite common in mammals where shuttling of nuclear receptors in and out of the nucleus has been the focus of in depth study. Association of steroid receptors with



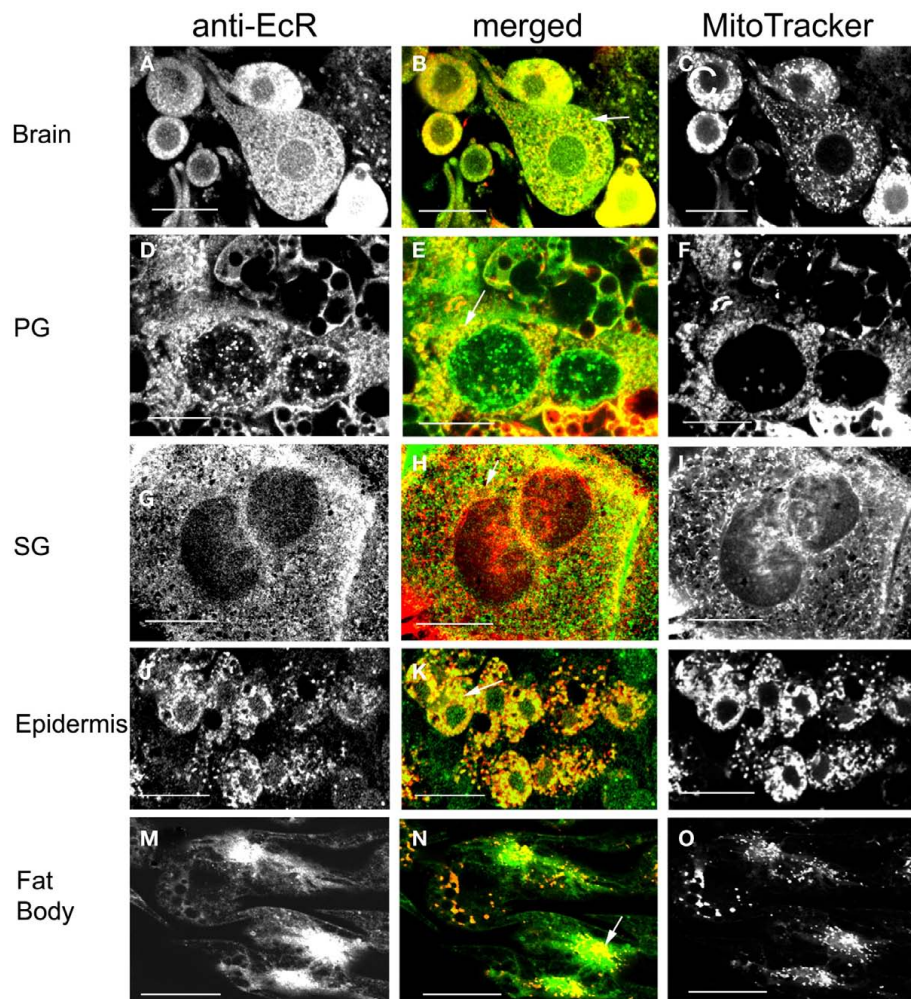


FIGURE 10 | Cells double-labeled with anti-EcR (left column, green) and MitoTracker (right column, red). Co-localization is shown as yellow/orange in the merged images of left and right in the middle column. Brain neurons

(A–C), PG cells (D–F), SG cells (G–I), epidermal cells (J–L), and fat body cells (M–O). Arrows in the merged images (B,E,H,K,N) show co-localization as yellow dots. Scale bars = 10 μ m.

MTs has been reported, both for the ligand-free receptor (e.g., GR, Akner et al., 1991; reviews by Akner et al., 1995 and by Dvorák et al., 2004) and for the ligand-bound receptor (e.g., estrogen receptor α , Azuma et al., 2004; Manavathi et al., 2006; progesterone receptor, Shimazu, 2003; GR, Galigniana et al., 1998, 2001; Dvorák et al., 2005, 2007; Harrell et al., 2004; vitamin D receptor, Barsony et al., 1997). These precedents raise the prospect that MT may play a critical role in EcR shuttling in *Rhodnius* and potentially in insects in general.

Our present and previous data (Vafopoulou, 2009) showed that treatment of scotophase cells with the MT-stabilizing agent taxol resulted in a considerable reduction in nuclear EcR with the concomitant increase in cytoplasmic EcR. This finding suggests that MT stabilization inhibits receptor accumulation in the nucleus and further supports the notion that MTs may serve as movement machinery for EcR. Possibly, stabilization of MTs prevents movement of EcR to the nucleus by tethering it to MTs. Evidence in support of this idea was provided by Manavathi et al. (2006) who

found that taxol inhibited ER α transcriptional activity in human breast cancer cells and taxol increased tubulin association with the mineralocorticoid receptor (MR)–Hsp90 heterocomplex (Galigniana et al., 2010). We also observed that disruption of MTs in cells using colchicine (Vafopoulou, 2009 and present evidence) resulted in depletion of nuclear EcR, suggesting that destruction of cytoskeletal tracks also inhibited transport of EcR from cytoplasm to nucleus. A comparable inhibition of nucleocytoplasmic shuttling of GR and aryl hydrocarbon receptor by agents that disrupt MTs was reported by Dvorák et al. (2007). In colchicine-treated cells of *Rhodnius*, the association of EcR with tubulin was maintained but became fragmented into scattered dots in pockets of cytoplasm with the normal organized network of MTs being lost. This finding again supports the idea that nucleocytoplasmic shuttling of EcR requires an intact cytoskeleton. The directional movement through the cytoplasm to the nucleus using MTs implied by the above argument clearly indicates genomic action of EcR.

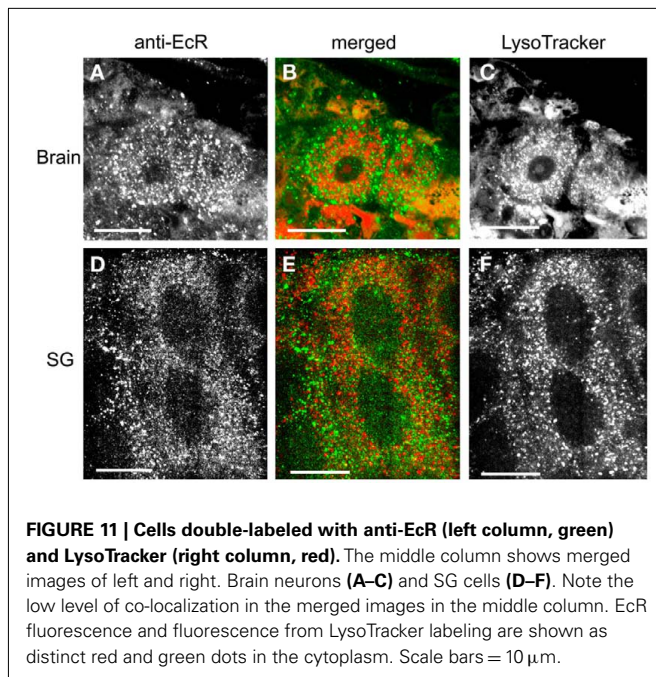


FIGURE 11 | Cells double-labeled with anti-EcR (left column, green) and LysoTracker (right column, red). The middle column shows merged images of left and right. Brain neurons (A–C) and SG cells (D–F). Note the low level of co-localization in the merged images in the middle column. EcR fluorescence and fluorescence from LysoTracker labeling are shown as distinct red and green dots in the cytoplasm. Scale bars = 10 μ m.

RELATIONSHIPS OF EcR WITH THE CHAPERONE Hsp90 AND THE FKBP52 IMMUNOPHILIN

Proteins require molecular chaperones for protection from proteolysis, normal folding, and maturation. Generally, steroid receptors form large multiprotein heterocomplexes with the ubiquitous and essential chaperone proteins, the heat shock proteins 90 and 70 (Hsp90 and Hsp70) and many co-chaperones including the immunophilins FKBP51 and FKBP52 that bind to an acceptor site on Hsp90 via a tetratricopeptide repeat (TPR; reviews by Nollen and Morimoto, 2002; Pratt and Toft, 2003; Pratt et al., 2004a,b). Immunophilins are intracellular receptors for immunosuppressant drugs such as FK506, rapamycin, and cyclosporine A and have been implicated as modulators of steroid receptor function (Ratajczak et al., 2003).

We used antibodies against human Hsp90 and FKBP52 to localize intracellularly related proteins within *Rhodnius* SG cells. We used these cells as model cells for *Rhodnius* because of their large size, flat morphology, and expansive cytoplasmic area. Hsp90 is a ubiquitous and highly conserved protein crucial to cellular signaling involved in numerous cellular regulations including steroid hormone signaling, the regulation of folding, activity, and stability of a wide range of client proteins such as steroid receptors (reviews by Pratt et al., 2004a,b; Picard, 2006; Echeverría and Picard, 2010). The FK506-binding protein 52, FKBP52, is part of the mature steroid receptor heterocomplex and it plays a crucial role in the intracellular trafficking of receptors (reviews above). On Western blots of SG protein extracts, the antibody against human Hsp90 recognized a peptide around 90 kDa and the antibody against human FKBP52 recognized a peptide of molecular size about 45 kDa showing that *Rhodnius* contains immunoreactive peptides of similar molecular size to their human equivalents. Double immunolabels showed extensive and intimate co-localization of EcR with both the ubiquitous chaperone

Hsp90 and the co-chaperone FKBP52. These close spatial relationships provide the first evidence that EcR may associate with both chaperone proteins, suggesting that these proteins may form heterocomplexes with EcR in *Rhodnius* as they do with mammalian steroid receptors. Information is scarce about the requirement of chaperones or even their presence, for EcR function, with a few exceptions. For example, purified EcR/USP heterodimer from *Drosophila* acquires DNA binding activity only with the addition of chaperones such as Hsp90 and FKBP52 (Arbeitman and Hogness, 2000). Also, FKBP52 was immunoprecipitated along with EcR in the PGs of *M. sexta*, raising the possibility of a functional role of this immunophilin in this insect (Song et al., 1997).

Importantly, both Hsp90 and FKBP52 co-localize with MTs in *Rhodnius* SG cells. Association of FKBP52 with MTs and tubulin in particular has also been shown in mammalian cells (Perrot-Applanat et al., 1995; Chambraud et al., 2007). Since EcR co-localizes with both Hsp90 and FKBP52 and all three proteins also co-localize with MTs, it is reasonable to suggest that the EcR association with MTs occurs in the form of a EcR–Hsp90–FKBP52 heterocomplex as does its mammalian counterparts (see below).

Interestingly, the intimate association of EcR with either chaperone is maintained in both the photophase and scotophase. In the photophase, associations of EcR with either Hsp90 or FKBP52 appear as scattered fluorescent dots in the cytoplasm with no fluorescence present in the nucleus. On the other hand, in scotophase, both Hsp90 and FKBP52 fluorescence co-localize with EcR fluorescence in the nucleus. At the same time, the cytoplasm becomes largely devoid of fluorescent dots from co-localization of EcR with either chaperone, suggesting that the bulk of EcR has become transported to the nucleus as a complex with Hsp90 and FKBP52. In scotophase, we detected EcR-positive nuclei both with and without Hsp90 in the same tissue sample, which is consistent with the expectation that Hsp90 dissociates from the receptor within the nucleus following transport. Dissociation from FKBP52 may also occur inside the nucleus. A widely accepted model is that the receptor–Hsp90 based heterocomplex dissociates in the cytoplasm following receptor transformation by ligand binding. However, recent evidence showed that the MR–Hsp90–immunophilin complex accumulates in the nucleus in a hormone-dependent manner and dissociates within the nucleus (Galigniana et al., 2010), i.e., receptor transformation occurs *inside* the nucleus. Even in the absence of ligand, GR–Hsp90–immunophilin complex can translocate into the nucleus as an intact complex (Echeverría et al., 2009). Our results are consistent with the view that dissociation of EcR from the chaperones Hsp90 and FKBP52 occurs within the nucleus, indicating that transformation of the receptor occurs inside the nucleus. Considering the fact that daily EcR shuttling occurs in synchrony with daily ecdysteroid peaks in the hemolymph (Vafopoulou and Steel, 2006; review by Steel and Vafopoulou, 2006), we envisage that EcR is transformed rhythmically every day inside the nucleus in response to daily pulses of the ligand.

RELATIONSHIP OF EcR WITH CYTOPLASMIC DYNEIN AND ROLE OF THE COMPLEX IN EcR TRAFFICKING

The cytoskeleton is considered a vital biological network for integration of signal transduction pathways. Bi-directional transport

of cargo is achieved by motor-driven structures like MTs (review by Welte, 2004). MTs have plus and minus ends. They are organized in such a way that their minus ends are clustered around the centrosome, which is located near the nucleus and their plus ends are near the periphery. This arrangement is suitable for transport of cargo from the cytoplasm to the nucleus and back. Cytoplasmic dynein is a multisubunit high molecular weight ATPase that transports cargo to the minus end of MTs. In mammals, two of its components are the very closely related light chains 1 (DYNLL1 also designated DLC8 because of its low MW about 8 kDa, or PIN) and 2, which are ubiquitous and among the most highly conserved proteins among species (see review by Pfister et al., 2006). A Blast search revealed a 95% amino acid sequence similarity with DNLL1 of *Aedes aegypti* and *Culex quinquefasciatus* and the “cut-up” protein of *Drosophila melanogaster*. The *Drosophila* homolog to DYNLL1 (Cdlc1, also known as dclc1 and “cut-up”) is ubiquitously expressed during development and in the adult and is required for both embryogenesis and cell differentiation (review by Pfister et al., 2006). In *Rhodnius* SG cells, the antibody against human DNLL1/2 recognized a small protein of about 15 kDa on SDS-PAGE immunoblots that co-migrated with human DYNLL1, showing that *Rhodnius* possesses a peptide related to human DYNLL1.

We investigated the structural association between EcR and MTs in triple labeled experiments with the light chain dynein, DYNLL1 component of the dynein motor protein. We detected abundant dynein fluorescence in the cytoplasm of SG cells, substantial amounts of which co-localized with both EcR and with tubulin on MTs. Altogether, these findings imply that all four proteins EcR, Hsp90, FKBP52, and light chain dynein 1 are found together and with tubulin on MTs. Therefore, we suggest that EcR forms a heterocomplex with Hsp90 and FKBP52 that co-localizes on MTs with the motor protein dynein. These considerations suggest that the intracellular movement of EcR in *Rhodnius* cells employs the cytoskeletal tracks of MTs. The suggestion that MTs may use the EcR–Hsp90 heterocomplex as cargo for cytoplasmic transport has not been considered in any previous work. The relation of EcR with the MT network would also explain the present finding of EcR in axons of brain neurons in *Rhodnius*. Steroid receptors in axons have been detected in many mammalian systems (e.g., ER, Milner et al., 2005; AR, Milner et al., 2007). It is well-known that retrograde transport of cargo in axons requires cytoplasmic dynein and MTs (review by Hirokawa and Takemura, 2004).

There is a growing body of information, mostly derived from studies with the GR that supports the hypothesis that FKBP52 provides a link between the receptor–Hsp90–immunophilin heterocomplex and the cytoplasmic dynein motor complex (Harrell et al., 2004). For example, FKBP52 is required for dynein/dynactin-dependent retrograde movement of GR (Harrell et al., 2004), MR (Piwien Pilipuk et al., 2007; Galigniana et al., 2010), aryl hydrocarbon (Kazlauskas et al., 2001), p53 (Galigniana et al., 2004), and possibly estrogen receptor (Rayala et al., 2005). Interestingly, GR heterocomplexes isolated from the cytosol also contained tubulin, indicating that the dynein motor links the receptor heterocomplex to MTs (Harrell et al., 2004).

The above suggestions that EcR forms a complex with both Hsp90 and FKBP52 that attaches itself to the motor protein dynein on MTs for transport to the nucleus provides a mechanism by which EcR could exert its genomic effects. The complex seems to dissociate inside the nucleus. Therefore, we infer that the daily nucleocytoplasmic shuttling of EcR that occurs during defined periods of larval–adult development of *Rhodnius* employs cytoskeletal tracks for movement. Nucleocytoplasmic shuttling of EcR is further supported by the fact that EcRs in other species possess several nuclear export signals in addition to a nuclear import signal (Gwózdź et al., 2007; Betanska et al., 2011). Because the nuclear EcR rhythm is synchronous to the robust circadian rhythm of circulating ecdysteroids it is inferred that *Rhodnius* cells detect and respond to the daily signals in the rhythmic ecdysteroid titer.

These inferences raise some interesting questions. Is EcR transported to the nucleus alone or in the form of a heterodimer with Usp? It has been shown that EcR binds to ecdysteroids in the absence of its heterodimerization partner Usp (Grebe et al., 2000; Nieva et al., 2007) and EcR import to the nucleus increased in a hormone-dependent manner (Lammerding-Köppel et al., 1998; Nieva et al., 2007). Further, in a mammalian cell line which expresses either EcR or Usp, tagging of the proteins with the yellow fluorescent protein showed that Usp resides almost exclusively in the nucleus whereas EcR is found in both the nuclear and cytoplasmic compartments (Nieva et al., 2005; Gwózdź et al., 2007). Indeed, Usp possesses only nuclear localization signals but no nuclear export signals, whereas EcR possesses both (Gwózdź et al., 2007). Therefore, one view that we cannot exclude is the possibility that EcR in *Rhodnius* shuttles undimerized to the nucleus. Indeed, EcR undimerized with Usp induces transcription of glue genes in the SGs of *Drosophila* (Constantino et al., 2008). However, when both Usp and EcR are co-expressed in the above mammalian cell line, the presence of Usp favors nuclear localization of EcR (Gwózdź et al., 2007). Further, stable residency of EcR in the nucleus requires the formation of a heterodimer with Usp (Nieva et al., 2005). These findings support the opposite view that because EcR in *Rhodnius* cells resides in nuclei for many hours every night, it might require partnership with Usp in the nucleus. Such an arrangement would imply that Usp transport to the nucleus is also rhythmic in *Rhodnius*.

ASSOCIATION OF EcR WITH THE MITOCHONDRIA

A substantial amount of cytoplasmic EcR fluorescence does not co-localize with MTs. When we examined the association of EcR with mitochondria in double label experiments with a vital fluorescent dye that labels mitochondria, we detected substantial co-localization. Mitochondria are visible as punctate arrays of dots and rods that in many cases form dense aggregates, particularly in the perinuclear region. This perinuclear aggregation of mitochondria is a well-known distribution pattern of mitochondria within cells. The distribution pattern of EcR fluorescence in this area is similar to that of other nuclear receptors in mammalian cells (e.g., for GR, Scheller et al., 2000; for ER, Chen et al., 2004). Association of steroid receptors with mitochondria has been documented for many mammalian steroid receptors (references in Vafopoulou, 2009), where they are thought to influence mitochondrial gene activity. Indeed, hormone response elements in mitochondrial

DNA and active hormone receptors were found to be imported into mitochondria and enhance the transcription of mitochondrial genes (references in Vafopoulou, 2009). The association of EcR with mitochondria of several cell types in *Rhodnius* raises the possibility that EcR, like its mammalian counterparts, may be involved in the coordination of ecdysteroid-responsive genes in mitochondria. The present finding of EcR along nerve axons highly remote from the nucleus (as seen for other steroid hormones; see above), emphasizes the generality of such non-genomic functions of steroid hormones.

We did not find much association of EcR with acidic organelles in cells such as lysosomes. The absence of EcR from acidic organelles suggests that lysosomes may not be involved in the

removal of EcR from the cell. This is unlike estrogen receptor α presence in lysosomes of mammalian cells, which suggested a role for lysosomes in receptor degradation as it shuttles out of the nucleus (Qualmann et al., 2000).

Since EcR exhibits a daily rhythm in *Rhodnius* that is driven by the rhythm in circulating steroid hormone levels (Vafopoulou and Steel, 2006; review by Steel and Vafopoulou, 2006), it is likely that both genomic and non-genomic effects will show synchronous daily rhythms.

ACKNOWLEDGMENTS

This work is supported by Natural Sciences Research Council of Canada, Discovery Grant 6669.

REFERENCES

- Akner, G., Mossberg, K., Wikström, A. C., Sundqvist, K. G., and Gustafsson, J. A. (1991). Evidence for colocalization of glucocorticoid receptor with cytoplasmic microtubules in human gingival fibroblasts, using two different monoclonal anti-GR antibodies, confocal laser scanning microscopy and image analysis. *J. Steroid Biochem. Mol. Biol.* 39, 419–432.
- Akner, G., Wikström, A. C., and Gustafsson, J. A. (1995). Subcellular distribution of the glucocorticoid receptor and evidence for its association with microtubules. *J. Steroid Biochem. Mol. Biol.* 52, 1–6.
- Ampleford, E. J., and Steel, C. G. H. (1985). Circadian control of a daily rhythm in hemolymph ecdysteroid titer in the insect *Rhodnius prolixus* (Hemiptera). *Gen. Comp. Endocrinol.* 59, 453–459.
- Arbeitman, M. N., and Hogness, D. S. (2000). Molecular chaperones activate the *Drosophila* ecdysone receptor, an RXR heterodimer. *Cell* 101, 67–77.
- Azuma, K., Horie, K., Inoue, S., Ouchi, Y., and Sakai, R. (2004). Analysis of estrogen receptor α signalling complex at the plasma membrane. *FEBS Lett.* 577, 339–344.
- Barsony, J., Renyi, I., and McKoy, W. (1997). Subcellular distribution of normal and mutant vitamin D receptors in living cells. *J. Biol. Chem.* 272, 5774–5782.
- Betanska, K., Hönl, G., Spindler-Barth, M., and Spindler, K.-D. (2011). The importance of exportin and Ran for nucleocytoplasmic shuttling of the ecdysteroid receptor. *Arch. Insect Biochem. Physiol.* 76, 12–21.
- Chambraud, B., Belabes, H., Fontaine-Lenoir, V., Fellous, A., and Baulieu, E. E. (2009). The immunophilin FKBP52 specifically binds to tubulin and prevents microtubule formation. *FASEB J.* 21, 2787–2797.
- Chen, J. Q., Delannoy, M., Cooke, C., and Yager, J. D. (2004). Mitochondrial localization of ER α and ER β in human MCF7 cells. *Am. J. Physiol. Endocrinol. Metab.* 286, E1011–E1022.
- Constantino, B. F. B., Bricker, D. K., Alexandre, K., Shen, K., Merriam, J. R., Antoniewski, C., Callender, J. L., Henrich, V. C., and Andres, A. J. (2008). A novel ecdysone receptor mediates steroid-regulated developmental events during the mid-third instar of *Drosophila*. *PLoS Genet.* 4, e1000102. doi: 10.1371/journal.pgen.1000102
- Dick, T., Krishanu, R., Salz, H. K., and Chia, W. (1996). Cytoplasmic dynein (ddlc1) mutations cause morphogenetic defects and apoptotic cell death in *Drosophila melanogaster*. *Mol. Cell. Biol.* 16, 1966–1977.
- Dvorák, Z., Modrianský, M., Ulrichová, J., and Maurel, P. (2004). Speculations of the role of the microtubule network in glucocorticoid receptor signaling. *Cell Biol. Toxicol.* 20, 333–343.
- Dvorák, Z., Modrianský, M., Ulrichová, J., Maurel, P., Vilarem, M. J., and Pascucci, J. M. (2005). Disruption of microtubules leads to glucocorticoid receptor degradation in HeLa cell line. *Cell. Signal.* 17, 187–196.
- Dvorák, Z., Vrzal, R., Ulrichová, J., Macejová, D., Ondková, S., and Brtko, J. (2007). Expression, protein stability and transcriptional activity of retinoic acid receptors are affected by microtubules interfering agents and all-trans-retinoic acid in primary rat hepatocytes. *Mol. Cell. Endocrinol.* 267, 89–96.
- Echeverría, P. C., Mazaira, G., Erlejan, A., Gomez-Sanchez, C., Piwien Pilipuk, G., and Galigniana, M. D. (2009). Nuclear import of the glucocorticoid receptor-Hsp90 complex through the nuclear pore complex is mediated by its interaction with Nup62 and importin β . *Mol. Cell. Biol.* 29, 4788–4797.
- Echeverría, P. C., and Picard, D. (2010). Molecular chaperones, essential partners of steroid hormone receptors for activity and mobility. *Biochim. Biophys. Acta* 1803, 641–649.
- Elmog, M., Iwami, M., and Sakurai, S. (2004). Presence of membrane ecdysone receptor in the anterior silk gland of the silkworm *Bombyx mori*. *Eur. J. Biochem.* 271, 3171–3179.
- Elmog, M., Iwami, M., and Sakurai, S. (2007). Solubilization of the ecdysone binding protein from anterior silk gland cell membranes of the silkworm, *Bombyx mori*. *Zool. Sci.* 24, 971–977.
- Fujiwara, H., Jindra, M., Newitt, R., Palli, S. R., Hiruma, K., and Riddiford, L. M. (1995). Cloning of an ecdysone receptor homolog from *Manduca sexta* and the developmental profile of its mRNA in wings. *Insect Biochem. Mol. Biol.* 25, 845–856.
- Galigniana, M. D., Erlejan, A. G., Monte, M., Gomez-Sanchez, C., and Piwien Pilipuk, G. (2010). The hsp90-FKBP52 complex links the mineralocorticoid receptor to motor proteins and persists bound to the receptor in early nuclear events. *Mol. Cell. Biol.* 30, 1285–1298.
- Galigniana, M. D., Harrell, J. M., O'Hagen, H. M., Ljungman, M., and Pratt, W. B. (2004). Hsp90-binding immunophilins link p53 to dynein during p53 transport to the nucleus. *J. Biol. Chem.* 279, 22483–22489.
- Galigniana, M. D., Radanyi, C., Renoir, J. M., Housley, P. R., and Pratt, W. B. (2001). Evidence that the peptidylpropyl isomerase domain of the hsp90-binding immunophilin FKBP52 is involved in both dynein interaction and glucocorticoid receptor movement to the nucleus. *J. Biol. Chem.* 276, 14884–14889.
- Galigniana, M. D., Scruggs, L. J., Herington, J., Welsh, M. J., Carter-Su, C., Housley, P. R., and Pratt, W. B. (1998). Heat shock protein 90-dependent (geldanamycin-inhibited) movement of the glucocorticoid receptor through the cytoplasm to the nucleus requires intact cytoskeleton. *Mol. Endocrinol.* 12, 1903–1913.
- Grebe, M., Rauch, P., and Spindler-Barth, M. (2000). Characterization of subclones of the epithelial cell line from *Chironomus tentans* resistant to the insecticide RH5992, a non-steroidal moulting hormone agonist. *Insect Biochem. Mol. Biol.* 30, 591–600.
- Gwózdź, T., Dutko-Gwózdź, J., Nieva, C., Betanska, K., Orlowski, M., Kowalska, A., Dobrucki, J., Spindler-Barth, M., Spindler, K.-D., and Ozyhar, A. (2007). EcR and USP, components of the ecdysteroid nuclear receptor complex, exhibit differential distribution of molecular determinants directing subcellular trafficking. *Cell. Signal.* 19, 490–503.
- Harrell, J. M., Murphy, P. J., Morishima, Y., Chen, H., Mansfield, J. F., Galigniana, M. D., and Pratt, W. B. (2004). Evidence for glucocorticoid receptor transport on microtubules by dynein. *J. Biol. Chem.* 279, 54647–54654.
- Henrich, V. C. (2009). “The ecdysteroid receptor,” in *Insect Development: Morphogenesis, Molting and Metamorphosis*, ed. L. I. Gilbert (London, GR: Academic Press), 261–304.
- Hirokawa, N., and Takemura, R. (2004). Molecular motors in neuronal development, intracellular transport and diseases. *Curr. Opin. Neurobiol.* 14, 564–573.
- Jindra, M., Malone, F., Hiruma, K., and Riddiford, L. M. (1996). Developmental profiles and ecdysteroid regulation of the mRNAs for two ecdysone receptor isoforms in the epidermis and wings of the tobacco hornworm, *Manduca sexta*. *Dev. Biol.* 180, 258–272.

- Kazlauskas, A., Sundstrom, S., Poellinger, L., and Pongratz, I. (2001). The hsp90 chaperone complex regulates intracellular localization of the dioxin receptor. *Mol. Cell. Biol.* 21, 2594–2607.
- Lammerding-Köppel, M., Spindler-Barth, M., Steiner, E., Lezzi, M., Drews, U., and Spindler, K.-D. (1998). Immunohistochemical localization of ecdysteroid receptor and ultraspiracle in the epithelial cell line from *Chironomus thummi* (Insecta, Diptera). *Tissue Cell* 30, 187–194.
- Manavathi, B., Acconsia, F., Rayala, S. K., and Kumar, R. (2006). An inherent role of microtubule network in the action of nuclear receptor. *Proc. Natl. Acad. Sci. U.S.A.* 103, 15981–15986.
- Milner, T. A., Ayoola, K., Drake, C. T., Herrick, S. P., Tabori, N. E., and McEwen, B. S. (2005). Ultrastructural localization of estrogen receptor β immunoreactivity in the rat hippocampal formation. *J. Comp. Neurol.* 491, 81–95.
- Milner, T. A., Hernandez, F. J., Herrick, S. P., Pierce, J. P., Iadecola, C., and Drake, C. T. (2007). Cellular and subcellular localization of androgen receptor immunoreactivity relative to C1 adrenergic neurons in the rostral ventrolateral medulla of male and female rats. *Synapse* 61, 268–278.
- Nakagawa, Y., and Henrich, V. C. (2009). Arthropod nuclear receptors and their role in molting. *FEBS J.* 276, 6128–6157.
- Nieva, C., Gwózdź, T., Dutko-Gwózdź, J., Wiedenmann, J., Spindler-Barth, M., Wiczorek, E., Dobrucki, J., Dus, D., Henrich, V., Ozyhar, A., and Spindler, K.-D. (2005). Ultraspiracle promotes the nuclear localization of ecdysteroid receptor in mammalian cells. *Biol. Chem.* 386, 463–470.
- Nieva, C., Spindler-Barth, M., Azoitei, A., and Spindler, K.-D. (2007). Influence of hormone intracellular localization of the *Drosophila melanogaster* ecdysteroid receptor (EcR). *Cell. Signal.* 19, 2582–2587.
- Nollen, E. A., and Morimoto, R. I. (2002). Chaperoning signalling pathways: molecular chaperones as stress-sensing 'heat shock' proteins. *J. Cell. Sci.* 115, 2809–2816.
- Ou, Q., Magico, A., and King-Jones, K. (2012). Nuclear receptor DHR4 controls the timing of steroid hormone pulses during *Drosophila* development. *PLoS Biol.* 9, e1001160. doi: 10.1371/journal.pbio.1001160
- Perrot-Applanat, M., Cibert, C., Géraud, G., Renoir, J.-M., and Baulieu, E. E. (1995). The 59 kDa FK506-binding protein, a 90kDa heat shock protein binding immunophilin (FKBP59-HBI), is associated with the nucleus, the cytoskeleton and mitotic apparatus. *J. Cell. Sci.* 108, 2037–2051.
- Pfister, K. K., Shah, P. R., Hummerich, H., Russ, A., Cotton, J., Annur, A. A., King, S. M., and Fisher, E. M. C. (2006). Genetic analysis of the cytoplasmic dynein subunit families. *PLoS Genet.* 2, 11–26. doi: 10.1371/journal.pgen.0020001
- Picard, D. (2006). Chaperoning steroid hormone action. *Trends Endocrinol. Metab.* 17, 230–236.
- Piwil Pilipuk, G., Vinson, G. P., Sanchez, C. G., and Galigniana, M. D. (2007). Evidence for NL1-independent nuclear translocation of the mineralocorticoid receptor. *Biochem.* 46, 1389–1397.
- Pratt, W. B., Galigniana, M. D., Harrell, J. M., and DeFranco, D. B. (2004a). Role of hsp90 and the hsp90-binding immunophilins in signalling protein movement. *Cell. Signal.* 16, 857–872.
- Pratt, W. B., Galigniana, M. D., Morishima, Y., and Murphy, P. J. (2004b). Role of molecular chaperones in steroid receptor action. *Essays Biochem.* 40, 41–58.
- Pratt, W. B., and Toft, D. O. (2003). Regulation of signal protein function and trafficking by the hsp90/hsp70-based chaperone machinery. *Exp. Biol. Med.* 228, 111–133.
- Qualmann, B., Kessels, M. M., Thole, H. H., and Sierralta, W. D. (2000). A hormone pulse influences distributions and leads to lysosomal accumulation of the estradiol receptor α in target tissues. *Eur. J. Cell Biol.* 79, 383–393.
- Ratajczak, T., Ward, B. K., and Minchin, R. F. (2003). Immunophilin chaperones in steroid receptor signalling. *Curr. Top. Med. Chem.* 3, 1348–1357.
- Rayala, S. K., den Hollander, P., Balasenthil, S., Yang, Z., and Broadus, R. R. (2005). Functional regulation of oestrogen receptor pathway by the dynein light chain 1. *EMBO Rep.* 6, 538–545.
- Riddiford, L. M., Hiruma, K., Zhou, X. F., and Nelson, C. A. (2003). Insights into the molecular basis of the hormonal control of molting and metamorphosis from *Manduca sexta* and *Drosophila melanogaster*. *Insect Biochem. Mol. Biol.* 33, 1327–1338.
- Scheller, K., Sekeris, C. E., Krohne, G., Hock, R., Hansen, I. A., and Scheer, U. (2000). Localization of glucocorticoid hormone receptors in mitochondria of human cells. *Eur. J. Cell Biol.* 79, 299–307.
- Schlattner, U., Vafopoulou, X., Steel, C. G. H., Hormann, R. E., and Lezzi, M. (2006). Non-genomic ecdysone effects and the invertebrate nuclear steroid hormone receptor EcR – new role for an “old” receptor? *Mol. Cell. Endocrinol.* 247, 64–72.
- Shimazu, K. K. (2003). Expression and intracellular localization of progesterone receptors in cultured human gingival fibroblasts. *J. Periodont. Res.* 38, 242–246.
- Shu, Y., Du, Y., and Wang, J. (2011). Molecular characterization and expression patterns of *Spodoptera litura* heat shock protein 70/90 and their response to zinc stress. *Comp. Biochem. Physiol. A Mol. Integr. Physiol.* 158, 102–110.
- Song, Q., Alnemri, E. S., Litwack, G., and Gilbert, L. I. (1997). An immunophilin is a component of the insect ecdysone receptor (EcR) complex. *Insect Biochem. Mol. Biol.* 27, 973–982.
- Spindler, K.-D., Hönl, C., Tremmel, C. H., Braun, S., Ruff, H., and Spindler-Barth, M. (2009). Ecdysteroid hormone action. *Cell. Mol. Life Sci.* 66, 3837–3850.
- Steel, C. G. H., and Vafopoulou, X. (2006). Circadian orchestration of developmental hormones in the insect, *Rhodnius prolixus*. *Comp. Biochem. Physiol. A Mol. Integr. Physiol.* 144, 351–364.
- Vafopoulou, X. (2009). Ecdysteroid receptor (EcR) is associated with microtubules and with mitochondria in the cytoplasm of prothoracic gland cells of *Rhodnius prolixus* (Hemiptera). *Arch. Insect Biochem. Physiol.* 72, 249–262.
- Vafopoulou, X., and Steel, C. G. H. (1991). Circadian regulation of ecdysteroid synthesis in prothoracic glands of the insect, *Rhodnius prolixus* (Hemiptera). *Gen. Comp. Endocrinol.* 83, 1–9.
- Vafopoulou, X., and Steel, C. G. H. (2006). Ecdysteroid hormone nuclear receptor (EcR) exhibits circadian cycling in certain tissues, but not others, during development in *Rhodnius prolixus* (Hemiptera). *Cell Tissue Res.* 323, 443–455.
- Vafopoulou, X., Steel, C. G. H., and Terry, K. (2005). Ecdysteroid receptor (EcR) shows marked differences in temporal patterns between tissues during larval-adult development in *Rhodnius prolixus*: correlations with haemolymph ecdysteroid titres. *J. Insect Physiol.* 51, 27–38.
- Welte, M. A. (2004). Bidirectional transport along microtubules. *Curr. Biol.* 14, R525–R537.
- Wigglesworth, V. B. (1985). “Historical perspectives,” in *Comprehensive Insect Physiology, Biochemistry and Pharmacology. Vol. 7 Endocrinology I*, eds G. A. Kerkut and L. I. Gilbert (Oxford, GR: Pergamon Press), 1–24.
- Zhang, Q., and Denlinger, D. L. (2010). Molecular cloning of heat shock protein 90, 70 and 70 cognate cDNAs and their expression patterns during thermal stress and pupal diapause in the corn earworm. *J. Insect Physiol.* 56, 138–150.

Conflict of Interest Statement: The authors declare that the research was conducted in the absence of any commercial or financial relationships that could be construed as a potential conflict of interest.

Received: 09 October 2011; accepted: 06 March 2012; published online: 23 March 2012.

Citation: Vafopoulou X and Steel CGH (2012) Cytoplasmic travels of the ecdysteroid receptor in target cells: pathways for both genomic and non-genomic actions. *Front. Endocrin.* 3:43. doi: 10.3389/fendo.2012.00043

This article was submitted to *Frontiers in Experimental Endocrinology*, a specialty of *Frontiers in Endocrinology*.

Copyright © 2012 Vafopoulou and Steel. This is an open-access article distributed under the terms of the Creative Commons Attribution Non Commercial License, which permits non-commercial use, distribution, and reproduction in other forums, provided the original authors and source are credited.



The arginine residue within the C-terminal active core of *Bombyx mori* pheromone biosynthesis-activating neuropeptide is essential for receptor binding and activation

Takeshi Kawai¹, Jae Min Lee², Koji Nagata¹, Shogo Matsumoto², Masaru Tanokura¹ and Hiromichi Nagasawa^{1*}

¹ Department of Applied Biological Chemistry, Graduate School of Agricultural and Life Sciences, The University of Tokyo, Tokyo, Japan

² Molecular Entomology Laboratory, RIKEN Advanced Science Institute, Wako, Saitama, Japan

Edited by:

Joe Hull, USDA Agricultural Research Service, USA

Reviewed by:

Adrien Fónagy, Plant Protection Institute of Hungarian Academy of Sciences, Hungary

Ronald Nachman, US Department of Agriculture, USA

*Correspondence:

Hiromichi Nagasawa, Department of Applied Biological Chemistry, Graduate School of Agricultural and Life Sciences, The University of Tokyo, 1-1-1, Yayoi, Bunkyo-ku, Tokyo 113-8657, Japan.

e-mail: anagahi@mail.ecc.

u-tokyo.ac.jp

In most lepidopteran insects, the biosynthesis of sex pheromones is regulated by pheromone biosynthesis-activating neuropeptide (PBAN). *Bombyx mori* PBAN (BomPBAN) consists of 33 amino acid residues and contains a C-terminus FSPRLamide motif as the active core. Among neuropeptides containing the FXPRLamide motif, the arginine (Arg, R) residue at the second position from the C-terminus is highly conserved across several neuropeptides, which can be designated as RXamide peptides. The purpose of this study was to clarify the role of the Arg residue in the BomPBAN active core. We synthesized 10-residue peptides corresponding to the C-terminal part of BomPBAN with a series of replacements at the second position from the C-terminus, termed the C2 position, and measured their efficacy in stimulating Ca^{2+} influx in insect cells expressing a fluorescent PBAN receptor chimera (PBANR-EGFP) using the fluorescent Ca^{2+} indicator, Fura Red-AM. The PBAN analogs with the C2 position replaced with alanine (Ala, A), aspartic acid (Asp, D), serine (Ser, S), or L-2-aminooctanoic acid (Aoc) decreased PBAN-like activity. R^{C2}A (SKTRYFSPALamide) and R^{C2}D (SKTRYFSPDLamide) had the lowest activity and could not inhibit the activity of PBAN C10 (SKTRYFSPRLamide). We also prepared Rhodamine Red-labeled peptides of the PBAN analogs and examined their ability to bind PBANR. In contrast to Rhodamine Red-PBAN C10 at 100 nM, none of the synthetic analogs exhibited PBANR binding at the same concentration. Taken together, our results demonstrate that the C2 Arg residue in BomPBAN is essential for PBANR binding and activation.

Keywords: FXPRLamide peptides, GPCR, Lepidoptera, neuropeptide, PBAN, PBANR, sex pheromone silkworm

INTRODUCTION

Virgin female moths attract conspecific males using sex pheromone for species-specific mating. Pheromone biosynthesis and emission from the pheromone gland are activated during a calling period that is synchronized with the photoperiodic cycle through the function of pheromone biosynthesis-activating neuropeptide (PBAN), which is produced in the subesophageal ganglion (Kitamura et al., 1989; Raina et al., 1989; Raina, 1993; Rafaeli, 2002). In *Bombyx mori*, PBAN consists of 33 amino acid residues and contains as its active core a C-terminal FXPRLamide motif (X = S, T, G, or V) that is essential for PBAN activity (Kuniyoshi et al., 1992).

Several neuropeptides containing the FXPRLamide motif at the C-terminus have been identified from a number of insect orders including Lepidoptera, Diptera, and Orthoptera (Predel and Wegener, 2006). These peptides have been reported to regulate various biological activities such as initiation of *B. mori* embryonic diapause (Imai et al., 1991) and heliothine pupal (Xu and Denlinger, 2003), melanization of larvae in lepidopteran species (Matsumoto et al., 1990), hindgut/oviduct contraction in the

cockroach and the locust (Nachman et al., 1986; Schoofs et al., 1992), and acceleration of pupariation in several flies (Zdarek et al., 1998). Moreover, PRX or RXamide (X = F, L, V, or Y) peptides have also been identified in many organisms as biologically active peptides (Predel and Wegener, 2006; Walker et al., 2009). These peptides have been widely identified from insect species (Baggerman et al., 2002; Hummon et al., 2006; Hauser et al., 2008; Weaver and Audsley, 2008). The presence of a C-terminal amide and an Arg residue at the second position from the C-terminus, termed the C2 position, in so many diverse insect neuropeptides suggests some functional importance.

The receptors for many of the peptides discussed above have been identified as G protein-coupled receptors (GPCRs). The insect GPCRs have been identified using cultured cells such as HEK293, CHO mammalian cells (Iversen et al., 2002; Yamanaka et al., 2008), and Sf9 insect cells (Choi et al., 2003; Hull et al., 2004). The PBAN receptor (PBANR) was first cloned from the corn earworm, *Helioverpa zea*, as a homolog of the neuromedin U receptor (NmUR) in vertebrates that recognized FXPRNamide peptides (Fujii et al., 2000; Choi et al., 2003). Since then, PBANRs have been

identified as class-A GPCR family members from *B. mori*, *Heliothis virescens*, *Manduca sexta*, and *Plutella xylostella* (Hull et al., 2004; Kim et al., 2008; Lee et al., 2011). In *B. mori*, PBAN binding has been shown *in vitro* using isolated pheromone glands to trigger an influx of extracellular Ca^{2+} in the pheromone producing cells (Mastumoto, 2010), as well as insect cells transiently expressing PBANR (Choi et al., 2003; Hull et al., 2004).

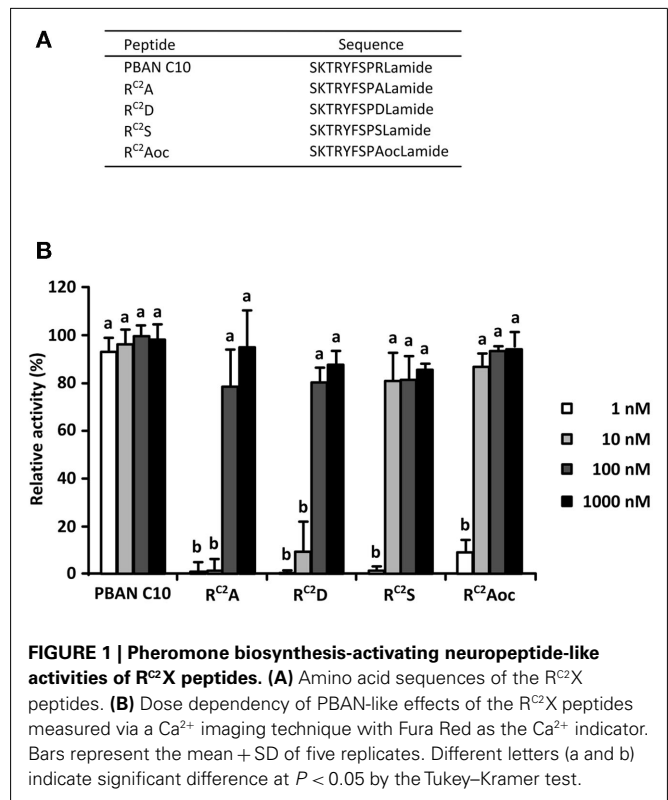
In the course of our study on the structure–activity relationship of PBAN and search for PBAN antagonists to control pests and to obtain a *B. mori* PBANR (BomPBANR)/ligand complex appropriate for crystallographic structural analysis, we established an *in vitro* PBAN assay system by observing Ca^{2+} influx into Sf9 cells, which had been prepared from immature ovaries of *Spodoptera frugiperda* (Vaughn et al., 1977), constitutively expressing BomPBANR–EGFP (Hull et al., 2011; Kawai et al., 2011). We first focused on the C6 residue and determined that a synthetic Y^{C6N} [SKTRNFSPRLamide] was a partial agonist (Kawai et al., 2010). Next, we prepared cyclic peptides, cyclo Y^{C6} [cyclo(TCYFSPRL)] and cyclo N^{C6} [cyclo(TCNFSPRL)], from linear precursor peptides fused to an intein protein (Kimura et al., 2006) and determined that these partial peptides were also partial agonists (Kawai et al., 2011). These results showed that BomPBANR recognizes the amino acid residue at C6 position and type I β -turn secondary structure (Nachman et al., 1993). We also synthesized and examined a peptide substituted with D-Phe at C4 position [RYFdFPRamide, LA-4] which had been reported as a linear antagonist (Zeltser et al., 2000; Ben-Aziz et al., 2005) and demonstrated that LA-4 was a partial agonist to BomPBANR (Kawai et al., 2009).

In this study, we focused on the Arg residue at the C2 position in the PBAN active core, because this residue is highly conserved in not only PBAN but also many other related neuropeptides. We synthesized four PBAN analogs consisting of 10 amino acid residues, in which the Arg residue was substituted with Ala, Asp, Ser, or L-2-aminooctanoic acid (Aoc), and assessed their *in vitro* PBAN-like activities by a Ca^{2+} imaging assay using stably transformed Sf9 cells expressing BomPBANR–EGFP and a confocal laser scanning microscope.

RESULTS

AGONISTIC ACTIVITIES OF SYNTHETIC PBAN C-TERMINAL PEPTIDES

To investigate the effect of the Arg side chain on *in vitro* PBAN-like activity, we prepared four synthetic PBAN analogs, in which the Arg residue at the C2 position was substituted with amino acid residues exhibiting different side chain properties (Figure 1A). For this purpose, we selected Ala, Asp, Ser, and Aoc for the following reasons: Ala has a simple small side chain that lacks a functional group, Asp has a negatively charged carboxyl group, Ser has a hydroxyl group with an uncharged polarity, while the Aoc side chain is similar in length to the Arg side chain but lacks any functional groups. To determine the agonistic activities of the Ala (R^{C2A}), Asp (R^{C2D}), Ser (R^{C2S}), and Aoc (R^{C2Aoc}) analogs, we compared the Ca^{2+} response of the respective analogs with a corresponding PBAN analog composed of the C-terminal 10 residues (PBAN C10). Sf9 cells stably expressing BomPBANR–EGFP were loaded with Fura Red–AM, a fluorescent Ca^{2+} indicator, and their fluorescent profile in response to the each ligand was examined



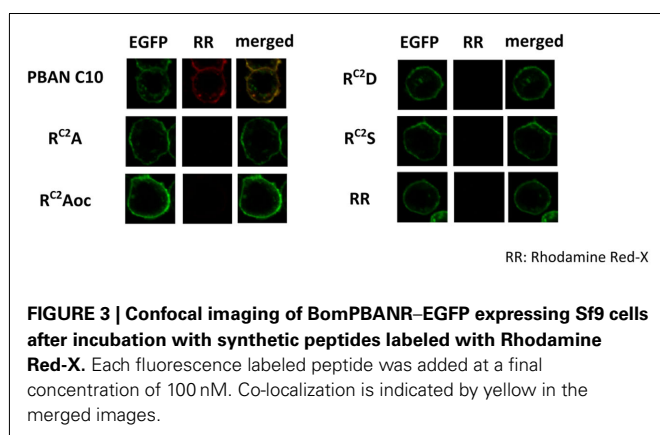
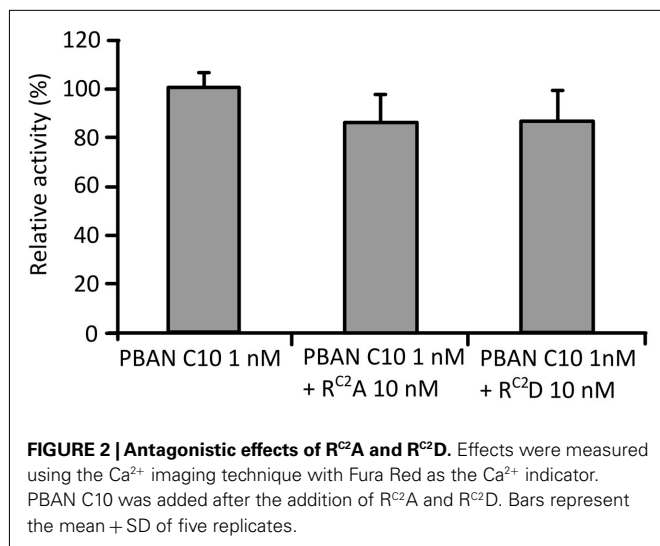
with a confocal laser scanning microscope (Kawai et al., 2011). As shown in Figure 1B, the PBAN-like activities of all of the R^{C2X} peptides were much lower than that of PBAN C10 at 1 nM. R^{C2A} and R^{C2D} showed full PBAN-like activity at 100 nM, while R^{C2S} and R^{C2Aoc} showed full activity at 10 nM.

EXAMINATION OF ANTAGONISTIC ACTIVITIES OF R^{C2X} PEPTIDES

Because R^{C2A} and R^{C2D} showed lower PBAN-like activities than the other two mutations, we also examined their antagonistic activities against PBAN C10. We found that the activity of PBAN C10 at 1 nM decreased to 87 and 85% following the addition of a 10-fold concentration of R^{C2A} and R^{C2D} , respectively (Figure 2), although this reduction in activity was not statistically significant.

FLUORESCENT BINDING ASSAY

To confirm the binding of the R^{C2X} mutations to BomPBANR–EGFP, we prepared fluorescent analogs of the synthetic peptides via conjugation with Rhodamine Red-X succinimidyl ester. As before, we used Sf9 cells stably expressing BomPBANR–EGFP to examine binding of each labeled peptide. Sf9 cells were imaged using a confocal laser scanning microscope using excitation at 488 and 560 nm for EGFP and Rhodamine Red-X, respectively. The binding intensity was assessed by the fluorescence ratio of Rhodamine Red-X to EGFP. Figure 3 shows the results. The expression of BomPBANR–EGFP on the cell surface was visualized as a ring of green fluorescence by EGFP in all cases. It was clearly demonstrated that PBAN C10 bound to BomPBANR–EGFP as observed as a red fluorescent ring on the cell surface, which was merged with green fluorescence to be yellow. However, the binding of



the R^{C2}X peptides to BomPBANR-EGFP could not be detected clearly.

DISCUSSION

Neuropeptides mediate various biological events in both vertebrates and invertebrates. Among them, there is a group of neuropeptides that share chemical characteristics of C-terminal amidation and the presence of Arg at the C2 position. PBAN, an insect neuropeptide, belongs to this group. In this study, we sought to clarify the role of the Arg residue in PBAN activity. Instead of an ordinary *in vivo* PBAN assay using female moths, we adopted a bioassay assessing PBAN-like activity *in vitro* by using insect (Sf9) cells artificially expressing BomPBANR-EGFP, which we have previously established (Mastumoto, 2010; Kawai et al., 2011). We synthesized and examined four synthetic peptides, in which Arg at the C2 position was replaced by each of four representative amino acid residues with different chemical properties from Arg.

The activity of R^{C2}A was significantly lower than PBAN C10, which is consistent with previous results demonstrating the effect of Ala substitutions of this position in a *Heliothis virescens* PBAN C-terminal hexapeptide (Kim et al., 2008). It has also been

reported that the substitution of Arg at the C2 position of neuropeptide Y, a vertebrate neuropeptide, with Ala reduced the affinity to both human Y₁ and Y₂ receptors (Beck-Sickinger et al., 1994). In addition, the reduced *in vivo* PBAN activity was reported following Gln, Lys, or norvaline substitution of Arg at the C2 position in *B. mori* (Kuniyoshi et al., 1991). While these results suggest the potential importance of the Arg guanidine group, the length of the side chain may also influence the activity. We consequently prepared a peptide with Aoc at the C2 position because Aoc has a side chain of similar length to Arg but without any functional groups, thus making it hydrophobic. Unexpectedly, the R^{C2}Aoc peptide, showed higher activity than R^{C2}A (Figure 1B). While the guanidino functional group is important for binding, it is apparent that the length of the side chain is also important.

Concerning the hydrophilicity of the side chain, we compared the activity of R^{C2}A with that of R^{C2}S. R^{C2}S was found to be more active than R^{C2}A, indicating some contribution of the hydroxyl group. However, the increased bulkiness of the Ser hydroxymethyl group over the Ala methyl group may also contribute to some extent. R^{C2}S was a little less active than R^{C2}Aoc, indicating the side chain length is more important than hydrophilicity. R^{C2}D, which carried a charge opposite to the natural peptide, showed activity stronger than R^{C2}A, but was weaker than R^{C2}S, indicating that a negative charge is not preferable for binding to the receptor.

Neither R^{C2}A nor R^{C2}D was able to inhibit the activity of 1 nM PBAN C10 even at a 10-fold higher concentration (10 nM), at which concentration that R^{C2}A and R^{C2}D exhibited almost no and very low agonistic activity, respectively. This result suggests that both R^{C2}A and R^{C2}D bind very weakly to BomPBANR; it is unlikely that they bind BomPBANR as strongly as PBAN C10 but cannot trigger the Ca²⁺ influx. The weak binding of the four synthetic analogs was directly demonstrated by observation of the Rhodamine Red-labeled conjugates. We therefore concluded that the Arg residue at C2 position is important for PBANR binding. Although the four mutants exhibited PBAN-like activity comparable to PBAN C10 at 100 nM, we failed to observe any binding at that concentration, perhaps because the Rhodamine Red-labeled analogs were weakly bound and removed during the final washing steps prior to imaging. It is unlikely that the Rhodamine Red-labeled analogs have lower activity than non-labeled peptides, because the possible labeling sites are the ε-amino group of Lys at the C9 position and the N-terminal amino group, which are far from the active core. Experiments at higher concentrations of labeled peptides will be needed.

MATERIALS AND METHODS

SYNTHESIS AND PURIFICATION OF PEPTIDES

Pheromone biosynthesis-activating neuropeptide analogs were synthesized with an automated peptide synthesizer Apex 369 (AAPPTec, Louisville, KY, USA) using the Fmoc solid-phase strategy according to the manufacturer's instructions. The Arg residue at the C9 position of all PBAN analogs was replaced with Lys for labeling with Rhodamine Red-X succinimidyl ester. After deprotection and cleavage from the resin, synthetic peptides were purified by HPLC with a PEGASIL ODS column (10 i.d. × 150 mm, Senshu Kagaku, Tokyo, Japan) using two solvents, 0.05% trifluoroacetic acid (TFA; solvent A) and 90% CH₃CN/0.05% TFA

(solvent B). Peptides were eluted at a flow rate of 4.0 ml/min using a step-gradient program starting from 0% B in 2.5 min, then to 75% B in 15 min, and then 100% B over the next 30 min. Reagents for peptide synthesis were purchased from WATANABE CHEMICAL IND., LTD (Hiroshima, Japan). Synthetic peptides were lyophilized and stored at -20°C until use.

PREPARATION OF FLUORESCENT PBAN ANALOGS

A 200- μl aliquot containing 250 μg Rhodamine Red succinimidyl ester (Life technologies, Tokyo, Japan) was added to a solution of 0.1 M sodium bicarbonate (pH 8.2) and 1.0 μmol synthetic peptide. The mixture was stirred overnight at room temperature and the conjugated peptide purified by HPLC under the same conditions as above. RR-C10 PBAN and RR- $\text{R}^{\text{C}2}\text{X}$ were stored at 4°C until use.

PREPARATION OF STABLE PBANR-EGFP TRANSFORMANTS

An expression plasmid encoding the BomPBANR fused with EGFP at its C-terminus was produced using a pIB/V5-His TOPO TA cloning kit (Life Technologies). Sf9 cells in IPL-41 insect cell medium (Life Technologies) supplemented with 10% fetal bovine serum (FBS) were transfected with the expression plasmid using Cellfectin (Life Technologies). Transfected Sf9 cells were selected using blasticidin S according to the manufacturer's procedures.

CONFOCAL LASER SCANNING MICROSCOPE-BASED Ca^{2+} IMAGING ASSAY

BomPBANR-EGFP stably expressing cells were harvested and incubated in 24 well glass bottom plate (AGC, Tokyo, Japan) at 28°C for 2 days with 10% FBS in IPL-41. On the day of experiment, cells were washed three times with IPL-41 and incubated in 250 μl of IPL-41 with 0.75 μl of Pluronic F-127 and 1 mM Fura Red AM (Life Technologies) for 30 min in the dark. After incubation, the cells were washed three times with IPL-41, and 300 μl IPL-41 was added to each well. The plate was left in the dark for 20 min to allow hydrolysis of the Fura Red AM ester bond. EGFP and Fura Red fluorescence were obtained on a FV-1000D confocal

laser microscope (OLYMPUS, Tokyo, Japan) using 488 and 548 nm laser lines, respectively. To measure agonistic activity, fluorescence was monitored for 40 scans (1.08 s/scan), and a 100- μl peptide solution which were prepared to the concentration of 1, 10, 100, and 1000 nM was added to the well after 10 scans. For measuring antagonistic activity of $\text{R}^{\text{C}2}\text{A}$ and $\text{R}^{\text{C}2}\text{D}$, the fluorescence was monitored for 50 scans. $\text{R}^{\text{C}2}\text{A}$ and $\text{R}^{\text{C}2}\text{D}$ solution (100 μl) was added to the well after 10 scans, and then 100 μl PBAN C10 was added after 25 scans. The Fura Red fluorescence was analyzed using the FV-1000D software "FluoView" (OLYMPUS). The data obtained were statistically analyzed using a Tukey-Kramer test. These experiments were performed with five replicates.

CONFOCAL LASER SCANNING MICROSCOPE-BASED PEPTIDE BINDING ASSAY

The binding ability of Rhodamine Red- $\text{R}^{\text{C}2}\text{X}$ peptides ($\text{X} = \text{Ala}$, Asp , Ser , and Aoc) to BomPBANR-EGFP was analyzed using a confocal laser scanning microscope. Sf9 cells adherently cultured on 35 mm glass bottom dishes (AGC, Tokyo, Japan) were transfected with 5 μg of expression plasmid containing BomPBANR-EGFP. Sixteen hours after transfection, the Sf9 cells were washed with 10% FBS/IPL-41 containing kanamycin at the final concentration of 200 $\mu\text{g}/\text{ml}$ and incubated for 1 day at 28°C . On the day of the experiment, transfected cells were washed with serum free IPL-41 medium and incubated at 4°C for 15 min. To examine the binding of the labeled peptides to BomPBANR-EGFP, transfected cells were incubated in 500 μl IPL-41 containing each RR-peptide at the concentration of 100 nM at 4°C for 60 min in the dark, and then fixed with 4% formaldehyde/PBS. The fluorescence of BomPBANR-EGFP and RR-peptides were obtained on a FV-1000D confocal laser scanning microscope with 488 and 548 nm laser lines, respectively.

ACKNOWLEDGMENTS

This research was supported by Targeted Proteins Research Program (TPRP) from the Ministry of Education, Culture, Sports, Science and Technology of Japan.

REFERENCES

- Baggerman, G., Cerstiaens, A., De Loof, A., and Schoofs, L. (2002). Peptidomics of the larval *Drosophila melanogaster* central nervous system. *J. Biol. Chem.* 277, 40368–40374.
- Beck-Sickinger, A. G., Wieland, H. A., Willim, K.-D., Rudolf, K., and Jung, G. (1994). Complete L-alanine scan of neuropeptide Y reveals ligands binding to Y1 and Y2 receptors with distinguished conformations. *Eur. J. Biochem.* 225, 947–958.
- Ben-Aziz, O., Zeltser, I., and Altstein, M. (2005). PBAN selective antagonists: inhibition of PBAN induced cuticular melanization and sex pheromone biosynthesis in moth. *J. Insect Physiol.* 51, 305–314.
- Choi, M. Y., Fuerst, E. J., Rafaei, A., and Jurenka, R. (2003). Identification of a G protein-coupled receptor for pheromone biosynthesis activating neuropeptide from pheromone glands of the moth *Helicoverpa zea*. *Proc. Natl. Acad. Sci. U.S.A.* 100, 9721–9726.
- Fujii, R., Hosoya, M., Fukusumi, S., Kawamata, Y., Habata, Y., Hinuma, S., and Onda, H. (2000). Identification of neuromedin U as the cognate ligand of the orphan G protein-coupled receptor FM-3. *J. Biol. Chem.* 275, 21068–21074.
- Hauser, F., Cazzamali, G., Williamson, M., Park, M., Li, B., Tanaka, Y., Predel, R., Neupert, S., Schachtner, J., Verleyen, P., and Gimmelikhuijzen, C. J. P. (2008). A genome-wide inventory of neurohormone GPCRs in the red flour beetle *Tribolium castaneum*. *Front. Neuroendocrinol.* 29, 142–165.
- Hull, J. J., Lee, H. M., and Matsumoto, S. (2011). Identification of specific sites in the third intracellular loop and carboxyl terminus of the *Bombyx mori* pheromone biosynthesis activating neuropeptide receptor crucial for ligand-induced internalization. *Insect Mol. Biol.* 20, 801–811.
- Hull, J. J., Ohnisi, A., Moto, K., Kawasaki, Y., Kurata, R., Suzuki, M. G., and Matsumoto, S. (2004). Cloning and characterization of the pheromone biosynthesis activating neuropeptide receptor from the silkworm, *Bombyx mori*: significance of the carboxyl terminus in receptor internalization. *J. Biol. Chem.* 279, 51500–51507.
- Hummon, A. B., Richmond, T. A., Verleyen, P., Baggerman, G., Huybrechts, J., Ewing, M. A., Vierstrate, E., Rodriguez-Zas, S. L., Schoofs, L., Robinson, G. E., and Sweedler, J. V. (2006). From the genome to the proteome: uncovering peptides in the Apis brain. *Science* 314, 647–649.
- Imai, K., Konno, T., Nakazawa, T., Komiya, T., Isobe, M., Koga, K., Goto, T., Yaginuma, T., Sakakibara, K., Hasegawa, K., and Yamashita, O. (1991). Isolation and structure of diapause hormone of the silkworm, *Bombyx mori*. *Proc. Jpn. Acad.* 67B, 98–101.
- Iversen, A., Cazzamali, G., Williamson, M., Hauser, F., and Gimmelikhuijzen, C. J. P. (2002). Molecular cloning of functional expression of a *Drosophila* receptor for the neuropeptides capa-1 and -2. *Biochem. Biophys. Res. Commun.* 299, 628–633.

- Kawai, T., Hull, J. J., Matsumoto, S., Nagata, J., Tanokura, M., and Nagasawa, H. (2010). "Studies on the structure-activity relationship of pheromone biosynthesis-activating neuropeptide (PBAN)," in *Peptide Science 2009: Proceedings of the 46th Japanese Peptide Symposium*, ed. K. Okamoto (Osaka: The Japanese Peptide Society Press), 231–234.
- Kawai, T., Nagata, K., Okada, K., Hayakawa, K., Hull, J. J., Lee, H. M., Matsumoto, S., Tanokura, M., and Nagasawa, H. (2011). "Structure-activity relationship studies of the pheromone biosynthesis-activating neuropeptide of the silkworm, *Bombyx mori*," in *Peptide science 2010: Proceedings of the Fifth International Peptide Symposium*, eds N. Fujii and Y. Kiso (Osaka: The Japanese Peptide Society Press), 126.
- Kawai, T., Sugisaka, A., Hull, J. J., Matsumoto, S., Nagata, K., Tanokura, M., and Nagasawa, H. (2009). "Development of a novel bioassay system for pheromone biosynthesis-activating neuropeptide (PBAN) using the *Bombyx* receptor expressed in insect cell," in *Peptide Science 2008: Proceedings of the 45th Japanese Peptide Symposium*, ed. M. Nomizu (Osaka: The Japanese Peptide Society Press), 287–288.
- Kim, Y. J., Nachman, R. J., Aimanova, K., Gill, S., and Adams, M. E. (2008). The pheromone biosynthesis activating neuropeptide (PBAN) receptor of *Heliothis virescens*: identification, functional expression, and structure-activity relationships of ligand analogs. *Peptides* 29, 268–275.
- Kimura, R. H., Tran, A.-T., and Camaero, J. A. (2006). Biosynthesis of the cyclotide Kalata B1 by using protein splicing. *Angew. Chem. Int. Ed. Engl.* 45, 973–976.
- Kitamura, A., Nagasawa, H., Kataoka, H., Inoue, T., Ando, T., and Suzuki, A. (1989). Amino acid sequence of pheromone biosynthesis-activating neuropeptide (PBAN) of the silkworm, *Bombyx mori*. *Biochem. Biophys. Res. Commun.* 163, 520–526.
- Kuniyoshi, H., Kitamura, A., Nagasawa, H., Chuman, T., Shimazaki, K., Ando, T., and Suzuki, A. (1991). "Structure-activity relationship of pheromone biosynthesis activating neuropeptide (PBAN) from the silkworm, *Bombyx mori*," in *Peptide Chemistry 1990: Proceedings of the 28th Symposium on Peptide Chemistry*, ed. Y. Shimonishi (Osaka: The Japanese Peptide Society Press), 251–254.
- Kuniyoshi, H., Nagasawa, H., Ando, T., Suzuki, A., Nachman, R. J., and Holman, G. M. (1992). Cross-activity between pheromone biosynthesis activating neuropeptide (PBAN) and myotropic pyrokinin insect peptides. *Biosci. Biotechnol. Biochem.* 56, 167–168.
- Lee, D. W., Shrestha, S., Kim, A. Y., Park, S. J., Yang, C. Y., Kim, Y., and Koh, Y. H. (2011). RNA interference of pheromone biosynthesis-activating neuropeptide receptor suppresses mating behavior by inhibiting sex pheromone production in *Plutella xylostella* (L.). *Insect Biochem. Mol. Biol.* 41, 236–243.
- Mastumoto, S. (2010). Molecular mechanisms underlying sex pheromone production in moths. *Biosci. Biotechnol. Biochem.* 74, 223–231.
- Matsumoto, S., Kitamura, A., Nagasawa, H., Kataoka, H., Orikasa, C., Mitsui, T., and Suzuki, A. (1990). Functional diversity of a neurohormone produced by the suboesophageal ganglion: molecular identification of melanization and reddish coloration hormone and pheromone biosynthesis activating neuropeptide. *J. Insect Physiol.* 53, 752–759.
- Nachman, R. J., Holman, G. M., and Cook, B. J. (1986). Active fragments and analogs of the insect neuropeptide leucopyrokinin; structure-function studies. *Biochem. Biophys. Res. Commun.* 137, 936–942.
- Nachman, R. J., Kuniyoshi, H., Roberts, V. A., Holman, G. M., and Suzuki, A. (1993). Active conformation of the pyrokinin/PBAN neuropeptide family for pheromone biosynthesis in the silkworm. *Biochem. Biophys. Res. Commun.* 193, 661–666.
- Predel, R., and Wegener, C. (2006). Biology of the CAPA peptides in insects. *Cell. Mol. Life Sci.* 63, 2477–2490.
- Rafaeli, A. (2002). Neuroendocrine control of pheromone biosynthesis in moths. *Int. Rev. Cytol.* 213, 41–49.
- Raina, A., Jaffe, K., Kempe, T. G., Keim, P., Blacher, R. W., Fales, H. M., Riley, C. T., Klun, J. A., Ridgway, R. L., and Hayes, D. K. (1989). Identification of neuropeptide hormone that regulates sex pheromone production in female moth. *Science* 244, 796–798.
- Raina, A. K. (1993). Neuroendocrine control of sex pheromone biosynthesis in lepidoptera. *Annu. Rev. Entomol.* 38, 329–349.
- Schoofs, L., Holman, G. M., Hayes, T. K., Nachman, R. J., Kochansky, J. P., and Deloof, A. (1992). Isolation identification and synthesis of locustamyotropin III and IV, two additional neuropeptides of *Locusta migratoria*; members of the locustamyotropin family. *Insect Biochem. Mol. Biol.* 22, 447–452.
- Vaughn, J. L., Goodwin, R. H., Tompkins, G. J., and McCawley, P. (1977). The establishment of two cell lines from the insect *Spodoptera frugiperda* (lepidoptera: noctuidae). *In vitro* 13, 213–217.
- Walker, R. J., Papaioannou, S., and Holden-Dye, L. (2009). A review of FMRFamide- and RFamide-like peptides in metazoan. *Invert. Neurosci.* 9, 111–153.
- Weaver, R. J., and Audsley, N. (2008). Neuropeptides of the beetle, *Tenebrio molitor*, identified using MALDI-TOF mass spectrometry and deduced sequences from the *Tribolium castaneum* genome. *Peptides* 29, 168–178.
- Xu, W.-H., and Denlinger, D. L. (2003). Molecular characterization of prothoracicotrophic hormone and diapause hormone in *Heliothis virescens* during diapauses, and a new role for diapauses hormone. *Insect Mol. Biol.* 12, 509–516.
- Yamanaka, N., Yamamoto, S., Zitnan, D., Watanabe, K., Kawada, T., Satake, H., Kaneko, Y., Himura, K., Tanaka, Y., Shinoda, T., and Kataoka, H. (2008). Neuropeptide receptor transcriptome reveals unidentified neuroendocrine pathway. *PLoS ONE* 3, e3048. doi:10.1371/journal.pone.0003048
- Zdarek, J., Nachman, R. J., and Hayes, T. K. (1998). Structure-activity relationships of insect neuropeptides of the pyrokinin/PBAN family and their selective action on pupariation in fresh fly (*Neobellera bullata*) larvae (diptera: sarcophagidae). *Eur. J. Entomol.* 95, 9–16.
- Zeltser, I., Glion, C., Ben-Aziz, O., Scheffler, I., and Altstein, M. (2000). Discovery of linear lead antagonist to the insect pheromone biosynthesis activating neuropeptide (PBAN). *Peptides* 21, 1457–1465.

Conflict of Interest Statement: The authors declare that the research was conducted in the absence of any commercial or financial relationships that could be construed as a potential conflict of interest.

Received: 09 November 2011; accepted: 05 March 2012; published online: 20 March 2012.

Citation: Kawai T, Lee JM, Nagata K, Matsumoto S, Tanokura M and Nagasawa H (2012) The arginine residue within the C-terminal active core of *Bombyx mori* pheromone biosynthesis-activating neuropeptide is essential for receptor binding and activation. *Front. Endocrin.* 3:42. doi: 10.3389/fendo.2012.00042

This article was submitted to *Frontiers in Experimental Endocrinology*, a specialty of *Frontiers in Endocrinology*. Copyright © 2012 Kawai, Lee, Nagata, Matsumoto, Tanokura and Nagasawa. This is an open-access article distributed under the terms of the Creative Commons Attribution Non Commercial License, which permits non-commercial use, distribution, and reproduction in other forums, provided the original authors and source are credited.



Molecular structure and diversity of PBAN/pyrokinin family peptides in ants

Man-Yeon Choi* and Robert K. Vander Meer*

United States Department of Agriculture, Agriculture Research Service, Center for Medical, Agricultural, and Veterinary Entomology, Gainesville, FL, USA

Edited by:

Joe Hull, USDA Agricultural Research Service, USA

Reviewed by:

Julang Li, University of Guelph, Canada

Jan Adrianus Veenstra, Université de Bordeaux, France

*Correspondence:

Man-Yeon Choi and Robert K. Vander Meer, United States Department of Agriculture, Agriculture Research Service, Center for Medical Agricultural and Veterinary Entomology, 1600 SW 23rd Dr. Gainesville, FL 32608, USA.
e-mail: mychoi@ars.usda.gov;
bob.vandermeer@ars.usda.gov

Neuropeptides are the largest group of insect hormones. They are produced in the central and peripheral nervous systems and affect insect development, reproduction, feeding, and behavior. A variety of neuropeptide families have been identified in insects. One of these families is the PBAN/pyrokinin family defined by a common FXPRLamide or similar amino acid fragment at the C-terminal end. These peptides, found in all insects studied thus far, have been conserved throughout evolution. The most well studied physiological function is regulation of moth sex pheromone biosynthesis through the pheromone biosynthesis activating neuropeptide (PBAN), although several developmental functions have also been reported. Over the past years we have extended knowledge of the PBAN/pyrokinin family of peptides to ants, focusing mainly on the fire ant, *Solenopsis invicta*. The fire ant is one of the most studied social insects and over the last 60 years a great deal has been learned about many aspects of this ant, including the behaviors and chemistry of pheromone communication. However, virtually nothing is known about the regulation of these pheromone systems. Recently, we demonstrated the presence of PBAN/pyrokinin immunoreactive neurons in the fire ant, and identified and characterized PBAN and additional neuropeptides. We have mapped the fire ant PBAN gene structure and determined the tissue expression level in the central nervous system of the ant. We review here our research to date on the molecular structure and diversity of ant PBAN/pyrokinin peptides in preparation for determining the function of the neuropeptides in ants and other social insects.

Keywords: ant, social insect, PBAN, pyrokinin, neuropeptide, gene structure, diversity

PBAN/PYROKININ PEPTIDES IN INSECTS

Neuropeptides are part of a large group of neurohormones that have important regulatory functions and are found in most animals. The pheromone biosynthesis activating neuropeptide (PBAN)/pyrokinin family is a major group of insect neuropeptides, and they are expected to be found in all insect groups, and to have multiple functions during insect development and reproduction. The first peptide identified from the pyrokinin family of peptides was leukopyrokinin from the cockroach, *Leucophaea maderae* (Holman et al., 1986). Leukopyrokinin has a pyroglutamate at its N-terminal end, and it functions by stimulating the contraction of hindgut muscles in cockroaches, locusts, and crickets (Nachman et al., 1986; Schoofs et al., 1990a,b, 1991; Holman et al., 1991; Predel et al., 1995, 1997; Predel and Nachman, 2001). Independently, the first PBAN was isolated from *Helicoverpa zea* (Raina et al., 1989), since then many PBAN family peptides have been identified from different insect groups based on their ability to stimulate sex pheromone biosynthesis in moths and/or peptide sequence homology (Rafaeli, 2009; Choi et al., 2010; Jurenka and Rafaeli, 2011).

The PBAN/pyrokinin peptide family is defined by a similar 5-amino-acid C-terminal sequence (ex: FXPRLamide) that is the minimal sequence required for physiological activity (Raina and Kempe, 1990, 1992; Fonagy et al., 1992b; Kuniyoshi et al., 1992).

This motif has been identified in a variety of orders as well as some crustaceans, and has been shown to regulate a variety of insect functions: (1) stimulate pheromone biosynthesis in female moths (Raina et al., 1989); (2) induce melanization in moth larvae (Matsumoto et al., 1990; Altstein et al., 1996); (3) induce embryonic diapause and seasonal polyphenism in moths (Suwan et al., 1994; Uehara et al., 2011); (4) stimulate visceral muscle contraction in cockroaches (Nachman et al., 1986; Predel and Nachman, 2001); (5) accelerate puparium formation in several flies (Zdarek et al., 1997; Verleyen et al., 2004); (6) terminate pupal diapause in heliothine moths (Sun et al., 2003; Xu and Denlinger, 2003). To date, about 200 PBAN/pyrokinin family peptides have been reported from over 40 species (GenBank and unpublished). It is one of the largest neuropeptide families in insects; however, the physiological function of most of these peptides is unknown.

Although a variety of fire ant pheromones have been identified, little is known about the regulation of their production and release. PBAN is synthesized in the subesophageal ganglion (SG), located near the brain (Br), and released into the hemolymph, where it acts on pheromone glands to stimulate pheromone biosynthesis in moths. The mechanism of PBAN control over pheromone production is well understood for sex pheromone biosynthesis in a number of lepidopteran moths (Tillman et al., 1999; Rafaeli,

2009; Jurenka and Rafaeli, 2011). However, thus far no other insect group has been shown to regulate pheromone biosynthesis using PBAN. PBAN acts directly on pheromone glands by stimulating specific receptor linked G-proteins to open a ligand-gated calcium channel to allow the influx of extracellular Ca^{2+} , which is the critical second messenger for PBAN signal transduction (Jurenka et al., 1991, 1994; Fonagy et al., 1992a; Rafaeli and Soroker, 1994; Ma and Roelofs, 1995a; Matsumoto et al., 1995a,b; Choi et al., 2003; Choi and Jurenka, 2004, 2006). Signal transduction is activated quickly once PBAN binds with the specific PBAN receptor (Choi et al., 2003; Hull et al., 2004; Rafaeli et al., 2007; Zheng et al., 2007; Kim et al., 2008; Jurenka and Nusawardani, 2011; Lee et al., 2011). Details of the PBAN mode of action regarding pheromone biosynthesis in moths is reviewed in the regulatory role of PBAN in moths (Jurenka and Rafaeli, 2011).

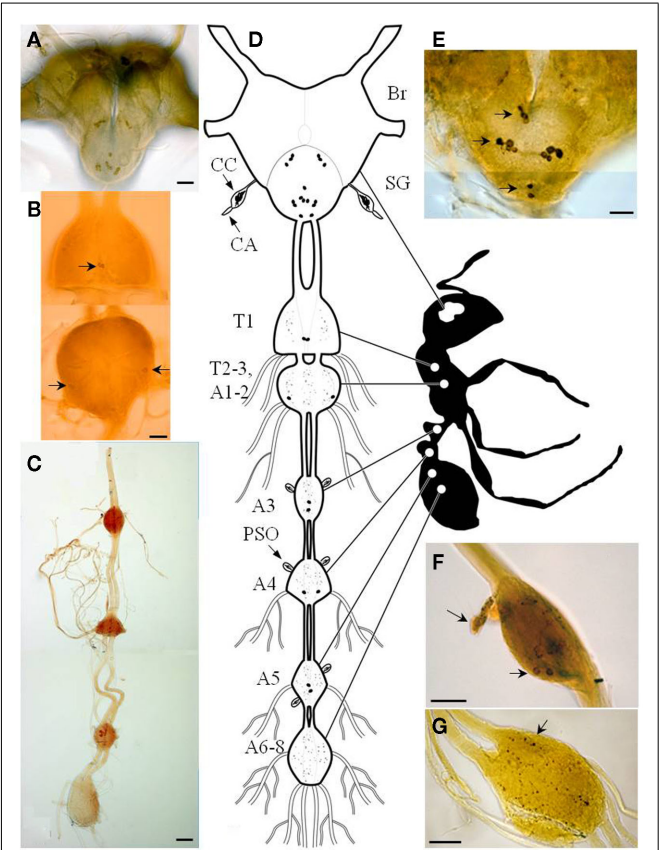


FIGURE 1 | Diagram of the central nervous system of the fire ant adult. Photomicrographs of brain and subesophageal ganglion (A), immunoreactive neurons in thoracic ganglia [(B), arrows], and abdominal ganglia (C). Schematic drawing of fire ant adult CNS and PBAN-like immunoreactivity (D). Posterior view of an adult Br-SG complex showing somata in the SG and near the esophageal foramen [(E), arrows]. Immunoreactive neurons projecting into perisymphetic organs in abdominal ganglion [(F), arrows]. Terminal ganglion (sixth–eighth neuromeres) containing a densely stained region of varicosities [(G), arrow; Br, brain; SG, subesophageal ganglion; CC, corpora cardiaca; CA, corpora allata; PSO, perisymphetic organ; T1–3, first–third thoracic ganglia; A1–8, first–eight abdominal ganglia]. Bar = 50 μm (Choi et al., 2009).

LOCATION OF PBAN/PYROKININ IN ANTS

Immunocytochemical tools were used to locate PBAN/pyrokinin peptides in the central nervous system (CNS) of the fire ant (Choi et al., 2009). This system visualized PBAN immunoreactivity in dissected Br, SG, and ventral nerve cord (VNC) of the fire ant (Figure 1). The number and location of PBAN-like immunoreactive neurons showed a similar pattern for all sexual forms and workers (sterile). The distribution pattern of PBAN-like immunoreactive materials in the fire ant CNS was similar to that already shown in moths (Blackburn et al., 1992; Kingan et al., 1992; Sato et al., 1994; Ma and Roelofs, 1995b; Davis et al., 1996; Ma et al., 1996; Duportets et al., 1998; Sun et al., 2003; Choi et al., 2004; Wei et al., 2008), locust (Tips et al., 1993), and *Drosophila* (Choi et al., 2001). However, unlike moths, the last fire ant abdominal ganglion (AG) does not contain PBAN immunoreactive neurons (Figure 1G). Three clusters of neurons were found in the SG (Figures 1A,D,E) and five pairs of neurons in the ventral nervous system (Figures 1B,C,D). The three cell clusters present in the SG are composed of one pair in the most posterior, four pairs in the medial, and three pairs in the anterior ganglia (Figure 1E). The ganglia in the VNC contained five pairs of PBAN-like immunoreactive neurons (Figures 1B–D). One pair was located in the first thoracic ganglion, and another pair in the second thoracic ganglion (Figure 1B). Neurites along the midline and lateral side

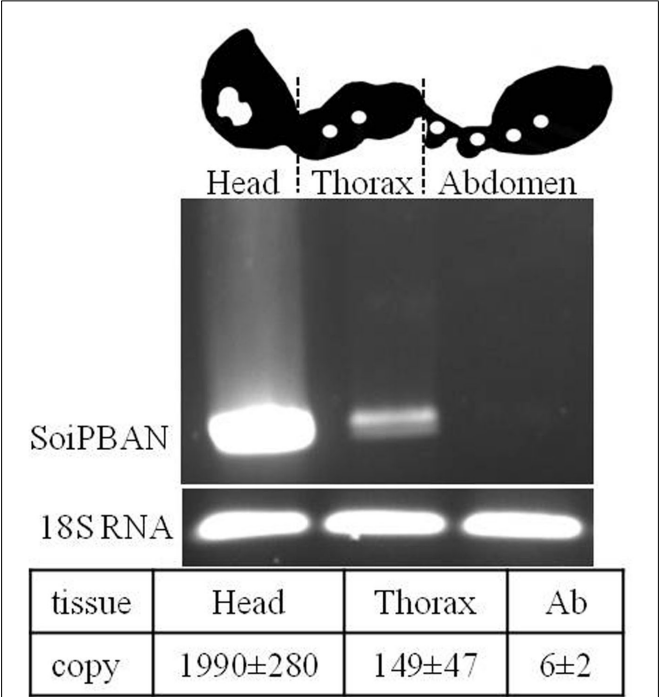
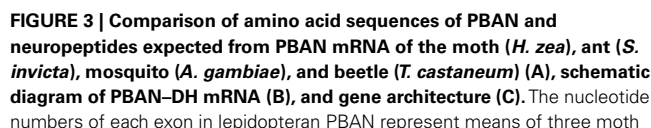


FIGURE 2 | Schematic drawing of fire ant tissues for SoipBAN mRNA transcription levels analyzed by reverse transcription (RT) (upper) and quantitative (Q)-PCR (lower). Total RNAs from head, thorax, and abdomen (Ab) were amplified by RT-PCR and gene copies were quantified by Q-PCR. Gene copies per microgram RNA were significantly different (*t*-test, $P < 0.05$, $N = 3$). The fire ant 18S rRNA gene is a positive control (Choi et al., 2011).

The VNC in ancestral insects has been shown to consist of eight discrete AGs. In evolutionarily advanced insects, the number of AGs varies. In most cases, the first abdominal and/or the terminal AGs are fused with one or more neuromeres; therefore, the number of discrete ganglia is reduced (Niven et al., 2008). The ventral nerve structure of fire ant female alates and queens shows only two thoracic and four AGs. The pro-thoracic ganglion (T1) is discrete, but the meso- (T2), and meta- (T3) thoracic ganglia, and the first (A1) and second (A2) AGs are fused together to form the second structurally discrete thoracic ganglia, as found in most insects. Of the four discrete AGs, A3, A4, and A5 are distinct ganglia; however, the last three AGs (A6, A7, A8) are likely fused forming the single terminal ganglion in the fire ant. A similar fusion pattern for both thoracic and abdominal neuromeres in the VNC has been shown in lepidopteran and hymenopteran species (Niven et al., 2008).

Recently, the results for SoiPBAN (*Solenopsis invicta* PBAN) mRNA expression levels in different tissues of fire ants (Choi et al., 2011) contradicted the strong PBAN immunoreactivity detected in the fire ant VNC (Choi et al., 2009). As anticipated, the strongest transcriptional signal and maximum number of SoiPBAN gene copies were detected in the head (**Figure 2**), indicating that the gene products including PBAN are actively produced in the SG as shown in **Figure 1**. SoiPBAN gene transcription and copies in the thoracic tissue were relatively low. However, only a minimal level of PBAN gene transcription was observed in abdominal tissue (**Figure 2**), in contrast to the strong PBAN-like immunoreactivity observed from abdominal neurons associated with the PSO in the AG (**Figure 1**). If these peptides were only from SoiPBAN gene products, then gene expression and copy number in abdominal tissue would be expected to be at least similar to or higher than the thorax tissue. Therefore, these results suggest that a FXPRL peptide is dominantly expressed in the abdomen that is derived from a gene other than the SoiPBAN gene. Thus far, only two gene families are known to produce FXPRL peptides: PBAN and the capability (CAPA) genes in insects. PBAN (-DH) genes produce four or five FXPRL or similar sequenced peptides including PBAN and the diapause hormone (DH). The CAPA gene encodes one FXPRL neuropeptide with a very conserved motif, WFGPRL at the C-termini (Predel and Wegener, 2006).

PBAN anti-sera reacts with any C-terminus FXPR peptide sequence regardless of what gene is producing the peptide, thus the cross-reactivity does not allow the determination of the number of genes responsible for the observed reactivity. Interestingly, the



species. DH, diapause hormone homolog; α , β , and γ : neuropeptides encoded from the cDNA; PBANs are translated from exon 3 in ants, and exons 4 and 5 in moths, respectively. The shaded area represents PBAN coding regions. Open areas represent untranslated regions. The alignment was made with Genetx-Tree software (ver. 10: Choi and Vander Meer, 2009; Choi et al., 2011).

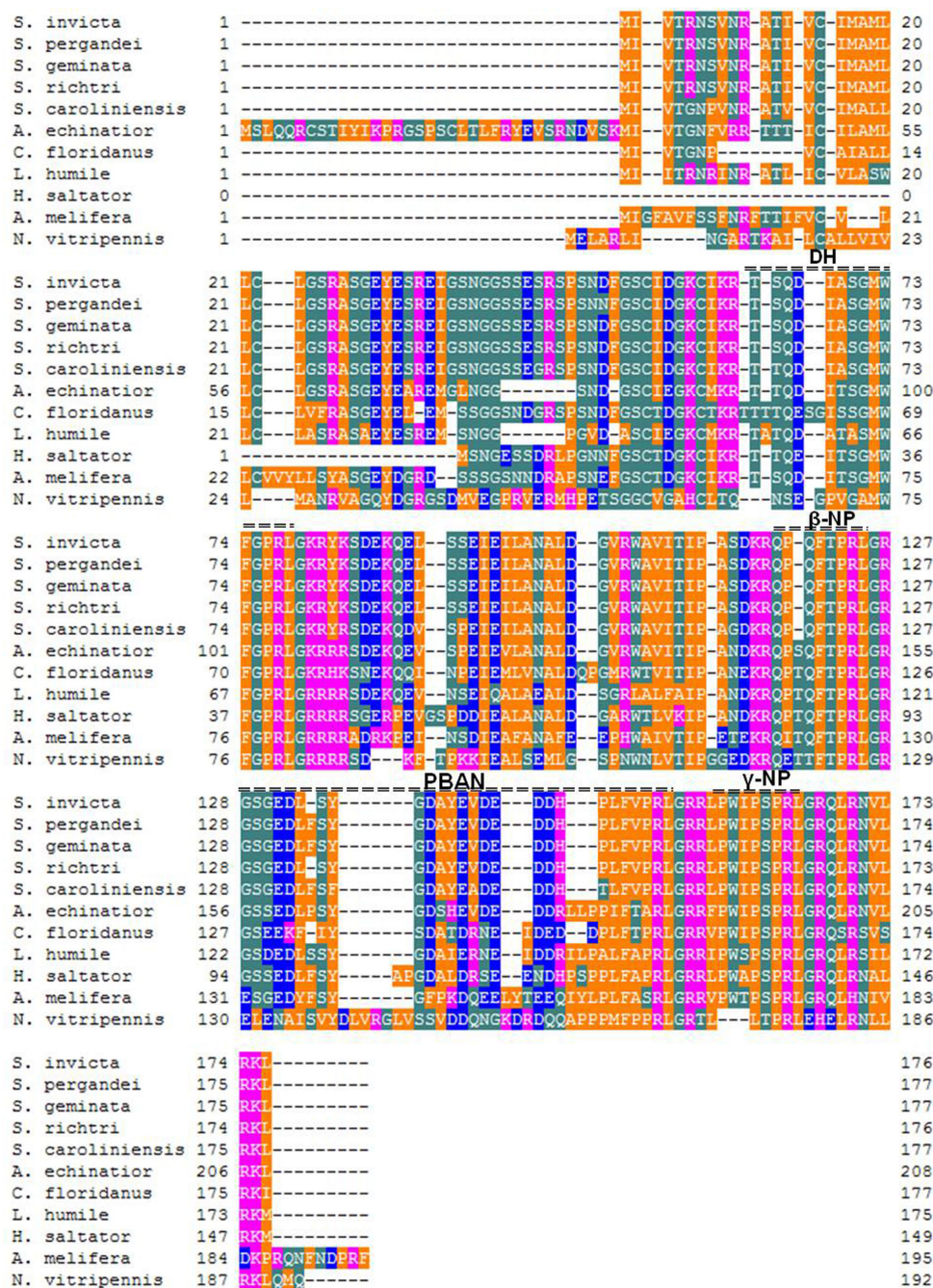


FIGURE 4 | Alignment of PBAN/pyrokinin peptides for hymenopteran insects. The species names are follow: ants (*Solenopsis invicta*, *S. pergandei*, *S. geminata*, *S. richteri*, *S. carolinensis*, *Acromyrmex echinator*, *Camponotus floridanus*, *Linepithema humile*,

and *Harpegnathos saltator*), honeybee (*Apis mellifera*), and wasp (*Nasonia vitripennis*). The alignment was made with Genetyx-Tree software (ver. 10). The translated peptide domains are indicated by double dashes above the aligned sequences.

immunocytochemistry and the transcription studies strongly suggest that PBAN/pyrokinin-like peptides are encoded from both PBAN/pyrokinin and CAPA genes. Many FXPRL peptides encoded from the CAPA gene have been isolated from the abdominal neurohemal organs of several insect groups (Predel and Wegener, 2006). Recently, we identified a fire ant specific CAPA gene

(unpublished data). Though PBAN/pyrokinin family peptides, characterized by the conserved penta-peptide at the C-terminus, have been found independently in various insect groups, it is clear that the PBAN gene is well conserved in Insecta, and probably extends to the entire Arthropod phylum (Neupert et al., 2009).

MOLECULAR STRUCTURE OF ANT PBANs

The first ant PBAN was identified from the fire ant, *S. invicta*, and specifically named SoiPBAN (Choi and Vander Meer, 2009), subsequently four additional PBAN genes were reported from the fire ant species complex (Choi et al., 2010). SoiPBAN cDNA contains 531 nucleotides covering the entire open reading frame (ORF) and encoding 176-amino acids (AA), including four FXPRL-NH₂ peptide domains. The structures of the four FXPRL peptides and their homology with the known insect PBAN/pyrokinin peptides are: (1) DH = 15-AA (TSQDIASGMWFGPRL-NH₂); (2) β -neuropeptide = 8-AA (QPQFTPRL-NH₂); (3) PBAN = 26-AA (GSGEDLSYGDAYEVEDD DHPLFVPRL-NH₂); and (4) γ -neuropeptide (NP) = 9-AA (LPWIPSPRL-NH₂; **Figure 3A**). Unlike the five peptides, DH, α , β , PBAN, and NPs, encoded from PBAN genes of lepidopteran moths, the domain of α -NP is not present in the PBAN genes of ants, mosquitoes, or beetles based on peptide homology (**Figures 3A,B**). Although C-terminal pentapeptide sequences are slightly different from moths, all four peptides from SoiPBAN cDNA induced inappropriate sex pheromone biosynthesis in *H. zea* females (Choi and Vander Meer, 2009).

The entire *S. invicta* PBAN gene (Choi et al., 2011) is composed of 13,358 nucleotides (**Figure 3C**). The gene is comprised of three exons (94, 242, and 195 nucleotides translated, respectively) interrupted by two large intron gaps; intron 1 and 2. SoiPBAN cDNA encodes a DH-homolog peptide, which is translated from the second exon, and the other peptides, β -NP, γ -NP, and SoiPBAN, are translated from the third exon. The ant PBAN gene has three exons and relatively large intron gaps compared to moth PBAN genes that consist of six exons (Xu et al., 1999; Zhang et al., 2005; Jing et al., 2007). A search of two hymenopteran species, *Apis mellifera* (accession No: NP_001104182) and *Nasonia vitripennis* (accession No: NP_001161197) genomic DNAs from the NCBI database revealed that these PBAN genes are also composed of three exons as in the fire ant PBAN gene, but contrary to the fire ant PBAN gene they contain very short intron sequence gaps. A comparison of hymenopteran and lepidopteran PBAN genes suggests that exon 1 for both translates the signal peptide. The hymenopteran exon 2 and 3 corresponds to moth PBAN gene exons 2–3 and exons 4–6, respectively (**Figure 3C**).

MOLECULAR DIVERSITY OF ANT PBANs

The *Solenopsis* group is a large genus with 185 described species (Pitts et al., 2005). The genus is difficult taxonomically due to the lack of reliable diagnostic characters. Most recently they have been re-classified into four complexes: *S. virulens*, *S. tridens*, *S. geminata*, and *S. saevissima* (Pitts et al., 2005). Since the elucidation of the first ant PBAN gene (Choi and Vander Meer, 2009), PBAN genes from four additional *Solenopsis* species and a hybrid were identified: *S. richteri* and a *S. invicta*/*S. richteri* hybrid (*Sae-vissima* complex), *S. geminata* (*Geminata* complex), *S. pergandei*, and *S. carolinensis* (members of a large group classified as thief ants that live primarily underground; Choi et al., 2010). *Solenopsis* PBAN genes were divided into two groups of cDNAs translating 176-AA for *S. invicta*, *S. richteri*, and the hybrid, and 177-AA for *S. geminata*, *S. pergandei*, and *S. carolinensis* (**Figure 4**). The one additional amino acid residue (F) in the later group was associated with the PBAN domain. Comparison of the five fire ant PBAN/pyrokinin genes showed that *S. carolinensis* was the

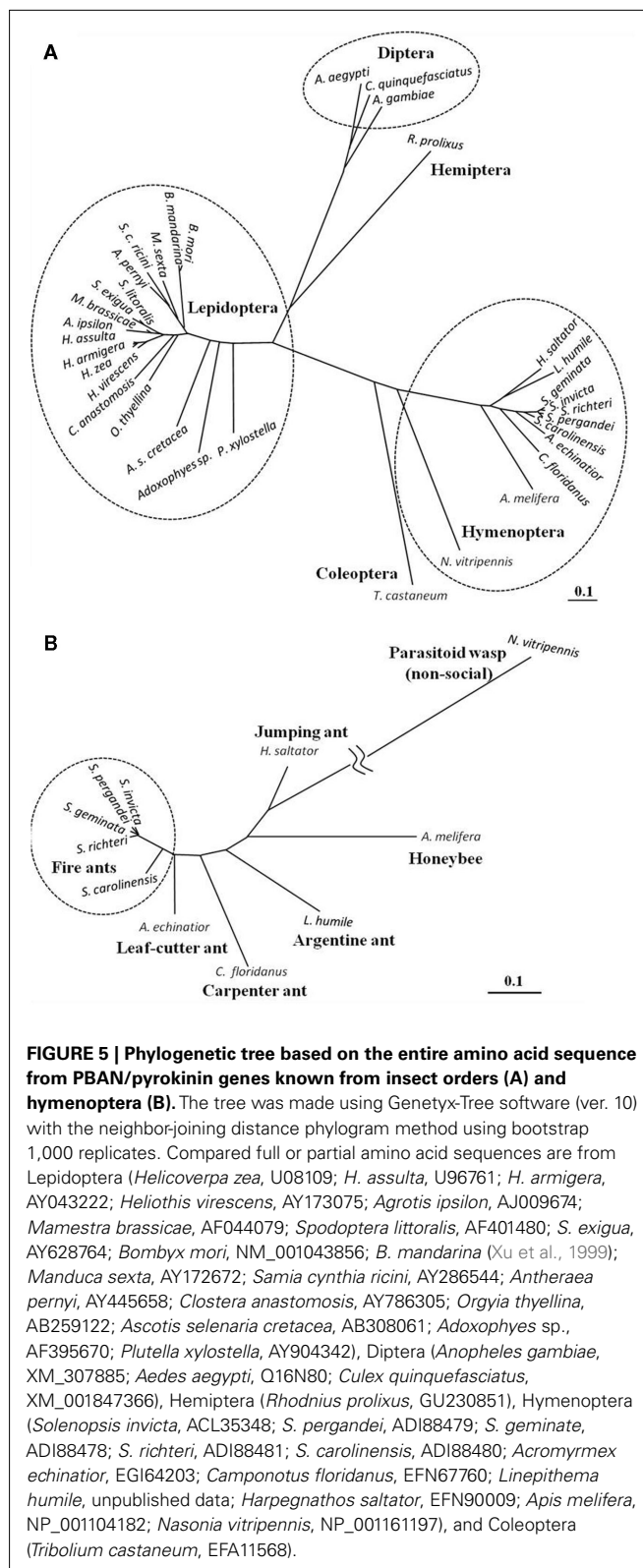


FIGURE 5 | Phylogenetic tree based on the entire amino acid sequence from PBAN/pyrokinin genes known from insect orders (A) and hymenoptera (B). The tree was made using Genetix-Tree software (ver. 10) with the neighbor-joining distance phylogram method using bootstrap 1,000 replicates. Compared full or partial amino acid sequences are from Lepidoptera (*Helicoverpa zea*, U08109; *H. assulta*, U96761; *H. armigera*, AY043222; *Heliothis virescens*, AY173075; *Agrotis ipsilon*, AJ009674; *Mamestra brassicae*, AF044079; *Spodoptera littoralis*, AF401480; *S. exigua*, AY628764; *Bombyx mori*, NM_001043856; *B. mandarina* (Xu et al., 1999); *Manduca sexta*, AY172672; *Samia cynthia ricini*, AY286544; *Antheraea pernyi*, AY445658; *Closteria anastomosis*, AY786305; *Orgyia thyellina*, AB259122; *Ascotis selenaria cretacea*, AB308061; *Adoxophyes sp.*, AF395670; *Plutella xylostella*, AY904342), Diptera (*Anopheles gambiae*, XM_307885; *Aedes aegypti*, Q16N80; *Culex quinquefasciatus*, XM_001847366), Hemiptera (*Rhodnius prolixus*, GU230851), Hymenoptera (*Solenopsis invicta*, ACL35348; *S. pergandei*, ADI88479; *S. geminata*, ADI88478; *S. richteri*, ADI88481; *S. carolinensis*, ADI88480; *Acromyrmex echinator*, EGI64203; *Camponotus floridanus*, EFN67760; *Linepithema humile*, unpublished data; *Harpegnathos saltator*, EFN90009; *Apis mellifera*, NP_001104182; *Nasonia vitripennis*, NP_001161197), and Coleoptera (*Tribolium castaneum*, EFA11568).

most distant from the other species based on nucleotide sequence homology (**Figures 4 and 5B**). This phylogenetic classification by neuropeptide sequence is consistent with the morphological cladistic analysis of the *Solenopsis* genus (Pitts et al., 2005), except

that *S. pergandei* most closely resembled *S. geminata*, and both were very distant from *S. carolinensis*, indicating significant evolutionary distance between the two thief ant species (Figure 5B). Although the PBAN gene products, neuropeptides, are not characterized functionally except for lepidopteran moths, the phylogenetic relationship of all known PBAN genes is similar to the taxonomic phylogeny based on the family level of classification and evolutionary tree of Insecta (Figure 5A). This indicates that neuropeptide gene sequences can be used to infer insect phylogenetic relationships. As anticipated, ant PBAN genes are similar within hymenopteran insects, but are distant from moth and mosquito species. Interestingly, if amino acid sequences of PBAN genes are compared in hymenopteran species, the non-social parasitoid wasp, *N. vitripennis*, is very distant from social insects including the honeybee (Figures 4 and 5B). Based on the amino acid sequences translated from PBAN genes from insects, the similarity is correlated with the basic taxonomic or phylogenetic classification of Insecta. The PBAN/pyrokinin gene is well conserved in Insecta, however, the translated pre-propeptides might vary with functional diversity, being retained or lost during the evolutionary process.

FUTURE DIRECTION

Although the amino acid sequences, gene transcription, and specific neuronal sites for ant PBAN/pyrokinin family peptides are

now known, their function in ants remains to be determined. The well documented fire ant could be an excellent social insect model to find a specific role of these neuropeptides during immature development, as well as in adult castes. To clarify specific physiological modes of action of PBAN/pyrokinin peptides in the fire ant the identification and characterization of specific receptor(s) for these peptides is required. The study includes measurement of binding activity of PBAN and other peptides to the PBAN receptor expressed in an *in vitro* system, and determination of the receptor location, e.g., tissue, gland, or organ, which would suggest a potential target site and role for PBAN/pyrokinin peptides. PBAN/pyrokinin peptides have been reported and/or identified from all insect orders investigated so far, thus these neuropeptides including PBAN are expected to have both general and specific roles, such as feeding, diapause, regulation of pheromone production, and/or other endocrinal functions. The work reviewed here lays the groundwork necessary for successfully determination of these functions, which will add significantly to our understanding of development, reproduction and social behavior in ants, and may lead to novel control possibilities for economical important invasive ants.

ACKNOWLEDGMENTS

We thank Drs. S. Allan and M. Coy for valuable comments to an earlier version.

REFERENCES

- Altstein, M., Gazit, Y., Aziz, O. B., Gabay, T., Marcus, R., Vogel, Z., and Barg, J. (1996). Induction of cuticular melanization in *Spodoptera littoralis* larvae by PBAN/MRCH: development of a quantitative bioassay and structure function analysis. *Arch. Insect Biochem. Physiol.* 31, 355–370.
- Blackburn, M. B., Kingan, T. G., Raina, A. K., and Ma, M. C. (1992). Colocalization and differential expression of PBAN- and FMRFamide-like immunoreactivity in the subesophageal ganglion of *Helicoverpa zea* (Lepidoptera: Noctuidae) during development. *Arch. Insect Biochem. Physiol.* 21, 225–238.
- Choi, M. Y., Fuerst, E. J., Rafaeli, A., and Jurenka, R. (2003). Identification of a G protein-coupled receptor for pheromone biosynthesis activating neuropeptide from pheromone glands of the moth *Helicoverpa zea*. *Proc. Natl. Acad. Sci. U.S.A.* 100, 9721–9726.
- Choi, M. Y., and Jurenka, R. A. (2004). PBAN stimulation of pheromone biosynthesis by inducing calcium influx in pheromone glands of *Helicoverpa zea*. *J. Insect Physiol.* 50, 555–560.
- Choi, M. Y., and Jurenka, R. A. (2006). Role of extracellular Ca^{2+} and calcium channel activated by a G protein-coupled receptor regulating pheromone production in *Helicoverpa zea* (Lepidoptera: Noctuidae). *Ann. Entomol. Soc. Am.* 99, 905–909.
- Choi, M. Y., Lee, J. M., Han, K. S., and Boo, K. S. (2004). Identification of a new member of PBAN family and immunoreactivity in the central nervous system from *Adoxophyes* sp. (Lepidoptera: Tortricidae). *Insect Biochem. Mol. Biol.* 34, 927–935.
- Choi, M. Y., Meer, R. K., Shoemaker, D., and Valles, S. M. (2011). PBAN gene architecture and expression in the fire ant, *Solenopsis invicta*. *J. Insect Physiol.* 57, 161–165.
- Choi, M. Y., Rafaeli, A., and Jurenka, R. A. (2001). Pyrokinin/PBAN-like peptides in the central nervous system of *Drosophila melanogaster*. *Cell Tissue Res.* 306, 459–465.
- Choi, M. Y., Raina, A., and Vander Meer, R. K. (2009). PBAN/pyrokinin peptides in the central nervous system of the fire ant, *Solenopsis invicta*. *Cell Tissue Res.* 335, 431–439.
- Choi, M. Y., and Vander Meer, R. K. (2009). Identification of a new member of the PBAN family of neuropeptides from the fire ant, *Solenopsis invicta*. *Insect Mol. Biol.* 18, 161–169.
- Choi, M. Y., Vander Meer, R. K., and Valles, S. M. (2010). Molecular diversity of PBAN family peptides from fire ants. *Arch. Insect Biochem. Physiol.* 74, 67–80.
- Davis, N. T., Homberg, U., Teal, P. E., Altstein, M., Agricola, H. J., and Hildebrand, J. G. (1996). Neuroanatomy and immunocytochemistry of the median neuroendocrine cells of the subesophageal ganglion of the tobacco hawkmoth, *Manduca sexta*: immunoreactivities to PBAN and other neuropeptides. *Microsc. Res. Tech.* 35, 201–229.
- Dupontets, L., Gadenne, C., Dufour, M. C., and Couillaud, F. (1998). The pheromone biosynthesis activating neuropeptide (PBAN) of the black cutworm moth, *Agrotis ipsilon*: immunohistochemistry, molecular characterization and bioassay of its peptide sequence. *Insect Biochem. Mol. Biol.* 28, 591–599.
- Fonagy, A., Matsumoto, S., Uchiumi, K., and Mitsui, T. (1992a). Role of calcium ion and cyclic nucleotides in pheromone production in *Bombyx mori*. *J. Pest. Sci.* 17, 115–121.
- Fonagy, A., Schoofs, L., Matsumoto, S., De Loof, A., and Mitsui, T. (1992b). Functional cross-reactivities of some locustamyotropins and *Bombyx* pheromone biosynthesis activating neuropeptide. *J. Insect Physiol.* 38, 651–657.
- Holman, G. M., Cook, B. J., and Nachman, R. J. (1986). Isolation, primary structure and synthesis of a blocked neuropeptide isolated from the cockroach, *Leucophaea maderae*. *Comp. Biochem. Physiol.* 85C, 219–224.
- Holman, G. M., Nachman, R. J., Schoofs, L., Hayes, T. K., Wright, M. S., and De Loof, A. (1991). The *Leucophaea maderae* hindgut preparation: a rapid and sensitive bioassay tool for the isolation of insect myotropins of other insect species. *Insect Biochem.* 21, 107–112.
- Hull, J. J., Ohnishi, A., Moto, K., Kawasaki, Y., Kurata, R., Suzuki, M. G., and Matsumoto, S. (2004). Cloning and characterization of the pheromone biosynthesis activating neuropeptide receptor from the silkworm, *Bombyx mori*. Significance of the carboxyl terminus in receptor internalization. *J. Biol. Chem.* 279, 51500–51507.
- Jing, T. Z., Wang, Z. Y., Qi, F. H., and Liu, K. Y. (2007). Molecular characterization of diapause hormone and pheromone biosynthesis activating neuropeptide from the black-back prominent moth, *Clostera anastomosis* (L.) (Lepidoptera, Notodontidae). *Insect Biochem. Mol. Biol.* 37, 1262–1271.

- Jurenka, R., and Nusawardani, T. (2011). The pyrokinin/pheromone biosynthesis-activating neuropeptide (PBAN) family of peptides and their receptors in Insecta: evolutionary trace indicates potential receptor ligand-binding domains. *Insect Mol. Biol.* 20, 323–334.
- Jurenka, R., and Rafali, A. (2011). Regulatory role of PBAN in sex pheromone biosynthesis of heliothine moths. *Front. Exp. Endocrinol.* 2:46, 1–8.
- Jurenka, R. A., Fabrias, G., Devoe, L., and Roelofs, W. L. (1994). Action of PBAN and related peptides on pheromone biosynthesis in isolated pheromone glands of the redbanded leafroller moth, *Argyrotaenia velutinana*. *Comp. Biochem. Physiol. Pharmacol. Toxicol. Endocrinol.* 108, 153–160.
- Jurenka, R. A., Jacquin, E., and Roelofs, W. L. (1991). Stimulation of pheromone biosynthesis in the moth *Helicoverpa zea*: action of a brain hormone on pheromone glands involves Ca^{2+} and cAMP as second messengers. *Proc. Natl. Acad. Sci. U.S.A.* 88, 8621–8625.
- Kim, Y. J., Nachman, R. J., Aimanova, K., Gill, S., and Adams, M. E. (2008). The pheromone biosynthesis activating neuropeptide (PBAN) receptor of *Heliothis virescens*: identification, functional expression, and structure-activity relationships of ligand analogs. *Peptides* 29, 268–275.
- Kingan, T. G., Blackburn, M. B., and Raina, A. (1992). The identification of pheromone-biosynthesis-activating neuropeptide (PBAN) immunoreactivity in the central nervous system of the corn earworm, *Helicoverpa zea*. *Cell Tissue Res.* 270, 229–240.
- Kuniyoshi, H., Nagasawa, H., Ando, T., Suzuki, A., Nachman, R. J., and Holman, G. M. (1992). Cross-activity between pheromone biosynthesis activating neuropeptide (PBAN) and myotropic pyrokinin insect peptides. *Biosci. Biotechnol. Biochem.* 56, 167–168.
- Lee, D. W., Shrestha, S., Kim, A. Y., Park, S. J., Yang, C. Y., Kim, Y., and Koh, Y. H. (2011). RNA interference of pheromone biosynthesis-activating neuropeptide receptor suppresses mating behavior by inhibiting sex pheromone production in *Plutella xylostella* (L.). *Insect Biochem. Mol. Biol.* 41, 236–243.
- Ma, P. W. K., and Roelofs, W. L. (1995a). Calcium involvement in the stimulation of sex pheromone production by PBAN in the European corn borer, *Ostrinia nubilalis* (Lepidoptera: Pyralidae). *Insect Biochem. Mol. Biol.* 25, 467–473.
- Ma, P. W. K., and Roelofs, W. L. (1995b). Sites of synthesis and release of PBAN-like factor in the female European corn borer, *Ostrinia nubilalis*. *J. Insect Physiol.* 41, 339–350.
- Ma, P. W. K., Roelofs, W. L., and Jurenka, R. A. (1996). Characterization of PBAN and PBAN-encoding gene neuropeptides in the central nervous system of corn earworm moth, *Helicoverpa zea*. *J. Insect Physiol.* 42, 257–266.
- Matsumoto, S., Kitamura, A., Nagasawa, H., Kataoka, H., Orikasa, C., Mitsui, T., and Suzuki, A. (1990). Functional diversity of a neurohormone produced by the subesophageal ganglion: molecular identity of melanization and reddish coloration hormone and pheromone biosynthesis activating neuropeptide. *J. Insect Physiol.* 36, 427–432.
- Matsumoto, S., Ozawa, R., Nagamine, T., Kim, G. H., Uchiyumi, K., Shono, T., and Mitsui, T. (1995a). Intracellular transduction in the regulation of pheromone biosynthesis of the silkworm, *Bombyx mori*: suggested involvement of calmodulin and phosphoprotein phosphatase. *Biosci. Biotechnol. Biochem.* 59, 560–562.
- Matsumoto, S., Ozawa, R., Uchiyumi, K., Kurihara, M., and Mitsui, T. (1995b). Intracellular signal transduction of PBAN action in the common cutworm, *Spodoptera litura*: effects of pharmacological agents on sex pheromone production in vitro. *Insect Biochem. Mol. Biol.* 25, 1055–1059.
- Nachman, R. J., Holman, G. M., and Cook, B. J. (1986). Active fragments and analogs of the insect neuropeptide Leucopyrokinin: structure-function studies. *Biochem. Biophys. Res. Commun.* 137, 936–942.
- Neupert, S., Russell, W. K., Predel, R., Russell, D. H., Strey, O. F., Teel, P. D., and Nachman, R. J. (2009). The neuropeptidomics of *Ixodes scapularis* synganglion. *J. Proteomics* 72, 1040–1045.
- Niven, J. E., Graham, C. M., and Burrows, M. (2008). Diversity and evolution of the insect ventral nerve cord. *Annu. Rev. Entomol.* 53, 253–271.
- Pitts, J. P., Mchugh, J. V., and Ross, K. G. (2005). Cladistic analysis of the fire ants of the *Solenopsis saevissima* species-group (Hymenoptera: Formicidae). *Zool. Scr.* 34, 493–505.
- Predel, R., Kellner, R., Kaufmann, R., Penzlin, H., and Gade, G. (1997). Isolation and structural elucidation of two pyrokinins from the retrocerebral complex of the American cockroach. *Peptides* 18, 473–478.
- Predel, R., Linde, D., Rapus, J., Vettermann, S., and Penzlin, H. (1995). Periviscerokinins (Pea-PVK): a novel myotropic neuropeptide from the perisymphathetic organs of the American cockroach. *Peptides* 16, 61–66.
- Predel, R., and Nachman, R. J. (2001). Efficacy of native FXPRLamides (pyrokinins) and synthetic analogs on visceral muscles of the American cockroach. *J. Insect Physiol.* 47, 287–293.
- Predel, R., and Wegener, C. (2006). Biology of the CAPA peptides in insects. *Cell. Mol. Life Sci.* 63, 2477–2490.
- Rafali, A. (2009). Pheromone biosynthesis activating neuropeptide (PBAN): regulatory role and mode of action. *Gen. Comp. Endocrinol.* 162, 69–78.
- Rafali, A., Bober, R., Becker, L., Choi, M. Y., Fuerst, E. J., and Jurenka, R. (2007). Spatial distribution and differential expression of the PBAN receptor in tissues of adult *Helicoverpa* spp. (Lepidoptera: Noctuidae). *Insect Mol. Biol.* 16, 287–293.
- Rafali, A., and Srooker, V. (1994). “Second messenger interactions in response to PBAN stimulation of pheromone gland cultures,” in *Insect Neurochemistry and Neurophysiology*, eds A. Borkovec and M. J. Loeb (Boca Raton, FL: CRC Press), 223–226.
- Raina, A. K., Jaffe, H., Kempe, T. G., Keim, P., Blacher, R. W., Fales, H. M., Riley, C. T., Klun, J. A., Ridgway, R. L., and Hayes, D. K. (1989). Identification of a neuropeptide hormone that regulates sex pheromone production in female moths. *Science* 244, 796–798.
- Raina, A. K., and Kempe, T. G. (1990). A pentapeptide of the C-terminal sequence of PBAN with pheromonotropic activity. *Insect Biochem.* 20, 849–851.
- Raina, A. K., and Kempe, T. G. (1992). Structure activity studies of PBAN of *Helicoverpa zea* (Lepidoptera: Noctuidae). *Insect Biochem. Mol. Biol.* 22, 221–225.
- Sato, Y., Ikeda, M., and Yamashita, O. (1994). Neurosecretory cells expressing the gene for common precursor for diapause hormone and pheromone biosynthesis-activating neuropeptide in the subesophageal ganglion of the silkworm, *Bombyx mori*. *Gen. Comp. Endocrinol.* 96, 27–36.
- Schoofs, L., Holman, G. M., Hayes, T. K., Kochansky, J. P., Nachman, R. J., and De Loof, A. (1990a). Locustat-achykinin III and IV: two additional insect neuropeptides with homology to peptides of the vertebrate tachykinin family. *Regul. Pept.* 31, 199–212.
- Schoofs, L., Holman, G. M., Hayes, T. K., Nachman, R. J., and De Loof, A. (1990b). Isolation, identification and synthesis of locustamyotropin II, an additional neuropeptide of *Locusta migratoria*: member of the cephalomyotropic peptide family. *Insect Biochem.* 20, 479–484.
- Schoofs, L., Holman, G. M., Hayes, T. K., Nachman, R. J., and De Loof, A. (1991). Isolation, primary structure, and synthesis of locustapyrokinin: a myotropic peptide of *Locusta migratoria*. *Gen. Comp. Endocrinol.* 81, 97–104.
- Sun, J. S., Zhang, T. Y., Zhang, Q. R., and Xu, W. H. (2003). Effect of the brain and subesophageal ganglion on pupal development in *Helicoverpa armigera* through regulation of FXPRLamide neuropeptides. *Regul. Pept.* 116, 163–171.
- Suwan, S., Isobe, M., Yamashita, O., Minakata, H., and Imai, K. (1994). Silkworm diapause hormone, structure-activity relationships indispensable role of C-terminal amide. *Insect Biochem. Mol. Biol.* 24, 1001–1007.
- Tillman, J. A., Seybold, S. J., Jurenka, R. A., and Blomquist, G. J. (1999). Insect pheromones – an overview of biosynthesis and endocrine regulation. *Insect Biochem. Mol. Biol.* 29, 481–514.
- Tips, A., Schoofs, L., Paemen, L., Ma, M., Blackburn, M., Raina, A., and Loof, A. D. (1993). Colocalization of locustamyotropin and pheromone biosynthesis activating neuropeptide-like immunoreactivity in the central nervous system of five insect species. *Comp. Biochem. Physiol. A Comp. Physiol.* 106, 195–207.
- Uehara, H., Senoh, Y., Yoneda, K., Kato, Y., and Shiomi, K. (2011). An FXPRLamide neuropeptide induces seasonal reproductive polyphenism underlying a life-history trade-off in the tussock moth. *PLoS ONE* 6, e24213. doi:10.1371/journal.pone.0024213
- Verleyen, P., Clynen, E., Huybrechts, J., Van Lommel, A., Vanden Bosch, L.,

- De Loof, A., Zdarek, J., and Schoofs, L. (2004). Fraenkel's pupariation factor identified at last. *Dev. Biol.* 273, 38–47.
- Wei, Z.-J., Hong, G.-Y., Jinag, S.-T., Tong, Z.-X., and Lu, C. (2008). Characters and expression of the gene encoding DH, PBAN and other FXPRLamide family neuropeptides in *Antheraea pernyi*. *J. Appl. Entomol.* 132, 59–67.
- Xu, W., Sato, Y., and Yamashita, O. (1999). Molecular characterization of the cDNA encoding diapause hormone and pheromone biosynthesis activating neuropeptide in *Bombyx mandarina*. *Nihon Sanshigaku Zasshi* 68, 373–379.
- Xu, W. H., and Denlinger, D. L. (2003). Molecular characterization of prothoracicotropic hormone and diapause hormone in *Heliothis virescens* during diapause, and a new role for diapause hormone. *Insect Mol. Biol.* 12, 509–516.
- Zdarek, J., Nachman, R. J., and Hayes, T. K. (1997). Insect neuropeptides of the pyrokinin/PBAN family accelerate pupariation in the fleshfly (*Sarcophaga bullata*) larvae. *Ann. N. Y. Acad. Sci.* 814, 67–72.
- Zhang, T. Y., Sun, J. S., Liu, W. Y., Kang, L., Shen, J. L., and Xu, W. H. (2005). Structural characterization and transcriptional regulation of the gene encoding diapause hormone and pheromone biosynthesis activating neuropeptide in the cotton bollworm, *Helicoverpa armigera*. *Biochim. Biophys. Acta* 1728, 44–52.
- Zheng, L., Lytle, C., Njauw, C. N., Altstein, M., and Martins-Green, M. (2007). Cloning and characterization of the pheromone biosynthesis activating neuropeptide receptor gene in *Spodoptera littoralis* larvae. *Gene* 393, 20–30.

Conflict of Interest Statement: The authors declare that the research was conducted in the absence of any commercial or financial relationships that could be construed as a potential conflict of interest.

Received: 21 November 2011; accepted: 09 February 2012; published online: 24 February 2012.

Citation: Choi M-Y and Vander Meer RK (2012) Molecular structure and diversity of PBAN/pyrokinin family peptides in ants. *Front. Endocrin.* 3:32. doi: 10.3389/fendo.2012.00032

This article was submitted to *Frontiers in Experimental Endocrinology*, a specialty of *Frontiers in Endocrinology*.

Copyright © 2012 Choi and Vander Meer. This is an open-access article distributed under the terms of the Creative Commons Attribution Non Commercial License, which permits non-commercial use, distribution, and reproduction in other forums, provided the original authors and source are credited.



Effects of starvation on brain short neuropeptide F-1, -2, and -3 levels and short neuropeptide F receptor expression levels of the silkworm, *Bombyx mori*

Shinji Nagata*, Sumihiro Matsumoto, Tomohiro Nakane, Ayako Ohara, Nobukatsu Morooka, Takahiro Konuma, Chiaki Nagai and Hiromichi Nagasawa

Department of Applied Biological Chemistry, Graduate School of Agricultural and Life Sciences, The University of Tokyo, Bunkyo-ku, Tokyo, Japan

Edited by:

Joe Hull, USDA Agricultural Research Service, USA

Reviewed by:

Hironori Ando, Niigata University, Japan

Joe Hull, USDA Agricultural Research Service, USA

Åsa M. E. Winther, Karolinska Institutet, Sweden

*Correspondence:

Shinji Nagata, Department of Applied Biological Chemistry, Graduate School of Agricultural and Life Sciences, The University of Tokyo, 1-1-1 Yayoi, Bunkyo-ku, Tokyo 113-8657, Japan.
e-mail: anagashi@mail.ecc.u-tokyo.ac.jp

In our previous report, we demonstrated the possibility that various regulatory neuropeptides influence feeding behavior in the silkworm, *Bombyx mori*. Among these feeding-related neuropeptides, short neuropeptide F (sNPF) exhibited feeding-accelerating activity when injected into *B. mori* larvae. Like other insect sNPFs, the deduced amino acid sequence of the cDNA encoding the sNPF precursor appears to produce multiple sNPF and sNPF-related peptides in *B. mori*. The presence of three sNPFs, sNPF-1, sNPF-2, and sNPF-3, in the brain of *B. mori* larvae was confirmed by direct MALDI-TOF mass spectrometric profiling. In addition, all three sNPFs are present in other larval ganglia. The presence of sNPF mRNA in the central nervous system (CNS) was also confirmed by Reverse transcription-polymerase chain reaction. Semi-quantitative analyses of sNPFs in the larval brain using matrix-assisted laser desorption ionization time-of-flight mass spectrometry further revealed that brain sNPF levels decrease in response to starvation, and that they recover with the resumption of feeding. These data suggest that sNPFs were depleted by the starvation process. Furthermore, food deprivation decreased the transcriptional levels of the sNPF receptor (BNGR-A10) in the brain and CNS, suggesting that the sNPF system is dependent on the feeding state of the insect and that the sNPF system may be linked to locomotor activity associated with foraging behavior. Since the injection of sNPFs accelerated the onset of feeding in *B. mori* larvae, we concluded that sNPFs are strongly related to feeding behavior. In addition, semi-quantitative MS analyses revealed that allatostatin, which is present in the larval brain, is also reduced in response to starvation, whereas the peptide level of Bommyosuppressin was not affected by different feeding states.

Keywords: *Bombyx mori*, feeding behavior, peptide, short neuropeptide F

INTRODUCTION

Although phytophagous insects feed on their preferred host plants, feeding is not continuous. A number of biochemical and behavioral studies have found that chemical components extracted from host plants serve as attractants or deterrents for plant feeders (Harborne, 1993; Hanson, 2003), and thus contribute to host selection. Therefore, it is believed that feeding behavior in phytophagous insects may be initiated by the chemical components present in their preferred host plants.

The biology and physiology of the mechanisms that regulate insect feeding behavior have been extensively investigated (Simpson, 1995). To date, sequential behaviors in regularly occurring feeding patterns have been monitored using a number of phytophagous insects, including orthopteran (Blaney et al., 1973; Simpson, 1982; Simpson and Ludlow, 1986) and lepidopteran species (Reynolds et al., 1986; Bowdan, 1988a,b; Timmins et al., 1988; Bernays and Woods, 2000; Nagata and Nagasawa, 2006). In the case of the silkworm, *Bombyx mori*, larvae exhibit characteristic feeding behavioral patterns that are generated independent of

circadian rhythms at regular intervals of approximately every 2 h (Nagata and Nagasawa, 2006). Since these characteristic behaviors are primarily timed by the mode-changing process from quiescent status to feeding status, we assumed that some process might be involved in the decision to initiate feeding activity.

Based on previous physiological reports, the feeding state of an insect can be defined according to the following two indicators: (1) duration elapsed from the end of the previous meal and (2) head-swaying behavior immediately before the onset of eating or under feeding-motivated states (Nagata et al., 2011a). These two physiologically defined feeding states, hunger and satiety, support the evaluation of feeding behavior in *B. mori* larvae by measuring the latency period prior to the initiation of feeding (Nagata et al., 2011b). We were previously able to identify several biologically active peptides as feeding modulators by measuring the length of the latency period prior to the initiation of feeding in *B. mori* larvae (Nagata et al., 2009, 2011a,b). Among these peptides, two classes of peptides with different biological activities on feeding behavior were characterized: (1) inhibitory peptides, which prolong the

latency to the initiation of feeding, and (2) acceleratory peptides, which shorten the latency to feeding initiation. Consistent with a previous proposal regarding control of invertebrate feeding behavior (Simpson, 1995), we found that FMRFamide-related peptides (FaRPs) and myosuppressin have inhibitory effects on the initiation of feeding behavior by peptide administration in *B. mori* larvae (Nagata et al., 2011b). In contrast, the administration of short neuropeptide F (sNPF) was shown to shorten the latency period, possibly resulting from the activation of locomotor activity. Quantitative analysis of sNPF levels during different feeding states, however, has not been fully examined.

The compiled genomic information from a number of insect species has allowed us to identify *in silico* various conserved factors, including the identification of sNPFs from a number of insect species. sNPFs belong to a very diverse neuropeptide group sharing a C-terminal RF-amide or RY-amide. In vertebrates, a representative RY-amide peptide, neuropeptide Y (NPY), has been characterized as a neuromodulator controlling feeding behaviors (Tatemoto et al., 1982). In invertebrates, a NPY homologous peptide has been identified in the tapeworm, *Moniezia expansa*, as a factor that regulates myo-stimulatory effects (Maule et al., 1991). By using an antibody against NPF [antiserum against Arg-X-Arg-Phe/Tyr-NH₂; serum code 792(3)], shorter peptides that share the C-terminal RF-amide sequence, subsequently designated as short NPF, have been identified in the Colorado potato beetle (Spittaels et al., 1996). However, the detailed function of sNPF *in vivo* remains to be elucidated.

A cDNA encoding sNPF was first identified in the fruit fly, *Drosophila melanogaster* (Vanden Broeck, 2001). The deduced amino acid sequence contained four sNPFs, which were predicted to be produced after the post-translational modification of a dibasic amino acid cleavage site and C-terminal amidation (Vanden Broeck, 2001). In *D. melanogaster*, sNPF has been shown to be pleiotropic including regulation of feeding behavior (Lee et al., 2004, 2008; Nassel and Wegener, 2011). sNPFs are conserved across arthropod species with the number of sNPF isoforms encoded by a single cDNA varying depending on the insect species (Nassel and Wegener, 2011). In *B. mori*, sNPF has been identified as a juvenile hormone (JH) regulating peptide that functions in tandem with allatotropin to regulate the secretion of JH from the corpora allata (Yamanaka et al., 2008). Identification of a cDNA encoding sNPFs revealed the presence of three sNPFs in *B. mori* (Mita et al., 2003; Roller et al., 2008; Yamanaka et al., 2008), which is consistent with reports in other insects of multiple sNPFs.

In *D. melanogaster*, the presence of sNPFs isoforms has been characterized by direct matrix-assisted laser desorption/ionization time-of-flight mass spectrometry (MALDI-TOF MS) profiling (Predel et al., 2004; Baggerman et al., 2005; Yew et al., 2009; Carlsson et al., 2010; Wegener et al., 2011). Although sNPF-2 and a partial fragment of sNPF-3 were purified from *B. mori* brain extracts (Yamanaka et al., 2008), there is currently no experimental evidence for the presence of all three sNPF isoforms at the peptide level in *B. mori*. We consequently performed direct mass spectrometric profiling of larval brains to reassess the presence of sNPFs. In addition, to further address the mechanisms underlying sNPF-mediated feeding behaviors, we semi-quantitatively measured the levels sNPFs during different feeding states in *B. mori*.

MATERIALS AND METHODS

CHEMICALS AND REAGENTS

Chemicals and reagents, α -cyano-4-hydroxycinnamic acid (CCA), ethidium bromide, agarose for electrophoresis and Trizma-base, and EDTA used in the present study were purchased from Nacal-tesque (Osaka, Japan). Methanol, diethylether, formic acid, trifluoroacetic acid (TFA), and acetonitrile for reversed-phase HPLC (RP-HPLC) were purchased from Kanto Chemicals (Tokyo, Japan). Fmoc derivatives of amino acids were purchased from Watanabe Chemical Industries (Hiroshima, Japan).

INSECTS

Silkworm eggs from the hybrid *B. mori* strain (Kinshu \times Showa) were purchased from UEDA SANSHU Ltd. (Ueda, Japan). Larvae were reared in plastic containers at $26 \pm 1^\circ\text{C}$ with $70 \pm 10\%$ relative humidity under long-day lighting conditions (16L: 8D) using SILKMATE 2S artificial diet purchased from NIPPON NOSAN Co. Ltd. (Yokohama, Japan). Larvae were provided with fresh diet on a daily basis. Only larvae whose growth was synchronized were utilized for the present experiments.

PREPARATION OF STARVED AND RE-FED *B. mori* LARVAE

Bombyx mori larvae were starved by food deprivation with feces frequently removed from the containers throughout starvation. Food deprivation was initiated in synchronously growing fifth instar, day-2 larvae (2.7 ± 0.3 g). Resumption of feeding was initiated with addition of an artificial diet block. One hour after resumption of feeding, the re-fed-larvae were anesthetized on ice. For mass spectrometric analyses, brains were dissected out from the prepared larvae.

PREPARATION OF SYNTHETIC PEPTIDES

Short neuropeptide Fs were chemically synthesized based on the Fmoc method using an automated peptide synthesizer (APEX-SC, apex396, Advanced ChemTech, Louisville, KY, USA) and deprotection as previously reported (Nagata et al., 2011b). In brief, after deprotection and cleavage from resins, the synthetic peptides in diethylether were collected by centrifugation. The resulting crude synthetic peptides were partially purified using Sep-Pak C18. The adsorbed sample was eluted with 60% acetonitrile/0.1% TFA. The eluate was subjected to RP-HPLC (Jasco SC 802, PU-880, UV-875, Jasco; Tokyo, Japan) on a Senshu Pak Pegasil-300 ODS column (4.6 mm i.d. \times 250 mm, Shenshu Kagaku, Tokyo, Japan) with a 25-min linear gradient of 10–60% acetonitrile containing 0.05% TFA at a flow rate of 1.0 ml/min. The purity of the synthetic peptide was confirmed by MALDI-TOF MS using a Voyager-DETMSTR (Applied Biosystems, CA, USA) in the positive ion mode and CCA as the matrix. A highly purified byproduct (m/z 983) of sNPF synthesis was used for semi-quantitative analyses in the present study.

REVERSE TRANSCRIPTION-POLYMERASE CHAIN REACTION

Total RNA was extracted from fat body, silk glands, foregut, midgut, hindgut, Malpighian tubules, hemocytes, central nervous ganglia, brain, ovary, and testis using TRI-ZOL reagent (Invitrogen, Carlsbad, CA, USA) according to the manufacturer's protocol. After treatment with DNase

I (TaKaRaBio, Shiga, Japan), cDNA was synthesized using a reverse transcriptase, Superscript III (Invitrogen), and an oligo-dT₃₀ primer. Gene specific primers were sNPF-Fw (5'-GATGCTCCTAAAGAAGACAAT-3') and sNPF-Rv (5'-TCAGGCTTTCCGGTGCTTCCG-3'). Primers for sNPF (BNGR-A10) were sNPF-Fw (5'-GCTACAATCCATTCCTCTATGCTT-3') and sNPF-Rv (5'-AGGTTCCCTTGCTGAAGAAATCAC-3'). Ribosomal protein 49 (*rp49*) was used as an experimental control with the following gene specific primer: Rp-Fw (5'-GACCTGTTTACAGGCCGACAATCG-3') and Rp-Rv (5'-TTATATTATTCACTCTCCTGGGAGCGGAG-3'). Amplified fragments were electrophoresed on a 1.2% agarose gel and detected by staining with ethidium bromide. The saturation of PCR products were observed after 35 cycles of amplification. We consequently performed our analyses at 30 cycles. To quantitate the sNPF expression levels (data not shown), gel images were analyzed using the public domain NIH Image program (the U.S. National Institutes of Health at <http://rsb.info.nih.gov/nih-image/>). The analyzed PCR product bands were normalized to bands derived from the PCR experimental control, *rp49*.

QUANTITATIVE RT-PCR

Extraction of total RNA and RT reaction were performed as described above. The primers for Quantitative RT-PCR (qRT-PCR) for sNPF were: forward 5'-TGCTTGCTCAACGAAACT-3'; reverse 5'-GAAAGCACCCAAACATGGAA-3'. As a control, the following primers for *rp49* were used: forward 5'-TGGGAGGTTTCCCCATT-3'; reverse 5'-CCATGCAGCAACCCTTGAT-3'. PCR was performed using a 7300 Real-Time PCR system (Applied Biosystems). Thermal cycling conditions were as follows: after initial denaturation at 95°C for 10 min, 40 cycles of 95°C, 15 s; 60°C, 1 min. The singly targeted qRT-PCR product was confirmed by constructing a melt curve to all reactions. The reaction was performed using Power SYBR® Green PCR Master Mix (Applied Biosystems) and 50 nM

of each primer. Data were analyzed using the 7300 Real-Time PCR system software v1.3 (Applied Biosystems). Results are represented as a ratio of sNPF and RpL3 by Ct method.

DIRECT MALDI-TOF MS ANALYSIS

Brain and other ganglia were isolated from *B. mori* larvae and placed in a drop of distilled water. After removal of excess water, the matrix solution was covered with the dried brain or ganglia prior to mass spectrometry analysis. Mass spectra were measured on a MALDI-TOF mass spectrometer with CCA as matrix in the positive ion mode. The matrix solution was prepared by saturating CCA in 60% acetonitrile containing 0.1% TFA.

SEMI-QUANTITATIVE ANALYSES USING MALDI-TOF MS

For semi-quantitative analyses, the intensities of the mass spectra ion peaks were evaluated by comparing with an exogenously added internal standard peptide as previously reported (Jimenez et al., 1997). The internal standard peptide, which is not observed in the spectrum of brain extracts, has a *m/z* 983 and is the byproduct of Fmoc chemical synthesis of sNPF-2 with Fmoc at the N-terminus of sNPF-2. The internal standard was added in extraction solution (90% methanol in 0.1% formic acid). The relative intensities of each ion peak were compared with the intensity of the ion peak corresponding to the internal standard peptide. Five samples were measured for analyses of ion peak intensities. At least three measurements were carried out per sample. Single measurement of MALDI-TOF MS was carried out by accumulation of more than 50 shots using the same laser desorption settings.

STATISTICAL ANALYSIS

The intensities of the semi-quantitative analyses of sNPF were statistically compared with control samples derived from brains of larvae fed *ad libitum* using one-way ANOVA. Significances were determined with Dunnett's *post hoc* test (data from larvae fed *ad libitum* were used as experimental controls for comparison).

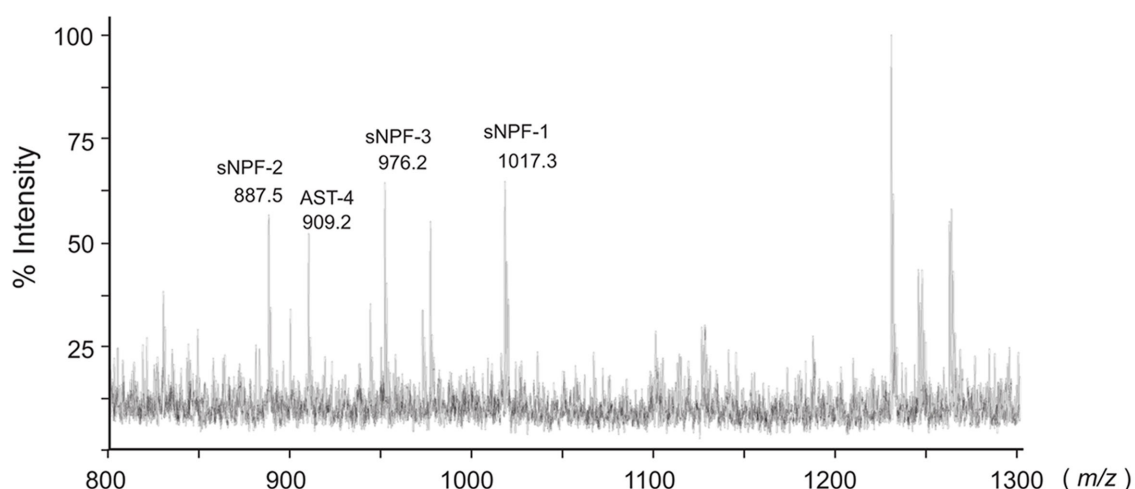


FIGURE 1 | *Bombyx mori* sNPF precursor and MS spectrum of *B. mori* larval brain. Representative MS spectrum of the *B. mori* larval brain. A fifth instar *B. mori* larval brain was isolated and directly analyzed by MALDI-TOF MS. The *B. mori* genomic database was used to facilitate identification of ion peaks in the spectrum.

RESULTS

sNPF IN THE SILKWORM, *BOMBYX MORI*

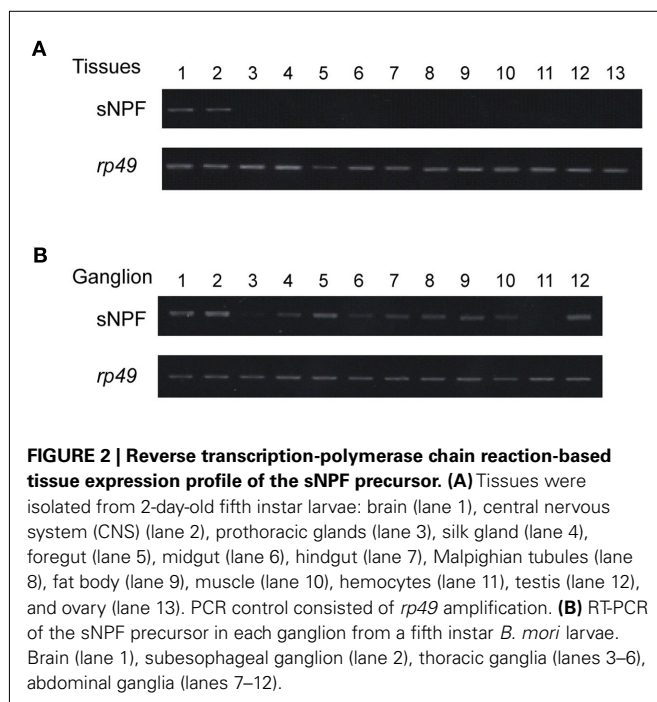
In *B. mori*, three sNPFs, sNPF-1, sNPF-2, and sNPF-3, are encoded by a single cDNA sequence (Yamanaka et al., 2008). Of these three sNPFs, sNPF-2 and a partial fragment of sNPF-3 were purified from brain extracts (Yamanaka et al., 2008). To confirm the presence of sNPFs in the central nervous system (CNS), we performed direct MALDI-TOF mass spectrometric analyses using the isolated brain of a last instar larva (Figure 1). In total, more than 15 detectable ion peaks were observed. As deduced from the cDNA sequence encoding the sNPF precursor, ion peaks at m/z 1017.2, 887.2, and 976.1 corresponding to sNPF-1, sNPF-2, and sNPF-3, respectively, were observed. These data suggest the presence of all three forms of sNPF in the brain. A database search revealed that these ion peaks coincided with those of known neuropeptides, including sNPFs (Figure 1).

RT-PCR ANALYSES OF *B. mori* sNPFs

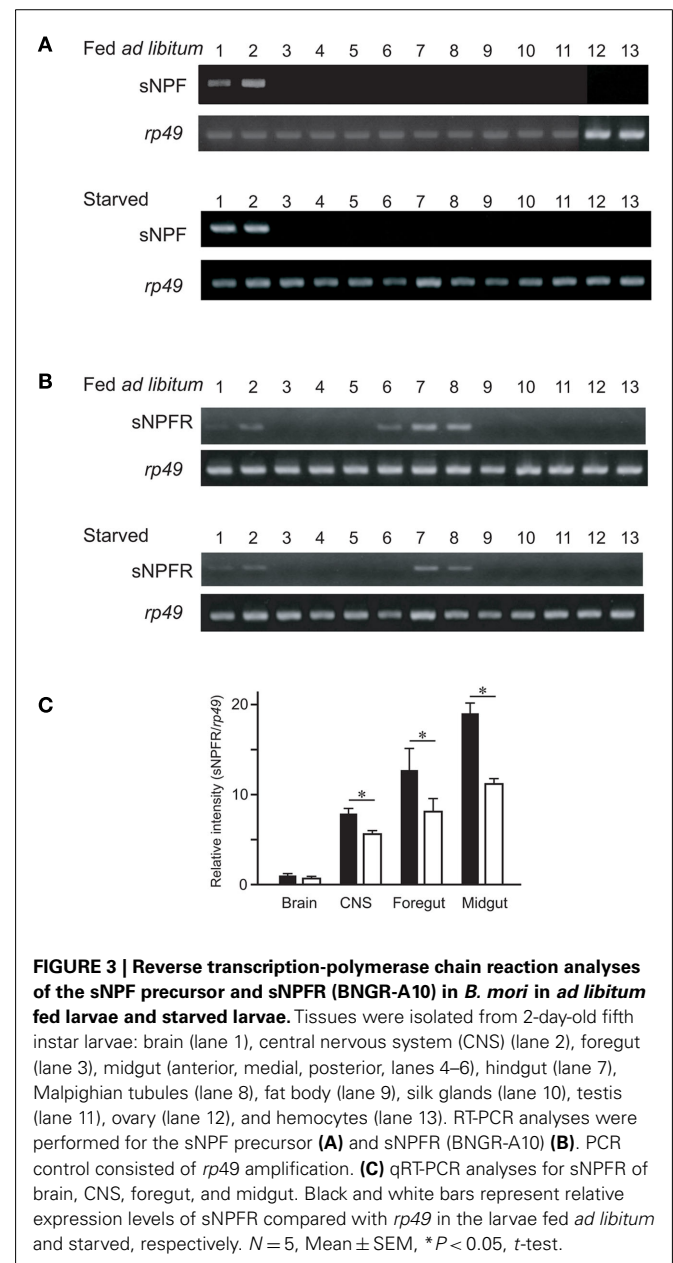
We subsequently confirmed the expression sites of the sNPF precursor transcript in *B. mori* larvae. Reverse transcription-polymerase chain reaction (RT-PCR) using specific primers for the sNPF precursor cDNA sequence revealed that the expression of sNPFs was observed in the brain and CNS (Figure 2A). To analyze the detailed location of sNPF expression, we examined the expression profile in each ganglion. We found that all ganglia expressed the sNPF precursor mRNA, even though biased cDNA amplification was observed (Figure 2B). These RT-PCR data are consistent with our MS data.

sNPF EXPRESSION DURING DIFFERENT FEEDING STATES

While determining the sNPF precursor expression profile, we observed clear differences in expression levels. The resulting RT-PCR products were compared between the tissues of *ad libitum*



fed larvae and starved larvae. These results showed similar levels for the sNPF precursor transcript in the brain and CNS in the different feeding states (Figure 3A). Furthermore, the transcriptional expression level of the sNPF receptor (sNPF-R, BNGR-A10) was also analyzed by RT-PCR. The widely distributed expression sites of the sNPF-R were reconfirmed, supporting previous reports (Yamanaka et al., 2008). Comparison of the transcriptional levels of the sNPF-R between RT-PCR products derived from tissues of *ad libitum* fed larvae and starved larvae revealed that starvation reduces sNPF-R transcript levels (Figure 3B). The reduced levels of sNPF-R transcript by starvation were confirmed using several sNPF-R expressing tissues, brain, CNS, midgut, and hindgut by qRT-PCR (Figure 3C). We observed a significant reduction in sNPF-R expression levels following starvation in all tissues



examined except for the brain, which likewise showed a slight albeit not significant reduction in sNPF.

SEMI-QUANTITATIVE ANALYSES OF sNPFs IN THE BRAIN

We next examined the peptide levels of sNPFs in the brain during different feeding states. The amount of brain sNPFs were semi-quantitatively analyzed by comparing the relative levels of sNPFs in crude larval brain extracts with an exogenous internal standard peptide. A byproduct of sNPF-2 chemical synthesis was used as an exogenous standard peptide after separation from sNPF-2 by RP-HPLC. In the resulting spectra, we observed ion peaks at m/z 1017.2, 887.2, and 976.1 corresponded to sNPF-1, sNPF-2, and sNPF-3, respectively. Reduced levels of sNPF-1 and sNPF-2 were observed in starved larval brains. The levels of sNPF-1 and sNPF-2 further decreased with an increase in the starvation period (Figure 4). A resumption of feeding returned the levels of brain sNPF-1 and sNPF-2 back to basal levels. It is noteworthy that sNPF-1 and sNPF-2 were significantly reduced by starvation, whereas sNPF-3 was not as clearly affected. However, there did appear to be a similar trend, albeit not statistically significant, in the reduction sNPF-3 levels, most noticeably after 2 days of starvation. The less pronounced reduction in sNPF-3 levels could be due to a lower ionization efficiency.

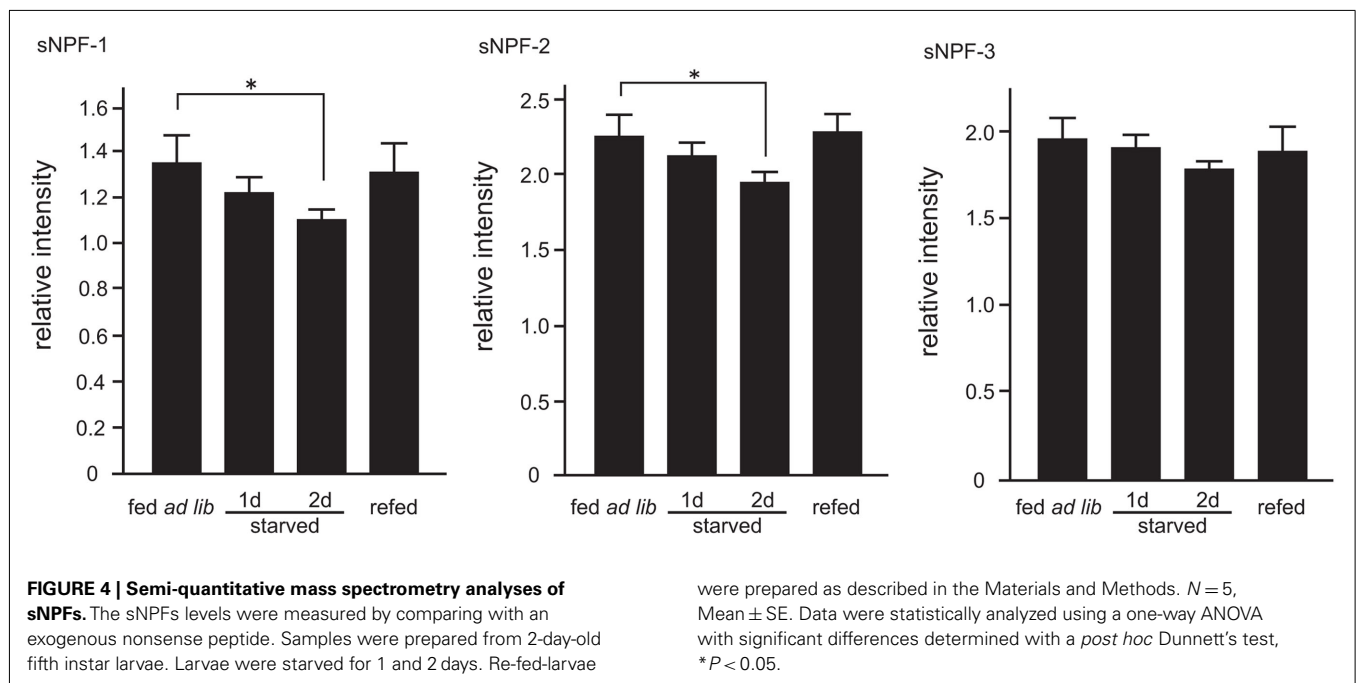
The mass spectral profiles (Table 1) obtained while performing the semi-quantitative analyses of sNPFs allowed us to examine the effects of starvation two other significant ion peaks. These ion peaks correspond to Bommyosuppressin (BMS) at m/z 1229.1 and allatostatin-4 (AST-4) at m/z 909.1, which have been suggested to be feeding-related peptides (Audsley and Weaver, 2009; Nagata et al., 2011b). We found that, similar to sNPF-1 and sNPF-2, AST-4 levels were reduced by starvation and were recovered following a resumption of feeding (Figure 5). In contrast, the levels of brain of BMS did not change significantly.

DISCUSSION

In *B. mori*, post-translational cleavage of the sNPF precursor yields three sNPF forms. In the current study, we examined the presence and expression profile of these three cleavage products and have shown that sNPF mRNA is expressed throughout the CNS with all three sNPF forms in each *B. mori* larval ganglion. Since sNPFs have been linked to the regulation of feeding behavior (Nagata et al., 2011b; Nassel and Wegener, 2011), the presence of sNPFs in all ganglia is consistent with a putative role in regulating feeding behavior in *B. mori*.

In other insect species, multiple sNPF forms (from one to five) are present (Nassel and Wegener, 2011). This is consistent with evidence showing the presence of three sNPFs in *B. mori*. For example, based on the deduced amino acid sequence of the sNPF precursor, the *D. melanogaster* sNPF gene appears to encode four separate sNPF forms (Vanden Broeck, 2001). The presence of these four sNPFs at the peptide level has been confirmed by direct mass spectrometry analyses (Predel et al., 2004; Baggerman et al., 2005; Yew et al., 2009; Carlsson et al., 2010). In the mass spectrum profiling, trypsin-like enzymatic processing of sNPFs appeared to generate shorter sNPF-like products (Baggerman et al., 2005; Wegener et al., 2011), which would suggest that at least six sNPF isoforms are present in the *D. melanogaster* larval CNS. In contrast, as demonstrated in Figure 1, no ion peaks corresponding to sNPF precursor-derived peptides were observed in the crude *B. mori* larval brain extract.

Both our direct mass spectrometry measurements and RT-PCR analyses of the *B. mori* CNS indicated that sNPF expression is localized, if not restricted to, the nervous tissues. However, it has been reported that, in addition to the CNS, *D. melanogaster* sNPFs are also expressed in the midgut (Reiher et al., 2011). In the case of *B. mori*, we were unable to detect any ion signals for sNPFs in the crude extract of the larval midgut nor could we detect sNPF



precursor mRNA in the midgut via RT-PCR. As sNPFs exert a number of biological events, including regulating feeding behavior, sNPFs in the midgut might function as enterogastric peptides in *D. melanogaster*. Although sNPF expression was not observed in the *B. mori* larval midgut, sNPFs secreted from the individual ganglia could potentially function in all tissues because receptor expression has been reported to be widespread in *B. mori* larvae (Yamanaka et al., 2008). Additionally, antiserum against RF-amide, which can recognize sNPFs in addition to other RF-amide peptides, indicated that RF-amide peptides are preset in many neurons (Walker et al., 2009; Nassel and Wegener, 2011). Consequently, even though sNPFs are not expressed in the midgut of *B. mori*, it is possible that they function in gastric control.

Even though sNPFs were initially identified based on cross-reactivity with an anti-neuropeptide F (NPF) antibody, our knowledge of their functionality remains limited. A number of studies, however, have proposed possible functions for sNPFs (Nassel and Wegener, 2011). For example, in *D. melanogaster*, sNPFs are produced in numerous small neurons in the brain that are thought to be associated with locomotor modulation and regulation as well as other various functions (Hanesch et al., 1989; Strauss, 2002; Kahsai and Winther, 2011). This possible function supports our previous data, which showed that the injection of sNPFs into *B. mori* larvae influenced the initiation of feeding behavior (Nagata et al., 2011b). sNPFs sometimes co-express with other peptide hormones in *D. melanogaster*, such as tachykinin and ion transport peptides, resulting in a proposal that sNPFs may regulate hormone release (De Lange et al., 1997; de Jong-Brink et al., 2001; Kahsai et al., 2010). In *B. mori*, sNPFs also appear to negatively act on the allatotropin producing organ, the corpora allata, such that JH secretion and biosynthesis are decreased (Yamanaka et al., 2008).

To have a better understanding of how sNPF may function in *B. mori*, we estimated the amount of sNPFs at both the transcriptional and peptide levels. The present data indicate that starvation has no effect on the transcriptional level of sNPFs (data not shown)

but did reduce the amount of mature sNPF peptides in the brain. Although the sNPF content of the remaining ganglia was not measured in this study, we found that the brain sNPF levels changed significantly in response to starvation (Figure 4). We speculate that a reduction in brain sNPFs, which likely results from functional consumption of the peptides, would trigger several biologically important events in *B. mori* larvae such as the activation of locomotor activity accompanied with other functions. This would be consistent with the observation that sNPFs drive locomotor activity in *D. melanogaster* (Kahsai et al., 2010).

Table 1 | Ion peaks detected by direct MALDI-TOF MS analyses of fifth instar *B. mori* larvae brain.

Observed ion peak	Peptide
830.1	n.d
887.2	sNPF-2
899.1	AST-6
909.1	AST-4
928.0	n.d
943.1	AST-5
951.2	AST-3
976.1	sNPF-3
1017.2	sNPF-1
1031.0	n.d
1100.9	PTSP
1127.0	n.d
1229.1	Bommysuppressin
1246.1	n.d
1267.0	n.d
1295.1	n.d

sNPF, short neuropeptide F; AST, allatostatin; PTST; prothoracicostatic hormone; n.d, not determined.

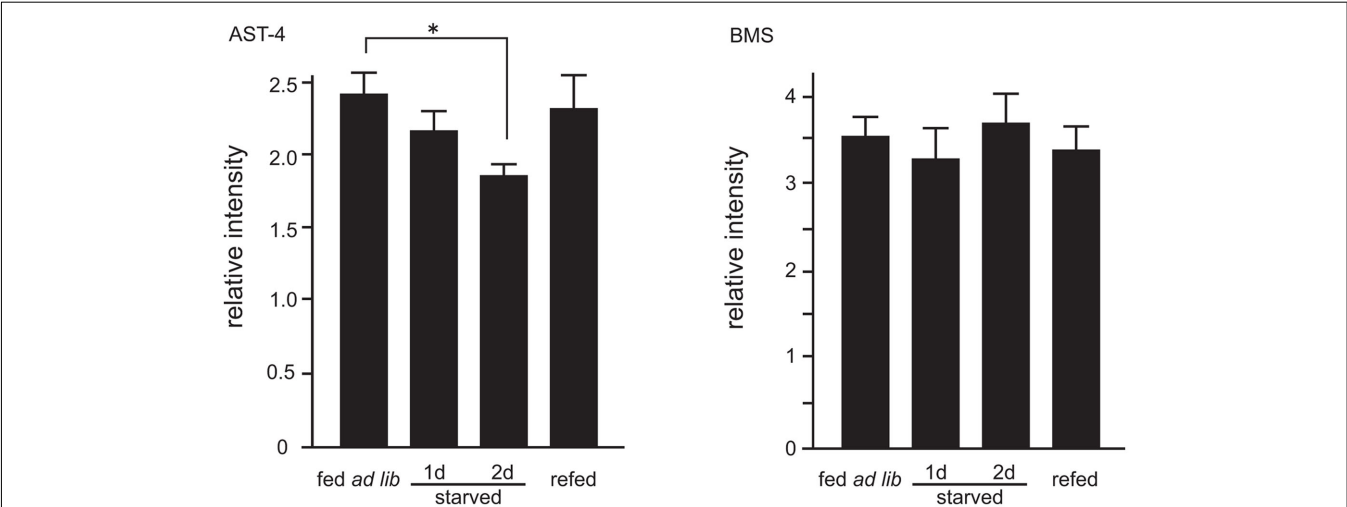


FIGURE 5 | Semi-quantitative analyses of allatostatin (AST)-4 and Bommyosuppressin (BMS). Ion peaks corresponding to AST-4 at *m/z* 909.1 and BMS at *m/z* 1229.1 were analyzed. Analytical conditions were the same

as those for sNPFs analyses. *N* = 5, Mean ± SE. Data was statistically analyzed by one-way ANOVA. Significant differences were determined by the *post hoc* Dunnett's test, **P* < 0.05.

Intriguingly, the sNPF receptor transcript levels were reduced in response to starvation (**Figures 3B,C**). Furthermore, different behavioral states were observed after short versus long starvation, with the latter showing much lower levels of locomotor activity (Wolfgang and Riddiford, 1987; Nagata and Nagasawa, 2006). As sNPFs are possible locomotor modulators (Kahsai et al., 2010), the reduction in sNPF levels is consistent with the fact that larvae starved for longer periods would exhibit decreased locomotor activity as a means of conserving crucial energy stores.

Database-assisted transcriptomic analyses revealed that several GPCRs might be allocated to receptors for RF-amide peptides in most insect species, including *D. melanogaster* (Mertens et al., 2002) and *Anopheles gambiae* (Hill et al., 2002). In *B. mori*, there are three sNPF receptors, BNGR-A10, BNGR-A11, and BNGR-A7 (data not shown, manuscript in preparation). Interestingly, these three receptors are expressed in almost all tissues of the larval body, but exhibit biases in distribution (Yamanaka et al., 2008; unpublished data by our group). This observation suggests that each receptor has different ligands or different functions *in vivo*. Therefore, careful analyses of sNPF expression levels, in addition to that of the associated receptors, are required to further develop our understanding of the mechanisms underlying sNPF-modulated feeding behavior.

REFERENCES

- Audsley, N., and Weaver, R. J. (2009). Neuropeptides associated with the regulation of feeding in insects. *Gen. Comp. Endocrinol.* 162, 93–104.
- Baggerman, G., Boonen, K., Verleyen, P., De Loof, A., and Schoofs, L. (2005). Peptidomic analysis of the larval *Drosophila melanogaster* central nervous system by two-dimensional capillary liquid chromatography quadrupole time-of-flight mass spectrometry. *J. Mass Spectrom.* 40, 250–260.
- Bernays, E. A., and Woods, H. A. (2000). Foraging in nature by larvae of *Manduca sexta* influenced by an endogenous oscillation. *J. Insect Physiol.* 46, 825–836.
- Blaney, W. M., Chapman, R. F., and Wilson, A. (1973). The pattern of feeding of *Locusta migratoria* (L.) (Orthoptera, Acrididae). *Acrida* 2, 119–137.
- Bowdan, E. (1988a). The effect of deprivation on the microstructure of feeding by the tobacco hornworm caterpillar. *J. Insect Behav.* 1, 31–50.
- Bowdan, E. (1988b). Microstructure of feeding by tobacco hornworm caterpillar, *Manduca sexta*. *Entomol. Exper. Appl.* 47, 127–136.
- Carlsson, M. A., Diesner, M., Schachtner, J., and Nassel, D. R. (2010). Multiple neuropeptides in the *Drosophila* antennal lobe suggest complex modulatory circuits. *J. Comp. Neurol.* 518, 3359–3380.
- De Lange, R., van Golen, F. A., and can Minnen, J. (1997). Diversity in cell specific co-expression of four neuropeptide genes involved in control of male copulation behaviour in *Lymnaea stagnalis*. *Neuroscience* 78, 289–299.
- de Jong-Brink, M., ter Maat, A., and Tensen, C. P. (2001). NPY in invertebrates: molecular answers to altered functions during evolution. *Peptides* 22, 309–315.
- Hanesch, U., Fischbach, K. F., and Heisenberg, M. (1989). Neuronal architecture of the central complex in *Drosophila melanogaster*. *Cell Tissue Res.* 257, 343–366.
- Hanson, J. B. (2003). “Phenolics,” in *Natural Products, Their Chemistry and Biological Significance*, eds J. Mann, J. B. Davidson, J. B. Hobbs, D. V. Banthorpe, and J. B. Harborne (Upper Saddle River, NJ: Prentice Hall), 362–388.
- Harborne, J. B. (1993). *Introduction to Ecological Biochemistry*, 4th Edn. London: Academic Press.
- Hill, C. A., Fox, A. N., Pitts, R. J., Kent, L. B., Tan, P. L., Chrystal, M. A., Cravchik, A., Collins, F. H., Robertson, H. M., and Zwiebel, L. J. (2002). G protein-coupled receptors in *Anopheles gambiae*. *Science* 298, 176–178.
- Jimenez, C. R., Li, K. W., Dreisewerd, K., Mansveldt, H. D., Brussaard, A. B., Reinhold, B. B., Van der Schors, R. C., Karas, M., Hillenkamp, F., Burbach, J. P. H., Costello, C. E., and Geraerts, W. P. M. (1997). Pattern changes of pituitary peptides in rat after salt-loading as detected by means of direct, semiquantitative mass spectrometric profiling. *Proc. Natl. Acad. Sci. U.S.A.* 94, 9481–9486.
- Kahsai, L., Martin, J. R., and Winther, A. M. (2010). Neuropeptides in the *Drosophila* central complex in modulation of locomotor behavior. *J. Exp. Biol.* 213, 2256–2265.
- Kahsai, L., and Winther, A. M. (2011). Chemical neuroanatomy of the *Drosophila* central complex: distribution of multiple neuropeptides in relation to neurotransmitters. *J. Comp. Neurol.* 519, 290–315.
- Lee, K. S., Kwon, O. Y., Lee, J. H., Kwon, K., Min, K. J., Jung, S. A., Kim, A. K., You, K. H., Tatar, M., and Yu, K. (2008). *Drosophila* short neuropeptide F signalling regulates growth by ERK-mediated insulin signalling. *Nat. Cell Biol.* 10, 468–475.
- Lee, K. S., You, K. H., Choo, J. K., Han, Y. M., and Yu, K. (2004). *Drosophila* short neuropeptide F regulates food intake and body size. *J. Biol. Chem.* 279, 50781–50789.
- Maule, A. G., Shaw, C., Halton, D. W., Thim, L., Johnston, C. F., Fairweather, I., and Buchanana, K. D. (1991). Neuropeptide F: a novel parasitic flatworm regulatory peptide from *Moniezia expansa* (Cestoda: Cyclophyllidae). *Parasitology* 102, 309–316.
- Mertens, I., Meeusen, T., Huybrechts, R., De Loof, A., and Schoofs, L. (2002). Characterization of the short neuropeptide F receptor from *Drosophila melanogaster*. *Biochem. Biophys. Res. Commun.* 297, 1140–1148.
- Mita, K., Morimyo, M., Okano, K., Koike, Y., Nohata, J., Kawasaki, H., Kadono-Okuda, K., Yamamoto, K., Suzuki, M. G., Shimada, T., Goldsmith, M. R., and Maeda, S. (2003). The construction of an EST database for *Bombyx mori* and its application. *Proc. Natl. Acad. Sci. U.S.A.* 100, 14121–14126.
- Nagata, S., Morooka, N., Asaoka, K., and Nagasawa, H. (2011a). Identification of a novel hemolymph peptide that modulates silkworm feeding motivation. *J. Biol. Chem.* 286, 7161–7170.
- Nagata, S., Morooka, N., Matsumoto, S., Kawai, T., and Nagasawa, H. (2011b). Effects of neuropeptides on feeding initiation in larvae of the silkworm, *Bombyx mori*. *Gen. Comp. Endocrinol.* 172, 90–95.
- Nagata, S., Morooka, N., Matsumoto, S., and Nagasawa, H. (2009). Characterization of feeding-delaying factors from the silkworm *Bombyx mori*. *Ann. N. Y. Acad. Sci.* 1163, 481–483.
- Nagata, S., and Nagasawa, H. (2006). Effects of diet-deprivation and physical stimulation on the feeding behaviour of the larvae of the silkworm, *Bombyx mori*. *J. Insect Physiol.* 52, 807–815.

CONCLUSION

In the present study, we monitored sNPF levels in the CNS and brain of *B. mori* larvae. The level of sNPFs in the *B. mori* brain was influenced by the feeding state of the specimens examined. As previously proposed, sNPFs may function as possible neuromodulators of locomotion in *B. mori* larvae. We suggest that one of the pleiotropic functions of sNPFs is neuromodulatory in nature in that they potentially drive feeding behavior associated locomotor activity in response to the animal's feeding state.

ACKNOWLEDGMENTS

This work was supported partly by Grants-in-Aid for Scientific Research [#18780083 and 22780099 (Shinji Nagata); #22-4193 (Nobukatsu Morooka); #22-1424 (Chiaki Nagai)] from the Ministry of Education, Science, Sports, and Culture of Japan.

- Nassel, D. R., and Wegener, C. (2011). A comparative review of short and long neuropeptide F signaling in invertebrates: any similarities to vertebrate neuropeptide Y signaling? *Peptides* 32, 1335–1355.
- Predel, R., Wegener, C., Russell, W. K., Tichy, S. E., Russell, D. H., and Nachman, R. J. (2004). Peptidomics of CNS-associated neurohemal systems of adult *Drosophila melanogaster*: a mass spectrometric survey of peptides from individual flies. *J. Comp. Neurol.* 474, 379–392.
- Reynolds, S. E., Yeomans, M. R., Timmins, W. A. (1986). The feeding behaviour of caterpillars (*Manduca sexta*) on tobacco and on artificial diet. *Physiol. Entomol.* 11, 39–51.
- Reiher, W., Shirras, C., Kahnt, J., Baumeister, S., Isaac, R. E., Wegener, C. (2011). Peptidomics and peptide hormone processing in the *Drosophila* midgut. *J. Proteome Res.* 10, 1881–1892.
- Roller, L., Yamanaka, N., Watanabe, K., Daubnerova, I., Zitnan, D., Kataoka, H., and Tanaka, Y. (2008). The unique evolution of neuropeptide genes in the silkworm *Bombyx mori*. *Insect Biochem. Mol. Biol.* 38, 1147–1157.
- Secher, T., Lenz, C., Cazzamali, G., Sorensen, G., Williamson, M., Hansen, G. N., Svane, P., and Grimmekhuijzen, C. J. (2001). Molecular cloning of a functional allatostatin gut/brain receptor and an allatostatin preprohormone from the silkworm *Bombyx mori*. *J. Biol. Chem.* 276, 47052–47060.
- Simpson, S. J. (1982). Patterns in feeding: a behavioural analysis using *Locusta migratoria* nymphs. *Physiol. Entomol.* 7, 325–336.
- Simpson, S. J. (1995). “The control of meals in chewing insects,” in *Regulatory Mechanisms of Insect Feeding*, eds R. F. Chapman and J. de Boer (New York: Chapman & Hall), 137–156.
- Simpson, S. J., and Ludlow, A. R. (1986). Why locusts start to feed? A comparison of causal factors. *Anim. Behav.* 34, 480–496.
- Spittaels, K., Verhaert, P., Shaw, C., Johnston, R. N., Devreese, B., and Van Beeumen, J. (1996). Insect neuropeptide F (NPF)-related peptides: isolation from Colorado potato beetle (*Leptinotarsa decemlineata*) brain. *Insect Biochem. Mol. Biol.* 26, 375–382.
- Strauss, R. (2002). The central complex and the genetic dissection of locomotor behaviour. *Curr. Opin. Neurobiol.* 12, 633–638.
- Tatemoto, K., Carlquist, M., and Mutt, V. (1982). Neuropeptide Y-a novel brain peptide with structural similarities to peptide YY and pancreatic polypeptide. *Nature* 296, 659–660.
- Timmins, W. A., Bellward, K., Stamp, A. J., and Reynolds, S. E. (1988). Food intake, conversion efficiency and feeding behaviour of tobacco hornworm caterpillar given artificial diet of carrying nutrient and water content. *Physiol. Entomol.* 13, 303–314.
- Vanden Broeck, J. (2001). Neuropeptides and their precursors in the fruitfly, *Drosophila melanogaster*. *Peptides* 22, 241–254.
- Walker, R. J., Papioannou, S., and Holden-Dye, L. (2009). A review of FMRFamide- and RFamide-like peptides in metazoan. *Invert. Neurosci.* 9, 111–153.
- Wegener, C., Hervet, H., Kahnt, J., Bender, M., and Rhea, J. M. (2011). Deficiency of prohormone convertase dPC2 (AMONTILLADO) results in impaired production of bioactive neuropeptide hormones in *Drosophila*. *J. Neurochem.* 118, 581–595.
- Wolfgang, W. J., and Riddiford, L. M. (1987). Cuticular mechanics during larval development of the tobacco hornworm, *Manduca sexta*. *J. Exp. Biol.* 128, 19–33.
- Yamanaka, N., Yamamoto, S., Zitnan, D., Watanabe, K., Kawada, T., Satake, H., Kaneko, Y., Hiruma, K., Tanaka, Y., Shinoda, T., and Kataoka, H. (2008). Neuropeptide receptor transcriptome reveals unidentified neuroendocrine pathways. *PLoS ONE* 3, e3048. doi:10.1371/journal.pone.0003048
- Yew, J. Y., Wang, Y., Barteneva, N., Dikler, S., Kutz-Naber, K. K., Li, L., and Kravitz, E. A. (2009). Analysis of neuropeptide expression and localization in adult *Drosophila melanogaster* central nervous system by affinity cell-capture mass spectrometry. *J. Proteome Res.* 8, 1271–1284.

Conflict of Interest Statement: The authors declare that the research was conducted in the absence of any commercial or financial relationships that could be construed as a potential conflict of interest.

Received: 15 September 2011; accepted: 04 January 2012; published online: 18 January 2012.

Citation: Nagata S, Matsumoto S, Nakane T, Ohara A, Morooka N, Konuma T, Nagai C and Nagasawa H (2012) Effects of starvation on brain short neuropeptide F-1, -2, and -3 levels and short neuropeptide F receptor expression levels of the silkworm, *Bombyx mori*. *Front. Endocrin.* 3:3. doi: 10.3389/fendo.2012.00003

This article was submitted to *Frontiers in Experimental Endocrinology*, a specialty of *Frontiers in Endocrinology*.

Copyright © 2012 Nagata, Matsumoto, Nakane, Ohara, Morooka, Konuma, Nagai and Nagasawa. This is an open-access article distributed under the terms of the Creative Commons Attribution Non Commercial License, which permits non-commercial use, distribution, and reproduction in other forums, provided the original authors and source are credited.



Regulatory role of PBAN in sex pheromone biosynthesis of heliothine moths

Russell Jurenka^{1*} and Ada Rafaeli²

¹ Department of Entomology, Iowa State University, Ames, IA, USA

² Department of Food Quality and Safety, Volcani Center, Agricultural Research Organization, Bet Dagan, Israel

Edited by:

Joe Hull, United States Department of Agriculture, USA

Reviewed by:

Taisen Iguchi, National Institute for Basic Biology, Japan

Sergio Polakof, French National Institute for Agricultural Research, France

Miriam Altstein, Agricultural Research Organization, Israel

*Correspondence:

Russell Jurenka, Department of Entomology, Iowa State University, Ames, IA 50011-3222, USA.
e-mail: rjurenka@iastate.edu

Both males and females of heliothine moths utilize sex-pheromones during the mating process. Females produce and release a sex pheromone for the long-range attraction of males for mating. Production of sex pheromone in females is controlled by the peptide hormone (pheromone biosynthesis activating neuropeptide, PBAN). This review will highlight what is known about the role PBAN plays in controlling pheromone production in female moths. Male moths produce compounds associated with a hairpencil structure associated with the aedeagus that are used as short-range aphrodisiacs during the mating process. We will discuss the role that PBAN plays in regulating male production of hairpencil pheromones.

Keywords: pheromone, PBAN, *Heliothis*, *Helicoverpa*, moth

BACKGROUND ON PBAN

The hormonal regulation of pheromone biosynthesis in moths was first demonstrated in the heliothine *Helicoverpa zea* (Raina et al., 1987) and a peptide isolated shortly thereafter (Raina et al., 1989). Pheromone biosynthesis activating neuropeptide (PBAN) was identified as a 33 amino acid C-terminal amidated peptide from the brain–subesophageal ganglion complex of adult female moths. Immunohistochemical procedures traced the neuronal production of PBAN to three groups of neurons in the subesophageal ganglion (Blackburn et al., 1992; Kingan et al., 1992; Rafaeli and Jurenka, 2003). The gene encoding for PBAN was subsequently identified (Davis et al., 1992; Ma et al., 1994, 1998). In addition to encoding for PBAN four other neuropeptides could be produced. One of these had been identified as the diapause hormone that regulates embryonic diapause in the silkworm moth (Imai et al., 1991). The analysis of mRNA from a number of moth species now indicates that five peptides could be produced by the PBAN gene (Choi et al., 2004). Evidence indicates that these peptides could be processed and released into circulation as active neuropeptides (Ma et al., 1996).

Sequence similarities to the pyrokinins became evident after it was determined that the minimum activity required was the last five C-terminal amino acids (Raina and Kempe, 1990, 1992). Leukopyrokinin was first identified in the cockroach *Leucophaea maderae* due to the stimulation of hindgut muscle contraction (Holman et al., 1986). A variety of PBAN/pyrokinin peptides have been found in all insects to date based on gene sequence and peptide isolation (Jurenka and Nusawardani, 2011). These peptides are found in neurons localized to the brain–subesophageal ganglion and ganglia of the ventral nerve cord. Most insects possess another peptide produced by the *capa* gene. This gene, first identified in *Drosophila melanogaster* (Kean et al., 2002), can produce

three peptides. Two of the peptides are periviscerokinins that usually have an FPRVamide C-terminal ending. Periviscerokinins are involved in a variety of functions including stimulating heart rate and affecting Malpighian tubule functions. The third peptide, that can be produced by the *capa* gene, is related to the diapause hormone because it has a WFGPRLamide C-terminal ending.

As indicated above the first functions described for the PBAN/pyrokinin family of peptides was stimulation of pheromone biosynthesis in female moths and stimulation of hindgut muscle contraction in cockroaches. Other functions were soon described for peptides in the family including induction of embryonic diapause in females and cuticle melanization in larvae of the silkworm moth, *Bombyx mori* (Matsumoto et al., 1990; Imai et al., 1991). Once the peptides were identified it became apparent that these peptides belong to the same family with cross-reactivity of function. Subsequently other functions were identified including acceleration of puparium formation in higher flies (Zdarek et al., 1997) and pupal diapause development in heliothine moths (Sun et al., 2003; Zhang et al., 2004). This list of functions indicates the pleiotropic nature of the PBAN/pyrokinin family of peptides across the Insecta. Other functions could potentially be found for the family because these peptides are found in all insects (Jurenka and Nusawardani, 2011).

The target tissue for the action of PBAN in adult female moths is the pheromone gland, which is found as intersegmental tissues located between the eighth and ninth abdominal segments of the ovipositor in heliothines (Rafaeli and Jurenka, 2003). Pheromone biosynthesis can be stimulated by either injecting peptides into intact female moths or peptides can be incubated with an isolated pheromone gland on saline. The *in vitro* studies demonstrate that the PBAN-receptors are located in the epidermal cells of the

pheromone gland. A biologically active biotinylated-PBAN analog was used to demonstrate specific binding to a protein from isolated pheromone glands (Rafaeli et al., 2003). Cloning and functional expression of a PBAN-receptor was first reported in *H. zea*, the same moth in which PBAN was first identified (Choi et al., 2003).

PBAN-RECEPTOR

The PBAN-receptor was identified based on sequence similarities with a group of three receptors from *D. melanogaster*. After the *D. melanogaster* genome was sequenced and annotated peptide G-protein coupled receptors (GPCR) were identified based on sequence alignment with known vertebrate peptide GPCRs (Hewes and Taghert, 2001). One group of three receptors (CG8784, CG8795, CG9918) had sequence similarities with the neuromedin U (NmU) receptor from mammals. The ligand, NmU, has a C-terminal ending of FRPRNamide, which is similar to the C-terminal ending of PBAN, FSPRLamide. Choi et al. (2003) demonstrated that the vertebrate NmU peptide stimulated pheromone biosynthesis in female moths indicating cross-reactivity and receptor activation. The *D. melanogaster* sequences were used in a PCR based sequencing approach to obtain the full-length sequence from pheromone glands of *H. zea*. The three receptors from *D. melanogaster* were also characterized as being activated by pyrokinins (Park et al., 2002) indicating that all of these receptors belong to a similar family.

The functional expression of the *H. zea* PBAN-receptor indicated that PBAN activated the receptor at a half-maximum effective concentration of 25 nM (Choi et al., 2003). Several other peptides produced by the PBAN-gene were also active at similar concentrations. Although, concentrations required to stimulate pheromone biosynthesis *in vitro* in *Helicoverpa armigera* showed that PBAN was active at 0.5 nM and the other peptides at significantly higher concentrations (Stern et al., 2007). PBAN-receptors have been characterized from several moths including *B. mori* (Hull et al., 2004), *Heliothis virescens* (Kim et al., 2008), and *Plutella xylostella* (Lee et al., 2011). These studies indicate that PBAN will activate receptors at concentrations in the low nanomolar range. Several other PBAN-receptors have been identified based on sequence homology from other moths including *H. armigera* (Rafaeli et al., 2007), *Spodoptera exigua* (Cheng et al., 2010), and *Spodoptera littoralis* (Zheng et al., 2007).

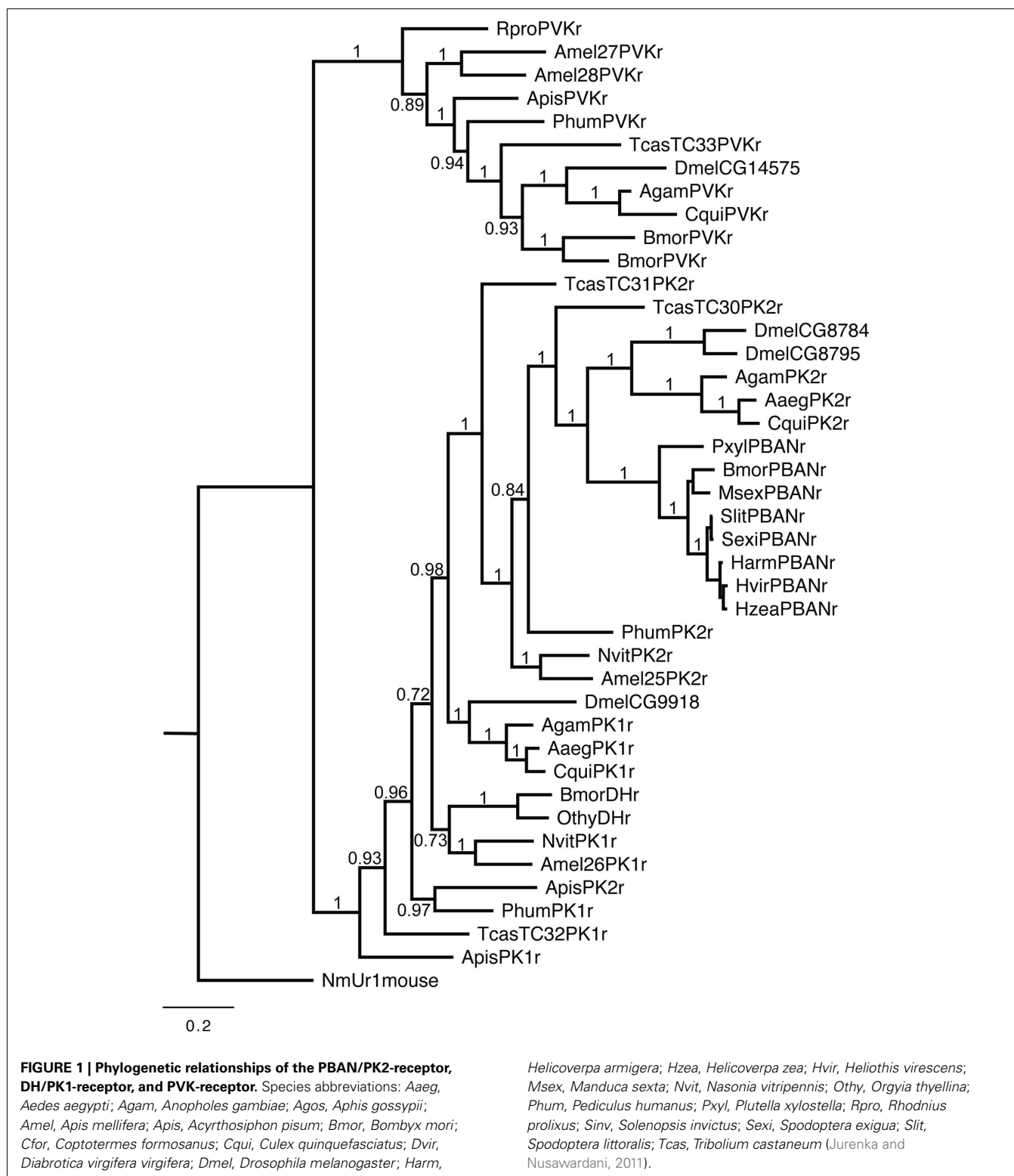
Only one PBAN-receptor sequence was identified from pheromone glands of *H. zea* (Choi et al., 2003). However, three PBAN-receptor sequences were identified from cDNA obtained from the central nervous system of *H. virescens* fourth instar larvae (Kim et al., 2008). All three receptor sequences were identical except for C-terminal extensions. The N-terminal and seven-transmembrane domain regions of the *H. virescens* PBAN-receptors are about 98.5% identical with the *H. zea* and *H. armigera* receptors. The *H. virescens* PBAN-receptor subtype C, was identified in pheromone glands of adult female *H. virescens*. The other two were identified from the larval central nervous system and did not have activity when tested in a calcium mobilization assay using a heterologous expression system (Kim et al., 2008). The C-terminal extension of *H. virescens* PBAN-receptor subtype C is similar to the C-terminal of the *B. mori* PBAN-receptor

(Hull et al., 2004). The C-terminal extension in the *B. mori* PBAN-receptor is involved in efficient internalization of the receptor after activation (Hull et al., 2004). It is interesting to note that the PBAN-receptors identified from pheromone glands of other moths have a shortened C-terminal ending similar to that of the *H. zea* PBAN-receptor. Functional significance of a short C-terminal ending indicates that the receptor could remain active in the pheromone gland cell membrane for a longer period of time. Time course studies on induction of pheromone biosynthesis in isolated pheromone glands indicated that the PBAN-receptor does remain active for a period of time after stimulation by PBAN (Choi et al., 2004).

The diapause hormone-receptor (DH-receptor) has high sequence homology to the PBAN-receptor especially in the transmembrane domains (Jurenka and Nusawardani, 2011). In Lepidoptera the DH-receptor has only been characterized from *B. mori* (Homma et al., 2006). Other insects have a pyrokinin 1-receptor (PK1-receptor) that is similar to the DH-receptor in sequence and are activated by DH-like peptides with an FGPRamide C-terminal ending. Other insects also have PK2-receptors that are similar to the PBAN-receptor. A third GPCR is the perivicerokinin-receptor (PVK-receptor) that is activated by PVKs but not by other PBAN/pyrokinin-like peptides (Iversen et al., 2002; Park et al., 2002; Olsen et al., 2007). Phylogenetic relationships of these receptors from insects indicate three groups of receptors that follow a typical evolutionary origin for orders of insects (Figure 1).

G-protein coupled receptors have a seven-transmembrane domain motif that appears to be structurally conserved. With the X-ray crystal structure of rhodopsin, β_1 and β_2 adrenergic receptors, and A_{2A} adenosine receptors published, it is possible to construct homology models based on these solved three-dimensional structures. A detailed model of the *H. zea* PBAN-receptor was built using the crystal structure of rhodopsin as a template and *in silico* binding studies indicated possible interactions with PBAN as a ligand (Stern et al., 2007). A putative ligand binding pocket was indicated in a study utilizing an evolutionary trace approach in comparing the insect PBAN-receptors (Jurenka and Nusawardani, 2011). The conserved nature of the transmembrane domains and structural features of the ligand binding pocket for GPCRs allows the prediction of ligand interactions in a binding pocket of the PBAN-receptor. A model illustrating a putative *H. zea* PBAN-receptor binding pocket is shown in Figure 2. This model will need to be verified with mutation studies to determine if the specified amino acids are involved in ligand binding.

Several mutation studies have been conducted to determine which domains of the PBAN-receptor are involved in ligand recognition and activation. One study utilized chimeras where the extracellular domains were exchanged sequentially between the *H. zea* PBAN-receptor and the *D. melanogaster* PK1-receptor (Choi et al., 2007). All extracellular domain chimeras reduced activity of the chimera receptor when challenged with PBAN. However the *H. zea* PBAN-receptor chimera with the third extracellular loop exchanged had increased activity when challenged with the diapause hormone. The *D. melanogaster* PK1-receptor chimera with the third extracellular loop exchanged had increased activity when challenged with PBAN. These results indicate that the third extracellular loop is important for peptide recognition and



could be involved in accepting the correct peptide for binding to a receptor activation site which is the ligand binding pocket located in the transmembrane domain area of the receptor. Alanine substitution mutations made in the third extracellular loop indicate

that specific amino acids could be involved in peptide recognition (Choi and Jurenka, 2010). Further studies will be required to validate these models and establish how this family of receptors recognize specific peptides and activate the receptor.

PBAN MODE OF ACTION

Pheromone biosynthesis activating neuropeptide activation of the receptor induces the influx of extracellular calcium and the subsequent increase in cytosolic calcium (Jurenka et al., 1991; Jurenka, 1996). In heliothine moths, as in all moth species examined to date, the presence of calcium in the extracellular medium is a prerequisite for PBAN action (Rafaeli, 1994; Choi et al., 2004; Choi and Jurenka, 2006) suggesting that the opening of cation channels and the concomitant influx of calcium are most likely conserved features of PBAN activation. In the absence of calcium or the presence of calcium-calmodulin inhibitors such as W7, pheromonotropic activity is abolished (Rafaeli and Gileadi, 1996a) and, conversely, the pheromonotropic effects of PBAN can be duplicated with calcium ionophores such as ionomycin, thapsigargin, and A23187 (Rafaeli and Gileadi, 1996a; Rafaeli and Jurenka, 2003).

However, unlike the signal transduction pathway determined for the silkworm *B. mori*, in the heliothine moths there is evidence that the increase in cytosolic calcium activates a calcium-calmodulin sensitive adenylate cyclase which in turn promotes the production of cyclic-AMP (Rafaeli and Soroker, 1989; Soroker and Rafaeli, 1995; Rafaeli and Gileadi, 1996a). Furthermore, pharmacological compounds that affect cyclic-AMP levels such as cyclic-AMP analogs, isobutyl methyl xanthine (a phosphodiesterase inhibitor), and forskolin (an adenylate cyclase activator) have been shown to stimulate downstream events and thereby pheromone biosynthesis in *H. armigera* (Rafaeli and Soroker, 1989; Rafaeli, 1994) and *H. zea* (Jurenka et al., 1991). In addition, in *H. armigera* sodium fluoride, a G-protein activator can induce intracellular cyclic-AMP levels and subsequent downstream events leading to pheromone production, independent of the ligand PBAN (Rafaeli and Gileadi, 1996b). As an outcome of the activation of the second

messengers, kinase, and/or phosphatase is activated, which, in their turn, stimulate fatty acid biosynthesis in the pheromone biosynthetic pathway (Figure 3).

What enzyme in the biosynthetic pathway is affected by the signal cascade brought about through PBAN binding to its receptor? Demonstration of the enzymatic key regulatory step in the biosynthesis of sex-pheromones primarily relies on following labeled precursors and intermediates into pheromone molecules in the absence and presence of PBAN. Thus, if production of a labeled pheromone component from incorporation of labeled precursor occurs in the absence of PBAN to the same extent as in its presence the labeled precursor must be acting downstream of the regulatory enzyme and therefore regulation must occur upstream. The effect of PBAN on the different steps in the biosynthetic pathway has been investigated in several Lepidopteran species including *B. mori* (Arima et al., 1991; Ozawa et al., 1993), *Thaumetopoea pityocampa* (Arseque et al., 1990), *S. littoralis* (Martinez et al., 1990; Fabrias et al., 1994), *Manduca sexta* (Fang et al., 1995; Tumlinson et al., 1997), *H. zea* (Jurenka et al., 1991), *H. armigera* (Tsfadia et al., 2008), and *Plodia interpunctella* (Tsfadia et al., 2008). Studies

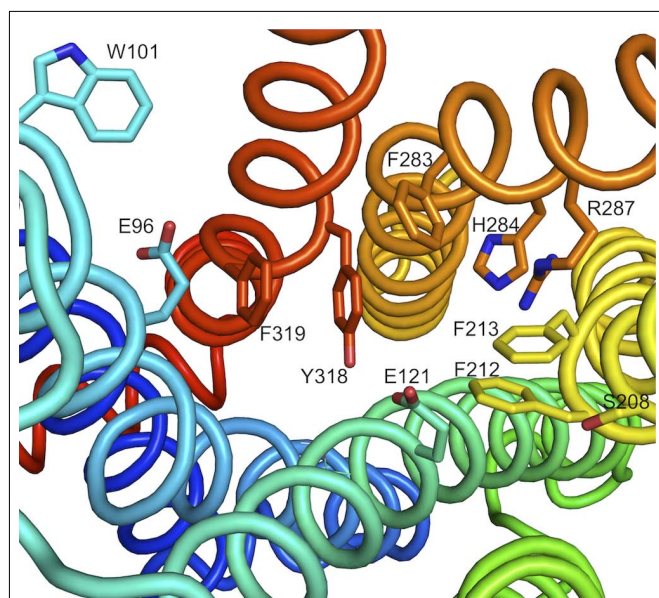


FIGURE 2 | A model of the *Helicoverpa zea* PBAN-receptor illustrating amino acids that could be involved in binding PBAN. Reproduced with permission from Jurenka and Nusawardani (2011).

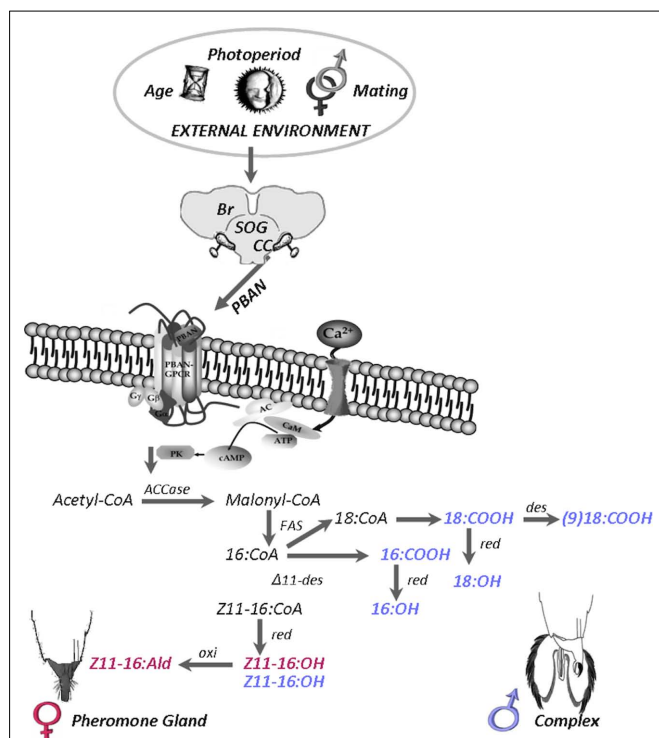


FIGURE 3 | A diagrammatic representation of sex pheromone biosynthesis resulting from PBAN release into the hemolymph and its interaction with the PBAN GPCR in female pheromone glands (PG) and male hairpencil-aedaeus-complexes of *Helicoverpa armigera*. Up-regulation of female components in red and male components in blue. (Male-complex illustration taken from Bober and Rafaeli, 2010 with permission). Abbreviations: AC, adenylate cyclase; ACCase, acetyl-CoA carboxylase; Br, brain; CaM, calcium-calmodulin; cAMP, cyclic-AMP; CC, corpora cardiaca; Δ11-des, Δ11 desaturase; FAS, fatty acid synthetase; GPCR, G-protein coupled receptor; oxi, oxidase; PBAN, pheromone biosynthesis activating neuropeptide; PK, protein kinase A; red, reductase; SOG, subesophageal ganglion.

of this nature have so far indicated that PBAN does not influence desaturase activity.

Using both stable isotopes and specific enzyme inhibitors the rate limiting step of PBAN pheromone biosynthesis regulation in *H. armigera* was determined (Tsfadia et al., 2008). These studies showed that only incorporation of labeled acetate is affected by PBAN and that this incorporation can be inhibited by the acetyl coenzyme A carboxylase (ACCase) inhibitor, tralkoxydim. Levels of incorporation of labeled malonyl CoA or palmitic acid (downstream of acetate) were unaffected by the presence or absence of PBAN (Tsfadia et al., 2008). Thus, in *H. armigera*, the rate limiting step for PBAN control is regulation of the ACCase which catalyzes the rate limiting enzyme of fatty acid biosynthesis, prior to the action of fatty acid synthetase (Figure 3). PBAN is also thought to influence ACCase activity in *Argyrotaenia velutinana* (Tang et al., 1989), *P. interpunctella* (Tsfadia et al., 2008), and *H. zea* (Jurenka et al., 1991). In contrast, in *B. mori*, *T. pityocampa*, *S. littoralis*, and *M. sexta* PBAN stimulates a reductase that converts an acyl-CoA to an alcohol precursor (Arsequell et al., 1990; Martinez et al., 1990; Ozawa et al., 1993; Fang et al., 1995). In *H. virescens* a two-step regulatory role for PBAN was demonstrated (Eltahlawy et al., 2007). This two-step theory entailed a push (ACCase) and a pull (acyl-CoA) for the action of PBAN and may explain the controversial hypotheses suggested for identifying the rate limiting steps controlled by PBAN in the different moth species.

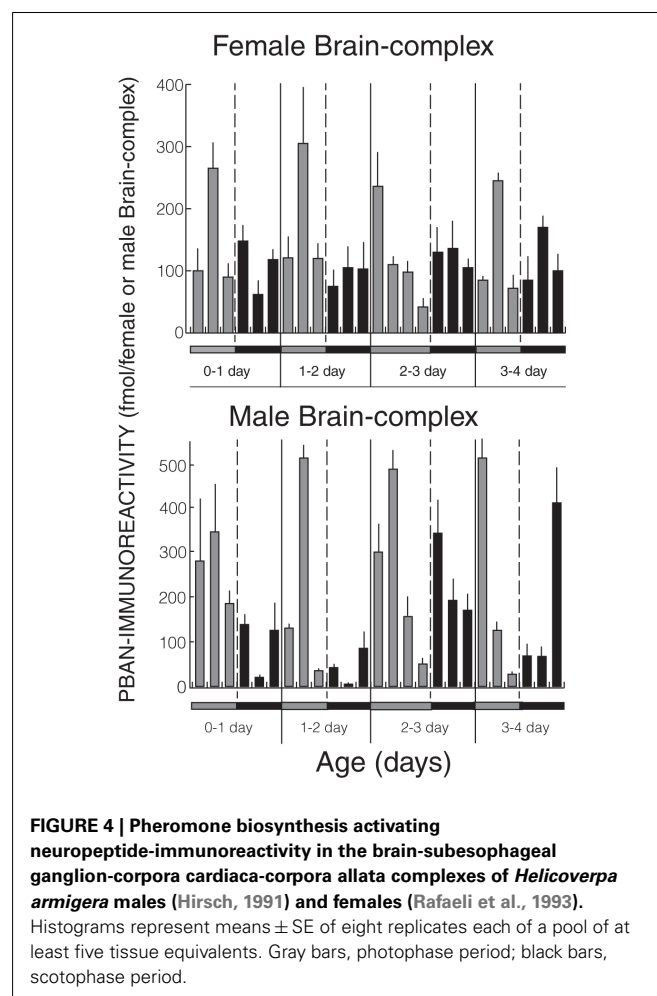
An interesting feature revealed by studies on the mode of PBAN action is that in those species in which PBAN has been shown to regulate reductase activity, cyclic-AMP has proven to be ineffective as a pheromonotropic agent whereas in those species in which PBAN regulates ACCase activity, cyclic-AMP appears to be involved as a second messenger. Moreover, it is interesting that different receptor subtypes maybe correlated with the different downstream intracellular signal cascades that are induced. It is apparent that at least two subtypes of PBAN-receptors could be located in pheromone glands: one with calcium signaling cascade including cyclic-AMP and a shorter C-terminal tail (*H. zea*, *H. armigera*); the other dependent only on calcium having a longer C-terminal tail (*B. mori*). Allocating these characteristics may be too premature until more evidence becomes available as to the involvement of cyclic-AMP in the signal transduction of other PBAN-receptor subtypes. For example, PBAN induces calcium elevations by the *P. xylostella* PBAN-receptor, which also has a short C-terminal tail; however cyclic-AMP levels were not analyzed in the *P. xylostella* study (Lee et al., 2011).

PBAN'S INFLUENCE ON MALE PHEROMONAL COMPONENTS

Male pheromone production has been studied in several insect species. Male insects often possess scent-releasing organs in the form of hairpencils, coremata, or androconial scales (Birch et al., 1990). In the Lepidoptera, studies have identified hairpencil secretions produced by several species (Chow et al., 1986; Phelan et al., 1986; Teal and Tumlinson, 1989; Heath et al., 1992; Thibout et al., 1994; Huang et al., 1996). The behavioral role of these secretions is not well understood, but most often these odors have been deemed important in courtship behavior. In general male pheromones can be considered to have many possible functions: they can act as aphrodisiacs to stimulate female receptivity during courtship

(Birch, 1974); they have been reported to induce female calling (Szentesi et al., 1975), females become immobile allowing copulation; and they have been reported to function as male-to-male inhibitory compounds, thereby minimizing male-competition (Hirai et al., 1978; Teal et al., 1984; Teal and Tumlinson, 1989; Wu et al., 1991; Huang et al., 1996). Odors released by male hairpencils are important in male acceptance by the female and may play a role in mate choice and species isolation (Hillier and Vickers, 2004; Lassance and Löfstedt, 2009). In the European corn borer, *Ostrinia nubilalis*, scents released during courtship by males provide critical information for female acceptance (Lassance and Löfstedt, 2009). Close-range chemical cues have also been proposed as a trait used by females to assess male quality (Eisner and Meinwald, 1995).

In species of Lepidoptera belonging to the Arctiidae and Danaidae, scent gland composition is related to host plant consumption and sequestration of compounds during the larval and adult stages (Birch and Hefetz, 1987). However, in other moth species, as in the heliothine moths, these male odors are derived from the fatty acid biosynthetic pathway, and as such are similar to the female sex-pheromone blends (Teal and Tumlinson, 1989; Huang et al., 1996). In *O. nubilalis* the male chemical signal is also analogous to the female signal in that structurally similar compounds are being used by both sexes and are governed by



the same genes encoding biosynthetic enzymes (Lassance and Löfstedt, 2009).

Pheromone biosynthesis activating neuropeptide was originally isolated from female *H. zea* subesophageal ganglia and its distribution in the female nervous system was studied using ELISA (Kingan et al., 1992) however the gene transcript was shown to be present in both the male and female central nervous system (Ma et al., 1998). Using an immunoassay, PBAN was also found in both female and male *H. armigera* central nervous systems and throughout the photoperiod (Figure 4; Hirsch, 1991; Rafaeli et al., 1993).

The function of PBAN in the males, however, has been a mystery since its discovery but its presence has been speculated to have other functional significances particularly in light of the pleiotropic action of PBAN and PBAN-like peptides in other insects. However, a recent temporal differential expression study of the PBAN-R revealed the presence of gene transcripts in both the male-complexes (hairpencil-aedeagus complex) and female pheromone glands of two moth species, *H. armigera* and *B. mori* (Bober et al., 2010) with levels dependent on the age of the adults and up-regulated on or just before eclosion. Whilst the presence of PBAN in males can be understood in terms of the ubiquitous characteristic of this peptide family, the presence, as well as the transcriptional regulation of its receptor in the male-complex

called for a re-examination of a possible function for PBAN and its receptor in this tissue.

As discussed above, and, since fatty acid-derived pheromonal compounds were identified in male-complexes of several moth species including heliothine moths, we aimed to determine whether PBAN plays a role in the regulation of the biosynthesis of these compounds in male *H. armigera*. We utilized both physiological bioassays and RNA interference (RNAi) technology to identify several male pheromone components that are responsive to PBAN stimulation and to photoperiod, and are also significantly affected by silencing of the PBAN-R (Bober and Rafaeli, 2010). We hypothesized that these components are key in the chemical communication between females and males during copulation (Figure 4). It remains to be demonstrated that those PBAN up-regulated male produced compounds are indeed responsible for a successful mating encounter by either arresting females for copulation, increasing their receptivity, or deterring co-specific males from competing.

ACKNOWLEDGMENTS

Research originating from the authors' laboratories was supported by Research Grant No. IS-4163-08C from BARD, The United States – Israel Binational Agricultural Research and Development Fund.

REFERENCES

- Arima, R., Takahara, K., Kadoshima, T., Numazaki, F., Ando, T., Uchiyama, M., Nagasawa, H., Kitamura, A., and Suzuki, A. (1991). Hormonal regulation of pheromone biosynthesis in the silkworm moth, *Bombyx mori* (Lepidoptera: Bombycidae). *Appl. Entomol. Zool. (Jpn.)* 26, 137–147.
- Arsekuell, G., Fabrias, G., and Camps, F. (1990). Sex pheromone biosynthesis in the processionary moth *Thaumetopoea pityocampa* by delta-13 desaturation. *Arch. Insect Biochem. Physiol.* 14, 47–56.
- Birch, M. C. (1974). "Aphrodisiac pheromones in insects", in *Pheromones*, ed. M. C. Birch (Amsterdam: North Holland), 115–134.
- Birch, M. C., and Hefetz, A. (1987). Extrusible organs in male moths and their role in courtship behavior. *Bull. Entomol. Soc. Am.* 33, 222–229.
- Birch, M. C., Poppy, G. M., and Baker, T. C. (1990). Scents and eversible scent structures of male moths. *Annu. Rev. Entomol.* 35, 25–58.
- Blackburn, M. B., Kingan, T. G., Raina, A. K., and Ma, M. C. (1992). Colocalization and differential expression of PBAN- and FMRF-like immunoreactivity in the subesophageal ganglion of *Helicoverpa zea* (Lepidoptera: Noctuidae) during development. *Arch. Insect Biochem. Physiol.* 21, 225–238.
- Bober, R., Azrieli, A., and Rafaeli, A. (2010). Developmental regulation of the pheromone biosynthesis activating neuropeptide-receptor (PBAN-R): re-evaluating the role of juvenile hormone. *Insect Mol. Biol.* 19, 77–86.
- Bober, R., and Rafaeli, A. (2010). Gene-silencing reveals the functional significance of pheromone biosynthesis activating neuropeptide receptor (PBAN-R) in a male moth. *Proc. Natl. Acad. Sci. U.S.A.* 107, 16858–16862.
- Cheng, Y., Luo, L., Jiang, X., Zhang, L., and Niu, C. (2010). Expression of pheromone biosynthesis activating neuropeptide and its receptor (PBANR) mRNA in adult female *Spodoptera exigua* (Lepidoptera: Noctuidae). *Arch. Insect Biochem. Physiol.* 75, 13–27.
- Choi, M.-Y., Fuerst, E.-J., Rafaeli, A., and Jurenka, R. (2003). Identification of a G protein-coupled receptor for pheromone biosynthesis activating neuropeptide from pheromone glands of the moth, *Helicoverpa zea*. *Proc. Natl. Acad. Sci. U.S.A.* 100, 9721–9726.
- Choi, M.-Y., Fuerst, E.-J., Rafaeli, A., and Jurenka, R. (2007). Role of extracellular domains in PBAN/Pyrokinin GPCRs from insects using chimera receptors. *Insect Biochem. Mol. Biol.* 37, 296–306.
- Choi, M.-Y., Lee, J. M., Han, K. S., and Boo, K. S. (2004). Identification of a new member of PBAN family and immunoreactivity in the central nervous system from *Adoxophyes sp.* (Lepidoptera: Tortricidae). *Insect Biochem. Mol. Biol.* 34, 927–935.
- Choi, M.-Y., and Jurenka, R. A. (2006). Role of extracellular calcium and calcium channel activated by a G protein-coupled receptor regulating pheromone production in *Helicoverpa zea* (Lepidoptera: Noctuidae). *Ann. Entomol. Soc. Am.* 99, 905–909.
- Choi, M.-Y., and Jurenka, R. A. (2010). Site-directed mutagenesis and PBAN activation of the *Helicoverpa zea* PBAN-receptor. *FEBS Lett.* 584, 1212–1216.
- Chow, Y. S., Lin, Y. M., and Teng, H. J. (1986). "Morphological and biological evidence for the presence of a male sex pheromone of the diamond-back moth," in *Diamondback Moth Management: Proceedings of the First International Workshop*, eds N. S. Talekar and T. D. Griggs (Shanghai: Asian Vegetable Research and Development Center), 103–108.
- Davis, M. B., Vakharia, V. N., Henry, J., Kempe, T. G., and Raina, A. K. (1992). Molecular cloning of the pheromone biosynthesis-activating neuropeptide in *Helicoverpa zea*. *Proc. Natl. Acad. Sci. U.S.A.* 89, 142–146.
- Eisner, T., and Meinwald, J. (1995). The chemistry of sexual selection. *Proc. Natl. Acad. Sci. U.S.A.* 92, 50–55.
- Eltahlawy, H., Buckner, J. S., and Foster, S. P. (2007). Evidence for two-step regulation of pheromone biosynthesis by the pheromone biosynthesis-activating neuropeptide in the moth *Heliothis virescens*. *Arch. Insect Biochem. Physiol.* 64, 120–130.
- Fabrias, G., Marco, M. P., and Camps, F. (1994). Effect of the pheromone biosynthesis activating neuropeptide on sex pheromone biosynthesis in *Spodoptera littoralis* isolated glands. *Arch. Insect Biochem. Physiol.* 27, 77–87.
- Fang, N., Teal, P. E. A., and Tumlinson, J. H. (1995). PBAN regulation of pheromone biosynthesis in female tobacco hornworm moths, *Manduca sexta* (L.). *Arch. Insect Biochem. Physiol.* 29, 35–44.
- Heath, R. R., Landolt, P. J., Dueben, B. D., Murphy, R. E., and Schneider, R. E. (1992). Identification of male cabbage looper sex pheromone attractive to females. *J. Chem. Ecol.* 18, 441–453.
- Hewes, R. S., and Taghert, P. H. (2001). Neuropeptides and neuropeptide receptors in the *Drosophila melanogaster* genome. *Genome Res.* 11, 1126–1142.
- Hillier, N. K., and Vickers, N. J. (2004). The role of Heliothine hair pencil compounds in female *Heliothis virescens* (Lepidoptera: Noctuidae) behavior and mate acceptance. *Chem. Senses* 29, 499–511.

- Hirai, K., Shorey, H. H., and Gaston, L. K. (1978). Competition among courting male moths: male-to-male inhibitory pheromone. *Science* 202, 844–845.
- Hirsch, J. (1991). *Distribution and Mode of Action of Pheromone Biosynthesis Activating Neuropeptide (PBAN) in the Moth Helicoverpa (Heliothis) Armigera*. M.Sc. thesis, The Hebrew University of Jerusalem, Faculty of Agriculture, Rehovot.
- Holman, G. M., Cook, B. J., and Nachman, R. J. (1986). Isolation, primary structure and synthesis of a blocked neuropeptide isolated from the cockroach, *Leucophaea maderae*. *Comp. Biochem. Physiol.* 85C, 219–224.
- Homma, T., Watanabe, K., Tsurumaru, S., Kataoka, H., Imai, K., Kamba, M., Niimi, T., Yamashita, O., and Yaginuma, T. (2006). G protein-coupled receptor for diapause hormone, an inducer of *Bombyx* embryonic diapause. *Biochem. Biophys. Res. Commun.* 344, 386–393.
- Huang, Y. P., Xu, S. F., Tang, X. H., Zhao, Z. W., and Du, J. W. (1996). Male orientation inhibitor of cotton bollworm: identification of compounds produced by male hairpencil glands. *Entomol. Sin.* 3, 172–182.
- Hull, J. J., Ohnishi, A., Moto, K. I., Kawasaki, Y., Kurata, R., Suzuki, M. G., and Matsumoto, S. (2004). Cloning and characterization of the pheromone biosynthesis activating neuropeptide receptor from the silkworm, *Bombyx mori*: significance of the carboxyl terminus in receptor internalization. *J. Biol. Chem.* 279, 51500–51507.
- Imai, K., Konno, T., Nakazawa, Y., Komiyama, T., Isobe, M., Koga, K., Goto, T., Yaginuma, T., Sakakibara, K., Hasegawa, K., and Yamashita, O. (1991). Isolation and structure of diapause hormone of the silkworm, *Bombyx mori*. *Proc. Jpn. Acad.* 67, 98–101.
- Iversen, A., Cazzamali, G., Williamson, M., Hauser, F., and Grimmelikhuijzen, C. J. P. (2002). Molecular cloning and functional expression of a *Drosophila* receptor for the neuropeptides cap-1 and -2. *Biochem. Biophys. Res. Commun.* 299, 628–633.
- Jurenka, R., and Nusawardani, T. (2011). The pyrokinin/pheromone biosynthesis-activating neuropeptide (PBAN) family of peptides and their receptors in Insecta: evolutionary trace indicates potential receptor ligand-binding domains. *Insect Mol. Biol.* 20, 323–334.
- Jurenka, R. A. (1996). Signal transduction in the stimulation of sex pheromone biosynthesis in moths. *Arch. Insect Biochem. Physiol.* 33, 245–258.
- Jurenka, R. A., Jacquin, E., and Roelofs, W. L. (1991). Control of the pheromone biosynthetic pathway in *Helicoverpa zea* by the pheromone biosynthesis activating neuropeptide. *Arch. Insect Biochem. Physiol.* 17, 81–91.
- Kean, L., Cazenave, W., Costes, L., Broderick, K. E., Graham, S., Pollock, V. P., Davies, S. A., Veenstra, J. A., and Dow, J. A. T. (2002). Two nitridergic peptides are encoded by the gene capability in *Drosophila melanogaster*. *Am. J. Physiol. Regul. Integr. Comp. Physiol.* 282, R1297–R1307.
- Kim, Y.-J., Nachman, R. J., Aimanova, K., Gill, S., and Adams, M. E. (2008). The pheromone biosynthesis activating neuropeptide (PBAN) receptor of *Heliothis virescens*: identification, functional expression, and structure-activity relationships of ligand analogs. *Peptides* 29, 268–275.
- Kingan, T. G., Blackburn, M. B., and Raina, A. K. (1992). The distribution of pheromone biosynthesis-activating neuropeptide (PBAN) immunoreactivity in the central nervous system of the corn earworm moth, *Helicoverpa zea*. *Cell Tissue Res.* 270, 229–240.
- Lassance, J.-M., and Löfstedt, C. (2009). Concerted evolution of male and female display traits in the European corn borer, *Ostrinia nubilalis*. *BMC Biol.* 7, 10. doi:10.1186/1741-7007-7-10
- Lee, D.-W., Shrestha, S., Kim, A. Y., Park, S. J., Yang, C. Y., Kim, Y., and Koh, Y. H. (2011). RNA interference of pheromone biosynthesis-activating neuropeptide receptor suppresses mating behavior by inhibiting sex pheromone production in *Plutella xylostella* (L.). *Insect Biochem. Mol. Biol.* 41, 236–243.
- Ma, P. W. K., Knipple, D. C., and Roelofs, W. L. (1994). Structural organization of the *Helicoverpa zea* gene encoding the precursor protein for pheromone biosynthesis-activating neuropeptide and other neuropeptides. *Proc. Natl. Acad. Sci. U.S.A.* 91, 6506–6510.
- Ma, P. W. K., Knipple, D. C., and Roelofs, W. L. (1998). Expression of a gene that encodes multiple neuropeptides in the central nervous system of corn earworm, *Helicoverpa zea*. *Insect Biochem. Mol. Biol.* 28, 373–385.
- Ma, P. W. K., Roelofs, W. L., and Jurenka, R. A. (1996). Characterization of PBAN and PBAN-encoding gene neuropeptides in the central nervous system of the corn earworm moth, *Helicoverpa zea*. *J. Insect Physiol.* 42, 257–266.
- Martinez, T., Gabrias, G., and Camps, F. (1990). Sex pheromone biosynthetic pathway in *Spodoptera littoralis* and its activity by a neurohormone. *J. Biol. Chem.* 265, 1381–1387.
- Matsumoto, S., Kitamura, A., Nagasawa, H., Kataoka, H., Orikasa, C., Mitsui, T., and Suzuki, A. (1990). Functional diversity of a neurohormone produced by the suboesophageal ganglion: molecular identity of melanization and reddish colouration hormone and pheromone biosynthesis activating neuropeptide. *J. Insect Physiol.* 36, 427–432.
- Olsen, S. S., Cazzamali, G., Williamson, M., Grimmelikhuijzen, C. J. P., and Hauser, F. (2007). Identification of one capa and two pyrokinin receptors from the malaria mosquito *Anopheles gambiae*. *Biochem. Biophys. Res. Commun.* 362, 245–251.
- Ozawa, R. A., Ando, T., Nagasawa, H., Kataoka, H., and Suzuki, A. (1993). Reduction of the acyl group: the critical step in bombykol biosynthesis that is regulated *in vitro* by the neuropeptide hormone in the pheromone gland of *Bombyx mori*. *Biosci. Biotechnol. Biochem.* 57, 2144–2147.
- Park, Y., Kim, Y.-J., and Adams, M. E. (2002). Identification of G protein-coupled receptors for *Drosophila* PRXamide peptides, CCAP, corazonin, and AKH supports a theory of ligand-receptor coevolution. *Proc. Natl. Acad. Sci. U.S.A.* 99, 11423–11428.
- Phelan, P. L., Silk, P. J., Northcott, C. J., Tan, S. H., and Baker, T. C. (1986). Chemical identification and behavioral characterization of male wing pheromone of *Ephesia elutella* (Pyralidae). *J. Chem. Ecol.* 12, 135–146.
- Rafaeli, A. (1994). Pheromonotropic stimulation of moth pheromone gland cultures *in vitro*. *Arch. Insect Biochem. Physiol.* 25, 287–299.
- Rafaeli, A., Bober, R., Becker, L., Choi, M. Y., Fuerst, E. J., and Jurenka, R. (2007). Spatial distribution and differential expression of the PBAN receptor in tissues of adult *Helicoverpa* spp. (Lepidoptera: Noctuidae). *Insect Mol. Biol.* 16, 287–293.
- Rafaeli, A., and Gileadi, C. (1996a). Down regulation of pheromone biosynthesis: cellular mechanisms of pheromonostatic responses. *Insect Biochem. Mol. Biol.* 26, 797–807.
- Rafaeli, A., and Gileadi, C. (1996b). “Multi-signal transduction of moth pheromone biosynthesis-activating neuropeptide (PBAN) and its modulation: involvement of G-proteins?,” in *The Peptidergic Neuron*, eds B. Kirsch and R. Mentlein (Basel: Birkhauser), 239–244.
- Rafaeli, A., and Jurenka, R. A. (2003). “PBAN regulation of pheromone biosynthesis in female moths,” in *Pheromone Biochemistry and Molecular Biology*, eds G. J. Blomquist and R. Vogt (San Diego: Academic Press), 107–136.
- Rafaeli, A., and Soroker, V. (1989). Cyclic-AMP mediation of the hormonal stimulation of [14 C]-acetate incorporation by *Heliothis armigera* pheromone glands *in vitro*. *Mol. Cell. Endocrinol.* 65, 43–48.
- Rafaeli, A., Soroker, V., Hirsch, J., Kamensky, B., and Raina, A. K. (1993). Influence of photoperiod and age on the competence of pheromone glands and on the distribution of immunoreactive PBAN in *Helicoverpa* spp. *Arch. Insect Biochem. Physiol.* 22, 169–180.
- Rafaeli, A., Zakharova, T., Lapsker, Z., and Jurenka, R. A. (2003). The identification of an age- and female-specific putative PBAN membrane-receptor protein in pheromone glands of *Helicoverpa armigera*: possible up-regulation by juvenile hormone. *Insect Biochem. Mol. Biol.* 33, 371–380.
- Raina, A., and Kempe, T. (1990). A pentapeptide of the C-terminal sequence of PBAN with pheromonotropic activity. *Insect Biochem.* 20, 849–851.
- Raina, A. K., Jaffe, H., Kempe, T. G., Keim, P., Blacher, R. W., Fales, H. M., Riley, C. T., Klun, J. A., Ridgway, R. L., and Hayes, D. K. (1989). Identification of a neuropeptide hormone that regulates sex pheromone production in female moths. *Science* 244, 796–798.
- Raina, A. K., Jaffe, H., Klun, J. A., Ridgway, R. L., and Hayes, D. K. (1987). Characteristics of a neurohormone that controls sex pheromone production in *Heliothis zea*. *J. Insect Physiol.* 33, 809–814.
- Raina, A. K., and Kempe, T. G. (1992). Structure activity studies of PBAN of *Helicoverpa zea* (Lepidoptera: Noctuidae). *Insect Biochem. Mol. Biol.* 22, 221–225.
- Soroker, V., and Rafaeli, A. (1995). Multi-signal transduction of the pheromonotropic response by pheromone gland incubations of *Helicoverpa armigera*. *Insect Biochem. Mol. Biol.* 25, 1–9.

- Stern, P. S., Yu, L., Choi, M.-Y., Jurenka, R. A., Becker, L., and Rafaeli, A. (2007). Molecular modeling of the binding of pheromone biosynthesis activating neuropeptide to its receptor. *J. Insect Physiol.* 53, 803–818.
- Sun, J.-S., Zhang, T.-Y., Zhang, Q.-R., and Xu, W.-H. (2003). Effect of the brain and subesophageal ganglion on pupal development in *Helicoverpa armigera* through regulation of FXPRLamide neuropeptides. *Regul. Pept.* 116, 163–171.
- Szentesi, A., Toth, M., and Dodrovolsky, A. (1975). Evidence and preliminary investigation on a male aphrodisiac and a female sex pheromone in *Mamestra brassicae* (L.) *Acta Phytopathol. Hung.* 10, 425–429.
- Tang, J. D., Charlton, R. E., Jurenka, R. A., Wolf, W. A., Phelan, P. L., Streng, L., and Roelofs, W. L. (1989). Regulation of pheromone biosynthesis by a brain hormone in two moth species. *Proc. Natl. Acad. Sci. U.S.A.* 86, 1806–1810.
- Teal, P. E. A., and Tumlinson, J. H. (1989). Isolation, identification and biosynthesis of compounds produced by male hairpencil glands of *Heliothis virescens* (F.) (Lepidoptera: Lepidoptera). *J. Chem. Ecol.* 15, 413–427.
- Teal, P. E. A., Tumlinson, J. H., McLaughlin, F. R., Heath, R. R., and Rush, R. A. (1984). (Z)-11-hexadecanol: a behavioral modifying chemical present in the pheromone gland of female *Heliothis zea* (Lepidoptera: Noctuidae). *Can. Entomol.* 116, 777–779.
- Thibout, E., Ferary, S., and Auger, J. (1994). Nature and role of sexual pheromones emitted by males of *Ascrolepiopsis assectella* (Lep.). *J. Chem. Ecol.* 20, 1571–1581.
- Tsfadia, O., Azrieli, A., Falach, L., Zada, A., Roelofs, W. L., and Rafaeli, A. (2008). Pheromone biosynthetic pathways: PBAN-regulated rate-limiting steps and differential expression of desaturase genes in moth species. *Insect Biochem. Mol. Biol.* 38, 552–567.
- Tumlinson, J. H., Fang, N., and Teal, P. E. A. (1997). “The effect of PBAN on conversion of fatty acyls to pheromone aldehydes in female,” in *Insect Pheromone Research: New Directions*, eds R. T. Cardé and A. K. Minks (New York: Chapman and Hall), 54–55.
- Wu, W. Q., Tang, X. H., Xu, S. F., and Du, J. W. (1991). The diel rhythm of calling behavior and sex pheromone production of *Helicoverpa armigera* (Hubner) (Lepidoptera: Noctuidae). *Contributions from Shanghai Institute of Entomology* 10, 57–62.
- Zdarek, J., Nachman, R. J., and Hayes, T. K. (1997). Insect neuropeptides of the pyrokinin/PBAN family accelerate pupariation in the fleshfly (*Sarcophaga bullata*) larvae. *Ann. N. Y. Acad. Sci.* 814, 67–72.
- Zhang, T.-Y., Sun, J.-S., Zhang, Q.-R., Xu, J., Jiang, R.-J., and Xu, W.-H. (2004). The diapause hormone-pheromone biosynthesis activating neuropeptide gene of *Helicoverpa armigera* encodes multiple peptides that break, rather than induce, diapause. *J. Insect Physiol.* 50, 547–554.
- Zheng, L., Lytle, C., Njauw, C.-N., Altstein, M., and Martins-Green, M. (2007). Cloning and characterization of the pheromone biosynthesis activating neuropeptide receptor gene in *Spodoptera littoralis* larvae. *Gene* 393, 20–30.

Conflict of Interest Statement: The authors declare that the research was conducted in the absence of any commercial or financial relationships that could be construed as a potential conflict of interest.

Received: 24 June 2011; accepted: 15 September 2011; published online: 10 October 2011.

Citation: Jurenka R and Rafaeli A (2011) Regulatory role of PBAN in sex pheromone biosynthesis of heliothine moths. *Front. Endocrin.* 2:46. doi: 10.3389/fendo.2011.00046

This article was submitted to *Frontiers in Experimental Endocrinology*, a specialty of *Frontiers in Endocrinology*.

Copyright © 2011 Jurenka and Rafaeli. This is an open-access article subject to a non-exclusive license between the authors and Frontiers Media SA, which permits use, distribution and reproduction in other forums, provided the original authors and source are credited and other Frontiers conditions are complied with.



Screening for the genes involved in bombykol biosynthesis: identification and functional characterization of *Bombyx mori* acyl carrier protein

Atsushi Ohnishi*, Misato Kaji, Kana Hashimoto and Shogo Matsumoto*

Molecular Entomology Laboratory, RIKEN Advanced Science Institute, Wako, Japan

Edited by:

Joe Hull, USDA Agricultural Research Service, USA

Reviewed by:

Honoo Satake, Suntory Institute for Bioorganic Research, Japan
Sheng Li, Chinese Academy of Sciences, China
Shunsuke Moriyama, Kitasato University, Japan

*Correspondence:

Atsushi Ohnishi and Shogo Matsumoto, Molecular Entomology Laboratory, RIKEN Advanced Science Institute, Hirosawa 2-1, Wako, Saitama 351-0198, Japan.
e-mail: aohnishi@riken.jp;
smatsu@riken.jp

Species-specific sex pheromones released by female moths to attract conspecific male moths are synthesized *de novo* in the pheromone gland (PG) via fatty acid synthesis (FAS). Biosynthesis of moth sex pheromones is usually regulated by a neurohormone termed pheromone biosynthesis activating neuropeptide (PBAN), a 33-aa peptide that originates in the subesophageal ganglion. In the silkworm, *Bombyx mori*, cytoplasmic lipid droplets (LDs), which store the sex pheromone (bombykol) precursor fatty acid, accumulate in PG cells prior to eclosion. PBAN activation of the PBAN receptor stimulates lipolysis of the stored LD triacylglycerols (TAGs) resulting in release of the bombykol precursor for final modification. While we have previously characterized a number of molecules involved in bombykol biosynthesis, little is known about the mechanisms of PBAN signaling that regulate the TAG lipolysis in PG cells. In the current study, we sought to further identify genes involved in bombykol biosynthesis as well as PBAN signaling, by using a subset of 312 expressed-sequence tag (EST) clones that are in either our *B. mori* PG cDNA library or the public *B. mori* EST databases, SilkBase and CYBERGATE, and which are preferentially expressed in the PG. Using RT-PCR expression analysis and an RNAi screening approach, we have identified another eight EST clones involved in bombykol biosynthesis. Furthermore, we have determined the functional role of a clone designated BmACP that encodes *B. mori* acyl carrier protein (ACP). Our results indicate that BmACP plays an essential role in the biosynthesis of the bombykol precursor fatty acid via the canonical FAS pathway during pheromonogenesis.

Keywords: bombykol, *Bombyx mori*, lipid droplet, triacylglycerol, acyl carrier protein

INTRODUCTION

In most moth species, sex pheromone biosynthesis is regulated by the pheromone biosynthesis activating neuropeptide (PBAN), a neurohormone consisting of 33 amino acid peptide that originates in the subesophageal ganglion and that is characterized by the core C-terminal FSPRLamide sequence. Initially purified and sequenced from the corn earworm, *Helioverpa zea* (Raina et al., 1989) and the silkworm, *B. mori* (Kitamura et al., 1989), PBAN has since been identified in numerous other lepidopteran species (Rafaeli and Jurenka, 2003). In most species including *B. mori*, PBAN is released into the hemolymph during a species-specific period after adult emergence and acts on the pheromone gland (PG) to trigger the production and release of species-specific sex pheromones (Rafaeli, 2002, 2009). The PG is a functionally differentiated organ in close proximity to the terminal abdominal tip which originates in the intersegmental membrane between the eighth and ninth abdominal segments (Percy and Weatherston, 1974; Fónagy et al., 2000; Matsumoto et al., 2007). In the silkworm, *Bombyx mori*, the sex pheromone, bombykol (E, Z-10, 12-hexadecadien-1-ol), is synthesized *de novo* within PG cells from acetyl-CoA via conventional long chain fatty acid synthesis (FAS; Bjostad et al., 1987; Jurenka, 2003). The straight

chain fatty acyl intermediate, palmitate, is converted stepwise to bombykol by the actions of a bifunctional Z11-10/12 fatty acyl desaturase, Bmpgdesat1, and a PG-specific fatty acyl reductase, pgFAR (Moto et al., 2003, 2004; Ohnishi et al., 2006). On the day before adult emergence, *B. mori* PG cells rapidly accumulate numerous lipid droplets (LDs) within the cytoplasm (Fónagy et al., 2001). These LDs play an essential role in bombykol biosynthesis by acting as a reservoir for the *de novo* synthesized bombykol precursor, 10,12-hexadecadienoate, which is deposited in the LDs in the form of triacylglycerols (TAGs) with the precursor predominantly sequestered at the *sn*-1 and *sn*-3 positions of the glycerides (Matsumoto et al., 2002). After adult emergence, the stored fatty acid is cleaved and converted to bombykol in response to PBAN stimulation (Matsumoto et al., 2007, 2010).

To identify functional proteins involved in bombykol biosynthesis, we generated a PG expressed-sequence tag (EST) database by constructing a normalized PG cDNA library prepared from newly emerged female *B. mori* moths of the inbred p50 strain (Yoshiga et al., 2000). We next screened *in silico* for PG-specific genes, using our own database as well as the public *B. mori* EST databases (SilkBase and CYBERGATE). Of the approximate 11,000 independent EST clones, we identified a number of clones that are

predominantly or specifically expressed in the *B. mori* PG. Apart from this type of approach, we also established a method of RNAi-mediated *in vivo* gene silencing in *B. mori* (Ohnishi et al., 2006). Using this methodological tool, we have characterized a number of genes that are specifically or predominantly expressed in the *B. mori* PG during pheromonogenesis. These genes, which are up-regulated on the day prior to adult emergence (i.e., *pgFAR*, *Bmpgdesat1*, *pgACBP*, *mgACBP*, *PBANR*, *BmFATP*, and *BmLsd1*), play critical roles in bombykol production triggered by the external PBAN signal (Matsumoto et al., 2001; Moto et al., 2003, 2004; Hull et al., 2004; Ohnishi et al., 2006, 2009, 2011). In the current study, we describe the further identification of eight EST clones involved in bombykol biosynthesis using similar methodologies. Among these clones, we have also determined the functional role of a clone (NRPG0659) that encodes the *B. mori* acyl carrier protein (BmACP) critical for bombykol biosynthesis.

MATERIALS AND METHODS

INSECTS

Larvae of the inbred p50 strain of *B. mori*, originally provided by T. Shimada of the University of Tokyo, were reared on an artificial diet and maintained under a 16L:8D photoperiod at 25°C (Fónagy et al., 1992). Pupal age was determined based on morphological characteristics as described (Matsumoto et al., 2002).

RAPID AMPLIFYING cDNA ENDS (RACE)

Messenger RNA was isolated from about 100 µg of PG total RNA by using a Micro-Fast Track kit (Invitrogen). RACE was performed using a GeneRacer kit (Invitrogen) according to the manufacturer's instructions. Computer-assisted sequence analyses were performed using GENETYX-MAC Ver.15.0.5 (Software Development Co., Tokyo, Japan).

RT-PCR ANALYSIS

Pheromone glands and other tissues were dissected into insect Ringer's solution [35 mM NaCl, 36 mM KCl, 12 mM CaCl₂, 16 mM MgCl₂, 274 mM glucose, and 5 mM Tris (pH 7.5)] and mechanically trimmed as described (Ozawa and Matsumoto, 1996). Total RNA was isolated from the trimmed PGs by the method of Chomczynski and Sacchi (1987). First-strand cDNA synthesis was performed with 500 ng total RNA using an RNA PCR kit (Takara Bio, Otsu, Japan) according to the manufacturer's instructions. Fragments of *BmACP* and *Actin* were amplified using a specific oligonucleotide primer set designed from the published sequence [for *BmACP*, NRPG0659-F (sense primer): 5'-GCACAATTAAAGCCGCTGTC-3' and NRPG0659-R (antisense primer): 5'-ATGTCTTTTGGTCTGACCAG-3'; for *Actin*, *Actin-F* (sense primer): 5'-AGATGACCCAGATCATGTTTG-3' and *Actin-R* (antisense primer): 5'-GAGATCCACATCTGCTGGAAG-3'). PCR was performed using thermacycler conditions consisting of 30 cycles at 94°C for 30 s, 55°C for 30 s, and 72°C for 60 s. PCR products (5 µL) were electrophoresed on a 1.5% agarose gel in Tris-acetate-EDTA buffer and stained with ethidium bromide.

SYNTHESIS AND INJECTION OF DOUBLE-STRANDED RNA (dsRNA)

Templates for the synthesis of dsRNAs corresponding to *BmACP* were prepared using gene specific primers containing

T7 polymerase sites [NRPG0659-T7-F (sense primer): 5'-CGGATCCTAATACGACTCACTATAGGGCGGCACAATTAA-3', NRPG0659-T7-R (antisense primer): 5'-CCGGATCCTAATACGACTCACTATAGGGCGGCAATACATTGC-3'; nucleotide sequences corresponding to the T7 promoter region are underlined]. PCR was performed using thermacycler conditions consisting of six cycles at 94°C for 30 s, 56.5°C for 30 s, 68°C for 90 s followed by 30 cycles at 94°C for 30 s, 66°C for 30 s, 68°C for 90 s using KOD-Plus – (Toyobo, Osaka, Japan) with the resulting products purified (Wizard SV Gel and PCR Clean-Up kit, Promega) and used as templates to generate dsRNAs using the AmpliScribe™T7 High Yield Transcription kit (Epicentre Technologies, Madison, WI, USA) according to the manufacturer's instructions. After synthesis, the dsRNAs were diluted with diethyl pyrocarbonate (DEPC) – treated H₂O, the RNA concentrations measured (Abs₂₆₀), and the products analyzed by gel electrophoresis to confirm annealing. Samples were diluted to the desired concentration (final volume 2 µL) and injected into 1-day-old pupae (i.e., pupae 1 day removed from the larval-pupal molt) using a 10 µL microsyringe (Hamilton, USA) as described (Ohnishi et al., 2006; Hull et al., 2009, 2010). Control pupae were injected with 2 µL DEPC-treated H₂O alone. After injection, pupae were maintained under normal conditions until adult emergence.

IN VIVO BOMBYKOL ANALYSIS

Adult females were decapitated within 3 h of emergence and maintained at 25°C for 24 h. They were then injected with either 2 µL (2.5 pmol/µL) *B. mori* PBAN in PBS or PBS alone. Abdominal tips were dissected 90 min after injection and bombykol production was measured by HPLC as described (Matsumoto et al., 1990) using a Senshu-Pak NO₂ column [Senshu Scientific Co., Tokyo, Japan; 4.6 mm inner diameter × 150 mm, pore size, 100 Å].

MICROSCOPIC EXAMINATION OF CYTOPLASMIC LIDS

PGs were dissected and mechanically trimmed from normal, decapitated, and RNAi-treated females. The excised glands were fixed with a 4% formalin/PBS solution and stained with Nile Red (a fluorescent probe for intracellular neutral lipids; Molecular Probes, Eugene, OR, USA) as described (Fónagy et al., 2001). Fluorescence microscopy was performed with an OLYMPUS BX-60 system equipped with a PM-30 exposure unit and a BH20-RFL-T3 light source (400× magnification). Nile Red imaging was done with a 330–385 nm band pass excitation filter, a 400 nm dichroic mirror, and a 420 nm long pass barrier filter (Olympus cube WU). Images were processed and merged using Photoshop CS (Adobe Systems).

ANALYSIS OF LD TRIACYLGLYCEROLS

Lipid droplets TAGs were analyzed as described previously (Matsumoto et al., 2002). Five trimmed PGs were prepared from the desired stages of female moths and dipped in 100 µL acetone for 10 min at room temperature. The dried acetone extracts were dissolved in *n*-hexane and loaded on either a Senshu-Pak PEGASIL-Silica 120-5 column (Senshu Scientific Co.; 4.6 mm inner diameter × 250 mm, pore size, 120 Å) equilibrated with *n*-hexane/acetic acid (99/1) or a SSC-C₂₂ docosil column (Senshu Scientific Co.; 4.6 mm inner diameter × 250 mm, pore size,

120 Å) equilibrated with acetonitrile/ethanol (6/4). Because various TAG components comprise the cytoplasmic LDs, the entire TAG fraction was separated and detected using an evaporative light scattering detector (ELSD; SEDEX model 75, Sedere, France). Fatty acyl groups in the TAGs were identified by fast atom bombardment mass spectrometry (FAB-MS) and tandem MS (MS/MS) analyses using a JMS HX/HX-110A tandem mass spectrometer (JEOL, Tokyo, Japan) as described (Matsumoto et al., 2002).

RESULTS

EXPRESSION ANALYSIS OF *B. MORI* EST CLONES USING RT-PCR

To identify proteins functionally involved in bombykol biosynthesis, we selected 88 PG-specific genes *in silico* from approximately 11,000 independent clones in our PG EST database and/or the public *B. mori* EST databases. To examine the *in vivo* expression patterns of the 88 gene transcripts, we performed RT-PCR analysis using various tissues including PG, which were prepared from *B. mori* females (p50 strain) before and after eclosion. The results indicated that 26 clones were specifically expressed in the PG and/or up-regulated the day prior to eclosion

(Table 1), suggesting potential functional roles for these genes in pheromonogenesis.

RNAi SCREENING FOR GENES INVOLVED IN *B. MORI* PHEROMONOGENESIS

We previously established a method of RNAi-mediated *in vivo* gene silencing in *B. mori* (Ohnishi et al., 2006). To confirm the *in vivo* function of the 26 genes described above, we performed dsRNA-mediated RNAi knockdown of these target genes and examined their inhibitory effect on bombykol production. Compared to control pupae injected with DEPC-treated H₂O, 1-day-old p50 female pupa injected with 10 µg dsRNA corresponding to the respective genes resulted in a significant reduction in bombykol production for 8 of the 26 genes (NRPG0074, NRPG0604, NRPG0659, NRPG0660, NRPG0873, NRPG0891, NRPG1860, and NRPG1885; Figure 1). Because no decrease in bombykol production was observed in control pupae injected with dsRNAs for unrelated proteins including enhanced green fluorescent protein (EGFP), these findings suggest that disruption of bombykol production results from specific knockdown of the target gene sequences (Figure 1). These eight EST clones include two clones

Table 1 | Expressed-sequence tag clones identified in the *Bombyx mori* pheromone gland.

EST clone name	GenBank homolog description	Accession no. ¹	E-value ²	PG expression ³	Up-regulation ⁴
NRPG0023	Triacylglycerol lipase (<i>Bombyx mori</i>)	DQ311322	5.00E-94	+	+
NRPG0034	Aldehyde dehydrogenase (<i>Bombyx mori</i>)	DQ311433	1.00E-100	+	+
NRPG0074	Chemosensory protein (<i>Bombyx mori</i>)	DQ855507	2.00E-66	+	+
NRPG0098	Scavenger receptor cysteine-rich protein (<i>Culex pungens</i>)	DS232623	1.00E-13	+	+
NRPG0203	B-cell receptor-associated protein 31 (<i>Acromyrmex echinator</i>)	GL888216	2.00E-10	+	
NRPG0204	ABC transporter (<i>Aedes aegypti</i>)	EAT43031	8.00E-43	+	+
NRPG0293	No homolog			+	
NRPG0414	No homolog				+
NRPG0476	No homolog			+	+
NRPG0604	Glycerophosphoryl diester phosphodiesterase (<i>Bombyx mori</i>)	AB115083	3.00E-96	+	+
NRPG0640	Serine protease (<i>Aedes aegypti</i>)	CH477825	3.00E-4	+	+
NRPG0659	Acyl carrier protein (<i>Bombyx mori</i>)	DQ443383	8.00E-76		+
NRPG0660	Cuticle protein (<i>Bombyx mori</i>)	BR000649	3.00E-98	+	+
NRPG0733	Arylsulfatase (<i>Culex quinquefasciatus</i>)	DS232119	2.00E-65	+	+
NRPG0825	No homolog			+	+
NRPG0857	Yellow protein (<i>Bombyx mori</i>)	DQ358081	1.00E-114	+	+
NRPG0873	Glucose dehydrogenase (<i>Aedes aegypti</i>)	EAT44639	4.00E-35	+	+
NRPG0891	Perilipin (<i>Bombyx mori</i>)	DQ311207	1.00E-110	+	+
NRPG1106	Aldehyde oxidase (<i>Bombyx mori</i>)	EU073423	1.00E-127	+	+
NRPG1147	VLC acyl-CoA synthetase (<i>Drosophila melanogaster</i>)	AY118315	6.00E-64	+	+
NRPG1187	Lipase 3 (<i>Drosophila melanogaster</i>)	CAA74737	4.00E-22	+	+
NRPG1431	No homolog			+	
NRPG1860	Fatty acid transport protein (<i>Bombyx mori</i>)	AB451529	1.00E-115	+	+
NRPG1885	Lipase (<i>Aedes aegypti</i>)	EAT48716	2.00E-17	+	+
fpheP04_F_A15	Alcohol dehydrogenase (<i>Bombyx mori</i>)	DQ512730	4.00E-23		+
fpheP07_F_F10	BmorCPR53 cuticle protein (<i>Bombyx mori</i>)	BR000544	3.00E-68	+	

¹Accession number of the GenBank homolog.

²E-value for the comparison of the EST sequence information and the GenBank homolog (BLASTX).

³+ Indicates a gene that is predominantly expressed in the PG.

⁴+ Indicates a gene that is up-regulated from the day prior to eclosion in the PG.

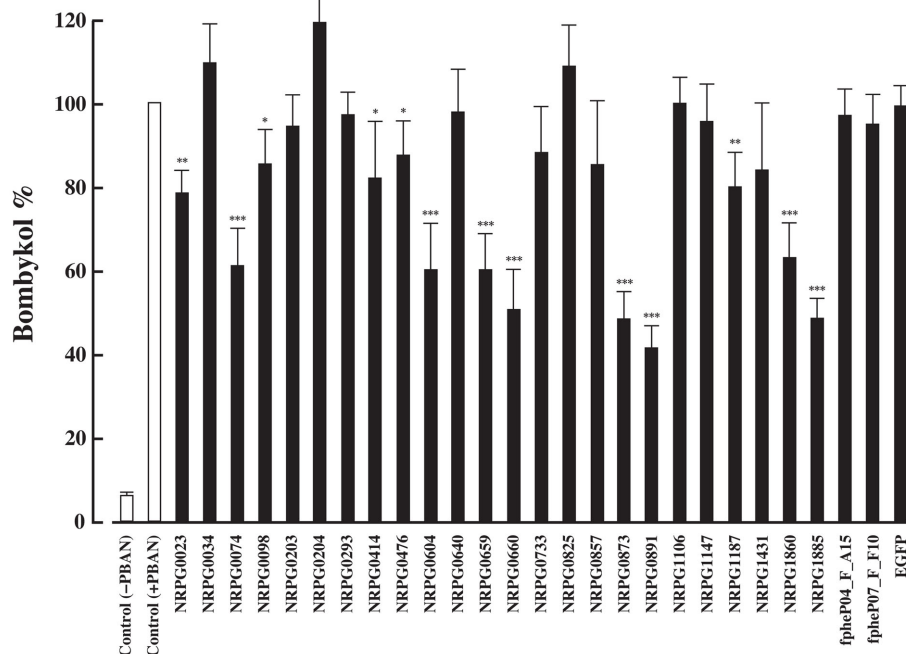


FIGURE 1 | Effect of RNAi treatment on *in vivo* bombykol production. One-day-old pupae were injected with 10 μ g dsRNA corresponding to the target genes or *EGFP*. Results are expressed relative to the mean value for

bombykol levels in non-RNAi-treated females following injection with 5 pmol PBAN (* $p < 0.05$; ** $p < 0.01$; *** $p < 0.001$). Bars represent mean values \pm SD from independent experimental animals ($n > 15$).

```

1 attaaagggttttggcaaccaggctttcggattcgcgatgagagagaattgctgaaagaaaataaagcatttcgtgagcttgaagaaatggc 90
1                                     M A 2
91 tgctgcgaatatatttccgaagtgccttcggtggtctattacggagatcaacaacgtatagaacgtccgtaacatgctgctcttcgaccgt 180
3  A A N I F R S A F G G L L R R S T T Y R T S V T C R L S T V 32
181 tgctgtgcagcaaaagttcagcacaattaaagccgctgtcaaaatatacaaaagtcaggcccttcagaatgggaacgagaacatggtat 270
33  A L Q Q K F S T I K A A V K I Y K S Q A L Q N G N E K H G I 62
271 ccgcaagtacagcgggtggccctccctcaccttagacctataaaaagtagagtactgcttgacttcaactttatgacaaaattaaccc 360
63  R K Y S G G P P L T L D L I K S R V L L V L Q L Y D K I N P 92
361 tgaacagttgactgtagatagccacttcatgaatgatctgggtcttgactcactggaccatgttgaggtcataatggcaatggaagatga 450
93  E Q L T V D S H F M N D L G L D S L D H V E V I M A M E D E 122
451 atttggaattgagataccggatggtgatgcagagagactggtcagacaaaagacattgtccaatacattgctgacaaggaagatatatta 540
123 F G F E I P D G D A E R L V R P K D I V Q Y I A D K E D I Y 152
541 tgaataataaaaaaaatataaaacttcataattttggaccagttgtatttttgaaacgataacaaacacacaaaattgcattttctta 630
153 E * 153
631 atttacaactggcctaaaagtattgttttagtgattagacaacttttgttttaattttacacaaacgttatcagtgcaacttcagaccattg 720
721 tgtaaaaagtgtgaagttttgtttttaattatagcctgttagaataagatcatttgatttcatttgatctggtggtacattatctgataa 810
811 taaaatagtaaatagatcaaaaaaaaaaaaaaaaaaaaaa 848

```

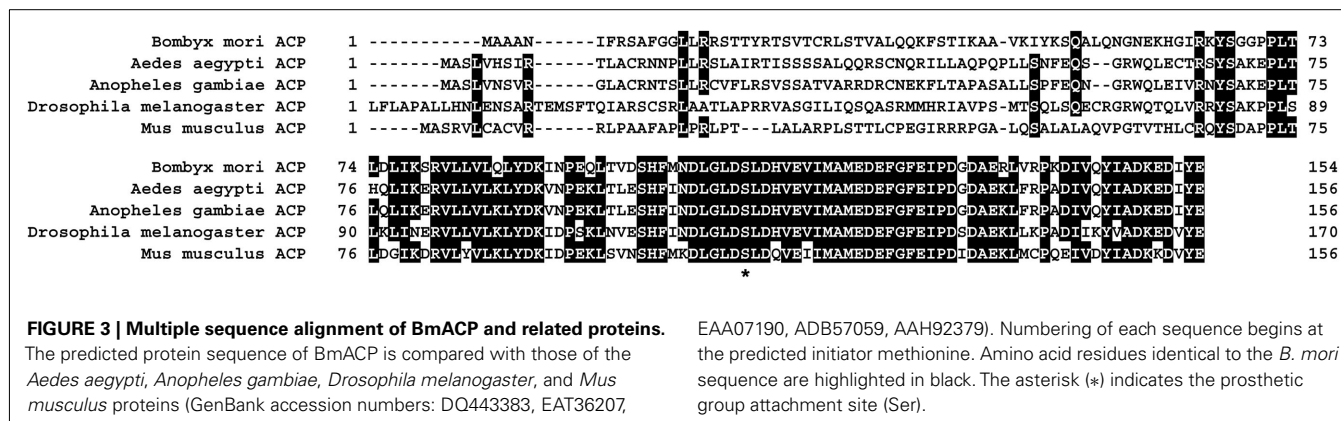
FIGURE 2 | cDNA and deduced amino acid sequence of BmACP.

that encode BmLsd1 and BmFATP (NRPG0891 and NRPG1860), which we have recently characterized functionally associated with LD dynamics during *B. mori* pheromogenesis (Ohnishi et al., 2009, 2011). From this group, five of the genes (NRPG0604, NRPG0659, NRPG0891, NRPG1860, and NRPG1885) are predicted to encode proteins involved in lipid metabolism (Table 1), which is consistent with a role in bombykol biosynthesis. The roles of the other three genes, which encode a chemosensory protein

(NRPG0074), a cuticle protein (NRPG0660), and a glucose dehydrogenase (NRPG0873), in bombykol biosynthesis have yet to be identified.

CHARACTERIZATION OF NRPG0659

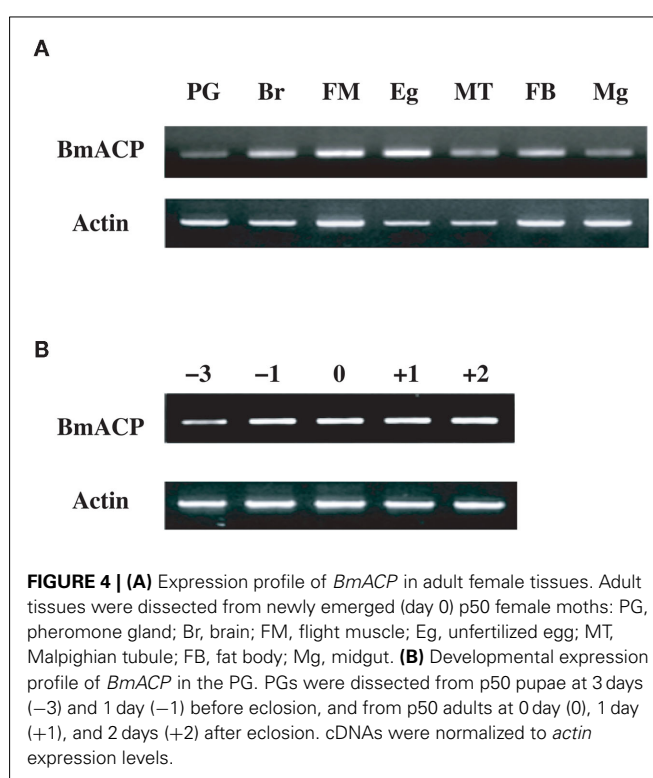
Our RNAi-mediated gene silencing screen suggested the involvement of NRPG0659 in bombykol production (Figure 1). NRPG0659 is predicted to encode an acyl carrier protein (Table 1),



which is known to be a universal and highly conserved carrier of acyl intermediates during FAS (Byers and Gong, 2007). Consequently, we sought to characterize the functional role of the BmACP expressed in the PG. Structural analysis using both 3'- and 5'-RACE confirmed that *BmACP* is comprised of a 848-nt ORF encoding a 153-aa protein flanked by a 85-nt 5'-UTR and a 304-nt 3'-UTR (Figure 2). Comparison of the BmACP sequence with sequences from other organisms revealed high similarities with the *Aedes aegypti* ACP, *Anopheles gambiae* ACP, *Drosophila melanogaster* ACP, and *Mus musculus* ACP (59, 59, 54, and 54% similarity, respectively; Figure 3). These ACPs including BmACP are characterized by a highly conserved C-terminal domain sequence that contains a conserved serine residue necessary for interacting with acyl proteins (Figure 3; Byers and Gong, 2007). While RT-PCR analysis revealed that *BmACP* is ubiquitously expressed in adult tissues (Figure 4A), it undergoes up-regulation 1 day prior to adult emergence in the PG (Figure 4B). This up-regulation profile is reminiscent of PG proteins crucial to bombykol biosynthesis (Matsumoto et al., 2001; Moto et al., 2003, 2004; Hull et al., 2004; Ohnishi et al., 2006, 2009, 2011).

IN VIVO EFFECT OF RNAi-MEDIATED BmACP KNOCKDOWN ON BOMBYKOL PRODUCTION

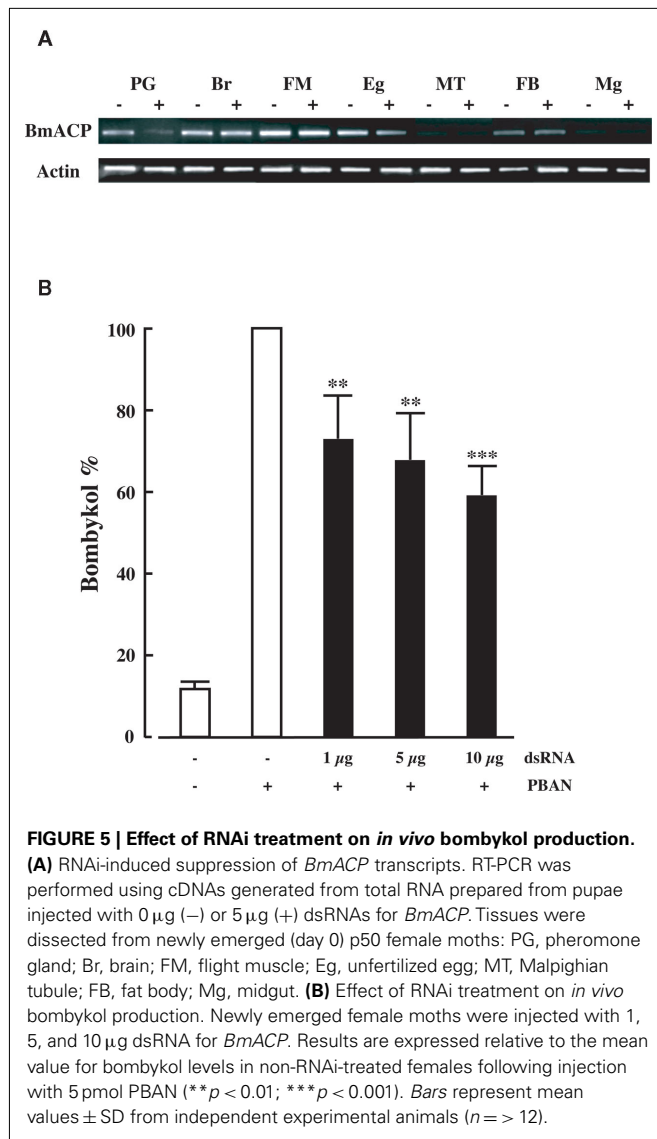
To confirm the *in vivo* function of BmACP, we returned to dsRNA-mediated RNAi knockdown and examined the effect on transcript levels. When we injected 10 μ g *BmACP* dsRNA into newly emerged adult p50 females, *BmACP* mRNA levels 2 days after injection in the PG were selectively reduced compared to those in other tissues as well as control females injected with DEPC-treated H₂O alone (Figure 5A). Although the reason for the PG-selective knockdown of BmACP is presently unknown, a similar PG-selective decrease in transcript levels was observed following knockdown of BmFATP and BmLsd1 (Ohnishi et al., 2009, 2011). Because *BmACP* dsRNA injections had no effect on pupal development or adult emergence, we next injected varying concentrations (1, 5, and 10 μ g) of *BmACP* dsRNA into newly emerged female moths. A dose-dependent reduction in bombykol production was observed with 1, 5, and 10 μ g dsRNA injections resulting in bombykol levels 73, 63, and 59% of the control level, respectively (Figure 5B). To confirm the knockdown effect by *BmACP*, we also examined other dsRNAs corresponding to non-overlapping 5' and 3' regions



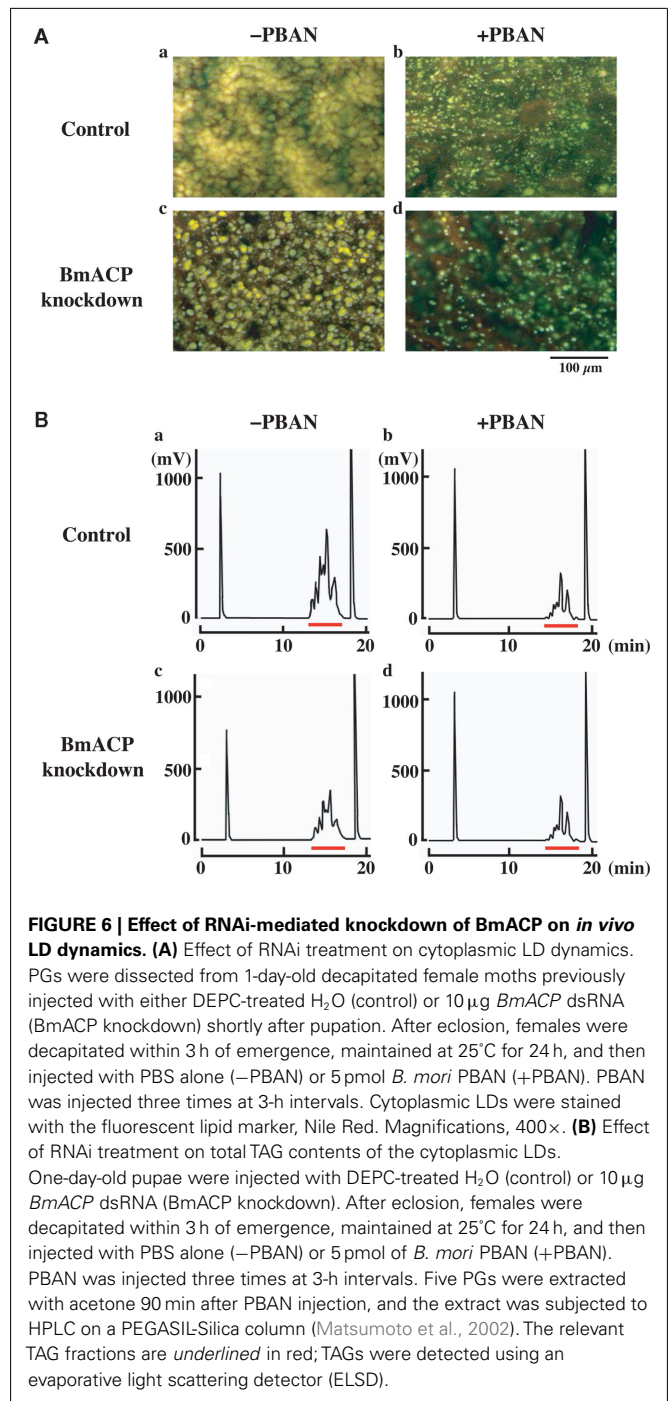
of *BmACP*; these dsRNAs had a similar knockdown effect on bombykol production (data not shown).

IN VIVO EFFECT OF RNAi-MEDIATED BmACP KNOCKDOWN ON CYTOPLASMIC LD DYNAMICS

We further examined the knockdown effect of BmACP on LD dynamics during pheromonogenesis (Figure 6). The most obvious characteristic feature of PG cells is the abundance of LDs within the cytoplasm (Fónagy et al., 2000, 2001). The role of the LDs in bombykol biosynthesis is to store the bombykol precursor fatty acid in the form of TAGs and release it in response to the external signal of PBAN (Matsumoto et al., 2002). To monitor the LD dynamics during pheromonogenesis, we have previously stained the LDs with the fluorescent lipid marker, Nile Red, and found that they appear 1–2 days before eclosion, rapidly



accumulate on the day of eclosion, and decrease in size and number after eclosion in response to PBAN (Fónagy et al., 2001). In RNAi-untreated controls, female moths accumulated numerous large LDs in the PG cell, which underwent a striking reduction following PBAN-induced LD lipolysis (Figure 6A,a,b, also see Ohnishi et al., 2009, 2011). In contrast, PGs of female moths treated with *BmACP* dsRNA accumulated noticeably smaller LDs (Figure 6A,a,c). Because these LDs store the bombykol precursor in the form of TAGs (14), we further examined the effects of BmACP knockdown on the fluctuation of total TAGs. Following extraction with acetone from dissected PGs, total TAG levels were measured by normal-phase HPLC on a PEGASIL-Silica column (Matsumoto et al., 1990). In BmACP knocked-down PGs, PBAN-induced TAG lipolysis was comparable to that of the non-RNAi-treated control (Figure 6B,b,d). In contrast, accumulation of TAG content was significantly reduced (38%) in BmACP-knockdown PGs compared to the RNAi-untreated control (Figure 6B,a,c). Taken together, these results indicate that BmACP is integral to



the bombykol biosynthetic pathway in that it plays an essential role in accumulating the bombykol precursor for TAG storage in the cytoplasmic LDs before eclosion.

IN VIVO EFFECT OF RNAi-MEDIATED BmACP KNOCKDOWN ON DE NOVO SYNTHESIS OF THE BOMBYKOL PRECURSOR

The TAGs that compose cytoplasmic LDs in the PGs comprise various TAG species in which the bombykol precursor is predominantly sequestered at the *sn*-1 and/or *sn*-3 position as a major

fatty acyl component (Matsumoto et al., 2002). Consequently, we sought to assess the effects of BmACP silencing on *de novo* synthesis of the bombykol precursor via the conventional FAS pathway. In agreement with our previous results (Matsumoto et al., 2002) and **Figure 7**, overall TAG contents in PGs of both control and RNAi-treated moths were dramatically reduced in response to PBAN (**Figures 6B** and **7**). In addition, the total amount of TAGs in RNAi-treated PGs was again reduced ~34% compared to that of

the non-RNAi-treated PGs (**Figures 7A,C**). Furthermore, there was a significant difference in the TAG elution profiles between non-RNAi-treated and RNAi-treated PGs before PBAN injection; silencing BmACP brought about a striking reduction in specific TAG peaks (see peaks 1, 1a, 2, 3 in **Figure 7**). MS analysis indicated that the TAG species eluted in these peaks are mainly comprised of the bombykol precursor fatty acid (**Table 2**; Matsumoto et al., 2002).

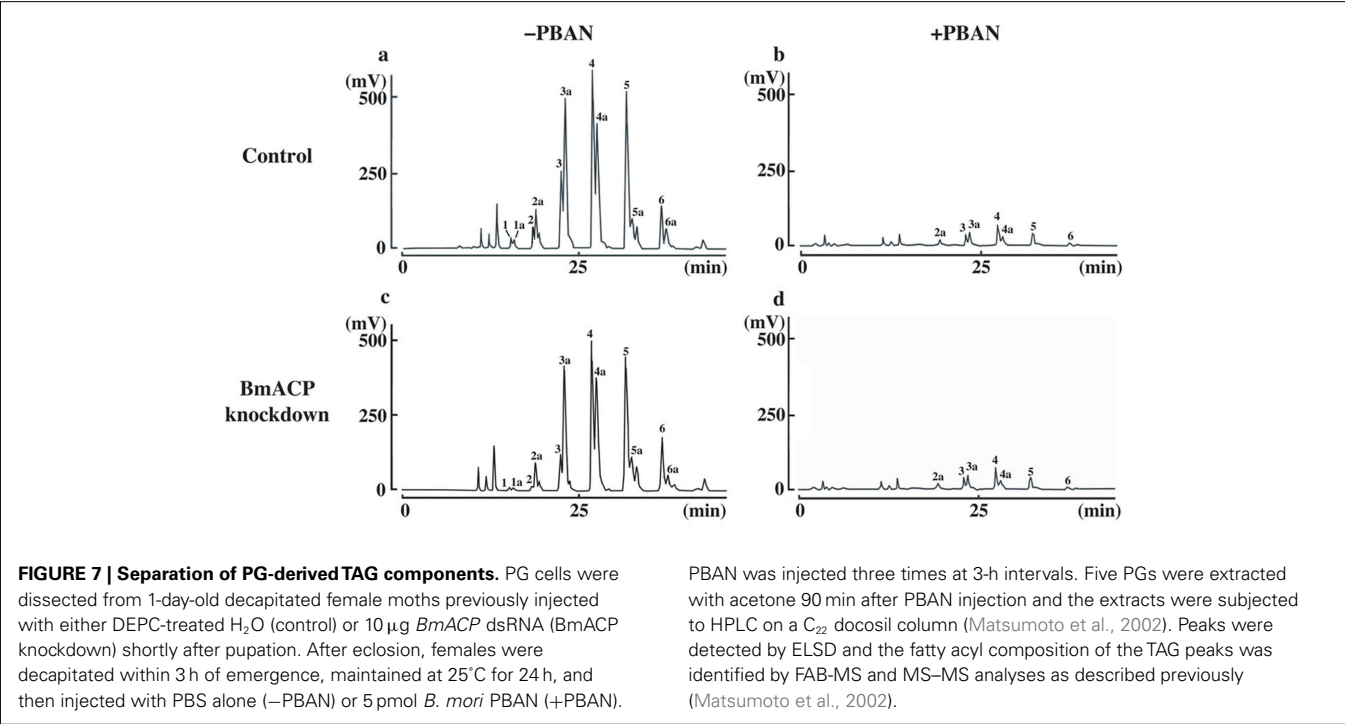


Table 2 | Comparison of peak areas in Figures 7A,C.

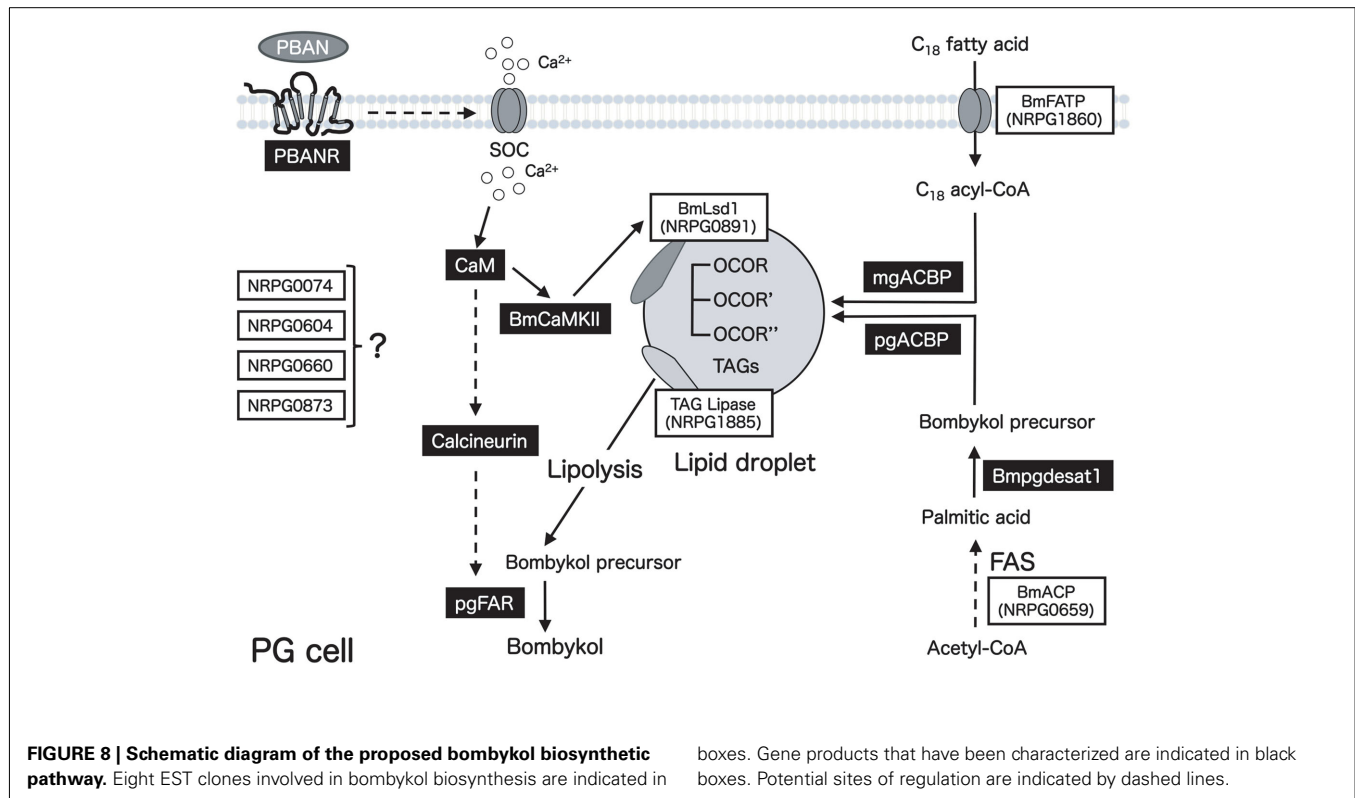
Peak#	Control (a) Avg. peak area (AU) SD	BmACP knockdown (c) Avg. peak area (AU) SD	Ratio (%) B/A × 100	Student's t-test ^a	Fatty acyl compositions ^b
1	143 ± 8	50 ± 6	35.0	***	(C16:2, C16:2, C16:2)
1a	134 ± 3	57 ± 11	42.2	***	(C16:2, C16:2, C18:3)
2	211 ± 12	118 ± 21	55.6	***	(C16:2, C18:2, C16:2)
2a	941 ± 166	678 ± 155	72.0	*	(C16:1, C18:3, C18:3) and (C16:2, C18:2, C18:3)
3	1,622 ± 204	492 ± 62	30.3	***	(C16:2, C18:1, C16:2)
3a	2,022 ± 318	1,691 ± 270	80.1	*	(C16:2, C18:1, C18:3)
4	2,169 ± 296	1,550 ± 329	71.5	**	(C16:2, C18:1, C16:1) and/or (C16:1, C18:1, C16:2)
4a	1,831 ± 318	1,333 ± 270	72.8	*	(C16:1, C18:1, C18:3), (C16:1, C18:2, C18:2), and (C16:2, C18:1, C18:2)
5	2,140 ± 248	1,638 ± 399	76.5	*	(C16:2, C18:1, C18:1) and/or (C18:1, C18:1, C16:2)
5a	689 ± 67	595 ± 116	86.4	NS	(C18:1, C18:1, C18:3) and (C18:1, C18:2, C18:2)
6	624 ± 72	552 ± 42	88.5	NS	(C16:1, C18:1, C18:1) and/or (C18:1, C18:1, C16:1)
6a	301 ± 49	221 ± 45	73.3	NS	(C18:1, C18:1, C18:2)

C16:1, Δ 11-hexadecenoate; C16:2, Δ 10,12-hexadecadienoate; C18:1, Δ 9-octadecenoate; C18:2, Δ 9,12-octadecadienoate; C18:3, Δ 9,12,15-octadecatrienoate. NS, not significant.

^aStatistical analysis of avg. peak area control samples vs. BmACP knockdown samples performed using Student's t-test (n = 5).

^bFatty acyl compositions of the TG(s) in each peak were identified with Fast Atom Bombardment MS and MS-MS analyses (Matsumoto et al., 2002).

*p < 0.05, **p < 0.01, ***p < 0.001.



DISCUSSION

We have developed a method to facilitate identification of the genes involved in bombykol biosynthesis, using RT-PCR expression analysis and RNAi-mediated *in vivo* gene silencing in conjunction with EST databases. In the current study, we identified eight EST clones that likely encode various proteins that play a role in bombykol production (Table 1; Figure 1). These eight EST clones include two clones that encode BmFATP and BmLsd1 (NRPG1860 and NRPG0891), two proteins that we have recently identified and shown to be functionally associated with LD dynamics during *B. mori* pheromonogenesis (Ohnishi et al., 2009, 2011). We have reported that BmFATP plays a role in stimulating the TAG synthesis required for LD accumulation via a process similar to the so-called vectorial acylation that couples the uptake of extracellular fatty acids with activation to CoA thioesters (Ohnishi et al., 2009). In contrast, BmLsd1 plays an essential role in the TAG lipolysis associated with bombykol biosynthesis via phosphorylation with activation of BmCaMKII by influx of extracellular Ca^{2+} (Ohnishi et al., 2011).

Of the eight clones identified in the current study, we further characterized the clone that encodes BmACP. ACP is a highly conserved 70–100-aa carrier of acyl intermediates during FAS (Byers and Gong, 2007). In yeast and mammals, ACP exists as a separate domain within a large multifunctional fatty acid synthase polypeptide (type I FAS), whereas it is a small monomeric protein in bacteria and plastids (type II FAS). Because many insect sex pheromones are synthesized *de novo* from acetyl-CoA via the conventional long chain FAS pathway within PG cells (Bjostad et al., 1987; Jurenka, 2003), identification of BmACP in the PG suggests that it plays a significant role in the early

steps of bombykol biosynthesis. Accordingly, RNAi-mediated gene silencing of BmACP *in vivo* resulted in a significant reduction in bombykol production, suggesting the functional relevance of BmACP in bombykol biosynthesis (Figure 5). In addition, RNAi treatment resulted in accumulation of noticeably smaller LDs in the PG (Figure 6), indicating that it plays an essential role in LD accumulation prior to eclosion. While similar results were observed when BmFATP gene expression was suppressed (Ohnishi et al., 2009), the analysis of TAG contents revealed a significant difference. BmACP suppression mainly reduced the TAGs containing the bombykol precursor fatty acid, whereas the BmFATP suppression mainly reduced the TAGs containing the essential C_{18} -fatty acids derived from diet (Figure 7). These results are consistent with the general properties of ACPs and strongly suggest that BmACP plays an essential role in the biosynthesis of the bombykol precursor palmitic acid via the canonical FAS pathway in PG cells during pheromonogenesis. These results also indicate that BmACP and BmFATP function cooperatively to populate the TAGs comprising the cytoplasmic LDs (Figure 8). In addition, our present results validate the methodological approach we have taken to mine EST databases for unidentified functional molecules that play a critical role in moth sex pheromone production.

ACKNOWLEDGMENTS

We thank Shinji Atsushima, Masaaki Kurihara, and Katsunori Ichinose for maintaining the *B. mori* colony. This work was supported by the Lipid Dynamics Research Program from RIKEN and the Targeted Proteins Research Program (TPRP) from the Ministry of Education, Culture, Sports, Science, and Technology of Japan.

REFERENCES

- Bjostad, L. B., Wolf, W. A., and Roelofs, W. L. (1987). "Pheromone biosynthesis in lepidopterans: desaturation and chain shortening," in *Pheromone Biochemistry*, eds G. D. Prestwich and G. J. Blomquist (Orlando, FL: Academic Press), 77–120.
- Byers, D. M., and Gong, H. (2007). Acyl carrier protein: structure-function relationships in a conserved multifunctional protein family. *Biochem. Cell Biol.* 85, 649–662.
- Chomczynski, P., and Sacchi, N. (1987). Single-step method of RNA isolation by acid guanidinium thiocyanate-phenol-chloroform extraction. *Anal. Biochem.* 162, 156–159.
- Fónagy, A., Matsumoto, S., Uchiyama, K., Orikasa, C., and Mitsui, T. (1992). Action of pheromone biosynthesis activating neuropeptide on pheromone glands of *Bombyx mori* and *Spodoptera litura*. *J. Pest Sci.* 17, 47–54.
- Fónagy, A., Yokoyama, N., and Matsumoto, S. (2001). Physiological status and change of cytoplasmic lipid droplets in the pheromone-producing cells of the silkworm, *Bombyx mori* (Lepidoptera, Bombycidae). *Arthropod Struct. Dev.* 30, 113–123.
- Fónagy, A., Yokoyama, N., Okano, K., Tatsuki, S., Maeda, S., and Matsumoto, S. (2000). Pheromone-producing cells in the silkworm, *Bombyx mori*: identification and their morphological changes in response to pheromonotropic stimuli. *J. Insect Physiol.* 46, 735–744.
- Hull, J. J., Lee, J. M., Kajigaya, R., and Matsumoto, S. (2009). *Bombyx mori* homologs of STIM1 and Orail are essential components of the signal transduction cascade that regulates sex pheromone production. *J. Biol. Chem.* 284, 31200–31213.
- Hull, J. J., Lee, J. M., and Matsumoto, S. (2010). Gq α -linked phospholipase C β 1 and phospholipase C γ are essential components of the pheromone biosynthesis activating neuropeptide (PBAN) signal transduction cascade. *Insect Mol. Biol.* 19, 553–566.
- Hull, J. J., Ohnishi, A., Moto, K., Kawasaki, Y., Kurata, R., Suzuki, M. G., and Matsumoto, S. (2004). Cloning and characterization of the pheromone biosynthesis activating neuropeptide receptor from the silkworm, *Bombyx mori*: Significance of the carboxyl terminus in receptor internalization. *J. Biol. Chem.* 279, 51500–51507.
- Jurenka, R. A. (2003). "Biochemistry of female moth sex pheromones," in *Insect Pheromone Biochemistry and Molecular Biology*, eds G. J. Blomquist and R. G. Vogt (Oxford: Elsevier Academic Press), 53–80.
- Kitamura, A., Nagasawa, H., Kataoka, H., Inoue, T., Matsumoto, S., Ando, T., and Suzuki, A. (1989). Amino acid sequence of pheromone-biosynthesis-activating neuropeptide (PBAN) of the silkworm, *Bombyx mori*. *Biochem. Biophys. Res. Commun.* 163, 520–526.
- Matsumoto, S., Fónagy, A., Yamamoto, M., Wang, F., Yokoyama, N., Esumi, Y., and Suzuki, Y. (2002). Chemical characterization of cytoplasmic lipid droplets in the pheromone-producing cells of the silkworm, *Bombyx mori*. *Insect Biochem. Mol. Biol.* 32, 1447–1455.
- Matsumoto, S., Hull, J. J., Ohnishi, A., Moto, K., and Fónagy, A. (2007). Molecular mechanisms underlying sex pheromone production in the silkworm, *Bombyx mori*: characterization of the molecular components involved in bombykol biosynthesis. *J. Insect Physiol.* 53, 752–759.
- Matsumoto, S., Kitamura, A., Nagasawa, H., Kataoka, H., Orikasa, C., Mitsui, T., and Suzuki, A. (1990). Functional diversity of a neurohormone produced by the subesophageal ganglion: molecular identity of melanization and reddish coloration hormone and pheromone biosynthesis activating neuropeptide. *J. Insect Physiol.* 36, 427–432.
- Matsumoto, S., Ohnishi, A., Lee, J. M., and Hull, J. J. (2010). Unraveling the pheromone biosynthesis activating neuropeptide (PBAN) signal transduction cascade that regulates sex pheromone production in moths. *Vitam. Horm.* 83, 425–445.
- Matsumoto, S., Yoshiga, T., Yokoyama, N., Iwanaga, M., Koshiba, S., Kigawa, T., Hirota, H., Yokoyama, S., Okano, K., Mita, K., Shimada, T., and Tatsuki, S. (2001). Characterization of acyl-CoA-binding protein (ACBP) in the pheromone gland of the silkworm, *Bombyx mori*. *Insect Biochem. Mol. Biol.* 31, 603–609.
- Moto, K., Suzuki, M. G., Hull, J. J., Kurata, R., Takahashi, S., Yamamoto, M., Okano, K., Imai, K., Ando, T., and Matsumoto, S. (2004). Involvement of a bifunctional fatty-acyl desaturase in the biosynthesis of the silkworm, *Bombyx mori*, sex pheromone. *Proc. Natl. Acad. Sci. U.S.A.* 101, 8631–8636.
- Moto, K., Yoshiga, T., Yamamoto, M., Takahashi, S., Okano, K., Ando, T., Nakata, T., and Matsumoto, S. (2003). Pheromone gland-specific fatty-acyl reductase of the silkworm, *Bombyx mori*. *Proc. Natl. Acad. Sci. U.S.A.* 100, 9156–9161.
- Ohnishi, A., Hashimoto, K., Imai, K., and Matsumoto, S. (2009). Functional characterization of the *Bombyx mori* fatty acid transport protein (BmFATP) within the silkworm pheromone gland. *J. Biol. Chem.* 284, 5128–5136.
- Ohnishi, A., Hull, J. J., Kaji, M., Hashimoto, K., Lee, J. M., Tsuneizumi, K., Suzuki, K., Dohmae, N., and Matsumoto, S. (2011). Hormone signaling linked to silkworm sex pheromone biosynthesis involves Ca $^{2+}$ /calmodulin-dependent protein kinase II (CaMKII)-mediated phosphorylation of the insect PAT family protein *Bombyx mori* lipid storage droplet protein-1 (BmLsd1). *J. Biol. Chem.* 286, 24101–24112.
- Ohnishi, A., Hull, J. J., and Matsumoto, S. (2006). Targeted disruption of genes in the *Bombyx mori* sex pheromone biosynthetic pathway. *Proc. Natl. Acad. Sci. U.S.A.* 103, 4398–4403.
- Ozawa, R., and Matsumoto, S. (1996). Intracellular signal transduction of PBAN action in the silkworm, *Bombyx mori*: involvement of acyl CoA reductase. *Insect Biochem. Mol. Biol.* 26, 259–265.
- Percy, J. E., and Weatherston, J. (1974). "Gland structure and pheromone production in insects," in *Pheromones*, ed. M. C. Birch (Amsterdam: North-Holland Publishing Co.), 11–34.
- Rafaeli, A. (2002). Neuroendocrine control of pheromone biosynthesis in moths. *Int. Rev. Cytol.* 213, 49–91.
- Rafaeli, A. (2009). Pheromone biosynthesis activating neuropeptide (PBAN): regulatory role and mode of action. *Gen. Comp. Endocrinol.* 162, 69–78.
- Rafaeli, A., and Jurenka, R. A. (2003). "PBAN regulation of pheromone biosynthesis in female moths," in *Insect Pheromone Biochemistry and Molecular Biology*, eds G. J. Blomquist and R. G. Vogt (Oxford: Elsevier Academic Press), 107–136.
- Raina, A. K., Jaffe, H., Kempe, T. G., Keim, P., Blacher, R. W., Riley, C. T., Klun, J. A., Ridgway, R. L., and Hayes, D. K. (1989). Identification of a neuropeptide hormone that regulates sex pheromone production in female moths. *Science* 244, 769–798.
- Yoshiga, T., Okano, K., Mita, K., Shimada, T., and Matsumoto, S. (2000). cDNA cloning of acyl-CoA desaturase homologs in the silkworm, *Bombyx mori*. *Gene* 246, 339–345.

Conflict of Interest Statement: The authors declare that the research was conducted in the absence of any commercial or financial relationships that could be construed as a potential conflict of interest.

Received: 26 September 2011; accepted: 18 November 2011; published online: 07 December 2011.

Citation: Ohnishi A, Kaji M, Hashimoto K and Matsumoto S (2011) Screening for the genes involved in bombykol biosynthesis: identification and functional characterization of *Bombyx mori* acyl carrier protein. *Front. Endocrin.* 2:92. doi: 10.3389/fendo.2011.00092

This article was submitted to *Frontiers in Experimental Endocrinology*, a specialty of *Frontiers in Endocrinology*.

Copyright © 2011 Ohnishi, Kaji, Hashimoto and Matsumoto. This is an open-access article distributed under the terms of the Creative Commons Attribution Non Commercial License, which permits non-commercial use, distribution, and reproduction in other forums, provided the original authors and source are credited.



Construction of an *in vivo* system for functional analysis of the genes involved in sex pheromone production in the silkworm, *Bombyx mori*

Ken-ichi Moto* and Shogo Matsumoto

Molecular Entomology Laboratory, RIKEN Advanced Science Institute, Wako, Saitama, Japan

Edited by:

Joe Hull, USDA Agricultural Research Service, USA

Reviewed by:

Honoo Satake, Suntory Institute for Bioorganic Research, Japan
Maxwell Scott, North Carolina State University, USA
Yukio Ishikawa, The University of Tokyo, Japan

*Correspondence:

Ken-ichi Moto, Molecular Entomology Laboratory, RIKEN Advanced Science Institute, Hirosawa 2-1, Wako, Saitama 351-0198, Japan.
e-mail: kmoto@riken.jp

Moths produce species-specific sex pheromones to attract conspecific mates. The biochemical processes that comprise sex pheromone biosynthesis are precisely regulated and a number of gene products are involved in this biosynthesis and regulation. In recent years, at least 300 EST clones have been isolated from *Bombyx mori* pheromone gland (PG) specific cDNA libraries with some of those clones [i.e., *B. mori* PG-specific desaturase 1 (*Bmpgdesat1*), PG-specific fatty acyl reductase, PG-specific acyl-CoA-binding protein, *B. mori* fatty acid transport protein, *B. mori* lipid storage droplet protein-1] characterized and demonstrated to play a role in sex pheromone production. However, most of the EST clones have yet to be fully characterized and identified. To develop an efficient system for analyzing sex pheromone production-related genes, we investigated the feasibility of a novel gene analysis system using the upstream region of *Bmpgdesat1* that should contain a PG-specific gene promoter in conjunction with *piggyBac* vector-mediated germ line transformation. As a result, we have been able to obtain expression of our reporter gene (enhanced green fluorescent protein) in the PG but not in other tissues of transgenic *B. mori*. Current results indicate that we have successfully constructed a novel *in vivo* gene analysis system for sex pheromone production in *B. mori*.

Keywords: *Bombyx mori*, pheromone gland, EST analysis, *piggyBac*, germ line transformation

INTRODUCTION

Many species of moths (Insecta: Lepidoptera) produce and release sex pheromones, which are species-specific multi-component blends of semiochemicals, that attract conspecific mates (Tamaki, 1985). A major class of sex pheromones produced by these female moths has been characterized by the presence of straight chain C₁₀–C₁₈ unsaturated aliphatic compounds containing an oxygenated functional group such as alcohol, aldehyde, or acetate ester. These components are synthesized *de novo* in the pheromone-producing cells from acetyl-CoA through fatty acid synthesis, chain shortening, desaturation, and reductive modification of the carbonyl carbon (Tillman et al., 1999). In this biosynthetic pathway, various combinations of limited chain shortening and regio- and stereo-specific desaturation steps are involved in the production of large numbers of species-specific pheromone blends in Lepidoptera. Physiologically, moth sex pheromone biosynthesis is regulated by pheromone biosynthesis activating neuropeptide (PBAN), a 33-amino acid neuropeptide amidated at its C terminus that originates from the subesophageal ganglion (Raina and Menn, 1993).

In the silkworm *Bombyx mori*, the sex pheromone bombykol, (*E*, *Z*)-10,12-hexadecadien-1-ol, is synthesized during photophase starting from the day of eclosion in the single layered epidermal cells located beneath the endocuticle between the eighth and ninth abdominal segments (Ando et al., 1988; Fónagy et al., 2001). Bombykol is biosynthesized *de novo* from acetyl-CoA through palmitate, which is stepwise converted to bombykol by $\Delta 11$

desaturation, $\Delta 10$, 12 desaturation, and reduction (Ando et al., 1988).

The public *B. mori* EST databases constructed from 36 cDNA libraries prepared using various tissues contains 35,000 EST clones, which together yield more than 11,000 independent EST clones (Mita et al., 2003). At least 300 independent EST clones have been isolated from cDNA libraries of the pheromone gland (PG), and some of which have recently been characterized and shown to function in sex pheromone production. *B. mori* PG-specific desaturase 1 (*Bmpgdesat1*), initially referred to as *Desat1* but since renamed, is a fatty acyl-CoA desaturase involved in $\Delta 11$ desaturation and $\Delta 10$, 12 desaturation (Yoshiga et al., 2000; Moto et al., 2004). PG-specific fatty acyl reductase (*pgFAR*) is involved in the reduction step (Moto et al., 2003b). PG-specific acyl-CoA-binding protein (*pgACBP*) is involved in the incorporation of the pheromone precursor fatty acyl groups in the triacylglycerols that comprise the cytoplasmic lipid droplets (Matsumoto et al., 2001; Ohnishi et al., 2006), while *B. mori* fatty acid transport protein (*BmFATP*) plays a role in both triacylglycerol synthesis and lipid droplet accumulation throughout the uptake of extracellular fatty acids following activation to CoA thioesters in the pheromone-producing cells (Ohnishi et al., 2009). *B. mori* lipid storage droplet protein-1 (*BmLsd1*), which is a member of the PAT family of proteins, plays an essential role in triacylglycerol lipolysis in the pheromone-producing cells (Ohnishi et al., 2011). Despite these efforts, the potential role the vast number of EST clones have in sex pheromone production has yet to be clarified.

In *B. mori*, some experimental methods for gene analysis have been established. Transient gene transfer methods such as electroporation and baculovirus infection are powerful tools for gene promoter analysis because these methods are suitable for expressing a fluorescent protein as a reporter for a short period of time (Moto et al., 1999, 2003a; Shiomi et al., 2003, 2005). However, because these methods include potential negative effects due to electric damage or pathogenic damage due to viral infection, their suitability for characterizing target gene function is subject to question. On the other hand, germ line transformation methods using *piggyBac* transposase might be suitable for characterizing the function of target genes if the transgene product has no deleterious effect on the insect itself (Tamura et al., 2000). The combination of germ line transformation with tissue-specific or cell-specific gene promoters has the potential to provide exquisite experimental results (Thomas et al., 2002; Inoue et al., 2005; Yamagata et al., 2008). In this paper, we report on the isolation of a novel PG-specific gene promoter. In addition, we demonstrate the feasibility of a gene analysis system using this promoter in combination with the *piggyBac* transposon vector in *B. mori*, and show using an enhanced green fluorescent protein (EGFP) report that expression is specific to the PG of transgenic progeny.

MATERIALS AND METHODS

SILKMOTH STRAINS

Two *B. mori* strains were used in this study. The inbred strain p50 was used to amplify the upstream regions of *Bmpgdesat1* and *pgFAR* from genomic DNA via PCR. The pnd-w1 (RK) strain, which is a non-diapausing strain that has non-pigmented eggs and eyes, was used for germ line transformation. Larvae were reared on an artificial diet (Nihon Nosan, Japan) at 25°C under 16:8 (light:dark).

EST ANALYSIS

The public *B. mori* EST database (CYBERGATE)¹ was used in this study. To determine the number of EST clones categorized as *Bmpgdesat1*, *pgFAR*, and *pgACBP* in each cDNA library, we performed blastn analysis using the EST database and DNA sequences corresponding to the open reading frame (ORF) of the three genes.

¹http://150.26.71.213/cgi-bin/main_MX

CONSTRUCTION OF TRANSFER VECTORS

When the following *piggyBac* vectors were constructed all of the PCR experiments were conducted using KOD-*plus* DNA polymerase (Toyobo, Japan) and PTC Thermo cycler (MJ Research, USA). The nucleotide sequences of all PCR products were confirmed by DNA sequencing. For construction of pBac/3xP3-DsRed2/Ds1USR-EGFP, a 3,870-bp DNA fragment comprising the upstream region of *Bmpgdesat1* was amplified by PCR from *B. mori* genomic DNA with the oligonucleotide primer pair, ds1USR-F1 (5'-AAGGCGCGCCGTACAGCCTACCGCTTAGCG-3') and ds1USR-EGFP-R (5'-TGCTCACCATTCTTAGTAATTTAGATTTC-3'), **Figure 1**. A 997-bp DNA fragment comprising the EGFP ORF and SV40 terminator was also amplified by PCR from pEGFP-1 (Clontech, USA) with the oligonucleotide primer pair, ds1USR-EGFP-F (5'-AATTACTAAAATGGTGAGCAAGGGCGAGG-3') and SV40T-R (5'-AAGGCCGCGCCATACATTGATGAGTTTGG-3'). Primers ds1USR-EGFP-F and ds1USR-EGFP-R were partially complementary to each other and were designed to connect the 3' end of the above PCR product containing the upstream region sequence of *Bmpgdesat1* and the 5' end of the above PCR product containing the EGFP ORF and the SV40 terminator. These two primers were also designed to overlap the initiation codon of *Bmpgdesat1* and that of the EGFP ORF. To link these two DNA fragments, PCR amplification was performed with primers ds1USR-F and SV40T-R1 using the above two PCR products as templates. The resultant product was digested at the *AscI* site in the ds1USR-F primer and the *FseI* site in the SV40T-R1 primer and inserted into the corresponding site of a pBac (3xP3-DsRed2) transformation vector that carries inverted repeats of the *piggyBac* element for integration and the *Drosophila* red fluorescent protein (DsRed) gene under the control of an artificial eye-specific promoter (3xP3) as a selectable marker (**Figure 2A**). For construction of pBac/3xP3-DsRed2/pgFARUSR-EGFP, a 929-bp DNA fragment comprising the upstream region of *B. mori* *pgFAR* was amplified by PCR from *B. mori* genomic DNA with the oligonucleotide primer pair, pgFARUSR-F (5'-AAGGCGCGCCTCTCCATAAGCCTTACGAGG-3') and pgFARUSR-EGFP-R (5'-TGCTCACCATTCTTGGAGATTACGCGG-3'; **Figure 1**). A 997-bp DNA fragment comprising the EGFP ORF and the SV40 terminator was amplified by PCR from pEGFP-1 (Clontech, USA) with the oligonucleotide primer pair, pgFARUSR-EGFP-F (5'-AATCTCCAAGATGGTGAGCAAGGGCGAGG-3') and SV40T-R1.

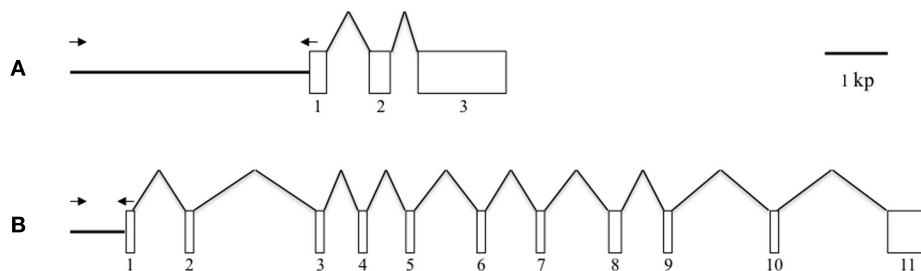


FIGURE 1 | Schematic representation of the gene structures of *Bmpgdesat1* and *pgFAR*. (A) *Bmpgdesat1*. (B) *pgFAR*. Exons and introns are indicated by boxes and broken lines connecting the exon boxes,

respectively. Arrows indicate the position and direction of primers used to amplify the upstream region of the genes in this study. Numbers denote the exon number.

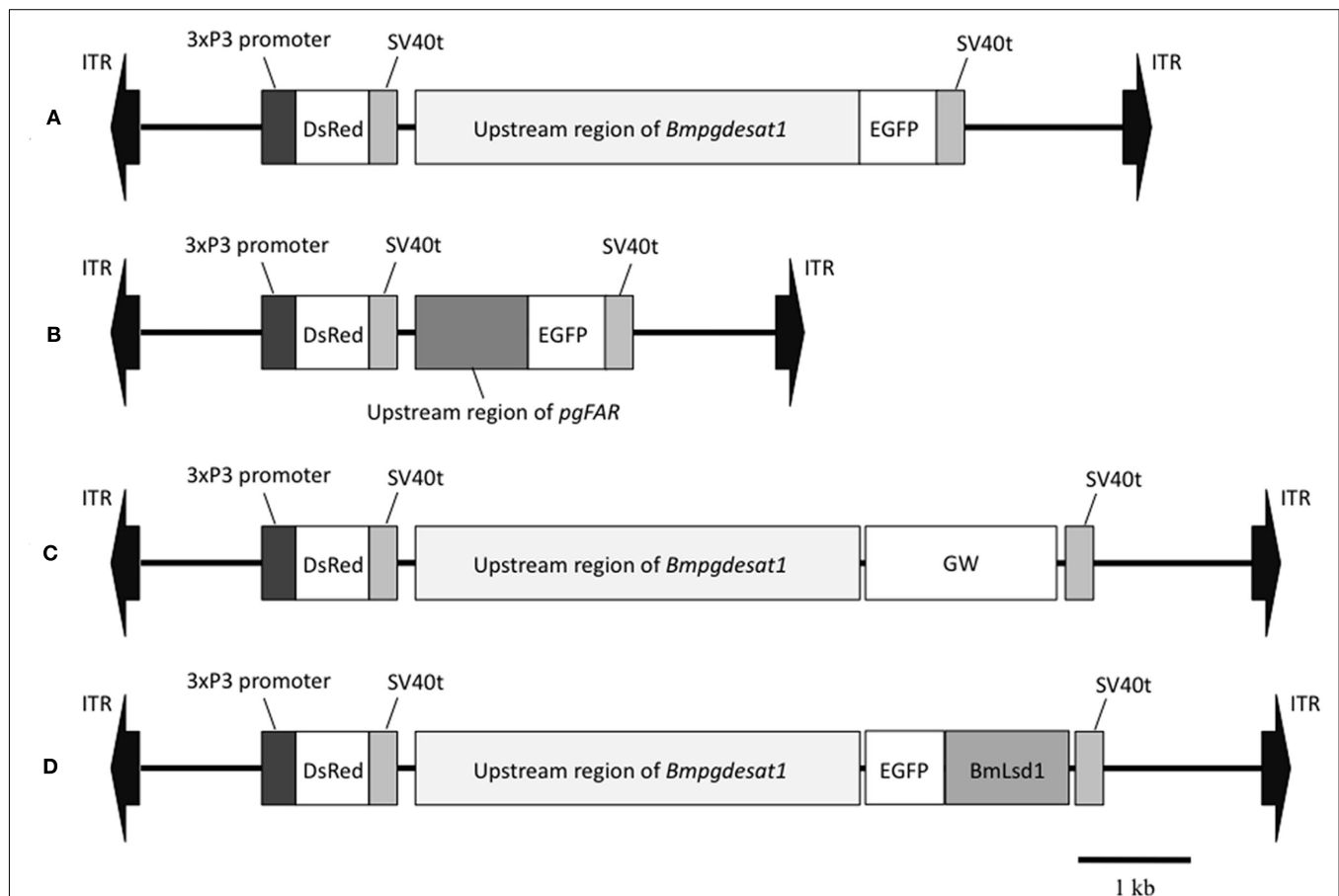


FIGURE 2 | Schematic representation of the *piggyBac* vectors used in this study. (A) pBac/3xP3-DsRed2/Ds1USR-EGFP. (B) pBac/3xP3-DsRed2/pgFARUSR-EGFP. (C) pBac/3xP3-DsRed2/Ds1USR-GW. (D) pBac/3xP3-DsRed2/Ds1USR-EGFP-BmLsd1. ITR, inverted terminal repeat of *piggyBac* transposon; DsRed, *Drosophila* red fluorescent protein; EGFP, enhanced green fluorescence protein coding region; SV40t, simian virus 40 terminator; GW, gateway recombination cassette.

Primers pgFARUSR-EGFP-F and pgFARUSR-EGFP-R were partially complementary to each other and were designed to connect the 3' end of the above PCR product containing the upstream region sequence of *pgFAR* and the 5' end of the above PCR product containing the EGFP ORF and the SV40 terminator. To link these two DNA fragments, PCR amplification was performed with primers pgFARUSR-F and SV40T-R1 using the above two PCR products as templates. The resultant product was digested at the *AscI* site in the pgFARUSR-F primer and the *FseI* site in the SV40T-R1 primer and inserted into the corresponding site of the pBac (3xP3-DsRed2) transformation vector (**Figure 2B**). For construction of pBac/3xP3-DsRed2/Ds1USR-GW, a 3,868-bp DNA fragment comprising the upstream region of *Bmpgdesat1* was amplified by PCR from *B. mori* genomic DNA with the oligonucleotide primer pair, ds1USR-F (5'-AAGGCGCGCCGTACAGCCTACCGCTTAGCG-3') and ds1USR-R (5'-TTACGCGTTTAGTAATTTAGATTTC-3'). The resultant product was digested at the *BssHII* site in the ds1USR-F primer and the *MluI* site in the ds1USR-R primer and inserted into the corresponding site of the pMCS5 cloning vector (MoBioTec, Germany). The resultant

plasmid was named pMCS5-Ds1USR. A 244-bp DNA fragment comprising the SV40 terminator was amplified by PCR from pEGFP-1 with the oligonucleotide primer pair, SV40T-F (5'-AAGCATGCGATCATAATCAGCCATACC-3') and SV40T-R2 (5'-AAAAGCTTACATACATTGATGAGTT-3'). The resultant product was digested at the *SphI* site in the SV40T-F2 primer and the *HindIII* site in the SV40T-R2 primer and inserted into the corresponding site of the plasmid pMCS5-Ds1USR. The resultant plasmid was named pMCS5-Ds1USR-SV40T. A 1730-bp DNA fragment comprising the Gateway recombination cassette was amplified by PCR from pYES-DEST52 (Invitrogen) with the oligonucleotide primer pair, GW-F (5'-AAAGATCTACAAGTTTGTACAAAAAAGC-3') and GW-R (5'-AAGGGCCACCCTTTGTACAAAGAAAGC-3'). The resultant product was digested at the *BglII* site in the GW-F primer and the *ApaI* site in the GW-R and inserted into the corresponding site of the plasmid pMCS5-Ds1USR-SV40T. The resultant plasmid was named pMCS5-Ds1USR-GW-SV40T. A 5,968-bp DNA fragment comprising the upstream region of *Bmpgdesat1*, the Gateway recombination cassette and the SV40 terminator was amplified from pMCS5-Ds1USR-GW-SV40T by PCR

with the oligonucleotide primer pair, ds1USR-F1 and SV40T-R1. The resultant product was digested at the *AscI* site in the pgFARUSR-F primer and the *FseI* site in the SV40T-R1 primer and inserted into the corresponding site of a pBac (3xP3-DsRed2) transformation vector (**Figure 2C**). For construction of pBac/3xP3-DsRed2/Ds1USR-EGFP-BmLsd1, a 745-bp DNA fragment comprising the EGFP ORF was amplified by PCR from pEGFP-1 with the oligonucleotide primer pair, CACC-EGFP-F (5'-AAAGATCTACAAGTTTGTACAAAAAAGC-3') and EGFP-A5-R (5'-AAGGGCCCACTTTGTACAAGAAAGC-3'). A 1,113-bp DNA fragment comprising the lipid storage droplet protein (BmLsd1) ORF was also amplified by PCR from EST clone NRPG0891, which contains the BmLsd1 ORF sequence and is derived from the NRPG cDNA library (**Table 1**; Mita et al., 2003), with the oligonucleotide primer pair, A5-BmLsd1-F (5'-GCAGCTGCAG CTGCAATGCC GAATCTTGAA-3') and BmLsd1-R (5'-TTAATTGACACCGTTAATGG-3'). The primers EGFP-A5-R and A5-BmLsd1-F were bridging primers and were designed to connect the 3' end of the above PCR fragment containing the BmLsd1 ORF sequence and the 5' end of the above PCR fragment containing the EGFP ORF sequence by the following PCR. To link these two DNA fragments, PCR amplification was performed with primers CACC-EGFP-F and BmLsd1-R using the above two PCR products as templates. The resultant product was cloned into pENTR/D-TOPO (Invitrogen) according to the manufacturer's instruction. Furthermore, this fusion protein ORF was cloned into the plasmid pBac/3xP3-DsRed2/Ds1USR-GW by *in vitro* recombination using LR Clonase (Invitrogen, **Figure 2D**).

INJECTION OF DNA INTO EMBRYOS

Plasmid DNAs for injection were purified using a Qiagen plasmid midi kit (Qiagen, Hilden, Germany) according to the manufacturer's instruction. A vector plasmid was co-injected with the helper plasmid pHA3PIG, which served as the of the *piggBac* transposase (Kanda and Tamura, 1991; Tamura et al., 2000). Vector and helper plasmid (each 200 ng/ μ l) were dissolved in distilled water and microinjected into eggs collected 3–6 after oviposition. The injected eggs represented generation 0 (G_0). After microinjection, the embryos were maintained at 25°C in a moist plastic case until hatching. The larvae were reared and G_0 adults were mated with the same family or recipient strain. The resulting generation 1 (G_1) progenies were screened for 3xP3 promoter-driven DsRed fluorescence in the stemma of their embryo. The DsRed-positive larvae G_1 were reared to adults and EGFP fluorescence was confirmed in the PG. Fluorescence was observed using a fluorescence microscope (Leica, MZ FL III) equipped with filter sets for DsRed and EGFP. Fluorescence imaging was obtained with an AxioCam HRC camera

(Carl Zeiss Microimaging GmbH) controlled by AxioVision Rel. 4.8 software (Carl Zeiss Microimaging GmbH).

CONFOCAL MICROSCOPY

Abdominal tips were dissected from female adults expressing the EGFP-BmLsd1 fusion protein and immersed in PBS. Under a dissecting microscope, the ovipositor portion of the abdominal tip was cut off and the resulting intersegmental membrane was spread open and trimmed by cleaning off all internal tissues attached (Fónagy et al., 2001). Fluorescence imaging was obtained with a Leica TCS NT confocal system using the 488-nm laser of an argon laser. Images were processed using Photoshop 6.0 (Adobe Systems, San Jose, CA, USA).

RESULTS

EST ANALYSIS

While more than 50 papers using transgenic *B. mori* have already been published, gene promoters related to PG-specific expression have yet to be reported. Based on Northern blot analysis, we previously reported that the genes, *Bmpgdesat1*, *pgACBP*, and *pgFAR*, are expressed predominantly in the PG and play essential roles in bombykol biosynthesis (Yoshiga et al., 2000; Matsumoto et al., 2001; Moto et al., 2003b, 2004). Consequently, we assumed that these three genes contain certain promoters for PG-specific expression. In the *B. mori* EST database (CYBERGATE)², there are >11,000 independent EST clones which have been generated from 36 cDNA libraries containing four PG cDNA libraries prepared by our group (**Table 1**; Mita et al., 2003). To investigate whether these three genes were expressed exclusively in the *B. mori* PG, we examined the relationship between these three genes and the number of the categorized EST clones in every cDNA library (**Table 2**). Although EST clones classified as *Bmpgdesat1* were present in our PG cDNA libraries as well as the famL cDNA library (prepared from antenna and Maxillary Galea of fifth instar larvae), the ratio of the EST clones of the famL cDNA library was significantly lower than that of the PG cDNA libraries. EST clones classified as *pgFAR* were likewise also present in the MFB cDNA library that was prepared from microbe-infected fat bodies of fifth instar larvae. However, as above, the ratio of the *pgFAR* EST clones in the MFB cDNA library was much lower compared to the PG cDNA libraries. Moreover, no EST clone classified as *pgFAR* was identified in the cDNA libraries prepared from non-infected fat bodies. In contrast to the other two genes, EST clones classified as *pgACBP* were present in various tissues. Compared with *Bmpgdesat1* and *pgFAR*, the ratio of the unexpected *pgACBP* EST clones was higher in other tissues. These results indicate that the gene promoters of *Bmpgdesat1* and *pgFAR* could be exploited for PG-specific expression of target genes of interest *in vivo*, but not that of *pgACBP*.

TRANSFORMATION EXPERIMENTS

Because the promoter regions of *Bmpgdesat1* and *pgFAR* have not been identified, we tried to obtain DNA sequence information for the upstream regions of these genes by using the Kaikoblast

Table 1 | List of the pheromone gland cDNA libraries in the *B. mori* EST database.

Library name	Strain	Type
pg	Shuko × ryuhaku	General cDNA library
P5PG	p50	General cDNA library
NRPG	p50	Normalized cDNA library
fphe	p50	Full-length cDNA library

²http://150.26.71.213/cgi-bin/main_MX

database³. The size of the defined upstream regions for *Bmpgdesat1* (GenBank accession numbers: AB693932) and *pgFAR* was 3,844 and 929-bp, respectively (Figure 1). To confirm whether the upstream regions contained PG-specific gene promoters, the corresponding DNA fragments were amplified by PCR using genomic DNA from the p50 strain with each fragment linked to the EGFP coding region and the SV40 terminator. Each expression cassette was then inserted into the cloning sites of a *piggyBac* vector, pBac (3xP3)-DsRed2 (Inoue et al., 2005). The resultant transformation vectors were named pBac/3xP3-DsRed2/Ds1USR-EGFP

and pBac/3xP3-DsRed2/pgFARUSR-EGFP (Figures 2A,B). These vectors were separately co-injected with a *piggyBac* transposase plasmid into pre-blastodermal eggs of *B. mori* pnd-w1 (RK) strain. Of the 686 eggs injected with the pBac/3xP3-DsRed2/Ds1USR|EGFP plasmid, 348 larvae survived to the first larval stage (Table 3). We recovered 114 females and 87 males. After sibling mating, five of the G₀ mating yielded progeny larvae with DsRed fluorescent eyes. The yield of mating in G₀ adults with transformed gametes was 5.3% (Table 3). Three lines of DsRed-positive G₁ females survived to adult. In two of these lines, EGFP fluorescence was detected in the PGs (Table 4; Figure 3), but not in other tissues (data not shown). We also confirmed that the *Bmpgdesat1* gene promoter did not drive

³<http://kaikoblast.dna.affrc.go.jp/>

Table 2 | The relationship between individual genes and the frequency of their identified EST clones amongst the cDNA libraries that comprise the *B. mori* EST database.

Library name	Organ tissue	Developmental stage	Total no. of EST clones in the library	No. of <i>Bmpgdesat1</i> EST clones (%)	No. of <i>pgFAR</i> EST clones (%)	No. of <i>pgACBP</i> EST clones (%)
pg	Pheromone gland	Newly eclosed adult	468	3 (0.6)	0 (0)	4 (0.85)
P5PG	Pheromone gland	Newly eclosed adult	811	10 (1.2)	3 (0.37)	9 (1.1)
NRPG	Pheromone gland	Newly eclosed adult	1,520	12 (0.8)	1 (0.064)	11 (0.72)
fphe	Pheromone gland	Newly eclosed adult	14,983	193 (1.3)	26 (0.17)	490 (3.3)
famL	Antenna + maxillary galea	Fifth-instar larva	25,972	2 (0.0077)	0 (0)	54 (0.21)
caL	Corpora allata	Fifth-instar larva	10,831	0 (0)	0 (0)	1 (0.0092)
fcaL	Corpora allata	Fifth-instar larva	33,462	0 (0)	0 (0)	58 (0.17)
fdpe	Diapause-destined embryos	12–40 h after oviposition	5,714	0 (0)	0 (0)	2 (0.035)
fe10	Embryo	100 h after fertilization	5,024	0 (0)	0 (0)	2 (0.040)
fe8d	Embryo	200 h after fertilization	17,551	0 (0)	0 (0)	21 (0.12)
fufe	Embryo	Unfertilized egg	17,095	0 (0)	0 (0)	66 (0.39)
ffbm	Fat body	Fifth-instar larva	9,843	0 (0)	0 (0)	32 (0.33)
MFBP	Microbe-infected fat body	Fifth-instar larva	5,846	0 (0)	1 (0.017)	6 (0.10)
fmvg	Maxillary galea	Fifth-instar larva	4,367	0 (0)	0 (0)	1 (0.023)
MSV3	Middle silk gland	Fifth-instar larva	4,829	0 (0)	0 (0)	3 (0.062)
msgV	Middle silk gland	Fifth-instar larva	632	0 (0)	0 (0)	1 (0.16)
fmgV	Midgut	Fifth-instar larva	38,020	0 (0)	0 (0)	23 (0.064)
fner	Nerve system + brain	Fifth-instar larva	37,074	0 (0)	0 (0)	32 (0.086)
ovS3	Ovary	Spinning stage	2,711	0 (0)	0 (0)	1 (0.037)
PSV3	Posterior silk gland	Fifth-instar larva	5,243	0 (0)	0 (0)	2 (0.038)
fprW	Prothoracic gland	Wandering stage	5,501	0 (0)	0 (0)	2 (0.036)
ftes	Testis	Fifth-instar larva	29,670	0 (0)	0 (0)	6 (0.020)
fwgP	Wing	Pupal stage	18,225	0 (0)	0 (0)	23 (0.13)
wdS2	Wing disk	Spinning stage	760	0 (0)	0 (0)	1 (0.13)
Total no.			296,152	220	31	853

Table 3 | Results of construct DNA injections into *pnd-w1* (RK) embryos.

Injected construct DNA	Number of injected embryos	Number of hatched embryos	Number of fertile moths		Number of total G ₁ broods	Number of DsRed-positive G ₁ broods
			Female	Male		
pBac/3xP3-DsRed2/Ds1USR-EGFP	686	348 (50.7%)	114	87	95	5 (5.3%)
pBac/3xP3-DsRed2/pgFARUSR-EGFP	803	276 (34.3%)	79	79	81	11 (13.6%)
pBac/3xP3-DsRed2/Ds1USR-EGFP-BmLsd1	522	122 (23.4%)	27	31	26	2 (7.7%)

Table 4 | Number of G₁ GFP-positive adults.

Lines	No. of DsRed-positive G ₁ larvae	No. of DsRed-positive moths		No. of GFP-positive Female
		Female	Male	
Ds1USR-EGFP no. 23	6	4	1	0
Ds1USR-EGFP no. 25	7	2	2	2
Ds1USR-EGFP no. 28	1	1	0	1
Ds1USR-EGFP no. 82	2	0	0	0
Ds1USR-EGFP no. 89	3	0	1	0
pgFARUSR-EGFP no. 5	1	0	0	0
pgFARUSR-EGFP no. 14	1	0	0	0
pgFARUSR-EGFP no. 19	5	0	2	0
pgFARUSR-EGFP no. 20	10	5	1	0
pgFARUSR-EGFP no. 23	1	1	0	0
pgFARUSR-EGFP no. 26	2	0	0	0
pgFARUSR-EGFP no. 29	2	1	0	0
pgFARUSR-EGFP no. 32	2	0	0	0
pgFARUSR-EGFP no. 45	4	2	1	0
pgFARUSR-EGFP no. 51	8	1	1	0
pgFARUSR-EGFP no. 52	3	0	0	0
Ds1USR-EGFP-BmLsd1 no. 2	5	2	1	2
Ds1USR-EGFP-BmLsd1 no. 8	2	1	0	0

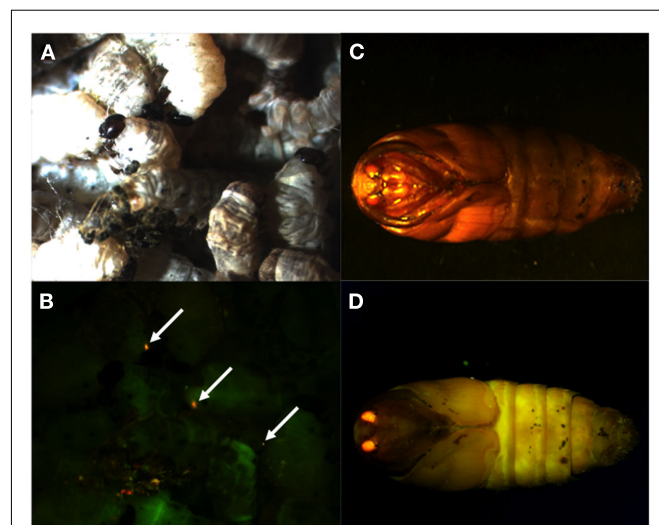


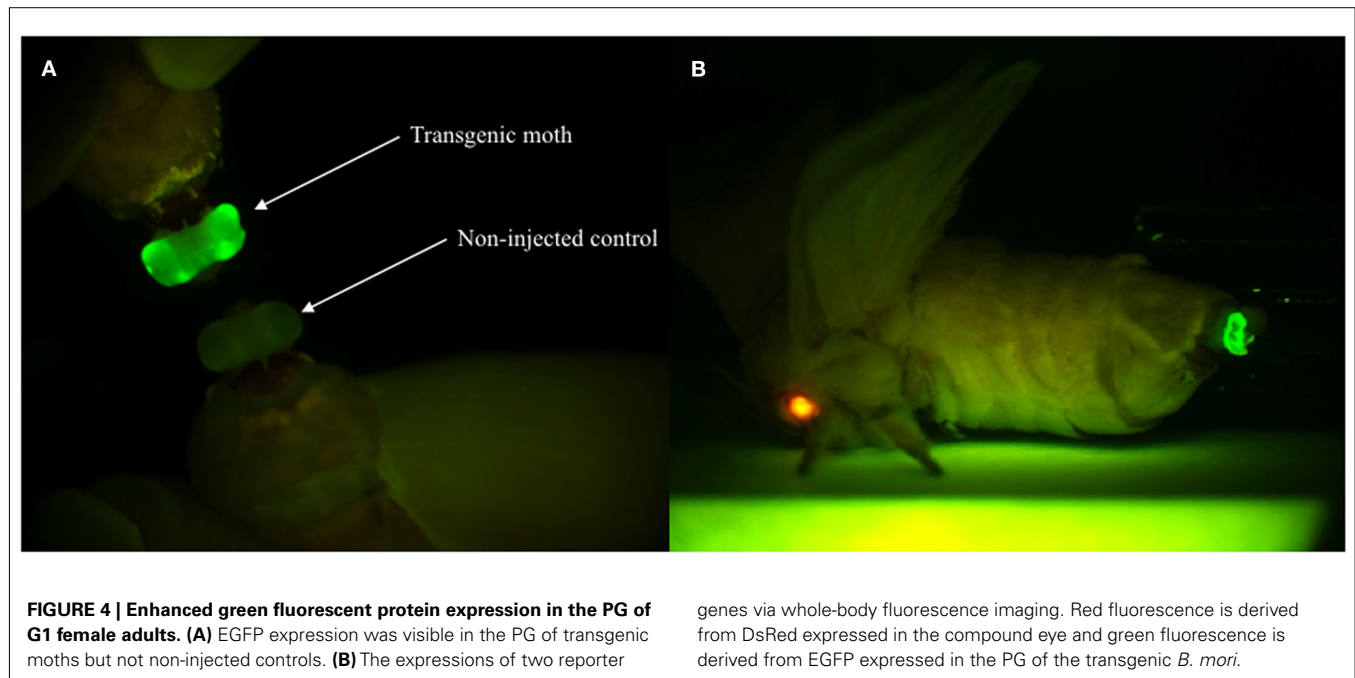
FIGURE 3 | DsRed expression in G₁ transgenic animals. DsRed expression was visible in the stemmata of larvae (**A,B**) and the compound eyes of pupa (**C,D**). (**A,C**) Bright-field images. (**B,D**) Fluorescence images. Arrows indicate DsRed expression in the stemmata.

expression in various tissues at different developmental stages (e.g., embryo, larvae, pupae, adult) for DsRed-positive G₂ females (data not shown). This result indicates that the PG-specific gene promoter resides within the 3,844-bp DNA sequence corresponding to the upstream region of *Bmpgdesat1*. Of the 803 eggs injected with the pBac/3xP3-DsRed2/pgFARUSR-EGFP plasmid,

348 larvae survived to the first larval stage (**Table 3**). We recovered 79 females and 79 males. After sibling mating, 11 of the G₀ mating yielded progeny larvae with DsRed fluorescent eyes. This yield was 13.6% (**Table 3**). Six lines of DsRed-positive G₁ females survived to adult. However, EGFP fluorescence was not detected in the PGs of all of the lines (**Table 4**). Because we confirmed that the EGFP reporter gene was specifically expressed in the PG of *B. mori* by using the above-mentioned 3,844-bp DNA sequence in conjunction with the conventional *piggyBac* transposon system, we next sought to construct a novel *piggyBac* vector pBac/3xP3-DsRed2/Ds1USR-GW containing the 3,844-bp DNA sequence and the Gateway recombination cassette (**Figure 2C**), which allows for various genes of interest to be fused to many reporters and tags through a simple and uniform procedure using the Gateway cloning technology (Walhout et al., 2000).

EXPRESSION AND LOCALIZATION OF AN EGFP FUSION PROTEIN

As an application of the gene transformation system in this study, we sought to investigate whether EGFP-tagged proteins responsible for sex pheromone production exhibit the expected sub-cellular localization pattern in the pheromone-producing cells of *B. mori*. NRPG0891 is one of the EST clones derived from the NRPG cDNA library (**Table 1** and **2**) and encodes a member of that PAT family of proteins known to localize to the surface of lipid droplets in Metazoan cells (Greenberg et al., 1991; Brasaemle et al., 1997; Heid et al., 1998; Wolins et al., 2001; Miura et al., 2002). This PAT family protein has recently been identified as BmLsd1 and shown to be involved in triacylglyceride lipolysis associated with sex pheromone production in *B. mori* (Ohnishi et al., 2011). Using immunocytochemistry, BmLsd1 was shown to localize to both the surface and core regions of lipid droplets, an inconsistency with the known localization pattern of mammalian PAT family proteins (Ohnishi et al., 2011). In the current study, we made a novel *piggyBac* vector pBac/3xP3-DsRed2/Ds1USR-EGFP-BmLsd1 to express EGFP-tagged BmLsd1 *in vivo* in the pheromone-producing cells of *B. mori* (**Figure 2D**). Of the 522 eggs injected with the pBac/3xP3-DsRed2/Ds1USR-EGFP-BmLsd1 plasmid, 122 larvae survived to the first larval stage (**Table 3**). We recovered 27 females and 31 males. After sibling mating, two of the G₀ matings yielded progeny larvae with DsRed eye fluorescence (**Table 3**). The yield of this mating was 7.7% (**Table 3**). Two lines of DsRed-positive G₁ females were maintained to adulthood. In one line, EGFP fluorescence was detected in the PGs (**Table 4**). After the abdominal tip was dissected from the EGFP-positive female and the ovipositor tip removed, the obtained intersegmental membrane was spread open and trimmed by cleaning all internal tissues attached to allow for confocal microscopic examination. The differential interference contrast image showed that lipid droplets were abundant in the pheromone-producing cells as described previously (**Figure 4**; Fónagy et al., 1999, 2001). The green fluorescence image showed that BmLsd1 was localized exclusively to the surface of the lipid droplets in the pheromone-producing cells of *B. mori* (**Figure 4**). This result is consistent with the localization of other PAT family proteins in Metazoa (Greenberg et al., 1991; Brasaemle et al., 1997; Heid et al., 1998; Wolins et al., 2001; Miura et al., 2002). While the reason for the discrepancy with



genes via whole-body fluorescence imaging. Red fluorescence is derived from DsRed expressed in the compound eye and green fluorescence is derived from EGFP expressed in the PG of the transgenic *B. mori*.

the immunocytochemistry results remains to be clarified, our present results on the specific localization of EGFP-tagged BmLsd1 strongly suggest that we can further apply this system, which uses a 3,844-bp DNA sequence corresponding to the upstream region of *Bmpgdesat1* and a fluorescence protein like EGFP in conjunction with the conventional *piggyBac*-mediated transposon system, for the functional identification of genes expressed in PG cells.

DISCUSSION

To date, at least 300 independent EST clones have been isolated from four different types of separately prepared *B. mori* PG cDNA libraries (Table 1). Using heterologous gene expression systems, a number of these genes have been characterized and their functional roles in bombykol production determined (Yoshiga et al., 2000, 2002; Matsumoto et al., 2001; Moto et al., 2003b, 2004; Hull et al., 2009, 2010); however, they have yet to be characterized *in vivo* in the PG of *B. mori* to unequivocally demonstrate their physiological functional significance. To address this issue, we sought to construct an *in vivo* system that could be utilized for functional analysis of genes involved in sex pheromone production in *B. mori*. In the current study, we successfully showed that genes of interest could be expressed specifically in the PG cells by utilizing the conventional *piggyBac* transposon system in conjunction with a 3,844-bp DNA sequence corresponding to the upstream region of *Bmpgdesat1*. Interestingly, EGFP expression was not observed in the line 23 carrying the Ds1USR-EGFP construct even though DsRed expression was present. We inferred that the absence of EGFP expression was due to the conventional chromosomal position effect as previously reported (Suzuki et al., 2005). On the other hand, we could not confirm the expression of the EGFP reporter gene in PG when we used the 929-bp DNA sequence corresponding to the upstream region of

pgFAR in this study. We were unable to adequately determine whether the PG-specific gene promoter is contained within the 929-bp DNA sequence corresponding to the upstream region of *pgFAR* because the number of the transgenic female moth examined in this study was too few. It is possible that the promoter region might not be contained in the fragment used in this study because the size of the fragment was too short or that the EGFP expression was not observed due to the chromosomal position effect.

Using this methodology with the 3,844-bp DNA sequence corresponding to the upstream region of *Bmpgdesat1*, we examined the *in vivo* localization of BmLsd1 in the pheromone-producing cells of *B. mori*. BmLsd1 is an insect PAT family protein associated with cytoplasmic lipid droplets and plays an essential role in bombykol biosynthesis via triacylglycerol lipolysis following Ca^{2+} /calmodulin-dependent protein kinase II phosphorylation (Ohnishi et al., 2011). In the previous study, BmLsd1 was shown using immunocytochemistry to localize to both the surface and core region of the lipid droplets (Ohnishi et al., 2011). In the current study, however, EGFP-tagged BmLsd1 localized specifically to the surface of the lipid droplets in PG cells, a distribution consistent with other general mammalian PAT family proteins (Figure 5; Greenberg et al., 1991; Brasaemle et al., 1997; Heid et al., 1998; Wolins et al., 2001; Miura et al., 2002). Consequently, the results suggest that the *piggyBac* transposon system used in the current study is more suitable than the traditional immunocytochemistry method to localize BmLsd1 in the pheromone-producing cells and thus help clarify the dynamics of pheromone production-related proteins *in vivo* in the living pheromone-producing cells of *B. mori*. For example, the dynamics of PBAN receptor and stromal interaction molecule 1 (i.e., STIM1), which have been shown in transient expression assays using fluorescent reporter-based chimeras in Sf9 cells to change their sub-cellular

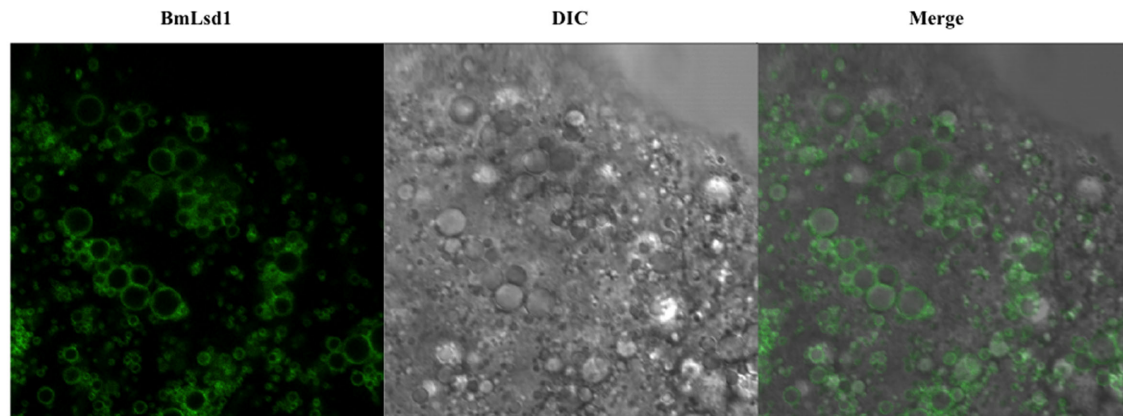


FIGURE 5 | Localization of BmLsd1 in the pheromone-producing cells of *B. mori*. Following dissection and trimming of the PG, pheromone-producing cells were analyzed by confocal microscopy. EGFP-BmLsd1 fluorescence image (BmLsd1), differential interference contrast image (DIC), and the merged image (merge) are shown.

localization in response to PBAN stimulation (Hull et al., 2004, 2005, 2009, 2010), could be clearly demonstrated *in vivo* in *B. mori* PGs.

Double-stranded RNA-mediated interference (RNAi) was originally applied in *Caenorhabditis elegans* and has been developed as a powerful tool for gene silencing in a range of organisms (Fire et al., 1998; Hannon, 2002; Agrawal et al., 2003). In *B. mori*, injection of dsRNAs for target genes provided unequivocal demonstrations for the roles of *Bmpgdesat1*, *pgFAR*, *pgACBP*, and *PBANR* in sex pheromone production (Ohnishi et al., 2006). This simple *in vivo* system using developing *B. mori* could also be applied to elucidating the molecular mechanisms underlying sex pheromone production in other Lepidoptera if DNA sequences of target genes are available. However, some genes related to sex pheromone production could be expressed in tissues other than PG (Matsumoto et al., 2001; Yoshiga et al., 2002; Ohnishi et al., 2009, 2011). In addition, because the insect circulatory system is an open system where hemolymph flows freely inside the body cavity, injection of target gene dsRNAs into the hemolymph might have unfavorable knockdown effects on tissues other than the PG. To prevent such side effects, our PG-specific gene expression system could be adapted as a novel *in vivo* PG-specific RNAi system that specifically expresses PG restricted dsRNAs for the target gene.

Sex pheromone production in *B. mori* is regulated by PBAN, which is released into the hemolymph after eclosion and acts directly on the PG to stimulate bombykol biosynthesis (Fónagy et al., 1992; Matsumoto et al., 2009). In contrast, transcriptional levels of the three pheromone production-related genes, *Bmpgdesat1*, *pgFAR*, and *pgACBP*, which are expressed predominantly in the PG, are synchronously up-regulated on the day prior to eclosion, indicating that transcription of these genes is regulated by factors other than PBAN (Yoshiga et al., 2000; Matsumoto et al., 2001; Moto et al., 2003b). It has been demonstrated that β -D-glucosyl-O-L-tyrosine, a humoral factor that appears in the pupal hemolymph 1 day prior to eclosion, regulates

pgACBP transcription (Ohnishi et al., 2005). Surprisingly, while β -D-glucosyl-O-L-tyrosine titers rise dramatically prior to eclosion and reach the maximum level on the day preceding eclosion, this factor had no effect on the transcription of *pgFAR* and *Bmpgdesat1*, indicating that the transcriptional mechanism of *pgACBP* is different from that of *pgFAR* and *Bmpgdesat1* (Matsumoto et al., 2010). The results of EST analysis in this study also suggest this discrepancy because almost all of the EST clones classified as *Bmpgdesat1* and *pgFAR* are obtained from the PG, whereas *pgACBP* EST clones are present in various tissues (Table 2). In this study, PG-specific expression of an EGFP reporter gene was observed when using a 3,844-bp DNA sequence corresponding to the upstream region of *Bmpgdesat1* but not the 929-bp DNA sequence corresponding to that of *pgFAR*, indicating that the 3,844-bp DNA sequence contains a transcriptional element involved in PG-specific gene expression. Further studies are needed to investigate the broader region surrounding *pgFAR* to identify the transcription element involved in the PG-specific expression of *pgFAR* (Figure 4). Consequently, it has yet to be determined whether the transcriptional mechanisms of the two respective genes are the same or not. It is possible that the transcriptional element in the 3,844-bp DNA sequence is novel as database searches failed to identify a transcriptional element. Therefore, further gene promoter analysis of *Bmpgdesat1* may define the novel transcriptional element and clarify a novel molecular mechanism of sex pheromone production apart from the PBAN signal transduction cascade.

ACKNOWLEDGMENTS

We thank Dr. Toshiki Tamura, Dr. Tishio Kanda, Dr. Hideki Sezutsu, Dr. Keiro Uchino, Dr. Masataka Suzuki, Masaaki Kurihara, Satoko Yasuda, and Kana Hashimoto for help with the preparation of transgenic animals. This research was supported by the Bioarchitect Research Program and Ministry of Education, Culture, Sports, Science and Technology of Japan grants-in-aid for Scientific Research (C) (20580058).

REFERENCES

- Agrawal, N., Dasaradhi, P. V., Mohammed, A., Malhotra, P., Bhatnagar, R. K., and Mukherjee, S. K. (2003). RNA interference: biology, mechanism, and applications. *Microbiol. Mol. Biol. Rev.* 67, 657–685.
- Ando, T., Hase, R., Funayoshi, A., Arima, R., and Uchiyama, M. (1988). Sex pheromone biosynthesis from C14-hexadecanoic acid in the silkworm moth. *Agric. Biol. Chem.* 52, 141–147.
- Brasaemle, D. L., Barber, T., Wolins, N. E., Serrero, G., Blanchette-Mackie, E. J., and Londos, C. (1997). Adipose differentiation-related protein is a ubiquitously expressed lipid storage droplet-associated protein. *J. Lipid Res.* 38, 2249–2263.
- Fire, A., Xu, S., Montgomery, M. K., Kostas, S. A., Driver, S. E., and Mello, C. C. (1998). Potent and specific genetic interference by double-stranded RNA in *Caenorhabditis elegans*. *Nature* 391, 806–811.
- Fónagy, A., Matsumoto, S., Uchiyama, K., Orisaka, C., and Mitsui, T. (1992). Action of pheromone biosynthesis activating neuropeptide on pheromone glands of *Bombyx mori* and *Spodoptera litura*. *J. Pest. Sci.* 17, 47–54.
- Fónagy, A., Yokoyama, N., and Matsumoto, S. (2001). Physiological status and change of cytoplasmic lipid droplets in the pheromone-producing cells of the silkworm, *Bombyx mori* (Lepidoptera, Bombycidae). *Arthropod. Struct. Dev.* 30, 113–123.
- Fónagy, A., Yokoyama, N., Okano, K., Tatsuki, S., Maeda, S., and Matsumoto, S. (1999). Pheromone-producing cells in the silkworm, *Bombyx mori*: identification and their morphological changes in response to pheromonotropic stimuli. *J. Insect Physiol.* 46, 735–744.
- Greenberg, A. S., Egan, J. J., Wek, S. A., Garty, N. B., Blanchette-Mackie, E. J., and Londos, C. (1991). Perilipin, a major hormonally regulated adipocyte-specific phosphoprotein associated with the periphery of lipid storage droplets. *J. Biol. Chem.* 266, 11341–11346.
- Hannon, G. J. (2002). RNA interference. *Nature* 418, 244–251.
- Heid, H. W., Moll, R., Schwetlick, I., Rackwitz, H. R., and Keenan, T. W. (1998). Adipophilin is a specific marker of lipid accumulation in diverse cell types and diseases. *Cell Tissue Res.* 294, 309–321.
- Hull, J. J., Lee, J. M., Kajigaya, R., and Matsumoto, S. (2009). *Bombyx mori* homologs of STIM1 and Orail are essential components of the signal transduction cascade that regulates sex pheromone. *J. Biol. Chem.* 284, 31200–31213.
- Hull, J. J., Lee, J. M., and Matsumoto, S. (2010). Functional role of STIM1 and Orail in silkworm (*Bombyx mori*) sex pheromone production. *Commun. Integr. Biol.* 3, 240–242.
- Hull, J. J., Ohnishi, A., and Matsumoto, S. (2005). Regulatory mechanisms underlying pheromone biosynthesis activating neuropeptide (PBAN)-induced internalization of the *Bombyx mori* PBAN receptor. *Biochem. Biophys. Res. Commun.* 334, 69–78.
- Hull, J. J., Ohnishi, A., Moto, K., Kawasaki, Y., Kurata, R., Suzuki, M. G., and Matsumoto, S. (2004). Cloning and characterization of the pheromone biosynthesis activating neuropeptide receptor from the silkworm, *Bombyx mori*. Significance of the carboxyl terminus in receptor internalization. *J. Biol. Chem.* 279, 51500–51507.
- Inoue, S., Kanda, T., Imamura, M., Quan, G. X., Kojima, K., Tanaka, H., Tomita, M., Hino, R., Yoshizato, K., Mizuno, S., and Tamura, T. (2005). A fibroin secretion-deficient silkworm mutant, Nd-sD, provides an efficient system for producing recombinant proteins. *Insect Biochem. Mol. Biol.* 35, 51–59.
- Kanda, T., and Tamura, T. (1991). Microinjection method for DNA in early embryos of the silkworm, *Bombyx mori*, using air pressure. *Bull. Natl. Inst. Seric. Entomol. Sci.* 2, 31–46.
- Matsumoto, S., Hull, J. J., and Ohnishi, A. (2009). Molecular mechanisms underlying PBAN signaling in the silkworm *Bombyx mori*. *Ann. N. Y. Acad. Sci.* 1163, 464–468.
- Matsumoto, S., Ohnishi, A., Lee, J. M., and Hull, J. J. (2010). Unraveling the pheromone biosynthesis activating neuropeptide (PBAN) signal transduction cascade that regulates sex pheromone production in moths. *Vitam. Horm.* 83, 425–445.
- Matsumoto, S., Yoshiga, T., Yokoyama, N., Iwanaga, M., Koshihara, S., Kigawa, T., Hirota, H., Yokoyama, S., Okano, K., Mita, K., Shimada, T., and Tatsuki, S. (2001). Characterization of acyl-CoA-binding protein (ACBP) in the pheromone gland of the silkworm, *Bombyx mori*. *Insect Biochem. Mol. Biol.* 31, 603–609.
- Mita, K., Morimyo, M., Okano, K., Koike, Y., Nohata, J., Kawasaki, H., Kadono-Okuda, K., Yamamoto, K., Suzuki, M. G., Shimada, T., Goldsmith, M. R., and Maeda, S. (2003). The construction of an EST database for *Bombyx mori* and its application. *Proc. Natl. Acad. Sci. U.S.A.* 100, 14121–14126.
- Miura, S., Gan, J. W., Brzostowski, J., Parisi, M. J., Schultz, C. J., Londos, C., Oliver, B., and Kimmel, A. R. (2002). Functional conservation for lipid storage droplet association among perilipin, ADRP, and TIP47 (PAT)-related proteins in mammals, *Drosophila*, and *Dictyostelium*. *J. Biol. Chem.* 277, 32253–32257.
- Moto, K., Abdel Salam, S. E., Sakurai, S., and Iwami, M. (1999). Gene transfer into insect brain and cell-specific expression of bombyxin gene. *Dev. Genes Evol.* 209, 447–450.
- Moto, K., Kojima, H., Kurihara, M., Iwami, M., and Matsumoto, S. (2003a). Cell-specific expression of enhanced green fluorescence protein under the control of neuropeptide gene promoters in the brain of the silkworm, *Bombyx mori*, using *Bombyx mori* nucleopolyhedrovirus-derived vectors. *Insect Biochem. Mol. Biol.* 33, 7–12.
- Moto, K., Yoshiga, T., Yamamoto, M., Takahashi, S., Okano, K., Ando, T., Nakata, T., and Matsumoto, S. (2003b). Pheromone gland-specific fatty-acyl reductase of the silkworm, *Bombyx mori*. *Proc. Natl. Acad. Sci. U.S.A.* 100, 9156–9161.
- Moto, K., Suzuki, M. G., Hull, J. J., Kurata, R., Takahashi, S., Yamamoto, M., Okano, K., Imai, K., Ando, T., and Matsumoto, S. (2004). Involvement of a bifunctional fatty-acyl desaturase in the biosynthesis of the silkworm, *Bombyx mori*, sex pheromone. *Proc. Natl. Acad. Sci. U.S.A.* 101, 8631–8636.
- Ohnishi, A., Hashimoto, K., Imai, K., and Matsumoto, S. (2009). Functional characterization of the *Bombyx mori* fatty acid transport protein (BmFATP) within the silkworm pheromone gland. *J. Biol. Chem.* 284, 5128–5136.
- Ohnishi, A., Hull, J. J., Kaji, M., Hashimoto, K., Lee, J. M., Tsuneizumi, K., Suzuki, T., Dohmae, N., and Matsumoto, S. (2011). Hormone signaling linked to silkworm sex pheromone biosynthesis involves Ca²⁺/calmodulin-dependent protein kinase II-mediated phosphorylation of the insect PAT family protein *Bombyx mori* lipid storage droplet protein-1 (BmLsd1). *J. Biol. Chem.* 286, 24101–24112.
- Ohnishi, A., Hull, J. J., and Matsumoto, S. (2006). Targeted disruption of genes in the *Bombyx mori* sex pheromone biosynthetic pathway. *Proc. Natl. Acad. Sci. U.S.A.* 103, 4398–4403.
- Ohnishi, A., Koshino, H., Takahashi, S., Esumi, Y., and Matsumoto, S. (2005). Isolation and characterization of a humoral factor that stimulates transcription of the acyl-CoA-binding protein in the pheromone gland of the silkworm, *Bombyx mori*. *J. Biol. Chem.* 280, 4111–4116.
- Raina, A. K., and Menn, J. J. (1993). Pheromone biosynthesis activating neuropeptide: from discovery to current status. *Arch. Insect Biochem. Physiol.* 22, 141–151.
- Shiomi, K., Fujiwara, Y., Atsumi, T., Kajiura, Z., Nakagaki, M., Tanaka, Y., Mizoguchi, A., Yaginuma, T., and Yamashita, O. (2005). Myocyte enhancer factor 2 (MEF2) is a key modulator of the expression of the prothoracicotropic hormone gene in the silkworm, *Bombyx mori*. *FEBS J.* 272, 3853–3862.
- Shiomi, K., Kajiura, Z., Nakagaki, M., and Yamashita, O. (2003). Baculovirus-mediated efficient gene transfer into the central nervous system of the silkworm, *Bombyx mori*. *J. Insect Biotechnol. Sericol.* 72, 149–155.
- Suzuki, M. G., Funaguma, S., Kanda, T., Tamura, T., and Shimada, T. (2005). Role of the male BmDSX protein in the sexual differentiation of *Bombyx mori*. *Evol. Dev.* 7, 58–68.
- Tamaki, Y. (1985). “Sex pheromones,” in *Comprehensive Insect Physiology, Biochemistry, and Pharmacology*, eds G. A. Kerkut and L. I. Gilbert (New York: Pergamon), 9, 145–191.
- Tamura, T., Thibert, C., Royer, C., Kanda, T., Abraham, E., Kamba, M., Komoto, N., Thomas, J. L., Mauchamp, B., Chavancy, G., Shirk, P., Fraser, M., Prudhomme, J. C., and Couble, P. (2000). Germline transformation of the silkworm *Bombyx mori* L. using a piggy-Bac transposon-derived vector. *Nat. Biotechnol.* 18, 81–84.
- Thomas, J. L., Da Rocha, M., Besse, A., Mauchamp, B., and Chavancy, G. (2002). 3xP3-EGFP marker facilitates screening for transgenic silkworm *Bombyx mori* L. from the embryonic stage onwards. *Insect Biochem. Mol. Biol.* 32, 247–253.
- Tillman, J. A., Seybold, S. J., Jurenka, R. A., and Blomquist, G. J. (1999). Insect pheromones – an overview of biosynthesis and endocrine

- regulation. *Insect Biochem. Mol. Biol.* 29, 481–514.
- Walhout, A. J., Temple, G. F., Brasch, M. A., Hartley, J. L., Lorson, M. A., van, den, Heuvel, S., and Vidal, M. (2000). GATEWAY recombinational cloning: application to the cloning of large numbers of open reading frames or ORFeomes. *Meth. Enzymol.* 328, 575–592.
- Wolins, N. E., Rubin, B., and Brasaemle, D. L. (2001). TIP47 associates with lipid droplets. *J. Biol. Chem.* 276, 5101–5108.
- Yamagata, T., Sakurai, T., Uchino, K., Sezutsu, H., Tamura, T., and Kanzaki, R. (2008). GFP labeling of neurosecretory cells with the GAL4/UAS system in the silkworm brain enables selective intracellular staining of neurons. *Zool. Sci.* 25, 509–516.
- Yoshiga, T., Okano, K., Mita, K., Shimada, T., and Matsumoto, S. (2000). cDNA cloning of acyl-CoA desaturase homologs in the silkworm, *Bombyx mori*. *Gene* 246, 339–345.
- Yoshiga, T., Yokoyama, N., Imai, N., Ohnishi, A., Moto, K., and Matsumoto, S. (2002). cDNA cloning of calcineurin heterosubunits from the pheromone gland of the silkworm, *Bombyx mori*. *Insect Biochem. Mol. Biol.* 32, 477–486.
- Conflict of Interest Statement:** The authors declare that the research was conducted in the absence of any commercial or financial relationships that could be construed as a potential conflict of interest.
- Received: 07 December 2011; accepted: 08 February 2012; published online: 27 February 2012.
- Citation: Moto K-I and Matsumoto S (2012) Construction of an *in vivo* system for functional analysis of the genes involved in sex pheromone production in the silkworm, *Bombyx mori*. *Front. Endocrin.* 3:30. doi: 10.3389/fendo.2012.00030
- This article was submitted to *Frontiers in Experimental Endocrinology*, a specialty of *Frontiers in Endocrinology*.
- Copyright © 2012 Moto and Matsumoto. This is an open-access article distributed under the terms of the Creative Commons Attribution Non Commercial License, which permits non-commercial use, distribution, and reproduction in other forums, provided the original authors and source are credited.



Biosynthetic pathway for sex pheromone components produced in a Plusiinae moth, *Plusia festucae*

Hayaki Watanabe, Aya Matsui, Sin-ichi Inomata, Masanobu Yamamoto and Tetsu Ando*

Graduate School of Bio-Applications and Systems Engineering, Tokyo University of Agriculture and Technology, Koganei, Tokyo, Japan

Edited by:

Shogo Matsumoto, Advanced Science Institute – RIKEN, Japan

Reviewed by:

Shogo Matsumoto, Advanced Science Institute – RIKEN, Japan
Russell Jurenka, Iowa State University, USA

*Correspondence:

Tetsu Ando, Graduate School of Bio-Applications and Systems Engineering, Tokyo University of Agriculture and Technology, Koganei, Tokyo 184-8588, Japan.
e-mail: antetsu@cc.tuat.ac.jp

While many Plusiinae species commonly secrete (Z)-7-dodecenyl acetate (Z7-12:OAc) as a key pheromone component, female moths of the rice looper (*Plusia festucae*) exceptionally utilize (Z)-5-dodecenyl acetate (Z5-12:OAc) to communicate with their partners. GC-MS analysis of methyl esters derived from fatty acids included in the pheromone gland of *P. festucae* showed a series of esters monounsaturated at the ω 7-position, i.e., (Z)-5-dodecenoate, (Z)-7-tetradecenoate, (Z)-9-hexadecenoate (Z9-16:Me), and (Z)-11-octadecenoate (Z11-18:Me). By topical application of D₃-labeled palmitic acid (16:Acid) and stearic acid (18:Acid) to the pheromone glands, similar amounts of D₃-Z5-12:OAc were detected. The glands treated with D₁₃-labeled monoenoic acids (Z9-16:Acid and Z11-18:Acid), which were custom-made by utilizing an acetylene coupling reaction with D₁₃-1-bromohexane, also produced similar amounts of D₁₃-Z5-12:OAc. These results suggested that Z5-12:OAc was biosynthesized by ω 7-desaturase with low substrate specificity, which could introduce a double bond at the 9-position of a 16:Acid derivative and the 11-position of an 18:Acid derivative. Additional experiments with the glands pretreated with an inhibitor of chain elongation supported this speculation. Furthermore, a comparative study with another Plusiinae species (*Chrysodeixis eriosoma*) secreting Z7-12:OAc indicated that the β -oxidation systems of *P. festucae* and *C. eriosoma* were different.

Keywords: pheromone biosynthesis, Lepidoptera, Noctuidae, incorporation of deuterated precursors, ω 7-desaturation, monoenyl fatty acid

INTRODUCTION

About 160,000 lepidopteran species are known world wide, and each species is believed to establish a species-specific mating communication system for species conservation. Not only nocturnal moths but also diurnal moths utilize special sex pheromones as a chemical cue. Lepidopteran sex pheromones have been identified from more than 600 moth species and about three-quarters of them are composed of C₁₀–C₁₈ unsaturated fatty alcohols, their acetates, and aldehyde derivatives, including one, two, or three C=C bonds (Type I pheromones; Ando et al., 2004; Ando, 2011; El-Sayed, 2011). These components are biosynthesized from saturated fatty acyl intermediates, into which double bonds are introduced at definite positions by desaturases working in a pheromone gland (Jurenka, 2004). The double bonds locate at various positions, i.e., from the terminal methyl group to the next carbon to the functional group. In addition to the different chain lengths and kinds of terminal functional groups, the chemical structural varieties are attributed to the different positions of the double bonds (Ando et al., 2004).

Plusiinae is a well-assembled subfamily in Noctuidae, which is the biggest family in Lepidoptera, and includes many pest species secreting Type I pheromones. Since a pioneering study on the chemical communication of the cabbage looper, *Trichoplusia ni* (Berger, 1966), sex pheromones have been identified from 22 Plusiinae species (Ando, 2011; El-Sayed, 2011). Most of them secrete (Z)-7-dodecenyl acetate (Z7-12:OAc) as a main pheromone component and blend some structurally related

compounds to make species-specific pheromones, suggesting that a primitive species in Plusiinae utilized Z7-12:OAc and speciated to many existing species while establishing the ability to produce new pheromone components. Z7-12:OAc is biosynthesized via Δ 11-desaturation of a saturated C₁₆ acyl compound (16:Acyl), probably a CoA-derivative of palmitic acid (16:Acid; Bjostad and Roelofs, 1983), and this key step has been confirmed by identification of the gene encoding Δ 11-desaturase from *T. ni* (Knipple et al., 1998). The Δ 11-desaturation is an important biosynthetic step because β -oxidation of the produced (Z)-11-hexadecenyl intermediate in different degrees yields a series of monoenyl compounds unsaturated at the ω 5-position, such as (Z)-9-tetradecenyl acetate (Z9-14:OAc) and (Z)-5-decenyl acetate (Z5-10:OAc). Among the Plusiinae species, Z9-14:OAc is secreted by *Macdunnoughia confusa*, and Z5-10:OAc is secreted by *Anadevidia peponis* as a minor pheromone component (Inomata et al., 2000).

On the other hand, the sex pheromone of the rice looper, *Plusia festucae*, is composed of (Z)-5-dodecenyl acetate (Z5-12:OAc) as a main component and (Z)-7-tetradecenyl acetate (Z7-14:OAc) as a minor component (Ando et al., 1995). Both components include a double bond at the ω 7-position, and the female moths produced no pheromone components unsaturated at the ω 5-position. This exceptional Plusiinae pheromone is noteworthy, and we are interested in the biosynthetic pathway of the ω 7-unsaturated components. Based on the information on the desaturation of many lepidopteran sex pheromones (Jurenka, 2004), we speculated that the *P. festucae* pheromone is produced by Δ 9-desaturation of

16:Acyl or Δ^{11} -desaturation of 18:Acyl. To clarify the pathway in *P. festucae*, we analyzed fatty acids in the pheromone glands by GC–MS at the start of the study. Next, deuterated C_{16} and C_{18} saturated and monoenoic fatty acids were treated to the pheromone glands, and the manner in which they were incorporated into Z5-12:OAc was compared. The results suggested that both desaturation made a contribution. The incorporation was also examined with a pheromone gland pretreated with an inhibitor of chain elongation to eliminate the possibility of the conversion of 16:Acid into 18:Acid. Furthermore, a similar biosynthetic experiment was carried out using another Plusiinae species, *Chrysodeixis eriosoma*, which secretes Z7-12:OAc as a main pheromone component (Komoda et al., 2000). Incorporation of deuterium was observed only in *C. eriosoma* females treated with the C_{16} acids, indicating different β -oxidation systems in *P. festucae* and *C. eriosoma* females.

MATERIALS AND METHODS

INSECTS

Larvae of three Plusiinae species (*P. festucae*, *C. eriosoma*, and *A. peponis*) were collected in a paddy field or a vegetable field of Tokyo University of Agriculture and Technology (Fuchu, Tokyo). The *P. festucae* larvae were also collected in a paddy field in Yamagata Prefecture. Rearing for successive generations was separately carried out on an artificial diet consisting mainly of kidney beans (Kawasaki et al., 1987) at 25°C under a 16L–8D cycle. The female pupae were separated from the males, and 2- to 3-day-old virgin females were used for experiments. Their sex pheromones are composed of the following monoenyl compounds: *P. festucae*, Z5-12:OAc, Z7-14:OAc, and Z5-12:OH (100:15:6; Ando et al., 1995); *C. eriosoma*, Z7-12:OAc and Z9-12:OAc (17:3; Komoda et al., 2000); *A. peponis*, Z7-12:OAc, Z5-10:OAc, and Z7-12:OH (10:5:1; Inomata et al., 2000).

LIPID EXTRACTION AND DERIVATIZATION

From 10 pheromone glands removed from the females of each species, lipids were extracted with a mixed solvent of chloroform and methanol (v/v = 2:1) and used for basic hydrolysis to yield fatty acids. After purification by preparative TLC, the free acids were converted to esters by diazomethane and quantitatively analyzed by GC–MS. The fatty acid methyl esters (FAMES) of *P. festucae* were also analyzed after derivatization with dimethyl disulfide (DMDS; Buser et al., 1983). The FAMES were dissolved in a mixture of DMDS (50 μ l) and diethyl ether (100 μ l) including iodine (500 μ g) and then warmed at 40°C overnight. The crude products, which were treated with a 5% sodium thiosulfate solution (0.5 ml), were extracted with hexane and analyzed by GC–MS.

ANALYTICAL INSTRUMENTS

^1H and ^{13}C NMR spectra were recorded by a Jeol Delta 2 Fourier transform spectrometer (JEOL Ltd., Tokyo, Japan) at 399.8 and 100.5 MHz, respectively, for CDCl_3 solutions containing TMS as an internal standard. GC–MS was conducted in the EI mode (70 eV) with an HP5973 mass spectrometer system (Hewlett-Packard) equipped with a split/splitless injector. A DB-23 column (0.25 mm ID \times 30 m, 0.25 μ m film, J & W Scientific, Folsom, CA,

USA) was commonly used for analyses of the pheromone components and FAMES, except for DMDS adducts, which were analyzed with an HP-5 column (0.25 mm ID \times 30 m, 0.25 μ m film, Hewlett-Packard, Wilmington, DE, USA). The temperature program for the DB-23 column was 80°C for 1 min and 8°C/min to 220°C, and that for HP-5 column was 100°C for 2 min, 15°C/min to 280°C, and held for 15 min. The carrier gas was He.

DEUTERIUM-LABELED PRECURSORS

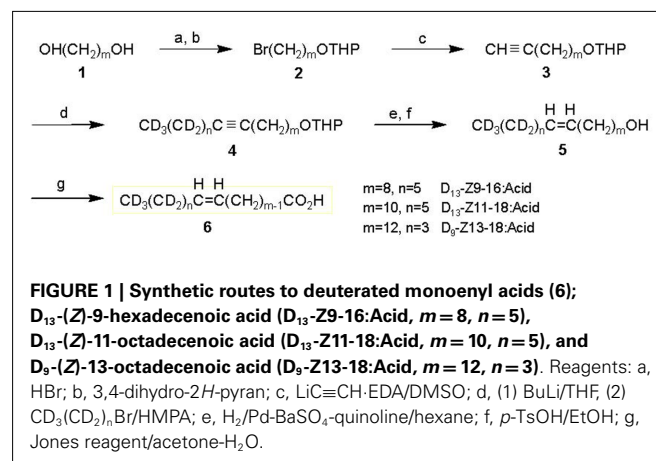
[16,16,16- D_3]Palmitic acid (D_9 -16:Acid, 99.7 atom% of D) and [18,18,18- D_3]stearic acid (D_3 -18:Acid, 99.7 atom% of D) were purchased from ISOTEC Inc. The synthesis of [13,13,14,14,15,15,16,16,16- D_9](Z)-11-hexadecenoic acid (D_9 -Z11-16:Acid) has been reported (Ando et al., 1998). Other deuterated monoenyl fatty acids were synthesized by the routes described below (shown in Figure 1).

D_{13} -Z9-16:Acid

[11,11,12,12,13,13,14,14,15,15,16,16,16- D_{13}](Z)-9-Hexadecenoic acid was prepared starting from 1,8-octanediol (**1**, $m = 8$). By half-bromination with HBr and protection of the remaining hydroxyl group by dihydropyran, this alcohol was converted into the THP ether of 8-bromooctan-1-ol (**2**, $m = 8$). The bromide was treated with lithium acetylide and the produced terminal acetylene compound (**3**, $m = 8$) was coupled with D_{13} -1-bromohexane (98 atom% of D, ISOTEC, Inc., OH, USA) to yield a hexadecyne derivative (**4**, $m = 8$, $n = 5$) that incorporated D_{13} . The triple bond of **4** was partially reduced to a double bond under hydrogen gas with a Pd–BaSO₄ catalyst poisoned with quinoline, and D_{13} -(Z)-9-pentadecen-1-ol (**5**, $m = 8$, $n = 5$) was obtained after cleavage of the THP protective group. This alcohol was oxidized with the Jones reagent to yield the D_{13} -Z9-16:Acid (**5**, $m = 8$, $n = 5$). NMR (δ ppm): ^1H : 1.30 (8H, broad), 1.63 (2H, tt, $J = 7.5$, 7.5 Hz), 2.02 (2H, dt, $J = 7$, 7 Hz), 2.35 (2H, t, $J = 7.5$ Hz), 5.34 (2H, m), ^{13}C : 24.7, 27.2, 29.1 ($\times 2$), 29.2, 29.7, 34.1, 129.8, 130.0, 180.2. GC–MS of methyl ester: Rt 13.75 min, m/z 281 (M^+ , 11%), 249 (38%), 74 (100%).

D_{13} -Z11-18:Acid

[13,13,14,14,15,15,16,16,17,17,18,18,18- D_{13}](Z)-11-Octadecenoic acid was synthesized starting from 1,10-decanediol (**1**, $m = 10$)



via a deuterated 11-octadecyne derivative (**4**, $m = 10$, $n = 5$), which was prepared by a coupling reaction between an acetylene compound (**3**, $m = 10$) and D_{13} -1-bromohexane. NMR (δ ppm); 1H : 1.29 (12H, broad), 1.64 (2H, tt, $J = 7.5$, 7.5 Hz), 2.01 (2H, dt, $J = 7$, 7 Hz), 2.34 (2H, t, $J = 7.5$ Hz), 5.34 (2H, m), ^{13}C : 24.7, 27.2, 29.1 ($\times 2$), 29.2 ($\times 3$), 29.4, 29.5, 29.8, 34.0, 129.9 ($\times 2$), 180.0. GC-MS of methyl ester: Rt 15.82 min, m/z 309 (M^+ , 10%), 277 (33%), 74 (100%).

***D*₉-Z13-18:Acid**

[15,15,16,16,17,17,18,18,18- D_9](*Z*)-13-Octadecenoic acid was synthesized starting from 1,12-dodecanediol (**1**, $m = 10$) via a deuterated 13-octadecyne derivative (**4**, $m = 12$, $n = 3$). This intermediate was prepared by a coupling reaction between an acetylene compound (**3**, $m = 12$) and D_9 -1-bromobutane, which was derived from D_{10} -1-butanol (98 atom% of D, ISOTEC, Inc.). NMR (δ ppm); 1H : 1.29 (14H, broad), 1.64 (2H, tt, $J = 7.5$, 7.5 Hz), 2.01 (2H, dt, $J = 7$, 7 Hz), 2.34 (2H, t, $J = 7.5$ Hz), 5.34 (2H, m), ^{13}C : 24.7, 27.2, 29.1, 29.2 ($\times 2$), 29.4, 29.5, 29.8, 34.0, 129.9 ($\times 2$), 180.1. GC-MS of methyl ester: Rt 15.80 min, m/z 305 (M^+ , 12%), 273 (41%), 74 (100%).

APPLICATION OF LABELED PRECURSORS AND AN ELONGATION INHIBITOR

Deuterated fatty acids were dissolved in dimethyl sulfoxide (DMSO) at a concentration of 20 $\mu g/\mu l$, and 1 μl of each solution was topically applied to the pheromone glands of 2-day-old virgin females of *P. festucae* and *C. eriosoma* 4 h after lights-off. Pheromone components were extracted from the glands with hexane 3 h after the application, and the extract was analyzed by GC-MS under a cyclic scan mode (from m/z 40 to m/z 500) or a selected ion monitoring (SIM) mode. The quantitative analysis of labeled and unlabeled compounds was accomplished by peak areas of $[M-60]^+$ ions, referring to calibration curves made with authentic standards. Five groups of the extract from five females were used for each treatment.

Conversion of D_3 -16:Acid was also examined with the *P. festucae* females, which lost their ability for chain elongation through treatment with an inhibitor, 2-hexadecynoic acid (Wood and Lee, 1981). The acid was synthesized by an acetylene coupling reaction between 1-pentadecyne and CO_2 in a similar manner as that reported for the preparation of 2-octadecynoic acid (Renobales et al., 1986). One microliter of the DMSO solution of the acid at a 20 $\mu g/\mu l$ concentration was topically applied to each pheromone gland 30 min before treatment with D_3 -16:Acid, and D_3 -Z5-12:OAc produced in the gland was quantitated by GC-MS.

RESULTS

FATTY ACIDS IN THE PHEROMONE GLANDS

Figure 2 shows the GC-MS analysis (total ion chromatogram, TIC) of FAMES derived from lipids in the pheromone gland of *P. festucae* females. In addition to a large amount of esters derived from generally observed fatty acids, such as methyl palmitate (**V**, Rt 13.74 min), stearate (**VIII**, Rt 15.63 min), and oleate (**IX**, Z9-18:Me, Rt 15.89 min), esters of several monoenoic acids were detected. Methyl (*Z*)-5-dodecenoate (**II**, Rt 9.48 min) and

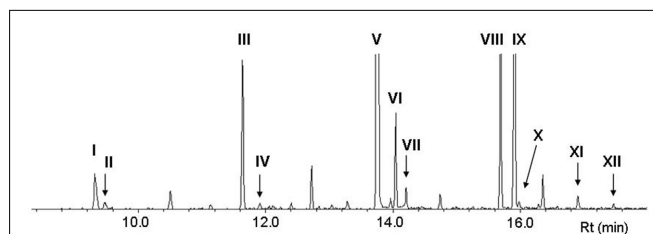


FIGURE 2 | GC-MS analysis (total ion chromatogram, TIC) of fatty acid methyl esters derived from the lipids in pheromone glands of *Plusia festucae*. I, methyl laurate (12:Me); II, methyl (*Z*)-5-dodecenoate (Z5-12:Me); III, methyl myristate (14:Me); IV, methyl (*Z*)-7-tetradecenoate (Z7-14:Me); V, methyl palmitate (16:Me); VI, methyl (*Z*)-9-hexadecenoate (Z9-16:Me); VII, methyl (*Z*)-11-hexadecenoate (Z11-16:Me); VIII, methyl stearate (18:Me); IX, methyl oleate (Z9-18:Me); X, methyl (*Z*)-11-octadecenoate (Z11-18:Me); XI, methyl linoleate (Z9,Z12-18:Me); XII, methyl linolenate (Z9,Z12,Z15-18:Me).

(*Z*)-7-tetradecenoate (**IV**, Rt 11.91 min) are expected to be direct precursors of the pheromone components of Z5-12:OAc and Z7-14:OAc, respectively. The Rts of **II** and **IV** coincided with authentic standards, and their chemical structures were further confirmed by mass spectra of DMDS adducts, i.e., characteristic fragment ions of DMDS adducts of **II** at m/z 161 and 145 and **IV** at m/z 189 and 145 revealed the double bond at the 5- and 7-positions, respectively. This DMDS experiment also confirmed the structure of other esters of monoenoic acids, methyl (*Z*)-9-hexadecenoate (**VI**, Z9-16:Me, Rt 14.04 min), (*Z*)-11-hexadecenoate (**VII**, Z11-16:Me, Rt 14.20 min), and (*Z*)-11-octadecenoate (**X**, Z11-18:Me, Rt 15.97 min). Among the esters corresponding to the two possible candidates for a biosynthetic intermediate with a long chain, the titer of Z9-16:Me was remarkably higher than that of Z11-18:Me.

To understand the characteristic profile of FAMES in *P. festucae*, the contents of C_{16} and C_{18} monoenoic acids were compared with those included in pheromone glands of the other two Plusiinae species, *C. eriosoma* and *A. peponis* (Table 1). These two species, which produce Z7-12:OAc as a main pheromone component, included more abundant Z11-16:Me than *P. festucae*, indicating $\Delta 11$ -desaturation of 16:Acid as a key step in their 7-12:OAc biosyntheses. On the other hand, while the titer of Z9-16:Me in *P. festucae* was lower than those of the two species, the ratio of Z9-16:Me to Z11-16:Me was notably higher than that of the others. Both the titer of Z11-18:Me and its ratio to Z9-18:Me in *P. festucae* were smaller than those of the other species.

INCORPORATION OF LABELED ACIDS INTO THE *P. festucae* PHEROMONE

Figure 3 shows GC-MS analysis (TIC and mass chromatograms) of the extracts, which were prepared from the glands treated with deuterated C_{16} acids. In addition to endogenous Z5-12:OAc (Rt 10.63 min) monitored by ions at m/z 166, 138, and 110, ion peaks of m/z 169, 141, and 113 at 10.58 min suggested the production of D_3 -Z5-12:OAc by the topical application of D_3 -16:Acid (Figure 3A). In the case of D_{13} -Z9-16:Acid, an ion peak of m/z 179 at 10.47 min suggested the production of D_{13} -Z5-12:OAc (Figure 3B). Ion peaks of m/z 151 and 123 at 10.47 min, which were diagnostic for D_{13} -Z5-12:OAc, were

Table 1 | Composition of monounsaturated fatty acids in the pheromone glands of three Plusiinae species^a.

Insect species	C ₁₆ Acid (methyl ester)			C ₁₈ Acid (methyl ester)		
	Titer (μg/gland) ^b		Ratio ^c	Titer (μg/gland) ^b		Ratio ^c
	Z9-Isomer (VI, ω7-ene)	Z11-Isomer (VII, ω5-ene)		Z9-Isomer (IX, ω9-ene)	Z11-Isomer (X, ω7-ene)	
<i>Plusia festucae</i>	1.65 ± 0.02	0.24 ± 0.13	6.88 ± 2.17 ^a	8.08 ± 2.64	0.17 ± 0.09	0.02 ± 0.01 ^a
<i>Chrysodeixis eriosoma</i>	2.36 ± 0.09	3.27 ± 0.37	0.72 ± 0.10 ^b	10.51 ± 0.53	0.48 ± 0.03	0.05 ± 0.01 ^b
<i>Anadevidia peponis</i>	1.97 ± 0.24	2.59 ± 1.29	0.76 ± 0.35 ^b	7.03 ± 1.04	0.73 ± 0.30	0.10 ± 0.05 ^b

^a Each acid was quantitatively analyzed by GC–MS as a methyl ester; Z9-16:Me (VI), Z11-16:Me (VII), Z9-18:Me (IX), and Z11-18:Me (X) (see **Figure 2**).

^b Mean ± SE (n = 4).

^c Values within each test followed by a different letter are significantly different at P < 0.05 by Tukey–Kramer Test.

very small because the fragment ions were also produced by Z5-12:OAc and an unknown component. By treatment with D₃-18:Acid and D₁₃-Z11-18:Acid, the corresponding deuterated pheromone components were detected in the pheromone gland extracts. **Table 2** shows the titers of unlabeled endogenous and deuterated exogenous pheromone components. The titers of D₃-Z5-12:OAc in the pheromone glands treated with D₃-16:Acid and D₃-18:Acid were almost equal. The titers of D₁₃-Z5-12:OAc derived from D₁₃-Z9-16:Acid and D₁₃-Z11-18:Acid were also almost equal. The incorporation ratios of D₁₃-Z9-16:Acid and D₁₃-Z11-18:Acid were higher than those of D₃-16:Acid and D₃-18:Acid.

EFFECT OF 2-HEXADECYNOIC ACID ON PHEROMONE BIOSYNTHESIS

The incorporation of D₃-16:Acid and D₁₃-Z9-16:Acid was examined with the *P. festucae* glands pretreated with 2-hexadecynoic acid. The GC–MS analysis of the pheromone gland extracts showed the following titers of deuterated pheromone components and the incorporation ratios; D₃-Z5-12:OAc (0.25 ± 0.09 ng/gland, 1.5 ± 0.7%, n = 3) from D₃-16:Acid and D₁₃-Z5-12:OAc (0.48 ± 0.22 ng/gland, 2.0 ± 0.8%, n = 3) from D₁₃-Z9-16:Acid. These values were similar to those in the glands untreated with the inhibitor (**Table 2**), indicating that the chain elongation inhibitor did not affect the pheromone biosynthesis.

INCORPORATION OF LABELED ACIDS INTO THE *C. ERIOSOMA* PHEROMONE

Experiments with labeled acids were also carried out with *C. eriosoma* females (**Table 2**). While D₃-16:Acid was converted into D₃-Z7-12:OAc, the labeled pheromone was not detected in the pheromone gland treated with D₃-18:Acid. Similarly, while D₉-Z11-16:Acid was converted into D₉-Z7-12:OAc, the labeled pheromone was not detected in the pheromone gland treated with D₉-Z13-18:Acid. The titer of D₉-Z7-12:OAc was higher than that of D₃-Z7-12:OAc. The incorporation ratio of D₃-16:Acid was about five times higher than that of D₉-Z11-16:Acid.

DISCUSSION

In Lepidoptera, biosynthesis of Type I pheromones has been studied with several species and the results have proposed the following pathway operating in pheromone glands; formation of saturated

fatty acyl compounds from acetyl CoA → desaturation → chain shortening or elongation → reduction of the acyl moiety to a hydroxyl group → acetylation of alcohols or oxidation to aldehydes (Jurenka, 2004). Pheromone glands usually include unsaturated fatty acyl intermediates, and they have been detected by GC–MS analysis of FAMES from lipids in the glands. For example, Z11-16:Me and Z9-14:Me were found in FAMES derived from lipids in *T. ni* females in addition to Z7-12:Me, which possessed the same chain structure as the main pheromone component (Z7-12:OAc; Bjostad and Roelofs, 1983; Roelofs and Bjostad, 1984). The key step for the biosynthesis in *T. ni* is Δ11-desaturation (ω5-desaturation) of 16:Acyl, and Z11-16:Me is the main ester derived from the pheromone gland lipids. Z11-16:Me was not the longest one among the esters of monoenoic acids. A trace amount of the ester of a C₁₈ acid unsaturated at the ω5-position (Z13-18:Me) was detected and estimated to be produced by chain elongation of a Z11-16:Acyl intermediate.

On the other hand, a series of acyl intermediates unsaturated at the ω7-position was found in the lipids of the *P. festucae* females, which secreted Z5-12:OAc as a main pheromone component (**Figure 2**). Z9-16:Me is most abundantly included among the esters unsaturated at the ω7-position and the ratio of Z9-16:Me to Z11-16:Me detected in *P. festucae* is higher than those of other Plusiinae species, *C. eriosoma* and *A. peponis* (**Table 1**), which secrete Z7-12:OAc as a main pheromone component, as *T. ni* does. The data suggest that Z9-16:Acyl, which is produced by Δ9-desaturation (ω7-desaturation) of 16:Acyl, is a key biosynthetic intermediate of Z5-12:OAc. The content of Z11-18:Me is very small in *P. festucae*, and the ratio of Z11-18:Me to Z9-18:Me detected in *P. festucae* was also smaller than those in the other two Plusiinae species (**Table 1**). We speculated that Z11-18:Me might not be derived from a key biosynthetic intermediate of *P. festucae*, similarly to Z13-18:Me found in the FAMES of *T. ni* females.

The biosynthetic pathway of Z5-12:OAc was confirmed by experiments with labeled fatty acids (**Table 2**). By topical application of D₃-16:Acid and D₁₃-Z9-16:Acid, D₃-Z5-12:OAc and D₁₃-Z5-12:OAc were respectively produced in the pheromone glands of *P. festucae*. The incorporation ratio of D₁₃-Z9-16:Acid was higher than that of D₃-16:Acid, supporting the desaturation step of 16:Acyl. Moreover, D₃-18:Acid and D₁₃-Z11-18:Acid were also incorporated into Z5-12:OAc. The incorporation ratios of

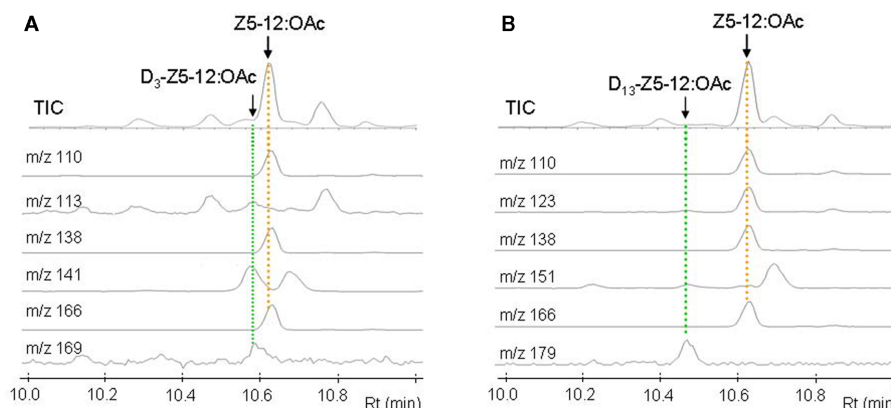


FIGURE 3 | GC-MS analysis of pheromone gland extracts of *Plusia festucae* females which were treated with D₃-palmitic acid [D₃-16:Acid (A)] and D₁₃-(Z)-9-hexadecenoic acid [D₁₃-Z9-16:Acid (B)]. The mass chromatograms indicated the

following unlabeled and labeled pheromone components; Z5-12:OAc by the ions at *m/z* 166, 138, and 110, D₃-Z5-12:OAc by the ions at *m/z* 169, 141, and 113, and D₁₃-Z5-12:OAc by the ions at *m/z* 179, 151, and 123.

Table 2 | Titters of endogenous and exogenous pheromone components in the sex pheromone glands of *Plusia festucae* and *Chrysodeixis eriosoma* females, which were treated with deuterated fatty acids^a.

Species	Treatment	Endogenous component		Exogenous component		Incorporation ratio (%) ^c [Y]/[X] × 100
		Structure	Titer [X] (ng/gland) ^b	Structure	Titer [Y] (ng/gland) ^b	
<i>P. festucae</i>	D ₃ -16:Acid	Z5-12:OAc	15.6 ± 8.0	D ₃ -Z5-12:OAc	0.22 ± 0.05	1.4 ± 0.5 ^a
	D ₃ -18:Acid	Z5-12:OAc	18.8 ± 8.8	D ₃ -Z5-12:OAc	0.23 ± 0.06	1.2 ± 0.4 ^a
	D ₁₃ -Z9-16:Acid	Z5-12:OAc	28.0 ± 12.4	D ₁₃ -Z5-12:OAc	0.59 ± 0.16	2.1 ± 0.2 ^b
	D ₁₃ -Z11-18:Acid	Z5-12:OAc	21.6 ± 4.4	D ₁₃ -Z5-12:OAc	0.56 ± 0.07	2.6 ± 0.6 ^b
<i>C. eriosoma</i>	D ₃ -16:Acid	Z7-12:OAc	102 ± 49	D ₃ -Z7-12:OAc	2.9 ± 1.4	2.9 ± 0.5 ^a
	D ₃ -18:Acid	Z7-12:OAc	141 ± 58	D ₃ -Z7-12:OAc	Undetected	0
	D ₉ -Z11-16:Acid	Z7-12:OAc	179 ± 80	D ₉ -Z7-12:OAc	25.0 ± 9.9	14.0 ± 4.2 ^b
	D ₉ -Z13-18:Acid	Z7-12:OAc	131 ± 47	D ₉ -Z7-12:OAc	Undetected	0

^aEach acetate was quantitatively analyzed by GC-MS.

^bMean ± SE (n = 3).

^cValues within each species followed by a different letter are significantly different at *P* < 0.05 by Tukey-Kramer Test.

D₃-16:Acid and D₃-18:Acid were not significantly different, and those of D₁₃-Z9-16:Acid and D₁₃-Z11-18:Acid are also similar. These results indicate that the above speculation for Z11-18:Me is incorrect. The very low content of Z11-18:Me suggests the rapid β-oxidation of Z11-18:Acyl. Thus, we concluded that not only Δ⁹-desaturation of 16:Acyl but also Δ¹¹-desaturation of 18:Acyl are at work in the pheromone biosynthesis in the *P. festucae* females, as shown in **Figure 4**, if D₃-16:Acid is not easily converted into D₃-18:Acid in the pheromone glands. Since this chain elongation seems to be a common reaction, we examined the incorporation of D₃-16:Acid using females pretreated with 2-hexadecynoic acid. This acetylene compound is a known inhibitor of chain elongation of 16:Acid (Wood and Lee, 1981). The inhibitor did not affect the incorporation in *P. festucae*, indicating that D₃-16:Acid was desaturated without elongation and D₃-Z9-16:Acid produced from D₃-16:Acid was converted into D₃-Z5-12:OAc (**Figure 4**).

As a comparative study, the biosynthesis of Z7-12:OAc in *C. eriosoma* was examined with labeled fatty acids (**Table 2**). The incorporation ratios of the deuterated C₁₆ acids demonstrated the Δ¹¹-desaturation of 16:Acyl as a key step similar to *T. ni* and other Plusiinae species (Komoda et al., 2000). On the contrary, deuterated C₁₈ acids were not incorporated into the pheromone. Chain shortening of the C₁₈ acids did not proceed in the pheromone gland of *C. eriosoma*, and it was interestingly revealed that the β-oxidation systems of *P. festucae* and *C. eriosoma* were different. The ability of β-oxidation of the C₁₈ chain is not necessary for the *C. eriosoma* females and the inability might fit their pheromone biosynthesis. The silkworm (*Bombyx mori*) secreted C₁₆ dienyl alcohol (bombykol) as a sex pheromone. Among a series of labeled fatty acids with a saturated C₁₂-C₁₈ chain, only 16:Acid was reliably incorporated into the bombykol (Ando et al., 1986). The other free acids did not enter into the biosynthetic pathway of

bombykol. Although it is difficult to generalize, chain shortening and elongation of exogenous free acids do not seem to happen easily in the *B. mori* females. If the enzymes in the pheromone glands of *P. festucae* perform only a minimum necessary function, our experiment with the labeled acids clearly revealed their contribution to both types of desaturation in pheromone production.

In Plusiinae, *Thysanoplusia intermixta* females secrete a mixture of Z7-12:OAc and (5E,7Z)-5,7-dodecadienyl acetate (E5,Z7-12:OAc) for mating communication (Ando et al., 1998). The biosynthesis of the dienyl component was also investigated with several deuterated acids (Ono et al., 2002). While the double bond at the 5-position in the monoenyl pheromone of *P. festucae* is introduced at an early stage of the biosynthesis, probably just after construction of C₁₆ and C₁₈ saturated fatty acids, desaturation at the same position in the dienyl pheromone of *T. intermixta* is achieved on Z7-12:Acyl, which is produced by Δ 11-desaturation of 16:Acyl and β -oxidation of the produced Z11-16:Acyl intermediate. This Δ 5-desaturation is, in other words, ω 7-desaturation. Some species in Plusiinae secrete pheromone components produced by ω 3-desaturation, such as Z9-12:OAc of *C. eriosoma* and Z7-10:OAc of *Diachrysia chrysitis* (Löfstedt et al., 1994). In these species, Δ 13-desaturation of 16:Acyl and Δ 11-desaturation of 14:Acyl might proceed. Experimental proof for the actual substrate of ω 3-desaturase is anticipated.

Whereas some Plusiinae species produce more than 10 components, only two or three compounds are essential for male attraction. Based on the chemical structures of these primary components, we have classified Plusiinae pheromones into nine groups (Ando et al., 2004; Inomata et al., 2005). All monoenyl components include the double bond at the ω 3-, ω 5-, or ω 7-position;

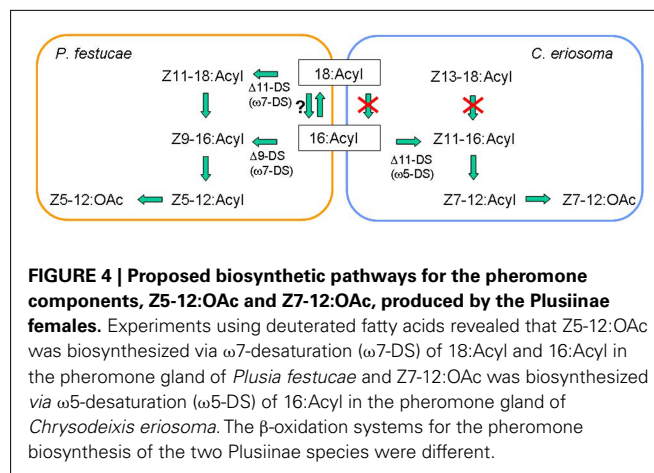


FIGURE 4 | Proposed biosynthetic pathways for the pheromone components, Z5-12:OAc and Z7-12:OAc, produced by the Plusiinae females. Experiments using deuterated fatty acids revealed that Z5-12:OAc was biosynthesized via ω 7-desaturation (ω 7-DS) of 18:Acyl and 16:Acyl in the pheromone gland of *Plusia festucae* and Z7-12:OAc was biosynthesized via ω 5-desaturation (ω 5-DS) of 16:Acyl in the pheromone gland of *Chrysodeixis eriosoma*. The β -oxidation systems for the pheromone biosynthesis of the two Plusiinae species were different.

thus, the pheromones are produced by a combination of one of three desaturases and specific β -oxidation enzyme(s). Genes of the desaturases expressed specifically in a pheromone gland have been characterized from more than 20 lepidopteran species (Jurenka, 2004; Wang et al., 2010; Fujii et al., 2011). While the first identification of the desaturase for pheromone biosynthesis of moths was accomplished with *T. ni* (Knipple et al., 1998), the enzymes have unfortunately not been identified from any other Plusiinae species. In addition to providing insights on the chemical structures and biosynthetic pathways of the sex pheromones, systematic studies of the enzymes acting in the Plusiinae species would clarify specification of this subfamily. The Plusiinae pheromones might be one of the most profitable targets for gaining an understanding of the evolution of moth species, and, therefore, further comprehensive studies are anticipated.

REFERENCES

- Ando, T. (2011). *Internet Database*. Available at <http://www.tuat.ac.jp/~antetsu/LepiPheroList.htm>
- Ando, T., Arima, R., Mori, A., and Uchiyama, M. (1986). Incorporation of ¹⁴C-fatty acids into bombykol, a female sex pheromone of the silkworm moth. *Agric. Biol. Chem.* 50, 1093–1095.
- Ando, T., Inomata, S., Shimada, R., Nomura, M., Uehara, S., and Pu, G.-Q. (1998). Sex pheromones of *Thysanoplusia intermixta* and *T. orichalcea*: identification and field tests. *J. Chem. Ecol.* 24, 1105–1116.
- Ando, T., Inomata, S., and Yamamoto, M. (2004). Lepidopteran sex pheromones. *Top. Curr. Chem.* 239, 51–96.
- Ando, T., Ohno, R., Kokuryu, T., Funayoshi, A., and Nomura, M. (1995). Identification of female sex pheromone components of rice looper, *Plusia festucae* (L.), (Lepidoptera: Noctuidae). *J. Chem. Ecol.* 21, 1181–1190.
- Berger, R. S. (1966). Isolation, identification, and synthesis of the sex attractant of the cabbage looper, *Trichoplusia ni*. *Ann. Entomol. Soc. Am.* 59, 767–771.
- Bjostad, L. B., and Roelofs, W. L. (1983). Sex pheromone biosynthesis in *Trichoplusia ni*: key steps involve delta-11 desaturation and chain-shortening. *Science* 220, 1387–1389.
- Buser, H.-R., Arn, H., Guerin, P., and Rauscher, S. (1983). Determination of double bond position in mono-unsaturated acetates by mass spectrometry of dimethyl disulfide adducts. *Anal. Chem.* 55, 818–822.
- El-Sayed, A. M. (2011). *Internet Database*. Available at <http://www.pherobase.com/>
- Fujii, T., Ito, K., Tatamatsu, M., Shimada, T., Katsma, S., and Ishikawa, Y. (2011). Sex pheromone desaturase functioning in a primitive *Ostrinia* moth is cryptically conserved in congeners' genomes. *Proc. Natl. Acad. Sci. U.S.A.* 108, 7102–7106.
- Inomata, S., Komoda, M., Watanabe, H., Nomura, M., and Ando, T. (2000). Identification of sex pheromones of *Anadevidia peponis* and *Macdunnoughia confusa*, and field tests of their role in reproductive isolation of closely related Plusiinae moths. *J. Chem. Ecol.* 26, 443–454.
- Inomata, S., Watanabe, A., Nomura, M., and Ando, T. (2005). Mating communication systems of four Plusiinae species distributed in Japan: identification of the sex pheromones and field evaluation. *J. Chem. Ecol.* 31, 1429–1442.
- Jurenka, R. (2004). Insect pheromone biosynthesis. *Top. Curr. Chem.* 239, 97–132.
- Kawasaki, K., Ikeuchi, M., and Hidaka, T. (1987). Laboratory rearing method for *Acanthoplusia agnate* (Lepidoptera: Noctuidae) without change of artificial diet. *Jpn. J. Appl. Entomol. Zool.* 31, 78–80.
- Knipple, D. C., Rosenfield, C.-L., Miller, S. J., Liu, W., Tang, J., Ma, P. W. K., and Roelofs, W. L. (1998). Cloning and functional expression of a cDNA encoding a pheromone gland-specific acyl-CoA Δ ¹¹-desaturase of the cabbage looper moth, *Trichoplusia ni*. *Proc. Natl. Acad. Sci. U.S.A.* 95, 15287–15292.
- Komoda, M., Inomata, S., Ono, A., Watanabe, H., and Ando, T. (2000). Regulation of sex pheromone biosynthesis in three Plusiinae moths: *Macdunnoughia confusa*, *Anadevidia peponis*, and *Chrysodeixis eriosoma*. *Biosci. Biotechnol. Biochem.* 64, 2145–2151.
- Löfstedt, C., Hansson, B. S., Tóth, M., Szöcs, G., Buda, V., Bengtsson, M., Ryrholm, N., Svensson, M., and Priesner, E. (1994). Pheromone differences between sibling taxa *Diachrysia chrysitis* (Linnaeus, 1758) and *D. tutti* (Kostrowicki, 1961) (Lepidoptera: Noctuidae). *J. Chem. Ecol.* 20, 91–109.
- Ono, A., Imai, T., Inomata, S., Watanabe, A., and Ando, T. (2002). Biosynthetic pathway for production of a conjugated dienyl sex pheromone of a Plusiinae moth, *Thysanoplusia intermixta*. *Insect Biochem. Mol. Biol.* 32, 701–708.

- Renobales, M., Wakayama, E. J., Halarnkar, P. P., Reitz, R. C., Pomonis, J. G., and Blomquist, G. J. (1986). Inhibition of hydrocarbon biosynthesis in the housefly by 2-octadecynoate. *Arch. Insect Biochem. Physiol.* 3, 75–86.
- Roelofs, W., and Bjostad, L. (1984). Biosynthesis of lepidopteran pheromones. *Bioorg. Chem.* 12, 279–298.
- Wang, H.-L., Lienard, M. A., Zhao, C.-H., Wang, C.-Z., and Löfstedt, C. (2010). Neofunctionalization in an ancestral insect desaturase lineage led to rare Δ^6 pheromone signals in the Chinese tussah silk-worm. *Insect Biochem. Mol. Biol.* 40, 742–751.
- Wood, R., and Lee, T. (1981). Metabolism of 2-hexadecynoate and inhibition of fatty acid elongation. *J. Biol. Chem.* 256, 12379–12386.
- Conflict of Interest Statement:** The authors declare that the research was conducted in the absence of any commercial or financial relationships that could be construed as a potential conflict of interest.
- Received: 26 September 2011; paper pending published: 18 October 2011; accepted: 26 October 2011; published online: 14 November 2011.
- Citation: Watanabe H, Matsui A, Inomata S-i, Yamamoto M and Ando T (2011) Biosynthetic pathway for sex pheromone components produced in a Plusiinae moth, *Plusia festucae*. *Front. Endocrin.* 2:74. doi: 10.3389/fendo.2011.00074
- This article was submitted to *Frontiers in Experimental Endocrinology*, a specialty of *Frontiers in Endocrinology*.
- Copyright © 2011 Watanabe, Matsui, Inomata, Yamamoto and Ando. This is an open-access article subject to a non-exclusive license between the authors and Frontiers Media SA, which permits use, distribution and reproduction in other forums, provided the original authors and source are credited and other Frontiers conditions are complied with.



Prostaglandins and their receptors in insect biology

David Stanley^{1*} and Yonggyun Kim²

¹ Biological Control of Insects Research Laboratory, Agricultural Research Service, United States Department of Agriculture, Columbia, MO, USA

² Department of Bioresource Sciences, Andong National University, Andong, Republic of Korea

Edited by:

Joe Hull, USDA Agricultural Research Service, USA

Reviewed by:

Qi Fang, Zhejiang University, China
Qisheng Song, University of Missouri, USA

*Correspondence:

David Stanley, Biological Control of Insects Research Laboratory, Agricultural Research Service, United States Department of Agriculture, 1503 South Providence Road, Columbia, MO 65203, USA.
e-mail: stanleyd@missouri.edu

We treat the biological significance of prostaglandins (PGs) and their known receptors in insect biology. PGs and related eicosanoids are oxygenated derivatives of arachidonic acid (AA) and two other C20 polyunsaturated fatty acids. PGs are mostly appreciated in the context of biomedicine, but a growing body of literature indicates the biological significance of these compounds extends throughout the animal kingdom, and possibly beyond. The actions of most PGs are mediated by specific receptors. Biomedical research has discovered a great deal of knowledge about PG receptors in mammals, including their structures, pharmacology, molecular biology and cellular locations. Studies of PG receptors in insects lag behind the biomedical background, however, recent results hold the promise of accelerated research in this area. A PG receptor has been identified in a class of lepidopteran hemocytes and experimentally linked to the release of prophenoloxidase. PGs act in several crucial areas of insect biology. In reproduction, a specific PG, PGE₂, releases oviposition behavior in most crickets and a few other insect species; PGs also mediate events in egg development in some species, which may represent all insects. PGs play major roles in modulating fluid secretion in Malpighian tubules, rectum and salivary glands, although, again, this has been studied in only a few insect species that may represent the Class. Insect immunity is a very complex defense system. PGs and other eicosanoids mediate a large number of immune reactions to infection and invasion. We conclude that research into PGs and their receptors in insects will lead to important advances in our understanding of insect biology.

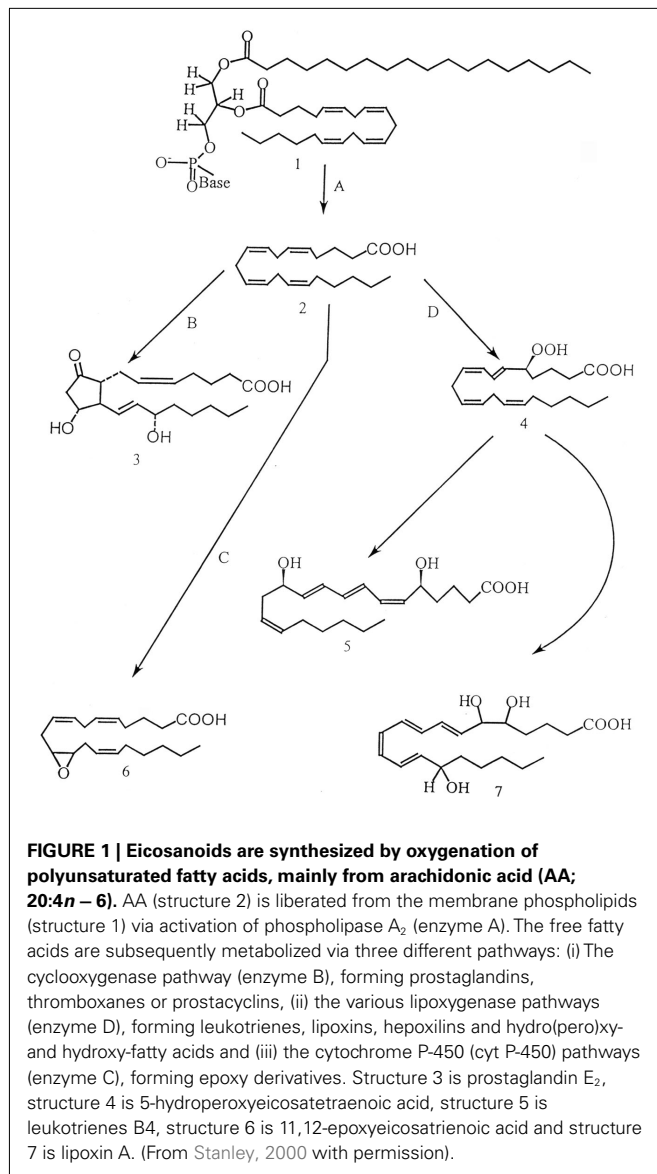
Keywords: prostaglandins, insect physiology, receptors, immunity, reproduction

INTRODUCTION

Prostaglandins (PGs) and other eicosanoids are oxygenated derivatives of arachidonic acid (AA) and two other C20 polyunsaturated fatty acids. Corey et al. (1980) put forth the term eicosanoid, based on the Greek word for 20, “eikosi.” Eicosanoid is a broad term for all biologically active AA metabolites. Three major groups of eicosanoids are recognized. The cyclooxygenase (COX) pathways lead to PGs; the lipoxygenase (LOX) pathways produce a myriad compounds, including the leukotrienes; and the cytochrome P-450 “epoxidase” pathways yield a group of epoxyeicosatrienoic acids. PGs and LOX products have been identified and exert biological actions in insect tissues. The epoxyeicosatrienoic acids act in mammalian tissues, but have not been reported for invertebrates. **Figure 1** presents a broad outline of eicosanoid biosynthesis; eicosanoid chemical structures and biosynthetic pathways are treated in detail elsewhere (Stanley, 2000, 2005).

The roots of endocrinology go back to the 1850s, first with Arnold Berthold’s castration/transplantation experiments on roosters (Benedum, 1999). He showed that castrating roosters led to atrophy of the comb and disinterest in hens. Also in the 1850s the French physiologist, Claude Bernard, discussed “internal secretions” that travel in blood circulation to distant target cells within the body. Eicosanoids are relative newcomers to biochemical signaling. The first known eicosanoids are dated to the 1930s, when von Euler (1936) reported that a substance(s) from

the human prostate gland stimulated contractions in isolated uterine smooth muscle preparations. The contraction-stimulating substances had the characters of an acidic lipid and von Euler named them “prostaglandins” after their source. There was no real progress on PGs until Bergström and Samuelsson (Bergström et al., 1962) reported the chemical structures of PGE, PGF₁ and PGF₂ nearly 30 years later. Once the chemical structures of these PGs were revealed, it became clear immediately that AA is the immediate precursor for all PGs. Although originally interested in cholesterol reaction mechanisms, after the structural work on PGs, Bergström devoted his research to understanding AA metabolism, during which he discovered other eicosanoids, including endoperoxides, leukotrienes and thromboxanes. The pharmacologist John Vane shared the 1982 Nobel Prize for Medicine or Physiology with Bergström and Samuelsson for their pioneering work on PGs and other eicosanoids. Vane’s contribution was his original demonstration that aspirin and other analgesics relieve discomforts associated with inflammation by inhibiting PG biosynthesis. Knowledge of the chemical structures and clinical significance of PGs and other eicosanoids launched a very large research enterprise in industry, academia and government. We now know that PGs and other eicosanoids are biosynthesized and exert important biological actions in virtually all mammalian tissues and body fluids. For a few examples, eicosanoids act in reproduction, immunity, smooth muscle contraction, ion transport and in mucosal protection.



The discovery of eicosanoids in a marine invertebrate came from a broad research program on marine natural products. In their 15th paper in a series, Weinheimer and Spraggins (1969) reported on two PG derivatives in the gorgonian octocoral, *Plexaura homomalla*. As a side note, this discovery came before PGs were available for physiological research. While *P. homomalla* became the first commercial source of PGs for research purposes, there were no insights into the biological significance of PGs or any eicosanoids in invertebrates. Destephano and Brady (1977) provided the first suggestion that PGs act in insect biology with their report on PG biosynthesis in reproductive tissues of the house cricket, *Acheta domesticus*. They also showed that injecting 100 µg of PGE₂ into gravid virgin females led to release of egg-laying behavior. This was the first report of a biological role of PGs in insects.

In the context of this issue of Frontiers in Experimental Endocrinology, we focus on PG receptor-mediated events in insect

physiology, including the release of egg-laying behavior in crickets, roles of PGs in insect egg development, a PG receptor in tick salivary glands and finally, a PG receptor-mediated action in insect immunity. The main points of the paper are that (1) in most cases, the PG receptors are postulated on the basis of specificity of PG actions, rather than studied directly; (2) PGs are crucial elements in insect physiology; (3) PG actions are receptor-mediated; and (4) research into insect PG receptors represents a very broad, newly illuminated frontier with profound implications in basic and applied biology.

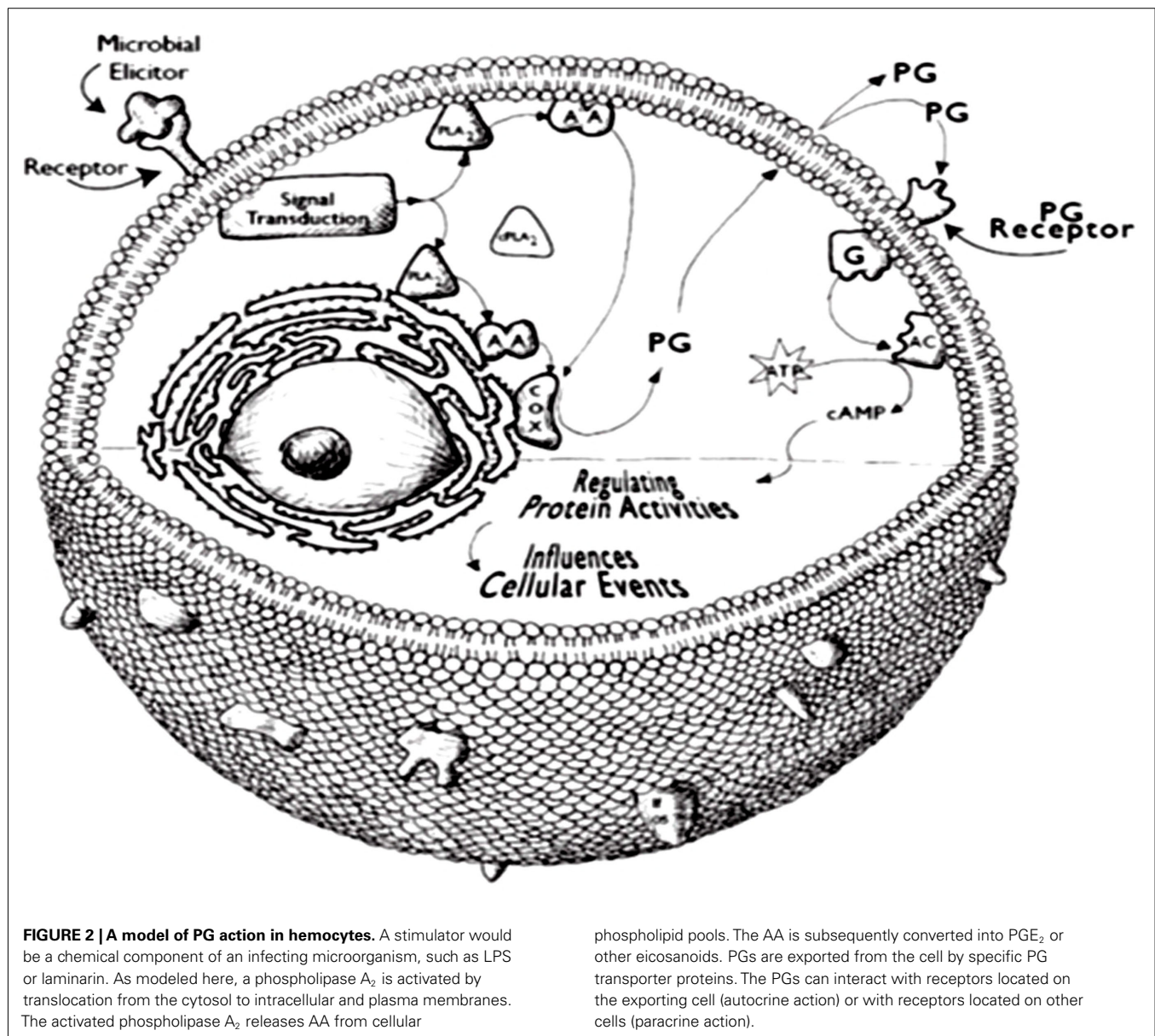
A BIOMEDICAL BACKGROUND ON PG RECEPTORS

Drawing on the biomedical model developed in studies of mammalian physiology and pathophysiology, PGs and at least some LOX products interact with specific cell surface receptors, particularly G protein coupled receptors (GPCRs) of the rhodopsin family (Breyer et al., 2001). Figure 2 presents a model of one mechanism of the influence of PGs on cellular events. The genes encoding GPCRs account for relatively large proportions of animal genomes; GPCRs are organized into a variety of families (Vanden Broeck, 2001). GPCRs selectively couple with various intracellular G proteins, each of which regulates the activities of specific cellular effector proteins, including adenylyl cyclase and others (Blenau and Baumann, 2001). Some mammalian PG receptors influence events related to homeostasis, such as ion transport physiology and others influence gene expression in target cells.

The detailed situation is still more complex. Whereas most PG receptors are thought to be located on cell surfaces, nuclear PG receptors also have been reported (Bhattacharya et al., 1999). Cell surface PG receptors also exist in various subtypes. PGs D, E, F, I, and Thromboxane A have specific receptors, each denoted by a letter associated with the PG and a P: DP, EP, FP, IP, and TP receptors. Still more complexity attends the EP receptors, which occur in subtypes, EP1, EP2, EP3, and EP4 and each of these interact with separate G proteins. EP3 receptors are further subdivided into variants due to splice variations (Hatae et al., 2002). All this variation in PG receptors allows various PGs to exert multiple and even contradictory influences on cells. For example, EP3 variant EP3A, once activated, can stimulate increased intracellular cAMP concentrations, while EP3 variant EP3B lowers intracellular cAMP concentrations. Compared to the huge body of literature on PG receptors in the biomedical literature, there is only scant knowledge these receptors in invertebrates. Here we assemble the diverse information into a unified picture.

PROSTAGLANDINS IN INSECT REPRODUCTION

In decades of detailed research Werner Loher and his students developed the most complete picture of a cricket mating system, studying the Australian field cricket, *Teleogryllus commodus*. Loher and Edson (1973) showed that mating exerts profound influences on female crickets. They reported the apparently odd situation that successful mating, *per se*, does not attenuate female receptivity; instead, males tend to corral females within mating arenas after mating until they deposit their eggs. Males call and court females, and this synchronizes sexual readiness in both sexes. Males produce spermatophores and express calling behavior on a circadian rhythm basis (Loher, 1984). Virgin



females express nightly locomotor behavior and are responsive to male calling songs, both behaviors also organized on circadian rhythms. Following successful mating (and not all copulations are successful because the long tubes of the spermatophores must find their way into the spermathecae), females stop their locomotor behaviors and lose interest in male calling songs (Loher, 1984). A third very important change in females is the onset of oviposition behavior that can last for hours and culminate in deposition of hundreds of fertile eggs, each individually deposited. Loher demonstrated that the physical stimulation of mating is not responsible for these profound changes in female behavior, because mating with castrated males does not produce the changes (Loher and Edson, 1973). He postulated that a chemical factor, produced in testes and sexually transferred to females, induced at least some of the behavioral changes in females.

In his first experiment to identify a chemical factor, Loher (1979) injected sexually mature virgins with PGE_2 (and saline into control females), then recorded egg-laying each day for the following 13 days. For the first 24 h following treatment, Loher recorded an average of about 6 eggs/female in controls and about 76 eggs/female in PG-treated experimental females. Over the whole experiment experimental females deposited about 217 eggs/female/day, compared to about 11 by the control females. This work laid a foundation for a lengthy research program on the roles and actions of PG in releasing oviposition behavior in female crickets.

The program began with analytic biochemistry to determine quantities of PGE_2 in spermathecae from virgin and mated females, using a high-performance liquid chromatography protocol, which at the time was sensitive to about 0.5 ng. They collected and analyzed pools of 100 spermathecae, from which they recorded

about 500 pg PGE₂/spermatheca in glands from mated females and none in spermathecae from virgins. Recalling that PGs took their name from the prostate gland, mammalian semen is generally rich in PGs. On the basis of mammalian semen, Loher guessed that cricket seminal fluids, which are transferred to females in spermatophores, would contain a fair amount of PG. Similar chemical determinations showed that spermatophores contain about 20 pg/spermatophore, far too little to account for the recorded 500 pg/spermathecae.

The next line of work was designed to determine PGE₂ biosynthesis in spermatophores and spermathecae. They used a fairly standard protocol in which the fluid contents of spermatophores and spermathecae were incubated in the presence of radioactive AA. After the incubations, the reactions were extracted and analyzed on thin-layer chromatography (TLC). This work showed that spermathecal preparations from virgin females did not produce PGs, while similar preparations from mated females and from spermatophores produced about 25–35 pmol PGE₂/h/tissue and about 12–13 pmol PGF_{2α}/h/tissue. Because the presence and biological significance of AA and other C20 polyunsaturated fatty acids was not appreciated at the time, the authors also recorded the presence of AA in spermathecae of virgin females at about 2% of total fatty acids. These findings became the basis of the “enzyme transfer model,” which specified that an enzyme with PG biosynthetic activity was transferred from male to female along with the other components of spermathecal seminal fluid; once in the spermathecae of newly mated females, the enzyme converts AA into PGE₂, which subsequently releases oviposition behavior (Loher et al., 1981). The model also prompted deeper study.

Stanley-Samuelson and Loher (1983) investigated the arrangement of AA in spermatophores and spermathecae. They found that spermathecae from mated females contained about 40-fold more AA than spermathecae from virgin females (0.008 mg AA/spermatheca for virgins and about 0.34 mg AA/spermatheca for mated females). The difference between virgin and mated females was roughly the amount of AA detected in spermatophores. Virtually all the AA in spermatophores was associated with phospholipids, with none in neutral lipids. Within phospholipids, AA made up about 4% of phosphatidylethanolamine fatty acids and about 25% of phosphatidylcholine fatty acids. This is a very unusual asymmetry in fatty acid arrangements, from which the authors inferred that AA is arranged in spermatophores for a special purpose.

All previous work had focused on the influence of a single PG, namely PGE₂, on releasing egg-laying behavior. Of course, there are many PGs, which raises questions about the specificity of PG actions in releasing oviposition behavior. If the PG mode of action were similar to the mammalian background, specific PG receptors would limit the number of different PGs that release oviposition behavior. Stanley-Samuelson et al. (1986) investigated the relation between PG structures and egg-laying. They used groups of 15-day-old virgin females. Some were untreated as negative controls, some were mated with intact males as positive controls and experimental groups were injected with 100 µg of a chemical. The outcomes of these experiments are tabulated in Stanley-Samuelson et al. (1986), where we see that the most effective treatments were the positive mating controls and treatments with 15-keto-PGE₂,

a metabolite of PGE₂. PGE₂ treatments also released egg-laying behavior, but at about 57% of the influence of mating. The authors interpreted the results in terms of PG receptors, which at that time were completely unknown in insect biology. There seemed to be a clear specificity for PGs with the ring features of PGE, that is, 9-keto, 11-hydroxy substitutions. PGD is similar to PGE, with 9-hydroxy, 11-keto substitutions, however, PGD treatments did not lead to deposition of substantial numbers of eggs. Hence, it would be postulated that PGs release egg-laying behavior via a specific receptor.

Oviposition behavior in *T. commodus* is a complex operation involving sense cells in the ovipositor used to assess the quality of an egg-laying substrate, followed by fertilization and inserting the ovipositor deep into the substrate. Eggs are moved into the substrate by oviduct musculature. As mentioned just above, males tend to guard their female partners until they have deposited their eggs, a behavior thought to reduce sperm competition because mated females remain receptive to other males even though they do not respond to calling songs. By analogy to the mammalian uterus, it was thought that PGs release oviposition behavior by stimulating contractions of the oviduct musculature. This idea was laid to rest by Loher (1984) and by Cook et al. (1984), who reported that PGs do not stimulate contractions of oviduct muscles in the cockroach, *Leucophaea maderae*. The *T. commodus* oviposition behavioral program is located in the terminal abdominal ganglion. The current untested hypothesis is that PGE₂ releases the oviposition via interactions with a PGE₂ receptor located in the terminal abdominal ganglion.

Prostaglandins act in releasing oviposition behavior in a few other insect species, including the 28 spotted ladybird, the rice brown planthopper and possibly the silk moth, all reviewed in Stanley (2000). Beyond this, PGs have been recorded in the female reproductive tracts of several insect species and mating leads to increases in PG titers (Stanley, 2000). Machado et al. (2007) were the first to report on a biological role for PGs within female reproductive tracts. They cultured ovarioles from the silk moth, *Bombyx mori* (Daizo strain), then determined the influence of PG biosynthesis inhibitors on ovarian development. *B. mori* ovarioles can be cultured *in vitro* and they can enter and complete choriogenesis autonomously. Machado et al. (2007) showed that treating cultured ovarioles with aspirin and other inhibitors of PG biosynthesis sharply reduced choriogenesis and the inhibitory influence could be reversed by adding PGF_{2α} to the cultures. They also used a commercial polyclonal antibody in western blots to record the presence of a COX protein, which increased as oogenesis moved toward choriogenesis. Thus, PGF_{2α} acts in ovarian development in *B. mori* and likely other insects. This is a specific PG action, which presumably takes place via a specific receptor.

The Machado research group has a long history of research on their model insect, the blood-sucking bug, *Rhodnius prolixus*. They reported on the roles of PGs and other eicosanoids in immune reactions of *R. prolixus* and the mosquito *Anopheles albimanus*, which we will discuss in the immunity section of this article (de Medeiros et al., 2009). They recently reported that fungal infection increased production of PGE₂ in *R. prolixus* and that the increased PGE₂ titers led to arrest of oogenesis in adult females. This work connects PG actions to the growing understanding of

ecological immunity, which informs understanding that immune reactions to infection and invasion entail considerable fitness costs, including reduced reproductive capacity (Rolff and Siva-Jothy, 2003). The positive influence of $\text{PGF}_{2\alpha}$ on ovarian development in *B. mori* and the inhibitory effect of PGE_2 on oogenesis in *R. prolixus* prompt the hypothesis that these two PGs exert opposite effects on ovarian development. The concept of two PGs exerting opposite effects within a single system is solidly based in the biomedical background, because each of the PGs has its individual receptor. Here we suggest insect ovarian tissues similarly express individual receptors allowing two PGs to express opposite effects. Recognizing the hypothesis suffers from recording the opposite effects in two insect species, it remains a testable idea.

PROSTAGLANDINS IN ION TRANSPORT PHYSIOLOGY

Prostaglandins influence ion transport physiology in invertebrates and in at least three insect ion transporting tissues, salivary gland, Malpighian tubules and rectum (Stanley, 2000). In the first suggestion that PGs act in insect biology, Dalton (1977a) reported that PGE_1 did not alter basal fluid secretion rates in salivary glands isolated from the blowfly, *Calliphora erythrocephala*, but did attenuate the normal stimulating influence of serotonin on fluid secretion rates. Serotonin influences fluid secretion via interaction with a cell surface receptor that increases intracellular cAMP concentrations. The attenuating effect of PGE_1 could be due to decreasing activity of adenylate cyclase, the enzyme responsible for cAMP production or by stimulating phosphodiesterase, the enzyme that metabolizes cAMP into an inactive form. Dalton (1977b) concluded that PGE_1 does not influence phosphodiesterase, but slows adenylate cyclase. This work added PGs to the biochemicals known to influence ion transport in insects, but the work was not carried forward, probably because a theoretical basis for PG actions in insect biology had not yet been established.

Petzel and Stanley-Samuelson (1992) hypothesized that PGs modulate fluid secretion rates in Malpighian tubules in female mosquitoes, *Aedes aegypti*. They used the classical Ramsey assay in which isolated sets of five Malpighian tubules in 20 μl saline drops were placed under light paraffin oil. Individual tubules were drawn into the oil. Fluid excreted by the tubules was visible in the oil and measured under a microscope. The experimental work showed that specific inhibitors of PG biosynthesis slowed the basal fluid secretion rates, while inhibitors of LOXs or epoxygenases did not influence fluid secretion. They concluded that PGs modulate basal fluid secretion in mosquito Malpighian tubules. In follow-up work, they used immunohistochemistry to localize PGE_2 in principal, but not stellate cells, within Malpighian tubules and also recorded the presence of AA in phospholipids, but not neutral lipids, prepared from isolated Malpighian tubules (Petzel et al., 1993). Using Ramsay procedures modified for very small insects, Van Kerkhove et al. (1995) reported that inhibitors of PG biosynthesis, but not inhibitors of LOXs or epoxygenase, severely restricted basal fluid secretion in Malpighian tubule preparations from the forest ant, *Formica polyctena*. Again, the authors concluded that PGs modulate Malpighian tubule fluid secretion in insects.

The insect rectum makes up a major component of insect renal function, acting to transport water and selected metabolites from

the rectal lumen back into hemolymph. The rectum of the locust, *Locusta migratoria*, is large enough to set up in an everted sac preparation to directly investigate regulation of rectal transport functions. Radallah et al. (1995) reported that treating everted rectal sacs with AA or with PGE_2 led to dose-dependent increases in fluid reabsorption. The experimental dosages were well within a physiological range (10^{-9} – 10^{-6} M) and similar treatments also led to increased intracellular Ca^{++} concentrations and increased phospholipase C activity. This work allows the hypothesis that PGE_2 acts via a specific receptor to stimulate the phospholipase C-driven signal pathway.

Salivary glands of the tick, *Amblyomma americanum*, and other tick species, produce copious amounts of PGs, which are injected into their hosts, along with salivary gland secretions which may also contain various pathogens. The PGs facilitate blood feeding by down-regulating host immune responses to the presence of the tick. The salivary glands also are responsible for renal functions during blood feeding on vertebrate hosts by injecting water and ions back into their hosts. The renal functions are regulated in part by PGE_2 , which acts via a specific receptor. Qian et al. (1997) used classical binding protocols to investigate a PGE_2 receptor from salivary glands of the tick, *A. americanum*. The receptor meets all criteria of a specific PG receptor. It is specific to PGE_2 , is reversible and is saturable. PGE_2 acts through this receptor to mediate two physiological processes in tick salivary glands. PGE_2 acts in salivary secretions and acts in receptor-mediated protein exocytosis (Qian et al., 1998). This work firmly establishes a PG receptor in tick renal function. Taken with all the work on the roles of PGs in fluid secretion, just described, we assert that PG-producing invertebrates also express GPCRs for the PGs. We turn, now, to insect immunity, another area of insect biology in which a specific PG receptor operates.

PROSTAGLANDINS AND OTHER EICOSANOIDS ACT IN INSECT IMMUNITY

Insects and other invertebrates have served as research model systems since the beginning of immunological research. For a couple of examples, Elie Metchnikoff, a Russian embryologist, placed splinters into the transparent bodies of bipinnaria stage starfish, and later observed phagocytes surrounding the splinter. Aside from the early work on vaccines, this is probably the first experiment in immunology. Another Russian, Serguei Metelnikov worked in the Pasteur Institute, where he conducted research on insect immunity in the 1920s. He is regarded as one of the founders of insect immunology.

Insects lack the antibody-based adaptive immune systems seen in vertebrates. Insect immunity is exclusively innate, that is, a naturally occurring, non-specific immunity that does not depend on previous infection experience. Nonetheless, insect immunity is a highly effective protection system. Insect immunology is studied from several perspectives. Direct studies of immune functions forms the basis of a large literature on the cellular and molecular mechanisms of immunity, and immune signaling, some of which has also guided biomedical research into mammalian immunity. The significance of research into insect immunity is underscored by recognition of Professor Jules Hoffmann, who led research into *Drosophila* immunity, with a share of the 2011 Nobel Prize

in Physiology or Medicine “for their discoveries concerning the activation of innate immunity.” Immune functions are biologically expensive and studies of ecological immunity are revealing physiological trade-offs, in which biologically expensive immune functions are traded off for other biological functions, including reproduction and migrations (Rolff and Siva-Jothy, 2003). For a single example, Schmid et al. (2008) reported that adult honeybees abandon cellular-based immunity in favor of prophenoloxidase-based immunity when they reach the foraging stage of their behavioral ontology. All this research highlights the breadth and depth of insect immunology, which is now beyond the capacity of individuals or even groups to comprehensively review. Let us begin with a brief glance of insect immune functions.

Insect integuments serve as exoskeletons and also as physical barriers to infectious agents. The gastrointestinal tract is a common entry to insect bodies, although it is not a completely open door for them. Insects express epithelial immunity in salivary glands (Abdelsadik and Roeder, 2010), guts (Cronin et al., 2009), Malpighian tubules (Davies and Dow, 2009), and tracheal epithelia (Wagner et al., 2008) of *Drosophila*. Epithelial immunity is a humoral response, based on induced expression of genes encoding anti-microbial peptides. After infectious agents get into hemolymph circulation, internal signaling coordinates and mediates humoral and cellular immune reactions. Humoral reactions, again, involve biosynthesis of anti-microbial peptides, the enzyme lysozyme and release of prophenoloxidase (PPO) from circulating encyotoids, a type of hemocyte. These peptides appear in the hemolymph of infected insects about 6–12 h post-infection (PI). Far more detailed descriptions of humoral immunity, including non-self surveillance and the signaling pathways that lead to anti-microbial peptide expression are available (Lemaitre and Hoffmann, 2007).

The hemolymph of most insects contains approximately $4\text{--}6 \times 10^6$ circulating hemocytes per ml. The main immune effector cells of Lepidoptera are plasmatocytes and granulocytes. These cells clear microbes from circulation by phagocytosis and a process called nodulation, a form of encapsulation. Nodulation begins with microaggregation of hemocytes with adhering microbes (Figure 3A), which grow into nodules. In the last phase of nodulation, plasmatocytes surround the nodule and activate a PPO system that melanizes nodules, which are finally attached to an internal organ or inner body wall. The darkened nodules remain in the body for the life of the insect and they are easily visible at $40\times$ (Figure 3B). Nodulation is responsible for clearing the majority of infecting microbes from circulation (Dunn and Drake, 1983). Invaders too large for phagocytosis, such as parasitoid eggs, are encapsulated in layers of hemocytes within resistant insects. These also are melanized and attached to the inner body wall or an internal organ. The melanization process produces reactive oxygen forms that may directly kill the invaders. Numbers of circulating hemocytes decline sharply during cellular responses and are replaced by hematopoiesis that takes place in small hematopoietic organs typically located in abdomens, but also in the thorax of some species. Millions of hemocytes may be invested in responses to a single infection event, which emphasizes the biological costs of hemocytic immunity (Stanley, 2006).

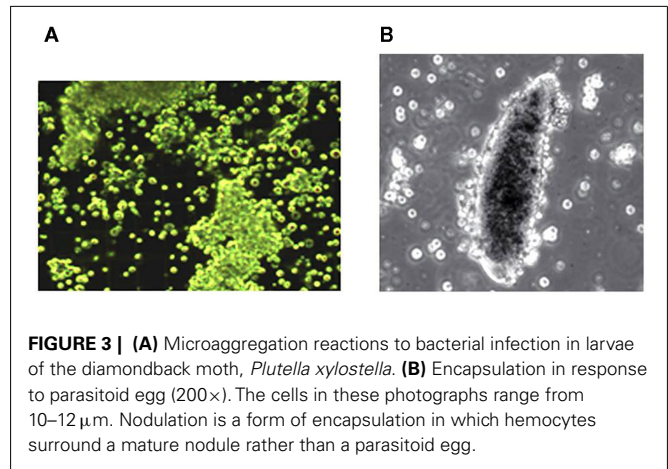


FIGURE 3 | (A) Microaggregation reactions to bacterial infection in larvae of the diamondback moth, *Plutella xylostella*. **(B)** Encapsulation in response to parasitoid egg (200 \times). The cells in these photographs range from 10–12 μm . Nodulation is a form of encapsulation in which hemocytes surround a mature nodule rather than a parasitoid egg.

Stanley-Samuelson and his colleagues investigated the hypothesis that eicosanoids mediate insect hemocytic immunity. They reported that injecting tobacco hornworms, *Manduca sexta*, with pharmaceutical inhibitors of eicosanoid biosynthesis (the non-steroidal anti-inflammatory drugs, NSAIDs) impaired the ability to clear injected bacteria from hemolymph circulation (Stanley-Samuelson et al., 1991). As all experiments were conducted within 2–4 h PI, it was suggested that eicosanoids mediated cellular, as opposed to humoral, immune reactions. A second paper reported that treating hornworms with inhibitors of eicosanoid biosynthesis impaired microaggregation and nodulation reactions to bacterial infection (Miller et al., 1994). These ground-breaking papers opened several lines of research. In one, several investigations of eicosanoid biochemistry documented the presence of eicosanoid precursor fatty acids in virtually all insects, recorded biosynthesis of PGs and other eicosanoids and demonstrated the presence of phospholipase A_2 (PLA $_2$) activity in immune and other insect tissues. These biochemical studies are beyond the scope of this article and specific citations more detailed reviews can be found elsewhere (Stanley, 2000, 2005, 2006; Stanley et al., 2009).

The biochemical work supported research into the influence of immune challenge on PLA $_2$ activity and PG biosynthesis. Jurenka et al. (1999) reported that bacterial infection increased biosynthesis of PGF $_{2\alpha}$ in true armyworms, *Pseudaletia unipuncta*, at 30 min post-infection. This work bolstered the idea that PGs and other eicosanoids are key mediators of insect cellular immunity. Later several authors reported that infection stimulated increased PLA $_2$ activity in tobacco hornworms (Tunaz et al., 2003), in whole flies, *Sarcophaga peregrine* (Yajima et al., 2003), in beet armyworms, *Spodoptera exigua* (Shrestha and Kim, 2007), and in the red flour beetle, *Tribolium castaneum* (Shrestha and Kim, 2010). Together, these publications allow a generalization that PLA $_2$ acts in insect cellular immunity.

In the context of PG receptors, we now consider specific cellular actions mediated by eicosanoids. In the early work, Miller et al. (1994) showed that eicosanoids mediate microaggregation and nodulation reactions to bacterial infection. Mandato et al. (1997) enhanced the list of eicosanoid-mediated actions, with their report that eicosanoids act in PPO activation, phagocytosis and cell spreading in larval *Galleria mellonella*. The influence

of eicosanoids on PPO activation is quite interesting because eicosanoids do not activate PPO in other species, such as a locust, *L. migratoria* (Goldsworthy et al., 2003). Figueiredo et al. (2008) also showed that inhibiting PLA₂ substantially reduced phagocytosis of the protozoan parasite, *Trypanosoma rangeli*, by *R. prolixus* hemocytes and that the inhibition was reversed by treating *R. prolixus* with AA. They concluded that eicosanoids mediate phagocytosis in *Rhodnius* and that *T. rangeli* somehow inhibited eicosanoid biosynthesis. Carton et al. (2002) reported that the PLA₂-inhibiting glucocorticoid, dexamethasone, inhibited encapsulation of parasitoid eggs in a resistant line of *D. melanogaster*. Similarly, Miller (2005) confirmed eicosanoid actions in *M. sexta* plasmacyte spreading. Hemocyte adhesion is crucial in clearing infecting bacteria from circulation. Marin et al. (2005) reported that AA increased adhesion of *G. mellonella* granulocytes, but not plasmacytes, to a glass surface. More recently, Merchant et al. (2008) reported that eicosanoids influence tobacco hornworm hemocyte migration in Boyden chambers. This may be a specific PG function because a LOX inhibitor, esculetin, did not influence hemocyte migration. Finally, Shrestha and Kim (2008) discovered that eicosanoids mediate release of PPO from encyctoids by inducing cell lysis in *S. exigua*. Hence, we have a list of specific eicosanoid actions beginning with microaggregation, encapsulation and nodulation as a form of encapsulation. These are large-scale, visible actions, each involving a large, but unknown number of discrete cell steps. For example, phagocytosis is a very complex action, which in *Drosophila* S2 cells involves at least 184 genes (Stroschein-Stevenson et al. (2006). Cell spreading and migration are similarly complex, although we do not have a direct comparator with respect to numbers of genes. We conclude that eicosanoids are crucial to the mediation and coordination of insect cellular immunity, but they exert their actions in concert with other biochemical signal systems, including biogenic amines and insect cytokines. Recent work suggests how eicosanoids interacts with other signal systems.

There are reports of specificity also in the broad groups of eicosanoids acting in immune functions. Lord et al. (2002) reported that eicosanoids, specifically LOXs products, but not by PGs, act in cellular immunity to the insect fungal pathogen, *Beauveria bassiana*. Similarly, PGs, but not LOXs products, appear to mediate microaggregation reactions to bacterial infection in isolated hemocyte preparations (Phelps et al., 2003). These reports also point to specific eicosanoid receptors, although the operational receptors have not been identified.

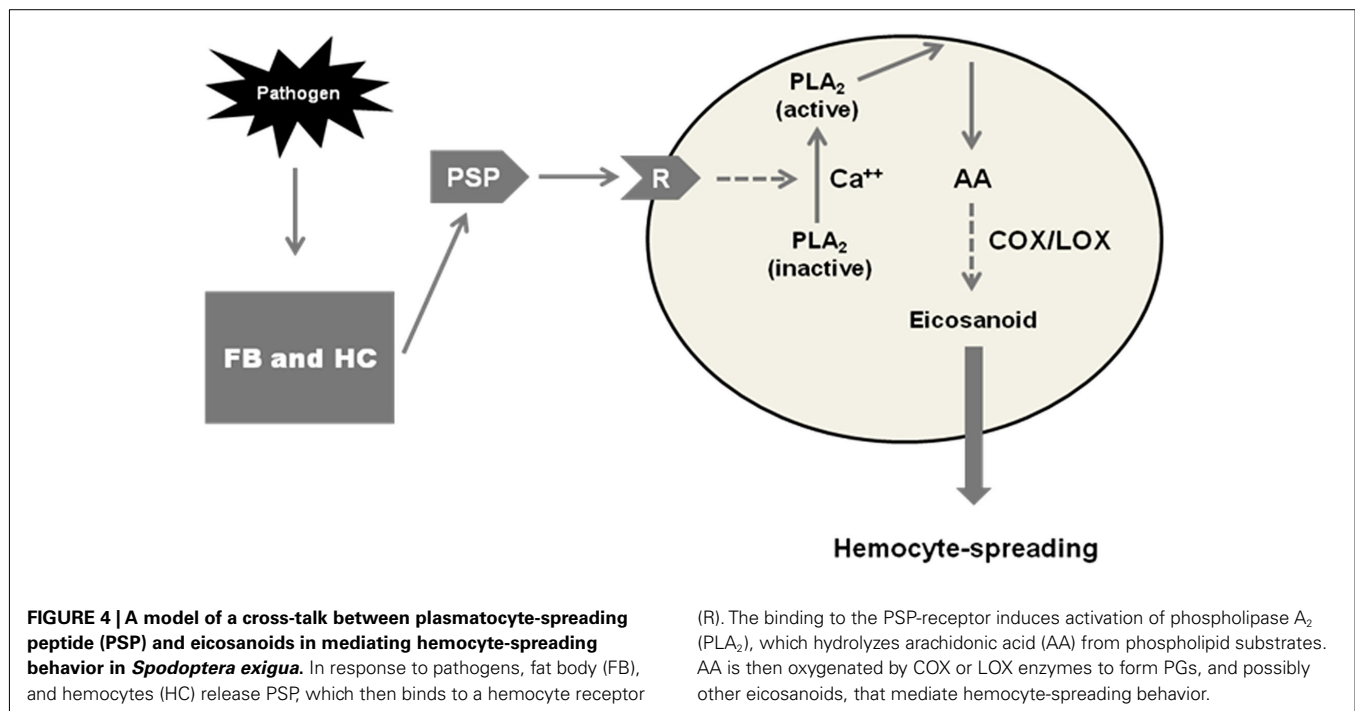
Baines et al. (1992) reported that two biogenic amines, octopamine (OA) and 5-hydroxy-tryptamine (5-HT), mediate phagocytosis and nodulation reactions to bacterial infection in the cockroach, *Periplaneta americana*, and subsequently showed that 5-HT acts through a GPCR that influences adenylate cyclase (Baines and Downer, 1992). Kim et al. (2009) were the first to investigate the intracellular interactions between eicosanoids and the biogenic amines in insect immunity. They showed that OA and 5-HT independently mediated phagocytosis and nodulation reactions in larvae of the lepidopteran, *S. exigua*. Two monoamine receptor antagonists, phentolamine and ketanserin, inhibited phagocytosis and nodulation and treating experimental larvae with the eicosanoid precursor fatty acid, AA, reversed

the inhibitory influence of the receptor antagonists. Similarly, the mediating influence of OA and 5-HT on phagocytosis and nodulation was inhibited in larvae treated with dexamethasone, a PLA₂ inhibitor that blocks all eicosanoid biosynthesis. The authors concluded that the immune-mediating influence of biogenic amines is expressed through stimulation of eicosanoid biosynthesis. This work demonstrated a solid intracellular connection between the actions of biogenic amines and eicosanoids in two cellular immune functions, phagocytosis and nodulation. This example of cross-talk between biogenic amine and eicosanoid signaling probably represents a common feature of signaling in insect immunity.

Plasmacyte-spreading peptide (PSP) is an insect cytokine, first identified in the soybean looper, *Pseudoplusia includens* (Clark et al., 1997). Pro-PSP is activated by cleavage into a 23-residue PSP that mediates plasmacytes spreading (PS; Clark et al., 1998). PSP acts through an approximately 190 kDa receptor to induce PS (Clark et al., 2004). PS is a crucial action in insect innate immunity. The process of nodule formation following microbial infection is completed by plasmacytes which spread over mature nodules, then activate a PPO to form a melanized, dark layer that completely encapsulates nodules. Plasmacyte spreading also acts in responses to wounding by spreading over wounds to participate in hemolymph clotting. PSP likely occurs in all insects that express cellular immune reactions because the *P. includens* PSP also acts in other lepidopterans, including *S. exigua* (Kim et al., 2008).

Srikanth et al. (2011) investigated the possible cross-talk between PSP and eicosanoid signaling in *S. exigua*. They showed that both PSP and PGE₂ independently mediate hemocyte spreading, that pharmaceutical inhibitors of PLA₂ inhibit hemocyte spreading in a dose-dependent manner and the same inhibitors inhibit PSP-stimulated hemocyte spreading, also in a dose-dependent manner. After cloning and sequencing the *S. exigua* gene encoding PSP, they showed that dsRNA designed to silence the gene effectively impaired cell spreading. The impairing influence of the dsRNA was rescued, in separate experiments, by treating dsRNA-injected larvae with AA and with PSP. The authors proposed a model (Figure 4) depicting the cross-talk between PSP and eicosanoid signaling. Infection stimulates production of activated PSP, which interacts with hemocytes through the PSP receptor. The PSP-receptor interaction activates a PLA₂, which in turn stimulates PGE₂ biosynthesis. The PSP-stimulated PGE₂ biosynthesis leads to plasmacytes spreading. This is another example of the cross-talk between eicosanoid and other signaling systems. This cross-talk between PSP and biogenic amine signaling establishes eicosanoids as an integral element of immune signaling in insect biology. The eicosanoid actions discussed in this section operate on the assumption of specific receptors for PGs and possibly other eicosanoids. Let us move on to the recent appreciation of a specific PG receptor operating in an *S. exigua* immune response.

Phenoloxidase (PO) is responsible for the melanization reactions to infection in insect and other invertebrates. These reactions are an enzyme-based element of humoral immune responses to infection, invasion and wounding. POs also act in other areas of insect biology, including tanning during post-embryonic development. Recent work on honeybee immunity emphasizes the significance of PO-based immunity, showing that adult honeybees abandon hemocytic immunity as they enter the foraging phase



of behavioral ontogeny; their PO-based immunity remains intact and even increases during foraging phase (Schmid et al., 2008). Inactive PPO is activated into PO by a series of serine proteases. In *S. exigua*, and likely most lepidopterans, PPO is produced and stored in specialized hemocytes, the encytoplasts. PPO is released from encytoplasts into hemolymph circulation by lysis and the lysis action is mediated by eicosanoids (Shrestha and Kim, 2008).

Shrestha et al. (2011) went on to show that a specific eicosanoid, PGE₂, is responsible for encytoplast lysis. PGE₂ acts through a GPCR, which they cloned and denoted Se-hcPGGPCR1. The receptor is expressed in all life stages, although rather faintly in eggs. Within larvae, it is expressed in hemocytes and gut, but not fat body or epidermis. Fluorescence *in situ* hybridization showed that the receptor is expressed in encytoplasts, but not the other hemocyte types, including the more abundant plasmatocytes and granulocytes. The receptor is constitutively expressed in low levels, which are increased following infection. PGE₂ also mobilizes intracellular Ca⁺⁺ during lysis (Shrestha and Kim, 2009). Shrestha et al. (2011) used a Ca⁺⁺ mobilization assay to establish a functional link between PGE₂ and Se-hcPGGPCR1. They used hemocytes prepared from *S. exigua* larvae that were untreated (controls) or injected with dsRNA specific to Se-hcPGGPCR1. PGE₂ treatments increased intracellular Ca⁺⁺ concentrations in a dose-dependent manner over the physiological range of 10⁻¹²–10⁻⁴ M in untreated control hemocyte preparations and in dsRNA treated preparations. Ca⁺⁺ mobilization was significantly reduced in the experimental preparations in which the gene encoding hcPGGPCR1 was silenced.

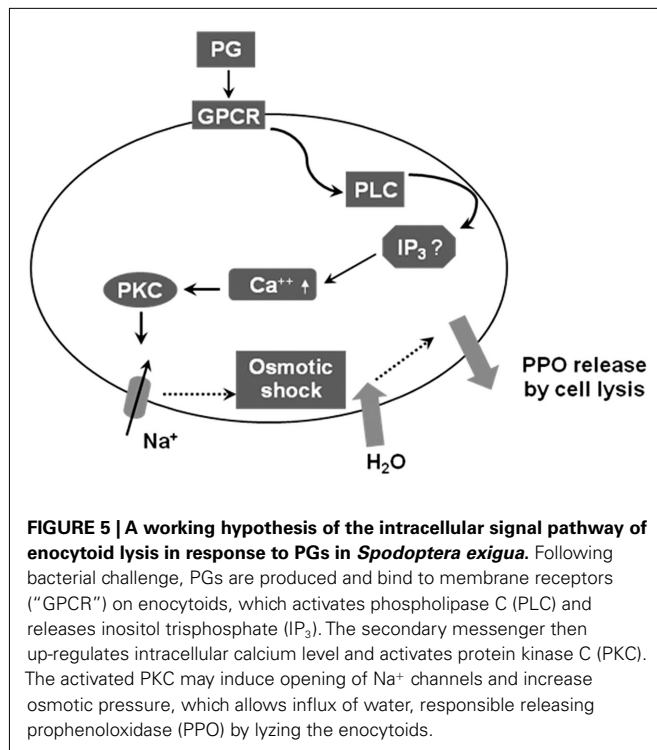
Downstream signaling of PGE₂ receptor binding was analyzed in encytoplast cell lysis (Shrestha and Kim, 2009). U-73122 (a specific inhibitor of phospholipase C) inhibited encytoplast lysis of

S. exigua significantly after bacterial infection. EGTA (a calcium chelator) treatment inhibited the cell lysis. Thus the encytoplast lysis depends on calcium signaling in response to PGE₂. Two PKC inhibitors (staurosporine and calphostin C) significantly inhibited the encytoplast lysis. Encytoplast lysis was likely induced by Na⁺ entry and subsequent osmotic shock because juvenile hormone analog, pyriproxyfen, which activates Na⁺–K⁺ ATPase and induces subsequent cell shrinkage, antagonized the effect of eicosanoid on cell lysis. Furthermore, ouabain (a specific Na⁺ pump inhibitor) significantly inhibited encytoplast lysis. These results suggest that eicosanoids mediate encytoplast lysis by activating the intracellular PKC pathway (Figure 5).

The specificity of PG actions in reproduction, fluid secretion and in encytoplast lysis supports the view that PG actions in insect biology are mediated via specific receptors. PGs express two general actions in cells. In one, they modulate homeostatic functions, such as basal fluid secretion rates, ovarian development and immune reactions. In another, PGs also influence expression of specific genes and proteins. Stanley et al. (2008) reported that challenging a cell line established from *Helicoverpa zea* (HzAM1 cells) with PGA₁ and PGE₁ led to changes in protein expression. The affected proteins included proteins in lipid metabolism, signal transduction, protection, cell functions and metabolism, however, each of the two PGs exerted different influences on protein expression. The specificity of the PG effects on protein expression also supports the view that PGs act through specific receptors.

SOME MICROBES CRIPPLE INSECT IMMUNITY VIA INHIBITION OF PLA₂

We close this article by looking at PG and other eicosanoid signaling from the perspective of some microbes. The point here is the



microbes produce and secrete compounds specifically tailored to the active sites of some PLA₂s. As described earlier, the first step in eicosanoid biosynthesis is a PLA₂ step that hydrolyzes AA from cellular phospholipid pools.

The entomopathic nematode, *Steinernema carpocapsae*, is a mutualistic symbiont with the bacterium, *Xenorhabdus nematophila*, a member of the family Enterobacteriaceae. After entering an insect body, free-living, non-feeding juvenile nematodes void *X. nematophila* into the hemolymph. The bacteria rapidly proliferate and kill the insect host. The freshly killed insect body serves the mutualistic nematode partner in two ways. First, the insect cadaver provides the nematode with an appropriate microhabitat to complete development and reproduce, supplying nutrients and restricting growth of other microbes. Second, *X. nematophila* protects the nematode from hemocytic encapsulation by impairing the host immune reactions to the foreign nematode. In their research into the beet armyworm, *S. exigua*, Park and Kim (2000) first suggested that the bacterium impairs host immunity by inhibiting eicosanoid biosynthesis. Outcomes of their experiments documented that treating the nematode-challenged host larvae with AA reduced mortality by about 40%. Deeper research revealed that *X. nematophila* produces and secretes heat-labile factors that directly inhibit secretory PLA₂ (sPLA₂) in the host. Moving beyond *S. exigua*, Park et al. (2003) reported that *X. nematophilus* similarly suppresses cellular immune reactions to infection by blocking eicosanoid biosynthesis in *M. sexta*. The bacterial inhibitory factor(s) occurred in the organic fraction of the bacterial culture medium and, as seen in the first experiment of Park and Kim (2000), the influence of the factor on cellular immunity was reversed by treating

experimental hornworms with AA. In direct experiments with isolated sPLA₂s, the authors demonstrated the bacterial factors are potent sPLA₂ inhibitors: they inhibit sPLA₂s from insect, prokaryotic and vertebrate sources (Park et al., 2004). The immunosuppressive action of the bacterium goes beyond Lepidoptera, to at least one cricket species, *Gryllus firmus* (Park and Stanley, 2006). Kim et al. (2005) showed that a related bacterium, *Photorhabdus temperata* (also a mutualistic partner of nematodes) similarly inhibits PLA₂ and nodulation in its host, *S. exigua*. The authors suggested that bacteria in the genera *Xenorhabdus* and *Photorhabdus* generally share the ability to inhibit PLA₂ in their hosts. The Enterobacteriaceae is a fairly large family of bacteria and it is not unreasonable to suppose other bacterial species in this family also impair insect host immunity by inhibition sPLA₂s.

The strategy of impairing host immunity via compromising eicosanoid biosynthesis is not limited to bacteria. Garcia et al. (2004) described the results of a subtle experiment in this area. They first fed fifth-instar blood-sucking bugs, *R. prolixus*, on blood containing juveniles of the protozoan *T. rangeli*. *T. rangeli* is non-pathogenic protozoan parasite of *R. prolixus*. A few days later, they injected additional *T. rangeli* into the insects. This double treatment resulted in reduced hemocyte phagocytosis and increased host mortality. These effects were reversed in experiments in which protozoans were co-injected with AA (at 10 µg/insect). The authors inferred that oral infection with *T. rangeli* inhibits the release of AA for eicosanoid biosynthesis. They also found that adding the glucocorticoid, dexamethasone, (which inhibits PLA₂ in an indirect manner) to the blood meals of *R. prolixus* inhibited phagocytosis. The inhibition was reversed by treating experimental *R. prolixus* larvae with AA or, separately, with platelet activating factor, a specialized phospholipid (Figueiredo et al., 2008). They also showed that *T. rangeli* cells inhibit phagocytosis and the inhibition was reversed by AA treatments. They used a fluorometric assay to determine that *T. rangeli* cells inhibit PLA₂ activity in *R. prolixus* hemocytes. This work shows that the protozoan parasite suppresses a host immune function, phagocytosis, by targeting the active site of PLA₂s that act in eicosanoid biosynthesis.

These findings support a broader generalization. Infectious organisms have evolved a very wide range of strategies to avoid or suppress insect immunity, most of which are outside the scope of this paper. These many strategies emerged from the tremendous selection forces on invaders. The fact that some of the invaders operate by inhibiting a key enzyme in eicosanoid signaling is a convincing argument that eicosanoids are crucial mediators of insect immunity.

ACKNOWLEDGMENTS

Thanks to Dr. Joe Hull, USDA/ARS, for the invitation to write this article. Mention of trade names or commercial products in this article is solely for the purpose of providing specific information and does not imply recommendation or endorsement by the U.S. Department of Agriculture. All programs and services of the U.S. Department of Agriculture are offered on a non-discriminatory basis without regard to race, color, national origin, religion, sex, age, marital status, or handicap.

REFERENCES

- Abdelsadik, A., and Roeder, T. (2010). Chronic activation of the epithelial immune system of the fruit fly's salivary glands has a negative effect on organismal growth and induces a peculiar set of target genes. *BMC Genomics* 11, 265. doi:10.1186/1471-2164-11-265
- Baines, D., DeSantis, T., and Downer, R. G. H. (1992). Octopamine and 5-hydroxytryptamine enhance the phagocytic and nodule formation activities of cockroach (*Periplaneta americana*) hemocytes. *J. Insect Physiol.* 41, 905–914.
- Baines, D., and Downer, R. G. H. (1992). 5-Hydroxytryptamine-sensitive adenylate cyclase affects phagocytosis in cockroach hemocytes. *Arch. Insect Biochem. Physiol.* 21, 303–316.
- Benedum, J. (1999). The early history of endocrine cell transplantation. *J. Mol. Med.* 77, 30–35.
- Bergström, S., Ryhage, R., Samuelson, B., and Sjövall, J. (1962). The structure of prostaglandin E, F1 and F2. *Acta Chem. Scand.* 16, 501–502.
- Bhattacharya, M., Varma, D. R., and Chemtob, S. (1999). Nuclear prostaglandin receptors. *Gene Ther. Mol. Biol.* 4, 323–338.
- Blenau, W., and Baumann, A. (2001). Molecular and pharmacological properties of insect biogenic amine receptors: lessons from *Drosophila melanogaster* and *Apis mellifera*. *Arch. Insect Biochem. Physiol.* 48, 13–38.
- Breyer, R. M., Bagdassarian, C. K., Myers, S. A., and Breyer, M. D. (2001). Prostanoid receptors: subtypes and signaling. *Annu. Rev. Pharmacol. Toxicol.* 41, 661–690.
- Carton, Y., Frey, F., Stanley, D. W., Vass, E., and Nappi, A. J. (2002). Dexamethasone inhibition of the cellular immune response of *Drosophila melanogaster* against a parasitoid. *J. Parasitol.* 288, 405–407.
- Clark, K. D., Garczynski, S. F., Arora, A., Crim, J. W., and Strand, M. R. (2004). Specific residues in plasmatocyte-spreading peptide are required for receptor binding and functional antagonism of insect human cells. *J. Biol. Chem.* 279, 33246–33252.
- Clark, K. D., Pech, L. L., and Strand, M. R. (1997). Isolation and identification of a plasmatocyte-spreading peptide from the hemolymph of the lepidopteran insect *Pseudoplusia includens*. *J. Biol. Chem.* 272, 23440–23447.
- Clark, K. D., Witherell, A., and Strand, M. R. (1998). Plasmatocyte spreading peptide is encoded by an mRNA differentially expressed in tissues of the moth *Pseudoplusia includens*. *Biochem. Biophys. Res. Commun.* 250, 479–485.
- Cook, B. J., Holman, G. M., and Meola, S. (1984). The oviduct musculature of the cockroach *Leucophaea maderae* and its response to various neurotransmitters and hormones. *Arch. Insect Biochem. Physiol.* 1, 167–178.
- Corey, E. J., Albright, J. O., Barton, A. E., and Hashimoto, S. (1980). Chemical and enzymic synthesis of 5-HPETE, a key biological precursor of slow-reacting substance of anaphylaxis (SRS) and 5-HETE. *J. Am. Chem. Soc.* 102, 1435–1436.
- Cronin, S. J. F., Nehme, N. T., Limer, S., Liegeois, S., Pospisilik, J. A., Schramek, D., Leibbrandt, A., de Matos Simoes, R., Gruber, S., Puc, U., Ebersberger, I., Zoranovic, T., Neely, G. G., von Haeseler, A., Ferrandon, D., and Penninger, J. M. (2009). Genome-wide RNAi screen identifies genes involved in intestinal pathogenic bacterial infection. *Science* 325, 340–343.
- Dalton, T. (1977a). Threshold and receptor reserve in the action of 5-hydroxytryptamine on the salivary glands of *Calliphora erythrocephala*. *J. Insect Physiol.* 23, 625–631.
- Dalton, T. (1977b). The effect of prostaglandin E1 on cyclic AMP production in the salivary glands of *Calliphora erythrocephala*. *Experientia* 33/10, 1329–1330.
- Davies, S.-A., and Dow, J. A. T. (2009). Modulation of epithelial innate immunity by autocrine production of nitric oxide. *Gen. Comp. Endocrinol.* 162, 113–121.
- de Medeiros, M. N., Belmonte, R., Soares, B. C. C., de Medeiros, L. N., Canetti, C., Freire-de-Lima, C. G., Maya-Monteiro, C. M., Bozza, P. T., Almeida, I. C., Masuda, H., Kurtensch, E., and Machado, E. A. (2009). Arrest of oogenesis in the bug *Rhodnius prolixus* challenged with the fungus *Aspergillus niger* is mediated by immune response-derived PGE2. *J. Insect Physiol.* 55, 151–158.
- Destephano, D. B., and Brady, U. E. (1977). Prostaglandin and prostaglandin synthetase in the cricket, *Acheta domesticus*. *J. Insect Physiol.* 23, 905–911.
- Dunn, P. E., and Drake, D. R. (1983). Fate of bacteria injected into naïve and immunized larvae of the tobacco hornworm *Manduca sexta*. *J. Invertebr. Pathol.* 41, 77–85.
- Figueiredo, M. B., Genta, F. A., Garcia, E. S., and Azambuja, P. (2008). Lipid mediators and vector infection: *Trypanosoma rangeli* inhibits *Rhodnius prolixus* hemocyte phagocytosis by modulation of phospholipase A2 and PAF-acetylhydrolase activities. *J. Insect Physiol.* 54, 1528–1537.
- Garcia, E. S., Machado, E. M. M., and Azambuja, P. (2004). Inhibition of hemocyte microaggregation reactions in *Rhodnius prolixus* larvae orally infected with *Trypanosoma rangeli*. *Exp. Parasitol.* 107, 31–38.
- Goldsworthy, G., Mullen, L., Opoku-Ware, K., and Chandrakant, S. (2003). Interactions between the endocrine and immune systems in locusts. *Physiol. Entomol.* 28, 54–61.
- Hatae, N., Sugimoto, Y., and Ichikawa, A. (2002). Prostaglandin receptors: advances in the study of EP3 receptor signaling. *J. Biochem.* 131, 781–784.
- Jurenka, R. A., Pedibhotla, V. K., and Stanley, D. W. (1999). Prostaglandin production in response to a bacterial infection in true armyworm larvae. *Arch. Insect Biochem. Physiol.* 41, 225–232.
- Kim, G. S., Nalini, M., Kim, Y., and Lee, D.-W. (2009). Octopamine and 5-hydroxytryptamine mediate hemocytic phagocytosis and nodule formation via eicosanoids in the beet armyworm, *Spodoptera exigua*. *Arch. Insect Biochem. Physiol.* 70, 162–176.
- Kim, Y., Ji, D., Cho, S., and Park, Y. (2005). Two groups of entomopathogenic bacteria, *Photorhabdus* and *Xenorhabdus*, share an inhibitory action against phospholipase A2 to induce host immunodepression. *J. Invertebr. Pathol.* 89, 258–264.
- Kim, Y., Jung, S., and Madanagopal, N. (2008). Antagonistic effect of juvenile hormone on hemocyte-spreading behavior of *Spodoptera exigua* in response to an insect cytokine and its putative membrane action. *J. Insect Physiol.* 54, 909–915.
- Lemaitre, B., and Hoffmann, J. (2007). The host defense of *Drosophila melanogaster*. *Annu. Rev. Immunol.* 25, 697–743.
- Loher, W. (1979). The influence of prostaglandin E2 on oviposition in *Teleogryllus commodus*. *Entomol. Exp. Appl.* 25, 197–199.
- Loher, W. (1984). "Behavioral and physiological changes in cricket-females after mating," in *Advances in Invertebrate Reproduction*, Vol. 3, ed. W. Engels (London: Elsevier), 189–201.
- Loher, W., and Edson, K. (1973). The effect of mating on egg production and release in the cricket, *Teleogryllus commodus*. *Entomol. Exp. Appl.* 16, 483–490.
- Loher, W., Ganjian, I., Kubo, I., Stanley-Samuelson, D. W., and Tobe, S. S. (1981). Prostaglandins: their role in egg-laying in the cricket *Teleogryllus commodus*. *Proc. Natl. Acad. Sci. U.S.A.* 78, 7835–7838.
- Lord, J. C., Anderson, S., and Stanley, D. W. (2002). Eicosanoids mediate *Manduca sexta* cellular response to the fungal pathogen *Beauveria bassiana*: a role for the lipoxigenase pathway. *Arch. Insect Biochem. Physiol.* 51, 46–54.
- Machado, E., Swevers, L., Sdralia, N., Medeiros, M. N., Mello, F. G., and Iatrou, K. (2007). Prostaglandin signaling and ovarian follicle development in the silkworm, *Bombyx mori*. *Insect Biochem. Mol. Biol.* 37, 876–885.
- Mandato, C. A., Diehl-Jones, W. L., Moore, S. J., and Downer, R. G. H. (1997). The effects of eicosanoid biosynthesis inhibitors on propenoloxidase activation, phagocytosis and cell spreading in *Galleria mellonella*. *J. Insect Physiol.* 43, 1–8.
- Marin, D., Dunphy, G. B., and Mandato, C. A. (2005). Cyclic AMP affects the hemocyte responses of larval *Galleria mellonella* to selected antigens. *J. Insect Physiol.* 51, 575–586.
- Merchant, D., Ertl, R. L., Rennard, S. I., Stanley, D. W., and Miller, J. S. (2008). Eicosanoids mediate insect hemocyte migration. *J. Insect Physiol.* 54, 215–221.
- Miller, J. S. (2005). Eicosanoids influence in vitro elongation of plasmatocytes from the tobacco hornworm, *Manduca sexta*. *Arch. Insect Biochem. Physiol.* 59, 42–51.
- Miller, J. S., Nguyen, T., and Stanley-Samuelson, D. W. (1994). Eicosanoids mediate insect nodulation responses to bacterial infections. *Proc. Natl. Acad. Sci. U.S.A.* 91, 12418–12422.
- Park, Y., and Kim, Y. (2000). Eicosanoids rescue *Spodoptera exigua* infected with *Xenorhabdus nematophilus*, the symbiotic bacteria to the entomopathogenic nematode *Steinernema carpocapsae*. *J. Insect Physiol.* 46, 1469–1476.
- Park, Y., Kim, Y., Putnam, S. M., and Stanley, D. W. (2003). The bacterium *Xenorhabdus nematophilus* depresses nodulation reactions to infection by inhibiting eicosanoid biosynthesis in tobacco hornworm, *Manduca sexta*. *Arch. Insect Biochem. Physiol.* 52, 71–80.
- Park, Y., Kim, Y., and Stanley, D. W. (2004). The bacterium *Xenorhabdus nematophila* inhibits phospholipases

- A2 from insect, prokaryote and vertebrate sources. *Naturwissenschaften* 91, 371–373.
- Park, Y., and Stanley, D. W. (2006). The bacterium *Xenorhabdus nematophilus* impairs insect immunity by inhibition of eicosanoid biosynthesis in adult cricket, *Gryllus firmus*. *Biol. Control* 38, 247–253.
- Petzel, D. H., Parrish, A. K., Ogg, C. L., Witters, N. A., Howard, R. H., and Stanley-Samuelson, D. W. (1993). Arachidonic acid and prostaglandin E2 in Malpighian tubules of yellow fever mosquitoes. *Insect Biochem. Mol. Biol.* 23, 431–437.
- Petzel, D. H., and Stanley-Samuelson, D. W. (1992). Inhibition of eicosanoid biosynthesis modulates basal fluid secretion in the Malpighian tubules of the yellow fever mosquito (*Aedes aegypti*). *J. Insect Physiol.* 38, 1–8.
- Phelps, P. K., Miller, J. S., and Stanley, D. W. (2003). Prostaglandins, not lipoxygenase products, mediate insect microaggregation reactions to bacterial challenge in isolated hemocyte preparations. *Comp. Biochem. Physiol.* 136, 409–416.
- Qian, Y., Essenberg, R. C., Dillwith, J. W., Bowman, A. S., and Sauer, J. R. (1997). A specific prostaglandin E2 receptor and its role in modulating salivary secretion in the female tick, *Amblyomma americanum* (L.). *Insect Biochem. Mol. Biol.* 27, 387–395.
- Qian, Y., Yuan, J., Essenberg, R. C., Bowman, A. S., Shook, A. S., Dillwith, J. W., and Sauer, J. R. (1998). Prostaglandin E2 in the salivary glands of the female tick, *Amblyomma americanum* (L.): calcium mobilization and exocytosis. *Insect Biochem. Mol. Biol.* 28, 221–228.
- Radallah, D., Nogaro, M., and Fournier, B. (1995). Arachidonic acid and prostaglandin E2 stimulate phospholipase C activity in the rectum of the African locust, *Locusta migratoria migratorioides*. *J. Insect Physiol.* 41, 7–16.
- Rolf, J., and Siva-Jothy, M. T. (2003). Invertebrate ecological immunology. *Science* 301, 472–475.
- Schmid, M. R., Brockmann, A., Pirk, C. W. W., Stanley, D. W., and Tautz, J. (2008). Adult honeybees (*Apis mellifera* L.) abandon hemocytic, but not phenoloxidase-based immunity. *J. Insect Physiol.* 54, 439–444.
- Shrestha, S., and Kim, Y. (2007). An entomopathogenic bacterium, *Xenorhabdus nematophila*, inhibits hemocyte phagocytosis of *Spodoptera exigua* by inhibiting phospholipase A2. *J. Invertebr. Pathol.* 96, 64–70.
- Shrestha, S., and Kim, Y. (2008). Eicosanoid mediates prophenoloxidase release from oenocytoids in the beet armyworm, *Spodoptera exigua*. *Insect. Biochem. Mol. Biol.* 38, 99–112.
- Shrestha, S., and Kim, Y. (2009). Oenocytoid cell lysis to release prophenoloxidase is induced by eicosanoid via protein kinase C. *J. Asia Pac. Entomol.* 12, 301–305.
- Shrestha, S., and Kim, Y. (2010). Activation of immune-associated phospholipase A2 is functionally linked to Toll/Imd pathways in the red flour beetle, *Tribolium castaneum*. *Dev. Comp. Immunol.* 34, 530–537.
- Shrestha, S., Stanley, D., and Kim, Y. (2011). PGE2 induces oenocytoid cell lysis via a G protein-coupled receptor in the beet armyworm, *Spodoptera exigua*. *J. Insect Physiol.* 57, 1568–1576.
- Srikanth, K., Park, J., Stanley, D., and Kim, Y. (2011). Plasmacyte spreading peptide influences hemocyte behavior via eicosanoids. *Arch. Insect Biochem. Physiol.* 78, 145–160.
- Stanley, D. W. (2000). *Eicosanoids in Invertebrate Signal Transduction Systems*. Princeton: Princeton University Press.
- Stanley, D. W. (2005). “Eicosanoids,” in *Comprehensive Insect Molecular Science*, Vol. 4, eds L. I. Gilbert, K. Iatrou, and S. S. Gill (Amsterdam: Elsevier), 307–339.
- Stanley, D. W. (2006). Prostaglandins and other eicosanoids in insects: biological significance. *Annu. Rev. Entomol.* 51, 25–44.
- Stanley, D. W., Goodman, C., An, S., McIntosh, A., and Song, Q. (2008). Prostaglandins A1 and E1 influence gene expression in an established insect cell line (BCIRL-HzAM1 cells). *Insect Biochem. Mol. Biol.* 38, 275–282.
- Stanley, D. W., Miller, J., and Tunaz, H. (2009). Eicosanoid actions in insect immunity. *J. Innate Immun.* 1, 282–290.
- Stanley-Samuelson, D. W., Jensen, E., Nickerson, K. W., Tiebel, K., Ogg, C. L., and Howard, R. W. (1991). Insect immune response to bacterial infection is mediated by eicosanoids. *Proc. Natl. Acad. Sci. U.S.A.* 88, 1064–1068.
- Stanley-Samuelson, D. W., and Loher, W. (1983). Arachidonic and other long-chain polyunsaturated fatty acids in spermatophores and spermathecae of *Teleogryllus commodus*: significance in prostaglandin-mediated reproductive behavior. *J. Insect Physiol.* 29, 41–45.
- Stanley-Samuelson, D. W., Pelloquin, J. J., and Loher, W. (1986). Egg-laying in response to prostaglandin injections in the Australian field cricket, *Teleogryllus commodus*. *Physiol. Entomol.* 11, 213–219.
- Stroschein-Stevenson, S. L., Foley, E., O’Farrell, P. H., and Johnson, A. D. (2006). Identification of *Drosophila* gene products required for phagocytosis of *Candida albicans*. *PLoS Biol.* 4, 87–99. doi:10.1371/journal.pbio.0040004
- Tunaz, H., Park, Y., Buyukguzel, K., Bedick, J. C., Nor Aliza, A. R., and Stanley, D. W. (2003). Eicosanoids in insect immunity: bacterial infection stimulates hemocytic phospholipase A2 activity in tobacco hornworms. *Arch. Insect Biochem. Physiol.* 52, 1–6.
- Van Kerkhove, E., Pirotte, P., Petzel, D. H., and Stanley-Samuelson, D. W. (1995). Eicosanoid biosynthesis inhibitors modulate basal fluid secretions rates in the Malpighian tubules of the ant, *Formica polyctena*. *J. Insect Physiol.* 41, 435–441.
- Vanden Broeck, J. (2001). Insect G protein-coupled receptors and signal transduction. *Arch. Insect Biochem. Physiol.* 48, 1–12.
- von Euler, U. S. (1936). On the specific vasodilating and plain muscle stimulating substances from accessory genital glands in men and certain animals (prostaglandin and vesiglandin). *J. Physiol.* 88, 213–234.
- Wagner, C., Isermann, K., Fehrenbach, H., and Roeder, T. (2008). Molecular architecture of the fruit fly’s airway epithelial immune system. *BMC Genomics* 9, 446. doi:10.1186/1471-2164-9-446
- Weinheimer, A. J., and Spraggins, R. L. (1969). The occurrence of two new prostaglandin derivatives (15-epi-PGA2 and its acetate, methyl ester) in the Gorgonian, *Plexaura homomalla*. *Chemistry of coelenterates. XV. Tetrahedron Lett.* 59, 5185–5188.
- Yajima, M., Takada, M., Takahashi, N., Kikuchi, H., Natori, S., Oshima, Y., and Kurata, S. (2003). A newly established in vitro culture using transgenic *Drosophila* reveals functional coupling between the phospholipase A2-generated fatty acid cascade and lipopolysaccharide-dependent activation of the immune deficiency (imd) pathway in insect immunity. *Biochem. J.* 371, 205–210.

Conflict of Interest Statement: The authors declare that the research was conducted in the absence of any commercial or financial relationships that could be construed as a potential conflict of interest.

Received: 31 October 2011; paper pending published: 01 December 2011; accepted: 05 December 2011; published online: 30 December 2011.

Citation: Stanley D and Kim Y (2011) Prostaglandins and their receptors in insect biology. *Front. Endocrin.* 2:105. doi: 10.3389/fendo.2011.00105

This article was submitted to *Frontiers in Experimental Endocrinology*, a specialty of *Frontiers in Endocrinology*.

Copyright © 2011 Stanley and Kim. This is an open-access article distributed under the terms of the Creative Commons Attribution Non Commercial License, which permits non-commercial use, distribution, and reproduction in other forums, provided the original authors and source are credited.



Recent topics on the regulatory mechanism of ecdysteroidogenesis by the prothoracic glands in insects

Yoshiaki Tanaka*

Insect Growth Regulation Research Unit, Division of Insect Science, National Institute of Agrobiological Sciences, Tsukuba, Japan

Edited by:

Shogo Matsumoto, Advanced Science Institute – RIKEN, Japan

Reviewed by:

Ryusuke Niwa, University of Tsukuba, Japan

Shinji Nagata, University of Tokyo, Japan

*Correspondence:

Yoshiaki Tanaka, Insect Growth Regulation Research Unit, Division of Insect Science, National Institute of Agrobiological Sciences, 1-2 Owashi, Tsukuba, Ibaraki, 3058634 Japan.
e-mail: yoshiaki@affrc.go.jp

Molting and metamorphosis are strictly regulated by steroid hormones known as ecdysteroids. It is now widely recognized that ecdysteroid biosynthesis (ecdysteroidogenesis) in the prothoracic gland (PG) is regulated by the tropic factor prothoracicotrophic hormone (PTTH). However, the importance of PTTH in the induction of molting and metamorphosis remains unclear, and other mechanisms are thought to be involved in the regulation of ecdysteroidogenesis by the PG. Recently, new regulatory mechanisms, prothoracicostatic factors, and neural regulation have been explored using the silkworm, *Bombyx mori*, and two circulating prothoracicostatic factors, prothoracicostatic peptide (PTSP) and Bommo-myosuppressin (BMS), have been identified. Whereas PTTH and BMS are secreted from the brain, PTSP is secreted from the peripheral neurosecretory system – the epiproctodeal gland – during the molting stage. The molecular basis of neural regulation of ecdysteroidogenesis has been revealed for the first time in *B. mori*. The innervating neurons supply both Bommo-FMRF related peptide (BRFa) and orcokinin to maintain low levels of ecdysteroids during the feeding stage. These complex regulatory mechanisms – involving tropic and static factors, peripheral neurosecretory cells as well as the central neuroendocrine system, and neural regulation in addition to circulating factors collaborate to regulate ecdysteroidogenesis. Thus, together they create the finely tuned fluctuations in ecdysteroid titers needed in the hemolymph during insect development.

Keywords: neuropeptide, prothoracicostatic factor, innervating neuron, prothoracic gland, *Bombyx mori*, ecdysteroidogenesis, peripheral neurosecretory cell

INTRODUCTION

Insects are an ideal model system for studying how the regulatory mechanisms of developmental timing are coordinated with growth. The developmental transitions of insects (i.e., molting and metamorphosis) are strictly regulated by steroid hormones known as ecdysteroids. The biosynthesis of ecdysteroids, referred to as ecdysteroidogenesis, occurs predominantly in the prothoracic glands (PGs) during larval development (Gilbert et al., 2002). Since Kopeć (1922) suggested that the larval brain of the gypsy moth *Lymantria dispar* secretes a factor necessary for molting, attempts have been made to purify and clone this insect “brain hormone” (subsequently called prothoracicotrophic hormone, PTTH). It is now widely recognized that ecdysteroid biosynthesis in the PGs is stimulated by PTTH (Kawakami et al., 1990; Mizoguchi et al., 1990); however, the importance of PTTH in the induction of molting and metamorphosis remains unclear. Removal of the brain in larvae does not result in developmental arrest, and such animals can often initiate metamorphic development, although their developments considerably delay both in the hawkmoth *Manduca sexta* (Truman, 1972) and in the silkworm *Bombyx mori* except for one hybrid race, J122 × C115 (Kobayashi, 1957). The loss of PTTH signal in the fruit fly, *Drosophila melanogaster*, does not cause mortality but leads to a delay in metamorphosis due to a low ecdysteroid titer, and the extended feeding period gives rise to bigger pupae and adults (McBrayer et al., 2007; Rewitz et al., 2009b). These data suggest that PTTH is required for the

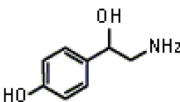
precise regulation of ecdysteroidogenesis but is not a crucial gate-keeper to initiate and maintain steroid biosynthesis in the PGs. In other words, other regulatory mechanisms may be involved in the regulation of ecdysteroidogenesis by the PGs.

In this review, recent studies on the regulatory mechanism of ecdysteroidogenesis by the PGs are described. In particular, I focus on humoral factors and on the neural control of ecdysteroidogenesis that have been mostly explored in *B. mori*.

HUMORAL FACTORS

The importance of the negative regulation of ecdysteroidogenesis has been recognized, and factors that inhibit ecdysteroidogenesis in several insect species have been described and characterized (Table 1). For example, hormonal inhibition of the PGs by the brain has been reported in locusts (Carlisle and Ellis, 1968). Crude extracts from the housefly, *Musca domestica*, reduce ecdysteroid synthesis and inhibit egg development when injected into the mosquito, *Aedes atropalpus* (Kelley et al., 1984). In the blow fly, *Calliphora vicina*, ecdysteroid synthesis in the larval ring gland appears to be regulated by a very potent inhibitory factor derived from the abdominal ganglion and subesophageal ganglion (Budd et al., 1993). A trypsin modulating oostatic factor (TMOF) isolated from the ovaries of adult females of flesh fly, *Neobellieria bullata*, is the first identified factor with prothoracicostatic activity (Hua et al., 1994). *N. bullata* TMOF inhibits ecdysteroid biosynthesis in the larval ring gland of flies (Hua and Koolman, 1995),

Table 1 | List of peptides and biogenic amine taken up in this review.

Name	Structure	Tropic/static	References
B. MORI			
PROTHORACICOTROPIC HORMONE (PTTH)	GNIQVENQAIPDPCTCKYKKEIEDLGENSEVPRFIET RNCNKTKQPTCRPPYICKESLYSITILKRRETKSQESL EIPNELKYRWVAESHPVSVACCLCTRDYQLRYNNN	Tropic	Kawakami et al. (1990)
PROTHORACICOSTATIC PEPTIDES (PTSPs)			
PTSP-I	AWQDLNSAWa	Static	Hua et al. (1999), Yamanaka et al. (2010)
PTSP-II	GWQDLNSAWa		
PTSP-III	APEKWAAFHGSWa		
PTSP-IV	GWNDISSVWa		
PTSP-V	AWQDMSSAWa		
PTSP-VI	AWSALHGTWa		
PTSP-VII	AWQDLNSVWa		
PTSP-VIII	AWSSLHSGWA		
BOMMO-MYOSUPPRESSIN (BMS)	pEDWHSFLRFa	Static	Yamanaka et al. (2005)
BOMMO-FMRF-AMIDE-RELATED PEPTIDE (BRFa)			
BRFa-I	SAIDRSMIRFa	Static	Yamanaka et al. (2006)
BRFa-II	SASFVRFa		
BRFa-III	DPSFIRFa		
BRFa-IV	ARNHFIRLa		
ORCOKININ			
Bommo-orc-I	NFDEIDESSLNTFV	Tropic	Roller et al. (2008), Yamanaka et al. (2011)
Bommo-orc-II	NFDEIDRSSMPFPYAI		
FXPRL-AMIDE			
Diapause hormone (DH)	TDMKDESDRGAHSERGalWFGPRLa	Tropic	Watanabe et al. (2007)
BIOGENIC AMINE			
Octopamine		Tropic	Hirashima et al. (1999)
OTHER INSECTS			
<i>N. bullata</i> TMOF	NPTNLH	Static	Hua et al. (1994), Hua and Koolman (1995)
<i>G. bimaculatus</i> AST-B1	GWQDLNGGWa	Static	Lorenz et al. (1998)
<i>H. armigera</i> DH-like peptide	NDVKDGAASGAHSdRLGLWFGPRLa	Tropic	Zhang et al. (2004)
<i>N. bullata</i> pyrokinin-II	SVQFKPRLa	Tropic	Verleyen et al. (2004)

but *N. bullata* TMOF is not present in the central nervous system of the larvae (Bylemans et al., 1996). Allatostatin-B (AST-B) isolated from adult brains of the cricket, *Gryllus bimaculatus*, has been observed to decrease the hemolymph ecdysteroid titer in the adult of *G. bimaculatus* (Lorenz et al., 1998) but the PGs do not produce physiologically significant amounts of ecdysteroids at this stage (Hoffmann et al., 1998). Thus, no endogenous prothoracicostatic factor had been identified until the isolation of prothoracicostatic peptide (PTSP) from larval brains of *B. mori* (Hua et al., 1999).

Prothoracicostatic peptide has the same sequence as Mansemyoinhibitory peptide-I (MIP-I), which was previously isolated from the nerve cord of the adult *M. sexta* (Blackburn et al., 1995). PTSP also shows high sequence homology to *G. bimaculatus* AST-B. This peptide inhibits both basal and PTTH-stimulated ecdysteroidogenesis *in vitro* in a dose-dependent manner, and injection of synthetic PTSP has been shown to temporally decrease the hemolymph ecdysteroid titer in fifth instar larvae of *B. mori*

(Liu et al., 2004). Interestingly, the peripheral neuroendocrine system – the epiproctodeal gland – is the principal site of neurohemal release of MIP in *M. sexta* (Davis et al., 2003): MIP-immunostaining in the epiproctodeal gland begins to increase during the first half of the molting period, and then most of the immunostaining is rapidly lost within several hours. This rapid loss of immunostaining suggests that a massive release of MIP from the epiproctodeal gland into hemolymph occurs at this stage, when there is a rapid decline in the ecdysteroid titer. The release of PTSP from the epiproctodeal gland also appears to occur at the same stage in *B. mori*, while the expression of *ptsp* in the brain is high during the feeding stage and low during the molting stage (Yamanaka et al., 2010).

Recently, a *B. mori* G protein-coupled receptor, which had previously been identified as an ortholog of the *Drosophila* sex peptide receptor (Yapici et al., 2008), is characterized as a functional PTSP receptor (Yamanaka et al., 2010). This receptor responds specifically to PTSP when examined using a heterologous expression

system. The receptor is expressed at low levels during the feeding stage, but is highly expressed in the PGs on the day before each larval and pupal ecdysis, when massive release of PTSP from the epiproctodeal gland occurs. These results suggest that PTSP secreted from the epiproctodeal gland acts on the PGs through the PTSP receptor during the molting cycle in *B. mori* and that the peripheral neurosecretory cells, as well as the neurosecretory system in the central nervous system, play a stage-specific role in regulating ecdysteroidogenesis. PTSP is unlikely to be involved in initiating the decrease in the ecdysteroid titer, but is probably involved in either full inactivation or suppression of re-activation of the PGs to finely regulate the ecdysteroid titer in the hemolymph (Yamanaka et al., 2010).

Another prothoracicostatic factor purified from pupal brains of *B. mori* is a decapeptide that shows the conserved structure of an insect myosuppressin, and has thus been named Bommo-myosuppressin (BMS; Yamanaka et al., 2005). Myosuppressin is a member of a larger peptide family of FMRF-amide-related peptides (FaRPs), which are known to regulate a wide range of processes from behavior to physiology in invertebrates (Mackey et al., 1987; Nelson et al., 1998; Nicols, 2003). BMS dose-dependently suppresses the cAMP level and inhibits ecdysteroidogenesis in the larval PGs at much lower concentrations than PTSP. The specific receptor for BMS is highly expressed in the PGs at the feeding stage. Together, these results suggest that BMS is secreted from the brain and plays an important role in maintaining low ecdysteroid levels during the feeding stage in the hemolymph. Vertebrates including humans have also been shown to possess peptides with RF-amide at the C-terminus (Yang et al., 1985), and at least one RF-amide peptide has been shown to inhibit steroid hormone release in experiments using an *in vitro* adrenal slice culture system (Labrousse et al., 1998). RF-amide peptides may modulate steroid hormone secretion throughout metazoans, thereby controlling post-embryonic development.

FXPRL-amide peptides, which are not homologous with PTTH, can stimulate ecdysteroidogenesis by the PGs. Diapause

hormone (DH) which was identified as an inducer of embryonic diapause in *B. mori* (Imai et al., 1991), stimulates ecdysteroidogenesis by the PGs of late fifth instar larvae of *B. mori* (Watanabe et al., 2007). The receptor for DH is expressed in the PGs, as well as in pupal pheromone glands and ovaries prior to eclosion, and the expression of this receptor in the PGs increases from the last half of the fifth instar stage to the first day of the pupal stage. These results suggest that DH regulates ecdysteroidogenesis during the late stages of fifth instar larvae in *B. mori*. Possible prothoracicotrophic effects of FXPRL-amide peptides have been reported in other insects. In the cotton bollworm *Helicoverpa armigera*, DH-like peptide can break the pupal diapause by activating the ecdysteroidogenesis by PGs in a temperature-dependent manner (Zhang et al., 2004). The pupariation of *N. bullata*, is accelerated by a FXPRL-amide peptide, *N. bullata* pyrokinin-II (Verleyen et al., 2004). Taken together, these results suggest that FXPRL-amide peptides can function as prothoracicotrophic factors across insect species and may play important roles in post-embryonic insect development.

NEURAL REGULATION

Since the first report of neural innervation in the PGs by Lyonet (1762; **Figure 1A**), the importance of PG-innervating neurons in the control of ecdysteroidogenesis has been well documented (Scharrer, 1964; Srivastava and Singh, 1968; Hintze-Podufal, 1970; Giebultowicz and Denlinger, 1985). In *B. mori*, the PGs are innervated by seven nerves starting from the subesophageal ganglion, prothoracic ganglia and mesothoracic ganglia, and by unpaired nerves between the above-mentioned ganglia (**Figure 1B**, Yokoyama, 1956). A positive correlation between the levels of electrical activity of PG-innervating neurons and the ecdysteroid titer during the course of development in the last larval instar has been reported in the American cockroach *Periplaneta americana* (Richter and Gersch, 1983), while the electrical activity shows an inverse relationship with ecdysteroid titer in the cabbage moth *Mamestra brassicae* (Okajima and Watanabe, 1989).

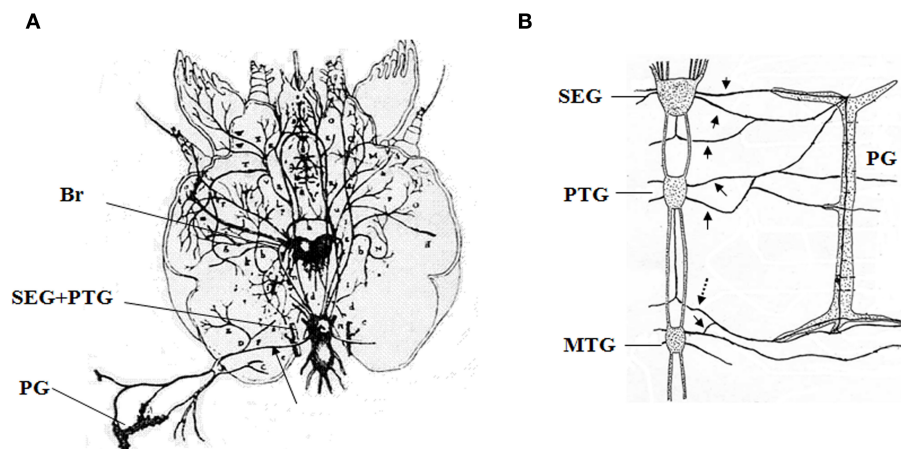


FIGURE 1 | Historical descriptions of neurons innervating the prothoracic gland. (A) The first description of innervating neurons of the moth by Lyonet (1762). **(B)** Innervating neurons in the larva of *Bombyx mori* reported by Yokoyama (1956). Br, brain; SEG, subesophageal ganglia; PTG, prothoracic

ganglia; MTG, mesothoracic ganglia; PG, prothoracic gland. Arrows indicate the neurons innervating the PGs, and a dotted arrow indicates the BRFa/Orcokinin-neuron. These figures are partially modified from the original ones.

However, studies revealing the molecular basis of regulation by the PGs have been restricted to hormonal factors throughout the last century.

Recently, for the first time we revealed the molecular basis of neural regulation of ecdysteroidogenesis in *B. mori* (Yamanaka et al., 2006). We found that Bommo-FMRF related peptide (BRFa) regulates ecdysteroidogenesis through direct innervation of the PGs in *B. mori*. BRFa is predominantly expressed in the prothoracic ganglion, and neurons in the prothoracic ganglion innervate the PGs and supply BRFa to the surface of PGs (Figure 1B). Electrophysiological recordings during development confirmed the increased firing activity of BRFa-expressing neurons in developmental stages of low PG activity and decreased ecdysteroid levels in the hemolymph. The prothoracicostatic function of BRFa has been confirmed by the report that BRFa neurons suppress the expression of several P450 genes induced by PTTH in the PGs (Yamanaka et al., 2007).

We found that other neuropeptides are delivered to the surface of the PGs through PG-innervating neurons (Yamanaka et al., 2011). Using direct mass spectrometric profiling of axons associated with the PGs, we detected several peptide peaks corresponding to *orcokinin* gene products in addition to BRFa. One of the two pairs of BRFa-expressing neurosecretory cells in the prothoracic ganglion co-expresses *orcokinin*, and these neurons project axons through the transverse nerve and terminate on the surface of the PGs (Figure 1B). Orcokinin was originally isolated from the nervous system of the spinycheek crayfish *Orconectes limosus* as a myostimulatory factor (Stangier et al., 1992). Orcokinin-like peptides have subsequently been identified in several insects (Pascual et al., 2004; Hofer et al., 2005; Liu et al., 2006; Christie, 2008; Roller et al., 2008; Clynen and Schoofs, 2009), although their physiological functions remain largely unknown except for a few cases (Hofer and Homberg, 2006). In *B. mori*, orcokinins have clear prothoracicotrophic activity and are able to cancel the static effect of BRFa on ecdysteroid biosynthesis, whereas the suppressive effect of BRFa on cAMP production remains unchanged in the presence of orcokinins (Yamanaka et al., 2011). The acute effects of prothoracicotrophic or prothoracicostatic factors which become manifest temporally during short-term *in vitro* incubation of the PG are mediated by translation and phosphorylation of intercellular molecules involved in the signal transduction of ecdysteroidogenesis (Gilbert et al., 2002; Huang et al., 2008; Rewitz et al., 2009a). On the other hand, the chronic effects of these factors which become obvious on a longer time scale during development are mediated by the transcriptional regulation of some genes encoding ecdysteroidogenic enzymes probably via cAMP-mediated pathway (Gilbert et al., 2002; Huang et al., 2008). The chronic effects of these factors are pharmacologically separable from the acute effects (Yamanaka et al., 2007). Thus, orcokinins might regulate ecdysteroidogenesis by the PGs via cAMP-independent way; that is, they specifically eliminate the acute prothoracicostatic effect of BRFa while maintaining the chronic inhibitory effect of BRFa. The signaling pathway of orcokinin at the molecular level needs to be elucidated to prove this hypothesis.

What is the functional significance of such a complex feature of the PG-innervating neurons in *B. mori*? It is known that a low level of ecdysteroid titer during the intermolt period has a complex

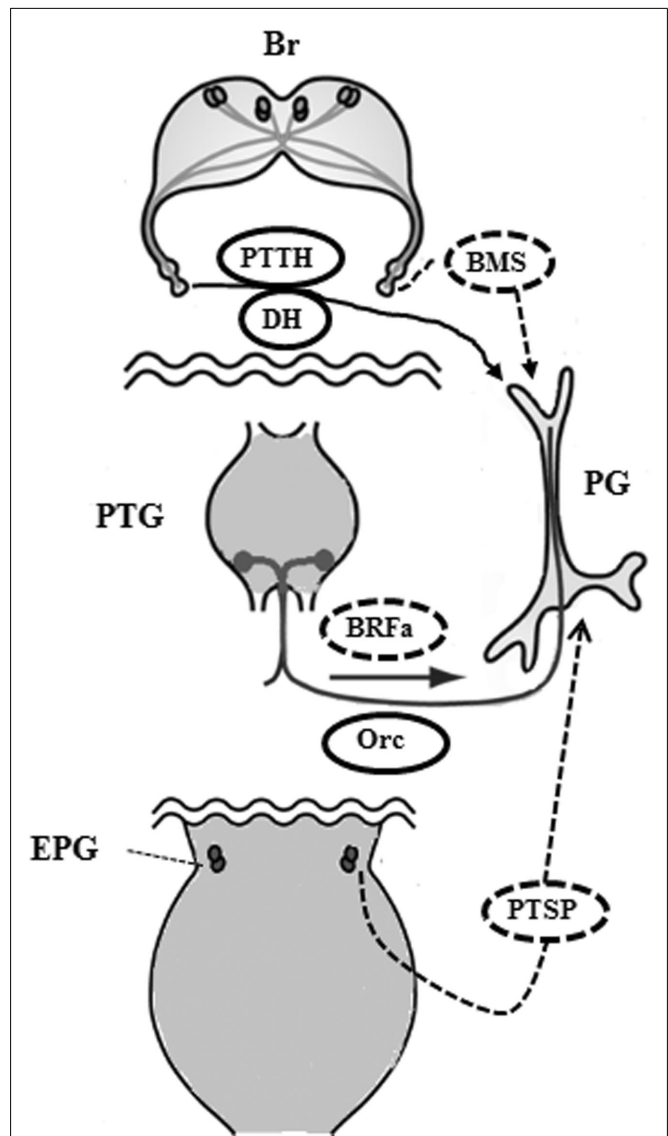


FIGURE 2 | Proposed regulatory mechanism of ecdysteroidogenesis by the prothoracic gland in the larva of *Bombyx mori*. During the feeding stage, BRFa and orcokinin are delivered through the innervating neurons to maintain low levels of ecdysteroid in collaboration with circulating BMS. Next, PTTH and DH are released to stimulate ecdysteroidogenesis after the release of inhibition by BRFa and BMS. PTSP is secreted from the epiproctodeal gland after the ecdysteroid level reaches a peak in order to decrease ecdysteroid levels rapidly. Br, brain; PTG, prothoracic ganglia; PG, prothoracic gland; EPG, epiproctodeal gland; Orc, orcokinin. Solid ovals indicate tropic factors and dotted ovals indicate static factors.

effect on the regulation of tissue growth and proliferation (Champlin and Truman, 1998; Colombani et al., 2005; Nijhout et al., 2007). Therefore, orcokinins might maintain a low ecdysteroid titer while BRFa suppresses full potentiation of the PGs prior to the ecdysteroid pulse generated by PTTH (Mizoguchi et al., 2001).

Prothoracic gland-innervating neurons of other lepidopteran insects are also stained by both FMRFa- and orcokinin-specific antibodies (Tanaka, unpublished data). In *D. melanogaster*, a pair

of bilaterally symmetric neurons located in the cerebral labrum portion of the brain directly innervate the PGs (Siegmund and Korge, 2001) and induce the production and secretion of ecdysone by delivering PTTH directly (McBrayer et al., 2007); however, it is not certain whether other peptides are delivered to the PGs through these innervating neurons. By contrast, PG-innervating neurons are not stained by PTTH-specific antibody in *B. mori* (Tanaka, unpublished data). Different peptidergic systems may regulate ecdysteroidogenesis among the various insect species.

FUTURE PROSPECTS

Bombyx mori has been a useful tool for insect endocrinology since the discovery of PG function by Fukuda (1944), and studies have shown that ecdysteroidogenesis by the PGs is under the control of a complex mechanism (Figure 2). Tropic and static factors, the peripheral neurosecretory system as well as the central neuroendocrine system, and neural regulation in addition to circulating factors all collaborate to regulate ecdysteroidogenesis by the PGs. Thus, together they create the finely tuned fluctuations in ecdysteroid titer needed in the hemolymph during the development of *B. mori*. Moreover, we should carefully re-investigate factors and mechanisms that have been ignored for a long time. For example, the roles of biogenic amines in ecdysteroidogenesis remain unclear, although it has been reported that octopamine stimulates the production of ecdysteroids by larval PGs of *B. mori* *in vitro* (Hirashima et al., 1999). How the PGs relay their con-

dition to the neural system is not yet fully understood, but the PG-innervating neurons may be involved in this communication. Three PG-innervating neurons contain afferent neurons as well as efferent ones in *M. brassicae* (Okajima and Watanabe, 1989). Although the function of these afferent neurons is unknown, the CNS may be monitoring the condition of the PGs via these neurons.

The neuropeptides responsible for the ecdysteroidogenesis in *B. mori* are commonly present among insect species, but their function in ecdysteroidogenesis remains to be elucidated in other insects. No prothoracicostatic factor has been identified as yet in *D. melanogaster*, and the importance of insulin signaling in regulating ecdysteroid production by the PGs has been recently highlighted (see the review by Marchal et al., 2010 and the recent topics by Gibbens et al., 2011). The regulatory mechanisms of ecdysteroidogenesis by the PGs may be diverse among insect species and need to be elucidated in different insect models in order to understand how the insects adapted to diverse environment.

ACKNOWLEDGMENTS

I specially thanks Drs. Naoki Yamanaka, Yue-Jin Hua, Ladislav Roller, Dusan Žitnan, Akira Mizoguchi, and Hiroshi Kataoka for the studies on PTSP, BMS, BRFa, and orcokinin. These studies were supported by the Grants-in-Aid for Scientific Research from the Japan Society for the Promotion of Science (JSPS, Grant 21380040).

REFERENCES

- Blackburn, M. B., Wagner, R. M., Kochansky, J. P., Harrison, D. J., Thomas-Laemont, P., and Raina, A. K. (1995). The identification of two myoinhibitory peptides, with sequence similarities to the galanins, isolated from the ventral nerve cord of *Manduca sexta*. *Regul. Pept.* 57, 213–219.
- Budd, E., Kauser, G., and Koolman, J. (1993). On the control of ecdysone biosynthesis by the central nervous system of blowfly larvae. *Arch. Insect Biochem. Physiol.* 23, 181–197.
- Bylemans, D., Verhaert, P., Janssen, I., Vanden Broeck, J., Borovsky, D., Ma, M., and De Loof, A. (1996). Immunolocalization of the oostatic and prothoracicostatic peptide, Neb-TMOF, in adults of the flesh fly, *Neobellieria bullata*. *Gen. Comp. Endocrinol.* 103, 273–280.
- Carlisle, D. B., and Ellis, P. E. (1968). Hormonal inhibition of the prothoracic gland by the brain in locusts. *Nature* 220, 706–707.
- Champlin, D. T., and Truman, J. W. (1998). Ecdysteroids govern two phases of eye development during metamorphosis of the moth, *Manduca sexta*. *Development* 125, 2009–2018.
- Christie, A. E. (2008). In silico analyses of peptide paracrine/hormones in Aphidoidea. *Gen. Comp. Endocrinol.* 159, 67–79.
- Clynen, E., and Schoofs, L. (2009). Peptidomic survey of the locust neuroendocrine system. *Insect Biochem. Mol. Biol.* 39, 491–507.
- Colombani, J., Bianchini, L., Layalle, S., Pondeville, E., Dauphin-Villemant, C., Antoniewski, C., Carre, C., Noselli, S., and Leopold, P. (2005). Antagonistic actions of ecdysone and insulins determine final size in *Drosophila*. *Science* 310, 667–670.
- Davis, N. T., Blackburn, M. B., Golubeva, E. G., and Hildebrand, J. G. (2003). Localization of myoinhibitory peptide immunoreactivity in *Manduca sexta* and *Bombyx mori*, with indications that the peptide has a role in molting and ecdysis. *J. Exp. Biol.* 206, 1449–1460.
- Fukuda, S. (1944). The hormonal mechanism of larval molting and metamorphosis in the silkworm. *J. Fac. Sci. Tokyo Imperial Univ. Sec. IV* 6, 477–532.
- Gibbens, Y. Y., Warren, J. T., Gilbert, L. I., and O'Connor, M. B. (2011). Neuroendocrine regulation of *Drosophila* metamorphosis requires TGFbeta/Activin signaling. *Development* 138, 2693–2703.
- Giebultowicz, J. M., and Denlinger, D. L. (1985). Identification of neurons innervating the ring gland of the flesh fly larva. *Sarcophaga crassipalpis* Macquart (Diptera: Sarcophagidae). *Int. J. Insect Morphol. Embryol.* 14, 155–161.
- Gilbert, L. I., Rybczynski, R., and Warren, J. T. (2002). Control and biochemical nature of the ecdysteroidogenic pathway. *Annu. Rev. Entomol.* 47, 883–916.
- Hintze-Podufal, C. (1970). Innervation of prothoracic glands of *Cerura vinula* L. (Lepidoptera). *Experientia* 26, 1269–1271.
- Hirashima, A., Hirokado, S., Ohta, H., Suetsugu, E., Sakaguchi, M., Kuwano, E., Taniguchi, E., and Eto, M. (1999). Titres of biogenic amines and ecdysteroids: effect of octopamine on the production of ecdysteroids in the silkworm *Bombyx mori*. *J. Insect Physiol.* 45, 843–851.
- Hofer, S., Dirksen, H., Tollback, P., and Homberg, U. (2005). Novel insect orckinins: characterization and neuronal distribution in the brains of selected dicondylarian insects. *J. Comp. Neurol.* 490, 57–71.
- Hofer, S., and Homberg, U. (2006). Evidence for a role of orckinin-related peptides in the circadian clock controlling locomotor activity of the cockroach *Leucophaea maderae*. *J. Exp. Biol.* 209, 2794–2803.
- Hoffmann, K. H., Lorenz, M. W., and Oeh, U. (1998). Ecdysteroid release by the prothoracic gland of *Gryllus bimaculatus* (Ensifera: Gryllidae) during larval-adult development. *J. Insect Physiol.* 44, 941–946.
- Hua, Y. J., Bylemans, D., De Loof, A., and Koolman, J. (1994). Inhibition of ecdysone biosynthesis in flies by a hexapeptide isolated from vitellogenic ovaries. *Mol. Cell. Endocrinol.* 104, R1–R4.
- Hua, Y.-J., and Koolman, J. (1995). An ecdysostatin from flies. *Regul. Pept.* 57, 263–271.
- Hua, Y. J., Tanaka, Y., Nakamura, K., Sakakibara, M., Nagata, S., and Kataoka, H. (1999). Identification of a prothoracicostatic peptide in the larval brain of the silkworm, *Bombyx mori*. *J. Biol. Chem.* 274, 31169–31173.
- Huang, X., Warren, J. T., and Gilbert, L. I. (2008). New players in the regulation of ecdysone biosynthesis. *J. Genet. Genomics* 35, 1–10.
- Imai, K., Konno, T., Nakazawa, Y., Komiya, T., Isobe, M., Koga, K., Goto, T., Yaginuma, T., Sakakibara, K., Hasegawa, K., and Yamashita, O. (1991). Isolation and structure of diapause hormone of the silkworm, *Bombyx mori*. *Proc. Jpn. Acad.* 67B, 98–101.

- Kawakami, A., Kataoka, H., Oka, T., Mizoguchi, A., Kimura-Kawakami, M., Adachi, T., Iwami, M., Nagasawa, H., Suzuki, A., and Ishizaki, H. (1990). Molecular cloning of *Bombyx mori* prothoracotropic hormone. *Science* 247, 1333–1335.
- Kelley, T. J., Birnbaum, M. J., Woods, C. W., and Borkovec, A. B. (1984). Effects of house fly oostatic hormone on egg development neurosecretory hormone action in *Aedes atropalpus*. *J. Exp. Zool.* 229, 491–496.
- Kobayashi, M. (1957). Studies on the neurosecretion in the silkworm, *Bombyx mori* L. *Bull. Sericult. Exp. Sta.* 15, 181–273.
- Kopeč, S. (1922). Studies on the necessity of the brain for the inception of insect metamorphosis. *Biol. Bull.* 42, 323–342.
- Labrousse, S., Laulin, J. P., Le Moal, M., Tramu, G., and Simonnet, G. (1998). Neuropeptide FF in the rat adrenal gland: presence, distribution and pharmacological effects. *J. Neuroendocrinol.* 10, 559–565.
- Liu, F., Baggerman, G., D'Hertog, W., Verleyen, P., Schoofs, L., and Wets, G. (2006). In silico identification of new secretory peptide genes in *Drosophila melanogaster*. *Mol. Cell. Proteomics* 5, 510–522.
- Liu, X., Tanaka, Y., Song, Q., Xu, B., and Hua, Y. (2004). *Bombyx mori* prothoracicostatic peptide inhibits ecdysteroidogenesis in vivo. *Arch. Insect Biochem. Physiol.* 56, 155–161.
- Lorenz, M. W., Lorenz, J. I., Treiblmayr, K., and Hoffmann, K. H. (1998). In vivo effects of allatostatins in crickets, *Gryllus bimaculatus* (Ensifera: Gryllidae). *Arch. Insect Biochem. Physiol.* 38, 32–43.
- Lyonet, P. (1972). *Traité anatomique de la chenille au rouge le bois de Saule*. Amsterdam: La Haye, P616.
- Mackey, S. L., Glanzman, D. L., Small, S. A., Dyke, A. M., Kandel, E. R., and Hawkins, R. D. (1987). Tail shock produces inhibition as well as sensitization of the siphon-withdrawal reflex of *Aplysia*: possible behavioral role for presynaptic inhibition mediated by the peptide Phe-Met-Arg-Phe-NH₂. *Proc. Natl. Acad. Sci. U.S.A.* 84, 8730–8734.
- Marchal, E., Vandersmissen, H. P., Badisco, L., Van de Velde, S., Verlinden, H., Iga, M., Van Wielendaale, P., Huybrechts, R., Simonet, G., Smaghe, G., and Vanden Broeck, J. (2010). Control of ecdysteroidogenesis in prothoracic glands of insects: a review. *Peptides* 31, 506–519.
- McBrayer, Z., Ono, H., Shimell, M., Parvy, J. P., Beckstead, R. B., Warren, J. T., Thummel, C. S., Dauphin-Villemant, C., Gilbert, L. I., and O'Connor, M. B. (2007). Prothoracotropic hormone regulates developmental timing and body size in *Drosophila*. *Dev. Cell* 13, 857–871.
- Mizoguchi, A., Ohashi, Y., Hosoda, K., Ishibashi, J., and Kataoka, H. (2001). Developmental profile of the changes in the prothoracicotropic hormone titer in hemolymph of the silkworm *Bombyx mori*: correlation with ecdysteroid secretion. *Insect Biochem. Mol. Biol.* 31, 349–358.
- Mizoguchi, A., Oka, T., Kataoka, H., Nagasawa, H., Suzuki, A., and Ishizaki, H. (1990). Immunohistochemical localization of prothoracotropic hormone-producing neurosecretory cells in the brain of *Bombyx mori*. *Dev. Growth Differ.* 32, 591–598.
- Nelson, L. S., Rosoff, M. L., and Li, C. (1998). Disruption of a neuropeptide gene, *flp-1*, causes multiple behavioral defects in *Caenorhabditis elegans*. *Science* 281, 1686–1690.
- Nicols, R. (2003). Signaling pathways and physiological functions of *Drosophila melanogaster* FMRamide-related peptides. *Annu. Rev. Entomol.* 48, 485–503.
- Nijhout, H. F., Smith, W. A., Schachar, I., Subramanian, S., Tobler, A., and Grunert, L. W. (2007). The control of growth and differentiation of the wing imaginal disks of *Manduca sexta*. *Dev. Biol.* 302, 569–576.
- Okajima, A., and Watanabe, M. (1989). Electrophysiological identification of neural pathway to the prothoracic gland and the change in electrical activities of the prothoracic gland innervating neurons during larval development of a moth, *Mamestra brassicae*. *Zool. Sci.* 6, 459–468.
- Pascual, N., Castresana, J., Valero, M. L., Andreu, D., and Belles, X. (2004). Orcokinin in insects and other invertebrates. *Insect Biochem. Mol. Biol.* 34, 1141–1146.
- Rewitz, K. F., Larsen, M. R., Lobner-Olesen, A., Rybczynski, R., O'Connor, M. B., and Gilbert, L. I. (2009a). A phosphoproteomics approach to elucidate neuropeptide signal transduction controlling insect metamorphosis. *Insect Biochem. Mol. Biol.* 39, 475–483.
- Rewitz, K. F., Yamanaka, N., Gilbert, L. I., and O'Connor, M. B. (2009b). The insect neuropeptide PTTH activates receptor tyrosine kinase torso to initiate metamorphosis. *Science* 326, 1403–1405.
- Richter, K., and Gersch, M. (1983). Electrophysiological evidence of nervous involvement in the control of the prothoracic gland in *Periplaneta americana*. *Experientia* 39, 917–918.
- Roller, L., Yamanaka, N., Watanabe, K., Daubnerova, I., Žitnan, D., Kataoka, H., and Tanaka, Y. (2008). The unique evolution of neuropeptide genes in the silkworm *Bombyx mori*. *Insect Biochem. Mol. Biol.* 38, 1147–1157.
- Scharrer, B. (1964). The fine structure of Blattarian prothoracic glands. *Z. Zellforsch. Mikrosk. Anat.* 64, 111–119.
- Siegmund, T., and Korge, G. (2001). Innervation of the ring gland of *Drosophila melanogaster*. *J. Comp. Neurol.* 431, 481–491.
- Srivastava, K. P., and Singh, H. H. (1968). On innervation of prothoracic glands in *Papilio demoleus* L. (Lepidoptera). *Experientia* 24, 838–839.
- Stangier, J., Hilbich, C., Burdzik, S., and Keller, R. (1992). Orcokinin: a novel myotropic peptide from the nervous system of the crayfish, *Orconectes limosus*. *Peptides* 13, 859–864.
- Truman, J. W. (1972). Physiology of insect rhythms I. Circadian organization of the endocrine events underlying the molting cycle of larval tobacco hornworms. *J. Exp. Biol.* 57, 805–820.
- Verleyen, P., Clynen, E., Huybrechts, J., Van Lommel, A., Vanden Bosch, L., De Loof, A., Zdzarek, J., and Schoofs, L. (2004). Fraenkel's pupariation factor identified at last. *Dev. Biol.* 273, 38–47.
- Watanabe, K., Hull, J. J., Niimi, T., Imai, K., Matsumoto, S., Yaginuma, T., and Kataoka, H. (2007). FXPRL-amide peptides induce ecdysteroidogenesis through a G-protein coupled receptor expressed in the prothoracic gland of *Bombyx mori*. *Mol. Cell. Endocrinol.* 273, 51–58.
- Yamanaka, N., Honda, N., Osato, N., Niwa, R., Mizoguchi, A., and Kataoka, H. (2007). Differential regulation of ecdysteroidogenic P450 gene expression in the silkworm, *Bombyx mori*. *Biosci. Biotechnol. Biochem.* 71, 2808–2814.
- Yamanaka, N., Hua, Y. J., Mizoguchi, A., Watanabe, K., Niwa, R., Tanaka, Y., and Kataoka, H. (2005). Identification of a novel prothoracicostatic hormone and its receptor in the silkworm *Bombyx mori*. *J. Biol. Chem.* 280, 14684–14690.
- Yamanaka, N., Hua, Y. J., Roller, L., Spalovska-Valachova, I., Mizoguchi, A., Kataoka, H., and Tanaka, Y. (2010). *Bombyx* prothoracicostatic peptides activate the sex peptide receptor to regulate ecdysteroid biosynthesis. *Proc. Natl. Acad. Sci. U.S.A.* 107, 2060–2065.
- Yamanaka, N., Roller, L., Žitnan, D., Satake, H., Mizoguchi, A., Kataoka, H., and Tanaka, Y. (2011). *Bombyx* orokinins are brain-gut peptides involved in the neuronal regulation of ecdysteroidogenesis. *J. Comp. Neurol.* 519, 238–246.
- Yamanaka, N., Žitnan, D., Kim, Y. J., Adams, M. E., Hua, Y. J., Suzuki, Y., Suzuki, M., Satake, H., Mizoguchi, A., Asaoka, K., Tanaka, Y., and Kataoka, H. (2006). Regulation of insect steroid hormone biosynthesis by innervating peptidergic neurons. *Proc. Natl. Acad. Sci. U.S.A.* 103, 8622–8627.
- Yang, H. Y., Fratta, W., Majane, E. A., and Costa, E. (1985). Isolation, sequencing, synthesis, and pharmacological characterization of two brain neuropeptides that modulate the action of morphine. *Proc. Natl. Acad. Sci. U.S.A.* 82, 7757–7761.
- Yapici, N., Kim, Y. J., Ribeiro, C., and Dickson, B. J. (2008). A receptor that mediates the post-mating switch in *Drosophila* reproductive behaviour. *Nature* 451, 33–37.
- Yokoyama, T. (1956). The morphology and innervation of the prothoracic gland in the silkworm, *Bombyx mori*. *J. Sericult. Sci. Jpn.* 25, 87–94.
- Zhang, T. Y., Sun, J. S., Zhang, Q. R., Xu, J., Jiang, R. J., and Xu, W. H. (2004). The diapause hormone-pheromone biosynthesis activating neuropeptide gene of *Helicoverpa armigera* encodes multiple peptides that break, rather than induce, diapause. *J. Insect Physiol.* 50, 547–554.

Conflict of Interest Statement: The author declares that the research was conducted in the absence of any commercial or financial relationships that could be construed as a potential conflict of interest.

Received: 28 October 2011; paper pending published: 10 November 2011; accepted: 06 December 2011; published online: 29 December 2011.

Citation: Tanaka Y (2011) Recent topics on the regulatory mechanism of ecdysteroidogenesis by the prothoracic glands in insects. *Front. Endocrin.* 2:107. doi: 10.3389/fendo.2011.00107

This article was submitted to *Frontiers in Experimental Endocrinology, a specialty of Frontiers in Endocrinology*.

Copyright © 2011 Tanaka. This is an open-access article distributed under the terms of the Creative Commons Attribution Non Commercial License, which permits non-commercial use, distribution, and reproduction in other forums, provided the original authors and source are credited.



Wolbachia as an “infectious” extrinsic factor manipulating host signaling pathways

Ilaria Negri^{1,2*}

¹ Department of Exploitation and Protection of the Agricultural and Forestry Resources, Università di Torino, Grugliasco, Italy

² Koiné – Environmental Consulting, Parma, Italy

Edited by:

Joe Hull, USDA Agricultural Research Service, USA

Reviewed by:

Sergio Polakof, French National Institute for Agricultural Research, France

Kostas Bourtzis, University of Western Greece, Greece

*Correspondence:

Ilaria Negri, Department of Exploitation and Protection of the Agricultural and Forestry Resources, Università di Torino, Via L. da Vinci, 44, 10095 Grugliasco, Italy.
e-mail: Ilaria.negri@unito.it

Wolbachia pipientis is a widespread endosymbiont of filarial nematodes and arthropods. While in worms the symbiosis is obligate, in arthropods *Wolbachia* induces several reproductive manipulations (i.e., cytoplasmic incompatibility, parthenogenesis, feminization of genetic males, and male-killing) in order to increase the number of infected females. These various phenotypic effects may be linked to differences in host physiology, and in particular to endocrine-related processes governing growth, development, and reproduction. Indeed, a number of evidences links *Wolbachia* symbiosis to insulin and ecdysteroid signaling, two multilayered pathways known to work antagonistically, jointly or even independently for the regulation of different molecular networks. At present it is not clear whether *Wolbachia* manipulates one pathway, thus affecting other related metabolic networks, or if it targets both pathways, even interacting at several points in each of them. Interestingly, in view of the interplay between hormone signaling and epigenetic machinery, a direct influence of the “infection” on hormonal signaling involving ecdysteroids might be achievable through the manipulation of the host’s epigenetic pathways.

Keywords: *Wolbachia*, insulin, ecdysone, nuclear receptors, epigenetic

INTRODUCTION

The maternally transmitted α -Proteobacterium *Wolbachia pipientis* (Rickettsiales) is a widespread endosymbiont of filarial nematodes and arthropods, including crustaceans, mites, spiders, scorpions, and especially insects, where it is estimated to infect up to 66% of the species (Werren et al., 2008).

While in worms *Wolbachia* are obligate symbionts, in arthropods they induce several reproductive manipulations in order to increase the number of infected females. Effects of the infection include cytoplasmic incompatibility, parthenogenesis, feminization of genetic males, and male-killing, as well as influences on host longevity and fecundity (Stouthamer et al., 1999; Werren et al., 2008). Such a host phenotypic variability is generally linked to the high genome plasticity of *Wolbachia*. However, experimental data also suggest a role for the symbiont in modulating the host sexual phenotypes by interaction with the hormonal signaling pathway. In particular, the various phenotypic effects may be due to differences in host physiology, and in particular to endocrine-related processes governing growth, development, and reproductive behavior which display a high variability in insects. In particular, a number of evidence links *Wolbachia* symbiosis to insulin and steroid (i.e., ecdysteroid) signaling. Many studies report antagonistic or cooperative relationships between steroid hormones and insulin. Indeed, an extensive crosstalk between the two hormonal signaling pathways has been demonstrated in regulating metabolism, development, and reproduction. For example, in the fly *Drosophila melanogaster* there is a mutual antagonistic relationship between these metabolic networks for nutrient homeostasis (Colombani et al., 2005). At a molecular level, for example, the expression of the ecdysone receptor (EcR)

co-activator DOR (which is misregulated in diabetic mammals) is controlled by insulin signaling via the forkhead transcription factor FOXO (Francis et al., 2010). The two hormonal signaling pathways may also cooperate: in mosquitoes they act in combination for the yolk protein precursor gene expression required for vitellogenesis (Roy et al., 2007). In the larval prothoracic gland, the insulin-signaling pathway modulates ecdysone release and influences both the duration and rate of larval growth (Shingleton, 2005); in adults, insulin-like peptides may trigger steroid synthesis by the follicular cells in insect ovaries (Wu and Brown, 2006). A parallel regulation by ecdysone and insulin has also been demonstrated in the *Drosophila*’s ovary where the hormones modulate the proliferation and self-renewal of germ-line stem cells independently (Ables and Drummond-Barbosa, 2010).

In the following sections, data on the involvement of *Wolbachia* in modulating both host hormonal pathways are discussed. Due to the complexity of such metabolic pathways, at present, it is not clear whether *Wolbachia* operates by attacking one pathway, thus affecting other related metabolic networks, or if the symbiont targets both pathways, even interacting at several points in each of them.

WOLBACHIA AND INSULIN SIGNALING

The insulin/IGF signaling (IIS) pathway plays key roles in growth, metabolism, reproduction, and longevity in different organisms. Recently, a specific interaction between IIS and *Wolbachia* has been demonstrated in *D. melanogaster*, where insulin-like peptide mutants display an extended lifespan if they harbor the symbiont (Grönke et al., 2010). Another research involves *Drosophila* insulin receptor mutants, characterized by a reduction

in IIS signaling with pleiotropic effects on many traits, including extreme dwarfism, sterility, increased fat levels, and shortened lifespan: interestingly, in presence of *Wolbachia* the IIS-related mutant phenotypes resulted in significant moderate effects (e.g., reduced fecundity and extended lifespan), suggesting that the symbiont acts to increase insulin signaling itself (Ikeya et al., 2009).

Wolbachia also seems to interact with *chico*, a gene encoding an insulin receptor substrate (Böhni et al., 1999). *Drosophila* carrying homozygous *chico*¹ alleles are sterile, but in presence of *Wolbachia* the females produce progeny, even if significantly smaller than their heterozygous siblings (Clark et al., 2005; Richard et al., 2005).

Additional data on the possible interaction between the symbiont and host IIS are provided by studies on crustaceans. *Wolbachia* is known to infect several species of crustaceans, and especially (but not exclusively) terrestrial isopods where the symbiont can induce the feminization of genetical males through an interaction with host hormonal signaling pathways (Bouchon et al., 2008). Crustacea are by default females, and male sex differentiation is triggered by an androgenic hormone (AH) secreted by the androgenic gland (AG; Legrand et al., 1987; Sagi and Khalaila, 2001). The current hypothesis about the feminizing action of *Wolbachia* is that the symbiont interacts either with the AG differentiation process or the AH receptors (Rigaud and Juchault, 1998; Bouchon et al., 2008). However, if *Wolbachia* bacteria are experimentally inoculated in adult males, the host soon develops female structures, despite the presence of the AG, which becomes even hypertrophic (Martin et al., 1973, 1999). This suggests that the AH receptors are no longer functional, favoring the hypothesis that *Wolbachia* induces feminization by targeting the receptor of the AH. Interestingly, the AH has been proven to be an insulin-like peptide (Manor et al., 2007): *in vivo* silencing of the gene induces an arrest of spermatogenesis, prevents the regeneration of male secondary sexual characteristics, and also induces a lag in molt and a growth reduction (Ventura et al., 2009). In sequential hermaphrodites, the silencing of the AG insulin-like factor induces the feminization of male-related phenotypes too (Rosen et al., 2010).

WOLBACHIA AND ECDYSONE SIGNALING

Among invertebrates *Wolbachia* is known to infect exclusively (!) Arthropoda and Nematoda, two Phyla belonging to the Ecdysozoa, a clade of animals which share the ability to replace the exoskeleton. This process is called ecdysis and is controlled hormonally by a class of steroids called ecdysteroids (Ewer, 2005).

In filarial worms, antibiotic curing of *Wolbachia* “infection” inhibits nematode fertility and development, suggesting a specific role for the symbiont in host oogenesis, embryogenesis, and molting (Casiraghi et al., 2002; Arumugam et al., 2008; Frank et al., 2010). In arthropods, several data suggest that the phenotypic effects induced by *Wolbachia* may be linked to steroid-related processes. As it is well known, insect steroids play key roles in the coordination of multiple developmental processes, and in adults they control important aspects of reproduction.

In particular, during development, insect molting is induced by the systemic hormone 20-hydroxyecdysone (20E). 20E acts on members of an evolutionarily conserved family of nuclear receptors: it binds to the heterodimeric EcR/Usf receptor

composed of EcR and USP (ultraspiracle, homologous to the vertebrate retinoid-X receptor), which shares many commonalities with the human thyroid hormone receptor. Then the EcR/USP complex activates the transcriptional processes underlying the cellular and morphogenetic molting cascade events (Gilbert et al., 2002). A biological action of 20E binding of un-partnered EcR has also been demonstrated (Spindler et al., 2009).

Despite the fact that ecdysteroids are present throughout the entire life of insects, their role in adults is quite elusive. Ecdysteroids, for example, may have a role in lifespan (Tricoire et al., 2009; Schwedes et al., 2011) or in stress responses, such as nutritional shortage, high temperature, dry starvation, and oxidative stress (Hirashima et al., 2000; Terashima et al., 2005; Ishimoto and Kitamoto, 2011). In adult flies ecdysone-mediated signaling is also involved in stressful social interactions and in homeostatic sleep regulation (Ishimoto and Kitamoto, 2011). Another unconventional role of the “molting” hormone is the control of important aspects of reproduction, including ovarian development and oogenesis (Raikhel et al., 2005). In many insect species 20E is directly involved in the regulation of vitellogenin biosynthesis by the female fat body, a metabolic tissue functionally analogous to the vertebrate liver; and it can also induce vitellogenin synthesis in males (Huybrechts and De Loof, 1977; Bownes et al., 1983; Zhu et al., 2007). The 20E has also been shown to affect sexual behavior (Ganter et al., 2007).

De Loof (2006) proposes that ecdysteroids may also act as sex hormones. In particular, 20E secreted by the follicle cells of the insect ovary could be the physiological equivalent of vertebrate estrogens, while E – the precursor of the active molting hormone 20E – should act as a distinct hormone, being the physiological equivalent of vertebrate testosterone (De Loof and Huybrechts, 1998; De Loof, 2006). Indeed, E can regulate a set of genes that are distinct from those controlled by 20E, thus confirming that it may exert different biological functions from 20E (Beckstead et al., 2007). However, in insects the existence of sex hormones is under debate, as the differentiation of primary and secondary sexual characteristics is generally considered under the exclusive control of the genotype of each single cell (Steinmann-Zwicky et al., 1989; Schütt and Nöthiger, 2000). However recent data demonstrate that in insects, as well as in vertebrates, non-autonomous (=hormonal) sex determination controls sex dimorphism (DeFalco et al., 2008; Casper and Van Doren, 2009). Thus, if ecdysteroids function as molting and sex hormones, this could explain why *Wolbachia* interferes with insect development and reproduction, as discussed in the following section.

Last but not least, it is worth noting that *Wolbachia* establish themselves in many host steroidogenic tissues, including the fat body and the ovarian follicular epithelium, as demonstrated in many insect species and shown in **Figure 1** (Sacchi et al., 2010; Gonella et al., 2011; Negri and Pellicchia, *in press*).

FEMINIZING WOLBACHIA: THE INDUCTION OF HOST FEMINE SEX DIFFERENTIATION DESPITE MASCULINE SEX DETERMINATION

Feminization, that is the development of genetical males into females, deals with sex differentiation much more directly than the other *Wolbachia*-induced phenotypes, thus offering the opportunity to shed light on the processes governing arthropod

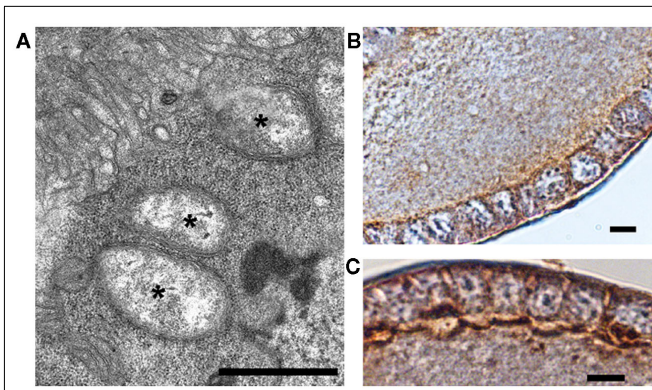


FIGURE 1 | Wolbachia's localization in the host's follicular epithelium of the gonad. (A) TEM micrograph of a *Wolbachia*-infected *Zyginidia pullula* (Hemiptera, Cicadellidae) follicle cell filled with bacteria (asterisks; bar = 0.9 μ m); **(B,C)** Immuno-histochemical reactions showing strong positivity (brown) to anti-wsp (*Wolbachia* surface protein) antibody in the leafhopper's follicular epithelium (bars = 10 μ m). Modified from Negri and Pellecchia (in press).

sex development, and on the involvement of the endosymbiont in such processes.

Until now, in insects, feminization induced by *Wolbachia* has been demonstrated in lepidopteran and hemipteran species (Hiroki et al., 2002; Kageyama and Traut, 2003; Negri et al., 2006; Sakamoto et al., 2007). In the butterfly *Eurema hecabe*, it has been demonstrated that the *Wolbachia* feminizing effect acts continuously throughout the larval development for the maintenance of the female phenotype (Narita et al., 2007). Accordingly, this suggests that the bacterium acts on the insect sex differentiation rather than sex determination, and ecdysteroids are the best candidate for such an interaction. Evidences are in fact provided by the effects of incomplete *Wolbachia* suppression by antibiotic treatments during lepidopteran larval stages. In particular some tetracycline-treated individuals show larval/pupal molting defects, and others do not pupate: the dissection of dead pupae reveals that many of them failed to escape from the pupal case (Narita et al., 2007). Similar molting defects may be obtained, for example, in ecdysone receptor knock-out individuals of *Blattella Germanica* and *D. melanogaster* EcR-mutants (Davis et al., 2005; Cruz et al., 2006). Moreover, antibiotic treatments in infected *E. hecabe* often induce also sexually intermediate traits in wings, gonads, and genitalia (Narita et al., 2007). Notably, in Lepidoptera a role for the ecdysteroid titer in regulating sexual dimorphism, including sex specific wing development, has been proved (Lobbia et al., 2003) strengthening the hypothesis of a link between *Wolbachia* and ecdysteroid signaling. In particular, we cannot exclude a host/symbiont co-adaptation where a partial symbiont removal leads to biological imbalance. This may also explain the origin of intersex individuals in *E. hecabe*, *Ostrinia scapularis*, and *O. furnacalis* partially cured by feminizing *Wolbachia* (Kageyama and Traut, 2003; Sakamoto et al., 2007). Intersexes are specimens characterized by a genetically homogeneous genotype (male in this case), but a mixture of male and female phenotypes (i.e., feminized tissues in this case): the appearance of these phenotypes may be the result of a partial but

evident conflict between male and female sex hormones and/or receptors.

In *Ostrinia* species, in addition, a complete feminization is fatal and genetical males die during the larval development (Kageyama and Traut, 2003; Sakamoto et al., 2007), while in other species the male-killing action of *Wolbachia* occurs during embryogenesis (Werren et al., 2008). As discussed above, the role played by ecdysteroids during the whole developmental cycle of insects is crucial. Embryogenesis, in particular, takes place in a steroid hormone-enriched environment, where steroids act for the coordination of morphogenetic movements (Kozlova and Thummel, 2003; Gaziova et al., 2004). Thus, if male-killing *Wolbachia* interacts with the host hormonal pathway involving ecdysteroids, this could affect the processes required for a normal development of males.

A sex-specific action of ecdysteroids during insect embryogenesis and development has been demonstrated in some studies concerning the effects of endocrine disrupting chemicals. Indeed, ecdysteroid agonists and antagonists (e.g., bisphenol A, tebufenozide, and ethinyl estradiol) are responsible for female-biased sex ratios in the treated populations (Hahn et al., 2001; Biddinger et al., 2006; Lee and Choi, 2007; Izumi et al., 2008). According to some authors, the observed sex-specific effect could be well explained by considering insect steroids as sex hormones. In particular, larval or embryo males die because they are subjected to an unsuitable, i.e., female, hormonal environment (Hahn et al., 2001).

WOLBACHIA, HOST OOGENESIS DEFECT RESCUING AND FECUNDITY ENHANCEMENT

In some cases *Wolbachia* is essential for insect reproduction, as in absence of the "infection" the host is not able to perform a normal oogenesis. For example, in the hymenopteran *Asobara tabida* the symbiosis with *Wolbachia* involves interference with the programmed cell death of nurse cells that is significantly higher in *Wolbachia*-cured insects (where the ovary completely lacks mature oocytes) than in naturally infected specimens (Dedeine et al., 2001; Pannebakker et al., 2007). The role of ecdysone in regulating cell apoptosis, a process required for insect development, is well known: during metamorphosis, for example, the steroid is a primary regulator of cell death in larval tissues which are destroyed or remodeled into an "adult" form (Tsuzuki et al., 2001; Mottier et al., 2004). Interestingly, in adults a higher level of 20E causes apoptosis of nurse cells which blocks the oogenesis process (McCall, 2004; Terashima et al., 2005; Ishimoto and Kitamoto, 2011). Therefore, it would be interesting to verify if *Wolbachia* interacts by modulating ecdysone signaling in *A. tabida*, thus influencing programmed cell death pathways occurring during host oogenesis.

In *D. melanogaster*, partial loss of function mutants of sex-lethal, the master regulator gene of the fly sex determination cascade, are sterile due to overproliferation of undifferentiated germ cells. In the infected line, *Wolbachia* is able to rescue oogenesis defects leading to partially fertile specimens (Starr and Cline, 2002). Stem cell behavior is regulated by intrinsic factors, signals from their niches and systemic hormones. Ecdysone is known to affect stem cell proliferation, also confirming current hypotheses

of an involvement of steroids in cancer: in particular, altered steroids signaling, as well as extensive molecular crosstalk between steroid and insulin/insulin-like growth factors, are commonly associated with cancer (Ables and Drummond-Barbosa, 2010). Accordingly, we may speculate that the occurrence of “cancer” germ cells could be due to a misregulation of ecdysone signaling in mutant flies that is rescued by *Wolbachia* infection.

Wolbachia has also been implicated in improving the fitness of several insect hosts (Dedeine et al., 2003).

New insights into the mechanisms underlying host fecundity enhancement are provided by a recent study on *D. mauritania*: *Wolbachia* improves fecundity both by enhancing stem cell proliferation and reducing programmed cell death in the germarium (Fast et al., 2011). The authors hypothesize that the presence of the bacterium in the germ-line stem cell niche modulates stem cell activity, although a contribution from systemic or stem cell intrinsic signals cannot be ruled out. It remains unclear, however, whether stem cells themselves sense and respond to *Wolbachia*. According to us, the role of ecdysone might be of primary importance, as the systemic hormone is known to stimulate directly germ-line stem cells in order to promote their self-renewal and activity (Ables and Drummond-Barbosa, 2010), with *Wolbachia* as the director of the scene.

INTERPLAY BETWEEN STEROID SIGNALING AND EPIGENETIC PATHWAYS

A growing body of data suggests a role for hormones in modulating epigenetic changes. In mammals, for example, steroids are able to induce epigenetic differences necessary for a correct sex differentiation of the brain (Nugent and McCarthy, 2011), and in adults they actively maintain DNA methylation patterns (Auger et al., 2011). An interaction between steroid/thyroid receptors and the epigenetic machinery (e.g., histone modifying enzymes and DNA methyltransferases) has been proposed too (Tsai et al., 2009; Haddad et al., 2010; Pathak et al., 2010). Novel insights into the mechanisms underlying such an interaction are provided by studies on nuclear receptor co-regulators (NRCs; i.e., co-activators and co-repressors). Strikingly, NRCs are key epigenetic regulators and utilize enzymatic activities to modify epigenetically the DNA and chromatin (Mahajan and Samuels, 2000; Rosenfeld et al., 2006; Hsia et al., 2010).

Thanks to studies on *Drosophila*, we now have compelling evidences of a direct interaction between steroids (specifically ecdysone) and epigenetic factors. For example, during fly development, neural circuit sculpting is due to cooperation between EcR and histone modifying enzymes (Kirilly et al., 2011). In addition, in the fly's ovary, ecdysone interacts with chromatin remodeling factors for modulating the proliferation and self-renewal of germ-line stem cells (Ables and Drummond-Barbosa, 2010). Ecdysone receptor signaling also needs direct cooperation with nucleosome remodeling complexes, and many EcR co-activators and co-repressors that contribute to the epigenetic memory have been identified and characterized (Kimura et al., 2008; Sawatsubashi et al., 2010; Kugler et al., 2011).

Interestingly, recent data demonstrate that *Wolbachia* infection is able to modulate the host genomic imprinting through methylation of the DNA (Negri et al., 2009a,b). In the leafhopper *Z.*

pullula, *Wolbachia*-infected genetic males develop into intersexes with a female phenotype. In particular, two kinds of intersexes are described: “intersex females” which are feminized males with ovaries, even able to produce progeny; and “intersex males” which bear testes and are characterized by a very low *Wolbachia* density (Negri et al., 2009a). Remarkably, *Wolbachia*-infected “intersex females” possess the same imprinting pattern of uninfected females, thus demonstrating that the infection disrupts the male imprinting (Negri et al., 2009a,b). In addition, the alteration occurs only if the bacterium exceeds a density threshold, as “intersex males” maintain a male genome-methylation pattern (Negri et al., 2009a). The epigenetic modifications affect the expression of genes involved in sex determination and development (Negri, unpublished data), thus avoiding the need for *Wolbachia* to interfere with each single gene separately.

In view of the interplay between hormone signaling and epigenetic machinery, data on the whole suggest that the manipulation of the host's epigenetic pathways might be achievable through a direct influence of *Wolbachia* on hormonal signaling involving ecdysteroids.

The model proposed in **Figure 2** tries to explain possible interactions. Once 20E is biosynthesized, it binds the nuclear receptor EcR which heterodimerizes with USP. The EcR/USP complex binds DNA and complexes with nuclear NRCs. Then, NRCs catalyze DNA methyltransferases for a correct methylation pattern of differentially methylated regions or directly function as histone modifying enzymes, thus activating proper selective transcriptional programs. In infected insects, *Wolbachia* may interact with the ecdysone pathway by synthesizing products competing with 20E or function as/interfere with NRCs. As a result, the EcR binding to DNA or the recruitment of DNA methyltransferases and/or histone modifying enzymes should be affected.

Accordingly, studies on *Wolbachia*–host interactions should give great attention for example to substances with an antagonist action on the ecdysone nuclear receptor; selective nuclear receptor modulators; or co-regulators of nuclear receptors, in view of their emerging role in integrating the transcriptional co-regulation with the epigenetic regulation (Rosenfeld et al., 2006; Kato et al., 2011).

CONCLUSION

Many experimental data support the role of *Wolbachia* in modulating the insect sexual phenotypes by interaction with the host hormonal signaling pathway. Indeed, the various phenotypic effects observed may be due to differences in host physiology and in particular to endocrine-related processes governing growth, development, and reproductive behavior.

In particular, a number of evidences links *Wolbachia* symbiosis to insulin and ecdysteroid signaling.

Several studies report an extensive crosstalk between the two hormonal signaling pathways, which may work antagonistically, jointly or even independently. Like many other symbiotic bacteria, *Wolbachia* could operate by attacking one crucial pathway in their hosts, thus affecting other metabolic networks, or by targeting both pathways, even interacting at several points in each of them for its own benefit (that is the manipulation of host reproduction and development in order to increase the number of infected females). In view of the interplay between hormone signaling and epigenetic

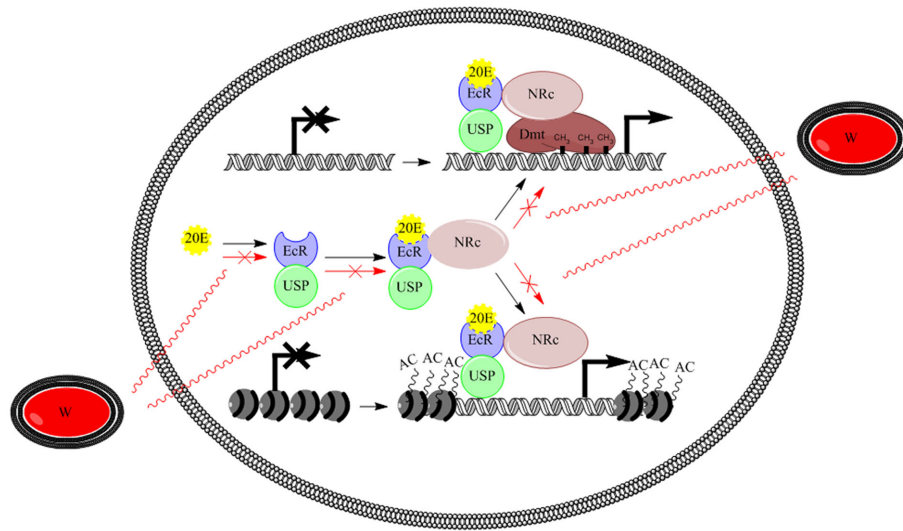


FIGURE 2 | Model illustrating the possible interplay between ecdysone signaling and epigenetic regulation, and *Wolbachia* action. 20E binds the nuclear receptor EcR which heterodimerizes with USP. Then, the EcR/USP complex binds DNA and complexes with nuclear receptor co-regulators, which catalyze DNA methyltransferases or directly function as histone

modifying enzymes, thus activating proper selective transcriptional programs. *Wolbachia* may interact by synthesizing products competing with 20E or function as/interfere with nuclear receptor co-regulators, respectively. 20E, 20-hydroxyecdysone; EcR, ecdysone receptor; USP, ultraspiracle; NRc, nuclear receptor co-regulator; Dmt, DNA-methyltransferase; W, *Wolbachia* bacteria

machinery, a direct influence of the “infection” on hormonal signaling involving ecdysteroids might be achievable through the manipulation of host epigenetic pathways.

Although further work is needed to fully clarify the genetic and molecular bases of such an interaction, new work hypotheses have been now offered for the study of the mechanisms used

by symbionts to dialog with their hosts. Likewise, the *Wolbachia*–host interaction should become an emerging model system for the study of hormone signaling orchestration made by microbial symbionts playing with nuclear receptors, and for shedding light on the role of NRCs in integrating the transcriptional co-regulation with the epigenetic regulation.

REFERENCES

- Ables, E. T., and Drummond-Barbosa, D. (2010). The steroid hormone ecdysone functions with intrinsic chromatin remodeling factors to control female germline stem cells in *Drosophila*. *Cell Stem Cell* 7, 581–592.
- Arumugam, S., Pfarr, K. M., and Hoerauf, A. (2008). Infection of the intermediate mite host with *Wolbachia*-depleted *Litomosoides sigmodontis* microfilariae: impaired L1 to L3 development and subsequent sex-ratio distortion in adult worms. *Int. J. Parasitol.* 38, 981–987.
- Auger, C. J., Coss, D., Auger, A. P., and Forbes-Lorman, R. M. (2011). Epigenetic control of vasopressin expression is maintained by steroid hormones in the adult male rat brain. *Proc. Natl. Acad. Sci. U.S.A.* 108, 4242–4247.
- Beckstead, R. B., Lam, G., and Thummel, C. S. (2007). Specific transcriptional responses to juvenile hormone and ecdysone in *Drosophila*. *Insect Biochem. Mol. Biol.* 37, 570–578.
- Biddinger, D., Hull, L., Huang, H., McPherson, B., and Loyer, M. (2006). Sublethal effects of chronic exposure to tebufenozide on the development, survival and reproduction of the tufted apple bud moth (Lepidoptera: Tortricidae). *J. Econ. Entomol.* 99, 834–842.
- Böhni, R., Riesgo-Escovar, J., Oldham, S., Brogiolo, W., Stocker, H., Andrus, B. F., Beckingham, K., and Hafen, E. (1999). Autonomous control of cell and organ size by CHICO, a *Drosophila* homolog of vertebrate IRS1–4. *Cell* 97, 865–875.
- Bouchon, D., Cordaux, R., and Grève, P. (2008). “Feminizing *Wolbachia* and the evolution of sex determination in isopods,” in *Insect Symbiosis*, eds K. Bourtzis and T. Miller (Boca Raton, FL: Taylor and Francis Group LLC), 273–294.
- Bownes, M., Blair, M., Kozma, R., and Dempster, M. (1983). 20E stimulates tissue-specific yolk-protein gene transcription in both male and female *Drosophila*. *J. Embryol. Exp. Morphol.* 78, 249–263.
- Casiraghi, M., McCall, J. W., Simoncini, L., Kramer, L. H., Sacchi, L., Genchi, C., Werren, J. H., and Bandi, C. (2002). Tetracycline treatment and sex-ratio distortion: a role for *Wolbachia* in the moulting of filarial nematodes? *Int. J. Parasitol.* 32, 1457–1468.
- Casper, A. L., and Van Doren, M. (2009). The establishment of sexual identity in the *Drosophila* germline. *Development* 136, 3821–3830.
- Clark, M. E., Anderson, C. L., Cande, J., and Karr, T. L. (2005). Widespread prevalence of *Wolbachia* in laboratory stocks and the implications for *Drosophila* research. *Genetics* 170, 1667–1675.
- Colombani, J., Bianchini, L., Layalle, S., Pondeville, E., Dauphin-Villemant, C., Antoniewski, C., Carré, C., Noselli, S., and Léopold, P. (2005). Antagonistic actions of ecdysone and insulins determine final size in *Drosophila*. *Science* 310, 667–670.
- Cruz, J., Mané Padrós, D., Belleés, X., and Martin, D. (2006). Functions of the ecdysone receptor isoform-A in the hemimetabolous insect *Blattella germanica* revealed by systemic RNAi in vivo. *Dev. Biol.* 297, 158–171.
- Davis, M. B., Carney, G. E., Robertson, A. E., and Bender, M. (2005). Phenotypic analysis of EcR-A mutants suggests that EcR isoforms have unique functions during *Drosophila* development. *Dev. Biol.* 282, 385–396.
- De Loof, A. (2006). Ecdysteroids: the overlooked sex steroids of insect? Males: the black box. *Insect Sci.* 13, 325–338.
- De Loof, A., and Huybrechts, R. (1998). “Insects do not have sex hormones”: a myth? *Gen. Comp. Endocrinol.* 111, 245–260.
- Dedeine, F., Bandi, C., Bouletreau, M., and Kramer, L. H. (2003). “Insights into *Wolbachia* obligatory symbiosis,” in *Insect Symbiosis*, eds K. Bourtzis and T. Miller (Boca Raton, FL: Taylor and Francis Group LLC), 267–282.
- Dedeine, F., Vavre, E., Fleury, F., Loppin, B., Hochberg, M. E., and Bouletreau, M. (2001). Removing symbiotic *Wolbachia* bacteria specifically inhibits oogenesis in a parasitic wasp. *Proc. Natl. Acad. Sci. U.S.A.* 98, 6247–6252.

- DeFalco, T., Camara, N., Le Bras, S., and Van Doren, M. (2008). Non-autonomous sex determination controls sexually dimorphic development of the *Drosophila* gonad. *Dev. Cell* 14, 275–286.
- Ewer, J. (2005). How the ecdysozoan changed its coat. *PLoS Biol.* 3, e349. doi:10.1371/journal.pbio.0030349
- Fast, E., Toomey, M., Panaram, K., Desjardins, D., Kolaczky, E., and Frydman, H. M. (2011). *Wolbachia* enhance *Drosophila* stem cell proliferation and target the germline stem cell niche. *Science* 334, 990–992.
- Francis, V. A., Zorzano, A., and Teleman, A. A. (2010). dDOR is an EcR coactivator that forms a feed-forward loop connecting insulin and ecdysone signalling. *Curr. Biol.* 20, 1799–1808.
- Frank, K., Frank, K., and Heald, R. D. (2010). The emerging role of *Wolbachia* species in heartworm disease. *Compend. Contin. Educ. Vet.* 32, E1–E5.
- Ganter, G. K., Walton, K. L., Merriam, J. O., Salmon, M. V., Brooks, K. M., Maddula, S., and Kravitz, E. A. (2007). Increased male male courtship in ecdysone receptor deficient adult flies. *Behav. Genet.* 37, 507–512.
- Gaziová, I., Bonnette, P. C., Henrich, V. C., and Jindra, M. (2004). Cell-autonomous roles of the ecdysoneless gene in *Drosophila* development and oogenesis. *Development* 131, 2715–2725.
- Gilbert, L. I., Rybczynski, R., and Warren, J. T. (2002). Control and biochemical nature of the ecdysteroidogenic pathway. *Annu. Rev. Entomol.* 47, 883–916.
- Gonella, E., Negri, I., Marzolari, M., Mandrioli, M., Sacchi, L., Pajoro, M., Crotti, E., Rizzi, A., Clementi, E., Tedeschi, R., Bandi, C., Alma, A., and Daffonchio, D. (2011). Bacterial endosymbiont localization in *Hyalesthes obsoletus*, the insect vector of bois noir in *Vitis vinifera*. *Appl. Environ. Microbiol.* 77, 1423–1435.
- Grönke, S., Clarke, D. F., Broughton, S., Andrews, T. D., and Partridge, L. (2010). Molecular evolution and functional characterization of *Drosophila* insulin-like peptides. *PLoS Genet.* 6, e1000857. doi:10.1371/journal.pgen.1000857
- Haddad, F., Jiang, W., Bodell, P. W., Qin, A. X., and Baldwin, K. M. (2010). Cardiac myosin heavy chain gene regulation by thyroid hormone involves altered histone modifications. *Am. J. Physiol. Heart Circ. Physiol.* 299, H1968–H1980.
- Hahn, T., Liess, M., and Schulz, R. (2001). Effects of the hormone mimetic insecticide tebufenozide on *Chironomus riparius* larvae in two different exposure setups. *Ecotoxicol. Environ. Saf.* 49, 171–178.
- Hirashima, A., Rauschenbach, I. Y., and Sukhanova, M. J. (2000). Ecdysteroids in stress responsive and nonresponsive *Drosophila virilis* lines under stress conditions. *Biosci. Biotechnol. Biochem.* 64, 2657–2662.
- Hiroki, M., Kato, Y., Kamito, T., and Miura, K. (2002). Feminization of genetic males by a symbiotic bacterium in a butterfly, *Eurema hecabe* (Lepidoptera: Pieridae). *Naturwissenschaften* 89, 67–70.
- Hsia, E. Y., Goodson, M. L., Zou, J. X., Privalsky, M. L., and Chen, H. W. (2010). Nuclear receptor coregulators as a new paradigm for therapeutic targeting. *Adv. Drug Deliv. Rev.* 62, 1227–1237.
- Huybrechts, R., and De Loof, A. (1977). Induction of vitellogenin synthesis in male *Sarcophaga bullata* by ecdysterone. *J. Insect Physiol.* 23, 1359–1362.
- Ikeya, T., Broughton, S., Alic, N., Grandison, R., and Partridge, L. (2009). The endosymbiont *Wolbachia* increases insulin/IGF-like signalling in *Drosophila*. *Proc. Biol. Sci.* 276, 3799–3807.
- Ishimoto, H., and Kitamoto, T. (2011). Beyond molting – roles of the steroid molting hormone ecdysone in regulation of memory and sleep in adult *Drosophila*. *Fly (Austin)* 5, 215–220.
- Izumi, N., Yanagibori, R., Shigeno, S., and Sajiki, J. (2008). Effects of bisphenol A on the development, growth and sex ratio of the housefly *Musca domestica*. *Environ. Toxicol. Chem.* 27, 1343–1353.
- Kageyama, D., and Traut, W. (2003). Opposite sex-specific effects of *Wolbachia* and interference with the sex determination of its host *Ostrinia scapularis*. *Proc. Biol. Sci.* 271, 251–258.
- Kato, S., Yokoyama, A., and Fujiki, R. (2011). Nuclear receptor coregulators merge transcriptional coregulation with epigenetic regulation. *Trends Biochem. Sci.* 36, 272–281.
- Kimura, S., Sawatsubashi, S., Ito, S., Kouzmenko, A., Suzuki, E., Zhao, Y., Yamagata, K., Tanabe, M., Ueda, T., Fujiyama, S., Murata, T., Matsukawa, H., Takeyama, K., Yaegashi, N., and Kato, S. (2008). *Drosophila* arginine methyltransferase 1 (DART1) is an ecdysone receptor co-repressor. *Biochem. Biophys. Res Commun.* 371, 889–893.
- Kirilly, D., Wong, J. J., Lim, E. K., Wang, Y., Zhang, H., Wang, C., Liao, Q., Wang, H., Liou, Y. C., Wang, H., and Yu, F. (2011). Intrinsic epigenetic factors cooperate with the steroid hormone ecdysone to govern dendrite pruning in *Drosophila*. *Neuron* 72, 86–100.
- Kozlova, T., and Thummel, C. S. (2003). Essential roles for ecdysone signaling during *Drosophila* mid-embryonic development. *Science* 301, 1911–1914.
- Kugler, S. J., Gehring, E. M., Walckamm, V., Krüger, V., and Nagel, A. C. (2011). The Putzig-NURF nucleosome remodeling complex is required for ecdysone receptor signaling and innate immunity in *Drosophila melanogaster*. *Genetics* 188, 127–139.
- Lee, S.-B., and Choi, J. (2007). Effects of bisphenol A and ethynyl estradiol exposure on enzyme activities, growth and development in the fourth instar larvae of *Chironomus riparius* (Diptera, Chironomidae). *Ecotoxicol. Environ. Saf.* 68, 84–90.
- Legrand, J. J., Legrand-Hamel, E., and Juchault, P. (1987). Sex determination in Crustacea. *Biol. Rev.* 62, 439–470.
- Lobbias, S., Niitsu, S., and Fujiwara, H. (2003). Female-specific wing degeneration caused by ecdysteroid in the tussock moth, *Orgyia recens*: hormonal and developmental regulation of sexual dimorphism. *J. Insect Sci.* 3, 1–7.
- Mahajan, M. A., and Samuels, H. H. (2000). A new family of nuclear receptor coregulators that integrate nuclear receptor signaling through CREB-binding protein. *Mol. Cell. Biol.* 20, 5048–5063.
- Manor, R., Weil, S., Oren, S., Glazer, L., Alfalo, E. D., Ventura, T., Chalifa-Caspi, V., Lapidot, M., and Sagi, A. (2007). Insulin and gender: an insulin-like gene expressed exclusively in the androgenic gland of the male crayfish. *Gen. Comp. Endocrinol.* 150, 326–336.
- Martin, G., Juchault, P., and Legrand, J. J. (1973). Mise en évidence d'un micro-organisme intracytoplasmique symbiote de l'oisillon *Armadillidium vulgare* Latreille dont la présence accompagne l'intersexualité ou la féminisation totale des mâles génétiques de la lignée thélygène. *C. R. Acad. Sci. Paris* 276, 2313–2316.
- Martin, G., Sorokine, O., Moniatte, M., Bulet, P., Hetru, C., and Van Dorsselaer, A. (1999). The structure of a glycosylated protein hormone responsible for sex determination in the isopod, *Armadillidium vulgare*. *Eur. J. Biochem.* 262, 727–736.
- McCall, K. (2004). Eggs over easy: cell death in the *Drosophila* ovary. *Dev. Biol.* 274, 3–14.
- Mottier, V., Siauxat, D., Bozzolan, F., Auzoux-Bordenave, S., Porcheron, P., and Debernard, S. (2004). The 20-hydroxyecdysone-induced cellular arrest in G2 phase is preceded by an inhibition of cyclin expression. *Insect Biochem. Mol. Biol.* 34, 51–60.
- Narita, S., Kageyama, D., Nomura, M., and Fukatsu, T. (2007). Unexpected mechanism of symbiont-induced reversal of insect sex: feminizing *Wolbachia* continuously acts on the butterfly *Eurema hecabe* during larval development. *Appl. Environ. Microbiol.* 73, 4332–4341.
- Negri, I., Franchini, A., Gonella, E., Daffonchio, D., Mazzoglio, P. J., Mandrioli, M., and Alma, A. (2009a). Unravelling the *Wolbachia* evolutionary role: the reprogramming of the host genomic imprinting. *Proc. Biol. Sci.* 276, 2485–2491.
- Negri, I., Mazzoglio, P. J., Franchini, A., Mandrioli, M., and Alma, A. (2009b). Male or female? The epigenetic conflict between a feminizing bacterium and its insect host. *Commun. Integr. Biol.* 2, 1–2.
- Negri, I., and Pelliccia, M. (in press). “Sex steroids in insects and the role of the endosymbiont *Wolbachia*: a new perspective,” in *Sex Hormones*, ed R. H. Dubey (InTech Publisher).
- Negri, I., Pelliccia, M., Mazzoglio, P. J., Patetta, A., and Alma, A. (2006). Feminizing *Wolbachia* in *Zyginidia pullula* (Insecta, Hemiptera), a leafhopper with an XX/X0 sex-determination system. *Proc. Biol. Sci.* 273, 2409–2416.
- Nugent, B. M., and McCarthy, M. M. (2011). Epigenetic underpinnings of developmental sex differences in the brain. *Neuroendocrinology* 93, 150–158.
- Pannebakker, B. A., Loppin, B., Eleman, C. P., Humblot, L., and Vavre, F. (2007). Parasitic inhibition of cell death facilitates symbiosis. *Proc. Natl. Acad. Sci. U.S.A.* 104, 213–215.
- Pathak, S., D'Souza, R., Ankolkar, M., Gaonkar, R., and Balasnor, N. H. (2010). Potential role of estrogen in regulation of the Insulin-like growth factor2-H19 locus in the rat testis. *Mol. Cell. Endocrinol.* 314, 110–117.
- Raikhel, A. S., Brown, M., and Belles, X. (2005). “Hormonal control of reproductive processes,” in *Comprehensive Insect Physiology, Biochemistry, Pharmacology and Molecular Biology*, eds L. Gilbert, S. Gill, and K. Iatrou (Boston: Elsevier Press), 433–491.

- Richard, D. S., Rybczynski, R., Wilson, T. G., Wang, Y., Wayne, M. L., Zhou, Y., Partridge, L., and Harshman, L. G. (2005). Insulin signaling is necessary for vitellogenesis in *Drosophila melanogaster* independent of the roles of juvenile hormone and ecdysteroids: female sterility of the chico1 insulin signaling mutation is autonomous to the ovary. *J. Insect Physiol.* 51, 455–464.
- Rigaud, T., and Juchault, P. (1998). Sterile intersexuality in an isopod induced by the interaction between a bacterium (*Wolbachia*) and the environment. *Can. J. Zool.* 76, 493–499.
- Rosen, O., Manor, R., Weil, S., Gafni, O., Linial, A., Aflalo, E. D., Ventura, T., and Sagi, A. (2010). A sexual shift induced by silencing of a single insulin-like gene in crayfish: ovarian upregulation and testicular degeneration. *PLoS ONE* 5, e15281. doi:10.1371/journal.pone.0015281
- Rosenfeld, M. G., Lunyak, V. V., and Glass, C. K. (2006). Sensors and signals: a coactivator/corepressor/epigenetic code for integrating signal-dependent programs of transcriptional response. *Genes Dev.* 20, 1405–1428.
- Roy, S. G., Hansen, I. A., and Raikhel, A. S. (2007). Effect of insulin and 20-hydroxyecdysone in the fat body of the yellow fever mosquito, *Aedes aegypti*. *Insect Biochem. Mol. Biol.* 37, 1317–1326.
- Sacchi, L., Genchi, M., Clementi, E., Negri, I., Alma, A., Ohler, S., Sasser, D., Bourtzis, K., and Bandi, C. (2010). Bacteriocyte-like cells harbour *Wolbachia* in the ovary of *Drosophila melanogaster* (Insecta, Diptera) and *Zyginidia pulula* (Insecta, Hemiptera). *Tissue Cell* 42, 328–333.
- Sagi, A., and Khalaila, I. (2001). The crustacean androgen: a hormone in an isopod and androgenic activity in decapods. *Am. Zool.* 41, 477–484.
- Sakamoto, H., Kageyama, D., Hoshizaki, S., and Yshikawa, Y. (2007). Sex specific death in the Asian corn borer moth (*Ostrinia furnacalis*) infected by *Wolbachia* occurs across larval development. *Genome* 50, 645–652.
- Sawatsubashi, S., Murata, T., Lim, J., Fujiki, R., Ito, S., Suzuki, E., Tanabe, M., Zhao, Y., Kimura, S., Fujiyama, S., Ueda, T., Umetsu, D., Ito, T., Takeyama, K., and Kato, S. (2010). A histone chaperone, DEK, transcriptionally coactivates a nuclear receptor. *Genes Dev.* 24, 159–170.
- Schütt, C., and Nöthiger, R. (2000). Structure, function and evolution of sex-determining systems in Dipteran insects. *Development* 127, 667–677.
- Schwedes, C., Tulsiani, S., and Carney, G. E. (2011). Ecdysone receptor expression and activity in adult *Drosophila melanogaster*. *J. Insect Physiol.* 57, 899–907.
- Shingleton, A. W. (2005). Body-size regulation: combining genetics and physiology. *Curr. Biol.* 15, R825–R827.
- Spindler, K. D., Hönl, C., Tremmel, Ch., Braun, S., Ruff, H., and Spindler-Barth, M. (2009). Ecdysteroid hormone action. *Cell. Mol. Life Sci.* 66, 3837–3850.
- Starr, D. J., and Cline, T. W. (2002). A host parasite interaction rescues *Drosophila* oogenesis defects. *Nature* 418, 76–79.
- Steinmann-Zwicky, M., Schmid, H., and Nöthiger, R. (1989). Cell-autonomous and inductive signals can determine the sex of the germ line of *Drosophila* by regulating the gene Sxl. *Cell* 57, 157–166.
- Stouthamer, R., Breeuwer, J. A., and Hurst, G. D. (1999). *Wolbachia pipiensis*: microbial manipulator of arthropod reproduction. *Annu. Rev. Microbiol.* 53, 71–102.
- Terashima, J., Takaki, K., Sakurai, S., and Bownes, M. (2005). Nutritional status affects 20-hydroxyecdysone concentration and progression of oogenesis in *Drosophila melanogaster*. *J. Endocrinol.* 187, 69–79.
- Tricoire, H., Battisti, V., Trannoy, S., Lasbleiz, C., Pret, A. M., and Monnier, V. (2009). The steroid hormone receptor EcR finely modulates *Drosophila* lifespan during adulthood in a sex-specific manner. *Mech. Ageing Dev.* 130, 547–552.
- Tsai, H.-W., Grant, P. A., and Rissman, E. F. (2009). Sex differences in histone modifications in the neonatal mouse brain. *Epigenetics* 4, 47–53.
- Tsuzuki, S., Iwami, M., and Sakurai, S. (2001). Ecdysteroid-inducible genes in the programmed cell death during insect metamorphosis. *Insect Biochem. Mol. Biol.* 31, 321–331.
- Ventura, T., Manor, R., Aflalo, E. D., Weil, S., Raviv, S., Glazer, L., and Sagi, A. (2009). Temporal silencing of an androgenic gland-specific insulin-like gene affecting phenotypical gender differences and spermatogenesis. *Endocrinology* 150, 1278–1286.
- Werren, J. H., Baldo, L., and Clark, M. E. (2008). *Wolbachia*: master manipulators of invertebrate biology. *Nat. Rev. Microbiol.* 6, 741–751.
- Wu, Q., and Brown, M. R. (2006). Signaling and function of insulin-like peptides in insects. *Annu. Rev. Entomol.* 51, 1–24.
- Zhu, J., Chen, L., and Raikhel, A. S. (2007). Distinct roles of Broad isoforms in regulation of the 20-hydroxyecdysone effector gene, Vitellogenin, in the mosquito *Aedes aegypti*. *Mol. Cell. Endocrinol.* 267, 97–105.

Conflict of Interest Statement: The author declares that the research was conducted in the absence of any commercial or financial relationships that could be construed as a potential conflict of interest.

Received: 09 November 2011; paper pending published: 30 November 2011; accepted: 21 December 2011; published online: 09 January 2012.

Citation: Negri I (2012) *Wolbachia* as an “infectious” extrinsic factor manipulating host signaling pathways. *Front. Endocrin.* 2:115. doi: 10.3389/fendo.2011.00115

This article was submitted to *Frontiers in Experimental Endocrinology*, a specialty of *Frontiers in Endocrinology*.

Copyright © 2012 Negri. This is an open-access article distributed under the terms of the Creative Commons Attribution Non Commercial License, which permits non-commercial use, distribution, and reproduction in other forums, provided the original authors and source are credited.